

Guibin Jiang · Xiangdong Li *Editors*

# A New Paradigm for Environmental Chemistry and Toxicology

From Concepts to Insights

 Springer

---

# A New Paradigm for Environmental Chemistry and Toxicology

---

Guibin Jiang • Xiangdong Li  
Editors

# A New Paradigm for Environmental Chemistry and Toxicology

From Concepts to Insights

 Springer

*Editors*

Guibin Jiang  
State Key Laboratory of Environmental  
Chemistry and Ecotoxicology  
Research Center for Eco-environmental  
Sciences, Chinese Academy of Sciences  
Beijing, China

Xiangdong Li  
Department of Civil and Environmental  
Engineering, Faculty of Construction  
and Environment  
The Hong Kong Polytechnic University  
Hong Kong, China

ISBN 978-981-13-9446-1      ISBN 978-981-13-9447-8 (eBook)  
<https://doi.org/10.1007/978-981-13-9447-8>

© Springer Nature Singapore Pte Ltd. 2020

This work is subject to copyright. All rights are reserved by the Publisher, whether the whole or part of the material is concerned, specifically the rights of translation, reprinting, reuse of illustrations, recitation, broadcasting, reproduction on microfilms or in any other physical way, and transmission or information storage and retrieval, electronic adaptation, computer software, or by similar or dissimilar methodology now known or hereafter developed.

The use of general descriptive names, registered names, trademarks, service marks, etc. in this publication does not imply, even in the absence of a specific statement, that such names are exempt from the relevant protective laws and regulations and therefore free for general use.

The publisher, the authors and the editors are safe to assume that the advice and information in this book are believed to be true and accurate at the date of publication. Neither the publisher nor the authors or the editors give a warranty, expressed or implied, with respect to the material contained herein or for any errors or omissions that may have been made. The publisher remains neutral with regard to jurisdictional claims in published maps and institutional affiliations.

This Springer imprint is published by the registered company Springer Nature Singapore Pte Ltd.  
The registered company address is: 152 Beach Road, #21-01/04 Gateway East, Singapore 189721, Singapore

---

## Foreword

Researchers from every academic discipline strive to understand the world around them and to solve the big problems facing humanity. When they have made new discoveries, they share them with their peers. With respect to these objectives, environmental chemists and toxicologists are unexceptional. Sometimes, we advance the field by publishing journal articles reporting the unexpected occurrence of a new family of contaminants, a previously unrecognized response to chemical exposure or a new way of understanding toxicokinetics. At other times, our contributions involve peer-reviewed critical reviews or perspective articles that use existing data to propose new ways of categorizing and explaining environmental phenomena. And sometimes progress comes in the form of a research monograph.

Unlike scientific journals, which sometimes sacrifice pedagogy for brevity and rapid publication, a research monograph provides authors with the opportunity to fully describe the relevant background and motivation for their work along with its importance and the future research opportunities that their research creates. A monograph also provides its editors with a chance to advance the field in a manner that may not be evident to the individual teams of authors. The editors of a research monograph carefully choose the authors and topics of individual chapters in much the same way as an artist creates a mosaic. Every individual chapter of the monograph describes the most recent developments in a specific field, but it is the holistic, overall view of the field that the reader gets by considering all of the chapters *in toto* that advances the discipline. For the newcomer to the field, a research monograph can be a point of entry that connects what might otherwise seem like a disconnected set of topics. For the experienced professional, a research monograph can open up opportunities to build connections and to tailor the next set of research studies to topics that can advance the overall objectives of the community.

*A New Paradigm for Environmental Chemistry and Toxicology* challenges our community to embrace a paradigm shift in the way that it operates. In the book's final chapter, Jin, Jiang and Li advocate for systems-level thinking to address the seemingly daunting challenge of responsibly managing chemicals in the Anthropocene. Their call for change could not have come from more qualified editors and it could not have come at a more opportune time. After a period of rapid development in the 1980s, the fields of environmental chemistry and toxicology have made incremental progress through the application of new analytical and bio-analytical tools, the extension of conceptual models to new families of contaminants and the analysis of data from long-term monitoring programs. Over the past 40 years, the number of peer-reviewed papers in the field has increased by over an order of magnitude as more countries join in the quest to protect the environment. But in light of civilization's exceedance of planetary boundaries, this is not enough.

As we learn more about the subtle impacts of chemical fate, transport and effects and as the industry continues to produce new families of chemicals in consumer products, crop protection products, medicines and fuels, it is becoming evident that a new approach is needed. Simply saying that we need to transcend disciplinary boundaries is not going to achieve this goal. No single investigator, no matter how brilliant and hardworking they may be, can master every aspect of this complex problem. We will always need researchers who can advance an

individual discipline by applying cutting-edge tools to advance understanding. However, if we want to be part of the solution to the world's problems, we have to find more effective ways to collaborate and to apply these tools simultaneously.

This research monograph brings together some of the leading environmental researchers interested in chemical fate, effects and treatment to create a mosaic that provides the reader with an understanding of where the field has been and where it is going. Considered individually, every chapter provides the reader with a thorough understanding of some of the key issues where progress is being made in specific sub-disciplines. Considered in its entirety, *A New Paradigm for Environmental Chemistry and Toxicology* lives up to its name by providing the reader with the knowledge needed to engage in this exciting and challenging next stage of progress in the discipline.

Grenoble, France  
June 2019

David L. Sedlak  
Plato Malozemoff Professor  
Co-Director, Berkeley Water Center  
Deputy Director, NSF Engineering Research  
for Reinventing the Nation's Urban Water Infrastructure (ReNUWIt)  
Director of Institute for Environmental Science and Engineering (IESE)  
University of California, Berkeley, CA 94720, USA

---

## Acknowledgements

With the tremendous developments in environmental chemistry and toxicology in the past 50 years, new theories have emerged, innovative methods have been proposed, and fresh applications have been conducted for various environmental problems. However, we are facing more complicated ecosystems both locally and globally. To address a series of global environmental issues and the future health of our planet, current research has migrated from assessments of past segregated phenomenological exposure and its effects based upon case chemicals towards a more predictive and scientific system with generalized principles and translational evidence that are applicable for policymakers and managers alike.

To reflect the state-of-the-art research fronts on environmental chemistry and toxicology, we have edited a reference book to illustrate the new paradigm shift from concepts to insights. With Springer Nature expressing interest in publishing the book, our work started in August 2018 with an initial plan of major chapter contents and potential contributors. It took several months before we had written confirmation from most of the selected authors. As we would like to have the book launch ceremony in August 2019 during one of the largest environmental chemistry conferences (The 10th National Conference on Environmental Chemistry in China), we had to set a strict deadline (31st May 2019) for the full chapter submission. Even though several authors could not meet the deadline, we are still very pleased to have 16 chapters on cutting-edge progress in environmental chemistry and toxicology. We are most grateful for the authors' dedication and contributions. It has been a great experience working with them on these important and interesting book chapters.

There are many people we would like to acknowledge in preparing the book for publication. Dr. Ling Jin (Research Assistant Professor of The Hong Kong Polytechnic University) provided great help in planning the book chapters and recommending leading authors. He also helped in drafting the last chapter to summarize the recent developments in environmental chemistry and toxicology since the publication of *Silent Spring* in 1962. Miss Anisha Tsang (Research Institute for Sustainable Urban Development, The Hong Kong Polytechnic University) provided excellent secretarial support in liaising with chapter authors, copyright clearance, and final document submissions. Miss Cherry Ma, our Coordinating Editor at Springer Nature China Office, offered excellent help at every stage of the book development. We are very grateful for her patience and cooperation. We are also grateful for Mr. Leon Lee (our summer intern from the University of East Anglia) for his careful proof read of the whole book.

We are most thankful for Prof. David Sedlak's remarkable and inspiring "Foreword" to the book. We hope the readers find the collections of theoretical developments and technological breakthroughs in environmental chemistry and toxicology useful and valuable.

July 2019

Guibin Jiang  
Xiangdong Li

---

## Contents

### **The Exposome: Pursuing the Totality of Exposure**

- The Exposome: Pursuing the Totality of Exposure** . . . . . 3  
Vrinda Kalia, Robert Barouki, and Gary W. Miller

### **Insights into Exposure Sources, Processes, and Impacts**

- In Situ Passive Sampling Techniques for Monitoring Environmental Mixture Exposure** . . . . . 13  
Lian-Jun Bao, Rainer Lohmann, Derek Muir, and Eddy Y. Zeng

- In Vivo SPME for Bioanalysis in Environmental Monitoring and Toxicology** . . . . . 23  
Anna Roszkowska, Miao Yu, and Janusz Pawliszyn

- Dose-Dependent Transcriptomic Approach for Mechanistic Screening in Chemical Risk Assessment** . . . . . 33  
Xiaowei Zhang, Pingping Wang, and Pu Xia

- Synchrotron-Based Techniques for the Quantification, Imaging, Speciation, and Structure Characterization of Metals in Environmental and Biological Samples** . . . . . 57  
Yu-Feng Li and Chunying Chen

### **Modelling and Computational Approaches for Exposure, Processes, and Impacts**

- High-Throughput Screening and Hazard Testing Prioritization** . . . . . 75  
Caitlin Lynch, Srilatha Sakamuru, Shuaizhang Li, and Menghang Xia

- Mixture Modelling and Effect-Directed Analysis for Identification of Chemicals, Mixtures and Effects of Concern** . . . . . 87  
Peta A. Neale and Beate I. Escher

- Mining Population Exposure and Community Health via Wastewater-Based Epidemiology** . . . . . 99  
Phil M. Choi, Kevin V. Thomas, Jake W. O'Brien, and Jochen F. Mueller

- Mechanistically Modeling Human Exposure to Persistent Organic Pollutants** . . . . . 115  
Frank Wania, Li Li, and Michael S. McLachlan

### **Solutions for Mitigating Hazardous Exposures**

- The Development and Challenges of Oxidative Abatement for Contaminants of Emerging Concern** . . . . . 131  
Stanisław Waclawek, Miroslav Černík, and Dionysios D. Dionysiou



---

<b>Biochar for Water and Soil Remediation: Production, Characterization, and Application</b> .....	153
Hao Zheng, Chenchen Zhang, Bingjie Liu, Guocheng Liu, Man Zhao, Gongdi Xu, Xianxiang Luo, Fengmin Li, and Baoshan Xing	
<b>Nanotechnology as a Key Enabler for Effective Environmental Remediation Technologies</b> .....	197
Yi Jiang, Bo Peng, Zhishang Wan, Changwoo Kim, Wenlu Li, and John Fortner	
<b>Emerging Issues of Future Concern</b>	
<b>Disinfection: A Trade-Off Between Microbial and Chemical Risks</b> .....	211
Nicholas Wawryk, Di Wu, Angela Zhou, Birget Moe, and Xing-Fang Li	
<b>Plastic and Microplastic Pollution: From Ocean Smog to Planetary Boundary Threats</b> .....	229
Liang-Ying Liu, Lei Mai, and Eddy Y. Zeng	
<b>Size and Composition Matters: From Engineered Nanoparticles to Ambient Fine Particles</b> .....	241
Lung-Chi Chen and Polina Maciejczyk	
<b>Transforming Environmental Chemistry and Toxicology to Meet the Anthropocene Sustainability Challenges Beyond <i>Silent Spring</i></b>	
<b>Transforming Environmental Chemistry and Toxicology to Meet the Anthropocene Sustainability Challenges Beyond <i>Silent Spring</i></b> .....	263
Ling Jin, Guibin Jiang, and Xiangdong Li	

# **The Exposome: Pursuing the Totality of Exposure**

# The Exposome: Pursuing the Totality of Exposure

Vrinda Kalia, Robert Barouki, and Gary W. Miller

## Abstract

Environmental determinants of health need to be measured and analyzed using system approaches that account for interactions between different agents that can elicit a biological response. The exposome offers a useful framework to examine the totality of exposures and their contribution to health and disease. Advances in exposure science, analytical chemistry, molecular biology, and toxicology have primed us to investigate the health effects of exposure to mixtures and concomitant exposures.

built environment, and neighborhood-level characteristics such as access to healthy food and parks. Furthermore, it includes structural policies that control access to healthcare and influence other health-related behaviours and choices. Given how diverse the environmental health umbrella is, it is not surprising that there are several definitions of what the environment constitutes. For the purpose of this chapter, we define the environment as all nongenetic factors that can be measured in the human body which may contribute to variability in disease risk and burden in an individual and the population.

## 1 Introduction

The role of the environment in disease etiology has received increased attention over the past several years. The genome and genetic variations account for far less of the disease burden in the population than was previously thought and the variation in population burden of disease is now largely attributed to nongenetic factors. A meta-analysis of 2,748 twin studies reported that the environmental contribution to thousands of complex human phenotypes was nearly equal to that of genetics (Polderman et al. 2015). A study in monozygotic twins found that the average genetic risk attributed to 28 chronic diseases was just 19% (range: 3–49%) (Rappaport 2016).

The environment encompasses a broad range of factors in the physical world. It includes but is not limited to dietary factors, exposure to infectious and synergistic organisms, toxicant exposures through various media and routes, the

## 2 Historical Perspective

The effect of the environment on human health has been suggested for millennia. In 400 BC, Hippocrates penned “On Airs, Waters, and Places” discussing the possible role of air and water quality, and climate on human health (Hippocrates 1881). The ancient Romans were aware of the adverse effects from exposure to lead from pipes that conducted water. Vitruvius, a Roman architect and civil engineer, noted that using earthen pipes to transport water would be safer for health than using pipes that contained lead (Hodge 1981). In the nineteenth century, public health efforts were focused on preventing exposure to infectious agents in the environment. Using epidemiological approaches, John Snow discovered a point of water contamination as the cause of a cholera epidemic in London in 1854 (Ruths 2009). These findings and others led to changes in water distribution systems, sewage treatment, and food handling in London. Water and sanitation remain important environmental determinants of health in many developing countries.

Most modern environmental epidemiology studies begin with observations of regional differences in disease rates. Adverse health effects associated with exposure to air pollution were discovered through atmospheric inversion phenomena that led to greater exposure for an extended period over specific geographic regions like Donora in the USA

V. Kalia · G. W. Miller (✉)

Department of Environmental Health Sciences, Mailman School of Public Health, Columbia University, New York, NY 10032, USA

e-mail: [gm2815@cumc.columbia.edu](mailto:gm2815@cumc.columbia.edu)

R. Barouki

Unité UMR-S 1124 Inserm-Université Paris Descartes, Paris, France

(1948), London in the UK (1952), and the Meuse Valley in Belgium (1930) (Nemery et al. 2001; Bell et al. 2004; Jacobs et al. 2018). Several other ecological studies were seminal in establishing relationships between air pollution exposure and adverse health outcomes (Dockery 1753). In the 1960s–70s, research focus shifted toward chemical and physical agents in the environment that can affect human health. Several researchers and public health agencies studied the effect of exposure to volatile organic compounds, metals, particulate matter, pesticides, and radiation on health. Books like *Silent Spring* (1962) and *Our Stolen Future* (1996) were critical in raising public awareness in the US on the societal cost of exposure to persistent organic pollutants and endocrine-disrupting chemicals. Recently, the effects of natural disasters, the built environment and global climate change on health have also been investigated.

Increased research efforts in precision medicine have also benefited environmental health research. Advances in molecular techniques have made it possible to study gene x environment interactions that can alter disease risk. The human genome project provided tools to make environmental determinants of health personalized, offering the opportunity to discern how certain genotypes may be more susceptible to effects of an environmental exposure (Collins et al. 2003). Apart from the geographical and genotypic context, the life stage during exposure can also alter disease risk and susceptibility to exposure. The developmental origins of health and disease (DoHAD) hypothesis has led to the discovery of epigenetic transfer of information from parent to offspring and unveiled the vulnerability of the fetus to environmental toxicants and their effect on development and health in later life (Barker 2007).

Advances in environmental chemistry and toxicology have been critical in understanding environmental contributors of human disease. Environmental epidemiology uses both to assign exposure and to determine the biological plausibility of observed association between exposure and outcome.

### 3 The Exposome

In order to understand the mechanisms by which environmental exposures can affect human health, researchers and regulators have studied exposures in great detail and described the effect of exposure in isolation to a number of chemicals on various health outcomes. However, real-world exposures do not occur in isolation and are accompanied with other exposures and context-specific factors. Besides, human interaction with the environment is lifelong, constant, and spatiotemporally dynamic. Most epidemiological and toxicological studies do not account for this chronic, low-dose exposure to environmental chemicals. To account

for this reality, Christopher Wild formally introduced the concept of the exposome in 2005. He defined it as the “life-course environmental exposures (including lifestyle factors), from the prenatal period onwards” (Wild 2005). The formal definition has undergone several revisions but most versions agree that the exposome comprises the entire set of lifelong environmental exposures and the biological response associated with these exposures (Wild 2012; Rappaport 2011; Miller and Jones 2014; Miller 2014). Investigating the biological response to an exposure accounts for toxicity mechanisms and interindividual variability in response. It also allows for the measurement of transient exposures that would be invisible through traditional approaches of exposure assessment. Since the environment is dynamic across the life course, assessing all exposures appears a daunting task. However, recent advances in methods bring optimism and avenues for creativity in the field.

#### 3.1 Tools to Monitor the Exogenous Exposures at the Population Level

*Remote sensing* is the science of gaining information on objects from a distance and has been used to identify exposures related to the urban environment. Specifically, they can be used to estimate population-level exposure to air pollution, changes in temperature, amount of green space assessed using a normalized difference vegetation index, and provide information on outdoor light-at-night exposure (Larkin and Hystad 2018; Markevych et al. 2017; Turner et al. 2017; Kloog et al. 2008; Rybnikova et al. 2016). Further, remote sensing data from a number of satellites has been integrated to determine global fine particulate matter concentrations (van Donkelaar et al. 2010).

*Mobile and stationary sensing* monitors are usually used to make exposure measurements in specific locations. They can be a part of national networks of measurement or be related to study-specific measurement campaigns. National networks tend to have limited coverage but can be used as part of a distributed sensor network, which uses low-cost sensors to fill in spatial gaps that national networks are unable to meet. These have been implemented in West Oakland, California (West Oakland Air Quality Study), and in Eindhoven, The Netherlands (AERIAS Project). However, low-cost sensors still require rigorous validation, limiting their widespread application (Curto et al. 2018). Mobile measurement campaigns have been implemented more recently in a few places, like Karlsruhe, Germany, and Zurich, Switzerland (Hagemann et al. 2014; Hasenfratz et al. 2015).

*Modeling* approaches find utility in distilling GIS and satellite data or spatial resolution. Models such as land use regression, kriging, and maximum entropy models have

been considered by researchers and will need to be elaborated (Jerrett et al. 2010). Data generated from population-level exposure assessments provides opportunity to create ecological studies that can provide links between exposure and population health. Most of these data sources, however, are ineffective at determining individual exposure levels. They will need to be integrated with individual-level measures for validation.

### 3.2 Tools to Monitor the Exogenous Exposures at the Individual Level

*External sensors* can be used to track a myriad of personal information. Personal location data obtained through GPS devices enable integration of exposure maps with individual location markers to get personal exposure estimates (Asimina et al. 2018). Accelerometers and other activity tracking personal devices like Jawbone, FitBit, Apple Watch, and Polar (Loh 2017) can be used to ascertain both external exposures and certain lifestyle factors related to exercise and diet. Personal sensing technologies can also be used to assess air pollution exposure, changes in ambient temperature, and presence of green space (Nieuwenhuijsen et al. 2014). Passive dosimeters like silicone wristbands can also be used for personal exposure assessment and provide valuable semi-quantitative information on several chemicals (O'Connell et al. 2014).

*Smartphone-based sensors and assessments* can integrate data from personal sensors like accelerometers, GPS, barometers, thermometers, and ambient light sensors to record personal exposures. Their high penetrance worldwide provides a unique opportunity to obtain large amounts of personal data from diverse individuals (Murphy and King 2016; van Wel et al. 2017).

*Personal sensors* to monitor heart rate, glucose levels, blood pressure, muscle activity, body temperature, and sweat production are being developed and will require validation before their implementation in large population studies. Compared to measurements of external exposure, individual-level data is more actionable, can be used for personalized advice, and can be related to internal dose and associated biological responses.

### 3.3 Tools to Measure Endogenous Response and the Exposome

Techniques in molecular biology have shown exponential advancement in the past three decades. These advances have increased the resolution at which biological response to perturbations from environmental exposures is measured. Exposures to environmental factors can induce local and

global changes in gene expression, enzyme activity, metabolite pathway alterations, and protein synthesis/folding. Deep molecular phenotyping can provide information on acute biological responses and also provide measures of long-term changes in physiology which can be viewed as markers of exposure memory (Go and Jones 2016; Weinhold 2006; Jeanneret et al. 2014).

**Metabolomics.** The metabolome is comprised of small molecules in a biological matrix that is <2000 Daltons in molecular mass. It is thought of as the functional output of genes and proteins, and their interaction with the environment. Recent advances in mass spectrometric techniques have made it possible to capture previously undetected small molecules, with estimates suggesting the metabolome may comprise of more than 1 million chemical features (Uppal et al. 2016). Chemical signals derived from a biological sample can arise from an endogenous metabolism, environmental chemical exposures, diet, the microbiome, personal care products, and drugs (Petrick et al. 2017; Liu et al. 2016; Jones 2016; Walker et al. 2019; Walker et al. 2016). Using an untargeted approach, metabolomics can expand surveillance of environmental chemicals, detect new xenobiotic chemicals, and identify unknown pollutants (Bonvalot et al. 2013; Roca et al. 2014; Jamin et al. 2014). Historically, metabolomics has not focused on those exogenous chemicals, but recent efforts are increasing the identity of environmental chemicals through these untargeted approaches. By simultaneously measuring exposure and biological response, metabolomics offers the opportunity to link exposure to molecules associated with exposure. While the identity of most chemical features that are measured using untargeted high-resolution metabolomics remain unknown, the technique offers a powerful opportunity for hypothesis generation and identification of unknown chemicals of interest related to a health outcome.

**Transcriptomics.** Gene expression is the process by which genetic data encoded by DNA is transcribed to RNA, which then initiates and directs protein synthesis in a cell. Cellular function regulation involves a complex series of steps that control the amount of RNA, and in turn, protein that is synthesized. Thus, exposures that alter functional regulation in the cell can be detected using transcriptomic and metabolomic analyses. Chemical exposures have been linked with distinct gene expression profiles that have been seen in humans and model organisms (Hamadeh et al. 2002). Transcriptomic analyses in human samples involve DNA microarray hybridization, which uses 40,000–50,000 molecular probes to seek RNA transcripts (McHale et al. 2009; Spira et al. 2004; Fry et al. 2007). Next-generation sequencing has made it possible to measure the effect of exposures on different types of RNA in a sample, including mRNA, microRNA, small interfering RNA, and long non-coding RNA. Databases that curate gene expression

profiles across different exposures and model organisms provide opportunities to compare experimental data with previously generated gene expression profiles (Grondin et al. 2018).

**Proteomics.** Protein measurement can elucidate signaling, inflammation, oxidative stress, and tissue damage in a biological sample. Levels of proteins and their posttranslational modifications are closer to function than gene expression data. Measuring proteins can be targeted using enzyme-linked immunosorbent assays (ELISA), or newer multiplexed bead-based assays that are capable of measuring more than 50 proteins in a small amount of biological material (Elshal and McCoy 2006; Tighe et al. 2015). While the use of high-resolution mass spectrometers in untargeted proteomics is insightful, it is also challenging due to difficulties in detecting low-abundance proteins. Chemical exposure to reactive electrophiles has been achieved through protein adductomics platforms, which can measure more than 100 human serum albumin adducts at the Cys34 site. Protein adductomics has been used to assess exposure to lifestyle factors, indoor air pollution, and ambient air pollution (Rappaport et al. 2012; Grigoryan et al. 2016; Liu et al. 2018).

**Epigenomics.** Epigenetic changes on DNA can alter gene expression. These changes can occur through the addition or removal of methyl groups on CpG dinucleotides, or through histone modifications. These modifications can be long term and have the potential to be transferred to the next generation if they occur in germ cells. Different stressors including chemical exposures can lead to specific epigenetic signatures that persist even after the stressor has been removed (Fernandez et al. 2012). Thus, epigenetic profiles can be used to monitor exposure history and to assess acute or chronic stress (Go and Jones 2016; Go and Jones 2014). High-throughput assays based on parallel sequencing of DNA with bisulfite conversions can measure up to 850,000 CpG sites within the human genome. Epigenome-wide association studies have revealed distinct methylation patterns associated with chemical exposures, providing insight into the mechanisms underlying the biological responses (Bollati et al. 2007; Seow et al. 2014; Hou et al. 2012).

**Multi-omics assessment of the exposome.** Information from different layers of the biochemical dogma can be integrated to paint a holistic picture of biological response to an environmental perturbation (Fig. 1). Using approaches from systems biology, we can gain a deeper understanding of environmental influences on human health by integrating across epigenomic, transcriptomic, proteomic, and metabolomic changes associated with exposures. The integration of high-dimensional data has benefited from the development of statistical approaches that identify interactions among biological response networks (Uppal et al. 2018; Kalia et al. 2019). The continued use of deep molecular phenotyping of

cohort studies will generate data needed to spur new discoveries and methods (Vineis 2017; Vrijheid 2014; Li et al. 2017; Barouki et al. 2018; Carvaillo et al. 2019).

### 3.4 Considerations in Measuring Exposure and Biological Response

We have learned several lessons from environmental epidemiology about associations between exposure and disease. Investigators have recognized the importance of accuracy and precision while measuring exposure. Accurate exposure assessment is essential to detect and quantify a dose–response relationship. Inaccuracy can lead to mis-measurement of a continuous exposure measure or can lead to misclassification of a dichotomous exposure status, which can severely bias results toward the null. Using biomarkers of exposure has several advantages: 1. Detection of the biomarker proves absorption of the compound, 2. It accounts for bioavailability of the compound, and 3. It integrates measures over all routes of exposure. However, it remains hard to tell where in the environment the compound came from, posing the need to compare internal dose data with data collected from external monitors and measurements. Further, since biomarker collection is expensive and relies on access to biological matrix availability, we can also validate other less expensive measurement methods by validation against biomarkers measured in a subset of the population. Epidemiological studies that provide causal interpretation of observations have good study designs. These study designs account for all variables that can confound relationships between exposure and response, and provide the means to uncover temporal relationships.

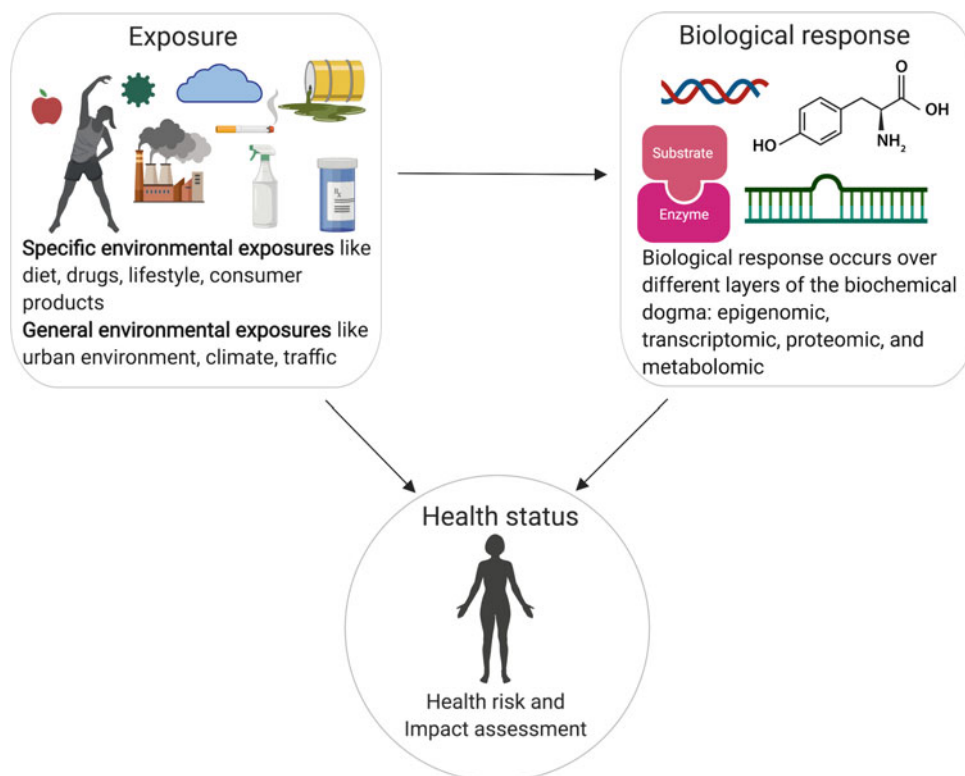
---

## 4 An International Perspective

Chris Wild’s article (Wild 2005) describing the exposome concept raised a huge interest in the scientific community, which did not translate immediately into identified projects in Europe until the European commission launched research calls on the exposome within the seventh framework (FP7). In 2012 and 2013, three projects were launched, HELIX, Exposomics, and then HEALS. The concept was not to develop facilities, but rather to form integrated projects that would encompass the complexity of the exposome. Each project had its own perspective. HELIX, for example, focused on the pregnancy exposome by studying several EU birth cohorts (Maitre et al. 2018), Exposomics focused on the short and long-term effects of exposure to water and air pollutants (Turner et al. 2018), and HEAL focused on modeling and multidisciplinary to develop a new “exposome” cohort (Steckling et al. 2018). More recently, the

**Fig. 1 The exposome concept**

Environmental exposures can derive from individual factors (like diet) and from general sources (like air pollution). Exposures that affect health leave a biological fingerprint that can be measured through changes in biological response in different biochemical layers. Integrating measures of external exposure and internal biological response create the exposomic framework to assess health status through risk and impact assessment. (Created with BioRender)



European Commission launched a new call within the H2020 framework, which will support 4–5 projects with a clear focus on the development of an exposome toolbox that should be coordinated by a cluster gathering of those projects. It is fair to say that several other projects within the EU are inspired by or address one of the exposures that constitute the exposome (Karjalainen et al. 2017). As an example, the EU biomonitoring program, HBM4EU, focuses on chemical exposures, while the project Lifepath addresses primarily socioeconomic aspects. There are other projects addressing urban exposures or the eco-exposome. While all these projects do not focus per se on technology developments, they do allow significant technological progress, most notably in analytical methodologies, sensor technology, biostatistics, and bioinformatics. Clearly, the upcoming exposome toolbox cluster will highlight and further develop these methodologies with the aim to support public health and regulatory decisions as well as informed individual prevention.

## 5 Environmental Chemistry and the Exposome

Chemicals released into the environment usually undergo transformations under different environmental conditions to produce intermediate chemicals. Several tools have been developed (Ruttikies 2016; Djoumbou-Feunang et al. 2019)

which can help predict and identify unknown chemical signals measured in human and environmental samples. Efforts are underway to use high-resolution mass spectrometers to characterize all chemicals present in an environmental sample. Methods have been developed to identify “known unknown” chemicals using spectral fragmentation patterns that can help deduce chemical structure and identity (Schymanski et al. 2015; Gago-Ferrero et al. 2015).

In an epidemiological setting, Liang and colleagues used high-resolution metabolomics to characterize plasma and saliva samples from participants of a traffic-related air pollution exposure study. They measured a number of traffic-related air pollutants using external monitors and measured the association between exposure and metabolic profiles of the participants. Chemical features of interest that were significantly associated with exposure belonged to metabolic pathways related to inflammation and oxidative stress, including leukotriene and vitamin E metabolism (Liang et al. 2018).

## 6 The Exposome and Toxicology

More than 85,000 chemicals are registered with the EPA for manufacture, import, and use in commercial products. Approximately, 112,000 chemicals and compounds are registered with the US Food and Drug Administration as drugs or food additives (Niedzwiecki et al. 2019).

A majority of these chemicals have little information on their health effects at low concentrations and their influence as complex mixtures seen in real-world scenarios. This poses a significant challenge that requires expertise across several disciplines. Toxicologists have been systematically working through this list of chemicals that contribute to the chemical exposome. High-throughput screening assays have gained popularity for their efficiency and the high resolution of data they produce. They both conserve time and provide valuable insight for researchers toward the affected organ system or pathway that may be perturbed due to an exposure. The National Toxicology Program in the US has been leading a shift in current toxicological research, moving away from in vivo testing and incorporating high-throughput in vitro assays, model organisms, and computational models to study the adverse effects of exposure to chemical mixtures (Council 2007). Some of these methods are discussed below.

**Structure–activity relationship (SAR).** This method uses physical and chemical characteristics to predict toxicity based on the similar-property principle, i.e., similar structure = similar biological activity (Tong et al. 2003). These methods can be quantitative (mathematical modeling) or qualitative (recognize substructures that afford toxic properties). They have found utility in predicting toxicokinetics, half-lives, and the ability of chemicals to cross the blood brain barrier.

**In vitro testing.** Human cell lines and animal cell lines transfected to express human genes can be used to create assays to measure molecular changes due to different exposures. Modifying assay parameters and changing culture conditions can alter the context of exposures to answer specific biological questions. As an example, in vitro cell lines have been used to study the effect of exposure to mixtures on receptor ligand binding and activation. A group of researchers found that at low concentrations, a combination of two known pregnane X receptor (PXR) ligands resulted in a synergistic effect on activation of the receptor, which was not observed with each chemical alone. The researchers suggested that the two ligands together form a “supermolecular ligand” within the ligand-binding pocket of the nuclear receptor (Delfosse 2015). Findings such as these support the exposome concept in toxicological studies.

Cell-based in vitro assays can be used for high-throughput screens, which offer an economical way to screen a large number of chemicals in a short period. These screens are widely accepted in the pharmaceutical industry to predict therapeutic action, pharmacokinetics, interactions with enzymes, biotransformation, metabolic products, and have been used to rapidly detect interactions of drugs with genetic polymorphisms. Further, all methods described to

measure biological response (Sect. 3.3.) can be applied on a cellular level to ascertain changes in gene expression, protein expression, metabolism, and epigenetic modifications due to an exposure.

**Model organisms.** While cell-based assays serve as excellent screening tools, single cells don't represent complex tissue interactions of a whole organism. To this end, model organisms like *Caenorhabditis elegans* (worms) and *Danio rerio* (zebrafish) have been gaining popularity as toxicological models. The short generation times of *C. elegans* make them excellent models to study aging and life course specific changes in response to exposure. Several molecular pathways have been conserved across evolution-making discoveries and observations in these models relevant for the human context. In a metabolomic study, Jones and colleagues described changes in metabolism in *C. elegans* as a result of exposure to a mixture of the heavy metal nickel and the pesticide chlorpyrifos. The authors noted changes in metabolism of the branched-chain amino acids and tricarboxylic acid cycle intermediates. They also found changes in reproduction (brood size) due to exposure to this mixture of toxicants (Jones et al. 2012).

---

## 7 Conclusion and Future Directions

Understanding the relationship between the totality of environmental exposures and health poses many challenges. Many exposures are largely involuntary and dynamic, and not all environmental exposures have been fully characterized. Studying the exposome thus relies on cutting-edge technologies that can detect and identify chemicals we are exposed to, moving beyond a targeted list of known chemicals of interest. Analysis and interpretation of this data requires various data analytical techniques: dimension reduction techniques, data integration, network analysis, and longitudinal analysis to name a few. Apart from novel data analytical applications, the field will also need to think about confounders and effect modifiers when measuring associations between exposure and disease. For example, how should social class or socioeconomic status be treated in a model—as a confounder, effect modifier, or a determinant of exposure? Uncovering the exposome will need input from scientists working in the fields of environmental chemistry, toxicology, exposure science, epidemiology, molecular biology, analytic chemistry, bioinformatics, and engineering. Thus, a multifaceted problem will be best tackled with multidisciplinary research teams.

**Acknowledgements** National Institutes of Health ES023839 and ES030163, Inserm, and University of Paris Descartes-USPC.



## References

- Asimina S et al (2018) Assessing and enhancing the utility of low-cost activity and location sensors for exposure studies. *Environ Monit Assess* 190(3):155
- Barker DJP (2007) The origins of the developmental origins theory. *J Internal Med* 261(5):412–417
- Barouki R et al (2018) Integration of the human exposome with the human genome to advance medicine. *Biochimie* 152:155–158
- Bell ML, Davis DL, Fletcher T (2004) A retrospective assessment of mortality from the London smog episode of 1952: the role of influenza and pollution. *Environ Health Perspect* 112(1):6–8
- Bollati V et al (2007) Changes in DNA methylation patterns in subjects exposed to low-dose benzene. *Cancer Res* 67(3):876–880
- Bonvallot N et al (2013) Metabolomics tools for describing complex pesticide exposure in pregnant women in Brittany (France). *PLoS ONE* 8(5):e64433
- Carvaillo J-C et al (2019) Linking Bisphenol S to adverse outcome pathways using a combined text mining and systems biology approach. *Environ Health Perspect* 127(4):47005
- Collins FS, Morgan M, Patrino A (2003) The human genome project: lessons from large-scale biology. *Science* 300(5617):286–290
- Council NR (2007) Toxicity testing in the 21st century: a vision and a strategy
- Curto A et al (2018) Performance of low-cost monitors to assess household air pollution. *Environ Res* 163:53–63
- Delfosse V et al (2015) Synergistic activation of human pregnane X receptor by binary cocktails of pharmaceutical and environmental compounds. *Nat Commun* 6
- Djoubbou-Feunang Y et al (2019) BioTransformer: a comprehensive computational tool for small molecule metabolism prediction and metabolite identification. *J Cheminformatics* 11(1):2
- Dockery DW et al An association between air pollution and mortality in six U.S. cities. *New England J Med* 329(24):1753–1759
- Elshal MF, McCoy JP (2006) Multiplex bead array assays: performance evaluation and comparison of sensitivity to ELISA. *Methods (San Diego, Calif.)* 38(4):317–323
- Fernandez AF et al (2012) A DNA methylation fingerprint of 1628 human samples. *Genome Res* 22(2):407–419
- Fry RC et al (2007) Activation of inflammation/NF-kappaB signaling in infants born to arsenic-exposed mothers. *PLoS Genet* 3(11):e207
- Gago-Ferrero P et al (2015) Extended suspect and non-target strategies to characterize emerging polar organic contaminants in raw wastewater with LC-HRMS/MS. *Environ Sci Technol* 49(20):12333–12341
- Go Y-M, Jones DP (2014) Redox biology: interface of the exposome with the proteome, epigenome and genome. *Redox Biol* 2:358–360
- Go Y-M, Jones DP (2016) Exposure memory and lung regeneration. *Ann Am Thoracic Soc* 13(Suppl 2):S452–S461
- Grigoryan H et al (2016) Adductomics pipeline for untargeted analysis of modifications to Cys34 of human serum albumin. *Anal Chem* 88(21):10504–10512
- Grondin CJ et al (2018) Accessing an expanded exposure science module at the comparative toxicogenomics database. *Environ Health Perspect* 126(1):014501
- Hagemann R et al (2014) Spatial variability of particle number concentrations and NOx in the Karlsruhe (Germany) area obtained with the mobile laboratory 'AERO-TRAM'. *Atmos Environ* 94:341–352
- Hamadeh HK et al (2002) Gene expression analysis reveals chemical-specific profiles. *Toxicol Sci Off J Soc Toxicol* 67(2):219–231
- Hasenfratz D et al (2015) Deriving high-resolution urban air pollution maps using mobile sensor nodes. *Pervasive Mob Comput* 16:268–285
- Hippocrates et al (1881) Hippocrates on airs, waters and places. Wyman & Sons, London, p 124
- Hodge AT (1981) Vitruvius, lead pipes and lead poisoning. *Am J Archaeol* 85(4):486–491
- Hou L et al (2012) Environmental chemical exposures and human epigenetics. *Int J Epidemiol* 41(1):79–105
- Jacobs ET, Burgess JL, Abbott MB (2018) The Donora smog revisited: 70 years after the event that inspired the clean air act. *Am J Pub Health* 108(Suppl 2):S85–S88
- Jamin EL et al (2014) Untargeted profiling of pesticide metabolites by LC-HRMS: an exposomics tool for human exposure evaluation. *Anal Bioanal Chem* 406(4):1149–1161
- Jeanneret F et al (2014) Human urinary biomarkers of dioxin exposure: analysis by metabolomics and biologically driven data dimensionality reduction. *Toxicol Lett* 230(2):234–243
- Jerrett M, Gale S, Kontgis C (2010) Spatial modeling in environmental and public health research. *Int J Environ Res Pub Health* 7(4):1302–1329
- Jones DP (2016) Sequencing the exposome: a call to action. *Toxicol Rep* 3:29–45
- Jones OAH et al (2012) Potential new method of mixture effects testing using metabolomics and *Caenorhabditis elegans*. *J Proteome Res* 11(2):1446–1453
- Kalia V, Jones DP, Miller GW (2019) Networks at the nexus of systems biology and the exposome. *Curr Opin Toxicol*
- Karjalainen T, Hoeveler A, Draghia-Akli R (2017) European union research in support of environment and health: building scientific evidence base for policy. *Environ Int* 103:51–60
- Kloog I et al (2008) Light at night co-distributes with incident breast but not lung cancer in the female population of Israel. *Chronobiol Int* 25(1):65–81
- Larkin A, Hystad P (2018) Evaluating street view exposure measures of visible green space for health research. *J Expo Sci Environ Epidemiol*
- Li S et al (2017) Metabolic phenotypes of response to vaccination in humans. *Cell* 169(5):862–877.e17
- Liang D et al (2018) Use of high-resolution metabolomics for the identification of metabolic signals associated with traffic-related air pollution. *Environ Int* 120:145–154
- Liu KH et al (2016) High-resolution metabolomics assessment of military personnel: evaluating analytical strategies for chemical detection. *J Occup Environ Med* 58(8 Suppl 1):S53–S61
- Liu S et al (2018) Cys34 Adductomes differ between patients with chronic lung or heart disease and healthy controls in Central London. *Environ Sci Technol* 52(4):2307–2313
- Loh M et al (2017) How sensors might help define the external exposome. *Int J Environ Res Pub Health* 14(4)
- Maitre L et al (2018) Human Early Life Exposome (HELIX) study: a European population-based exposome cohort. *BMJ Open* 8(9):e021311
- Markevych I et al (2017) Exploring pathways linking greenspace to health: theoretical and methodological guidance. *Environ Res* 158:301–317
- McHale CM et al (2009) Changes in the peripheral blood transcriptome associated with occupational benzene exposure identified by cross-comparison on two microarray platforms. *Genomics* 93(4):343–349
- Miller GW (2014) The exposome: a primer. Academic Press, Waltham
- Miller GW, Jones DP (2014) The nature of nurture: refining the definition of the exposome. *Toxicol Sci* 137(1):1–2
- Murphy E, King EA (2016) Smartphone-based noise mapping: integrating sound level meter app data into the strategic noise mapping process. *Sci Total Environ* 562:852–859
- Nemery B, Hoet PHM, Nemmar A (2001) The Meuse Valley fog of 1930: an air pollution disaster. *Lancet* 357(9257):704–708

- Niedzwiecki MM et al (2019) The exposome: molecules to populations. *Ann Rev Pharmacol Toxicol* 59(1):107–127
- Nieuwenhuijsen MJ et al (2014) Using personal sensors to assess the exposome and acute health effects. *Int J Environ Res Pub Health* 11(8):7805–7819
- O'Connell SG, Kincl LD, Anderson KA (2014) Silicone wristbands as personal passive samplers. *Environ Sci Technol* 48(6):3327–3335
- Patrick L et al (2017) An untargeted metabolomics method for archived newborn dried blood spots in epidemiologic studies. *Metabolomics* 13(3):27
- Polderman TJC et al (2015) Meta-analysis of the heritability of human traits based on fifty years of twin studies. *Nat Genetics* 47(7):702–709
- Rappaport SM (2011) Implications of the exposome for exposure science. *J Expos Sci Environ Epidemiol* 21(1):5–9
- Rappaport SM (2016) Genetic factors are not the major causes of chronic diseases. *PLoS ONE* 11(4):e0154387
- Rappaport SM et al (2012) Adductomics: characterizing exposures to reactive electrophiles. *Toxicol Lett* 213(1):83–90
- Roca M et al (2014) Comprehensive analytical strategy for biomonitoring of pesticides in urine by liquid chromatography–orbitrap high resolution mass spectrometry. *J Chromatogr A* 1374:66–76
- Ruths MB (2009) The lesson of John Snow and the broad street pump. *AMA J Ethics* 11(6):470–472
- Ruttkies C et al (2016) MetFrag relaunched: incorporating strategies beyond in silico fragmentation. *J Cheminformatics* 8
- Rybnikova NA, Haim A, Portnov BA (2016) Does artificial light-at-night exposure contribute to the worldwide obesity pandemic? *Int J Obes* 40(5):815–823
- Schymanski EL et al (2015) Non-target screening with high-resolution mass spectrometry: critical review using a collaborative trial on water analysis. *Anal Bioanal Chem* 407(21):6237–6255
- Seow WJ et al (2014) Epigenome-wide DNA methylation changes with development of arsenic-induced skin lesions in Bangladesh: a case-control follow-up study. *Environ Mol Mutagen* 55(6):449–456
- Spira A et al (2004) Effects of cigarette smoke on the human airway epithelial cell transcriptome. *Proc Natl Acad Sci USA* 101(27):10143–10148
- Steckling N et al (2018) Biomarkers of exposure in environment-wide association studies—opportunities to decode the exposome using human biomonitoring data. *Environ Res* 164:597–624
- Tighe PJ et al (2015) ELISA in the multiplex era: potentials and pitfalls. *Proteomics Clin Appl* 9(3–4):406–422
- Tong W et al (2003) Structure-activity relationship approaches and applications. *Environ Toxicol Chem* 22(8):1680–1695
- Turner MC et al (2017) Assessing the exposome with external measures: commentary on the state of the science and research recommendations. *Ann Rev Pub Health* 38(1):215–239
- Turner MC et al (2018) EXPOsOMICS: final policy workshop and stakeholder consultation. *BMC Pub Health* 18(1):260
- Uppal K et al (2016) Computational metabolomics: a framework for the million metabolome. *Chem Res Toxicol* 29(12):1956–1975
- Uppal K et al (2018) xMWAS: a data-driven integration and differential network analysis tool. *Bioinform (Oxford, England)* 34(4):701–702
- van Donkelaar A et al (2010) Global estimates of ambient fine particulate matter concentrations from satellite-based aerosol optical depth: development and application. *Environ Health Perspect* 118(6):847–855
- van Wel L et al (2017) Context-sensitive ecological momentary assessments; integrating real-time exposure measurements, data-analytics and health assessment using a smartphone application. *Environ Int* 103:8–12
- Vineis P et al (2017) The exposome in practice: design of the EXPOsOMICS project. *Int J Hyg Environ Health* 220(2 Pt A):142–151
- Vrijheid M (2014) The exposome: a new paradigm to study the impact of environment on health. *Thorax* 69(9):876–878
- Walker DI et al (2016) High-resolution metabolomics of occupational exposure to trichloroethylene. *Int J Epidemiol* 45(5):1517–1527
- Walker DI et al (2019) Multigenerational metabolic profiling in the Michigan PBB registry. *Environ Res* 172:182–193
- Weinhold B (2006) Epigenetics: the science of change. *Environ Health Perspect* 114(3):A160–A167
- Wild CP (2005) Complementing the genome with an “exposome”: the outstanding challenge of environmental exposure measurement in molecular epidemiology. *Cancer Epidemiol Prev Biomark* 14(8):1847–1850
- Wild CP (2012) The exposome: from concept to utility. *Int J Epidemiol* 41(1):24–32

# Insights into Exposure Sources, Processes, and Impacts



# In Situ Passive Sampling Techniques for Monitoring Environmental Mixture Exposure

Lian-Jun Bao, Rainer Lohmann, Derek Muir, and Eddy Y. Zeng

## Abstract

A large number of passive sampler devices have been developed for in situ sensing of polar and nonpolar organic chemicals in the environment. This chapter compiles and analyzes available information on the current progress in quantitation theories and technological improvements. The results show that it is critical to determine sorbent phase-water partition coefficients and sampling rates of target analytes for quantitation with the equilibrium and kinetic sampling strategies. Compared to passive sampling of organic contaminants in air, overlying water and sediment porewater, which has been extensively documented, measurements of organic contaminants in soil and at the air–soil interface have been largely unsuccessful with passive samplers. In addition, the combination of in situ passive sampling devices and bioassays could be a promising tool for directly assessing air and water quality with biological effects.

## Keywords

Passive sampling • Organic contaminants • Field application • Biological effects

## 1 Introduction

A large number of organic chemicals are synthesized and registered, with the total number registered by government agencies reaching almost 394,000 worldwide (<http://support.cas.org/>). Most organic chemicals can be released into the environment through a variety of pathways, such as direct atmospheric emissions and domestic, industrial, and agricultural wastewater discharge, etc., which poses potential health hazards to organisms and humans. Monitoring of organic contaminants in the environment is necessary for examining their occurrence and ecological risk though a mixture of exposures. Of particular note is that gaseous or freely dissolved organic contaminants are considered bioavailable for organisms. Conventional active sampling methods involve relatively complex and time-consuming procedures only provide instantaneous concentrations of target analytes. Comparatively, passive sampling techniques, on the principle of “like dissolves like” with sorbent phases, are easy to operate and often yield time-weighted average concentrations. Due to a great enrichment in the sorbent phase, the detection limits of a mixture of organic contaminants for passive sampling techniques can be lower than those using active sampling methods if the sampling costs are similar.

Because passive sampling techniques are simple to operate and cost-effective, they have opened up a new opportunity for in situ tracking dissolved organic chemicals including polar and nonpolar in air, water, and sediment. For instance, the Global Atmospheric Passive Sampling (GAPS) Network initiated in December 2004 has conducted measurements of persistent organic pollutants (POPs) and priority chemicals in the atmosphere with passive air samplers (Poza et al. 2009). The GAPS monitoring program has covered more than 55 sites on 7 continents in urban, rural, and remote regions (Koblizkova et al. 2012). In 2010, Lohmann and Muir (2010) called for the establishment of a monitoring network of POPs in global aquatic environments using passive sampling devices, especially with polyethylene (PE) as a sorption phase. In

---

L.-J. Bao (✉) · D. Muir · E. Y. Zeng  
Guangdong Key Laboratory of Environmental Pollution and Health, School of Environment, Jinan University, Guangzhou, 511443, China  
e-mail: [baolianjun@jnu.edu.cn](mailto:baolianjun@jnu.edu.cn)

R. Lohmann  
Graduate School of Oceanography, University of Rhode Island, Narragansett, Rhode Island, 02882-1197, USA

D. Muir  
Aquatic Contaminants Research Division, Environment and Climate Change Canada, 867 Lakeshore Road, Burlington, ON L7S 1A1, Canada

2016, two workshops, initiated by the co-authors of this chapter and with the participation of more than a dozen experts, were held in Guangzhou, China to discuss the key steps for establishing the Aquatic Global Passive Sampling network and launch the first round of global sampling activities (Lohmann et al. 2017).

Over the decades, an increasing number of in situ passive sampler devices have been developed with different sorbent phases. The corresponding quantitation methods have also been established and tested in under field conditions. Some in situ passive sampler devices, such as semipermeable membrane device (SPMD) and PE diffusion bag, have gradually been adopted as routine monitoring tools by local and national government agencies (Interstate Technology and Regulatory Council 2004; Huckins and Alvarez 2019). To date, new materials have been synthesized and used as novel sorbent phases (Ren et al. 2018; Zheng et al. 2018). A recent innovation is the development of samplers using multi-material 3D printing to produce low-cost passive sampler devices with porous membranes, which were initially used for evaluating the uptake of atrazine in water (Kalsoom et al. 2018).

This chapter reviews the latest developments in typical passive samplers for sensing polar and nonpolar organic chemicals in environments in an attempt to comprehend the current progress in quantitation theories and technological improvements of in situ passive sampling devices.

## 2 Quantitation Theory

The essential and principal objective of in situ passive samplers is to quantify the gaseous or freely dissolved organic contaminants in air, water, or sediment. Generally, the quantitation methods have been developed based on the partition process of a target analyte between the sorbent phase and environmental matrix within a passive sampler (Fig. 1). Here, two quantitation methods for in situ sampling on equilibrium partitioning and kinetically controlled diffusion respectively are introduced.

### 2.1 Equilibrium Sampling

When a target analyte in an environmental matrix (air or water) equilibrates with that in the sorbent phase of a passive sampler, its gaseous or freely dissolved concentration (defined as  $C_f$ ) can be derived by

$$C_f = C_s/K_f \quad (1)$$

where  $C_s$  is the analyte concentration in the sorbent phase at equilibrium and  $K_f$  is the equilibrium partition coefficient of

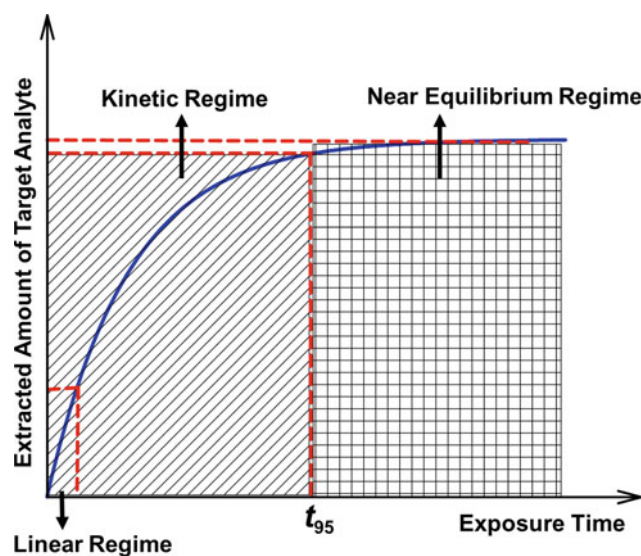


**Fig. 1** Typical extraction profile of a target analyte in a passive sampler's sorbent phase (Ouyang and Pawliszyn 2008)

the analyte between the sorbent phase and environmental matrix. The determination of  $K_f$  is the key step for both quantitation methods.

Over the decades, the  $K_f$  values for a large number of organic contaminants in different sorbent phases have been determined and summarized in some review articles. For example, Difilippo and Eganhouse (2010) compiled 55 references to evaluate the experimentally determined polydimethylsiloxane (PDMS)-water  $K_f$  for polycyclic aromatic hydrocarbons (PAHs), polychlorinated biphenyls (PCBs), chlorinated benzenes, DDT compounds, hexachlorocyclohexanes, chlorinated cyclodienes, organophosphorus insecticides, pyrethroids, carbamates, triazines, polybrominated diphenyl ethers (PBDEs), and BTEX at different temperatures and with different coating thicknesses of PDMS coating in freshwater or seawater. Lohmann (2012) also summarized a list of  $K_f$  for PAHs, PCBs, PBDEs, organochlorine pesticide, triclosan, etc. between low-density polyethylene (LDPE) and water. Recently, Lao et al. (2017) experimentally determined  $K_f$  values of 112 moderately hydrophobic organic compounds including PAHs, PBDEs, PCBs, and pesticides between poly(methyl methacrylate) and water. Smedes (2018) also measured silicone-water  $K_f$  values of 80 organic compounds, such as phthalates, musks, organophosphorus flame retardants, chlorobenzenes, pesticides, selected PCBs, and a number of miscellaneous compounds using a cosolvent method. Collectively, it is interesting to note that the relationships between  $\log K_f$  and  $\log K_{ow}$  (octanol-water partition coefficients) were established for unknown compounds in these four aforementioned and other references (Bao et al. 2011; Yang et al. 2006). It has been debated for years whether the relationship between  $\log K_f$  and  $\log K_{ow}$  should continue to be linear or

become nonlinear as  $\log K_{ow}$  reaches 7–7.5 and beyond. Several factors, such as poor mass balance, low solubility for very hydrophobic organic chemicals (VHOCs), loss of VHOCs to container surfaces by sorption, nonequilibrium state, chemical molecular volume, and energy barrier for chemical diffusion into polymer structure have been implicated as the causes for the aforementioned relationships (Lao et al. 2017; Bao et al. 2011). Apparently, further investigations into the correlative relationship between  $\log K_f$  and  $\log K_{ow}$  are necessary and beneficial for extending the application of passive samplers to nontarget VHOCs. In addition, the effects of temperature, ionic strength, and pressure on the  $K_f$  have been reported and should also be taken into account in developing passive sampling methods.

## 2.2 Kinetic Sampling

Compared to equilibrium sampling, the advantage of kinetic sampling is the relatively shorter sampling time required, which would somewhat reduce the likelihood for loss or damage of passive samplers in field deployment. On the other hand, the detection limits with the same amount of sorbent phase is greater for kinetic sampling than for equilibrium sampling for obvious reasons. Generally, the kinetically controlled diffusion process for HOCs is divided into two regimes, i.e., linear and curvilinear (Fig. 1). Within the linear uptake regime,  $C_f$  can be calculated by

$$C_f = N/R_s t \quad (2)$$

where  $N$  is the analyte mass in the sorbent phase at sampling time  $t$  and  $R_s$  is the sampling rate. Within the curvilinear uptake regime,  $C_f$  can be determined by

$$C_f = \frac{C_s^t}{K_f(1 - \exp(-\frac{R_s t}{K_f m_s}))} \quad (3)$$

where  $C_s^t$  is the analyte concentration in the sorbent phase at sampling time  $t$  and  $m_s$  is the mass of the sorbent phase. Obviously, it is critical to determine  $R_s$  for estimating  $C_f$ .

To in situ calibrate  $R_s$  of target analytes, the best approach is to spike performance reference compounds (PRCs) into the sorbent phase before deployment, assuming that the isotropic exchange kinetics between the uptake of the target analytes to the sorbent phase and the dissipation of PRCs from the sorbent phase to ambient environment are the same. Under this assumption,  $C_f$  can be expressed as

$$C_f = \frac{C_s^t}{K_f(1 - \frac{q}{q_0})} \quad (4)$$

where  $q$  and  $q_0$  are the amounts of a PRC at time  $t$  and 0 on the sorbent phase. Equation (4) indicates that  $C_f$  can be

directly determined from the initial and remaining amounts of the PRC in the sorbent phase and the equilibrium partition coefficient  $K_f$ . For the best calibration, the PRCs should be the isotopically labeled analogues of the target analytes. If isotopically labeled PRCs are not available, unlabeled and homologous chemicals which have similar physiochemical properties with the target analytes but are seldom detected in the environment can be used as PRCs. Several calibration methods, such as non-linear least squares regression (Booij and Smedes 2010), molar volume adjustment (Tomaszewsky and Luthy 2008), correlation between  $\log R_s$  and  $\log K_{ow}$  (Yao et al. 2016), one-dimensional model (Fernandez et al. 2009), and exposure adjustment factors (Huckins et al. 2002), have been developed to estimate the  $R_s$  of a suite of analytes without isotopically labeled PRCs. However, the limitations of PRCs calibration methods (Liu et al. 2013a), such as high cost and retained fraction, have been recognized. Hysteretic desorption of PRCs from PE and PDMS occurred with in situ passive sampling HOCs in sediment porewater under stagnant conditions, resulting in anisotropic exchange kinetics of PRCs and target analytes (Bao et al. 2016; Choi et al. 2016). Such anisotropic exchange kinetics in sediment requires more complicated use of PRC-based calibration methods; several of these have been detailed in the literature (Fernandez et al. 2009; Sanders et al. 2018; Thompson et al. 2015). To deal with this issue pragmatically, periodic agitation was introduced for in situ passive sampling of VHOCs in sediment porewater (Jalalizadeh and Ghosh 2017).

Besides dynamic conditions, complex environmental matrices also exhibit some effects on kinetic sampling. Lin et al. (2018) found that the dissipation rates of HOCs from PDMS fiber in water were enhanced by a factor of 70 and 34 with addition of humic acid and 2-hydroxypropyl- $\beta$ -cyclodextrin, respectively. They also developed a quantitative structure–activity relationship model to associate the experimental dissipation rates of the target HOCs with their physical–chemical properties and dissolved organic matter contents (Lin et al. 2018), which may be applied in estimating dissipation rates of HOCs in natural environments.

Kinetic sampling is often adopted for polar organic chemicals. Similar to HOCs, the quantitation methods for most polar passive samplers, such as Chemcatcher<sup>TM</sup> and polar organic chemical integrative sampler (POCIS), are also based on the uptake profiles of target analytes in the sorbent phase (Gong et al. 2018). As a result, Eq. (3) has been used to calculate the concentrations of polar organic chemicals in water with the aforementioned passive samplers. However, it should be noted that the PRC calibration method is not suitable for in situ calibration of the sampling rates of polar organic chemicals because of the anisotropic kinetics (Guibal et al. 2015; Fauvelle et al. 2012). Given the common structures of polar passive samplers, such as POCIS and

diffusive gradients in thin film technology (DGT), diffusive layer is usually designed to ensure that the uptake of target analytes into the samplers is a linear process. Under this circumstance, Eq. (2) can be used to quantify concentrations of polar organic compounds in water or sediment porewater. Alternatively, the concentration of a target analyte can be obtained by (Davison and Zhang 1994)

$$C_f = \frac{M\Delta g}{DA t} \quad (5)$$

where  $M$  is the analyte mass in the receiving or sorbent phase;  $\Delta g$  is the thickness of diffusive layer;  $D$  is the diffusion coefficient of the analyte through the diffusive layer; and  $A$  and  $t$  are the exposed area and sampling time, respectively. In addition, a series of environmental factors, such as hydrodynamic conditions, temperature, pH, ionic strength, and dissolved organic matter, have some impacts on passive sampling of polar organic chemicals. These issues were recently reviewed by Gong et al. (2018). Also, standardization of the sampler layout has been recommended to better calculate the sampling rates of polar organic compounds with passive samplers (Booij and Chen 2018).

## 3 Method Development

### 3.1 Polar Organic Chemicals

Chemcatcher<sup>TM</sup> and POCIS are the common passive samplers for measuring polar organic chemicals in water. Their configurations with different receiving phases or sorbent phases have been described in previous studies (Bernard et al. 2019; Kingston et al. 2000; Ahrens et al. 2018). Here, a newly developed promising sampler is introduced as an example of recent progress in method development.

The emerging sampler is organic-DGT, named as o-DGT. In fact, DGT has been widely used to measure free elements in aquatic environments since 1994 (Davison and Zhang 1994). Recently, it was modified for polar organic chemicals by replacing inorganic diffusive gel and receiving phase with organic gels. The superiority of o-DGT over Chemcatcher<sup>TM</sup> and POCIS is the independence of sampling rates with hydrodynamic conditions (Challis et al. 2016). Collectively, the main configurations of all o-DGT samplers are similar, with a protected filter, diffusive phase, and binding agent (receiving phase), which looks like a sandwich. The materials for diffusive phases and binding agents of o-DGT samplers vary with different applications. For example, Challis et al. (2018) used o-DGT sampler with a 0.75 mm Waters OASIS HLB binding gel and outer diffusive gel of same thickness, both of which were made of 1.5% agarose, to determine 27 pharmaceuticals and 7 pesticides along the

Red River from the United States–Canada border. Two novel o-DGT samplers were developed, which consist of XAD18 and HLB, respectively, as binding phases to measure perfluoroalkyl substances and organophosphorus flame retardants in aquatic system (Zou et al. 2018; Guan et al. 2018). Chen et al. (2015) used o-DGT samplers with a 0.5 mm XAD18 resin gel as a binding phase, 0.8 mm agarose diffusive gel, and polyethersulfone filter membrane to in situ measure the concentrations and fluxes of four antibiotics in soils. XDA-1 resin was used as binding phase of o-DGT sampler for measuring endocrine disrupting chemicals in seawaters (Xie et al. 2018). Of particular note is that a porous carbon material from metal–organic framework was used as novel binding gel to in situ measure antibiotics in water (Ren et al. 2018). The cyclodextrin polymer membrane was also adopted as the novel binding phase of DGT sampler to determine the concentrations of triclosan, triclocarbon, and methyl triclosan in rivers (Wei et al. 2019). In summary, o-DGT samplers are an important and emerging passive technique for in situ sampling of polar organic chemicals and moderate HOCs in water and soil.

### 3.2 Nonpolar Organic Chemicals

#### 3.2.1 Polyurethane Foam Disk

Polyurethane foam (PUF) has been used to collect gaseous HOCs with an active high-volume air sampler. It is also employed as a sorbent phase (PUF disk) in passive air sampling—this is one of a few passive samplers that actually also collects HOCs on particles (Rauert et al. 2018; Francisco et al. 2017). Generally, a PUF disk consists of two stainless steel domes or bowls with external diameters of 30 and 20 cm, respectively. Polyurethane foam as the sorbent phase PUF is housed inside the lower dome, and target compounds in the air are allowed to freely pass through the gap between the domes and holes in the bottom surface of the lower dome and sorbed into the PUF (Pozo et al. 2004). The domes are designed to protect the PUF from potential damage by precipitation, particle deposition, sunlight (for degradation of the target chemicals), and wind. Another type of passive air sampler, i.e., polymer-coated glass, contains the same shelter as the PUF disk, but has a thin layer of ethylene vinyl acetate as the sorbent phase. Apparently, this PUF is supposed to sense HOCs in the gaseous phase. Abdallah and Harrad (2010) modified the PUF disk for monitoring brominated flame retardants in the vapor and particulate phases in indoor air. In their design, the PUF was mounted from the middle of the lower dome to the top of the upper dome and a glass fiber filter (GFF) was suspended in the middle of the lower dome for collection of depositing particulates. Similarly, Tao et al. (2007) used PUF and GFF to construct a passive air sampler capable of collecting

gaseous and particle-affiliated PAHs. The shelter is a stainless steel cylinder with an upper cover and a porous bottom plate, and air can easily flow over the cylinder through the holes in the bottom plate. Particulates are trapped by the GFF suspended in the cylinder at the height of 10 mm, while gaseous PAHs are sorbed by the PUF attached to the top cover. The GFF and PUF are supported by backup plates fastened over a certain screw stem with nuts.

Passive air samplers with PUF as the sorbent phase are the most widely used devices in field monitoring of HOCs. The impregnation of ground XAD resins into PUF also greatly improves the sensitivity of detecting HOCs in field application (Koblizkova et al. 2012). The PUF disk has been used to measure PAHs, PCBs, PBDEs, OCPs, and polychlorinated naphthalenes (PCNs) in the atmosphere of Europe, Chile, and other countries (Pozo et al. 2004; Jaward et al. 2004a, b; Wilford et al. 2004). The sampling time of PUF disk for chemicals with  $\log K_{OA}$  greater than 8.5 can be several weeks or even months (e.g., 100 and 450 days) (Wilford et al. 2004; Shoeib and Harner 2002). Because sampling rates are strongly dependent on wind speed, prolonged sampling time can lead to large uncertainties for quantitative measurements (Wilford et al. 2004; Shoeib and Harner 2002; Tuduri et al. 2006). Additionally, small amounts of particulates enriched with low volatile HOCs may be accumulated by the PUF disk during outdoor exposure (Wilford et al. 2004; Jaward et al. 2004), undermining the measurement accuracy for gaseous HOCs. This was probably the main reason for adjusting the position of PUF and adding GFF for collecting particles in modified PUF disks (Wilford et al. 2004; Jaward et al. 2004). While this can undermine the measurement accuracy for gaseous HOCs, it has major benefits for determining total airborne concentrations of semi-volatile compounds. Further studies with dome-enclosed PUF disk samplers has demonstrated that they accumulate particles, ranging in size from 250 to 4140 nm, with no discrimination compared to conventional PS-1-type active air samplers (Markovic et al. 2015).

### 3.2.2 XAD

XAD-2 (styrene-divinylbenzene copolymer) resins have long been used for high-volume active air sampling. A novel passive sampler using the same resin was first reported by Wania et al. (2003). The sampler consists of a narrow resin-filled cylinder made of a fine stainless steel mesh placed in a protective sampling shelter with an opening at the bottom and under the cap at the top. Comparison of XAD and PUF-passives, as well as active XAD-PUF sandwich (high volume and low volume) sampling for pesticides in air, showed that all four yielded similar concentrations with no systematic bias among them Hayward et al. (2010). However, the XAD-passive had slower update rates than PUF-passives and thus appears to be best for long-term

deployments while PUF-PAS deployed for 3-month periods are able to reveal seasonal patterns quite clearly (Gouin et al. 2008). XAD-2 is more dense (bulk density =  $640 \text{ kg m}^{-3}$  vs.  $20\text{--}40 \text{ kg m}^{-3}$  for PUF) and less porous (porosity = 0.41 for XAD-2 vs. 0.97 for PUF) than PUFs. XAD-based passives are also less likely to accumulate airborne particles than PUF-passives due to sampler design and the very small pore diameter of XAD-2 ( $90 \text{ \AA}$ ) (Armitage et al. 2013). Sampling rates for XAD-passives have been shown to be sensitive to temperature and thus results are often reported in terms of nanograms per sampler rather than converted to concentrations. XAD-passives have been used for numerous studies of global air concentrations of relatively volatile organics such as volatile methyl siloxanes (Xu and Wania 2013) and perfluoroalkyl substances (Gawor et al. 2014), as well as for current use pesticides (Shunthirasingham et al. 2010).

### 3.2.3 Polyethylene

Because of its cost-effectiveness and ease to handle, polyethylene (PE), especially low-density polyethylene (LDPE), has emerged as the widest applied sorbent phase for in situ passive samplers. Under field conditions, the structure of PE-based devices is often quite simple. In earlier applications, bare PE films with different thicknesses ranging from 25 to  $100 \text{ }\mu\text{m}$  (Fig. 2a) were used to sense HOCs in air, overlying water, and sediment porewater (Cornelissen et al. 2008; Ruge et al. 2018; Apell and Gschwend 2016). Over the years, certain external supporting frames have gradually been designed to handle LDPE films more easily or to determine concentration profiles of HOCs in porewater and/or at the sediment–water interface. For example, Lohmann et al. (2017) designed a stainless steel cage to hold a total of 24 LDPE or silicone rubber sheets, each sized in  $4 \text{ cm}$  (width)  $\times$   $8 \text{ cm}$  (length), for measuring HOCs in freshwater and seawater across the globe. Oen et al. (2011) fixed LDPE films to a stainless steel sediment-penetrating rod and deployed it in San Francisco Bay, California, USA for determining vertical pore water profiles of PCBs. Lin et al. (2015) designed a central probe (Fig. 2c) with a tripod frame for landing on sediment bed to sense concentration profiles of HOCs from 30 cm above to 30 below the sediment–water interface. The probe is a hollow stainless steel tube attached with 24 depressions wrapped by PE films at 2.5 cm intervals. In addition, a sampling box for collecting PAHs and PCBs in soil air was designed to contain LDPE strips strung on a carrier, which were deployed on a grate above the soil (Donald and Anderson 2017).

Our group has also developed a series of in situ passive samplers (Fig. 2b, d, e, and f) with PE as the sorbent phase, including open water passive sampler, multi-section passive sampler, sediment–water interface passive sampler, and air–water passive sampler, which can be used to determine



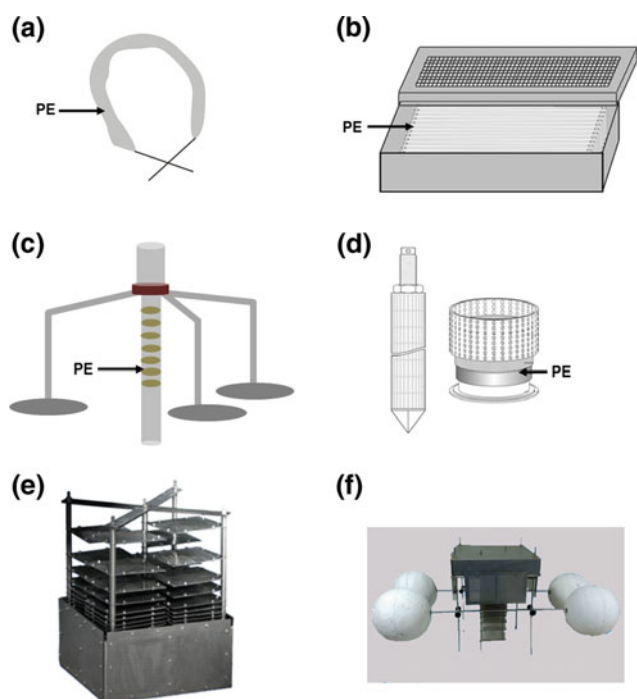


**Fig. 2** Typical passive samplers based on polyethylene (PE) or polyoxymethylene (POM) film: **a** PE membrane (Adams et al. 2007); **b** Passive water sampler (Bao et al. 2012); **c** A probe for measuring concentration profiles of HOCs at the sediment–water interface (Lin et al. 2015); **d** multi-section passive sampler (Liu et al. 2013b); **e** passive sampling device for measuring sediment-water diffusion fluxes of hydrophobic organic chemicals (Liu et al. 2013c); **f** air–water passive sampler for measuring concentration profiles of HOCs at the air–water interface (Wu et al. 2016)

concentrations, depth profiles, and exchange fluxes of HOCs in overlying water, sediment porewater, and sediment–water/air–water interfaces, respectively. All samplers were so designed to prevent large particles from adhesion onto LDPE film by adding GFF and porous shield. With this protective mechanism, target chemicals are allowed to freely penetrate through the porous shield and GFF and diffuse into LDPE phase. Specifically, the open water sampler (Fig. 2b) is composed of a rectangular copper box with two open frames, which are filled with two stainless steel porous plates, and GFF (Bao et al. 2012). Strips of LDPE in the copper box are fastened in a bracket of comb-like structures (Bao et al. 2012). The sediment porewater sampler (Fig. 2d) consists of a series of sampling cells isolated from each other with seclusion rings (Liu et al. 2013b). The sediment porewater sampler is able to measure concentration profiles of sediment porewater HOCs at 2 cm intervals (Liu et al. 2013b). The sediment–water interface sampler (Fig. 2e) is comprised of one upper and one lower section, intended for collecting HOCs in overlying water and sediment porewater, respectively (Liu et al. 2013c). In the upper section, the sampling cells are in a horizontal spiral arrangement and

isolated by stainless steel spacers of different thicknesses. In the lower section, the sampling cells, like sandwiched LDPE strips, are arranged vertically and isolated by stainless steel grating panels at an identical interval of 0.2 cm. Similarly, the air–water sampler (Fig. 2f) consists of two parts, intending for sensing gaseous and freely dissolved HOCs in air and water, respectively (Wu et al. 2016). For the upper part, an external setup was designed to protect the sampler from rainfall and photolysis of target analytes from sunlight. Four floats are fastened in two parallel support rods to ensure the sampler floating in water. The consecutive sampling units are placed horizontally and separated by stainless steel spacers of different thicknesses.

### 3.2.4 Silicone Rubber

Silicone rubber is a silicon–oxygen polymer with high content of PDMS, the commonly used sorbent phase for solid-phase microextraction. As a polymer sorbent phase, silicone rubber has been used as different bare shapes, such as rods, sheets, and tubes, for in situ passive sampling of HOCs in surface water (Emelogu et al. 2013a; Silva-Barni et al. 2019; van Pinxteren et al. 2010). It can be cut into trips similar to PE film and acts as the sorbent phase for the aforementioned sampling devices. It should be noted that silicone rubber membrane is softer and stickier than PE film at the same thickness, thereby relatively thicker silicone rubber (often 0.5 mm) can be adopted. Compared to PE, silicone rubber exhibits greater accumulation of moderate and light HOCs and is allowed to sense HOCs with a wider range of  $\log K_{ow}$  in water (Pintado-Herrera et al. 2016; Allan et al. 2013).

Besides field measurement of organic contaminants, silicone rubber has been widely used in toxicological tests with in vitro and in vivo bioassays by exposing test organisms, genes, and cells to extracts of in situ passive samplers (Emelogu et al. 2013b; De Baat et al. 2019). For example, Liscio et al. (2014) observed anti-androgenic effects in extracts from silicone strips, which were deployed for 14 days in a river contaminated by wastewater effluent. Novak et al. (2018) also observed quantifiable endocrine disruption effects in extracts of silicone rubber samplers with 5-d deployment in the Danube River. Obviously, the combination of passive sampling techniques, not limited to silicone rubber, and bioassays may be a promising tool for directly assessing water quality and identifying new and emerging nontarget analytes with biological effects.

## 4 Conclusions

Passive sampling techniques have been widely used to in situ measure the concentrations of organic contaminants in the environment, determine their exchange fluxes between

sediment–water and air–water interfaces, and assess the biological effects with in vitro and in vivo bioassays. The determination of sorbent phase-water partition coefficients and sampling rates of the target analytes is critical for quantitation with passive samplers, and the relationships between  $\log K_f$  and  $\log K_{ow}$  for VHOCs merit additional research efforts. Finally, in situ passive sampling devices for collecting organic chemicals in soil and at the air-soil interface need to be developed in the future.

## References

- Abdallah MA-E, Harrad S (2010) Modification and calibration of a passive air sampler for monitoring vapor and particulate phase brominated flame retardants in indoor air: application to car interiors. *Environ Sci Technol* 44:3059–3065
- Adams RG, Lohmann R, Fernandez LA, Macfarlane JK, Gschwend PM (2007) Polyethylene devices: passive samplers for measuring dissolved hydrophobic organic compounds in aquatic environments. *Environ Sci Technol* 41:1317–1323
- Ahrens L, Daneshvar A, Lau AE, Kreuger J (2018) Concentrations, fluxes and field calibration of passive water samplers for pesticides and hazard-based risk assessment. *Sci Total Environ* 637:835–843
- Allan IJ, Harman C, Raneklev SB, Thomas KV, Grung M (2013) Passive sampling for target and nontarget analyses of moderately polar and nonpolar substances in water. *Environ Toxicol Chem* 32:1718–1726
- Apell JN, Gschwend PM (2016) In situ passive sampling of sediments in the Lower Duwamish waterway superfund site: replicability, comparison with ex situ measurements, and use of data. *Environ Pollut* 218:95–101
- Armitage JM, Hayward SJ, Wania F (2013) Modeling the uptake of neutral organic chemicals on XAD passive air samplers under variable temperatures, external wind speeds and ambient air concentrations (PAS-SIM). *Environ Sci Technol* 47:13546–13554
- Bao L-J, You J, Zeng EY (2011) Sorption of PBDE in low-density polyethylene film: implications for bioavailability of BDE-209. *Environ Toxicol Chem* 30:1731–1738
- Bao L-J, Xu S-P, Zeng EY (2012) Development and field validation of a low-density polyethylene-containing passive sampler for measuring dissolved hydrophobic organic compounds in open waters. *Environ Toxicol Chem* 31:1012–1018
- Bao L-J, Wu X, Jia F, Zeng EY, Gan J (2016) Isotopic exchange on solid-phase micro extraction fiber in sediment under stagnant conditions: Implications for field application of performance reference compound calibration. *Environ Toxicol Chem* 35:1978–1985
- Bernard M, Boutry S, Lissalde S, Guibaud G, Saut M, Rebillard JP, Mazzella N (2019) Combination of passive and grab sampling strategies improves the assessment of pesticide occurrence and contamination levels in a large-scale watershed. *Sci Total Environ* 651:684–695
- Booij K, Chen S (2018) Review of atrazine sampling by polar organic chemical integrative samplers and Chemcatcher. *Environ Toxicol Chem* 37:1786–1798
- Booij K, Smedes F (2010) An improved method for estimating in situ sampling rates of nonpolar passive samplers. *Environ Sci Technol* 44:6789–6794
- Challis JK, Hanson ML, Wong CS (2016) Development and calibration of an organic-diffusive gradients in thin films aquatic passive sampler for a diverse suite of polar organic contaminants. *Anal Chem* 88:10583–10591
- Challis JK, Stroski KM, Luong KH, Hanson ML, Wong CS (2018) Field evaluation and in situ stress testing of the organic-diffusive gradients in thin-films passive sampler. *Environ Sci Technol* 52:12573–12582
- Chen C-E, Chen W, Ying G-G, Jones KC, Zhang H (2015) In situ measurement of solution concentrations and fluxes of sulfonamides and trimethoprim antibiotics in soils using o-DGT. *Talanta* 132:902–908
- Choi Y, Wu Y, Luthy RG, Kang S (2016) Non-equilibrium passive sampling of hydrophobic organic contaminants in sediment pore-water: PCB exchange kinetics. *J Hazard Mater* 318:579–586
- Cornelissen G, Pettersen A, Broman D, Mayer P, Breedveld GD (2008) Field testing of equilibrium passive samplers to determine freely dissolved native polycyclic aromatic hydrocarbon concentrations. *Environ Toxicol Chem* 27:499–508
- Davison W, Zhang H (1994) In situ speciation measurements of trace components in natural waters using thin-film gels. *Nature* 367:546–548
- De Baat ML, Kraak MHS, Van der Oost R, De Voogt P, Verdonchot PFM (2019) Effect-based nationwide surface water quality assessment to identify ecotoxicological risks. *Water Res* 159:434–443
- DiFilippo EL, Eganhouse RP (2010) Assessment of PDMS-water partition coefficients: implications for passive environmental sampling of hydrophobic organic compounds. *Environ Sci Technol* 44:6917–6925
- Donald CE, Anderson KA (2017) Assessing soil-air partitioning of PAHs and PCBs with a new fugacity passive sampler. *Sci Total Environ* 596:293–302
- Emelogu ES, Pollard P, Robinson CD, Webster L, McKenzie C, Napier F, Steven L, Moffat CF (2013a) Identification of selected organic contaminants in streams associated with agricultural activities and comparison between autosampling and silicone rubber passive sampling. *Sci Total Environ* 445:261–272
- Emelogu ES, Pollard P, Dymond P, Robinson CD, Webster L, McKenzie C, Dobson J, Bresnan E, Moffat CF (2013b) Occurrence and potential combined toxicity of dissolved organic contaminants in the Forth estuary and Firth of Forth, Scotland assessed using passive samplers and an algal toxicity test. *Sci Total Environ* 461:230–239
- Fauvelle V, Mazzella N, Delmas F, Madarassou K, Eon M, Budzinski H (2012) Use of mixed-mode ion exchange sorbent for the passive sampling of organic acids by polar organic chemical integrative sampler (POCIS). *Environ Sci Technol* 46:13344–13353
- Fernandez LA, Harvey CF, Gschwend PM (2009) Using performance reference compounds in polyethylene passive samplers to deduce sediment porewater concentrations for numerous target chemicals. *Environ Sci Technol* 43:8888–8894
- Francisco AP, Harner T, Eng A (2017) Measurement of polyurethane foam-air partition coefficients for semivolatile organic compounds as a function of temperature: application to passive air sampler monitoring. *Chemosphere* 174:638–642
- Gawor A, Shunthirasingham C, Hayward SJ, Lei YD, Gouin T, Mmereki BT, Masamba W, Ruepert C, Castillo LE, Shoeib M, Lee SC, Harner T, Wania F (2014) Neutral polyfluoroalkyl substances in the global Atmosphere. *Environ Sci Process Impacts* 16:404–413
- Gong X, Li K, Wu C, Wang L, Sun H (2018) Passive sampling for monitoring polar organic pollutants in water by three typical samplers. *Trends Environ Anal Chem* 17:23–33
- Gouin T, Wania F, Ruepert C, Castillo LE (2008) Field testing passive air samplers for current use pesticides in a tropical environment. *Environ Sci Technol* 42:6625–6630
- Guan D-X, Li Y-Q, Yu N-Y, Yu G-H, Wei S, Zhang H, Davison W, Cui X-Y, Ma LQ, Luo J (2018) In situ measurement of perfluoroalkyl substances in aquatic systems using diffusive gradients in thin-films technique. *Water Res* 144:162–171

- Guibal R, Lissalde S, Charriau A, Guibaud G (2015) Improvement of POCIS ability to quantify pesticides in natural water by reducing polyethylene glycol matrix effects from polyethersulfone membranes. *Talanta* 144:1316–1323
- Hayward SJ, Gouin T, Wania F (2010) Comparison of four active and passive sampling techniques for pesticides in air. *Environ Sci Technol* 44:3410–3416
- Huckins J, Alvarez D Semipermeable membrane device. <http://www.cerc.usgs.gov/pubs/center/pdfdocs/spmd.pdf>. Accessed June 2019
- Huckins JN, Petty JD, Lebo JA, Almeida FV, Booij K, Alvarez DA, Cranor WL, Clark RC, Mogensen BB (2002) Development of the permeability/performance reference compound approach for in situ calibration of semipermeable membrane devices. *Environ Sci Technol* 36:85–91
- Interstate Technology and Regulatory Council 2004
- Jalalizadeh M, Ghosh U (2017) Analysis of measurement errors in passive sampling of porewater PCB concentrations under static and periodically vibrated conditions. *Environ Sci Technol* 51:7018–7027
- Jaward FM, Farrar NJ, Harner T, Sweetman AJ, Jones KC (2004a) Passive air sampling of PCBs, PBDEs, and organochlorine pesticides across Europe. *Environ Sci Technol* 38:34–41
- Jaward FM, Farrar NJ, Harner T, Sweetman AJ, Jones KC (2004b) Passive air sampling of polycyclic aromatic hydrocarbons and polychlorinated naphthalenes across Europe. *Environ Toxicol Chem* 23:1355–1364
- Kaloom U, Hasan CK, Tedone L, Desire C, Li F, Breadmore MC, Nesterenko PN, Paull B (2018) Low-cost passive sampling device with integrated porous membrane produced using multimaterial 3D printing. *Anal Chem* 90:12081–12089
- Kingston JK, Greenwood R, Mills GA, Morrison GM, Persson LB (2000) Development of a novel passive sampling system for the time-averaged measurement of a range of organic pollutants in aquatic environments. *J Environ Monit* 2:487–495
- Koblizkova M, Genualdi S, Lee SC, Harner T (2012) Application of sorbent impregnated polyurethane foam (SIP) disk passive air samplers for investigating organochlorine pesticides and polybrominated diphenyl ethers at the global scale. *Environ Sci Technol* 46:391–396
- Lao W, Hong Y, Tsukada D, Maruya KA, Gan J (2017) A new film-based passive sampler for moderately hydrophobic organic compounds. *Environ Sci Technol* 50:13470–13476
- Lin D, Eek E, Oen A, Cho YM, Cornelissen G, Tommerdahl J, Luthy RG (2015) Novel probe for in situ measurement of freely dissolved aqueous concentration profiles of hydrophobic organic contaminants at the sediment-water interface. *Environ Sci Technol Lett* 2:320–324
- Lin W, Jiang R, Shen Y, Xiong Y, Hu S, Xu J, Ouyang G (2018) Effect of dissolved organic matter on pre-equilibrium passive sampling: a predictive QSAR modeling study. *Sci Total Environ* 635:53–59
- Liscio C, Abdul-Sada A, Al-Salhi R, Ramsey MH, Hill EM (2014) Methodology for profiling anti-androgen mixtures in river water using multiple passive samplers and bioassay-directed analyses. *Water Res* 57:258–269
- Liu H-H, Wong CS, Zeng EY (2013a) Recognizing the limitations of performance reference compound (PRC)-calibration technique in passive water sampling. *Environ Sci Technol* 47:10104–10105
- Liu H-H, Bao L-J, Feng W-H, Xu S-P, Wu F-C, Zeng EY (2013b) A multisection passive sampler for measuring sediment porewater profile of dichlorodiphenyltrichloroethane and its metabolites. *Anal Chem* 85:7117–7124
- Liu H-H, Bao L-J, Zhang K, Xu S-P, Wu F-C, Zeng EY (2013c) Novel passive sampling device for measuring sediment-water diffusion fluxes of hydrophobic organic chemicals. *Environ Sci Technol* 47:9866–9873
- Lohmann R (2012) Critical review of low-density polyethylene's partitioning and diffusion coefficients for trace organic contaminants and implications for its use as a passive sampler. *Environ Sci Technol* 46:606–618
- Lohmann R, Muir D (2010) Global aquatic passive sampling (AQUA-GAPS): using passive samplers to monitor POPs in the waters of the world. *Environ Sci Technol* 44:860–864
- Lohmann R, Muir D, Zeng EY, Bao LJ, Allan IJ, Arinaitwe K, Booij K, Heln P, Kaserzon S, Mueller JF, Shibata Y, Smedes F, Tsapakis M, Wong CS, You J (2017) Aquatic global passive sampling (AQUA-GAPS) revisited: First steps toward a network of networks for monitoring organic contaminants in the aquatic environment. *Environ Sci Technol* 51:1060–1067
- Markovic MZ, Prokop S, Staebler RM, Liggio J, Harner T (2015) Evaluation of the particle infiltration efficiency of three passive samplers and the PS-1 active air sampler. *Atmos Environ* 112:289–293
- Novak J, Vrana B, Rusina T, Okonski K, Grabic R, Neale PA, Escher BI, Macova M, Ait-Aissa S, Creusot N, Allan I, Hilscherova K (2018) Effect-based monitoring of the Danube River using mobile passive sampling. *Sci Total Environ* 636:1608–1619
- Oen AMP, Janssen EML, Cornelissen G, Breedveld GD, Eek E, Luthy RG (2011) In situ measurement of PCB pore water concentration profiles in activated carbon-amended sediment using passive samplers. *Environ Sci Technol* 45:4053–4059
- Ouyang G, Pawliszyn J (2008) A critical review in calibration methods for solid-phase microextraction. *Anal Chim Acta* 627:184–197
- Pintado-Herrera MG, Lara-Martin PA, Gonzalez-Mazo E, Allan IJ (2016) Determination of silicone rubber and low-density polyethylene diffusion and polymer/water coefficients for emerging contaminants. *Environ Toxicol Chem* 35:2162–2172
- Pozo K, Harner T, Shoeib M, Urrutia R, Barra R, Parra O, Focardi S (2004) Passive-sampler derived air concentrations of persistent organic pollutants on a north-south transect in Chile. *Environ Sci Technol* 38:6529–6537
- Pozo K, Harner T, Lee SC, Wania F, Muir DCG, Jones KC (2009) Seasonally resolved concentrations of persistent organic pollutants in the global atmosphere from first year of the GAPS study. *Environ Sci Technol* 43:796–803
- Rauert C, Harner T, Schuster JK, Eng A, Fillmann G, Castillo LE, Fentanes O, Ibarra MV, Miglioranza KSB, Rivadeneira IM, Pozo K, Zuluaga BHA (2018) Atmospheric concentrations of new persistent organic pollutants and emerging chemicals of concern in the Group of Latin America and Caribbean (GRULAC) region. *Environ Sci Technol* 52:7240–7249
- Ren S, Tao J, Tan F, Cui Y, Li X, Chen J, He X, Wang Y (2018) Diffusive gradients in thin films based on MOF-derived porous carbon binding gel for in-situ measurement of antibiotics in waters. *Sci Total Environ* 645:482–490
- Ruge Z, Muir D, Helm P, Lohmann R (2018) Concentrations, trends, and air-water exchange of PCBs and organochlorine pesticides derived from passive samplers in Lake Superior in 2011. *Environ Sci Technol* 52:14061–14069
- Sanders JP, Andrade NA, Ghosh U (2018) Evaluation of passive sampling polymers and nonequilibrium adjustment methods in a multiyear surveillance of sediment porewater PCBs. *Environ Toxicol Chem* 37:2487–2495
- Shoeib M, Harner T (2002) Characterization and comparison of three passive air samplers for persistent organic pollutants. *Environ Sci Technol* 36:4142–4151
- Shunthirasingham C, Oyiliagu CE, Cao XS, Gouin T, Wania F, Lee SC, Pozo K, Harner T, Muir DCG (2010) Spatial and temporal pattern of pesticides in the global atmosphere. *J Environ Monit* 12:1650–1657

- Silva-Barni MF, Smedes F, Fillmann G, Miglioranza KSB (2019) Passive sampling of pesticides and polychlorinated biphenyls along the Quequen Grande River watershed, Argentina. *Environ Toxicol Chem* 38:340–349
- Smedes F (2018) Silicone-water partition coefficients determined by cosolvent method for chlorinated pesticides, musks, organo phosphates, phthalates and more. *Chemosphere* 210:662–671
- Tao S, Liu Y, Xu W, Lang C, Liu S, Dou H, Liu W (2007) Calibration of a passive sampler for both gaseous and particulate phase polycyclic aromatic hydrocarbons. *Environ Sci Technol* 41:568–573
- Thompson JM, Hsieh CH, Luthy RG (2015) Modeling uptake of hydrophobic organic contaminants into polyethylene passive samplers. *Environ Sci Technol* 49:2270–2277
- Tomaszewsky JE, Luthy RG (2008) Field deployment of polyethylene devices to measure PCB concentrations in pore water of contaminated sediment. *Environ Sci Technol* 42:6086–6091
- Tuduri L, Harner T, Hung H (2006) Polyurethane foam (PUF) disks passive air samplers: wind effect on sampling rates. *Environ Pollut* 144:377–383
- van Pinxteren M, Paschke A, Popp P (2010) Silicone rod and silicone tube sorptive extraction. *J Chromatogr A* 1217:2589–2598
- Wania F, Shen L, Lei YD, Teixeira C, Muir DCG (2003) Development and calibration of a resin-based passive sampling system for monitoring persistent organic pollutants in the atmosphere. *Environ Sci Technol* 37:1352–1359
- Wei MB, Yang XH, Watson P, Yang FF, Liu HH (2019) A cyclodextrin polymer membrane-based passive sampler for measuring triclocarban, triclosan and methyl triclosan in rivers. *Sci Total Environ* 648:109–115
- Wilford BH, Harner T, Zhu J, Shoeib M, Jones KC (2004) Passive sampling survey of polybrominated diphenyl ether flame retardants in indoor and outdoor air in Ottawa, Canada: implications for source and exposure. *Environ Sci Technol* 38:5312–5318
- Wu C-C, Yao Y, Bao L-J, Wu F-C, Wong CS, Tao S, Zeng EY (2016) Fugacity gradients of hydrophobic organics across the air-water interface measured with a novel passive sampler. *Environ Pollut* 218:1108–1115
- Xie H, Chen Q, Chen J, Chen C-EL, Du J (2018) Investigation and application of diffusive gradients in thin-films technique for measuring endocrine disrupting chemicals in seawaters. *Chemosphere* 200:351–357
- Xu S, Wania F (2013) Chemical fate, latitudinal distribution and long-range transport of cyclic volatile methylsiloxanes in the global environment: a modeling assessment. *Chemosphere* 93:835–843
- Yang ZY, Zeng EY, Xia H, Wang JZ, Mai BX, Maruya KA (2006) Application of a static solid-phase microextraction procedure combined with liquid-liquid extraction to determine poly(dimethyl)siloxane-water partition coefficients for selected polychlorinated biphenyls. *J Chromatogr A* 1116:240–247
- Yao Y, Meng XZ, Wu C-C, Bao L-J, Wang F, Wu F-C, Zeng EY (2016) Tracking human footprints in Antarctica through passive sampling of polycyclic aromatic hydrocarbons in inland lakes. *Environ Pollut* 213:412–419
- Zheng J, Huang JL, Yang Q, Ni CY, Xie XT, Shi YR, Sun JF, Zhu F, Ouyang GF (2018) Fabrications of novel solid phase microextraction fiber coatings based on new materials for high enrichment capability. *Trends Anal Chem* 108:135–153
- Zou Y-T, Fang Z, Li Y, Wang R, Zhang H, Jones KC, Cui X-Y, Shi X-Y, Yin D, Li C, Liu Z-D, Ma LQ, Luo J (2018) Novel method for in situ monitoring of organophosphorus flame retardants in waters. *Anal Chem* 90:10016–10023



# In Vivo SPME for Bioanalysis in Environmental Monitoring and Toxicology

Anna Roszkowska, Miao Yu, and Janusz Pawliszyn

## Abstract

Solid-phase microextraction (SPME) is a well-established sample preparation technique in the field of environmental and toxicological studies. The application of SPME has extended from the headspace extraction of volatile compounds to the capturing of short-lived and unstable components of the ecosystem extracted from the living organism via direct immersion of SPME probes into the tissue (in vivo SPME). The development of biocompatible coatings and availability of different calibration approaches enables in vivo sampling of exogenous and endogenous compounds from the living plants and animals without the need for tissue collection. In addition, new geometry designs such as thin-film coatings, needle trap devices, recession needles, coated tips or blades has increased the sensitivity and robustness of in vivo sampling. Here, we present the fundamentals of in vivo SPME technique, including the types of extraction mode, geometry design of the coatings, calibration methods and data analysis methods used in untargeted in vivo SPME. We also discuss recent applications of in vivo SPME in environmental studies and in the analysis of pollutants in plant and animal tissues in addition to in vivo human saliva, breath and skin analysis. In summary, in vivo SPME technique shows great potential for both targeted and untargeted screening of small molecules in the living organisms exposed to the surrounding environment.

## Keywords

SPME • In vivo sampling • Environment • Toxicology • Contaminants • Calibration • Bioanalysis

## 1 Introduction

Solid-phase microextraction (SPME) was first introduced in 1989 as a novel sample preparation technique for environmental analysis. Since then, SPME has received particular attention as breakthrough “green” technology—not only in the field of environmental and toxicological studies but also in food analysis and biomedical research (Arthur and Pawliszyn 1990; Bojko and Pawliszyn 2014; Souza-Silva et al. 2015). One of the principal features that significantly distinguishes SPME from other techniques is that SPME integrates sampling, sample clean-up, and analyte pre-concentration into a single step, a feat which cannot be achieved with the use of traditional sample preparation protocols. This unique integrative feature of SPME not only facilitates fast, simple, and efficient extraction of analytes of interest from a variety of matrices, its superior clean-up enables easy coupling of SPME to different instrumental methods such as GC-MS and LC-MS, among others. Furthermore, new advances in SPME have enabled the direct coupling of SPME to MS for measurements of extracted compounds, an attractive option that shortens total analysis times while reducing errors related to sample handling (Reyes-Garcés et al. 2018).

While SPME has gained considerable attraction in environmental studies as a leading method for analysis of volatile organic compounds (VOCs), the applicability of the technique has broadened over the past few years to allow for the analysis of a wide variety of environmental pollutants, including pharmaceutical and personal care products (PPCPs), pesticides, and metal–organic compounds, as well as the analysis of endogenous compounds of plants and

A. Roszkowska · M. Yu · J. Pawliszyn  
Department of Chemistry, University of Waterloo, Waterloo, ON,  
Canada

A. Roszkowska (✉)  
Department of Pharmaceutical Chemistry,  
Medical University of Gdansk, Gdansk, Poland  
e-mail: [anna.roszkowska@gumed.edu.pl](mailto:anna.roszkowska@gumed.edu.pl)

M. Yu  
Department of Environmental Medicine and Public Health, Icahn  
School of Medicine at Mount Sinai, New York, NY, USA

animals exposed to contaminants (Llompart et al. 2019; Wang et al. 2009; Zhang et al. 2018). SPME has also been optimized for several on-site applications, such as analysis of toxins present in inanimate and animate components of the environment and evaluation studies concerning the impact of emitted pollutants on the functioning of ecosystems.

Owing to its advantageous *in vivo* capabilities, SPME has also been largely applied in environmental *in vivo* studies, where non-lethal extraction of small molecules can be performed on living organisms (Ouyang et al. 2011b; Vuckovic et al. 2011). This feature of SPME facilitates monitoring of the fate of pollutants in living organisms and allows for investigations concerning the distribution and accumulation of pollutants within an individual organism as a response to the exposome. *In vivo* sampling via SPME additionally enables the capture of short-lived and unstable metabolites by stabilizing highly reactive small molecules of endogenous and exogenous origin, thus preventing their degradation during sample handling and storage. Recently, SPME technique has been also applied for direct measurements of free drug concentration in solid tissue by a series of experiments performed in the laboratory and also *in silico* by using a mathematical model developed in COMSOL Multiphysics (Huq et al. 2019). The applied strategy facilitated calculations of local depletion of the analyte by a coating and also the mass transfer kinetics of SPME coating. The extraction by SPME coating did not affect the free concentration of the drug in solid tissue as the depletion of drug concentration surrounding the fiber was negligible, therefore the measurements of analyte distribution with the use of SPME technique are feasible. Therefore, *in vivo* SPME does not disturb homeostasis within investigated systems, as only a small portion of metabolites is extracted from the system under study (negligible depletion), thus enabling repeated SPME sampling of the same tissue or organ in individual organisms (Reyes-Garcés et al. 2018). More importantly, the capture of low-molecular-weight compounds via *in vivo* SPME may provide additional information concerning metabolic changes in exposome-wide association studies (EWAS) and also in a toxicological analysis. Important compounds derived from natural or anthropogenic sources of contamination, such as biomarkers of exposure, or toxicants and their metabolites, could be extracted with the use of this technology.

This chapter begins with an overview of the fundamentals of *in vivo* SPME and related techniques. We next discuss the most important topics regarding *in vivo* SPME: development of *in vivo* SPME devices, calibration methods, and data analysis for *in vivo* SPME sampling. A review of the main applications of this technique in environmental monitoring and toxicology studies of plant, animal, and human systems

is then presented. This chapter closes with future perspectives of SPME and its potential in environmental studies.

---

## 2 Fundamentals of *In Vivo* SPME

### 2.1 *In Vivo* SPME and Related Techniques

SPME can be performed in headspace (HS) or direct immersion (DI) mode for extraction of analytes from a variety of matrices. Extraction is carried out for a predetermined period of time with the use of an SPME device (e.g., blades, fibers) coated with an extraction phase (Godage and Gionfriddo 2019; Pawliszyn 2012; Vuckovic 2013). Application of HS-SPME and DI-SPME in environmental and toxicological studies has been reported for analysis of different elements (living and inanimate) of the ecosystem, including water, soil, plants, and animals. Following extraction, the SPME device can be directly introduced to GC for thermal desorption or desorbed using an optimized solvent that is subsequently injected into LC-MS, or directly coupled to MS.

The availability of different SPME devices and their biocompatibility make SPME technology a convenient tool for *in vivo* analysis, with minimum invasiveness to living organisms (Vuckovic et al. 2010). The availability of different calibration approaches for quantitative analysis enables optimal extraction and analysis of a broad range of analytes with different polarities from environmental and biological samples. Given that a derivatization step is necessary for the analysis of nonvolatile pollutants, an on-fiber derivatization technique, developed to combine the derivatization reaction and extraction steps during SPME, is also available for such applications (Martos and Pawliszyn 1998). In-tube SPME, on the other hand, enables direct analysis of nonvolatile compounds in aqueous matrices, and has been applied in the targeted analysis of environmental pollutants (Moliner-Martinez et al. 2015).

SPME can also be optimized for *in vivo* sampling via coating optimization. A matrix-compatible, PDMS-overcoated SPME fiber can be directly used in living systems for *in vivo* sampling, whereas coatings with HLB particles can extend the range of extracted compounds, making such coatings ideal for comprehensive or untargeted analyses of potential pollutants (Gionfriddo et al. 2017; Godage and Gionfriddo 2019). The constant development of SPME coatings aims to both improve coverage of compounds and minimize the invasiveness of the procedure on sampled animals during *in vivo* sampling.

The free concentration of a given pollutant in a living system can reflect *in vivo* exposure levels, while its total

concentration might reflect the long-term risk of the pollutant with respect to different living systems. While SPME fibers can directly measure free concentrations via non-exhaustive extraction, attainment of both the free concentration and total concentration of a given pollutant would allow for a more comprehensive and dynamic investigation of their environmental behavior and risk (Boyacı et al. 2018). In such cases, needle trap devices (NTD), which allow for exhaustive extraction, can be used to this end as passive sampling devices in air pollution monitoring (Lord et al. 2010). The NTD approach uses small needles containing a packed sorbent bed to briefly trap both fluid-borne analytes and particles. Similar to the SPME fiber, NTD can be directly coupled to a GC injection system to release the adsorbed analytes. An analytical approach exploiting both NTD and SPME fiber can thus enable parallel measurements of free concentrations and total concentrations of pollutants in air, enabling a more comprehensive evaluation of risk for living systems with respect to pollutants found in the environment (Niri et al. 2009).

Thin-film SPME (TFME) was developed in recent years for applications that demand higher extraction efficiency and sensitivity (Jiang and Pawliszyn 2012). TFME employs a larger surface area to extraction phase volume ratio so as to increase surface contact with the sample. Different TFME membranes are available for coupling with GC and LC instrumentation. Depending on the aim of research and the specific group(s) of compounds under study, analysts may choose to employ either thermally stable TFME membranes for gas chromatography or solvent-stable TFME membranes for liquid chromatography. The cold fiber technique presents yet another approach to increasing method sensitivity (Menezes et al. 2013). Briefly, the technique works by introducing cold air into a needle-based SPME apparatus. This causes a temperature difference between the extraction phase and sample, which enables faster and higher extraction of compounds into the cooling SPME fiber. The cold fiber technique has been applied in soil and sediment analyses as a way to enhance method sensitivity for volatile compounds (Martendal and Carasek 2011; Ghiasvand et al. 2006). These two methods, TFME and cold fiber SPME, can also be combined to further enhance method sensitivity for specific applications, such as to measure fragrance compounds in air (Jiang and Pawliszyn 2014).

Other geometries of SPME are also available for specific in vivo environmental analysis purposes. For instance, recession needles protect the extraction phase from mechanical damage due to the presence of a recession notch in the needles where the coating is housed (Poole et al. 2017). This research has been used in the untargeted analysis for living fish. Coated tips and mini tips, on the other hand, can be employed for extraction from small sample amounts (<10 uL) such as blood from mice (Piri-Moghadam et al.

2016; Vasiljevic et al. 2019). In addition to the advantages described above, such technologies also offer direct coupling with mass spectrometry for high-throughput analysis, and can be applied for nontarget analysis, features that are highly beneficial in exposome studies (Gómez-Ríos et al. 2018; Augusto Gomez-Rios et al. 2017). Prior to in vivo sampling, simulation-based experiments can be carried out to optimize the geometry of the device in view of the intended purpose of the research and the target sample (Alam et al. 2015).

## 2.2 Calibration Approaches

SPME is a non-exhaustive extraction method in which only a free fraction of the analyte is extracted from the sample matrix. Such a feature is particularly important in environment-wide association studies (EWAS) and toxicological studies, given that it is the unbound fraction of the toxicant that determines its activity in living systems. Quantitative analysis of targeted compounds is carried out by first determining the relationship between extracted amounts by the SPME coating and the analyte concentration in the biomatrix. To this end, various calibration methods have been developed to quantify concentrations of target analytes in biological samples (Ouyang and Pawliszyn 2008). In the equilibrium calibration method, the analyte in the extraction phase equilibrates with that in the sample matrix, and the extracted amount in the extraction phase can be expressed as

$$n_e = C_0 \frac{K_{fs} V_s V_f}{K_{fs} V_f + V_s} \quad (1)$$

where  $n_e$  is the amount extracted,  $C_0$  is the initial concentration of the target analyte in the sample,  $V_s$  is the sample volume,  $V_f$  is the volume of extraction phase, and  $K_{es}$  is the distribution coefficient of the analyte between the extraction phase and the sample matrix. However, in most in vivo SPME applications, the volume of the sample matrix is very large ( $V_s \gg K_{fs} V_f$ ), and Eq. (1) can be rewritten to the following equation:

$$n_e = C_0 K_{fs} V_f \quad (2)$$

In addition, under equilibrium conditions, calibration is independent of hydrodynamic variables, such as blood flow in a living system. However, due to the extended amount of time required for some compounds to equilibrate with the fiber, other calibration methods are often preferred for field and on-site SPME analysis applications, namely on-fiber kinetic calibration and sampling rate calibration (Bai et al. 2013). The kinetic calibration model has been used in several animal studies, and is based on the preloading of the fiber with a deuterated analog, which after introduction to a

biological matrix is desorbed from the fiber while the analytes from the sample matrix are extracted. The free concentration of the analyte is then calculated based on the isotropy of desorption of the deuterated analog from the extraction phase and the simultaneous extraction of the analyte from the sample. Use of this calibration method improves the accuracy and precision of analysis while also accounting for the influence of certain environmental factors, such as temperature, on extracted amounts. However, one of the main limitations of this calibration approach is that it is not suitable for some *in vivo* studies, e.g., human studies, since the introduction of exogenous substances to the living system is forbidden. In such cases, use of pre-equilibrium extraction approach may be considered for *in vivo* studies. In this calibration method, the linear regime of the SPME extraction process is required and the rate of mass transfer (sampling rate) must remain constant throughout the duration of sampling. Several factors, including sample matrix and the type of SPME coating employed, influence the ratio between the concentration of target analyte in the sample matrix and the extracted amount of analyte. Use of this diffusion-based calibration method allows for much shorter extraction times in comparison to the equilibrium extraction approach. This method has been employed in *in vivo* SPME fish studies; briefly, sampling rates were determined in laboratory conditions, then used to determine concentrations of analytes on-site (Ouyang et al. 2011a). The main advantage of this calibration approach is the elimination of standard addition or preloading of the SPME fiber. However, several factors in the analyzed matrix, such as blood flow and fluid content, may affect the amount of extracted analyte.

### 2.3 Data Analysis for *in Vivo* SPME

A major hindrance in SPME-based untargeted analysis is the annotation of obtained data (Domingo-Almenara et al. 2018). Since SPME can be performed on-site and *in vivo*, the scope of extracted and analyzed chemicals is beyond our current knowledge. This is called the “unknown unknown” paradox for research performed at the metabolites level: we want to identify unknown analytes as “markers”, but since unknown compounds are annotated in a database, we have no prior knowledge of these unknown compounds to identify them. Thus, we become restricted to identifying “known” compounds. For exposome studies, the major restriction in data interpretation is that although we already have databases with thousands of small molecules, we still don’t know whether there are other short-life compounds or trace metabolites totally ignored by the current knowledge scope, especially exogenous compounds (Vuckovic et al. 2011).

To address this issue, reaction/structure directed analysis was developed for SPME-based analysis (Yu et al. 2019).

Instead of using inductive rules and statistical properties from known compounds, statistical properties of peaks from real samples are considered for data mining. The qualitative information obtained from high-resolution mass spectrometry is the accurate mass-to-charge ratio ( $m/z$ ) of compounds. However, multiple compounds could share the same mass-to-charge ratios, while a single compound could also generate multiple mass-to-charge ratios such as adducts, neutral loss, or isotopologues. In this case, the single mass-to-charge ratio is not a very useful parameter for the annotation step. However, distances between mass-to-charge ratios could indicate certain types of reactions or structures; such an approach is called paired-mass distance (PMD) analysis. For instance, a PMD of 15.99 Da is always associated with an oxidation process. A randomly generated dataset would not show a PMD of 15.99 Da, while in real samples, a PMD of 15.99 Da will likely always appear with high frequency. In addition, PMDs can also reveal structure information for particular compounds. For instance, a PMD of 14.02 Da is associated with a-CH<sub>2</sub>-bond, while the PMD 42.01 Da is associated with a peptide bond. In this case, the use of local statistical properties (frequency of PMDs) to screen reaction level bio-information is preferred over trying to annotate each unknown compound. By quantitatively checking structure or reaction level changes from *in vivo* SPME sampling, we may capture the changes of short live metabolites’ profile.

---

### 3 Application of *in Vivo* SPME

Several organic compounds, such as PAHs, pesticides, PPCPs, and inorganic compounds (such as heavy metals) are constantly introduced to the ecosystem via a number of routes. Contaminants circulating in water and/or residing in sediments and soil eventually enter living organisms, where they affect the functioning of these biological systems (Miller et al. 2018). Even at very low concentrations, the constant persistence of such compounds in living organisms can exert adverse effects by acting on specific cellular processes at the genome, proteome, and metabolome levels. Due to their potential toxic, carcinogenic, and mutagenic activities, such chemicals have been labeled as emerging contaminants, indicating that their levels and distribution in the environment should be tightly controlled. Therefore, methods that will facilitate fast and efficient extraction and analysis of these environmental toxicants are highly desired.

Different analytical methodologies have been developed to investigate and determine trace levels of environmental toxins in animals and plants’ tissues. Typical sample preparation protocols include tissue homogenization followed by extraction of analytes with the use of organic solvents, whereupon the sample extract is cleaned-up prior



to instrumental analysis. In order to reduce the number of sampling/sample preparation steps, and so as to avoid sample collection that necessitates the sacrifice of living organisms, *in vivo* SPME has been introduced as a promising tool for non-lethal sampling of organic contaminants on-site. As already mentioned, *in vivo* SPME offers several advantages over conventional sample preparation protocols for extraction of analytes from complex matrices in field studies. Moreover, SPME can be directly coupled to GC-MS or LC-MS to provide close to real-time information about the types of toxicants present in living organisms as well as their levels in the analyzed matrices (Fig. 1). Given the advantages offered by *in vivo* SPME, application of this technique in the analysis of environmental contaminants in living plants and animals has been frequently reported (Xu et al. 2016; Zhang et al. 2016).

### 3.1 In Vivo SPME in Plant Analysis

Given that plants are important components of the food chain for many species, there is growing concern regarding the exposure of plants to contaminants present in the surrounding environment, including water, soil, and air. Once introduced to the plant body, toxins are distributed and reside in different parts of plants. Once plants are consumed, such toxins can also be forwarded to other hosts within the food chain, and affect the health status of those organisms.

Over the past years, multiple classes of emerging contaminants, including PAHs and PPCPs, have been detected in edible parts of plants from contaminated regions. However, extraction and quantitation of toxins in plants remain a challenging task due to the very complex nature of this matrix. Therefore, analytical methodologies that can track tissue distribution of contaminants in plants, such as SPME, are gaining increasing attention in food safety and environmental studies (Musteata et al. 2016). For instance, *in vivo* SPME was employed to monitor the fate of environmental contaminants such as chlorinated VOCs in living plants (Zhu et al. 2013). The optimized procedure facilitated extraction of methyl tert-butyl ether (MTBE), a component of a fuel, and prevented loss of this volatile compound, a loss previously observed during the traditional sample pre-treatment procedure (Reiche et al. 2013). The optimized technique facilitated monitoring of the level of MTBA present in reeds as a function of the season and water concentration levels. The accumulation and distribution of organochloride pesticides (OCPs) and organophosphorus pesticides (OPPs) via *in vivo* SPME were also investigated (Qiu et al. 2016). Custom-made PDMS fibers were introduced to different organs of living Malabar spinach plants, and concentrations of analyzed pesticides were calculated using the sampling rate calibration approach. Several factors, including the distribution concentration factor (DCF), have been used to assess the translocation and accumulation of toxins in different organs in order to improve our understanding of

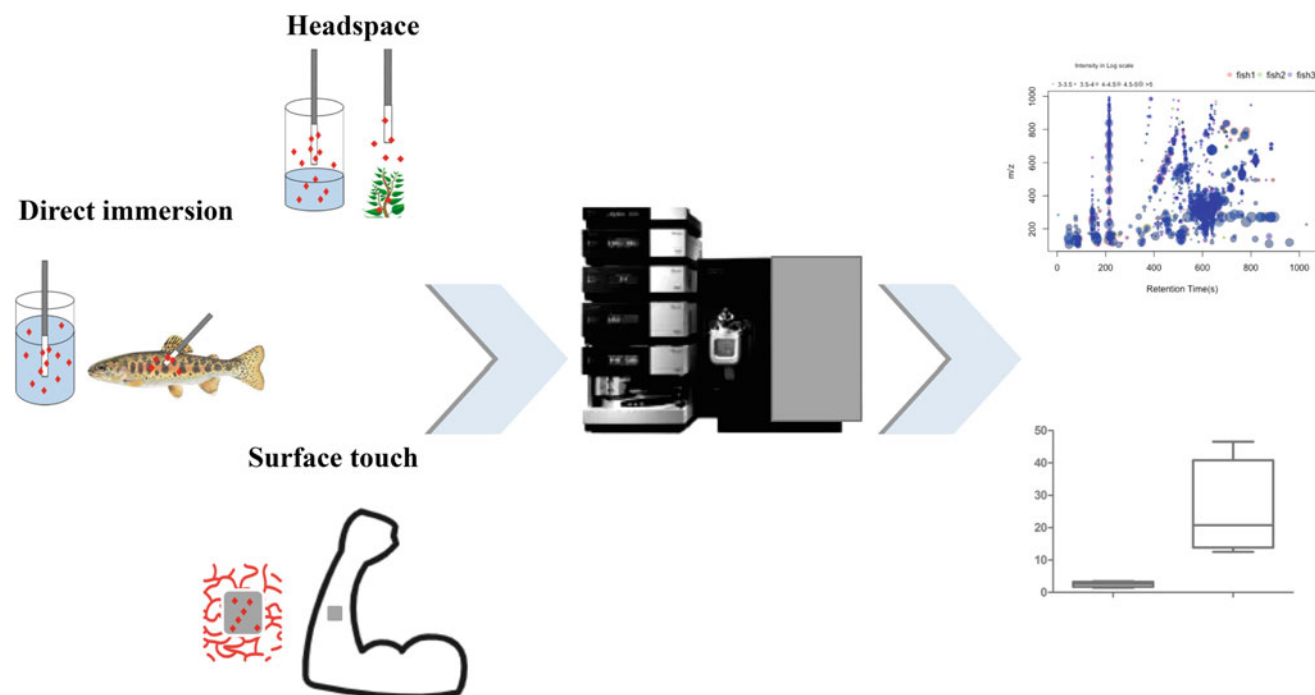


**Fig. 1** Application of SPME sampling along with the instrumental analysis and targeted/untargeted screening of metabolites in plant, animal and human studies

contaminant behavior in living plants. In addition, *in vivo* SPME was also applied for the analysis of metabolome profile and for detection of alterations in metabolite composition in fruits during maturation on the tree (Risticic et al., under review). Several classes of esters were upregulated in very mature 'Honeycrisp' apples, where the level of estragole was increasing with fruit ripening. Moreover, novel bioactive molecules, namely Amaryllidaceae alkaloids were extracted and successfully detected in the analyzed apples by two-dimensional gas chromatography–time-of-flight mass spectrometry (GCxGC-ToFMS). The applied *in vivo* SPME protocol facilitated a metabolite quenching and extraction of unique fruit components at different maturity stages. These were not previously reported in apples, possibly due to the use of sample preparation approaches that could disturb real metabolite composition in fruits via induction of enzymatic degradation and oxidation processes.

### 3.2 In Vivo SPME in Animal Studies

SPME has been considered an easy and efficient tool for *in vivo* analysis of contaminants present in the tissues and organs of animals exposed to environmental toxins. The ability to monitor the distribution of trace contaminants in living organisms is a significant advantage of SPME over conventional techniques, where complex sample preparation prior to instrumental analysis may result in a loss of compounds, especially those characterized by a volatile and/or highly reactive nature. One of the first reports describing the application of *in vivo* SPME in toxicological analysis in animal species detailed a pharmacokinetic study of a VOC, toluene, in the hippocampus of mice exposed to this toxin via inhalation (Nakajima et al. 2006). It had been previously observed on animal models that toluene can cause severe or chronic toxicity related to central nervous system disturbances. However, due to the fast vaporization of toluene during the traditional sampling steps, data regarding the exact level and pharmacokinetics of this compound in the brain had been inconsistent. Measurements of levels of toluene via SPME probes directly inserted into the hippocampus of freely moving rats provided reliable information regarding the half-life of this toxin. *In vivo* SPME followed by GC-MS instrumental analysis revealed that the concentration of toluene in mice brains reached a maximum within 30 min, and decreased rapidly in the next 90 min upon exposure to the VOC. In another study, *in vivo* SPME sampling was applied for analysis of the effects of intraperitoneally administered toluene on the composition of amino acids in the brain of living mice (Win-Shwe et al. 2007). The attained results helped to shed light into the relationship between high doses of toluene and increasing

levels of glutamate and taurine in the hippocampus suggesting that exposure to this toxin leads to the activation of neuroprotective mechanisms in the brain.

Few laboratory and field-based studies have also demonstrated the suitability of SPME technology for the extraction of emerging contaminants present in aquatic organisms. For instance, *in vivo* SPME has been applied for measurement of a variety of PPCPs in fish muscles. Quantitative analysis of a wide range of pharmaceuticals, including carbamazepine, naproxen, diclofenac, gemfibrozil, bisphenol A, fluoxetine, ibuprofen, and atrazine, was carried out with use of an SPME technique initially optimized in laboratory conditions (Wang et al. 2011). In controlled lab exposures, concentrations of the targeted compounds in fish were found to be related to exposure concentrations in effluents in a dose-dependent manner. Next, the optimized technique was applied to a field study of wild fish exposed to municipal wastewater effluents (MWWE). *In vivo* SPME allowed for monitoring of dynamic bioaccumulation processes of selected contaminants in the tissues of living organisms. Wild fish sampling via *in vivo* SPME enabled extraction of a selected group of emerging contaminants of concern from the tissues of several fish species, yielding results comparable to those attained via traditional monitoring methods. Togunde et al. developed an SPME method for *in vivo* sampling of the dorsal–epaxial muscle of rainbow trout (*Oncorhynchus mykiss*) in an 8-day laboratory exposure to selected pharmaceuticals (carbamazepine, fluoxetine, sertraline, paroxetine, atorvastatin, diclofenac, and venlafaxine). Concentrations of extracted analytes were measured *in vivo* with custom-made SPME fibers (Togunde et al. 2013). Due to the low invasiveness of the SPME probes used in this study, the optimized method was also applied for an on-site study of wild fish exposed to MWWE. The uptake and bioconcentration of waterborne contaminants, such as pharmaceutical residues in the muscles of Muskellunge (*Esox masquinongy*) were measured as a part of this wild fish study. In another study, Ouyang et al. developed a rapid *in vivo* SPME approach based on the sampling rate calibration method for both laboratory and field studies (Ouyang et al. 2011a). The SPME probe was inserted in fish dorsal–epaxial muscle for 20 min for extraction of certain pharmaceuticals (atrazine, carbamazepine, and fluoxetine). The method developed in the laboratory also facilitated the detection of trace levels of analytes within muscles in wild fish, yielding analytical results comparable to those of traditional sample preparation techniques involving lethal sampling followed by tissue liquid extraction with the use of organic solvents.

Recently, *in vivo* SPME was applied in an EWAS for monitoring of toxicants as well as for an assessment of the biochemical response of sixty white suckers (*Catostomus commersonii*) to exposure to potential contaminants

(Roszkowska et al. 2019). SPME probes were placed into dorsal–epaxial muscle for untargeted analysis of contaminants present in tissues of fish collected in the oil sands development region and outside the deposit (pulp and paper mill discharge region). Several organic compounds potentially related to industrial and workplace toxins, such as aliphatic and aromatic hydrocarbons, pesticides and PPCPs, including unstable and highly reactive compounds, were extracted via SPME probes from almost all sampling regions. In addition, this study revealed the presence of petroleum-related compounds in the fish muscle tissue, providing important information regarding the exposome of the organism to the surrounding environment as well as alterations in the biochemical profile of fish muscles caused by such exposures. The applied *in vivo* SPME technology for wild fish studies presents an interesting alternative to other techniques for biomonitoring studies aiming to track alterations in organisms exposed to environmental contaminants.

### 3.3 In Vivo SPME in Human Studies

*In vivo* sampling of different human matrices, including biofluids and solid tissues, can reveal real-time changes in certain metabolic pathways and also the presence of exogenous compounds as a response to environmental exposures (Vereb et al. 2011). SPME and related techniques have been applied in such studies as minimally invasive approaches capable of capturing short-lived species and endogenous compounds. For instance, HS-SPME has been used as a noninvasive diagnostic tool in breath analysis, where a commercially available SPME device was modified for direct, real-time extraction and quantitative determination of ethanol, acetone, and isoprene in human breath (Grote and Pawliszyn 1997). Recently, needle trap device (NTD) technology coupled with thermal-desorption photoionization time-of-flight mass spectrometry (TD-PI-TOFMS) was used during *in vivo* breath sampling to evaluate human exposure to smoke (Kleeblatt et al. 2015). In this work, several xenobiotic substances (benzene, toluene, styrene, and ethylbenzene) were successfully extracted and identified in the breath of smoking individuals. Another interesting human matrix for application of the *in vivo* SPME technique is saliva. As a complex biological matrix that can be easily collected in a noninvasive manner, saliva is essentially composed of filtered blood, and is thus potentially able to reflect human real-time exposure conditions to pollutants. In a nontargeted EWAS, a TFME device was immersed into saliva for *in vivo* monitoring of saliva with the aim of investigating associations between environmental exposure and chronic diseases (Bessonneau et al. 2013). To further increase the sensitivity of the saliva sampling method, TFME was also applied in *in vivo* saliva extraction by placing

the TFME device directly in the mouth of participants for a 5 min sampling period (Bessonneau et al. 2015; Shigeyama et al. 2019). The method was validated for simultaneous quantification of 49 prohibited substances, and can be used in doping tests. This optimized technique facilitated detection of trace levels of endogenous steroid hormones. Skin odor, on the other hand, is capable of revealing environmental exposure conditions as well as alterations in endogenous metabolites; to this end, HS-SPME has been used for *in vivo* skin analysis of human fragrance profiles (Duffy et al. 2017). In contrast to the SPME fiber, a TFME membrane can be directly applied onto the skin surface, enabling better sensitivity for semi- and low- volatility compounds in *in vivo* analysis (Jiang et al. 2013). Due to the minimal invasiveness of this technique, its non-depletive extraction mode and biocompatibility, *in vivo* SPME shows great potential for real-time monitoring of exposure of human tissues and organs to environmental contaminants and other toxins.

## 4 Conclusions and Future Perspectives

Increasing concern for ecosystem protection continues to extend the application of SPME in *in vivo* environmental and toxicological studies to the analysis of the accumulation and metabolism of contaminants, as well as to a wide range of exposome studies. SPME technology facilitates tracing of the behavior of certain toxins in living systems while also offering the possibility for monitoring of biochemical responses of organisms to exposure to environmental contaminants. *In vivo* SPME sampling provides more accurate and reliable information about the distribution of target compounds as it enables minimally invasive, real-time extraction of small molecules from living systems without the need for sample pre-treatment or animal sacrifices. This is especially important for low-abundance populations of animals and plants, for which traditional sampling can be problematic. Development of novel SPME devices and extraction phases as well as direct coupling of SPME probes to MS will extend the application of SPME techniques in EWAS and toxicological analyses; this in turn can provide further insight into the composition of exogenous substances and endogenous profiles of individual organisms. Use of this technique in cause–effect relationship studies of metabolome response of living organisms to exposure to contaminants may allow for the identification of novel biomarkers of the exposome, and provide crucial information necessary for a better understanding of the persistence and effects of pollutants in the environment.

**Acknowledgements** This monograph was developed within the framework of the Environment Canada through the Environmental Damages Fund (grant EC-129114).

## References

- Alam MN, Ricardez-Sandoval L, Pawliszyn J (2015) Numerical modeling of solid-phase microextraction: binding matrix effect on equilibrium time. *Anal Chem* 87:9846–9854. <https://doi.org/10.1021/acs.analchem.5b02239>
- Arthur CL, Pawliszyn J (1990) Solid phase microextraction with thermal desorption using fused silica optical fibers. *Anal Chem* 62:2145–2148. <https://doi.org/10.1021/ac00218a019>
- Augusto Gomez-Rios G, Vasiljevic T, Gionfriddo E, Yu M, Pawliszyn J (2017) Towards on-site analysis of complex matrices by solid-phase microextraction-transmission mode coupled to a portable mass spectrometer via direct analysis in real time. *Analyst*. <https://doi.org/10.1039/C7AN00718C>
- Bai Z, Pilote A, Sarker PK, Vandenberg G, Pawliszyn J (2013) In vivo solid-phase microextraction with in vitro calibration: determination of off-flavor components in live fish. *Anal Chem* 85:2328–2332. <https://doi.org/10.1021/ac3033245>
- Bessonneau V, Bojko B, Pawliszyn J (2013) Analysis of human saliva metabolome by direct immersion solid-phase microextraction LC and benchtop orbitrap MS. *Bioanalysis* 5:783–792. <https://doi.org/10.4155/bio.13.35>
- Bessonneau V, Boyaci E, Maciazek-Jurczyk M, Pawliszyn J (2015) In vivo solid phase microextraction sampling of human saliva for non-invasive and on-site monitoring. *Anal Chim Acta* 856:35–45. <https://doi.org/10.1016/j.aca.2014.11.029>
- Bojko B, Pawliszyn J (2014) In vivo and ex vivo SPME: a low invasive sampling and sample preparation tool in clinical bioanalysis. *Bioanalysis* 6:1227–1239. <https://doi.org/10.4155/bio.14.91>
- Boyaci E, Bojko B, Reyes-Garcés N, Poole JJ, Gómez-Ríos GA, Teixeira A, Nicol B, Pawliszyn J (2018) High-throughput analysis using non-depletive SPME: challenges and applications to the determination of free and total concentrations in small sample volumes. *Sci Rep* 8. <https://doi.org/10.1038/s41598-018-19313-1>
- Domingo-Almenara X, Montenegro-Burke JR, Benton HP, Siuzdak G (2018) Annotation: a computational solution for streamlining metabolomics analysis. *Anal Chem* 90:480–489. <https://doi.org/10.1021/acs.analchem.7b03929>
- Duffy E, Jacobs MR, Kirby B, Morrin A (2017) Probing skin physiology through the volatile footprint: discriminating volatile emissions before and after acute barrier disruption. *Exp Dermatol* 10:919–925. <https://doi.org/10.1111/exd.13344>
- Ghiasvand AR, Hosseinzadeh S, Pawliszyn J (2006) New cold-fiber headspace solid-phase microextraction device for quantitative extraction of polycyclic aromatic hydrocarbons in sediment. *J Chromatogr A ExTech* 2006 (1124):35–42. <https://doi.org/10.1016/j.chroma.2006.04.088>
- Gionfriddo E, Boyaci E, Pawliszyn J (2017) New generation of solid-phase microextraction coatings for complementary separation approaches: a step toward comprehensive metabolomics and multiresidue analyses in complex matrices. *Anal Chem* 89:4046–4054. <https://doi.org/10.1021/acs.analchem.6b04690>
- Godage NH, Gionfriddo E (2019) A critical outlook on recent developments and applications of matrix compatible coatings for solid phase microextraction. *TrAC Trends Anal Chem* 111:220–228. <https://doi.org/10.1016/j.trac.2018.12.019>
- Gómez-Ríos GA, Tascon M, Pawliszyn J (2018) Coated blade spray: shifting the paradigm of direct sample introduction to MS. *Bioanalysis* 10:257–271. <https://doi.org/10.4155/bio-2017-0153>
- Grote C, Pawliszyn J (1997) Solid-phase microextraction for the analysis of human breath. *Anal Chem* 69:587–596. <https://doi.org/10.1021/ac960749l>
- Huq M, Tascon M, Nazdragic E, Roszkowska A, Pawliszyn J (2019) Measurement of free drug concentration from biological tissue by solid-phase microextraction: in Silico and experimental study. *Anal Chem*. <https://doi.org/10.1021/acs.analchem.9b00983>
- Jiang R, Cudjoe E, Bojko B, Abaffy T, Pawliszyn J (2013) A non-invasive method for in vivo skin volatile compounds sampling. *Anal Chim Acta* 804:111–119. <https://doi.org/10.1016/j.aca.2013.09.056>
- Jiang R, Pawliszyn J (2014) Cooled membrane for high sensitivity gas sampling. *J Chromatogr A* 1338:17–23. <https://doi.org/10.1016/j.chroma.2014.02.070>
- Jiang R, Pawliszyn J (2012) Thin-film microextraction offers another geometry for solid-phase microextraction. *TrAC Trends Anal Chem* 39:245–253. <https://doi.org/10.1016/j.trac.2012.07.005>
- Kleeblatt J, Schubert JK, Zimmermann R (2015) Detection of gaseous compounds by needle trap sampling and direct thermal-desorption photoionization mass spectrometry: concept and demonstrative application to breath gas analysis. *Anal Chem* 87:1773–1781. <https://doi.org/10.1021/ac5039829>
- Llompart M, Celeiro M, Garcia-Jares C, Dagnac T (2019) Environmental applications of solid-phase microextraction. *TrAC Trends Anal Chem* 112:1–12. <https://doi.org/10.1016/j.trac.2018.12.020>
- Lord HL, Zhan W, Pawliszyn J (2010) Fundamentals and applications of needle trap devices: a critical review. *Anal Chim Acta* 677(1):3–18. A selection of papers presented at the 11th International Symposium on Advances in Extraction Technologies (ExTech2009). <https://doi.org/10.1016/j.aca.2010.06.020>
- Martendal E, Carasek E (2011) A new approach based on a combination of direct and headspace cold-fiber solid-phase microextraction modes in the same procedure for the determination of polycyclic aromatic hydrocarbons and phthalate esters in soil samples. *J Chromatogr A* 1218:1707–1714. <https://doi.org/10.1016/j.chroma.2011.01.074>
- Martos PA, Pawliszyn J (1998) Sampling and determination of formaldehyde using solid-phase microextraction with on-fiber derivatization. *Anal Chem* 70:2311–2320. <https://doi.org/10.1021/ac9711394>
- Menezes HC, Paiva MJN, Santos RR, Sousa LP, Resende SF, Saturnino JA, Paulo BP, Cardeal ZL (2013) A sensitive GC/MS method using cold fiber SPME to determine polycyclic aromatic hydrocarbons in spring water. *Microchem J* 110:209–214. <https://doi.org/10.1016/j.microc.2013.03.010>
- Miller TH, Bury NR, Owen SF, MacRae JI, Barron LP (2018) A review of the pharmaceutical exposome in aquatic fauna. *Environ Pollut* 239:129–146. <https://doi.org/10.1016/j.envpol.2018.04.012>
- Moliner-Martinez Y, Herráez-Hernández R, Verdú-Andrés J, Molins-Legua C, Campíns-Falcó P (2015) Recent advances of in-tube solid-phase microextraction. *TrAC Trends Anal Chem* 71:205–213. <https://doi.org/10.1016/j.trac.2015.02.020>
- Musteata FM, Sandoval M, Ruiz-Macedo JC, Harrison K, McKenna D, Millington W (2016) Evaluation of in vivo solid phase microextraction for minimally invasive analysis of nonvolatile phytochemicals in Amazonian plants. *Anal Chim Acta* 933:124–133. <https://doi.org/10.1016/j.aca.2016.05.053>
- Nakajima D, Tin-Tin-Win-Shwe Kakeyama M, Fujimaki H, Goto S (2006) Determination of toluene in brain of freely moving mice using solid-phase microextraction technique. *Neuro Toxicol* 27: 615–618. <https://doi.org/10.1016/j.neuro.2005.12.006>
- Niri VH, Eom I-Y, Kermani FR, Pawliszyn J (2009) Sampling free and particle-bound chemicals using solid-phase microextraction and needle trap device simultaneously. *J Sep Sci* 32:1075–1080. <https://doi.org/10.1002/jssc.200800603>
- Ouyang G, Oakes KD, Bragg L, Wang S, Liu H, Cui S, Servos MR, Dixon DG, Pawliszyn J (2011a) Sampling-rate calibration for rapid and nonlethal monitoring of organic contaminants in fish muscle by solid-phase microextraction. *Environ Sci Technol* 45:7792–7798. <https://doi.org/10.1021/es201709j>

- Ouyang G, Vuckovic D, Pawliszyn J (2011b) Nondestructive sampling of living systems using in vivo solid-phase microextraction. *Chem Rev* 111:2784–2814. <https://doi.org/10.1021/cr100203t>
- Ouyang G, Pawliszyn J (2008) A critical review in calibration methods for solid-phase microextraction. *Anal Chim Acta* 627:184–197. <https://doi.org/10.1016/j.aca.2008.08.015>
- Pawliszyn J (2012) *Handbook of solid phase microextraction*. Elsevier. <https://doi.org/10.1016/C2011-0-04297-7>
- Piri-Moghadam H, Ahmadi F, Gómez-Ríos GA, Boyacı E, Reyes-Garcés N, Aghakhani A, Bojko B, Pawliszyn J (2016) Fast quantitation of target analytes in small volumes of complex samples by matrix-compatible solid-phase microextraction devices. *Angew Chem Int Ed* 55:7510–7514. <https://doi.org/10.1002/anie.201601476>
- Poole JJ, Grandy JJ, Yu M, Boyacı E, Gómez-Ríos GA, Reyes-Garcés N, Bojko B, Heide HV, Pawliszyn J (2017) Deposition of a sorbent into a recession on a solid support to provide a new, mechanically robust solid-phase microextraction device. *Anal Chem*. <https://doi.org/10.1021/acs.analchem.7b01382>
- Qiu J, Chen G, Xu J, Luo E, Liu Yan, Wang F, Zhou H, Liu Yuan, Zhu F, Ouyang G (2016) In vivo tracing of organochloride and organophosphorus pesticides in different organs of hydroponically grown malabar spinach (*Basella alba* L.). *J Hazard Mater* 316:52–59. <https://doi.org/10.1016/j.jhazmat.2016.05.024>
- Reiche N, Mothes F, Fiedler P, Borsdorf H (2013) A solid-phase microextraction method for the in vivo sampling of MTBE in common reed (*Phragmites Australis*). *Environ Monit Assess* 185:7133–7144. <https://doi.org/10.1007/s10661-013-3089-3>
- Reyes-Garcés N, Gionfriddo E, Gómez-Ríos GA, Alam MN, Boyacı E, Bojko B, Singh V, Grandy J, Pawliszyn J (2018) Advances in solid phase microextraction and perspective on future directions. *Anal Chem* 90:302–360. <https://doi.org/10.1021/acs.analchem.7b04502>
- Risticciv S, Souza-Silva EA, Gionfriddo E, DeEll JR, Cochran J, Hopkins WS, Pawliszyn J Application of in vivo solid phase microextraction (SPME) in capturing metabolome of apple (*Malus × domestica* Borkh.) fruit, under review (*Frontiers in Plant Science*)
- Roszkowska A, Yu M, Bessonneau V, Ings J, McMaster M, Smith R, Bragg L, Servos M, Pawliszyn J (2019) In vivo solid-phase microextraction sampling combined with metabolomics and toxicological studies for the non-lethal monitoring of the exposome in fish tissue. *Environ Pollut* 249:109–115. <https://doi.org/10.1016/j.envpol.2019.03.024>
- Shigeyama H, Wang T, Ichinose M, Ansai T, Lee S-W (2019) Identification of volatile metabolites in human saliva from patients with oral squamous cell carcinoma via zeolite-based thin-film microextraction coupled with GC–MS. *J Chromatogr B* 1104:49–58. <https://doi.org/10.1016/j.jchromb.2018.11.002>
- Souza-Silva EA, Gionfriddo E, Pawliszyn J (2015) A critical review of the state of the art of solid-phase microextraction of complex matrices II. Food analysis. *TrAC Trends Anal Chem* 71:236–248. <https://doi.org/10.1016/j.trac.2015.04.018>
- Togunde OP, Lord H, Oakes KD, Servos MR, Pawliszyn J (2013) Development and evaluation of a new in vivo solid-phase microextraction sampler. *J Sep Sci* 36:219–223. <https://doi.org/10.1002/jssc.201200839>
- Vasiljevic T, Singh V, Pawliszyn J (2019) Miniaturized SPME tips directly coupled to mass spectrometry for targeted determination and untargeted profiling of small samples. *Talanta* 199:689–697. <https://doi.org/10.1016/j.talanta.2019.03.025>
- Vereb H, Dietrich AM, Alfeeli B, Agah M (2011) The possibilities will take your breath away: breath analysis for assessing environmental exposure. *Environ Sci Technol* 45:8167–8175. <https://doi.org/10.1021/es202041j>
- Vuckovic D (2013) High-throughput solid-phase microextraction in multi-well-plate format. *TrAC Trends Anal Chem* 45:136–153. <https://doi.org/10.1016/j.trac.2013.01.004>
- Vuckovic D, de Lannoy I, Gien B, Shirey RE, Sidisky LM, Dutta S, Pawliszyn J (2011) In Vivo Solid-Phase Microextraction: Capturing the Elusive Portion of Metabolome. *Angew Chem Int Ed* 50:5344–5348. <https://doi.org/10.1002/anie.201006715>
- Vuckovic D, Zhang X, Cudjoe E, Pawliszyn J (2010) Solid-phase microextraction in bioanalysis: new devices and directions. *J Chromatogr Mass Spectrom Innov Appl Part VI* 1217:4041–4060. <https://doi.org/10.1016/j.chroma.2009.11.061>
- Wang S, Oakes KD, Bragg LM, Pawliszyn J, Dixon G, Servos MR (2011) Validation and use of in vivo solid phase micro-extraction (SPME) for the detection of emerging contaminants in fish. *Chemosphere* 85:1472–1480. <https://doi.org/10.1016/j.chemosphere.2011.08.035>
- Wang Y, Zhang J, Ding Y, Zhou J, Ni L, Sun C (2009) Quantitative determination of 16 polycyclic aromatic hydrocarbons in soil samples using solid-phase microextraction. *J Sep Sci* 32:3951–3957. <https://doi.org/10.1002/jssc.200900420>
- Win-Shwe T-T, Mitsushima D, Nakajima D, Ahmed S, Yamamoto S, Tsukahara S, Kakeyama M, Goto S, Fujimaki H (2007) Toluene induces rapid and reversible rise of hippocampal glutamate and taurine neurotransmitter levels in mice. *Toxicol Lett* 168:75–82. <https://doi.org/10.1016/j.toxlet.2006.10.017>
- Xu J, Chen G, Huang S, Qiu J, Jiang R, Zhu F, Ouyang G (2016) Application of in vivo solid-phase microextraction in environmental analysis. *TrAC Trends Anal Chem* 85:26–35. <https://doi.org/10.1016/j.trac.2016.03.003>
- Yu M, Olkowicz M, Pawliszyn J (2019) Structure/reaction directed analysis for LC-MS based untargeted analysis. *Anal Chim Acta* 1050:16–24. <https://doi.org/10.1016/j.aca.2018.10.062>
- Zhang L, Gionfriddo E, Acquaro V, Pawliszyn J (2018) Direct immersion solid-phase microextraction analysis of multi-class contaminants in edible seaweeds by gas chromatography-mass spectrometry. *Anal Chim Acta* 1031:83–97. <https://doi.org/10.1016/j.aca.2018.05.066>
- Zhang Q-H, Zhou L-D, Chen H, Wang C-Z, Xia Z-N, Yuan C-S (2016) Solid-phase microextraction technology for in vitro and in vivo metabolite analysis. *TrAC Trends Anal Chem* 80:57–65. <https://doi.org/10.1016/j.trac.2016.02.017>
- Zhu F, Xu J, Ke Y, Huang S, Zeng F, Luan T, Ouyang G (2013) Applications of in vivo and in vitro solid-phase microextraction techniques in plant analysis: a review. *Anal Chim Acta* 794:1–14. <https://doi.org/10.1016/j.aca.2013.05.016>

# Dose-Dependent Transcriptomic Approach for Mechanistic Screening in Chemical Risk Assessment

Xiaowei Zhang, Pingping Wang, and Pu Xia

## Abstract

Omics approaches can monitor responses and alterations of biological pathways at a genome scale, which are useful to predict potential adverse effects from environmental toxicants. However, high-throughput application of transcriptomics in chemical assessment is limited due to the high cost and lack of “standardized” toxicogenomic methods. Here, we have developed a reduced transcriptome approach as an alternative strategy to facilitate testing a wide range of chemical concentrations, which targets a reduced set of genes to focus on key toxic response genes and associated pathways. The reduced transcriptomic approach allows full dose range testing of hundreds of chemicals or mixtures using human cells or zebrafish embryos. Points of departure of genes and pathways can be used for potency ranking and to classify chemicals by disrupted biological pathways. It is anticipated that reduced transcriptomic approaches will significantly advance pathway-based high-throughput screening of potentially toxic substances.

(Zhang et al. 2018). Toxicity pathway profiling could help to predict potential apical toxicity and prioritize and guide subsequent testing of the chemicals. To support chemical risk assessment, analytical frameworks such as the use of adverse outcome pathways (AOPs) have been adopted to describe cascading chains of causal events occurring at different levels of biological organization that result in a measurable ecotoxicological effect (Conolly et al. 2017). In particular, the AOP framework has gained traction in regulatory science as it offers an efficient and effective means for linking toxicological mechanisms with the standardized toxicity end points required for regulatory assessments, increasing their relevance as predictors of ecosystem effects. Nevertheless, among the many challenges and limitations that must be addressed to realize the full potential of the AOP framework in regulatory decision-making, one prominent task is the development of appropriate *in vitro* bioassays to capture all possible molecular initiating events (MIEs) and/or key events (KEs) that could be generated by thousands of untested chemicals (Knäpen et al. 2018).

Traditionally, monitoring and assessment of mixtures have relied on chemistry analyses. Although high-throughput targeted and nontargeted analytical methods have been developed for the detection of hundreds of chemicals present in complex environmental samples, chemical-focused analyses cannot detect contaminants with unknown structure, and cannot explain the cumulative toxicity of mixtures (Altenburger et al. 2015). Effect-based approaches such as high content screening can provide assessments of biological activity of environmental mixture. However, most current cell-based HTS assays are limited in their coverage of biological pathways, and subsequently their ability to predict a wide range of potential adverse outcomes (Escher et al. 2014).

Integrating genomic dose-response modeling into the hazard characterization with wide-range doses has shown to be valuable in risk assessment, particularly when applied to lower, more environmentally relevant doses. Omics technologies have the ability to provide a global view of the

## 1 Introduction

A major challenge in regards to prioritizing environmental chemicals and/or assessing the hazard of complex mixtures is the lack of sufficient toxicological information for thousands of chemicals and endless possibility of mixtures

### Electronic supplementary material

The online version of this chapter ([https://doi.org/10.1007/978-981-13-9447-8\\_4](https://doi.org/10.1007/978-981-13-9447-8_4)) contains supplementary material, which is available to authorized users.

X. Zhang (✉) · P. Wang · P. Xia

State Key Laboratory of Pollution Control & Resource Reuse,  
School of the Environment, Nanjing University, Nanjing, 210023,  
People's Republic of China  
e-mail: [zhangxw@nju.edu.cn](mailto:zhangxw@nju.edu.cn)

cellular processes of an individual in response to chemical exposure, and to do so in a high-throughput manner with the advancement of bioinformatics (Zhang et al. 2011). Therefore, the widespread adoption of omics can increase the efficacy, efficiency, and timeliness of chemical assessment, and generate new knowledge on the underlying mechanisms contributing to adverse effects (Zhang et al. 2018). Genomic studies on wide-range doses could help to determine new biomarkers and to derive points of departure for chemical risk assessment. For instance, certain endocrine-disrupting chemicals have been reported to alter gene expression in a nonmonotonic manner at low doses, which indicates a potential novel molecular mechanism. In addition, application of multiple doses with single replicate using human cells or zebrafish embryo has been shown to effectively identify vulnerable genes and pathways (Hermesen et al. 2012). Concentration-dependent bioactivity of chemicals or mixtures could indicate potential early responses. Pathway analysis based on the active values of differentially concentration-dependent genes implicates the potential bioactivity of samples, which can be used in diagnostic analysis of chemical profiles (Wang et al. 2018). However, utilization of biological-pathway responses derived from concentration-dependent genomic data is still limited in hazard characterization.

The development of reproducible, dose-dependent omics protocols for chemical testing is urgently needed to support the incorporation of omics technologies into chemical risk assessment (Zhang et al. 2018). While omics have been widely used to investigate whole-genome alteration for MOA prediction and classification of chemicals, consistent protocols for generation, processing, and interpretation of omics data should be established before such methodologies are incorporated into regulatory assessment. Great efforts have been made on the standardization of transcriptomics to profile genome expression. For instance, the MicroArray Quality Control (MAQC) project has been launched to evaluate the reproducibility of inter- and intraplatform microarray technologies. In ecotoxicology, a few studies have highlighted standardized transcriptomic protocols, ranging from RNA extracts to full bioinformatic pipelines, potentially improving interlaboratory comparability. One suggested advantage of concentration-dependent transcriptomic data is the generation of point of departure (POD) values. We also note that some concentration-dependent transcriptomics studies have been conducted using inconsistent bioinformatic methods for data filtering, concentration–response modeling, and quantitative characterization of genes and pathways. This makes comparison across studies problematic, and as such, we recommend that future studies consider the development of standardized protocols for concentration-dependent transcriptomic characterization of chemicals (Zhang et al. 2018).

As an alternative strategy to sequencing of the whole transcriptome, reduced transcriptome analysis targets a reduced set of genes to focus on key toxic response genes and associated pathways to facilitate testing a wide range of chemical concentrations (Xia et al. 2017). A key supporting principle is that a subset of representative genes in a network may function as surrogates for all genes of that network. The use of reduced transcriptomes has been proposed to measure a subset of genes to focus on toxicologically relevant genes; this reduces the complexity of such studies, which in turn supports extending the range of chemical concentrations being tested—a key statistical consideration. The principle supporting the use of reduced transcriptomes is that the expression of key genes can provide a proxy for expression of all genes in networks or pathways of interest. Recent examples of the use of gene subsets include the library of integrated network-based cellular signatures (LINCS) project, which has designed a key gene set of 978 human genes, and the National Institute of Environmental Health Sciences (NIEHS) has proposed the S1500 gene set consisting of 1500–3000 human genes, which were computationally selected from thousands of gene expression data sets in Gene Expression Omnibus (GEO) to be representative of the whole human transcriptome.

---

## 2 Development of Reduced Transcriptome for Human and Zebrafish

We have recently developed streamlined reduced transcriptome approaches using human cells (RHT) and zebrafish embryos (RZT) for the assessment of toxic substances (Fig. 1) (Xia et al. 2017; Wang et al. 2018). Two principles were employed when selecting genes for reduced transcriptomes: (1) maximal coverage of biological pathways and (2) toxicological relevance. Firstly, to cover comprehensive biological pathways, we selected all genes from existing biological-pathway databases such as the Kyoto Encyclopedia of Genes and Genomes (KEGG) or Gene Ontology (GO), followed by computational inference of a small set of genes playing central roles in entire gene networks. Secondly, toxicologically relevant genes were retrieved from existing toxicology testing databases, including all gene end points tested in ToxCast (<https://www.epa.gov/chemical-research/toxicity-forecaster-toxcasttm-data>) and all genes associated with MIEs and KEs in AOP-Wiki (<https://aopwiki.org/aops>). The above steps generated RHT and RZT gene sets consisted of 1200 human genes and 1637 zebrafish genes, respectively (Tables 1 and 2, Tables S1 and S2). In silico evaluation was performed to validate the coverage of biological pathways by RHT and RZT gene sets, which showed >90% KEGG and GO pathways were covered by at least one gene in each gene set.

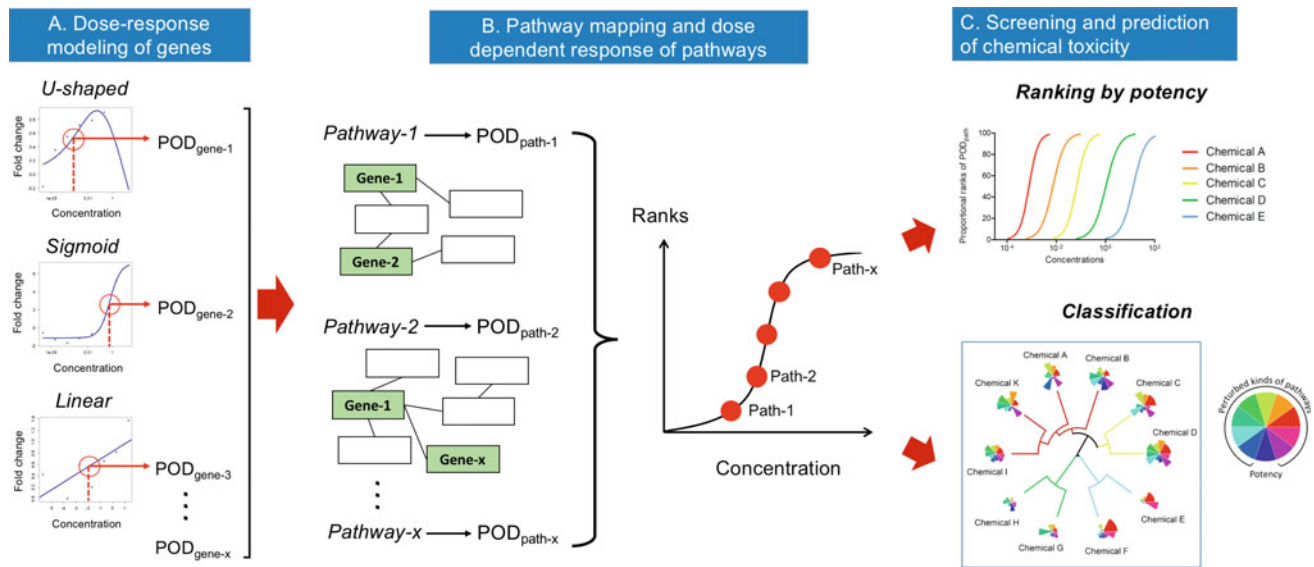


**Fig. 1** A streamlined workflow for reduced transcriptomic analysis of toxic substance by dose-response modeling. (1) Determination of point of departure of genes ( $POD_{gene}$ ); (2) Derivation of point of departure of pathways ( $POD_{path}$ ) and development of dose-dependent response of pathways by ranking of  $POD_{path}$ ; (3) Screening chemical by ranking of potency and chemical classification by disrupted biological pathways

**Table 1** Sources of the 1200 genes in the reduced human transcriptome (RHT)

Main category of genes	Number of genes	Source
Signaling and metabolism pathways	917	Pathway reporter genes (Bluhm et al. 2014)
Molecular initiating events and key events	42	AOP wiki ( <a href="http://aopwiki.org">http://aopwiki.org</a> )
Associated with endocrine disruption	143	Graphical gene model
Associated with genotoxicity	67	KEGG (Kyoto Encyclopedia of Genes and Genomes)
All endpoints tested in ToxCast bioassays	329	ToxCast ( <a href="http://www.epa.gov/ncct/toxcast/">http://www.epa.gov/ncct/toxcast/</a> )
In Total	1200	

**Table 2** Sources of reduced zebrafish transcriptome (RZT) gene panel

Category of genes	Number of zebrafish orthologs	Sources
Public databases	1019	Pathway reporter genes
	1022	L1000 landmark genes
	4260	KEGG database
Core genes	1000	Central roles of public databases
Toxicology-relevant genes	326	ToxCast
	173	AOP
	176	Graphical gene model
	152	Retrieved from references (Jiang et al. 2014; Li et al. 2014; Guiu et al. 2014; Verleyen et al. 2014; Wanglar et al. 2014; Xu et al. 2014a, b; Bluhm et al. 2014)
RZT gene panel	1637	Core genes and toxicology-relevant genes



Further, the ability of RHT and RZT to represent the entire transcriptome was validated using existing transcriptome data sets, where reduced transcriptomes were seen to faithfully represent clustering patterns in entire transcriptomes. Finally, genes in reduced transcriptomes were multiplexed and PCR-amplified, followed by simultaneous measurement of amplicon abundance (RNA-ampliseq). Below RZT was used as an example to illustrate the development procedure for reduced transcriptome.

**Design of a Gene Set for Reduced Zebrafish Transcriptome.** The RZT gene set was selected to represent the key biological pathways and toxicologically relevant processes in zebrafish (*Danio rerio*) genome. First, a list of genes associated with key biological pathways (in Entrez ID formats) was curated from three databases, including Kyoto Encyclopedia of Genes and Genomes (KEGG), zebrafish orthologs of L1000 landmark genes and zebrafish orthologs of pathway reporter genes (Table 2). The centrality values of genes were calculated using CentiScaPe in Cytoscape software. Centrality values are node parameters demonstrating the relevant position of nodes in a whole network. Higher centrality value suggests more central roles of a gene in biological pathways. Then the numbers of significantly enriched KEGG pathways and GO terms (adjusted  $p$ -value  $< 0.05$ ) were calculated in clusterProfiler by walking down the list of curated genes from high to low centrality values by adding 100 genes each time. We selected a minimum number of genes playing central roles in biological pathways, which may significantly represent the maximum number of biological pathways. Additionally, a list of toxicology-relevant genes was curated to include the following: (1) genes measured as end points in ToxCast, (2) genes corresponding to molecular initiating events (MIEs) and key events (KEs) associated with adverse outcome pathways (AOPs) described in the AOP-Wiki ([https://aopwiki.org/wiki/index.php/Main\\_Page](https://aopwiki.org/wiki/index.php/Main_Page)), (3) genes listed in graphical model of the fish hypothalamic–pituitary–gonadal (HPG) axis, and (4) a set of manually retrieved genes associated with development. Finally, to avoid potential amplification bias during mRNA quantification, the combined genes were submitted for online multiplex primers designed by Ion Ampliseq Designer, where the genes with high transcript abundance across zebrafish transcriptome were removed from the RZT gene set.

**In Silico Validation of RZT.** The numbers of KEGG pathways or GO terms covered by genes in the RZT gene set were calculated to evaluate the biological coverage of RZT. Additionally, the numbers of significantly enriched KEGG pathways and GO terms associated with the RZT gene set were compared to a randomly selected gene set (repeated  $N = 1000$ ) using clusterProfiler. Furthermore, to evaluate the

representation of RZT gene set on the global expression patterns and sensitivity of whole zebrafish transcriptome, five microarray data sets of transcriptomic experiments were used during in silico simulation analysis, which covers five distinct life stages of zebrafish (Table 3). The global expression patterns of the previous study were simulated with principal component analysis (PCA) by using genes from RZT gene set and whole genome using edgeR. The sensitivities of zebrafish transcriptome to toxicants in two concentration-dependent whole transcriptome data sets were evaluated by transcriptional point of departure ( $POD_t$ ) calculated by ten previously reported approaches using RZT gene set and whole transcriptome. The  $POD_t$  values estimated for the RZT gene set were compared with those for the whole transcriptome and the lowest observed adverse effect level (LOAEL) of apical end points.

**Methods for estimating transcriptional point of departure ( $POD_t$ ).** The values of  $POD_t$  based on RZT gene set or whole transcriptome were derived from data of chemical toxicity testing on zebrafish embryo by ten approaches previously described by Farmahin1. In approach 1, 2, 3, 4, and 5, transcriptional benchmark dose (BMDt) values were derived from pathway level. In approach 6, 7, 8, 9, and 10, BMDt values were derived from gene level. The BMDt values derived from each approach were used for estimating  $POD_t$ . The details are as following:

**Calculation of BMDt of genes.** BMDExpress2 was used for dose-response modeling and calculation of BMDt of each gene. First, raw counts of transcriptomic data were submitted to one-way ANOVA analysis in BMDExpress to identify genes significantly regulated in at least one treatment group compared to the vehicle control group. Then a best-fit model (Hill, Power, Linear, Polynomial 2°, or Polynomial 3°) for each gene was identified by the default parameters with slight changes as following: the Hill model was fagged if the “k” parameter was  $< 1/3$  of the lowest positive dose. In that situation, Hill model was excluded from the best-fit model selection of that gene.

**Calculation of fold changes of genes.** In approach 7, the 20 genes with the largest fold changes relative to controls were used. The normalized raw counts of genes were submitted to R package, edgeR3 to calculate fold change of each gene. 20 genes with the largest fold changes across all treatment were selected for further analysis.

**Calculation of BMDt of pathways.** Genes with calculated BMDt were submitted to R package, clusterProfiler4 to identify pathways of Gene Ontology Biological Process (GO BP) terms. A pathway enriched by at least three genes was assigned with the mean BMDt of genes matched to that pathway.

**Table 3** Description of transcriptome data of zebrafish for in silico validation of RZT gene set

Zebrafish stage	Treatment	Dose ranges	Dose unit	Accession number	Literature reference	Usage for in silico analysis
24 hpf (10 somites and 18 somites)	Pbx knockdown <sup>a</sup>			GSE8428	Maves et al. (2007)	PCA
48 hpf	Triclosan <sup>b</sup>	7.37	μM	GSE80955	Haggard et al. (2016)	PCA
96 hpf	ZnO nanoparticles <sup>b</sup>	2.64	mg/L	GSE77148	Choi et al. (2016)	PCA
	ZnSO <sub>4</sub> <sup>b</sup>	7.75	mg/L			
Larvae	Bisphenol A <sup>b</sup>	500, 1500 and 4500	μg/L	GSE22634	Lam et al. (2011)	PCA
Adult	Heart ventricle amputation <sup>c</sup>			GSE33981	Hofsteen et al. (2013)	PCA
24 hpf	Flusilazole <sup>b</sup>	0.28, 0.6, 1.35, 2.8, 6, 13.5, 28, and 60	μM	E-MTAB-832	Hermsen et al. (2012)	POD
72 hpf	Isoniazid	0.5, 1.67 and 5	mM	GSE55618	Driessen et al. (2015)	POD

<sup>a</sup>Genetic treatment condition; <sup>b</sup>Chemical treatment condition; <sup>c</sup>Physical treatment condition; <sup>d</sup>GEO accession number; <sup>e</sup>ArrayExpress accession number; PCA means principal component analysis; POD means calculation of transcriptional point of departure

**Estimating PODt by each approach.** Bootstrap was used to present the distribution of BMDt estimated by each approach. For each approach, BMDt of genes or pathways was randomly sampled with replacement. Mean BMDt of genes (in terms of approach 6, 7, 8, 9, and 10) or mean BMDt of pathways (in terms of approach 1, 2, 3, 4, and 5) were used for each bootstrap. 2000 bootstraps were used to simulate the distribution of BMDt for each of the ten approaches. Finally, the distribution of BMDt for each approach was presented by boxplot, and the mean values were used as the PODt for each approach (except approach 7 that used median values).

The developed RZT gene set consists of 1637 zebrafish Entrez ID genes, including a list of 1000 genes with greatest pathway centrality scores and a list of 724 toxicology-relevant genes. The 1000 pathway-central genes were shown to be the minimum number of genes representing the maximum biological pathways in terms of GO BP terms and KEGG pathways (Fig. 2a). Toxicology-relevant genes (n = 724) were selected to provide linkages between molecular mechanism and apical end points (Table 2). Then 44 genes were removed by the online designer either because their background expression was too high or too low, or because effective multiplexed primers could not be designed. This resulted in 1637 genes as the final RZT gene set.

The RZT gene set showed a broad coverage of biological pathways, where 95% KEGG pathways and 94% GO BP terms were represented by at least one gene in RZT gene set (Fig. 2b and c). The uncovered pathways were mainly

associated with basic metabolic processes. Furthermore, the RZT gene set of 1637 genes were significantly enriched in 29 KEGG pathways and 839 GO BP terms (adjusted  $p < 0.05$ ) respectively, which was a 48-fold and 17-fold more than the average number of KEGG pathways and GO BP terms enriched by randomly selected genes from zebrafish transcriptome.

The RZT gene set could faithfully represent the global expression patterns and sensitivities of a zebrafish's whole transcriptome to toxicants. The similar clustering patterns of samples were revealed by PCA analysis using the RZT gene set and whole genome on five transcriptomic studies across 24 hpf to adult zebrafish. Furthermore, the RZT gene set quantitatively represented the sensitivity of whole transcriptome for estimating PODt in response of toxicants. The PODt estimated by the RZT gene set was similar to that of whole transcriptome, where the overall ratios of PODt between RZT to whole genome were less than 1.5 more than 80% of the time (Fig. 2d and e). For the data set with recorded LOAEL, the overall PODt values calculated by RZT gene set were within threefold of whole transcriptomic LOAEL (Fig. 2d). For data sets without LOAEL, the overall PODt values calculated by the RZT gene set were still within tenfold ranges of LOAEL retrieved from other literature (Fig. 2e). The PODt values calculated from pathway-based approaches (approach 1, 2, 3, and 5) showed robust consistency between whole transcriptome and the RZT gene set, suggesting that pathway-based approaches may be applicable for estimating PODt by RZT.

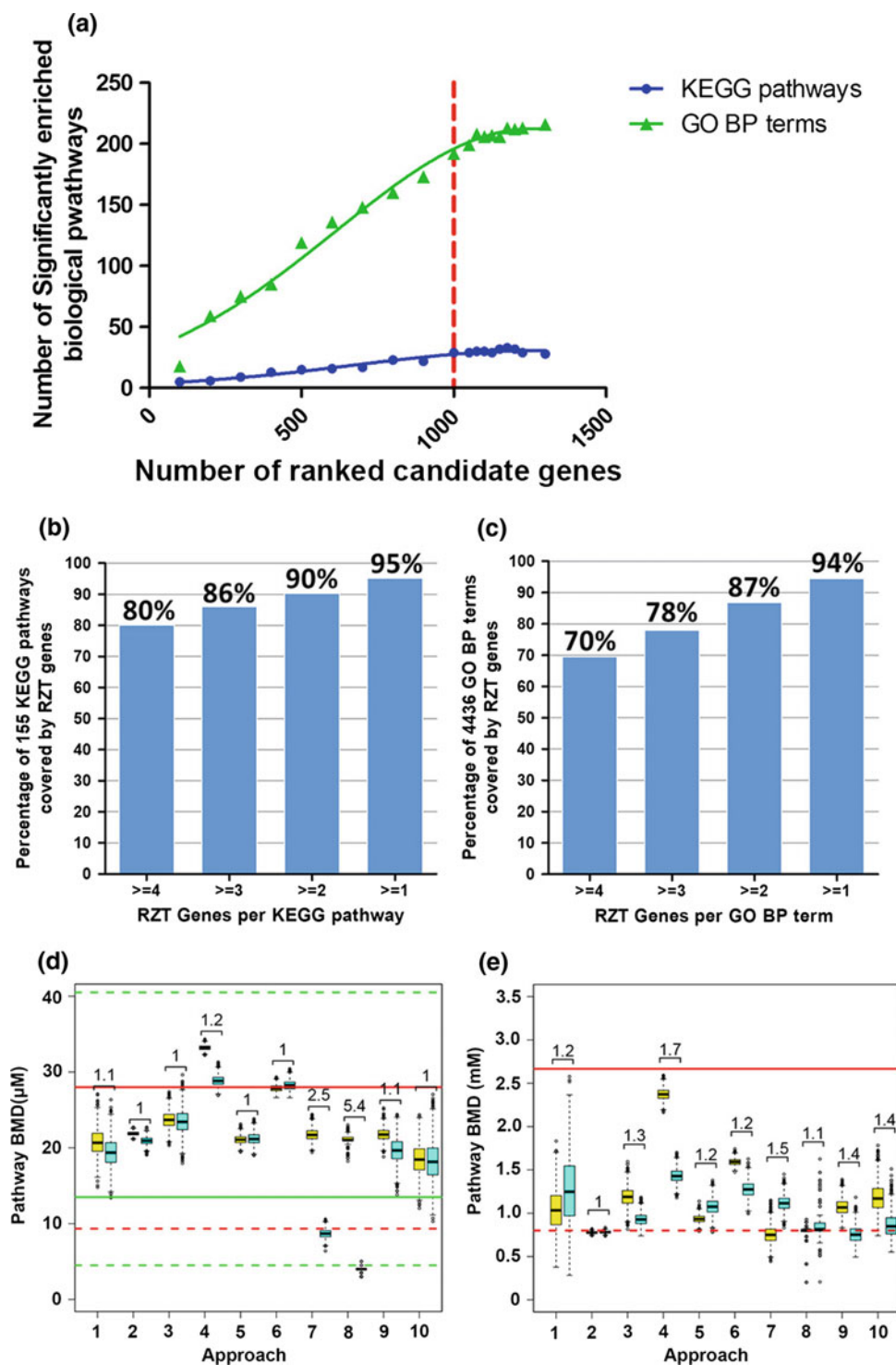


**Fig. 2** In silico evaluation of RZT gene set. **a** Investigation of minimal number of candidate genes for representing the maximal biological pathways including KEGG pathways and GO BP terms. The red dash line means the cutoff of 1000, where the number of top-ranked candidate genes is low enough for representing maximal biological pathways. The percentage of biological pathways coverage of **b** KEGG pathways and **c** GO BP terms by 1637 genes from RZT gene set. **d**, **e** Comparison on the distributions of transcriptional point of departure (PODt) estimated by RZT gene set (blue boxes) and the whole transcriptome (yellow boxes) using data from previously published

studies (EMTAB-832 and GSE55618, respectively). The black bold lines within boxes represent PODt. The number above boxes represents the ratio of PODt between by RZT gene set and whole genome (larger value to smaller value). In plot **(d)**, the solid lines in red and green represent LOAEL (13.5  $\mu\text{M}$ ) for pericardial edema (green line), and LOAEL (28  $\mu\text{M}$ ) for malformed heart (red line) induced by flusilazole in zebrafish embryo at 24 hpf. The dash lines in red and green represent threefold ranges of corresponding LOAELs. In plot **(e)**, the red solid and dash lines represent 1/3 and 1/10 values of LOAEL (8 mM) for liver damage induced by isoniazid in zebrafish embryo reported

### 3 Pipeline of Dose-Dependent Transcriptomes for High-Throughput Chemical Testing

A standardized pipeline for quantitative characterization of chemicals by dose-dependent reduced transcriptomes was developed (Fig. 1). Our study design employed wide-range doses (eight serial dilutions) with single biological replicates in human cells or zebrafish embryo for a specified exposure period, followed by RNA extraction for Ampliseq RNA library and HTS analysis. For example, the bioinformatics protocol for RHT contains four steps: (1) filtering genes which are unresponsive (counts < 5) to toxic substance exposure; (2) identifying the best-fit model for each gene to calculate POD values of genes ( $POD_{gene}$ ); (3) interpreting genes in the context of the biological pathways they influence; and (4) deriving POD values of pathways ( $POD_{path}$ ) to support sample-based quantitative assessment. In subsequent dose–response modeling, the transcriptional expression of filtered genes against concentrations are fitted to nonlinear models (e.g., parabolic, linear, sigmoid) by assigning a best-fit model (least akaike information criterion (AIC) value) for each gene.  $POD_{gene}$  values are determined according to the best-fit models (Fig. 3, Table 4). The  $POD_{path}$  value for a specific biological pathway can then be derived from the average value of  $POD_{gene}$  according to genes assigned to that pathway.

The  $POD_{path}$  estimate can characterize and quantify biological pathways potentially disrupted by toxic substances by identifying potentially sensitive pathways. This knowledge can inform understanding of responses at the molecular level in terms of molecular initiating events (MIEs) or key events (KEs) of chemical toxicity. The potency values ( $POD_{gene}$  or  $POD_{path}$ ) each provide critical information on the bioactivity of the chemicals. Moreover, altered pathways identified by this process can provide insight into substance mode of action, which can be used to predict likely adverse outcomes, guiding chemical cross read. In an RZT analysis

of zebrafish embryos following 8–32 h of exposure post fertilization (hpf) to  $10E-5-10 \mu\text{M}$  bisphenol A (BPA), the most sensitive pathways ( $POD_{path} < 0.001 \mu\text{M}$ ) identified were those involved in neurogenesis-related processes (e.g., central nervous system development, nervous system development, locomotion), which was concordant with a previously reported adverse effect of hyperactivity under BPA exposure.

Furthermore, the altered pathways and their corresponding  $POD_{path}$  value by reduced transcriptomics can be used to prioritize chemicals or environmental mixtures based on biological activity. RHT in two human cell lines (HepG2 and MCF7) and RZT in zebrafish embryos have been applied to a set of water samples ranging from wastewater to drinking water using a concentration-dependent transcriptomics protocol. Both RHT and RZT approaches were responsive, identifying a wide spectrum of biological activities associated with water-extracts exposure. Moreover, the most sensitive biological pathways were successfully identified, and were linked to adverse reproductive, genotoxic, and developmental outcomes. In this way, water quality was benchmarked by the sensitivity distribution curve of biological pathways, where the  $POD_{path}$  values of different samples can be ranked to discriminate polluted and clean samples. Overall, RHT and RZT approaches provided efficient and cost-effective tools to prioritize toxic substances based on the responsiveness of biological pathways.

Although used as a representative approach to whole transcriptomes, reduced transcriptomes may lose signals of unmeasured genes or pathways covered by only few genes. Computational methods have been developed to infer the remainder of whole transcriptomes, but regions of poor inference remain due to limitations of existing knowledge and differences among cell types. Currently, the reduced transcriptome approach can only be applied successfully for organisms with well-annotated genomes. In the future, however, reduced transcriptome approaches will be extended to other species as knowledge improves. It is also worth

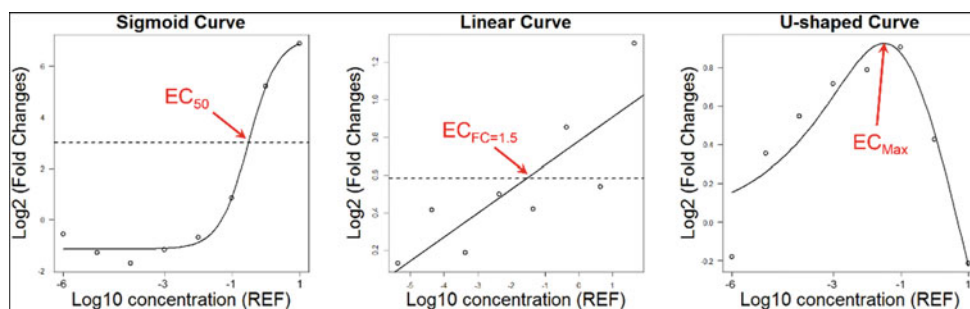


**Fig. 3** Overview of three types of concentration–effect curves for calculating effect concentration of DEGs identified by reduced transcriptomic analysis. The red symbols stand for effective concentrations (ECs) used for each type of concentration–effect curve.  $EC_{50}$ ,

$EC_{FC=1.5}$ , and  $EC_{Max}$  stand for median effective concentration, concentration causing 1.5-fold change and concentration inducing maximum effect, respectively

**Table 4** Concentration–effect models used for fitting fold changes of genes identified by reduced transcriptome analysis

Curve type	Model name	Equation	Parameters
Sigmoid	Three-parameter log-logistic	$y = \frac{d}{1 + \exp(b(\log(x) - \log(e)))}$	$d$ = upper limit; $e$ = inflection point; $b$ = slope
	Four-parameter log-logistic	$y = c + \frac{d-c}{1 + \exp(b(\log(x) - \log(e)))}$	$c$ = lower limit; $d$ = upper limit; $e$ = inflection point; $b$ = slope
	Michaelis–Menten	$y = c + \frac{d-c}{1 + e/x}$	$c$ = lower limit; $d$ = upper limit; $e$ = dose yielding a response halfway between $c$ and $d$
	Weibull I	$y = c + (d - c)\exp(-\exp(b(\log(x) - \log(e))))$	$c$ = lower limit; $d$ = upper limit; $e$ = inflection point; $b$ = slope
	Weibull II	$y = c + (d - c)(1 - \exp(-\exp(b(\log(x) - \log(e))))$	$c$ = lower limit; $d$ = upper limit; $e$ = inflection point; $b$ = slope
Linear	Linear	$y = E_0 + \delta x$	$E_0$ = intercept; $\delta$ = slope
	Linear-log	$y = E_0 + \delta \log(x + off)$	$E_0$ = intercept; $\delta$ = slope; $off$ = a fixed offset parameter
U-shaped	Gaussian	$y = c + (d - c)\exp\left(-0.5\left(\frac{\log(x) - \log(e)}{b}\right)^2\right)$	$c$ = back ground effect; $d$ = peak effect; $e$ = peak position; $b$ = width
	Gaussian-log	$y = c(d - c)\exp\left(-0.5\left(\frac{x-e}{b}\right)^2\right)$	$c$ = back ground effect; $d$ = peak effect; $e$ = peak position; $b$ = width

$y$  = response;  $x$  = concentration

adding that the genes curated in reduced transcriptomes should be optimized, updating toxicology databases such as AOP-Wiki, when both existing and new AOPs are under development.

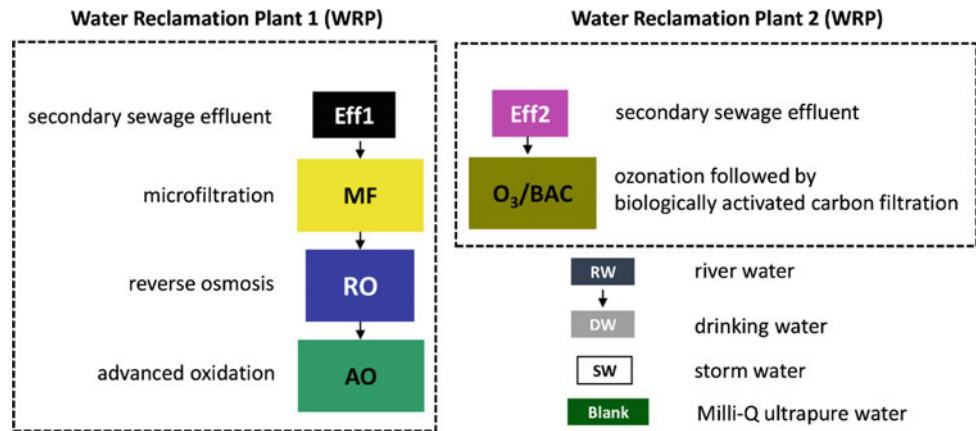
#### 4 Benchmarking Water Quality from Wastewater to Drinking Waters Using Reduced Transcriptome of Human Cells

One of the major challenges in environmental science is monitoring and assessing the risk of complex environmental mixtures. In vitro bioassays with limited key toxicological end points have been shown to be suitable to evaluate mixtures of organic pollutants in wastewater and recycled water. Omics approaches such as transcriptomics can monitor biological effects at the genome scale. However, few studies have applied omics approaches in the assessment of mixtures of organic micropollutants. Here, an omics approach was presented to profile the biological activity of water samples in human cells by RHT approach and dose-response models. A pair of widely used in vitro cell models in human toxicology, human hepatoma (HepG2), and human mammary cancer (MCF7) cells was used to assess the transcriptomic response induced by the mixtures. Cells were exposed to eight serial dilutions of each sample, and the transcriptional expression of 1200 selected genes was quantified by an RNA

amplicon-seq technology. To evaluate the performance of RHT for benchmarking water mixtures, the samples tested in this study were a set of ten water extracts that has been previously characterized by a battery of in vitro assays and chemical analysis. The objectives of the study were (1) to identify the mRNA expression profiles of the 1200 RHT genes in the HepG2 and MCF7 cells exposed to water samples in serial dilutions, (2) to evaluate the ability of RHT to assess biological activity of water samples in comparison with in vitro bioassays, and (3) to compare the concentration-dependent distribution of biological activity by mixture to that of chemical profiles.

#### Methods

**Water samples.** The ten water samples (Fig. 4) were collected and extracted with solid-phase extraction (SPE) as previously described (Escher et al. 2014). The dried extracts were stored in  $-80$  °C until analysis. Samples were dissolved in DMSO as stock solutions with relative enrichment factor (REF) of 10 000. The REF represents the concentrations of water samples (e.g., a REF of ten means tenfold concentrated sample; a REF of 0.1 means a tenfold diluted sample). All the ten samples have been tested by 103 in vitro bioassays covering the relevant steps of cellular toxicity pathways, including the activation of nuclear receptors, disruption of hormone synthesis, genotoxicity, adaptive stress response, and cytotoxicity.

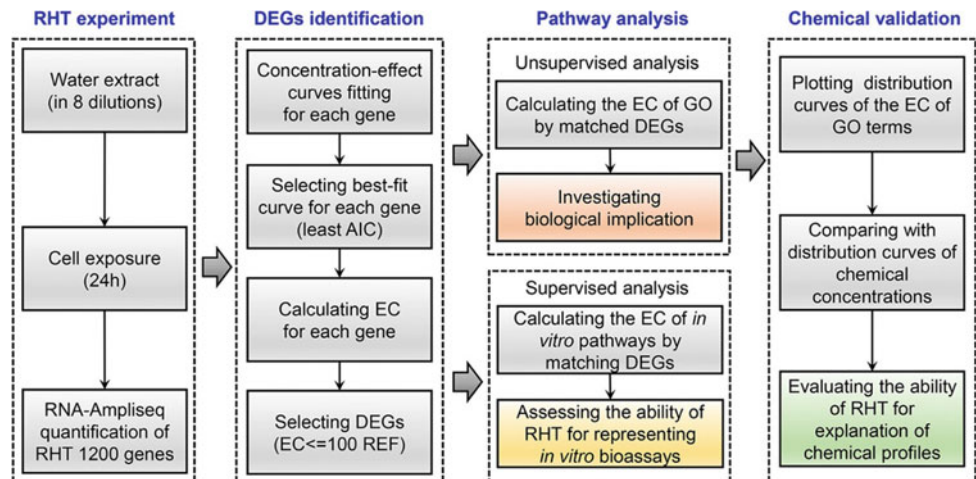
**Fig. 4** Description of ten water samples

**Cell Culture and Cytotoxicity Assay.** HepG2 and MCF7 (ATCC) cells were maintained in DMEM medium with 10% fetal bovine serum (FBS) in a humidified atmosphere of 5% CO<sub>2</sub> at 37 °C. After 24 h of incubation, cells seeded into 96 well plates with  $1 \times 10^5$  cells/mL were dosed with twofold serial dilutions of water samples (DMSO = 0.1%). After 24 h of exposure, cell viability was measured using 96 Aqueous One Solution Reagent (Promega, Madison, WI) according to the manufacturer's instruction.

**Transcriptome Analysis Using RHT.** The transcriptional expression of 1200 selected genes was measured by an amplicon-seq technology (Fig. 5, Table 1, and Table S1).

**RHT Experiment.** Cells in 12 well plates with  $1 \times 10^5$  cells/mL were treated with 8 5-fold noncytotoxic dilutions (from 10 to 0.000 128 REF for all ten samples in MCF7; from 2 to 0.000 0256 REF for sample Eff2, and from 10 to 0.000 128 REF in the other nine samples in HepG2) of water samples with a single replicate, in addition to two vehicle control. After 24 h of dosing, cells were harvested for total

RNA isolation using an RNeasy Mini Kit (Qiagen, Hilden, Germany). A total of 164 RNA samples (80 treatments and 2 vehicle controls for HepG2 and MCF7, respectively) were stored at  $-80$  °C until used. RNA concentrations were measured using QuBit fluorometer 2.0 (Thermo Fisher Scientific, Waltham, MA) with Quant-iT RNA HS Assay Kit according to the manufacturer's procedure. Libraries were prepared from 10 ng of RNA of each sample using Ion AmpliSeq Library Kit 2.0 and Ion AmpliSeq custom panels (Thermo Fisher Scientific, Waltham, MA), followed by high-throughput sequencing of RHT panel on Ion Torrent Proton (Thermo Fisher Scientific, Waltham, MA). Briefly, the 1200 human genes of RHT panel were multiplex-amplified, and then the counts of genes were quantified using the coverageAnalysis plugin on Ion Torrent Service. To examine the suitable sequence depth of RHT for each sample, Monte Carlo simulations were performed on the samples with maximum counts in HepG2 and MCF7, respectively (Text S1). Genes whose counts were not detected in vehicle control groups were removed, followed by normalization of counts between libraries using the R

**Fig. 5** Workflow of reduced human transcriptome (RHT) analysis of water samples. AIC, Akaike's Information Criterion; EC, effect concentration; DEGs, differentially expressed genes; REF, relative enrichment factor; GO, Gene Ontology

package edgeR. Fold changes of genes in each treatment were calculated by dividing the counts in treatment by the mean of counts in two vehicle controls.

**Concentration Effect Analysis.** For each gene, the fold change against concentration was first subjected to linear regression analysis using the R function `cor.test` (method “Pearson”). Next, the significant genes (p-value of <0.05) were subjected to automatic concentration–effect curves fitting analysis using `drc` and `DoseFinding`. Briefly, log<sub>2</sub>-transformed fold changes of each gene in log<sub>10</sub>-transformed concentrations were fitted with any of the nine concentration–effect models (Table 4). The model with the least akaike’s information criterion (AIC) value was identified as the best-fit model for that gene. Genes whose best-fit models showed significant curve-fitting performance (p-value of <0.05) were identified as differentially expressed genes (DEGs). The best-fit models of DEGs were used to derive the effect concentrations (ECs) of DEGs (Fig. 1). Briefly, for sigmoidal curves in which the maximum response could be defined, the concentrations causing 50% maximum effect were used as the ECs. For linear concentration–effect curves in which no maximum response can be defined, the concentrations causing absolute 1.5-fold change were used as the ECs of the gene. For the gene with U-shaped concentration–effect curves, its EC was assigned by the concentration causing the maximum response. A value of 100 REF was an inflection point of all ranked EC values, above which a small portion of DEGs ( $EC \geq 100$  REF) were defined as extrapolation artifacts and removed from further analysis. Finally, concentration-dependent sequences of molecular events were investigated by network analysis of DEGs using `stringApp` in Cytoscape.

**Pathway Analysis.** An unsupervised gene ontology (GO) analysis was performed to investigate potential bioactivity of each sample identified by RHT. First, DEGs of each sample were matched to their corresponding GO terms. GO terms with less than three DEGs were removed because three was the minimum number to calculate mean and standard deviation (SD). Then the EC of each GO term was calculated as the geometric mean of the ECs of matched DEGs. A previous study has used the mean of benchmark dose of DEGs for GO analysis, in which a narrow range of concentrations across only one or two orders of magnitude was assessed. However, a wide range of concentrations across six orders of magnitude was used here. The geometric mean rather than mean value of ECs of DEGs was used to represent the EC of each GO term to avoid heavy influence by DEGs with high EC values. Principal component analysis (PCA) was performed on ECs of GO in all samples using `FactoMineR`.

**Representation of In Vitro Pathways.** A supervised approach was used to assess the RHT representation of the previous in vitro bioassay. First, gene sets associated with cellular toxicity pathways tested by in vitro bioassays were manually curated from WikiPathways and Gene Ontology. Next, the EC of each pathway was calculated by the geometric mean of the ECs of matched DEGs. To be consistent with in vitro bioassays, the EC values of in vitro pathways of >30 REF were all assigned with 30 REF. For the in vitro pathways matched by single DEG, only the single DEG with acceptably high efficacy (the maximum absolute fold changes across all treatment being >1.5) was considered to be robust to represent the perturbation of its matched pathway (s). For in vitro pathways that were not matched by any DEGs, their ECs were assigned with 30 REF. Finally, the EC values of in vitro pathways identified by RHT analysis in each cell line were presented as a heatmap using the R package `gplot`. For biological end points tested by multiple bioassays, the geometric mean of EC values from multiple bioassays was calculated to provide a single integrated EC value for the corresponding pathways. The patterns of hierarchical clusters of water samples identified by RHT analysis were compared with the results of in vitro bioassays.

**Comparison of Bioactivity Potency with Chemical Profiles.** Chemical profiles in water samples may indicate biological effects of mixture, although there may be a lack of explanation for overall bioactivity. A total of 54 chemicals were previously characterized in 6 of 10 water samples at concentrations above the limit of detection (LOD). The RHT profiles were compared with chemical profiles of water samples. The overall biological potency of each sample was characterized by fitting proportionally ranked EC values of GO into a four-parameter dose–response curve using `GraphPad` (`GraphPad Prism 5.0` software, San Diego, CA), which was defined as biological potency distribution curve (BDC). BDC was not fitted for samples with GO terms of <20, which provided too few dots for fitting meaningful distribution curves. The overall chemical profile of each sample was characterized by fitting proportionally ranked concentrations of detected chemicals into a four-parameter dose–response curve defined as chemical concentrations distribution curve (CDC). Furthermore, relative biological potency (REP) and relative chemical contamination (REC) of each sample were calculated according to BDC and CDC using Formulas 1 and 2, respectively:

$$REP_i = \frac{MB_{Ref}}{MB_i} \quad (1)$$

$MB_{Ref}$  and  $MB_i$  are the median values calculated from BDC of the reference sample and sample *i*, respectively:

$$\text{REC}_i = \frac{\text{MC}_i}{\text{MC}_{\text{Ref}}} \quad (2)$$

$\text{MC}_{\text{ref}}$  and  $\text{MC}_i$  are the median values calculated from CDC of reference sample and sample  $i$ , respectively. Sample Eff2 showed the highest biological activity and chemical contamination among all water samples and thus was selected as the reference sample for calculation of REP and REC. Finally, the REP of each sample was compared to its REC.

## Results and Discussions

**Analysis of RHT by Mixture Samples.** Only sample Eff2 showed cytotoxicity at  $\text{REF} > 2$  in HepG2, while none of the samples showed any cytotoxicity at  $\text{REF} \leq 10$  in MCF7. The RHT experiment on serial noncytotoxic dilutions of total 164 samples showed sequence counts that ranged from 327 000 to 8 327 170 in HepG2 and from 158 025 to 3 025 355 in MCF7 (Fig. 6a, b). Monte Carlo simulations revealed that sequence depth of 300,000 reads is needed for detective signals (counts of  $>5$ ) of at least 750 genes. For the only five samples sequenced with counts  $<300\,000$ , even the sample with the lowest counts of 158 025 (the sixth dilution of O3/BAC in MCF7) still showed

coverage of  $>100$  counts for each gene, suggesting that the sequence depth of each sample was adequate for further data analysis. Out of the RHT 1200 gene list, 756 and 767 genes were expressed in HepG2 and MCF7, respectively, with 667 common genes (Fig. 7). The 95% percentile ranges of  $\log_2$ -fold changes across all ten samples in HepG2 was 0.03–9.51, relatively narrower than 0.02–163.14 in MCF7 (Fig. 8a). The sequence data was deposited in the NCBI BioProject database (accession no. PRJNA385238; <https://www.ncbi.nlm.nih.gov/bioproject/>).

The number of DEGs selected by the nine dose–response models across all ten samples ranged from 24 to 109 in HepG2 and from 7 to 157 in MCF7, respectively (Fig. 8b). The DEGs responsive at low dose range ( $\text{ECs} \leq 1 \text{ REF}$ ) were mainly fitted with U-shaped models (Fig. 9a, b), which suggest that the mode of hormesis dominates the low dose response of transcriptome. Taking the DEGs of Eff2 in HepG2, for instance, (Fig. 10), CSF1R, SIRT3, and TEK were potentially early response genes ( $\text{ECs} \leq 0.1 \text{ REF}$ ) associated with the regulation of ERK1/2 cascade, which were all fitted with the Gaussian model. It has been widely reported that the translocation of ERK1/2 was involved in early gene response. Secondary and adverse biological effects were identified by DEGs with higher EC values, including the regulation of signal transduction (such as

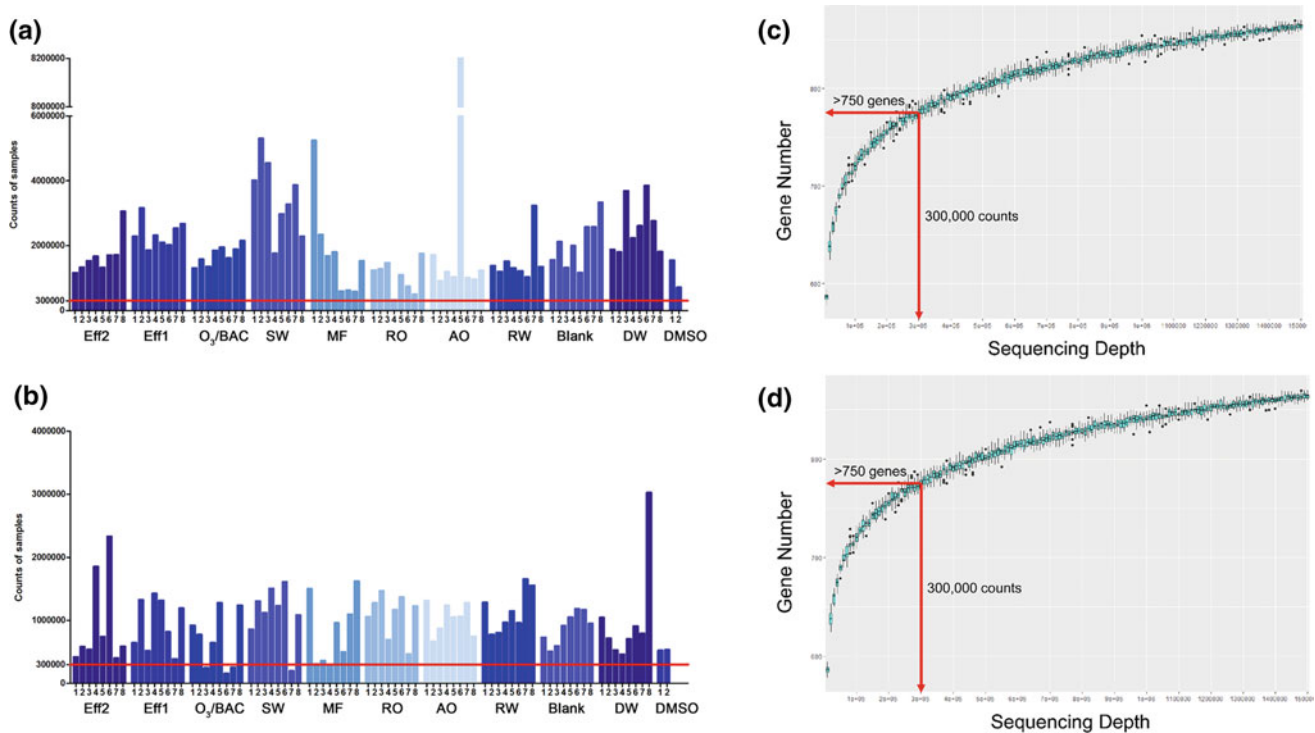


**Fig. 6** Sequencing counts of ten water samples across eight fivefold dilutions and two DMSO controls in **a** HepG2 and **b** MCF7. The number 1–8 of water samples stands for dilutions of samples from highest concentrations to the lowest concentrations. The numbers 1 and

2 of DMSO mean two replicates of vehicle controls. The red lines stand for the sequencing depth of 300,000 for detecting at least 750 genes, which was calculated by Monte Carlo simulation of sequencing counts of **c** fifth dilution of AO in HepG2 **d** eighth-dilution of DW in MCF7



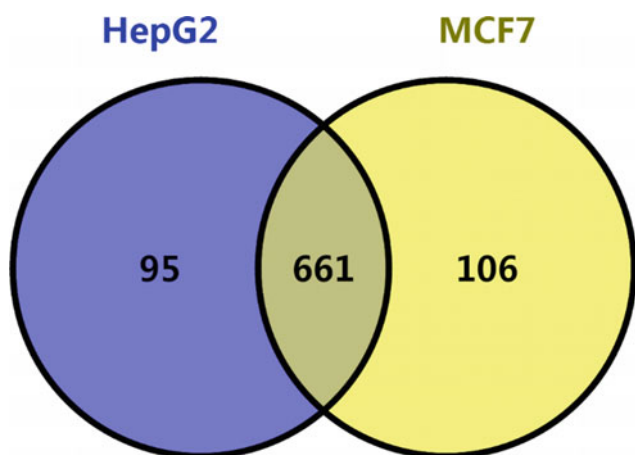


**Fig. 7** Venn diagram of RHT detective genes (counts >0 in both two vehicle control) in HepG2 and MCF7

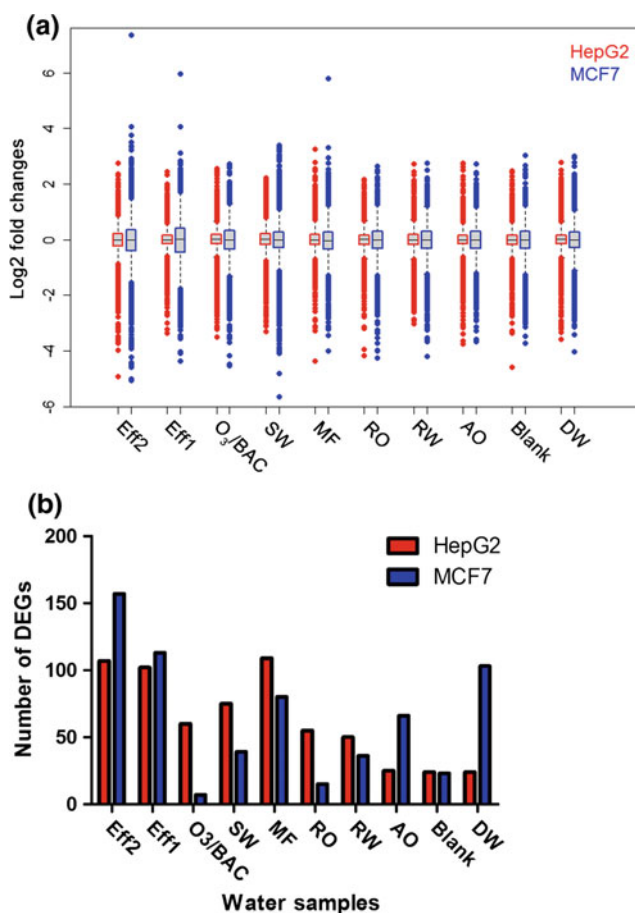


**Fig. 8** **a** Log<sub>2</sub>-fold changes of all genes identified by RHT analysis across all ten water samples in HepG2 and MCF7, respectively. **b** Number of differentially expressed genes (DEGs) of ten water samples identified by RHT analysis in HepG2 and MCF7, respectively

CDKN2A, DUSP3, and FOXP1,  $0.1 < EC \leq 1$  REF), regulation of cell proliferation (such as CSF1, FYN, and MAPK1,  $1 < EC \leq 10$  REF), and regulation of apoptosis

(all four DEGs including RTN4, CDKN1A, SRC, and HMOX1,  $EC > 10$  REF). Genes responsive at high dose ranges ( $ECs > 10$  REF) were mainly fitted with linear models, which may be due to severely secondary effects specifically induced at high doses. These results indicated that the dose–response profiles of DEGs identified by RHT analysis could differentiate low dose response from a wide spectrum of biological activities by water samples.

The RHT profiles in both HepG2 and MCF7 demonstrated significant responses to the polluted water samples. Most of the DEGs were identified in three polluted samples (Eff2, Eff1, and MF) in both HepG2 and MCF7. For all three polluted samples, 7 and 36 DEGs, mainly involved with cellular response to toxic substance, were identified by RHT in HepG2 and MCF7, respectively. Furthermore, three DEGs (ABCC3, CYP1A1, and KLF9) were identified in all the three polluted samples in both HepG2 and MCF7. CYP1A1 encodes a member of the cytochrome P450 superfamily of enzymes well known for metabolism of xenobiotics. ABCC3 encodes a member of the superfamily of ATP-binding cassette (ABC) transporter involved in multidrug resistance. KLF9 encodes a transcription factor has been widely reported to be involved in response to oxidative stress. The results suggested that polluted water samples prevalently induced a cellular stress response that could be commonly identified by HepG2 and MCF7. Moreover, 29, 23, and 13 DEGs were commonly identified by HepG2 and MCF7 for Eff2, Eff1, and MF, suggesting that HepG2 and MCF7 may be consistent in identification of positive responses in polluted samples.

Fewer DEGs were identified in blank sample in both HepG2 and MCF7 compared with the polluted water samples, suggesting that relatively low response was identified in HepG2 and MCF7 for blank sample. The DEGs of blank sample in HepG2 and MCF7 were mainly associated with nonspecific cellular response, but only four and nine DEGs of the blank sample in HepG2 and MCF7, respectively, showed an absolute fold change of  $\geq 1.5$  across all dilution treatments, suggesting very low biological effects induced by blank sample. The results are consistent with the previous results that the blank sample could induce slight nonspecific bioactivity, which may be due to the tiny impurities present in the solvent during SPE extract of samples. In addition, MGMT, encoding the O-6-methylguanine-DNA methyltransferase involved in DNA repair, showed an upregulation trend in HepG2, which may explain the observed genotoxicity previously reported in the blank sample.

The RHT profiles in both HepG2 and MCF7 may show specific response to water samples in middle or lower contaminated situation. The number of DEGs of DW in MCF7 was 103, which was significantly greater than the 25 DEGs of blank sample. However, only 24 DEGs of DW were identified in HepG2, which was equal to the DEGs number

**Fig. 9** Histogram of the effective concentration (EC) values of differentially expressed genes (DEGs) across ten water samples in **a** HepG2 and **b** MCF7, respectively

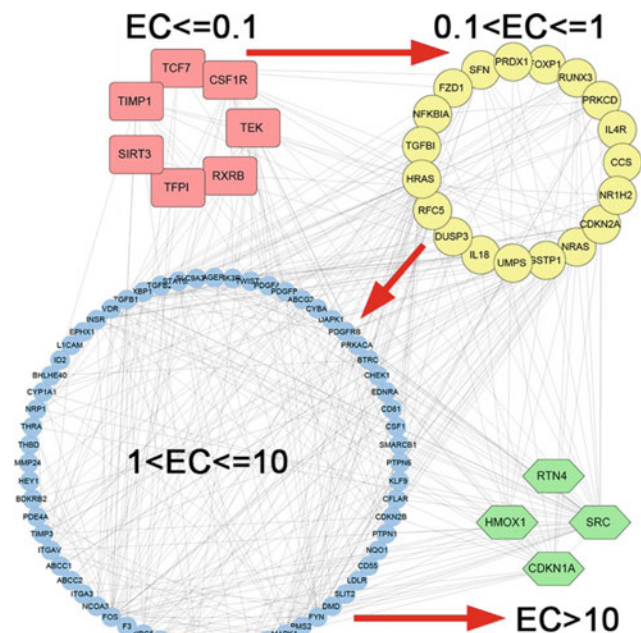
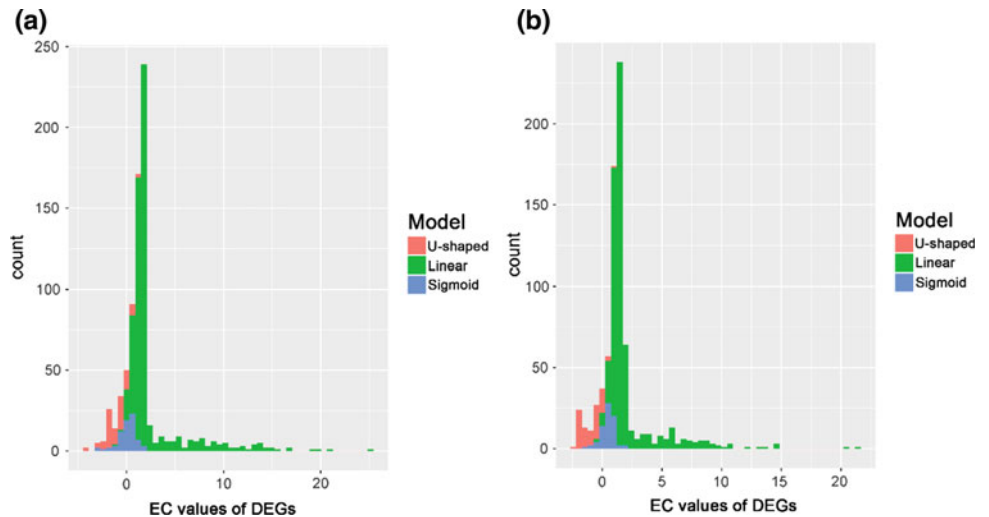


**Fig. 10** Concentration-dependent gene network of DEGs identified by RHT analysis in HepG2 cells treated by Eff2. The EC of DEGs is expressed as the relative enrichment factor (REF) of the water sample

of blank sample. It is suggested that the RHT analysis of MCF7 was more sensitive in response to DW sample than that of HepG2. Previous studies have reported that the DW sample induced broad bioactivity of xenobiotic metabolism and genotoxicity. The formation of disinfection by-products increases the toxicity of DW as compared to RW. Disinfection by-products may become more electrophilic after metabolic activation, resulting in enhanced biological effects, such as genotoxicity. The relatively weak effects of DW in HepG2 may be due to the poor expression of drug-metabolizing enzymes in HepG2.

**Unsupervised GO Analysis of RHT.** GO analysis of RHT profiles may implicate distinct bioactivity between water samples. The number of identified GO terms was proportional to the number of identified DEGs for a sample. For HepG2, the fewest GO terms were identified at blank sample (4) and the most at MF (170). For MCF7, the fewest GO terms were identified at O3/BAC (0) and the most at Eff2 (288). A small number of GO terms enriched by the RHT profiles of blank sample in HepG2 (4) and MCF7 (6) suggest low biological activities of blank sample. Change of the identified GO terms suggests potential changes of bioactivity of water samples from initial to advanced treatment processes. A total of 60 GO terms identified in Eff1 diminished after MF treatment, while 89 GO terms were specifically identified in MF in HepG2 (Fig. 11a). The reduced 60 GO terms of Eff1 were mainly associated with basic cellular response such as cellular oxidant detoxification, while the newly introduced GO terms in MF were associated with more adverse responses such as programmed necrotic cell death. It is suggested that extra and severe bioactivity was produced after MF treatment, which may be explained as the process of chloramination during MF treatment. The remaining six GO terms after the advanced treatment process of AO may be explained as background effect introduced during sample extract, which was similar to the blank sample. The three remaining GO terms identified in all Eff1 (MF, RO, and AO) were annotated to biological processes including that of cellular response to DNA damage stimulus (GO: 0006974), suggesting potential remaining of genotoxicity, which was observed in the previous study. Furthermore, principal component analysis (PCA) of ECs of identified GO terms showed that polluted and clean samples were distinctly separated in both HepG2 and MCF7 cells (Fig. 11b, c), suggesting that GO analysis may distinguish polluted and clean samples by bioactivity. However, in

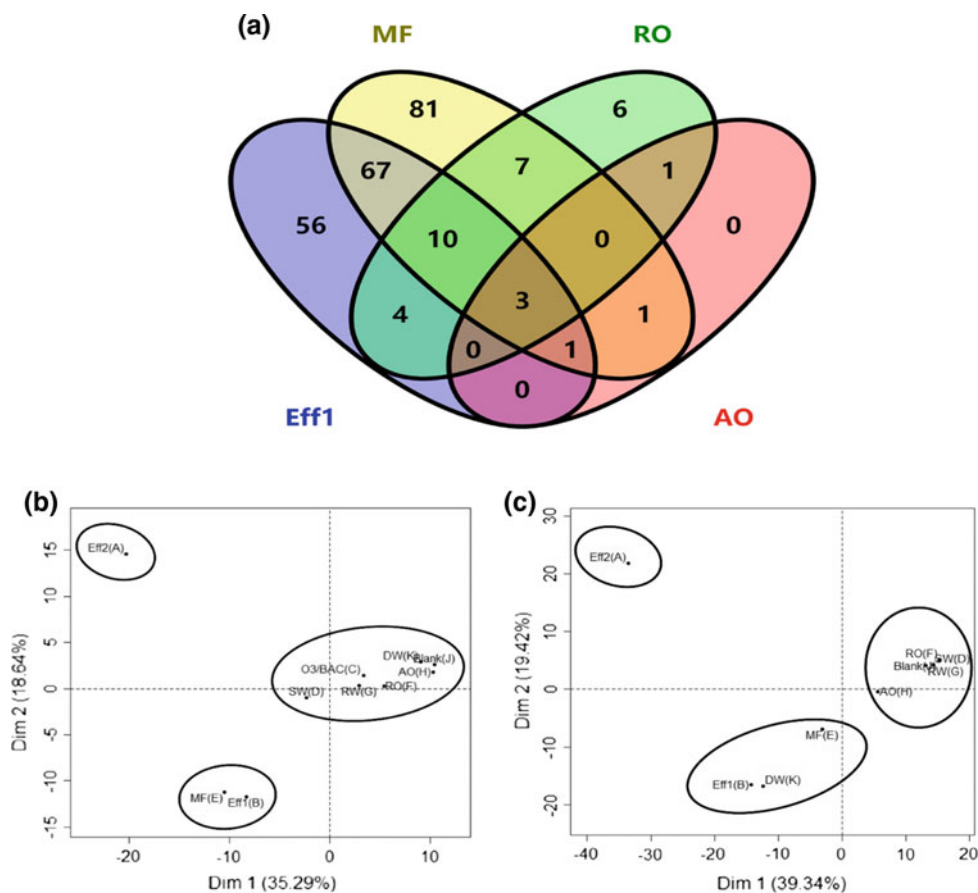
MCF7 cells, DW, a presumed clean sample, was grouped with polluted samples Eff2 and MF, suggesting that HepG2 and MCF7 cells demonstrated cell-type-specific responses.

**Cell-type-specific responses identified by GO analysis of RHT profiles in HepG2 and MCF7.** GO terms associated with DNA damage such as mismatch repair of DW sample were identified by RHT analysis in MCF7. However, in HepG2, only nonspecific biological responses such as regulation of cell growth were identified by RHT analysis of DW. Moreover, the cell-type-specific responses may be explained by the GO terms with top lowest EC values, which may represent low dose effects. For instance, in Eff2, the GO with the top ten lowest EC values in HepG2 was mainly associated with immune response, such as transmembrane receptor protein tyrosine kinase signaling pathway, negative regulation of inflammatory response, and natural killer cell mediated cytotoxicity, but the GO terms with the top lowest EC values in MCF7 were only annotated to pathways associated with xenobiotic metabolism, such as canonical Wnt signaling pathway.

**Supervised Analysis of RHT for Comparison with In Vitro Bioassays.** The RHT profiles of water samples in HepG2 and MCF7 both showed similar patterns with in vitro

bioassays, as biological effects were mainly identified in polluted samples (Fig. 12). For end points of xenobiotic metabolism, PXR, CAR, and AHR pathways in both two cell lines showed high responses in less-treated samples and nearly no response in clean samples, which was highly consistent with in vitro assays. Consistent with the results of in vitro assays, the overall activity of pathways associated with PPAR (PPAR $\alpha$ , PPAR $\delta$ , and PPAR $\gamma$ ) across ten water samples identified by RHT analysis was relatively low compared with other xenobiotic metabolism pathways. The PPAR $\alpha$  and PPAR $\delta$  pathway showed slight activity (EC > 10 REF) only at RW in HepG2. The PPAR $\gamma$  pathway showed high responses (EC  $\leq$  10 REF) only at polluted samples (Eff1 and MF) in MCF7, partially accordant with in vitro assays. For specific MOA, the ACHE pathway showed no response at either of the two cell lines, indicating that HepG2 and MCF7 were not suitable for identification of neurotoxic response. The activity of ER and AR pathways was similar to in vitro assays. A slight difference was shown in HepG2, in which the activity of AR pathway was identified in clean samples O3/BAC and AO but at very high REF (EC  $\geq$  20). For other hormone receptors, the PR pathway showed responses only at polluted samples in MCF7, while no active response of PR was observed in HepG2. The responses of the GR pathway were similar

**Fig. 11** a Venn diagram of GO terms identified by RHT analysis in Eff1, MF, RO, and AO in HepG2; Principle component analysis of the EC values of GO terms of ten water samples identified by RHT analysis in b HepG2 c MCF7, respectively



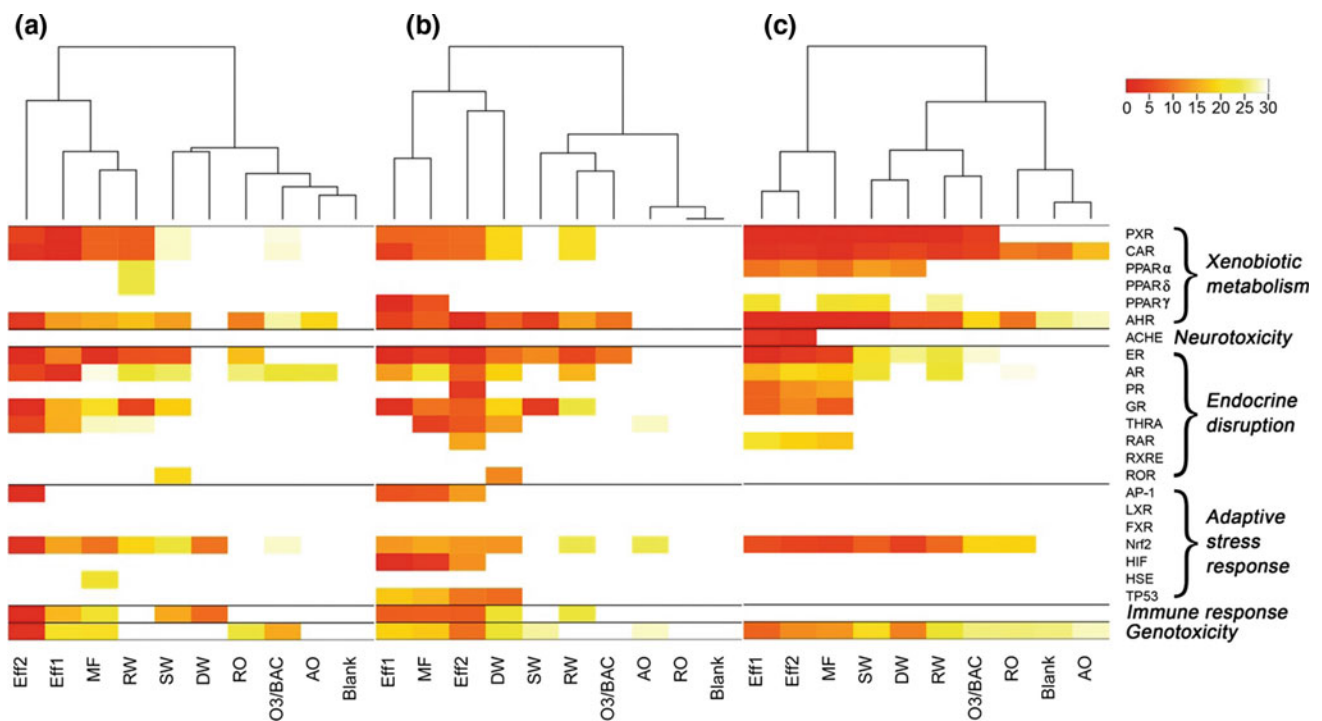


**Fig. 12** Heatmap of ECs of the 24 in vitro pathways calculated from RHT analysis in **a** HepG2, **b** MCF7, and **c** in vitro bioassays previously analyzed

between in vitro assays and RHT profiles in both HepG2 and MCF7, whereas GR activity was specifically shown in MCF7. TR activity was not identified by in vitro assays in any samples, while TR was identified to be activated at multiple samples by RHT analysis in both HepG2 and MCF7. No response of TR activity was observed in previous in vitro thyroid receptor gene bioassays, which has been explained as nonexistence of thyroid agonists and goitrogens in extraction of SPE. Nevertheless, RHT analysis in both HepG2 and MCF7 identified TR activity by multiple samples, which might be due to the “cross-talk effect” between molecular pathways or nongenomic modulation of thyroid hormone signaling pathways on transcript levels.

For reactive MOA, activity of pathways associated with adaptive stress responses and genotoxicity was identified in HepG2 and MCF7 exposed to polluted samples, which was consistent with the results of in vitro assays. Specific end points associated with adaptive stress responses, such as the Nrf2 and AP-1 pathways in sample Eff2 showed higher activity in HepG2 than in MCF7, suggesting that HepG2 may be more sensitive in response to adaptive stress responses than MCF7. Although immune-related response was not identified in any samples by in vitro assays, obvious immune responses were identified in RHT analysis in polluted samples. Only THP1 cytokine assay in antagonist mode was conducted in a previous in vitro bioassay to measure immunotoxicity. It has previously reported a poor

correlation between immunosuppressive chemicals and immunosuppressive activity identified by THP1 assay in water samples. RHT analysis could complement in vitro assays by providing measurement of a broader range of immune-related responses.

Overall, integration of the RHT profiles of HepG2 and MCF7 may provide a broad representation of bioactivity identified by the 103 in vitro assays. In the previous study, the 103 in vitro bioassays included multiple cell lines including 11 types of human cell lines, 2 types of rat cell lines and zebrafish embryos as well as lower organisms such as yeast and *Escherichia coli*, which were used to measure integrative end points across cellular toxicity pathway. Although the results might not be comparable between in vitro bioassays with different platform background on cell types and species, the RHT analysis of water samples with less cell lines, HepG2 and MCF7, was shown to be capable of reflecting patterns identified by in vitro bioassays. Furthermore, our results support the importance of the utilization of multiple cells in RHT analysis of water samples. HepG2 cell line was more specific in identification of adaptive stress response, and the MCF7 cell line was more specific in response to endocrine disruption effects. To assess the biological responses related to other toxicological end points, such as neurotoxic potential of water samples, other functional cell types, such as a human neuronal cell line, would be necessary.

**Comparison of Chemical Profiles with Bioactivity Identified by RHT.** Distribution curve of the EC values of GO is a novel approach to estimate the potency of overall biological activities by water samples. Although the RHT profiles in both HepG2 and MCF7 cells showed the decreasing potency of overall biological activities after serial water treatment processes, cell-type-specific signatures can be observed in the two cell lines (Fig. 13a, b). For the BDC in both HepG2 and MCF7, Eff2 showed the highest biological potency, followed by Eff1, and the clean samples such as SW and AO showed relatively low biological potency. MF and DW showed relatively high potency close to Eff1 in MCF7, and DW showed an even greater potency than its source water RW. However, in HepG2, both MF and DW showed lower potency than their upstream samples Eff1 and RW, respectively. This might be due to genotoxic and oxidative stress effects of disinfection by-products existing in water samples such as MF and DW. Endocrine tissue origin MCF7 cells may be more sensitive than hepatocyte HepG2 cells for identifying the bioactivity of water samples.

The relative potencies of water samples estimated by RHT profile were consistent with chemical contamination level of the samples. A total of six water samples (Eff2, Eff1, O3/BAC, MF, SW, and RO) have been previously characterized by chemistry analysis. Although the concentration of a chemical does not necessarily reflect overall contamination level, the chemical profiles showed distinct separation between polluted samples (Eff2, Eff1, and MF) and clean samples (SW, O3/BAC, and RO) (Fig. 13c). The CDC showed that Eff2 was the most contaminated sample, followed by Eff1 and MF, which was highly accordant with the ranks of biological potency reflected by GO distribution. For clean samples, the CDC showed SW may be more contaminated than O3/BAC and RO, which was also consistent with the GO distribution and the results of previous *in vitro* bioassays, in which SW showed higher potency than O3/BAC and RO.

The relative biological potencies may quantitatively reflect the alteration of chemical contamination. The overall values of REPs and REC of the ten samples were mainly within one magnitude (Fig. 13d and Table 5). The REP of polluted samples, Eff1 and MF, in MCF7 was both similar to their REC values, implicating that RHT analysis using MCF7 may be sensitive for reflecting the relatively small alteration of chemical profiles between polluted or less-treated water samples. Although the REPs of polluted samples in HepG2 were quite inconsistent with REC, the REP of clean samples, O3/BAC and RO, in HepG2 was similar to their REC values. It is suggested that RHT analysis using HepG2 was more appropriate for quantitatively inferring the alteration of chemical status of clean samples. More samples and more comprehensive chemical profiles are needed to validate suitability of MCF7 and HepG2 cells

in assessing specific biological response by water samples in future study.

The chemical profiles may help to explain the biological activity identified by RHT analysis. The occurrence of chemicals such as organophosphate pesticides (chlorpyrifos and diazinon) and steroids (17- $\beta$ -Estradiol) in Eff2 might contribute to the activation of immune response pathway, which was also suggested by the results of GO terms analysis of Eff2. Chlorpyrifos and diazinon are two kinds of organophosphate pesticides and have been reported to induce immunotoxicity in human cells. 17- $\beta$ -Estradiol has been widely reported to be able to induce immune response and may be synergistic with organophosphate pesticides. In a relatively clean sample SW, bisphenol A was the dominant chemical with the highest detected concentrations, suggesting that bisphenol A may partially contribute to the biological effects of SW. Bisphenol A is a well-known endocrine-disrupting chemical capable of affecting multiple nuclear receptors such as AR, ER, and AHR, which may explain the effects of AR, ER, and AHR identified by RHT analysis in SW sample. In a clean sample of O3/BAC, although few chemicals were detected, CYP1A1 was identified as DEG by RHT analysis in both HepG2 and MCF7, which may be related to the N, N-diethyl-meta-toluamide (DEET) detected in O3/BAC. Studies have reported that DEET may induce CYP1A1 enzyme in human liver cells. However, knowledge gaps exist in the mixture toxicology of environmental samples, such as response from unknown chemicals and a combined effect. To directly link the observed biological response with the measure chemicals, an effect-directed analysis (EDA) is necessary. The RHT analysis could provide a novel untargeted bioassay in EDA analysis of toxicants in the mixture.

Overall, the RHT method provides a highly dynamic approach to assess the biological response and to benchmark the potencies of water samples. The RHT profiles in two cell lines, HepG2 and MCF7, provided a comparable biological characterization on the water samples by the previous 103 *in vitro* bioassays, which could significantly increase the efficiency and throughput of assessment. Concentration-dependent bioactivity of water samples could be identified to indicate potential early responses. Pathway analysis based on the active values of differentially concentration-dependent genes implicates the potential bioactivity of samples, which can be used in diagnostic analysis of chemical profiles. The data analysis strategies developed here are also applicable to other omics approaches, such as metabolomics and proteomics, which have also been applied in mixture toxicology. Furthermore, our results highlight the value of the integration of multiple approaches, targeted *in vitro* assays, and untargeted omics approach, together with a higher resolution of chemical analysis in the study of mixtures. Finally, the selection of cell types that are

**Fig. 13** Distribution curves of EC values of GO of water samples identified by RHT analysis in **a** HepG2 and **b** MCF7 and **c** distribution curves of concentrations of chemicals detected in water samples, which were used to derive **d** REP and REC for comparison between biological potency and chemical contamination

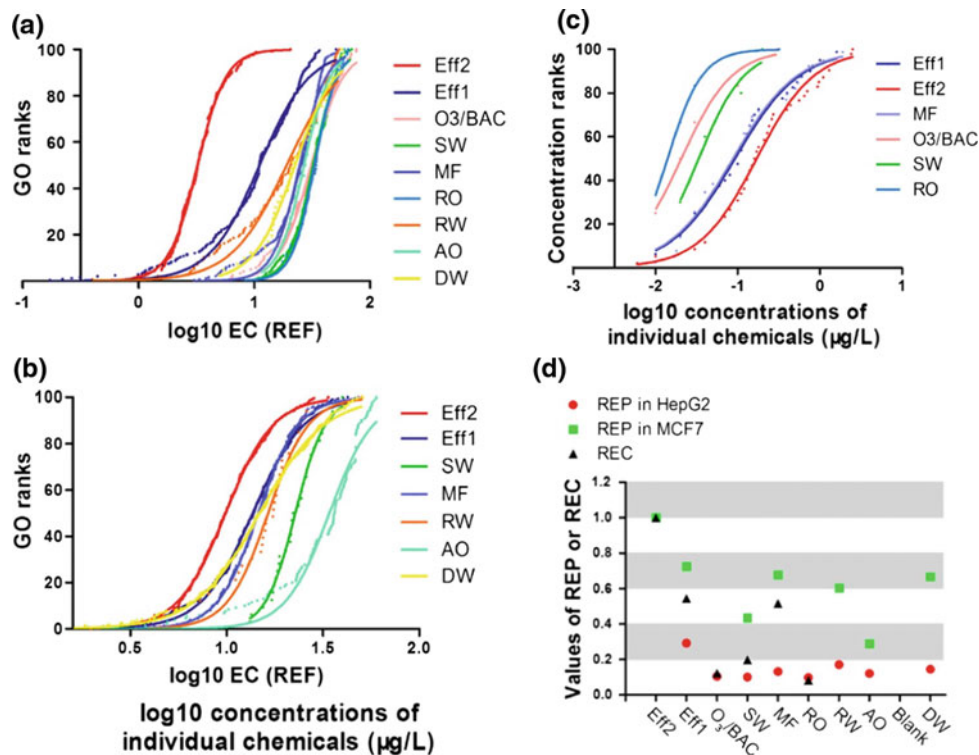


**Table 5** Relative biological potency (REP) and relative chemical contamination (REC) values of water samples

	Eff2	Eff1	O3/BAC	SW	MF	RO	RW	Blank	AO	DW
REP in HepG2	1	0.29	0.10	0.10	0.13	0.10	0.17	0.12	NA	0.14
REP in MCF7	1	0.72	NA	0.43	0.68	NA	0.60	0.29	NA	0.67
REC	1	0.54	0.12	0.20	0.51	0.08	NA	NA	NA	NA

NA means no available distribution curves for that sample

relevant to toxicological end points is essential in the assessment of mixture by RHT approach. Future studies should explore the utility of other cell types, such as human primary cells and embryonic stem cells, to increase the coverage of biological activities and improve the implications for human health.

## 5 Assessing Environmental Toxicants Using Zebrafish Embryo Test

Here, a reduced zebrafish transcriptome (RZT) approach was developed to represent the whole transcriptome and to profile bioactivity of chemical and environmental mixtures in zebrafish embryo. RZT gene set of 1637 zebrafish Entrez genes was designed to cover a wide range of biological processes, and to faithfully capture gene-level and pathway-level changes by toxicants compared with the whole transcriptome. Concentration–response modeling was

used to calculate the effect concentrations (ECs) of DEGs and corresponding molecular pathways. To validate the RZT approach, quantitative analysis of gene expression by RNA-ampliseq technology was used to identify differentially expressed genes (DEGs) at 32 hpf following exposure to seven serial dilutions of reference chemical BPA (10–10E–5 µM) or each of four water samples ranging from wastewater to drinking water (relative enrichment factors 10–6.4 × 10–4). The RZT-ampliseq-embryo approach was both sensitive and able to identify a wide spectrum of biological activities associated with BPA exposure. Water quality was benchmarked based on the sensitivity distribution curve of biological pathways detected using RZT-ampliseq-embryo. Finally, the most sensitive biological pathways were identified, including those linked with adverse reproductive outcomes, genotoxicity, and development outcomes. RZT-ampliseq-embryo approach provides an efficient and cost-effective tool to prioritize toxicants based on responsiveness of biological pathways.

The objectives of this study were threefold. The first was to curate a reduced gene list from zebrafish transcriptome (RZT) that can comprehensively represent biological pathways and toxicologically relevant processes, and be quantified by Ion Ampliseq Technology (RZT-ampliseq). Second, we aimed to develop a chemical test protocol integrating RZT-ampliseq and dose–response modeling in zebrafish embryo (RZT-ampliseq-embryo). Bisphenol A (BPA), a well-studied endocrine disruptor frequently detected in water samples, was selected as a reference chemical. Finally, we wanted to evaluate the performance of RZT-ampliseq-embryo for use in hazard assessment of environmental mixtures. The mixture samples tested in this study were a set of water extracts previously characterized by the RHT method.

**Zebrafish Embryo Culture and Exposure.** Embryos at 1 hpf were obtained from group spawns and incubated in buffered embryo medium at 28 °C until 8 hpf. Then, 1 mL of exposure solution was prepared in buffered embryo medium with a series of concentrations of single chemical or mixture (Table 5) with a final vehicle concentration of 0.1% dimethyl sulfoxide (DMSO; Sigma-Aldrich). Ten embryos were added to each well of 24 well microtiter plates. Plates were sealed with parafilm and incubated at 28 °C on a 14 h/10 h, light/dark cycle. At 32 hpf, the zebrafish embryos were collected for RNA isolation. The basal transcriptional expression of RZT gene set was evaluated on three replicates of 0.1% DMSO treatment sampled from six batches of culture.

**Single Chemical.** Stock solutions of BPA (Sigma-Aldrich) were prepared in DMSO. First, a single concentration experiment (0.1 and 10  $\mu$ M BPA) with three replicates was conducted to validate the gene expression profiling of RZT-ampliseq platform by comparing with the whole transcriptome evaluated using microarray. Second, embryos were dosed to a serial tenfold dilutions of BPA (10–10E–5  $\mu$ M) with a single replicate, in addition to three vehicle control (0.1% DMSO).

**Environmental Mixtures.** Four water extract samples previously characterized as representing high-, medium-, and low-toxic potencies (11) were tested by the RZT-ampliseq-embryo approach. The dried extracts were stored at –80 °C until analysis. Stock solutions of samples were prepared in DMSO with relative enrichment factor (REF) of 10 000, followed by 8–32 hpf embryo exposure. The REF represents the concentration in the ambient water samples (e.g., REF of ten means tenfold concentrated sample; REF of 0.1 means tenfold diluted sample).

**mRNA Expression Profiling by Ampliseq.** At 32 hpf, zebrafish embryos were collected for total RNA extraction using RNeasy mini kit (QIAGEN, GmbH, Hilden). RNA quantification was performed by using Agilent 2100 Bioanalyzer (Agilent technologies, Santa Clara, CA). Ten ng total RNA from each sample were reverse transcribed into cDNA by poly-A priming followed by PCR preamplification (15 cycles) according to the protocol supplied with the Ion AmpliSeq RNA Library Kit (Life Technologies, Carlsbad, CA). The library was amplified, purified, and stored at –20 °C. Amplicon size and DNA concentration were measured using Agilent High Sensitivity DNA Kit (Agilent Technologies, Waldbronn, Germany) according to the manufacturer’s recommendation. The resulting libraries were sequenced by Ion Proton (Life Technologies).

**Gene Expression Analysis Pipeline.** Raw reads were automatically quantified by using Torrent Mapping Alignment Program. Then log<sub>2</sub>-fold change of each gene was calculated using edgeR package. Differentially expressed genes (DEGs) of a single BPA concentration were identified by the threshold of absolute fold change  $\geq 1.5$  and Benjamini–Hochberg adjusted  $p < 0.05$ . For full dose–response profiling, log<sub>2</sub>-fold change of genes against concentrations was submitted to dose–response modeling analysis using drc and DoseFinding as described previously with minor modification. Briefly, nine dose–response models (Table 4) were fitted for each gene. The best-fit model, with the lowest akaike’s information criterion (AIC) value, was used for calculation of effect concentration (EC) values for genes whose best-fit model showed significant curve-fitting performance ( $p$ -value  $< 0.05$ ). Finally, genes whose EC  $\leq$  LOEC (BPA) or  $\leq 30$  REF (water samples, NO effect concentration) were defined as DEGs.

**Robustness Analysis of RZT-Ampliseq.** The zebrafish embryos treated with 0.1% DMSO were used to evaluate the basal expression of RZT genes, since 0.1% DMSO is frequently used as a control in toxicological studies. To evaluate the optimum sequencing depth of RZT-ampliseq-embryo for consistently detecting most genes, mRNA sample of 32 hpf zebrafish embryo exposed to 0.1% DMSO with 300 000 sequencing counts of RZT-ampliseq (coverage of  $\sim 200$  counts for each gene) was used. The optimum sequencing depth of samples was determined by a Monte Carlo simulation conducted using R language. Each sequenced depth was repeated 100 times to calculate the detected number of genes (Reads  $> 0$ , Reads  $> 20$ ) and the coefficient of variation (CV) (SD/Mean) of each gene’s expression abundance. For each gene, the relationship between CV and sequencing depth was fitted with loess model and then the minimum sequencing

depth of ensuring CV < 15% was calculated. To evaluate the mRNA profiling performance of ampliseq on the RZT gene set, the number of detected and undetected genes, as well as each gene expression abundance measured by RZT-ampliseq was compared to that by microarray platform (GSE43186) and RNA-seq platform on 36 hpf zebrafish embryo. Correlations of the gene expression abundance between different technologies were calculated using number of reads per amplicon for RZT-ampliseq, RPKM (reads per kilo base per million reads) values for RNA-seq and signal intensity values for microarray technology. Finally, to evaluate the repeatability of RZT-ampliseq, the CV of RZT gene set in zebrafish embryos of 0.1% DMSO ( $n = 3$ ) from six batches was analyzed using the edge package.

**Pathway-Level and Biological Process Validation.** For single dose experiment, functional enrichment analysis of identified DEGs was performed using a one-sided Fisher's exact test on GO of biological process (BP), and KEGG pathways with RZT gene list (Table S2) as background. For full dose experiment, the EC values of GO terms and KEGG pathways were calculated as the geometric mean of EC values of matched DEGs. Only GO terms or KEGG pathways matched by at least three genes were included in EC calculation and further analysis. Finally, to analyze the overall biological potency of each sample, the proportionally ranked distribution of GO and KEGG of EC values was fitted with a four-parameter dose-response curve using GraphPad Prism 5.0 software (San Diego, CA).

The molecular responses profiling (DEGs, KEGG pathways of DEGs) of 0.1  $\mu\text{M}$  BPA treatment by RZT-ampliseq were compared with whole transcriptome analysis of BPA archived in NCBI. To compare RZT-ampliseq-embryo approach with existing Toxcast high-throughput in vitro assays with regard to biological activities associated with BPA exposure, the responsive gene end points and molecular pathways (KEGG, GO BP terms) identified by both methods were evaluated. The responsive molecular gene end points were DEGs captured of dose-response model analysis of RZT-ampliseq-embryo. The responsive genes of Toxcast in vitro assay were downloaded from (<https://www.epa.gov/chemical-research/toxicity-forecaster-toxcasttm-data>). The responsive molecular end points were converted to zebrafish orthologous genes.

**Comparison of RZT with In Vitro Bioassays and RHT Method on Mixtures.** A supervised approach was used to assess the RZT representation of the previous in vitro bioassays. First, gene sets associated with cellular toxicity pathways tested by in vitro bioassays were manually curated from Wiki Pathways and Gene Ontology, KEGG. Then the EC of each pathway was calculated by the geometric mean of the ECs of matched DEGs. Pathway patterns identified by

the RZT approach were shown by heatmap using gplot package. The hierarchical clusters of water samples identified by RZT analysis were compared with the results of in vitro bioassays.

To evaluate the sensitivity and specificity of RZT-ampliseq-embryo in identification of bioactivity of mixtures, the results of RZT-ampliseq-embryo were compared to that of RHT-ampliseq using human HepG2 and MCF7 cells on the same sample set. Briefly, the sensitivity of 50% biological potency of water samples identified by RZT was compared with those identified by RHT in HepG2 and MCF7 cells in terms of KEGG or GO. In addition, linear regression was conducted on values of 50% biological potency identified by RZT and RHT. Finally, the coverage of the most sensitive pathways (top 20 sensitive KEGG pathways) of Eff2, the sample with potential highest and broadest bioactivity was compared between RZT and RHT approaches.

**RZT Assessment of a Classical Chemical: BPA.** The RZT approach showed good repeatability for quantifying transcriptional response to chemical by zebrafish embryo. Common CV of 32 hpf embryo mRNA samples exposed to 0.1% DMSO from 8 to 32 hpf was 13% (biological replication within one batch), 14% (biological replication among six batches) for RZT-ampliseq-embryo. This variation was acceptably low when compared with other RNA profiling technology, such as qPCR (CV: 1 ~ 15%), microarray (CV: 5 ~ 15%) or RNA-seq (CV: 10 ~ 15%). After exposure of two independent batches of embryos to a single dose of 10  $\mu\text{M}$  BPA, 67, 45 DEGs (ANOVA,  $p < 0.05$ ), respectively, were identified by RZT-ampliseq-embryo and 26 DEGs were common to both batches. Moreover, the fold change values of all expressed genes showed significant correlation between batches ( $R^2 = 0.62$ ) and the difference among the DEGs of two batches was nearly within twofold.

The full dose-response analysis of an RZT profile following exposure to BPA provided a distinct DEGs profile compared to that detected following single doses. Following 24-h exposure to 0.1 or 10  $\mu\text{M}$  BPA (single dose), 67 and 58 DEGs, respectively, were captured by RZT-ampliseq-embryo and 31 DEGs were commonly expressed. Eight GO BP terms and five KEGG terms were shared between 10 and 0.1  $\mu\text{M}$  BPA concentration groups. Transcriptional changes associated with DNA damage (DNA repair, cellular response to DNA damage stimulus) and central nervous system development were only captured after 0.1  $\mu\text{M}$  BPA exposure. Oocyte meiosis was only identified after 10  $\mu\text{M}$  BPA exposure. Moreover, there were no common DEGs in RZT-ampliseq-embryo and the published microarray data in embryo exposed to 8–32 hpf 0.1  $\mu\text{M}$  BPA. Three common KEGG pathways (counts of mapped gene  $\geq 3$ ) were identified in two platforms, but



these were only involved in fundamental apoptosis process (FoxO signaling pathway, p53 signaling pathway) and regulation of actin cytoskeleton. However, 98 DEGs were identified by dose–response analysis of the embryo exposed to the seven, tenfold, dilutions of BPA ( $10 \sim 10^{-5} \mu\text{M}$ ). Three and five of the DEGs identified by dose–response analysis were also detected as DEGs in embryos exposed to 10 and  $0.1 \mu\text{M}$ , respectively.

One significant advantage of dose–response analysis by RZT-ampliseq is the sensitivity analysis of genes and biological pathways in response to chemicals, which could aid inference regarding the potentially sensitive apical end point effects. The responsive DEGs were mainly fitted with U-shaped models, which suggest that the mode of hormesis dominates the low dose response of transcriptome. However, there are alternative interpretations other than true hormesis. For example, the time course of dynamic transcriptional response may change at different doses; in higher doses, for example, the transcript abundance can peak earlier, but falls by 32 h. Alternatively, perhaps there is a developmental delay at the higher doses, associated with triggering more and more AOPs in the organism, thereby causing more and more disruption of normal development. What is effectively a monotonic response to the chemical may produce a non-monotonic dose–response for a given snapshot in time. The response genes ( $EC < 0.001 \mu\text{M}$ ) (foxa3, dhra3a, src, rpa3, myb, csf1ra, flt4) were mainly fitted with Gaussian model (Fig. 14a) and were primarily associated with pathways of cell-based process, responses to external stimuli, immune system, and neurogenesis. The significant enrichment of neurogenesis-related processes (central nervous system development, nervous system development, locomotion) at very low concentrations of BPA ( $EC < 0.001 \mu\text{M}$ ) was corroborated by hyperactivity behavior ( $0.0068 \mu\text{M}(35)$ ) and increased neuronal development(35) observed in previous study. Moreover, hyperactivity behavior showed a nonmonotonic concentration-dependent response and was induced only at very low effect concentrations, which was consistent with the Gaussian model of the relevant DEGs. For the DEGs with EC between 0.001 and  $0.01 \mu\text{M}$ , only apoptosis relevant FOXO signaling pathway ( $FDR = 0.057$ , covered four genes) was enriched. Previous research reported BPA could induce apoptosis of mice spermatocytes and zebrafish embryo. A larger number of pathways, which included liver development, regulation of nucleobase-containing compound metabolic process, sensory organ morphogenesis, and DNA binding, were associated with the DEGs with EC between 0.01 and  $0.1 \mu\text{M}$ . The DEGs with EC ( $0.1\text{--}10 \mu\text{M}$ ), close to the LOEC ( $10 \mu\text{M}$ ),

were mainly associated with carbohydrate metabolic process and blood vessel development process.

The coverage of enriched pathways and the corresponding sensitivity detected following full dose–response profiling using RZT-ampliseq-embryo were compared with ToxCast in vitro results for BPA. Not only was there consistency with ToxCast in terms of the coverage of biological pathways, the RZT-ampliseq-embryo method appeared more sensitive (Fig. 14b–d). Bisphenol A was tested with regard to 821 ToxCast assay end points. Out of 96 genes that aligned with the 390 relevant assays, 78 genes had a corresponding orthologous zebrafish gene. In total, 5 KEGG pathways and 15 GO BP terms were commonly identified by ToxCast and RZT, although only five genes were identified by both approaches (Fig. 14b–d). Furthermore, the sensitivity rank of common genes (ptgre2a, tcf7l1b, src, xbp1, tfap2b) and KEGG pathways (metabolic pathways, MAPK signaling pathway, focal adhesion, endocytosis, adhere junction) was similar across two platforms (Fig. 14b, c). However, RZT-ampliseq-embryo was more sensitive than in vitro tests in ToxCast with 2.3, 2.9, and 2.8 magnitude difference at gene, KEGG, and GO BP level, respectively.

**RZT Assessment of Mixtures in Zebrafish Embryo.** The RZT-ampliseq-embryo was able to discriminate the relatively clean water samples from the polluted environmental samples by the relative potency of altered genes and molecular pathways. The DEGs responsive at low dose range ( $ECs \leq 0.1 \text{ REF}$ ) were mainly fitted with U-shaped models (Fig. 15). For example, the DEGs of MF were mainly associated with altered metabolic process (ar, smad1, prpf40a, ak2, uqcr2b, polr2g1, smc3, gtf2b, psmc1a, rpl7a, gars, ndufv2, htatsf1, rps24, u2af2b, cwc15, zgc:86599, nup85, psmc5, tcf7, hnrnp1, ikbkap, nup107), developmental process (such as kif1 bp, atp6v1e1b, flt4, sema3d, cttnb1, smad1, raf1a, tgfb2, ak2, rpl6, tgfb3, rps24, sumo1, tcf7, cyp26c1, plod3, ikbkap, hdac6), and cellular response to stimulus (such as ar, flt4, sema3d, smad1, raf1a, tgfb2, smc3, ssr4, psmc1a, tgfb3, psmc5, tcf7, ephb2b). The number of DEGs selected by the nine dose–response models across all four samples ranged from 78 to 300 (SI Fig. 15). Although the number of DEGs did not directly correlate with decreasing pollution level, the sensitivity distribution curve of biological pathways indicated the decrease of pollution level ( $\text{Eff2} > \text{MF} > \text{RW} > \text{DW}$ ). The EC values of the most sensitive KEGG or GO pathways of DW samples were 1–2 orders of magnitude higher than those of effluent samples, suggesting relatively weak biological effects were induced by D.

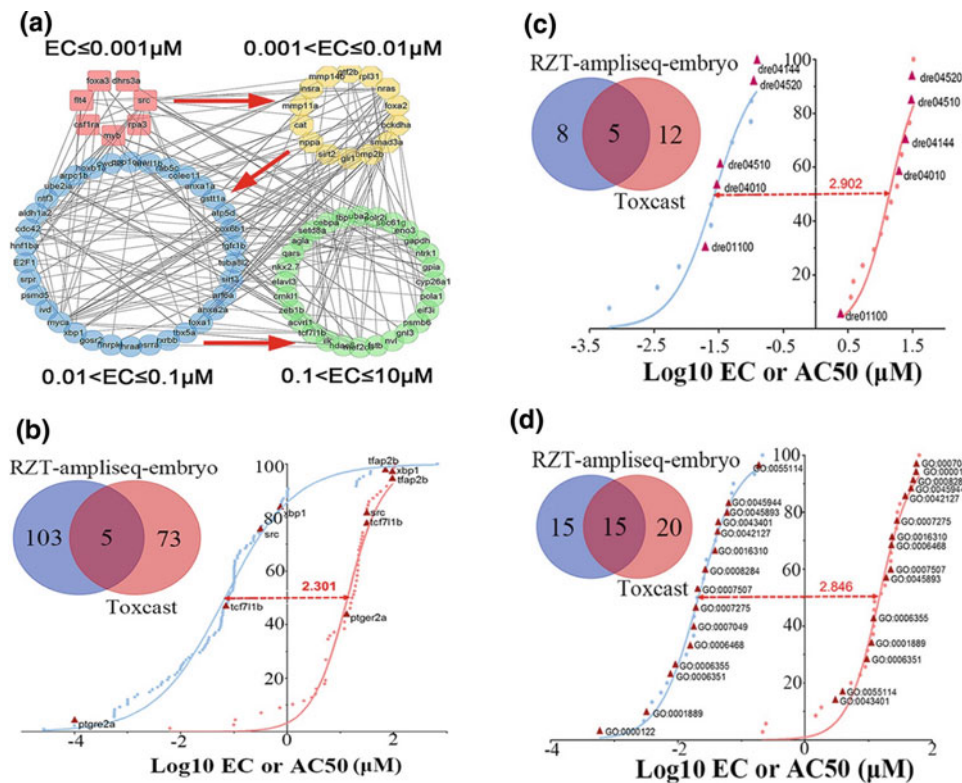


**Fig. 14** Concentration-dependent network of differentially expressed genes (DEGs) ( $p < 0.05$ ) in 32 hpf zebrafish embryo treated by BPA in RZT-ampliseq-embryo (blue,  $\text{log}_{10}$  EC value) and Toxcast in vitro assays (orange,  $\text{log}_{10}$  AC50 value) at gene level (b), KEGG pathway level (c) and GO BP term (d). For KEGG pathways and GO BP terms, only those with counts of mapped genes  $\geq 3$  were included in this

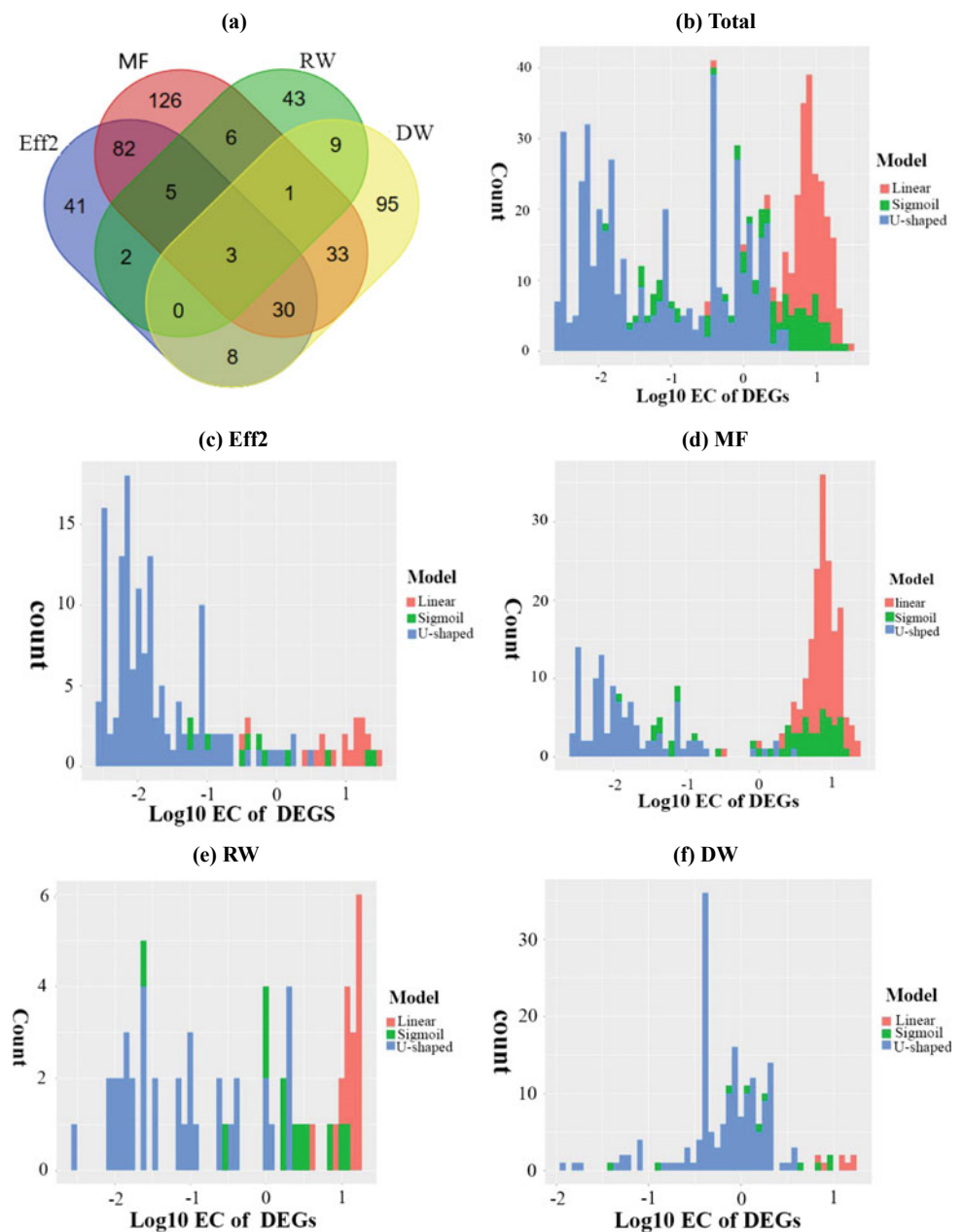
analysis. Common molecular end points were labeled by red triangle. Pathway scores (EC or AC50 value) were the geometric mean of the effect concentrations (ECs) (RZT-ampliseq-embryo) or AC50 (Toxcast) values of the relevant genes. The horizontal distance of 50% biological potency between RZT-ampliseq-embryo and Toxcast in vitro was labeled in red

The enriched pathways in RZT analysis could be used to prioritize potential biological end points for future assessment. Specifically, the most sensitive KEGG or GO BP pathways may be linked with adverse outcomes. All development relevant pathways (GO terms, each covered at least three DEGs suggested Eff2 and MF samples might induce potential development toxicity while RW and DW samples may not (Fig. 16a). The predicted adverse outcomes were corroborated by zebrafish embryo 48hpf lethality and 120hpf sublethal development experiment.

**Comparison between RZT-Embryo and RHT Cell Profiles of Water Samples.** RZT-embryo also provided different profiles of altered genes and pathways of the four water samples from that by RHT approach, which might be due to the greater biological complexity represented by a fish embryo compared to a single cell type. The most sensitive pathways identified by RZT following exposure to the water samples were distinct with those by RHT in HepG2 and

MCF7. Take Eff2 for example (Fig. 16b), only four KEGG pathways were overlapped between the 20 most sensitive pathways (with lowest EC values) identified by RZT-embryo and RHT in HepG2 and MCF7 cells. Nine of the 20 most sensitive pathways uniquely identified by RZT-embryo were associated with basic biological processes, which may suggest that rapidly developing and differentiating zebrafish embryos were more sensitive to alterations of basic processes, such as oxidative phosphorylation, than the single cell type in vitro system. Moreover, the most sensitive KEGG pathways identified by RHT in HepG2 and RHT in MCF7 showed cell-type responses, such as pathways involved in immune response and cellular communication, which were not among the most sensitive KEGG pathways by RZT-embryo assay. However, some cell-type-specific responses, including endocrine response in MCF7 and metabolism response in HepG2, were also identified by RZT as sensitive KEGG pathways responding to Eff2.

**Fig. 15** a Venn diagram of DEGs by four water samples identified by RZT-ampliseq-embryo in 32 hpf. Histogram of log<sub>10</sub> EC values of differentially expressed genes (DEGs) across total four water samples (b) and by each water sample (c), (d), (e), and (f)



A distinct pathway sensitivity distribution in response to the MF sample was identified by RZT-embryo compared to RHT in HepG2 and MCF7 cells. Although the potency of the median sensitive pathway (50% biological potency) following exposure to MF was lower than that of RW and DW in RZT-embryo, MF was more potent than that of RW and DW at the most sensitive pathways which were profiled by the RZT-embryo. These highly sensitive biological responses induced by MF were primarily related to embryo development (e.g., heart jogging, embryo pattern specification, notochord development, determination of left/right

symmetry) (Fig. 16a), which might be related to developmentally toxic pollutants present in the MF sample. The MF sample was water taken after microfiltration using filters disinfected by chlorination to avoid biofouling in a water reclamation plant, in which micropollutants such as carbamazepine, a teratogen, with the highest detected concentrations (1.9 µg/L) out of ten samples were present. Carbamazepine has been reported to disturb embryonic development with increasing hatching rate, body length, swim bladder appearance, and yolk sac absorption rate at 1 µg/L. However, knowledge gaps associated with unknown

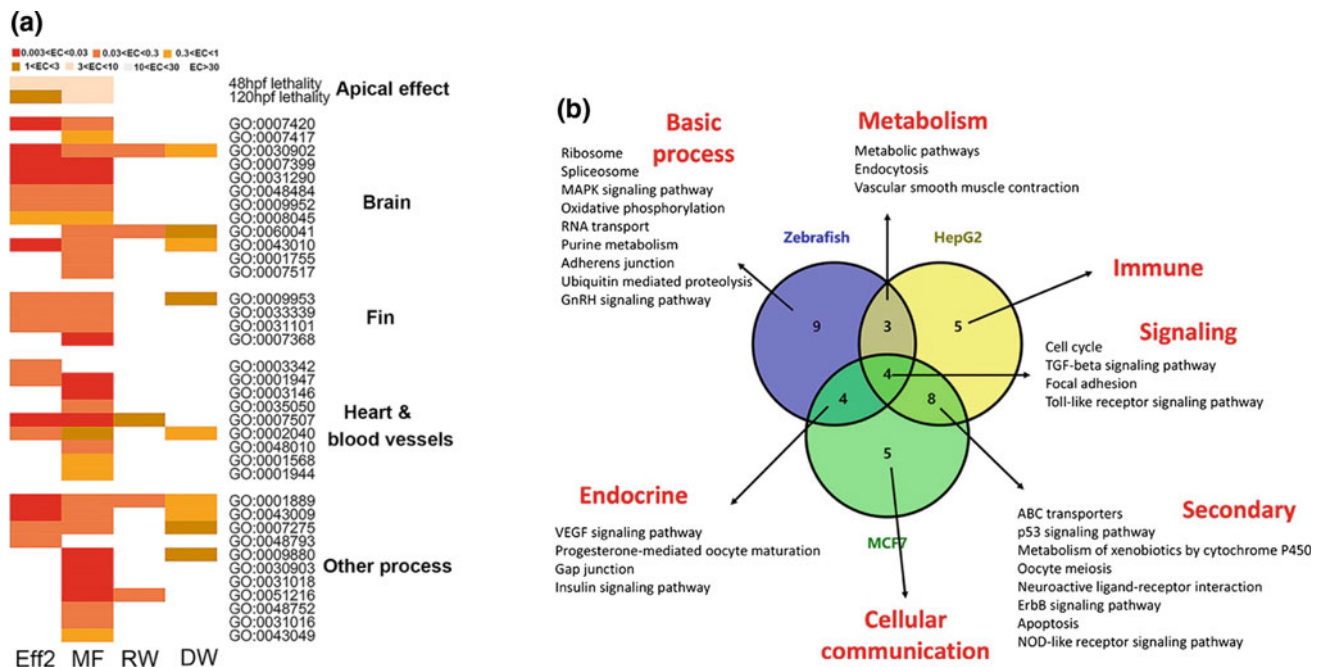


**Fig. 16** **a** Development-related biological processes affected by four water samples from RZT-ampliseq-embryo in 32 hpf. Plotted were log 10 EC values with a unit of relative enrichment factor (REF). **b** Venn diagram of top 20 sensitive KEGG pathways ranked by EC values identified by RZT, RHT in HepG2, and RHT in MCF7, respectively,

for Eff2 sample. The labels of “zebrafish” in blue, “HepG2” in yellow, and “MCF7” in green stand for approaches of RZT, RHT in HepG2, and RHT in MCF7, respectively. The labels in red stand for the main function of KEGG pathways

chemicals present in the mixtures and their potential combined effects still exist in toxicological assessment of these environmental samples. An effect-directed analysis (EDA) integrating extract fractionation and instrument analysis with the sensitive RZT approach may be used to identify the chemicals responsible for the observed effect in future.

In conclusion, we developed reduced transcriptome approaches (RHT and RZT) by integrating reduced transcriptome, RNA-ampliseq technology, and human cells or zebrafish embryo test to assess environmental toxicants. Firstly, the concentration-dependent transcriptomic approach could identify early molecular response and molecular mechanism of single chemical which would help to predict apical effect. The reduced transcriptome approach has potential to be used to evaluate and prioritize chemicals for further testing and potentially to predict adverse outcomes. These results demonstrate a promising and powerful tool for screening hundreds of chemicals or mixtures by potency ranking and to classify chemicals by the spectrum of disrupted biological pathways. The omics-based biological pathway strategy can also be used in the characterization of potential toxicity by environmental mixtures. It is anticipated that reduced transcriptomic approaches will significantly advance pathway-based high-throughput screening of potentially toxic substances.

## References

- Altenburger R, Ait-Aissa S, Antczak P, Backhaus T, Barcelo D, Seiler TB, Brion F, Busch W, Chipman K, de Alda ML, de Aragao Umbuzeiro G, Escher BI, Falciani F, Faust M, Focks A, Hilscherova K, Hollender J, Hollert H, Jager F, Jahnke A, Kortenkamp A, Krauss M, Lemkine GF, Munthe J, Neumann S, Schymanski EL, Scrimshaw M, Segner H, Slobodnik J, Smedes F, Kughathas S, Teodorovic I, Tindall AJ, Tollefsen KE, Walz KH, Williams TD, Van den Brink PJ, van Gils J, Vrana B, Zhang X, Brack W (2015) Future water quality monitoring—adapting tools to deal with mixtures of pollutants in water resource management. *Sci Total Environ* 512–513:540–551
- Bluhm, K.; Otte, J. C.; Yang, L.; Zinsmeister, C.; Legradi, J.; Keiter, S.; Kosmehl, T.; Braunbeck, T.; Straehle, U.; Hollert, H., Impacts of Different Exposure Scenarios on Transcript Abundances in Danio rerio Embryos when Investigating the Toxicological Burden of Riverine Sediments. *Plos One* **2014**, *9* (9)
- Choi JS, Kim RO, Yoon S, Kim WK (2016) Developmental toxicity of zinc oxide nanoparticles to zebrafish (*Danio rerio*): a transcriptomic analysis. *11* (8), e0160763
- Conolly RB, Ankley GT, Cheng W, Mayo ML, Miller DH, Perkins EJ, Villeneuve DL, Watanabe KH (2017) Quantitative adverse outcome pathways and their application to predictive toxicology. *Environ Sci Technol* 51(8):4661–4672
- Diressen M, Vitins AP, Pennings JL, Kienhuis AS, Water B, van der Ven LT (2015) A transcriptomics-based hepatotoxicity comparison between the zebrafish embryo and established human and rodent in vitro and in vivo models using cyclosporine A, amiodarone and acetaminophen. *Toxicol. Lett.* 232(2), 403–412

- Escher BI, Allinson M, Altenburger R, Bain PA, Balaguer P, Busch W, Crago J, Denslow ND, Dopp E, Hilscherova K, Humpage AR, Kumar A, Grimaldi M, Jayasinghe BS, Jarosova B, Jia A, Makarov S, Maruya KA, Medvedev A, Mehinto AC, Mendez JE, Poulsen A, Prochazka E, Richard J, Schifferli A, Schlenk D, Scholz S, Shiraishi F, Snyder S, Su G, Tang JY, van der Burg B, van der Linden SC, Werner I, Westerheide SD, Wong CK, Yang M, Yeung BH, Zhang X, Leusch FD (2014) Benchmarking organic micropollutants in wastewater, recycled water and drinking water with in vitro bioassays. *Environ Sci Technol* 48(3):1940–1956
- Guiu J, Bergen DJM, De Pater E, Islam ABMMK, Ayllon V, Gama-Norton L, Ruiz-Herguido C, Gonzalez J, Lopez-Bigas N, Menendez P, Dzierzak E, Espinosa L, Bigas A (2014) Identification of *Cdca7* as a novel Notch transcriptional target involved in hematopoietic stem cell emergence. *J Exp Med* 211(12):2411–2423
- Haggard DE, Noyes PD, Waters KM, Tanguay RL (2016) Phenotypically anchored transcriptome profiling of developmental exposure to the antimicrobial agent, triclosan, reveals hepatotoxicity in embryonic zebrafish. *Toxicol Appl Pharmacol* 308:32–45
- Hermesen SA, Pronk TE, van den Brandhof EJ, van der Ven LT, Piersma AH (2012) Concentration-response analysis of differential gene expression in the zebrafish embryotoxicity test following flusilazole exposure. *Toxicol Sci* 127(1):303–312
- Hofsteen P, Mehta V, Kim MS, Peterson RE, Heideman W (2013) TCDD inhibits heart regeneration in adult zebrafish. *Toxicological sciences: an official journal of the Society of Toxicology* 132(1):211–221
- Jiang J, Wu S, Wu C, An X, Cai L, Zhao X (2014) Embryonic exposure to carbendazim induces the transcription of genes related to apoptosis, immunotoxicity and endocrine disruption in zebrafish (*Danio rerio*). *Fish Shellfish Immunol* 41(2):493–500
- Knapen D, Angrish MM, Fortin MC, Katsiadaki I, Leonard M, Margiotta-Casaluci L, Munn S, O'Brien JM, Pollesch N, Smith LC, Zhang X, Villeneuve DL (2018) Adverse outcome pathway networks I: development and applications. *Environ Toxicol Chem* 37(6):1723–1733
- Lam SH, Hlaing MM, Zhang X, Yan C, Duan Z, Zhu L, Ung CY, Mathavan S, Ong CN, Gong Z (2011) Toxicogenomic and phenotypic analyses of bisphenol-A early-life exposure toxicity in zebrafish. *PLoS ONE* 6(12):e28273
- Li Y, Qi X, Yang Y-W, Pan Y, Bian H-M (2014) Toxic effects of strychnine and strychnine N-oxide on zebrafish embryos. *Chin J Nat Med* 12(10):760–767
- Maves L, Waskiewicz AJ, Paul B, Cao Y, Tyler A, Moens CB, Tapscott SJ (2007) Pbx homeodomain proteins direct Myod activity to promote fast-muscle differentiation. *Development (Cambridge, England)* 134(18):3371–3382
- Verleyen D, Luyten FP, Tylzanowski P (2014) Orphan G-Protein Coupled Receptor 22 (*Gpr22*) Regulates cilia length and structure in the zebrafish kupffer's vesicle. *Plos One* 9(10)
- Wang P, Xia P, Yang J, Wang Z, Peng Y, Shi W, Villeneuve DL, Yu H, Zhang X (2018) A reduced transcriptome approach to assess environmental toxicants using zebrafish embryo test. *Environ Sci Technol* 52(2):821–830
- Wanglar C, Takahashi J, Yabe T, Takada S (2014) *Tbx* protein level critical for clock-mediated somite positioning is regulated through interaction between *Tbx* and *ripply*. *Plos One* 9(9)
- Xia P, Zhang X, Zhang H, Wang P, Tian M, Yu H (2017) Benchmarking water quality from wastewater to drinking waters using reduced transcriptome of human cells. *Environ Sci Technol* 51(16):9318–9326
- Xu M, Liu D, Dong Z, Wang X, Wang X, Liu Y, Baas PW, Liu M (2014a) Kinesin-12 influences axonal growth during zebrafish neural development. *Cytoskeleton* 71(10):555–563
- Xu M, Liu D, Dong Z, Wang X, Wang X, Liu Y, Baas PW, Liu M (2014b) Kinesin-12 influences axonal growth during zebrafish neural development. *Cytoskeleton* 71(10):555–563
- Zhang X, Wiseman S, Yu H, Liu H, Giesy JP, Hecker M (2011) Assessing the toxicity of naphthenic acids using a microbial genome wide live cell reporter array system. *Environ Sci Technol* 45(5):1984–1991
- Zhang X, Xia P, Wang P, Yang J, Baird DJ (2018) Omics advances in ecotoxicology. *Environ Sci Technol* 52(7):3842–3851

# Synchrotron-Based Techniques for the Quantification, Imaging, Speciation, and Structure Characterization of Metals in Environmental and Biological Samples

Yu-Feng Li and Chunying Chen

## Abstract

This chapter introduces state-of-the-art synchrotron-based techniques in quantification, imaging, speciation of metals, and structure characterization of metal-binding biomolecules in environmental and biological samples. SRXRF has been widely applied in quantification of metals in different samples. The focused synchrotron-based X-ray can image metals down to nm resolution at two or three dimensions. XAS has been used for chemical speciation of different metals. In combination with SRXRF and XAS, it can also realize spatial and chemical imaging. The structure of metal-binding biomolecules can be characterized by PX and/or XAS. In all, quantification, imaging, speciation of metals, and the probing of the sub-molecular structure of metals in interactions with their surrounding environment through synchrotron-based techniques can help to unravel the speciation of toxic metals in linkage with their mobility in the environment and potential toxicity to organisms and humans.

## Keywords

Quantification • Imaging • Speciation • Structure characterization • Synchrotron radiation • SRXRF • XAS

## 1 Introduction

Many metals (and metalloids) play vital roles in the chemistry of life. For example, copper serves as a cofactor in many redox enzymes like cytochrome c oxidase, which influences respiratory electron transport chain of mitochondria while selenium plays a key role in host oxidative defense through selenoenzymes and selenoproteins (Hu et al. 2013). Over 30% of the proteins in biological systems are believed to require a metal cofactor like iron, zinc, copper, selenium, or molybdenum (Mounicou et al. 2009). On the other hand, many metals and metalloids including those essential metals are toxic to living organisms at inappropriate levels. Besides, the toxicity of metals and metalloids to organisms and human beings is highly linked with their speciation and bioavailability in the environment. Furthermore, the study on the absorption, distribution, metabolism, and excretion (ADME) of metals and metalloids will help us to understand the mechanisms underlying their toxic effects (Li et al. 2016a).

Many approaches were applied to study the levels, speciation and distribution, bioavailability of metals and metalloids in biological systems and the environment (Chen et al. 2010; Li et al. 2009; Szpunar 2004). Synchrotron radiation (SR) is an advanced light source providing from infrared up to hard X-rays with high brilliance (many orders of magnitude more than conventional light sources) and pulsed light emission (pulse durations at or below one nanosecond). The light produced by SR is highly polarized, tunable, and collimated and can be focused over a small area with much more photons than conventional sources. All of these properties make SR-based techniques outstanding tools in multidisciplinary research like physics, chemistry, life science, materials science, environmental science, etc. (Mai 2013). Like techniques using conventional lights sources, synchrotron-based techniques are developed through their interactions with matters, i.e., the absorption and the scattering. X-ray absorption spectrometry (XAS), Fourier

Y.-F. Li

CAS Key Laboratory for Biological Effects of Nanomaterials and Nanosafety, and HKU-IHEP Joint Laboratory on Metallomics, Institute of High Energy Physics, Chinese Academy of Sciences, Beijing, 100049, China  
e-mail: [liyf@ihep.ac.cn](mailto:liyf@ihep.ac.cn)

C. Chen (✉)

CAS Key Laboratory for Biological Effects of Nanomaterials and Nanosafety, National Center for Nanoscience and Technology, Beijing, 100190, China  
e-mail: [chenchy@nanoctr.cn](mailto:chenchy@nanoctr.cn)

transformed infrared spectroscopy (FTIR), ultraviolet–visible spectroscopy (UV–vis), soft/hard X-ray microscopy (scanning transmission X-ray microscopy, STXM; transmission X-ray microscopy, TXM), X-ray computed tomography (X-CT), etc. are based on the absorption of synchrotron radiation by matters. X-ray diffraction (XRD), protein X-ray crystal diffraction (PX), circular dichroism (CD), small angle X-ray scattering (SAXS), elastic/inelastic scattering (Raman spectroscopy), etc. are based on the scattering of synchrotron radiation by matters. Besides, the detection of the emission of secondary particles like X-ray photoelectron spectroscopy (XPS) and X-ray fluorescence spectrometry (XRF) are also developed using synchrotron radiation (Li et al. 2015b, c).

With the rapid growth in the number of synchrotron radiation facilities around the world, more and more synchrotron-based techniques are applied in studies of the environmental chemistry and toxicity of metals. In this chapter, we summarize the application of synchrotron-based techniques, especially the recent advances in quantification, imaging, speciation of metals, and structure characterization of metal-binding biomolecules in environmental and biological samples.

## 2 Quantification of Metals

The measurement of trace metal concentrations in environmental and biological samples can be achieved through different techniques like atomic absorption spectrometry (AAS), atomic fluorescence spectrometry (AFS), etc. Inductively coupled plasma based optical emission spectrometry (ICP-OES) and inductively coupled plasma mass spectrometry (ICP-MS) can quantify multi-trace metals rapidly and simultaneously in one run with the detection limit as low as parts per trillion (ppt) level. ICP-MS can detect most elements in biological systems, but sulfur, phosphorous, and halogens are not efficiently ionized by the ICP owing to their high ionization energies. A number of polyatomic interferences also hinder the detection of S, P, and transition elements like Fe and V using ICP-MS (Szpunar 2005). For ICP-MS, most liquid and gaseous samples can be directly introduced into the system, but solid samples require pretreatment such as digestion and/or ashing. This is both time-consuming and runs the risk of contamination during sample pretreatment. Neutron activation analysis (NAA) can simultaneously measure more than 30 elements in one sample with the detection limits from  $10^{-6}$  to  $10^{-13}$  g/g (Chai et al. 1992). The principal advantage of NAA is that it does not need sample digestion or dissolution. Therefore, there is little opportunity for reagent or laboratory contamination. Additionally, it is nearly free of any matrix interference effects as the vast majority of samples are

completely transparent to both the probe (the neutron) and the analytical signal (the gamma ray) (Chai and Zhu 1994). The major concern for NAA analysis is the radioactivity in the sample after neutron activation, which requires special caution and qualified operators.

X-ray fluorescence analysis (XRF) is a nondestructive, multielemental (from C to the end of the periodic table) analytical technique which is based on the detection of characteristic fluorescence after excited by a primary particle beam with sufficient energy (Jenkins 1999; Ji 2012). The particle beam can be electrons (Cantino and Hutchinson 1982), an X-ray beam (Ji 2012), or a proton beam (Johansson 1989). The detection limit for commercial XRF (using X-ray tube) is around part per million (ppm) level while with the introduction of synchrotron-based X-ray (SRXRF), it can be further lowered to around 1 part per billion (ppb) for Zn (Ji 2012; Van Langevelde and Vis 1991; Zhao and Xian 1997).

SRXRF has been applied to quantify trace elements in environmental and biological samples (Gordon et al. 1990; Kang et al. 2001; Piacenti da Silva et al. 2009). Urban air quality research is important since it has a strong effect on human health. The most critical pollutant in atmospheric aerosols is fine particulate matter (PM<sub>2.5</sub>) (i.e., particles with aerodynamic diameters smaller than 2.5  $\mu\text{m}$ ). Strong evidence suggests that PM<sub>2.5</sub> causes more severe health effects than particles with larger aerodynamic diameters (Mei et al. 2018). Air quality issues of international airports are becoming more and more important due to the dynamic growth of air traffic. Size-resolved sampling of particles according to their aerodynamic diameter was collected through cascade impactors. The particles collected on collector plates can be used directly as reflectors for SRXRF analysis (e.g., silicon wafers, Plexiglas, or quartz carriers). Trace elements (S, Cl, K, Ca, Ti, Fe, Cu, Zn, Se, Br, Sr, Pb) were analyzed in airport-related aerosols samples, which found typical elements coming from combustion processes (Zn, Pb), aircraft-related emissions (Cu), as well as road salting processes (Cl) (Groma et al. 2008). Trace elements like Cr, Mn, Co, Ni, and Cu in water samples were also quantified by SR-XRF, with comparable results got from ICP-MS (Wang et al. 2016).

Prostate cancer is the most frequently diagnosed form of noncutaneous cancer in men and the second leading cause of male cancer death in many countries. The differences in the elemental concentrations (e.g., P, S, K, Ca, Fe, Cu, Zn, and Rb) in samples of human prostate tissues with cancer, benign prostate hyperplasia, and normal tissues were analyzed utilizing SRXRF, which found that there was a reduction in the concentration of S, K, Ca, Fe, Zn, and Rb on the two pathologies studied when compared to the concentrations obtained in normal tissues (Leitão et al. 2014). The changes of some trace elements (Ti, V, Fe, Cu, Zn, As, Br, Rb, Sr,

Mo) in the cells of lung and cervix cancer before and after apoptosis were also studied, which found remarkable changes in some elements (Ti, As, Mo, and Fe) (Huang et al. 2001; Wu et al. 1997).

Zn serves numerous biological functions including protein synthesis, bone formation, and mineralization, as well as the development and maintenance of dental tissues. On the other hand, Pb exerts adverse effects on developing teeth, showing an increased incidence of dental caries and delays in enamel mineralization and tooth eruption. Co-administration of Zn is known to reduce tissue and organ Pb concentrations in animal models (Bandhu et al. 2006). SRXRF was used to measure the levels of Zn and Pb in the ameloblasts of developing Wistar rat teeth. It showed that intranuclear concentrations of Zn were greater than levels in the cytoplasm. Furthermore, nuclear and cytoplasmic concentrations of Zn in the maturation stage ( $742 \pm 27$  and  $424 \pm 25$  ppm, respectively) were significantly higher than that observed in the nucleus and cytoplasm of presecretory stage ameloblasts ( $132 \pm 10$  and  $109 \pm 10$  ppm, respectively) ( $p < 0.05$ ) (Arora et al. 2007).

In all synchrotron-radiation-based XRF can quantify multi-trace elements in environmental and biological samples in nondestructive manner. Besides, the detection limits for SRXRF can reach ppb range under total reflection mode, which is suitable for the detection of many biological-related trace elements (Leitão et al. 2014; Wang et al. 2016; Zhao and Xian 1997).

### 3 Imaging of Metals

Besides quantifying the levels of metals in the environmental and biological samples, it is also important to know their distribution, which can give information on the trafficking and deposition of metals in samples. The mapping of introduced radioactive or stable isotopic tracers or artificial dyes can only give information on the trafficking and distribution of specific metals introduced into the environmental or biological systems (Lee et al. 2007; Zhu et al. 2009). The imaging of metals without the assistance of isotopic tracers or artificial dyes can be achieved through mass-spectrometry-based and X-ray-fluorescence-based techniques.

Mass-spectrometry-based techniques include laser ablation-ICP-MS (LA-ICP-MS) and microscopic secondary ion mass spectrometry (SIMS). LA-ICP-MS has become a powerful tool in the analysis of trace element distribution in situ owing to the very high sensitivity of ICP-MS and direct laser sampling. LA-ICP-MS is well established for elemental mapping in the environmental samples (Devos et al. 2000; Meurer and Claeson 2002) and biological tissues such as plant leaves (Punshon et al. 2004), rat brains

(Jackson et al. 2006), human brains, and teeth (Becker et al. 2007; Kang et al. 2004). SIMS works by analyzing secondary ions removed from the sample by sputtering, which can give information on isotopic compositions of small samples (Wilson et al. 1989) with a detection limit of ng/kg level and lateral resolution down to 50 nm (Moore et al. 2012). However, both LA-ICP-MS and SIMS are locally destructive techniques, which may not be a suitable techniques for precious samples or live biological samples. Besides, the SIMS method only allows analysis under high vacuum conditions.

The X-ray-fluorescence-based imaging techniques include microscopic EDX (energy-dispersive X-ray fluorescence) or WDX (wavelength-dispersive x-ray fluorescence) and microscopic proton-induced X-ray emission (PIXE). EDX/WDX coupled to electron microscope can provide very good spatial resolution at about 10 nm, but the detection limit is at about g/kg level (Motelica-Heino et al. 1998) which may hold back their application in trace elements detection in biological samples. PIXE can simultaneously detect over 20 elements with an enhanced sensitivity up to 100 times that of EDX/WDX methods, which has been applied to elemental distribution in plant and animal tissues (Kramer et al. 1997; Sie and Thresher 1992; Tylko et al. 2007) and human blood cells and tumors (Johansson et al. 1987). The spatial resolution of 4  $\mu\text{m}$  for PIXE can be achieved by using characteristic Ti-K-X-rays (4.558 keV) produced by 3 MeV protons with beam spot size of  $\sim 1 \mu\text{m}$  (Ishii et al. 2007).

These methods are, however, limited by either high detection limits or poor spatial resolution. The synchrotron X-ray-fluorescence-based imaging techniques, i.e., SRXRF at the most advanced third-generation synchrotron radiation sources, on the other hand, can be effectively used to study trace element distribution in small spatial regions (down to 10 nm) with low detection limits (with absolute detection limit below  $10^{-17}$  g) in two or three dimension (Schroer et al. 2005; Yan et al. 2018).

#### 3.1 Two-Dimensional Imaging

By regulating synchrotron X-rays with a slit or focusing system, such as the Kirkpatrick-Baez mirror system (Ortega et al. 2004), refractive lenses (Snigirev et al. 1996), Fresnel zone plate (Snigirev et al. 1996), and multilayer Laue lens (Yan et al. 2018), the beam size can be changed into micron or nanometer level. Raster scanning of the specimen and acquisition of the entire X-ray spectrum yields quantitative topographical maps for a wide range of elements (Fahrni 2007). Different cells (Yang et al. 2005), tissues (Ide-Ektessabi et al. 2002; Wang et al. 2007), and organ slices (Iida and Noma 1993; Wang et al. 2008) has been



successfully studied using this two-dimensional (2D) SRXRF (Iida 1997; Paunesku et al. 2006).

Mercury (Hg) is one of the most hazardous toxic elements while selenium (Se) is an essential element for animals and human beings (Li et al. 2018a, 2019a). Although the antagonistic effect between Hg and Se in animals has been widely studied, their antagonism in plants remains less explored. The Hg and Se interaction was studied using rice as a model plant. SRXRF with micrometer level was applied to study the distribution of Hg and Se in different tissues of rice (Fig. 1) (Zhao et al. 2014b). It was found that Hg was mainly localized in the epidermis and the pericycle of the rice root. For Se/Hg co-exposed rice, the distribution of Se correlates well with that of Hg in the rice roots, and both of them principally concentrate in the epidermis and pericycle of the rice root. A substantial decrease in Hg accumulation in the epidermis and stele of the rice root can be found when co-exposed to Se. The content of Hg in the leaves collected from the Hg/Se co-exposed rice plant was much less than that of the Hg-exposed group, indicating the inhibitive effect of Se on Hg transportation from the roots to the leaves through the vascular cylinder. In rice grain, Hg was principally concentrated on the surface of it (the aleurone layer), especially along the growth site of the embryo. The concentration of Hg in the embryo part of the rice grain from Se and Hg co-exposed rice was much lower than that of the rice exposed to Hg alone. In addition, SRXRF also showed that the essential elements (Fe, Cu, Zn, K, Ca, etc.) were mainly concentrated in the embryo of the rice grain. This suggests that the essential nutrient elements, rather than the toxic elements, can be selectively accumulated in the rice grain. Therefore, SRXRF clearly shows that Se treatment can inhibit Hg uptake and transportation from the rice root to the aerial part, which finally leads to lowered Hg accumulation in the rice grain, especially in the aleurone layer and embryo. Following the knowledge gathered from the laboratory work, a field study was performed, which confirmed that treatment with appropriate level of Se is an efficient way to reduce Hg accumulation in rice and increase rice yield and quality, which in turn protects the health of the rice-dependent populations in Hg-contaminated area (Li et al. 2015a). Iron plaque and different forms of sulfur were also found to reduce mercury absorption and accumulation in roots and the above-ground parts of rice plants (Bai et al. 2019; Li et al. 2016b, 2017, 2018b, 2019b).

SRXRF with beam size at submicrometer level is well suited for quantitative elemental mapping of single cells with subcellular resolution. The subcellular distribution of copper in mouse fibroblast cells was studied with a  $0.2 \times 0.2 \mu\text{m}^2$  X-ray beam focused by Fresnel zone plate (Yang et al. 2005). The SRXRF confirmed the subcellular localization of Cu in mitochondria and the Golgi apparatus as found by fluorescence microscope. Besides, significant co-localization

of Cu and S was also found, suggesting that Cu might be primarily coordinated by S-donor ligands.

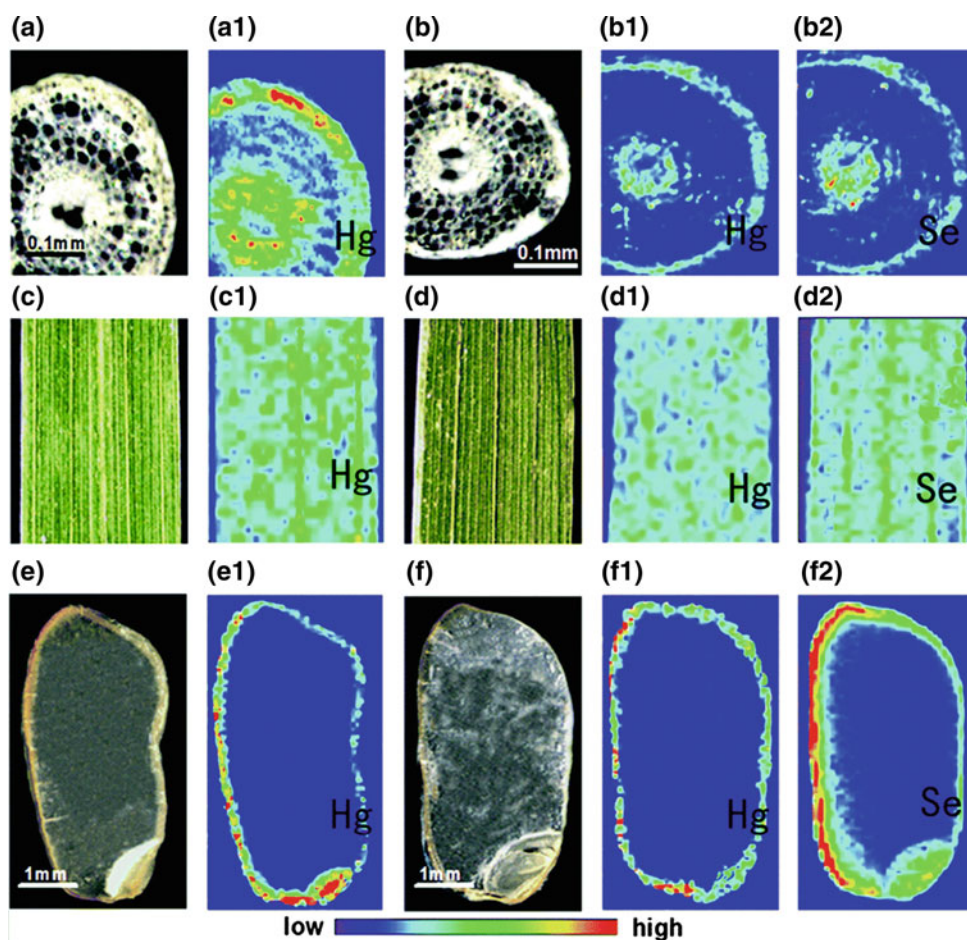
SRXRF with beam size at nanometer level has been applied to study the elemental imaging of Pt-stained human chromosome samples (Yan et al. 2016). Ag, Pt, Ba, and Cl were imaged in the chromosome with a single 2D raster imaging. High concentration of Ag was found, which came from the precursor used in the preparation process of the platinum blue stain due to an incomplete rinse during the preparation. The strong Ba signal corresponds to an unintended contamination particle introduced into the sample while Cl exists at multiple stages of the preparation process. The distribution of Pt is of the most interest since it binds to DNA. A large clump of Pt is seen, which results from excessive Pt accumulating along the edge of the sample as the stain evaporates. The nano SRXRF has also been applied to measure trace element (As, Ca, Cr, Cu, Fe, Mn, Ni, S, and Zn) distribution in *Spartina alterniflora* root epidermis and endodermis during dormancy (Feng et al. 2017). It was found that the elemental concentrations in the epidermis, outer endodermis, and inner endodermis were significantly different, with the levels of these elements higher in the endodermis than that in the epidermis. Furthermore, the elemental concentrations in the outer endodermis were significantly higher than those in the inner endodermis. These results suggest that the Casparian strip may play a role in governing the aplastic transport of these elements. Furthermore, most of the elements were found to be significantly correlated, suggesting that these elements may share the same transport pathways.

Besides the imaging of metals in organelles, cells, tissues, and organs, 2D SRXRF has also been applied to identify the metalloproteins after separation by two-dimensional gel electrophoresis. For example, the study on metalloproteins in human liver cytosol by SRXRF combined with gel filtration chromatography and isoelectric focusing separation found 2 Zn-containing bands, 11 Fe-containing bands, and some Cu-containing bands (Gao et al. 2005). The quantification of metals in metalloproteins was also possible. For example, the Se level in a total of 157 selenoproteins in Se-enriched yeast was found to be  $126.56 \mu\text{g/g}$ , which showed good recovery of Se in the selenoproteins (Zhao et al. 2015).

### 3.2 Three-Dimensional Imaging

Two-dimensional elemental mapping is performed along the sample surface. Therefore, the information retrieved is a product of the incident X-rays, penetration capability, and the self-absorption correction dependent on both the energy of the exciting radiation and the energy of the fluorescence radiation, which is not explicitly depth-sensitive. X-ray photons of sufficient energy can penetrate very deeply (in the

**Fig. 1** The distribution of Hg and Se in different tissues of rice measured by SRXRF. **a** The cross section of the root tip from rice under Hg exposure (**a1**, Hg XRF image); **b** the cross section of the root tip from rice under Hg and Se exposure (**b1**, Hg XRF image; **b2**, Se XRF image); **c** the leaf from Hg-exposed rice; **d** the leaf from Hg and Se co-exposed rice; **e** the rice grain from Hg-exposed rice; **f** the rice grain from Hg and Se co-exposed rice (Zhao et al. 2014b) Reproduced by permission of The Royal Society of Chemistry



order of several hundred microns, even mm range in soft materials) into the sample being analyzed (Kanngießer et al. 2007). Therefore, depth analysis using X-ray can be performed in a nondestructive and noninvasive way, which leads to three-dimensional (3D) imaging. 3D XRF imaging is achieved by one of two means; either specialized optics are used on both the X-ray source and detector (confocal XRF) (Kanngießer et al. 2003; Vincze et al. 2004) or via the use of pencil-shaped primary X-ray beams and reconstruction algorithms similar to those used in CT (i.e., SRXRF tomography) (Bleuet et al. 2010; Gan et al. 2006).

The confocal XRF has a depth resolution down to 10  $\mu\text{m}$  and detection limits of sub-mg/kg level (Janssens et al. 2004; Kanngießer et al. 2003; Kouichi Tsuji 2007; Muradin 2000; Vincze et al. 2004). Three-dimensional (3D) micro-XRF has been successfully applied in biological samples like the root of common duckweed (Kanngießer et al. 2007) and human joint bone (Zoeger et al. 2008) and heritage objects like ancient painting, ceramics, and Dead Sea Scroll parchment samples (Mantouvalou et al. 2011; Yi et al. 2016). One of the obvious advantages of confocal XRF is that the

elemental imaging in cross section can be achieved without the need to cut the samples into thin slices (Kanngießer et al. 2007).

The freshwater crustacean *Daphnia magna* is a frequently used ecotoxicological model organism to investigate the mechanisms of toxicity of metals. An ecotoxicological experiment was performed to determine in which tissues Zn accumulation occurs following exposure of *D. magna* to an elevated Zn concentration. Dynamic scanning confocal  $\mu\text{-XRF}$  was used to obtain virtual dorsoventral sections of the samples (De Samber et al. 2010). A distinct accumulation in the eggs, gut epithelium, ovaries, gills, and the carapace of the exposed *Daphnia* was found. Different subregions of interest, such as eggs (Fig. 2a), gut, and gill tissue (Fig. 2b) were also analyzed in more detail. Confocal micro-XRF can easily analyze the elemental distributions in different planes of interest. As shown in Fig. 2c, a sagittal section was visualized, enabling it to link specific metal accumulation patterns to corresponding biological/physiological features. Different hemoglobin currents inside the organism become confluent at the median dorsal ridge of the carapace (see Fig. 2a.i and c.i)

before returning to the pericardium around the heart (see Fig. 2c.ii). A more detailed analysis of the ovary located in the front of the gut (see Fig. 2b.iii and c.iii) regarding the reproductive toxicity of dietary Zn exposure.

The SRXRF tomography measurement is achieved through measuring a series of projected distributions under various angles and back projected using the appropriate mathematical algorithms (Gan et al. 2006; Vincze et al. 2001). Since this method involves rotation of the sample over 180° or 360° relative to the primary beam, it is limited to the investigation of relatively small objects. The spatial resolutions for XRF tomography are situated at the  $\mu\text{m}$  level or even less (Bleuet et al. 2010; Hansel et al. 2002b; Laforce et al. 2017).

SRXRF tomography has been used to characterize Fe plaques and associated metals on the surface of roots from the aquatic plants *Phalaris arundinacea* (reed canary grass) and *Typha latifolia* (cattail). By use of this technique, Pb and Fe were found to accumulate on the surface of the root in a similar pattern, forming a covering on the root surface while As was isolated to distinct regions on the exterior and interior of the root (Hansel et al. 2001, 2002a). Similarly, it was found that As was sequestered by Fe(III) oxyhydroxides within cattail root plaques from a contaminated wetland (Blute et al. 2004). However, because of the aquatic and metal excluding nature of the plants, these studies were limited to the roots only.

A Ni hyperaccumulator *Alyssum murale* “Kotodesh” was selected as a model to study the metal compartmentalization and concentration throughout plant tissues by SRXRF tomography (Fig. 3) (McNear et al. 2005). It was revealed that Ni is concentrated in stem and leaf dermal tissues and, together with Mn, in distinct regions associated with the

Ca-rich trichomes on the leaf surface (Fig. 3). In stems, nickel was concentrated in the xylem and absent from the phloem (Fig. 3) and cortex. In the root, Ni was isolated in the stele or vascular tissues of the finer root (Fig. 3 inset in root tomogram). The opposite pattern was seen for the coarser root, which is devoid of metals on the interior but covered in a “coating” of well-correlated Fe, Zn, and Ni.

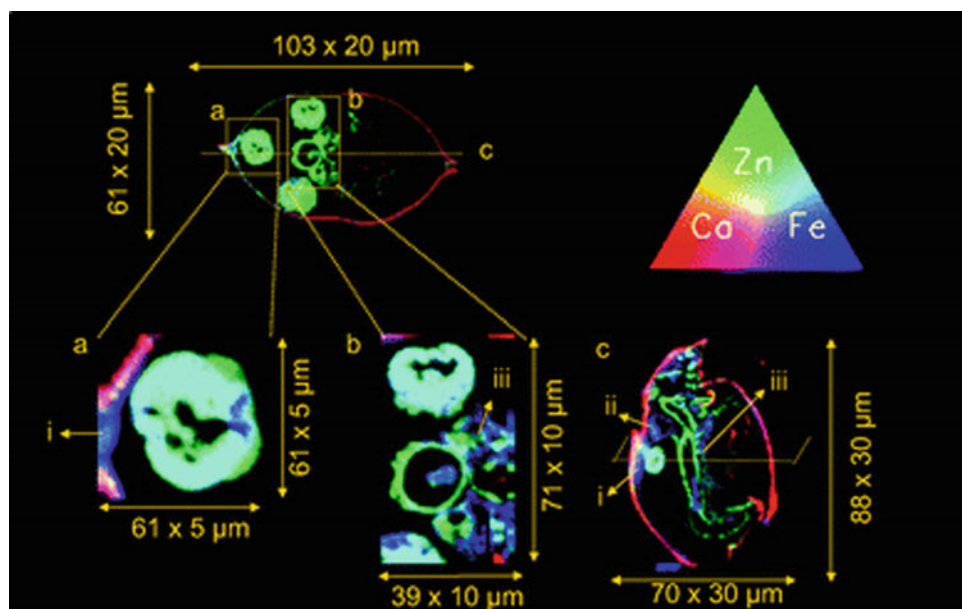
In general, SRXRF tomography involves long measuring times and challenging data treatment, making it a complex task for 3D determination/visualization of the elemental distributions within a given sample. In contrast, confocal XRF does not require a tomographic reconstruction procedure, and it enables the local analysis of arbitrary sub-volumes inside the sample (De Samber et al. 2010).

#### 4 Speciation of Metals

The biological effect of an element is not only dependent on the total concentration but also highly related to their chemical species. For example, dialkylmercury derivatives are extremely toxic while mercuric selenide has a relatively low toxicity and accumulates as an apparently benign detoxification product in marine animals (Wagemann et al. 1998), and methylmercury cysteine proves to be much less toxic than methylmercury chloride in a zebrafish larvae model system (Harris et al. 2003). The analytical activities of identifying and/or measuring the quantities of one or more individual chemical species in a sample are defined as speciation analysis by IUPAC (Templeton et al. 2000).

The general scheme for speciation analysis is as following: different species in samples are first extracted using acid, base, enzyme, or just diluted, then the extraction solution is

**Fig. 2** Illustration of the local analysis capabilities of confocal micro-XRF. The top image shows a dorsoventral scan through *Daphnia magna* (step size 20  $\mu\text{m}$ ). Detail a shows a scan of the egg (step size 5  $\mu\text{m}$ ). Detail b shows a detail of the gut and gill tissue (step size 10  $\mu\text{m}$ ). Detail c shows a sagittal scan through the sample. (i) Dorsal ridge of carapace, (ii) pericardium, (iii) ovary. Reproduced from Ref. De Samber et al. (2010) with permission from The Royal Society of Chemistry



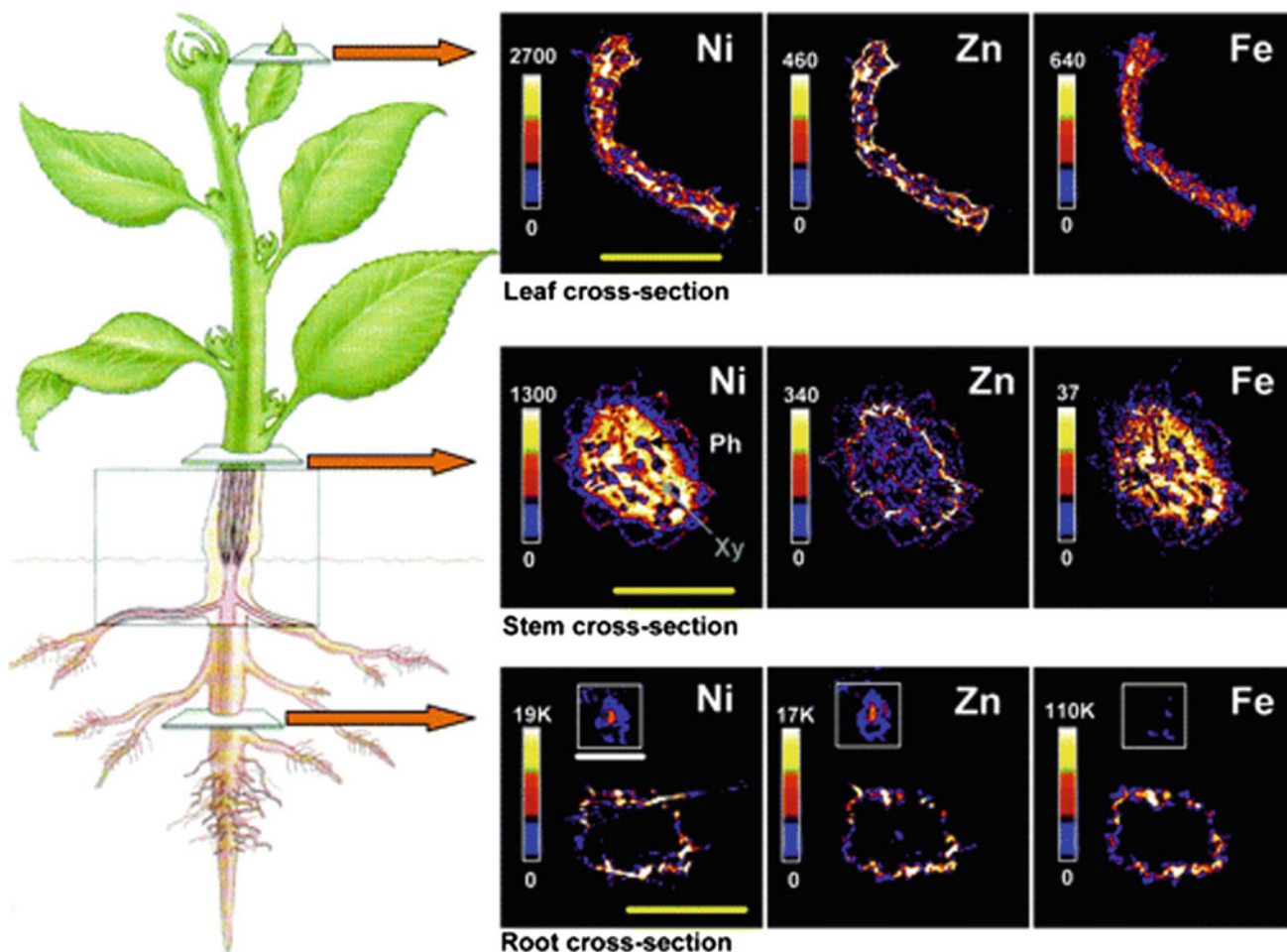


**Fig. 3** Ni, Fe, and Zn fluorescence CMT images of a leaf, stem, coarse, and fine root cross sections from *Alyssum murale* “Kotodesh”. Inset in root tomogram is of a finer root. The colorimetric scale maps region-specific relative metal concentrations ( $\mu\text{g/g}$ ) for each element, with brighter colors indicating areas of higher enrichment. The slight streakiness of the coarser root Ni image is most likely due to beam

hardening by very high Ni spots on the root surface. The lower thresholds for the tomograms were adjusted up slightly to suppress background noise and thereby improve image quality. The yellow scale bar represents  $\sim 500 \mu\text{m}$  and the white scale bar (root inset) represents  $\sim 100 \mu\text{m}$ . Reprinted with permission from (McNear et al. 2005). Copyright (2005) American Chemical Society

separated by the powerful selective separation techniques like HPLC, gas chromatography (GC), gel electrophoresis (GE), or electrochromatography (EC) and monitored by a sensitive and element-specific detector like ICP-MS and NAA (Chai et al. 2002; Li et al. 2007). However, the extraction process may destroy or change the chemical species in samples. Synchrotron-radiation-based X-ray absorption spectroscopy (XAS) provides an alternative which can study the chemical form of metals directly in gas phase, solution, or solid state (Chen et al. 2010; Li et al. 2008). This powerful technique for probing the local structure around almost any specific element in the periodic table (except the lightest) gives information on the number and chemical identities of near neighbors and the average interatomic distances without the requirement for preparation of crystalline samples.

Typical X-ray absorption spectra generally have three regions, including the pre-edge, X-ray absorption near-edge structure (XANES), including the first 50–150 eV after the absorption edge and extended X-ray absorption fine structure (EXAFS), which can be detected in suitable samples till 1000 eV and more behind the edge, respectively (Koningsberger and Prins 1988).

#### 4.1 Qualitative and Quantitative Speciation of Metals

XANES spectra can be used to determine the average oxidation state of the element and the coordination environment of the absorbing atom in the sample. By comparing to

known references, the oxidation state of metals in unknown samples could be identified.

It is known that methylmercury in fish is the primary dietary source for the general public. A comparison of the Hg L<sub>III</sub> XANES spectrum of swordfish skeletal muscle with the solution spectra of selected standard compounds found that the chemical form of methylmercury should be methylmercury cysteine, which is much less toxic than methylmercury chloride (Harris et al. 2003). More examples include Se metabolism of the purple bacterium *Rhodobacter sphaeroides* (Van Fleet-Stalder et al. 2000), reduction of As in Indian Mustard (Pickering et al. 2000a), Fe oxidation states in tissues (Kwiatak et al. 2001), Mn in mitochondria isolated from brain, liver, and heart (Gunter et al. 2004), Cu and Zn intake by *Bradybaena similaris* (land snail) (Yasoshima et al. 2001), Ni speciation in hyperaccumulator and non-accumulator *Thlaspi* species (Kramer et al. 2000), and Cu and Zn in copper–zinc superoxide dismutase isoforms (Chevreux et al. 2008).

XANES can also be applied to quantitative speciation. This is because XAS is a local probe technique, which implies no long-range order in sample is required. For many systems, XANES analysis based on linear combinations of known spectra from “model compounds” is sufficient to estimate ratios of different species.

Selenium (Se)-enriched yeast has probably been the most widely investigated food supplement. The direct speciation of Se species with minimal pretreatment steps was carried out with XANES. By comparison of the XAS spectra of Se-enriched yeast samples with that of the standard Se species, organic R–Se–R (represented by selenomethionine) was found to be the main chemical form of Se (Fig. 4). Quantitative speciation through principal component analysis (PCA) and least-squares linear combination (LC) fitting the Se-enriched yeast samples found 83, 85, and 81% of R–Se–R (probably selenomethionine which is known to exist in yeast) for commercial Se-enriched yeast, which is in agreement with those from HPLC–ICP–MS analysis (Li et al. 2010). The quantitative speciation of Se species was also got in stream insects. Organic selenides (R–Se–R), modeled as selenomethionine, were found to be the most abundant among all selenium compounds tested, ranging from 36 to 98%. Together with organic diselenides (R–Se–Se–R), these organic forms account for more than 85% of selenium in all nymphal and larval insects measured (Andrahennadi et al. 2007).

## 4.2 Spatial Speciation of Metals

Spatial analysis of absorbing atoms of interest is fascinating in elucidating the uptake and biotransformation of different species. The transformation of arsenic (Na<sub>2</sub>HAsO<sub>4</sub> or

NaAsO<sub>2</sub>) by arsenic hyperaccumulator, Cretan brake (*Pteris cretica* L. var *nervosa* Thunb) was studied (Huang et al. 2004). It was found that As<sup>5+</sup> tended to be reduced to As<sup>3+</sup> after it was taken up into the root, and arsenic was kept as As<sup>3+</sup> when it was transported to the above-ground tissues like petioles and pinnae.

A combination of XAS with elemental imaging techniques like SRXRF can provide speciation information at specific locations of interest (Yun et al. 1998; Zhao et al. 2014a). *Cardamine ensheensis* is a Se hyperaccumulator plant found in Enshi, a typical seleniferous area in southwestern Hubei Province, Central China. The spatial speciation of Se in roots, shoots, and leaves of *C. ensheensis* was studied using SRXRF and in situ Se K-edge XANES (Cui et al. 2018). It was found that Se was primarily located in the cortex, endodermis, and vascular cylinder in roots, though it was also in the epidermis, cortex, and vascular bundle of shoots and concentrated in the leaf veins and the peripheral parts. In situ XANES analysis showed that the root vascular tissue contained 16% SeO<sub>4</sub><sup>2-</sup>, 19% C–Se<sup>-</sup> (using selenocysteine, SeCys as model compound) and 65% C–Se–C (using methylselenocysteine, MeSeCys as model compound), and shoot vascular bundle contained 10% SeO<sub>4</sub><sup>2-</sup>, 28% C–Se<sup>-</sup> and 62% C–Se–C while leaves had 84% C–Se<sup>-</sup> and 16% SeO<sub>3</sub><sup>2-</sup> (Fig. 5).

## 4.3 Chemical Speciation Imaging

XAS can also be applied in chemically specific imaging. In the soft X-ray region, scanning transmission X-ray microscopy (STXM) is used in an approach called XANES “stack” imaging, as a stack of repeated 2D scans is acquired. Changing the incident photon energy and taking images with other photon energies gives an image sequence that includes both chemical information and topographical information. The third dimension becomes the XANES spectra, and each spatial pixel in the image contains a XANES spectrum and spatially resolved chemical speciation information (Lombi et al. 2011).

In the hard X-ray region, the fluorescence signal is often used when acquiring XANES spectra. The spatial distribution and chemical species of selenium in another Se hyperaccumulator *Astragalus bisulcatus* (two-grooved poison or milk vetch), a plant capable of accumulating up to 0.65% of its shoot dry biomass as Se in its natural habitat was studied by selectively tuning incident X-ray energies close to the Se K-absorption edge (Pickering et al. 2000b). Plants exposed to selenate for 28 days contained predominantly selenate in the mature leaf tissue, whereas the young leaves and the roots almost exclusively contained organoselenium, indicating that the ability to biotransform selenate is either inducible or developmentally specific. The concentration of

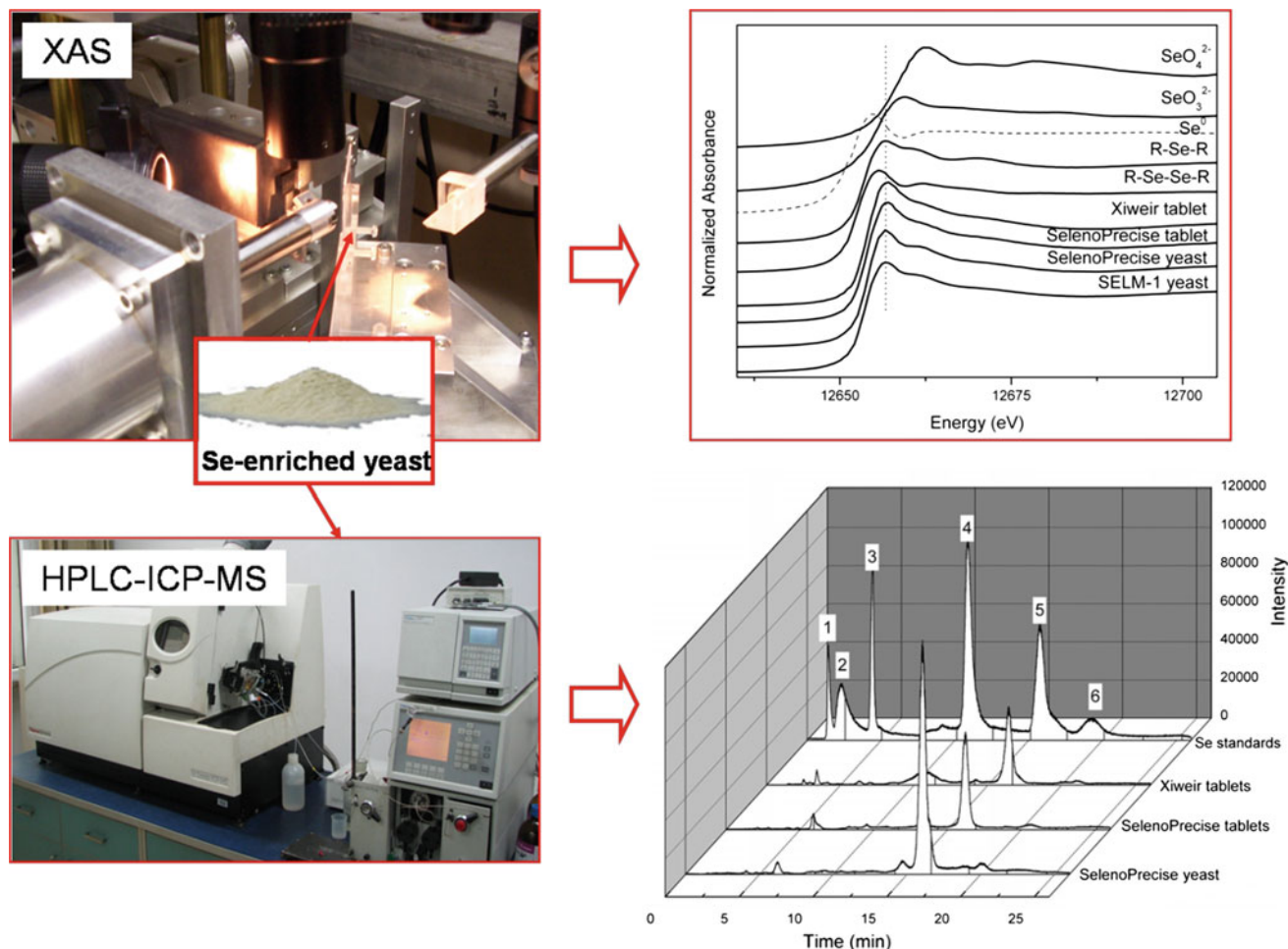


**Fig. 4** Se K near-edge spectra of standards species and yeast samples and chromatogram of Se standards ( $50 \mu\text{g Se L}^{-1}$ ) and enzymatic extracts of Se-enriched yeasts and tablets.  $\text{SeO}_4^{2-}$  (selenate),  $\text{SeO}_3^{2-}$  (selenite),  $\text{Se}^0$  (elemental Se), R–Se–R (selenomethionine), R–Se–Se–R (selenocystine). Column: Symmertryshield RP18,  $150 \times 3.9 \text{ mm}$ ,

mobile phase: 0.3%  $\text{CH}_3\text{OH} + 0.1\% \text{ HFBA}$ , flow rate:  $1 \text{ mL min}^{-1}$ , injection volume:  $100 \mu\text{L}$ . The Se standards are selenite (1), selenate (2), selenocystine (3), selenourea (4), selenomethionine (5), and selenocystamine (6) (Li et al. 2010). Reproduced by permission of The Royal Society of Chemistry

organoselenium in the majority of the root tissue was much lower than that of the youngest leaves, and isolated areas on the extremities of the roots contained concentrations of organoselenium of an order of magnitude greater than the rest of the root (Fig. 6).

## 5 Structure Characterization of Metal-Binding Biomolecules

In structure characterization of metalloproteins, protein crystallography (PX) is the most powerful tool for the determination of macromolecular 3D structure at a resolution of 0.15–2 nm. However, few studies at a higher resolution could be found up to now owing to: (i) the limited diffraction power of most crystals; (ii) photoreduction, or radiation damage, of the protein during data collection; and (iii) microheterogeneity of

samples (Ascone et al. 2005). This is not sufficient for illuminating the structural basis related to activities of the metal centers in functional metalloproteins, where the structural changes to the metal coordination during redox or substrate-binding reactions happen generally at  $\leq 0.01 \text{ nm}$ . On the other hand, XAS provides an alternative tool for the local structure around certain atoms at a resolution of as low as 1 femtometer, depending on the circumstances (Aksenov et al. 2001; Dalba et al. 1999; Pettifer et al. 2005). The combination of crystallographic information and XAS, specifically EXAFS, is a powerful approach for studying the structure–function relationship of proteins, particularly when subtle structural changes are associated with a chemical reaction. Cheung et al. made direct use of three-dimensional information from crystal structures of azurin in the analysis of EXAFS data for the oxidized and reduced form of the protein (Cheung et al. 2000). Subtle structural changes ( $<0.01 \text{ nm}$ ) take place at

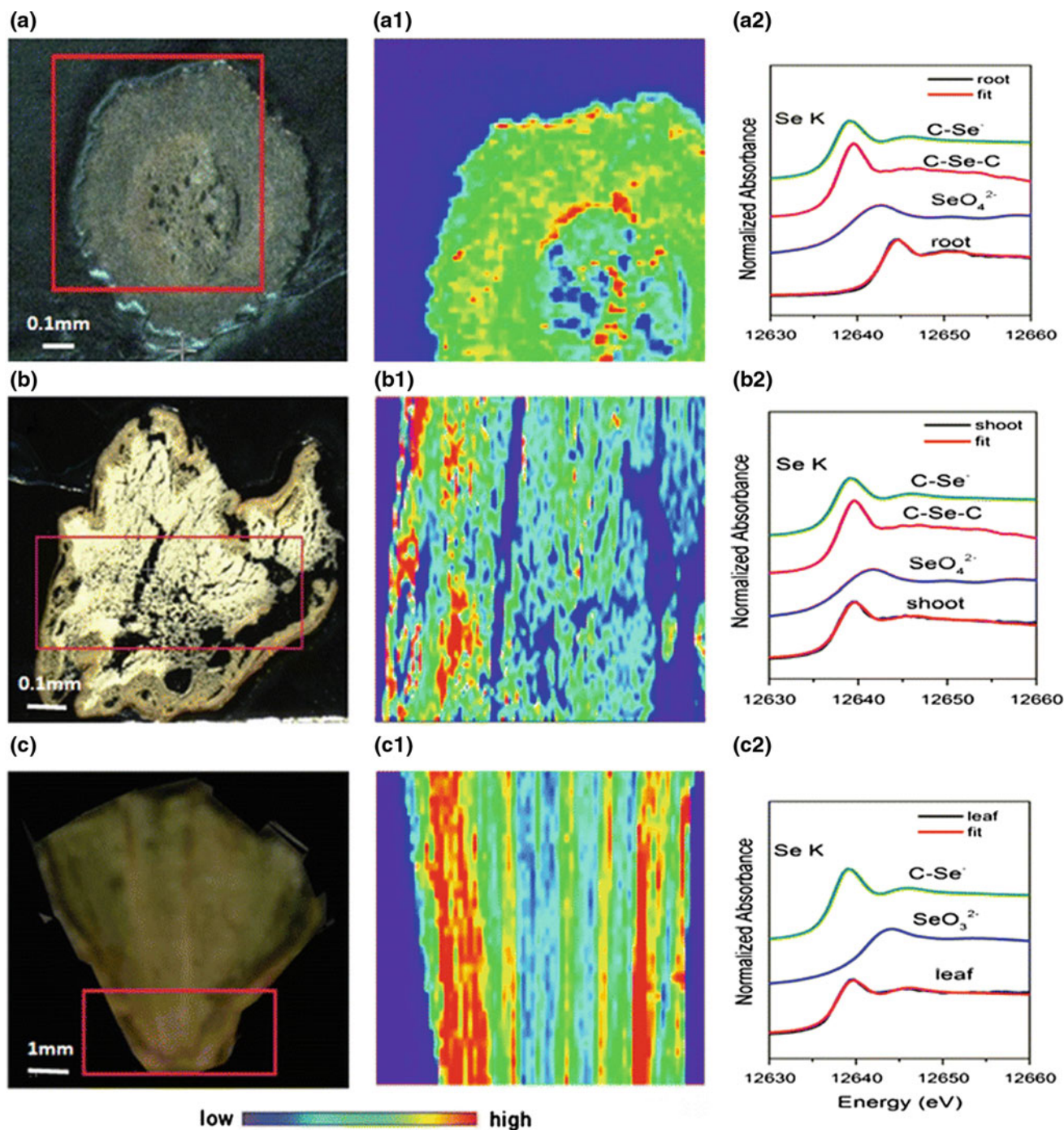


**Fig. 5** Optical image,  $\mu$ -SRXRF mapping of Se and least-square fitting of  $\mu$ -XANES spectra for roots (cross section, **a**, **a1**, **a2**), shoots (cross section, **b**, **b1**, **b2**), and leaves (**c**, **c1**, **c2**) in *C. enshiensis*. The red boxed area in **a**, **b**, and **c** is those for  $\mu$ -SRXRF mapping in **a1**, **b1**, and **c1**. In **a2**, **b2** and **c2**,  $\text{SeO}_3^{2-}$  (selenite),  $\text{SeO}_4^{2-}$  (selenate), C–Se<sup>–</sup> (using

selenocystine as model compound), and C–Se–C (using methylselenocysteine as model compound) were used for least-square fitting. Reprinted by permission from (Cui et al. 2018). Copyright (2018) Springer

the Cu site during a single-electron redox process. This approach is likely to be of most interest in cases where crystallographic information is available for some state of a protein. Under such conditions, EXAFS data on different states of the protein may be solved by the combined approach to predict

structural changes and examine how these intermediated states perturb the metal at the catalytic site.

XAS can also provide additional information for PX. An example is described for formate dehydrogenaseH (FDHH) of *Escherichia coli* containing molybdenum and

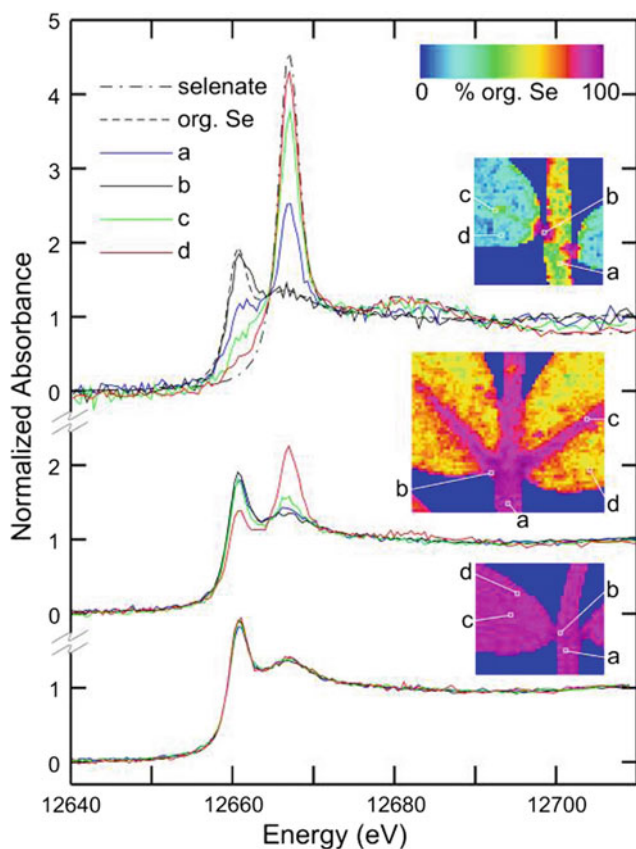


**Fig. 6** Spatially resolved X-ray absorption near-edge spectra recorded by using a  $100 \times 100 \mu\text{m}^2$  beam from selected portions of mature (Top), intermediate (Middle), and young (Bottom) leaves. The spectra of selenate and selenomethionine (org. Se) are also included. The Insets show maps of the percentage of total Se as organoselenium (balance selenate) and indicate the spatial location for the spectra. The percentages of selenate in each leaf specimen as determined by near-edge fitting for **a** (stem), **b** (petiole), **c** (mid-vein), and **d** (leaf blade), respectively, are mature 36, 0, 69, 88; intermediate 3, 0, 7, 28; young 3, 0, 1, 1 (Pickering et al. 2000b). Copyright (2000) National Academy of Sciences

selenocysteine at its active site (George et al. 1998b). The crystal structure was reported indicating an unusual des-oxo molybdenum site with four MoS ligands at 0.24 nm, one MoOH (or MoOH<sub>2</sub>) at 0.21 nm, and a coordinated selenocysteine with MoSe of 0.26 nm (Boyington et al. 1997). A des-oxo molybdenum site with four MoS (0.235 nm), one MoO (0.210 nm), and one MoSe ligand (0.262 nm) has been confirmed by subsequent EXAFS analysis at the Mo K-edge (George et al. 1998a). Selenium EXAFS at the Se K-edge is also in good accordance with that of molybdenum and, furthermore, indicates the presence of SeS ligation at 0.219 nm, which had been missed in the crystal structure (George et al. 1998a). The crystallographic analysis suggested a close Se...S contact of 0.29 nm with one of the MoS ligands. EXAFS, however, indicated that the active site of the formate dehydrogenase H of *E. coli* contained a novel

seleno-sulfide ligand to molybdenum, whereas sulfur was likely originated from one MoS ligand (George et al. 1998a, b).

The three-dimensional structure determinations of biological macromolecules such as proteins and nucleic acids by PX have improved our understanding of many of the mysteries involved in biological processes. At the same time, these results have clearly reinforced the commonly held belief that H atoms and water molecules around proteins and nucleic acids play a very important role in many physiological functions. However, since it is very hard to identify H atoms accurately in protein molecules by X-ray diffraction alone, a detailed discussion of protonation and hydration sites can only be based upon speculations so far. In contrast, it is well known that neutron diffraction (NS) provides an experimental method of directly locating H atoms (Niimura and Bau 2008). The combination of NS, PX, and XAS can give the structural information including both the locating of H atoms and metal atoms (Winterer et al. 2002).

High-throughput (HT) techniques of structural characterization using XAS have been proposed. Scott and co-workers (Scott et al. 2005) designed a 25-well sample holder with 1.5 mm-diameter holes in a  $5 \times 5$  arrangement on a 100 wide polycarbonate holder that fits into a liquid helium-flow XAS cryostat. With the beam apertured to 1 mm  $\times$  1 mm, the cryostat and sample holder are rastered first to align the wells, then the metal distribution is determined with a multi-channel energy-discriminating solid-state fluorescence detector. The elemental distribution maps detected by XRF are used to target protein samples for further speciation (by XANES) and structural analysis (by EXAFS) with a 30-element intrinsic germanium detector. As a feasibility study, a significant fraction of the B2200 open reading frames (ORF) in the *Pyrococcus furiosus* (Pf) genome has been individually cloned, tagged, expressed, and purified by high-throughput techniques. Up to 25 Pf ORF products are loaded (3 mL per well, protein concentration 0.2–1 mM) in a single run. Two Ni-containing proteins and one Zn-containing protein are detected by XRF. Ni XANES speciation clearly differentiates the types of Ni binding sites and Zn EXAFS structural analysis, which shows the sensitivity available for determining metal-site structures.

## 6 Conclusions

In this chapter, state-of-the-art synchrotron-based techniques in quantification, imaging, speciation of metals, and structure characterization of metal-binding biomolecules in environmental and biological samples are introduced. SRXRF is a nondestructive, multielemental analytical technique based on the detection of characteristic fluorescence



after being excited by a primary particle beam with sufficient energy, which has been used in quantification of metals in different samples. The focused synchrotron-based X-ray has been applied to image metals down to nm resolution at two or three dimensions. XAS can probe the local structure around almost any specific element in the periodic table, which has been used for chemical speciation of different metals. In combination with SRXRF, it can also realize spatial and chemical imaging. The structure of metal-binding biomolecules can be characterized by PX and/or XAS.

The long exposure to X-ray beam could cause damage to the samples, especially the biological samples, which may cause significant artifacts in both element distribution and chemical speciation. It is therefore essential to preserve the sample using cryogenic conditions or preferably through reducing the radiation dose by using fast detector technologies. This can drastically reduce the exposure duration and radiation doses (Lombi et al. 2011). The development of next generation of modern synchrotron sources and high efficiency of multi-element detector will greatly improve the resolution and sensitivity for metals in environmental and biological samples (Yuan et al. 2019).

**Acknowledgements** The authors are grateful for the financial support from Ministry of Science and Technology of China (2016YFA0201600), National Natural Science Foundation of China (11475196), and Guizhou Department of Science and Technology (No. QKH-2016-2804). We gratefully acknowledge the staff from Beijing Synchrotron Radiation Facility, Shanghai Synchrotron Radiation Facility and National Synchrotron Radiation Laboratory for beam time allocation and assistance during data collection.

## References

- Aksenov VL, Kuzmin AY, Purans J, Tyutyunnikov SI (2001) EXAFS spectroscopy at synchrotron-radiation beams. *Phys Part Nucl* 32:1–33
- Andrahennadi R, Wayland M, Pickering IJ (2007) Speciation of selenium in stream insects using X-ray absorption spectroscopy. *Environ Sci Technol* 41:7683–7687. <https://doi.org/10.1021/es071399v>
- Arora M, Kennedy BJ, Ryan CG, Boadle RA, Walker DM, Harland CL, Lai B, Cai Z, Vogt S, Zoellner H, Chan SWY (2007) The application of synchrotron radiation induced X-ray emission in the measurement of zinc and lead in Wistar rat ameloblasts. *Arch Oral Biol* 52:938–944. <https://doi.org/10.1016/j.archoralbio.2007.04.003>
- Ascone I, Fourme R, Hasnain S, Hodgson K (2005) Metallogenomics and biological X-ray absorption spectroscopy. *J Synchrotron Rad* 12:1–3
- Bai X, Li Y, Liang X, Li H, Zhao J, Li Y-F, Gao Y (2019) Botanic metallomics of mercury and selenium: Current understanding of mercury-selenium antagonism in plant with the traditional and advanced technology. *Bull Environ Contam Toxicol* 102:628–634. <https://doi.org/10.1007/s00128-019-02628-8>
- Bandhu HK, Dani V, Garg ML, Dhawan DK (2006) Hepatoprotective role of zinc in lead-treated, protein-deficient rats. *Drug Chem Technol* 29:11–24. <https://doi.org/10.1080/01480540500408507>
- Becker JS, Zoriy M, Przybylski M, Becker JS (2007) High resolution mass spectrometric brain proteomics by MALDI-FTICR-MS combined with determination of P, S, Cu, Zn and Fe by LA-ICP-MS. *Int J Mass Spectrom* 261:68–73
- Bleuet P, Gergaud P, Lemelle L, Bleuet P, Tucoulou R, Cloetens P, Susini J, Delette G, Simionovici A (2010) 3D chemical imaging based on a third-generation synchrotron source. *TrAC Trends Anal Chem* 29:518–527. <https://doi.org/10.1016/j.trac.2010.02.011>
- Blute NK, Brabander DJ, Hemond HF, Sutton SR, Newville MG, Rivers ML (2004) Arsenic sequestration by ferric Iron plaque on Cattail toots. *Environ Sci Technol* 38:6074–6077. <https://doi.org/10.1021/es049448g>
- Boyington JC, Gladyshev VN, Khangulov SV, Stadtman TC, Sun PD (1997) Crystal structure of Formate Dehydrogenase H: Catalysis involving Mo, molybdopterin, selenocysteine, and an Fe4S4 cluster. *Science* 275:1305–1308. <https://doi.org/10.1126/science.275.5304.1305>
- Cantino ME, Hutchinson TE (1982) Electron probe X-ray microanalysis. *Trends Biochem Sci* 7:132–134. [https://doi.org/10.1016/0968-0004\(82\)90201-8](https://doi.org/10.1016/0968-0004(82)90201-8)
- Chai Z, Zhu H (eds) (1994) Introduction to trace element chemistry. Atomic Energy Press, Beijing
- Chai Z, Sun J, Ma S (1992) Neutron activation analysis in environmental sciences, biological and geological sciences. Atomic Energy Press, Beijing
- Chai Z, Mao X, Hu Z, Zhang Z, Chen C, Feng W, Hu S, Ouyang H (2002) Overview of the methodology of nuclear analytical techniques for speciation studies of trace elements in the biological and environmental sciences. *Anal Bioanal Chem* 372:407–411
- Chen C, Chai Z, Gao Y (2010) Nuclear analytical techniques for metallomics and metalloproteomics. RSC publishing, Cambridge
- Cheung KC, Strange RW, Hasnain SS (2000) 3D EXAFS refinement of the Cu site of structural change at the metal centre in an oxidation-reduction process: an integrated approach combining EXAFS and crystallography. *Acta Crystallogr D* 56:697–704
- Chevreaux S, Roudeau S, Frayssé A, Carmona A, Devès G, Solari PL, Weng TC, Ortega R (2008) Direct speciation of metals in copper-zinc superoxide dismutase isoforms on electrophoresis gels using X-ray absorption near edge structure. *J Anal At Spectrom* 23:1117–1120
- Cui L, Zhao J, Chen J, Zhang W, Gao Y, Li B, Li Y-F (2018) Translocation and transformation of selenium in hyperaccumulator plant *Cardamine ensliensis* from Enshi, Hubei, China. *Plant Soil* 425:577–588. <https://doi.org/10.1007/s11104-018-3587-8>
- Dalba G, Fornasini P, Grisenti R, Purans J (1999) Sensitivity of extended X-ray-absorption fine structure to thermal expansion. *Phys Rev Lett* 82:4240
- De Samber B, Silversmit G, De Schampelaere K, Evens R, Schoonjans T, Vekemans B, Janssen C, Masschaele B, Van Hoorebeke L, Szalóki I, Vanhaecke F, Rickers K, Falkenberg G, Vincze L (2010) Element-to-tissue correlation in biological samples determined by three-dimensional X-ray imaging methods. *J Anal At Spectrom* 25:544–553. <https://doi.org/10.1039/B918624G>
- Devos W, Senn-Luder M, Moor C, Salter C (2000) Laser ablation inductively coupled plasma mass spectrometry (LA-ICP-MS) for spatially resolved trace analysis of early-medieval archaeological iron finds. *Fresenius' J Anal Chem* 366:873–880
- Fahrni CJ (2007) Biological applications of X-ray fluorescence microscopy: exploring the subcellular topography and speciation of transition metals. *Curr Opin Chem Biol* 11:121–127
- Feng H, Qian Y, Cochran JK, Zhu Q, Hu W, Yan H, Li L, Huang X, Chu YS, Liu H, Yoo S, Liu C-J (2017) Nanoscale measurement of trace element distributions in *Spartina alterniflora* root tissue during dormancy. *Sci Rep* 7:40420. <https://doi.org/10.1038/srep40420>

- Gan H, Gao H, Zhu H, Chen J, Zhu P, Xian D (2006) X-ray fluorescence tomography. *Laser Optoelectr Prog* 43:56–64
- Gao Y, Liu Y, Chen C, Li B, He W, Huang Y, Chai Z (2005) Combination of synchrotron radiation X-ray fluorescence with isoelectric focusing for study of metalloprotein distribution in cytosol of hepatocellular carcinoma and surrounding normal tissues. *J Anal At Spectrom* 20:473–475
- George GN, Colangelo CM, Dong J, Scott RA, Khangulov SV, Gladyshev VN, Stadtman TC (1998a) X-ray absorption spectroscopy of the molybdenum site of escherichia coli formate dehydrogenase. *J Am Chem Soc* 120:1267–1273
- George GN, Hedman B, Hodgson KO (1998b) An edge with XAS. *Nat Struct Biol* 5:645–647
- Gordon BM, Hanson AL, Jones KW, Pounds JG, Rivers ML, Schidlovsky G, Spanne P, Sutton SR (1990) The application of synchrotron radiation to microprobe trace-element analysis of biological samples. *Nucl Instrum Methods Phys Res B* 45:527–531. [https://doi.org/10.1016/0168-583X\(90\)90892-X](https://doi.org/10.1016/0168-583X(90)90892-X)
- Groma V, Osan J, Alseccz A, Torok S, Meirer F, Strelci C, Wobruschek P, Falkenberg G (2008) Trace element analysis of airport related aerosols using SR–TXRF. *Quart J Hung Meteorol Service* 112:83–97
- Gunter TE, Miller LM, Gavin CE, Eliseev R, Salter J, Buntinas L, Alexandrov A, Hammond S, Gunter KK (2004) Determination of the oxidation states of manganese in brain, liver, and heart mitochondria. *J Neurochem* 88:266
- Hansel CM, Fendorf S, Sutton S, Newville M (2001) Characterization of Fe plaque and associated metals on the roots of mine-waste impacted aquatic plants. *Environ Sci Technol* 35:3863–3868. <https://doi.org/10.1021/es0105459>
- Hansel CM, La Force MJ, Fendorf S, Sutton S (2002a) Spatial and temporal association of As and Fe species on aquatic plant roots. *Environ Sci Technol* 36:1988–1994. <https://doi.org/10.1021/es015647d>
- Hansel CM, La Force MJ, Fendorf S, Sutton S (2002b) Spatial and temporal association of As and Fe species on aquatic plant roots. *Environmen Sci Technol* 36:1988–1994
- Harris HH, Pickering IJ, George GN (2003) The chemical form of mercury in fish. *Science* 301:1203–1203 <https://doi.org/10.1126/science.1085941>
- Hu L, He B, Wang Y, Jiang G, Sun H (2013) Metallomics in environmental and health related research: Current status and perspectives. *Chin Sci Bull* 58:169–176. <https://doi.org/10.1007/s11434-012-5496-1>
- Huang Y, Wu Y, Zhao L, Li G, He W, Yuan L, Chen J, Li J, Zhang T, Cao E (2001) Beijing synchrotron radiation total-reflection X-ray fluorescence analysis facility and its applications on trace element study of cells. *Spectrochim Acta B* 56:2057–2062. [https://doi.org/10.1016/S0584-8547\(01\)00283-X](https://doi.org/10.1016/S0584-8547(01)00283-X)
- Huang Z, Chen T, Lei M, Hu T, Huang Q (2004) EXAFS study on arsenic species and transformation in arsenic hyperaccumulator. *Sci China C Life Sci* 47:124–129
- Ide-Ektessabi A, Fujisawa S, Sugimura K, Kitamura Y, Gotoh A (2002) Quantitative analysis of zinc in prostate cancer tissues using synchrotron radiation microbeams. *X-Ray Spectrom* 31:7–11
- Iida A (1997) X-ray spectrometric applications of a synchrotron X-ray microbeam. *X-Ray Spectrom* 26:359–363
- Iida A, Noma T (1993) Synchrotron X-ray muprobe and its application to human hair analysis. *Nucl Instrum Methods Phys Res Sec B* 82:129–138
- Ishii K, Matsuyama S, Watanabe Y, Kawamura Y, Yamaguchi T, Oyama R, Momose G, Ishizaki A, Yamazaki H, Kikuchi Y (2007) 3D-imaging using micro-PIXE. *Nucl Instrum Methods Phys Res, Sect A* 571:64–68
- Jackson B, Harper S, Smith L, Flinn J (2006) Elemental mapping and quantitative analysis of Cu, Zn, and Fe in rat brain sections by laser ablation ICP–MS. *Anal Bioanal Chem* 384:951–957
- Janssens K, Proost K, Falkenberg G (2004) Confocal microscopic X-ray fluorescence at the HASYLAB microfocus beamline: characteristics and possibilities. *Spectrochim Acta B* 59:1637–1645
- Jenkins R (1999) X-ray fluorescence spectrometry. Wiley, New York
- Ji A (2012) Development of X-ray fluorescence spectrometry in the 30 Years. *Rock Mineral Anal* 31:383–398
- Johansson E (1989) PIXE: a novel technique for elemental analysis. *Endeavour* 13:48–53
- Johansson E, Lindh U, Johansson H, Sundstrom C (1987) Micro-PIXE analysis of macro-and trace elements in blood cells and tumors of patients with breast cancer. *Nucl Instrum Methods Phys Res* 22:179–183
- Kang S, Shen X, Yao K, Sun X, Ju X, Huang Y, Xian D, Sun L, Wu Z (2001) SR–XRF in analysis of the trace elements in plants. *Progr Nat Sci* 11:273–277
- Kang D, Amarasingwardena D, Goodman A (2004) Application of laser ablation–inductively coupled plasma–mass spectrometry (LA–ICP–MS) to investigate trace metal spatial distributions in human tooth enamel and dentine growth layers and pulp. *Anal Bioanal Chem* 378:1608–1615
- Kanngießer B, Malzer W, Reiche I (2003) A new 3D micro X-ray fluorescence analysis set-up - first archaeometric applications. *Nucl Instrum Methods Phys Res B* 211:259–264
- Kanngießer B, Malzer W, Pagels M, Lühl L, Weseloh G (2007) Three-dimensional micro-XRF under cryogenic conditions: a pilot experiment for spatially resolved trace analysis in biological specimens. *Anal Bioanal Chem* 389:1171–1176
- Koningsberger DC, Prins R (1988) X-ray absorption: principles, applications, techniques of EXAFS, SEXAFS and XANES. John Wiley and Sons Inc., New York
- Kouchi Tsuji KN (2007) Development of confocal 3D micro-XRF spectrometer with dual Cr–Mo excitation. *X-Ray Spectrom* 36:145–149
- Kramer U, Grime GW, Smith JAC, Hawes CR, Baker AJM (1997) Micro-PIXE as a technique for studying nickel localization in leaves of the hyperaccumulator plant *Alyssum lesbiacum*. *Nucl Instrum Methods Phys Res B* 130:346–350
- Kramer U, Pickering IJ, Prince RC, Raskin I, Salt DE (2000) Subcellular localization and speciation of nickel in hyperaccumulator and non-Accumulator *Thlaspi* Species. *Plant Physiol* 122:1343–1354. <https://doi.org/10.1104/pp.122.4.1343>
- Kwiatk WM, Galka M, Hanson AL, Paluszkiwicz C, Cichocki T (2001) XANES as a tool for iron oxidation state determination in tissues. *J Alloys Compounds* 328:276–282
- Laforce B, Masschaele B, Boone MN, Schaubroeck D, Dierick M, Vekemans B, Walgraeve C, Janssen C, Cnudde V, Van Hoorebeke L, Vincze L (2017) Integrated three-dimensional microanalysis combining X-ray microtomography and X-ray fluorescence methodologies. *Anal Chem* 89:10617–10624. <https://doi.org/10.1021/acs.analchem.7b03205>
- Lee KJ, Nallathamby PD, Browning LM, Osgood CJ, Xu X-HN (2007) In vivo imaging of transport and biocompatibility of single silver nanoparticles in early development of zebrafish embryos. *ACS Nano* 1:133–143. <https://doi.org/10.1021/nn700048y>
- Leitão RG, Palumbo A, Souza PAVR, Pereira GR, Canellas CGL, Anjos MJ, Nasciutti LE, Lopes RT (2014) Elemental concentration analysis in prostate tissues using total reflection X-ray fluorescence. *Rad Phys Chem* 95:62–64
- Li Y-F, Chen C, Li B, Wang Q, Wang J, Gao Y, Zhao Y, Chai Z (2007) Simultaneous speciation of selenium and mercury in human urine samples from long-term mercury-exposed populations with

- supplementation of selenium-enriched yeast by HPLC-ICP-MS. *J Anal At Spectrom* 22:925–930
- Li Y-F, Chen C, Li B, Li W, Qu L, Dong Z, Nomura M, Gao Y, Zhao J, Hu W, Zhao Y, Chai Z (2008) Mercury in human hair and blood samples from people living in Wanshan mercury mine area, Guizhou, China: An XAS study. *J Inorg Biochem* 102:500–506
- Li Y-F, Gao Y, Chen C, Li B, Zhao Y, Chai Z (2009) High throughput analytical techniques in metallomics and the perspectives. *Sci Sin Chim* 39:1–10
- Li Y-F, Wang X, Wang L, Li B, Gao Y, Chen C (2010) Direct quantitative speciation of selenium in selenium-enriched yeast and yeast-based products by X-ray absorption spectroscopy confirmed by HPLC-ICP-MS. *J Anal At Spectrom* 25:426–430
- Li Y-F, Zhao J, Li Y, Li H, Zhang J, Li B, Gao Y, Chen C, Luo M, Huang R, Li J (2015a) The concentration of selenium matters: a field study on mercury accumulation in rice by selenite treatment in Qingzhen, Guizhou, China. *Plant Soil* 391:195–205. <https://doi.org/10.1007/s11104-015-2418-4>
- Li Y-F, Zhao J, Li Y, Xu X, Cui L, Zhang B, Shan S, Geng Y, Li J, Li B, Gao Y (2015b) Studies on the environmental health effects and ecotoxicology of mercury by synchrotron radiation-based techniques. *Sci Sin Chim* 45:1–17
- Li Y-F, Zhao J, Qu Y, Gao Y, Guo Z, Liu Z, Zhao Y, Chen C (2015c) Synchrotron radiation techniques for nanotoxicology. *Nanomed Nanotechnol Biol Med* 11:1531–1549. <https://doi.org/10.1016/j.nano.2015.04.008>
- Li Y-F, Sun H, Chen C, Chai Z (2016a) *Metallomics*. Science Press, Beijing
- Li Y, Zhao J, Zhang B, Liu Y, Xu X, Li Y-F, Li B, Gao Y, Chai Z (2016b) The influence of iron plaque on the absorption, translocation and transformation of mercury in rice (*Oryza sativa* L.) seedlings exposed to different mercury species. *Plant Soil* 398:87–97. <https://doi.org/10.1007/s11104-015-2627-x>
- Li Y, Zhao J, Guo J, Liu M, Xu Q, Li H, Li Y-F, Zheng L, Zhang Z, Gao Y (2017) Influence of sulfur on the accumulation of mercury in rice plant (*Oryza sativa* L.) growing in mercury contaminated soils. *Chemosphere* 182:293–300
- Li Y-F, Shang L, Zhao J, Hu H, Wang W (2018a) *Environmental bioinorganic chemistry of mercury*. Science Press, Beijing
- Li Y, Li H, Yu Y, Zhao J, Wang Y, Hu C, Li H, Wang G, Li Y, Gao Y (2018b) Thiosulfate amendment reduces mercury accumulation in rice (*Oryza sativa* L.). *Plant Soil* 430:413–422. <https://doi.org/10.1007/s11104-018-3726-2>
- Li P, Guo S, Zhao J, Gao Y, Li Y-F (2019a) Human biological monitoring of mercury through hair samples in China. *Bull Environ Contam Toxicol* 102:701–707. <https://doi.org/10.1007/s00128-019-02563-8>
- Li Y, Zhao J, Zhong H, Wang Y, Li H, Li Y-F, Liem-Nguyen V, Jiang T, Zhang Z, Gao Y, Chai Z (2019b) Understanding enhanced microbial MeHg production in mining-contaminated paddy soils under sulfate amendment: changes in Hg mobility or microbial methylators? *Environ Sci Technol* 53:1844–1852. <https://doi.org/10.1021/acs.est.8b03511>
- Lombi E, de Jonge MD, Donner E, Ryan CG, Paterson D (2011) Trends in hard X-ray fluorescence mapping: environmental applications in the age of fast detectors. *Anal Bioanal Chem* 400:1637–1644. <https://doi.org/10.1007/s00216-011-4829-2>
- Mai Z (2013) *Synchrotron radiation light source and its application*. Science Press, Beijing
- Mantouvalou I, Wolff T, Hahn O, Rabin I, Lühl L, Pagels M, Malzer W, Kanngiesser B (2011) 3D micro-XRF for cultural heritage objects: new analysis strategies for the investigation of the Dead Sea Scrolls. *Anal Chem* 83:6308–6315. <https://doi.org/10.1021/ac2011262>
- McNear DH, Peltier E, Everhart J, Chaney RL, Sutton S, Newville M, Rivers M, Sparks DL (2005) Application of quantitative fluorescence and absorption-edge computed microtomography to image metal compartmentalization in *Alyssum murale*. *Environ Sci Technol* 39:2210–2218. <https://doi.org/10.1021/es0492034>
- Mei M, Song H, Chen L, Hu B, Bai R, Xu D, Liu Y, Zhao Y, Chen C (2018) Early-life exposure to three size-fractionated ultrafine and fine atmospheric particulates in Beijing exacerbates asthma development in mature mice. *Part Fibre Toxicol* 15:13. <https://doi.org/10.1186/s12989-018-0249-1>
- Meurer WP, Claeson DT (2002) Evolution of crystallizing interstitial liquid in an arc-related cumulate determined by LA ICP-MS mapping of a large amphibole oikocryt. *J Petrol* 43:607–629. <https://doi.org/10.1093/petrology/43.4.607>
- Moore KL, Lombi E, Zhao F-J, Grovenor CRM (2012) Elemental imaging at the nanoscale: NanoSIMS and complementary techniques for element localisation in plants. *Anal Bioanal Chem* 402:3263–3273. <https://doi.org/10.1007/s00216-011-5484-3>
- Motelica-Heino M, Le Coustumer P, Thomassin JH, Gauthier A, Donard OFX (1998) Macro and microchemistry of trace metals in vitrified domestic wastes by laser ablation ICP-MS and scanning electron microprobe X-ray energy dispersive spectroscopy. *Talanta* 46:407–422
- Mounicou S, Szpunar J, Lobinski R (2009) Metallomics: the concept and methodology. *Chem Soc Rev* 38:1119–1138
- Muradin AK (2000) Capillary optics and their use in x-ray analysis. *X-Ray Spectrom* 29:343–348
- Niimura N, Bau R (2008) Neutron protein crystallography: beyond the folding structure of biological macromolecules. *Acta Cryst A* 64:12–22. <https://doi.org/10.1107/S0108767307043498>
- Ortega R, Bohic S, Tucoulou R, Somogyi A, Deves G (2004) Microchemical element imaging of yeast and human cells using synchrotron X-ray microprobe with Kirkpatrick-Baez optics. *Anal Chem* 76:309–314
- Paunesku T, Vogt S, Maser J, Lai B, Woloschak G (2006) X-ray fluorescence microprobe imaging in biology and medicine. *J Cell Biochem* 99:1489–1502
- Pettifer RF, Mathon O, Pascarelli S, Cooke MD, Gibbs MRJ (2005) Measurement of femtometre-scale atomic displacements by X-ray absorption spectroscopy. *Nature* 435:78–81
- Piacenti da Silva M, Zucchi OLAD, Ribeiro-Silva A, Poletti ME (2009) Discriminant analysis of trace elements in normal, benign and malignant breast tissues measured by total reflection X-ray fluorescence. *Spectrochim Acta B* 64:587–592. <https://doi.org/10.1016/j.sab.2009.05.026>
- Pickering IJ, Prince RC, George MJ, Smith RD, George GN, Salt DE (2000a) Reduction and coordination of arsenic in Indian mustard. *Plant Physiol* 122:1171–1178. <https://doi.org/10.1104/pp.122.4.1171>
- Pickering IJ, Prince RC, Salt DE, George GN (2000b) Quantitative, chemically specific imaging of selenium transformation in plants. *Proc Natl Acad Sci USA* 97:10717–10722. <https://doi.org/10.1073/pnas.200244597>
- Punshon T, Jackson BP, Bertsch PM, Burger J (2004) Mass loading of nickel and uranium on plant surfaces: application of laser ablation-ICP-MS. *J Environ Monit* 6:153–159
- Schroer C, Kurapova O, Patommel J, Boye P, Feldkamp J, Lengeler B, Burghammer M, Riekel C, Vincze L, Van der Hart A (2005) Hard X-ray nanoprobes based on refractive X-ray lenses. *Appl Phys Lett* 87:124103
- Scott RA, Shokes JE, Cospser NJ, Jenney FE, Adams MWW (2005) Bottlenecks and roadblocks in high-throughput XAS for structural genomics. *J Synchrotron Rad* 12:19–22. <https://doi.org/10.1107/S0909049504028791>

- Sie SH, Thresher RE (1992) Micro-PIXE analysis of fish otoliths: methodology and evaluation of first results for stock discrimination. *Int J PIXE* 2:357–379
- Snigirev A, Kohn V, Snigireva I, Lengeler B (1996) A compound refractive lens for focusing high-energy X-rays. *Nature* 384:49–51
- Szpunar J (2004) Metallomics: a new frontier in analytical chemistry. *Anal Bioanal Chem* 378:54–56
- Szpunar J (2005) Advances in analytical methodology for bioinorganic speciation analysis: metallomics, metalloproteomics and heteroatom-tagged proteomics and metabolomics. *Analyst* 130:442–465
- Templeton DM, Ariese F, Cornelis R, Danielsson LG, Muntau H, Van Leeuwen HP, Lobinski R (2000) Guidelines for terms related to chemical speciation and fractionation of elements. Definitions, structural aspects, and methodological approaches. *Pure Appl Chem* 72:1453–1470
- Tylko G, Mesjasz-Przybyłowicz J, Przybyłowicz WJ (2007) In-vacuum micro-PIXE analysis of biological specimens in frozen-hydrated state. *Nucl Instrum Methods Phys Res B* 260:141–148
- Van Fleet-Stalder V, Chasteen TG, Pickering IJ, George GN, Prince RC (2000) Fate of selenate and selenite metabolized by *Rhodobacter sphaeroides*. *Appl Environ Microbiol* 66:4849–4853. <https://doi.org/10.1128/aem.66.11.4849-4853.2000>
- Van Langevelde F, Vis RD (1991) Trace element determinations using a 15-keV synchrotron x-ray microprobe. *Anal Chem* 63:2253–2259. <https://doi.org/10.1021/ac00020a011>
- Vincze L, Vekemans B, Szaloki I, Janssens K, Van Grieken R, Feng H, Jones KW, Adams F (2001) High resolution X-Ray fluorescence micro-tomography on single sediment particles. In: Bonse Ulrich U (ed) 46th SPIE Annual Meeting International Symposium of Optical Science and Technology. San Diego, pp 240–245
- Vincze L, Vekemans B, Brenker FE, Falkenberg G, Rickers K, Somogyi A, Kersten M, Adams F (2004) Three-dimensional trace element analysis by confocal X-ray microfluorescence imaging. *Anal Chem* 76:6786–6791
- Wagemann R, Trebacz E, Boila G, Lockhart WL (1998) Methylmercury and total mercury in tissues of arctic marine mammals. *Sci Total Environ* 218:19–31
- Wang J, Chen C, Yu H, Sun J, Li B, Li YF, Gao Y, He W, Huang Y, Chai Z, Zhao Y, Deng X, Sun H (2007) Distribution of TiO<sub>2</sub> particles in the olfactory bulb of mice after nasal inhalation using microbeam SRXRF mapping techniques. *J Radioanal Nucl Chem* 272:527–531
- Wang J, Chen C, Liu Y, Jiao F, Li W, Lao F, Li Y, Li B, Ge C, Zhou G, Gao Y, Zhao Y, Chai Z (2008) Potential neurological lesion after nasal instillation of TiO<sub>2</sub> nanoparticles in the anatase and rutile crystal phases. *Toxicol Lett* 183:72–80
- Wang LL, Yu HS, Li LN, Wei XJ, Huang YY (2016) The development of TXRF method and its application on the study of trace elements in water at SSRF. *Nucl Instrum Methods Phys Res B* 375:49–55. <https://doi.org/10.1016/j.nimb.2016.03.046>
- Wilson RG, Stevie FA, Magee CW (1989) Secondary ion mass spectrometry. Wiley, New York
- Winterer M, Delaplane R, McGreevy R (2002) X-ray diffraction, neutron scattering and EXAFS spectroscopy of monoclinic zirconia: analysis by Rietveld refinement and reverse Monte Carlo simulations. *J Appl Cryst* 35:434–442. <https://doi.org/10.1107/S0021889802006829>
- Wu Y, Pan J, Pan G, Zhao L, Huang Y, Yuan L, Chen J (1997) A preliminary study of cell elemental spectroscopy with total reflection X-ray fluorescence analysis. *Nucl Technol* 20:164–168
- Yan H, Nazaretski E, Lauer K, Huang X, Wagner U, Rau C, Yusuf M, Robinson I, Kalbfleisch S, Li L, Bouet N, Zhou J, Conley R, Chu YS (2016) Multimodality hard-x-ray imaging of a chromosome with nanoscale spatial resolution. *Sci Rep* 6:20112. <https://doi.org/10.1038/srep20112>
- Yan H, Bouet N, Zhou J, Huang X, Nazaretski E, Xu W, Cocco AP, Chiu WKS, Brinkman KS, Chu YS (2018) Multimodal hard x-ray imaging with resolution approaching 10 nm for studies in material science. *Nano Futures* 2:011001. <https://doi.org/10.1088/2399-1984/aab25d>
- Yang L, McRae R, Henary MM, Patel R, Lai B, Vogt S, Fahrni CJ (2005) Imaging of the intracellular topography of copper with a fluorescent sensor and by synchrotron x-ray fluorescence microscopy. *Proc Natl Acad Sci USA* 102:11179–11184. <https://doi.org/10.1073/pnas.0406547102>
- Yasoshima M, Matsuo M, Kuno A, Takano B (2001) Studies on intake of heavy metals by *Bradybaena similaris*, land snails, by XAFS measurement. *J Synchrotron Rad* 8:969–971
- Yi L, Qin M, Wang K, Lin X, Peng S, Sun T, Liu Z (2016) The three-dimensional elemental distribution based on the surface topography by confocal 3D-XRF analysis. *Appl Phys A* 122:856. <https://doi.org/10.1007/s00339-016-0393-0>
- Yuan Q-X, Deng B, Guan Y, Zhang K, Liu Y-J (2019) Novel developments and applications of nanoscale synchrotron radiation microscopy. *Physics* 48:205–218
- Yun W, Pratt ST, Miller RM, Cai Z, Hunter DB, Jarstfer AG, Kemner KM, Lai B, Lee HR, Legnini DG, Rodrigues W, Smith CI (1998) X-ray Imaging and microspectroscopy of plants and fungi. *J Synchrotron Rad* 5:1390–1395. <https://doi.org/10.1107/S0909049598007225>
- Zhao L, Xian D (1997) Total reflection X-ray fluorescence analysis. *Physics* 661–665
- Zhao F-J, Moore KL, Lombi E, Zhu Y-G (2014a) Imaging element distribution and speciation in plant cells. *Trends Plant Sci* 19:183–192. <https://doi.org/10.1016/j.tplants.2013.12.001>
- Zhao J, Li Y-F, Li Y, Gao Y, Li B, Hu Y, Zhao Y, Chai Z (2014b) Selenium modulates mercury uptake and distribution in rice (*Oryza sativa* L.), in correlation to mercury species and exposure level. *Metallomics* 6:1951–1957
- Zhao J, Pu Y, Gao Y, Peng X, Li Y, Xu X, Li B, Zhu N, Dong J, Wu G, Li Y-F (2015) Identification and quantification of seleno-proteins by 2-DE-SR-XRF in selenium-enriched yeasts. *J Anal At Spectrom* 30:1408–1413
- Zhu MT, Feng WY, Wang Y, Wang B, Wang M, Ouyang H, Zhao YL, Chai ZF (2009) Particokinetics and extrapulmonary translocation of intratracheally instilled ferric oxide nanoparticles in rats and the potential health risk assessment. *Toxicol Sci* 107:342–351. <https://doi.org/10.1093/toxsci/kfn245>
- Zoeger N, Strelci C, Wobruschek P, Jokubonis C, Pepponi G, Roschger P, Hofstaetter J, Berzlanovich A, Wegrzynek D, China-Cano E, Markowicz A, Simon R, Falkenberg G (2008) Determination of the elemental distribution in human joint bones by SR micro XRF. *X-Ray Spectrom* 37:3–11. <https://doi.org/10.1002/xrs.998>

# **Modelling and Computational Approaches for Exposure, Processes, and Impacts**



# High-Throughput Screening and Hazard Testing Prioritization

Caitlin Lynch, Srilatha Sakamuru, Shuaizhang Li, and Menghang Xia

## Abstract

Tox21 is a collaborative effort among the National Center for Advancing Translational Sciences, the Environmental Protection Agency, the National Toxicology Program, and the Food and Drug Administration to elucidate the toxic effects of compounds found in the environment and/or created by humans. Since 2008, this program has screened many different pathways, targets, or phenotypes (more than 70 assays) using an in vitro quantitative high-throughput screening approach. Endocrine disruption and stress-related signaling pathways have been the main focus of the Tox21 screening program. Nuclear receptors play an important role in endocrine disruption, modulating many different biological processes and metabolism. It is therefore important to classify endogenous and exogenous compounds for their ability to alter the function or quantity of these nuclear receptors. Stress-related signaling pathways are necessary for body homeostasis and are involved in many disease states as well. Identifying compounds which induce stress signaling pathways in the body is prudent to fully determine the safety of an environmental chemical. This book chapter describes an in-depth analysis of Tox21, a summary of select examples of their assays, and the future plan for the screening program.

## Keywords

Acetylcholinesterase • Mitochondria • Nuclear receptor • Predictive toxicology • Quantitative high-throughput screening • Tox21

## 1 Introduction to Toxicology in the Twenty-First Century (Tox21)

An increasing amount of chemicals is released into the atmosphere each year, requiring more expedient and thorough screening techniques in order to effectively determine the toxicological effects on humans and the environment. Traditionally, the main source in identifying compound toxicity was in vivo animal models utilized to generate a detailed profile of each chemical (Greaves et al. 2004). These animal models were able to detect one specific toxicological endpoint (e.g., reproductive, oral, dermal, or developmental toxicity) per experiment (Shukla et al. 2010). However, these models may not fully represent the effects on humans, are performed at a low throughput, and/or are expensive to perform, leading to a lack in sufficient knowledge to evaluate safety concerns (NRC 1984). Regardless of these limitations, the preponderance of knowledge for a drug's toxicity and therapeutic window has mainly been founded based on these types of experiments, as a result of the lack of other robust in vitro options (Zurlo et al. 1994). Owing to these challenges, future chemical toxicity testing was suggested in a report by the National Research Council (NRC), which stated a predictive toxicology approach relying on identifying chemical modulators of cellular pathways using human cell-based in vitro assays and computational modeling was a novel method in tackling the identification of potential health risks (Gibb 2008). A collaborative effort, called Tox21, among the Environmental Protection Agency (EPA), the National Toxicology Program (NTP), and the National Chemical Genomics Center (NCGC) which is now a part of the National Center for Advancing Translational

C. Lynch · S. Sakamuru · S. Li · M. Xia (✉)  
National Center for Advancing Translational Sciences, National  
Institutes of Health (NIH), Bethesda, MD, USA  
e-mail: [mxia@mail.nih.gov](mailto:mxia@mail.nih.gov)

C. Lynch  
e-mail: [caitlin.lynych@nih.gov](mailto:caitlin.lynych@nih.gov)

S. Sakamuru  
e-mail: [sakamurus@mail.nih.gov](mailto:sakamurus@mail.nih.gov)

S. Li  
e-mail: [shuaizhang.li@nih.gov](mailto:shuaizhang.li@nih.gov)

Sciences (NCATS) was generated to bring compound toxicity testing into the twenty-first century. In 2010, the Food and Drug Administration (FDA) joined this effort. Since the inception of this esteemed program, over 200 peer-reviewed scientific articles related to the Tox21 program have been published within about 56 journals (Thomas et al. 2018). All data acquired throughout this program is also available online for public viewing (e.g., <https://tripod.nih.gov/tox21> and <https://pubchem.ncbi.nlm.nih.gov>), which is intended to progress toxicology and science beyond the scope that a single program could achieve.

Each of the collaborating entities plays a specific role throughout the Tox21 program. In 2004, NTP generated a vision for what science in the twenty-first century should look like, including the exploration of an alternative method to animal testing. The idea quickly led to establishing a high-throughput screening (HTS) program, which allowed for the testing of toxicity for thousands of environmental agents at a time (<https://ntp.niehs.nih.gov/results/tox21/history-index.html>). The EPA contributes to Tox21 by prioritizing toxic chemicals through the generation of data and predictive models using the Toxicity Forecaster (ToxCast, <https://www.epa.gov/chemical-research/toxicity-forecasting>). Building novel pathways to study the toxicity of the compounds, which the FDA regulates, fits into the overall theme of the Tox21 program. To fulfill this goal, the FDA has taken substantial strides toward the generation of comprehensive predictive toxic models (FDA's Predictive Toxicology Roadmap 2017). Lastly, NCATS' role for Tox21 includes performing the most advanced HTS models which the current technology has to offer so that more can be known about the hazards of commonly used chemicals in a quick and efficient manner (<https://ncats.nih.gov/tox21/about/goals>).

---

## 2 Tox21 Quantitative High-Throughput Assay Screening and Data Analysis

Quantitative HTS (qHTS) has become an innovative way to efficiently screen hundreds and thousands of chemical compounds at multiple concentrations in a short time. Each Tox21 qHTS assay is optimized into a 1536-well plate format so that each compound of the Tox21 10 K compound library, which includes ~ 8900 unique compounds, can be quickly tested at 15 different concentrations in triplicate. This compound collection, put together by NCATS, NTP, and the EPA, of environmental chemicals and clinically used drugs includes solvents, food additives, drinking water disinfection by-products, sunscreen additives, preservatives, industrial chemicals, flame retardants, synthesis by-products, natural product components, plasticizers, pesticide/herbicide additives and their metabolites, and therapeutic agents. Once

an initial optimization is complete, the Tox21 10 K compound primary screen is run and potential active compounds are selected for further studies (Fig. 1). Any compound going through mechanism-based assays also go through compound quality control (QC) to verify the purity and specific molecular weight of each selected compound.

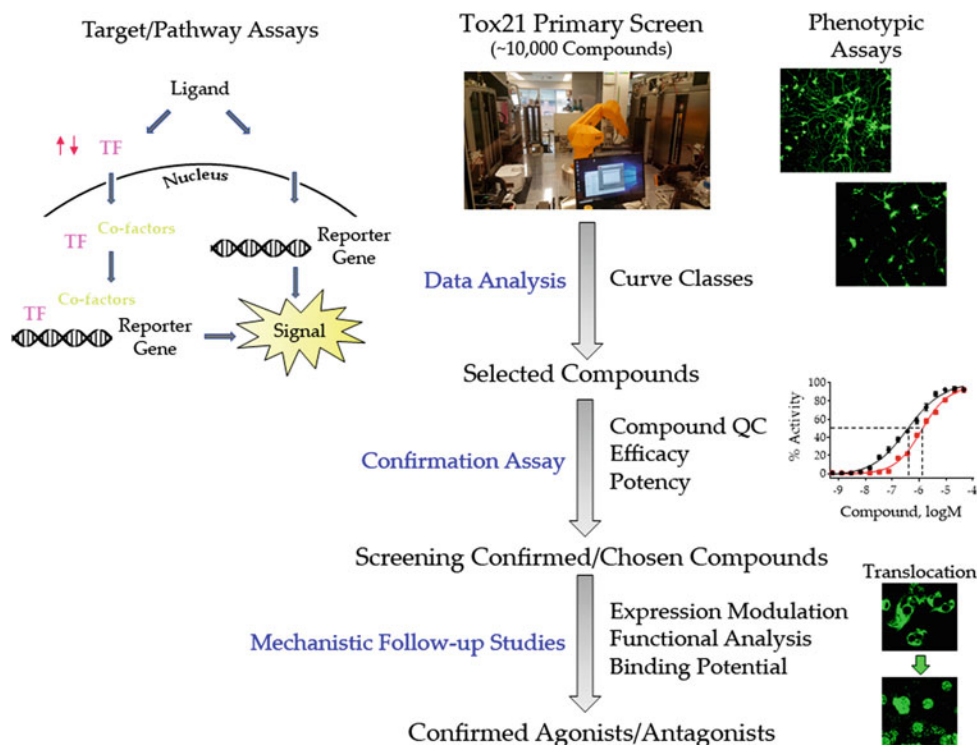
The assay types used for a primary screen are usually pathway-, target-, or phenotype-based assays. In this book chapter, we discuss certain target-specific assays (see Sects. 2.1 and 2.2); however, a more in-depth analysis and explanation of a few phenotypic assays can be found in a previous review paper (Hsu et al. 2017). Once the primary screen is complete, whether phenotypic, target, or pathway based, there is the potential ability to confirm certain compounds as agonists or antagonists for the specific endpoint being measured. Through a robust assay performance and a rigorous analysis of the data (see Sect. 2.3), Tox21 performs the initial step into profiling these potentially hazardous chemicals.

Owing to its ability to quickly and efficiently use a qHTS platform, Tox21 has performed more than 70 screens to identify the activity caused by environmental compounds in different signaling pathways and targets. Each screen was vigilantly optimized and tested to ensure robust performance data. A list of all current screens, performed by Tox21, is displayed in Table 1. The specific cell lines used for each assay target or pathway are shown alongside the endpoint readout followed by either a reference or where the cell line was acquired. For a few assay targets (androgen receptor, estrogen receptor  $\alpha$ , and estrogen-related receptor  $\alpha$ ), multiple engineered stable cell lines were utilized to fully identify compounds, from the Tox21 collection, which were active for those respective assays.

### 2.1 Nuclear Receptors

Nuclear receptors play a pivotal role in development, homeostasis, and/or disease states (Giguere 1999). Modulation of some nuclear receptors, through environmental chemicals and/or exogenous compounds, can be hazardous or beneficial to the human body depending on the extent of the alteration. Classifying these compounds as inhibitors or inducers of certain nuclear receptors would expound upon the knowledge of their toxic or therapeutic effect on humans. Modifying the androgen receptor (AR), estrogen receptor (ER), or estrogen-related receptor (ERR) pathways can lead to endocrine disruption and potentially cause reproductive and developmental disorders, as well as cancer (Gonzalez et al. 2019; Park et al. 2016). Altering the activity of the constitutive androstane receptor (CAR) or pregnane X receptor (PXR) can potentially be utilized for therapeutic purposes in certain disease states (Gao and Xie 2010; Hedrich et al. 2016) or identify potentially hazardous drug–drug interactions. The

**Fig. 1** Each screen starts with about 10,000 compounds from the Tox21 collection being assayed in a high-throughput screening manner, in either target/pathway or phenotypic-based platforms. The blue-colored words on the left side of the figure are the actions taken for each step to occur. The right side displays the endpoints used to generate a cutoff value for each future step, so that the collection can be further narrowed down in size based on significance. NR = nuclear receptor, TF = transcription factor



Tox21 program has screened different stably transfected cell lines for their activity on these nuclear receptors.

**AR Agonist Identification** The transcriptional factor AR regulates male sexual development, affects female fertility, and is involved in pathological processes which alter the state of certain diseases such as Kennedy's disease, Klinefelter's syndrome, and certain reproductive cancers (Culig et al. 2002; Pihlajamaa et al. 2015; Chang et al. 2014; Skakkebaek et al. 2014; Tanaka et al. 2012). Therefore, it is important to identify compounds, from the environment and elsewhere, which modify the activity of this important nuclear receptor. The Tox21 10 K chemical library was screened to categorize compounds as potential AR agonists if they generated AR activity in at least one of the two reporter gene cell lines utilized (Lynch et al. 2017). Through this endeavor, Tox21 scientists identified a potentially novel class of AR agonists—fluoroquinolone antibiotics. A binding assay was performed on the actives identified from the reporter gene assays to further define each compound as an AR agonist due to binding capability; an overall 72% concordance rate between binding and reporter assays demonstrated a high predictive ability of the cell-based primary screening results. Translocation of AR from the cytoplasm into the nucleus, the first step of activation, was also observed for 16 of the 17 most promising AR agonists, including GSK232420A, norethisterone enanthate, and prulifloxacin. This study was a first step in identifying certain compounds as potentially hazardous with respect to the AR pathway.

**ERR Modulation Profiling** Alongside its previously mentioned endocrine disruption involvement, ERR is also involved in energy homeostasis, as well as controlling mitochondrial oxidative respiration (Leone et al. 2005; Lin et al. 2004; Luo et al. 2003). A poor prognosis for breast, prostate, and endometrial cancer occurs when increases in  $ERR\alpha$  gene expression levels are found within the respective tumors (Fradet et al. 2016; Matsushima et al. 2016; Park et al. 2016). With all the pathways and disease states that ERR regulates, it is important to identify agonists (toxicants) and antagonists (potential therapeutics) to determine the full scope of internalizing these compounds. One of the unique features of this nuclear receptor is its crosstalk with peroxisome proliferator-activated receptor gamma co-activator 1 alpha ( $PGC-1\alpha$ ), which is sometimes a necessary component to  $ERR\alpha$  activation (Teng et al. 2014). When the Tox21 10 K compound library was screened for ERR agonists, a class of novel compounds was identified—statins (Lynch et al. 2018). Interestingly, this group of compounds had no effect in the  $PGC/ERR$  cell line, which implies activation of  $ERR\alpha$  independently of  $PGC-1\alpha$ . A known  $ERR\alpha$  inhibitor, XCT790, was co-treated with each statin and screened again using the ERR cell line. Each of the six statins showed concentration-dependent inhibition when co-treated with 0, 5, or 10  $\mu$ M XCT790, indicating ERR dependence. Two of the statins, cerivastatin sodium and fluvastatin, were also used to treat ERR siRNA transfected cells which showed an inhibition in three  $ERR\alpha$ -regulated genes, ERR, COX8, and



**Table 1** Cell Line and Assay Readouts for Tox21 Screens

Cell lines	Assay target	Assay readout	Cell lines acquired/Reference
AChE-SH-SY5Y	Acetylcholinesterase	Absorbance Fluorescence	Li et al. (2017a)
AhR-HepG2	Aryl hydrocarbon receptor	Luminescence	He et al. (2011)
AP1-ME180	Activator protein 1	Fluorescence	Invitrogen (Carlsbad, CA)
AR-HEK293	Androgen receptor (LBD)	Fluorescence	Lynch et al. (2017)
AR-MDA	Androgen receptor (full)	Luminescence	Lynch et al. (2017)
Aromatase-MCF7	Aromatase	Luminescence	Chen et al. (2015)
CAR-HepG2	Constitutive androstane receptor	Luminescence	Lynch et al. (2013, 2014, 2015, 2016, 2019a)
HepG2	Caspase-3 and Caspase-7	Luminescence	Huang et al. (2008)
DT40	DNA repair	Luminescence	Nishihara et al. (2016)
ELG1-HEK293	Telomere length regulation protein ELG1	Luminescence	Fox et al. (2012)
ER $\alpha$ -HEK293	Estrogen receptor $\alpha$	Fluorescence	Huang et al. (2011, 2014), Rotroff et al. (2014), Judson et al. (2015)
ER-MCF7	Estrogen receptor $\alpha$	Luminescence	Huang et al. (2014), Judson et al. (2015), Rotroff et al. (2014)
ER $\beta$ -HEK293	Estrogen receptor $\beta$	Fluorescence	Invitrogen
ERR-HEK293	Estrogen-related receptor $\alpha$	Luminescence	Lynch et al. (2018, 2019b), Teng et al. (2017)
ESRE-Hela	Endoplasmic reticulum stress response element	Fluorescence	Bi et al. (2015)
FXR-HEK293	Farnesoid X receptor	Fluorescence	Hsu et al. (2014, 2016a, 2016d)
GR-Hela	Glucocorticoid receptor	Fluorescence	Invitrogen
CHO	H2A histone family member X	Fluorescence	ATCC (Manassas, VA)
HCT116	HDAC I and HDAC II	Luminescence	Hsu et al. (2016c)
HRE-ME180	Hypoxia-inducible factors	Fluorescence Luminescence	Hsu et al. (2016b), Khuc et al. (2016)
HSE-Hela	Heat shock element	Fluorescence	Hancock et al. (2009)
MMP-HepG2-ME180	Mitochondrial membrane potential	Fluorescence	Li et al. (2017b), Sakamuru et al. (2012, 2016), Xia et al. (2018), Attene-Ramos et al. (2013, 2015)
NF $\kappa$ B	Nuclear factor-kappa B	Fluorescence	Miller et al. (2010)
Nrf2/ARE-HepG2	Antioxidant response element	Fluorescence	Shukla et al. (2012), Zhao et al. (2016)
p53-HCT-116	p53	Fluorescence	Witt et al. (2017)
PGC/ERR-HEK293	Estrogen-related receptor $\alpha$	Luminescence	Lynch et al. (2018, 2019b), Teng et al. (2014)
PPAR $\delta$ -HEK293	Peroxisome proliferator-activated receptor $\delta$	Fluorescence	Invitrogen
PPAR $\gamma$ -HEK293	Peroxisome proliferator-activated receptor $\gamma$	Fluorescence	Invitrogen
PR-HEK293	Progesterone receptor	Fluorescence	Invitrogen
PXR-HepG2	Pregnane X receptor	Luminescence	Shukla et al. (2011), Dr. Taochen Chen
RAR-C3H10T1/2	Retinoic acid receptor	Luminescence	Chen et al. (2016)
ROR $\gamma$ -CHO	Retinoic acid-related orphan receptor $\gamma$	Luminescence	Dr. Anton M. Jetten
RXR-HEK293	Retinoid X receptor	Fluorescence	Invitrogen
ShhGli1-3T3	Sonic hedgehog pathway	Luminescence	Dr. Yanling Chen Dr. David H. Reese
SMAD-HEK293	Smad signaling pathway	Fluorescence	Invitrogen
TRE-GH3	Thyroid hormone receptor	Luminescence	Freitas et al. (2014)
TRHR-HEK293	Thyrotropin-releasing hormone receptor	Fluorescence	Codex Biosolutions (Gaithersburg, MD)
TSHR-HEK293	Thyroid stimulating hormone Receptor	Fluorescence	Codex Biosolutions
VDR-HEK293	Vitamin D receptor	Fluorescence	Invitrogen

IDH3. Owing to the newly identified connection of statins with  $ERR\alpha$  agonism, it is plausible to assume that these compounds might potentiate a poor outcome or progression in different types of cancer. Further studies need to be performed to fully understand the implications of these initial studies performed by the Tox21 program.

A screen was performed on the Tox21 10 K compound collection to identify  $ERR\alpha$  antagonists as well (Lynch et al. 2019b). Two major groups, antineoplastic agents and pesticides, were classified as antagonists of  $ERR\alpha$  activity as well as some compounds inhibiting mRNA expression of five downstream genes (cytochrome c oxidase subunit 8A, COX8A; isocitrate dehydrogenase 3 (NAD(+)) alpha, IDH3 $\alpha$ ; peroxisome proliferator activated receptor alpha, PPAR $\alpha$ ; cytochrome c oxidase subunit 4I1, COX4I1; and cytochrome c). A heat map was also displayed showing the activity of each compound on multiple targets and pathways, including AR, nuclear factor erythroid 2-related factor 2/antioxidant response element (Nrf2/ARE), CAR, ER, ERR, farnesoid X receptor, thyroid hormone receptor, mitochondrial membrane potential, p53, PPAR $\gamma$ , progesterone receptor, retinoic acid receptor, retinoic acid-related orphan receptor, and sonic hedgehog. Most of the antineoplastic agents (artemisinin, bortezomib, carfilzomib, decitabine, etoposide, topotecan, and suberoylanilide hydroxamic acid) activated the p53 pathway which is consistent with a previous study (Guo et al. 2019), while most of them (artemisinin, bortezomib, carfilzomib, etoposide, gimatecan, methidichlorophen, topotecan, and suberoylanilide hydroxamic acid) also had antagonistic activity in the sonic hedgehog assay, which is a pathway known for being associated with tumor development (Jiang and Hui 2008). Interestingly, many of the pesticides demonstrated an activation of the antioxidant responsive element (ARE) pathway (Lynch et al. 2019b) which is known to counter oxidative stress (Johnson et al. 2008). However, it is likely these pesticides are causing the formation of free radicals, which induce oxidative stress, and ultimately, the increase in the ARE pathway would then occur. The Tox21 10 K compound study, for both agonist and antagonist identification of  $ERR\alpha$  modulation, was a major step into investigating the mechanism of action for many compounds, though future studies are certainly warranted and necessary to fully understand the scope of each specific compound and how they will interact in the body.

**CAR Agonist Classification** Classically, CAR had previously been known to regulate drug metabolizing enzymes and transporters which have an effect on all phases of drug metabolism (Qatanani and Moore 2005). It has recently been shown that CAR also plays an important role in energy homeostasis, as well as certain cancer progression and treatments (Gao and Xie 2010; Hedrich et al. 2016; Yamamoto et al. 2004). Owing to this novel function, it is important to identify any novel selective CAR agonists,

which is what the Tox21 10 K compound collection was screened for in a previous publication (Lynch et al. 2019a). Four compounds (neticonazole, diphenamid, phenothrin, and rimcazole) were identified to be hCAR activators through a confirmation study, using human primary hepatocytes, examining mRNA and protein expression of cytochrome P450 (CYP) 2B6 and CYP3A4. A nuclear translocation assay was also performed to display these four compounds exhibiting the first step of hCAR activation—translocation from the cytoplasm into the nucleus. Future studies will need to be performed to truly understand the usage of these compounds in a therapeutic capacity, as well as to identify possible drug–drug interactions which may occur.

## 2.2 Stress-Related Pathways

**Acetylcholinesterase Inhibitor Profiling** Acetylcholinesterase (AChE EC 3.1.1.7), found primarily in neuromuscular junctions and cholinergic brain synapses, is an enzyme involved in the termination of impulse transmission with a highly specific catalytic activity for hydrolyzing acetylcholine (ACh) into choline (Quinn 1987; Taylor and Radic 1994). After this transformation, choline is taken up into the pre-synaptic nerve and combined with acetyl-CoA to produce acetylcholine through the action of choline-acetyltransferase (Soreq and Seidman 2001). The majority of AChE can be found in an amphiphilic globular tetramer (G4) form or a monomeric G1 form (Fernandez et al. 1996; Wang and Tang 2005), inside either motor neurons or sensory fibers (Massoulie et al. 1993). Within these two forms, there are two subsites of the active site, which are called the anionic subsite and the esteratic subsite (Nachmansohn and Wilson 1951). The anionic subsite binds ACh and quaternary ligands, acting as competitive inhibitors to assist in inhibiting AChE (Mooser and Sigman 1974; Wilson and Quan 1958). In addition, one or more peripheral anionic sites, distinct from the choline-binding pocket, were also identified to bind ACh and other quaternary ligands acting as uncompetitive inhibitors (Taylor and Lappi 1975). In the esteratic subsite, the basic function of hydrolyzing ACh into acetate and choline is performed (Nachmansohn and Wilson 1951). Inhibition of AChE can lead to acetylcholine accumulation in the synaptic space, enhanced nicotinic and muscarinic receptor stimulation, as well as disrupted neurotransmission (Colovic et al. 2013). Therefore, AChE inhibitors play an important role in both toxicology and pharmacology, and it is important to identify compounds which can be associated as such.

Depending on the mode of action, AChE inhibitors can be divided into two subcategories: reversible and irreversible inhibitors. Reversible inhibitors, competitive or noncompetitive, have therapeutic applications, while irreversible inhibitors are more commonly associated with having toxic

side effects. Tacrine, a noncompetitive reversible AChE inhibitor, was the first approved drug for the treatment of Alzheimer's disease; however, due to its hepatotoxic side effects, the use of this drug has since been eradicated (Watkins et al. 1994). Other AChE inhibitors which have been approved by the U.S. Food and Drug Administration (FDA), to be utilized as drugs, include donepezil, rivastigmine, and galantamine (Bond et al. 2012). Carbamates, a group of reversible AChE inhibitors, are organic compounds which can be used as therapeutic drugs (for treating Alzheimer's disease, glaucoma, and Parkinson's disease), pesticides, parasiticides (in veterinary medicine), or as a prophylaxis of organophosphorus compound poisoning (Giacobini 2000). Organophosphorus pesticides exert their pesticidal activity by inhibiting AChE activity irreversibly, causing toxic effects such as headaches, impaired memory and concentration, disorientation, severe depression, irritability, drowsiness, or insomnia (Colovic et al. 2013). Many environmental pollutants, such as heavy metals, other pesticides, polycyclic aromatic hydrocarbons, and dioxins also show inhibition of AChE activity (Ademuyiwa et al. 2007; Kang and Fang 1997; Reddy and Philip 1994; Xie et al. 2013). Therefore, measurement of AChE activity has been widely used as a biomarker of toxic effects on the nervous system following exposure to organophosphate and carbamate pesticides (Lionetto et al. 2013). Although AChE inhibitors have significant consequences to human health, there are still a large number of compounds which have not been identified as irreversibly inhibiting AChE activity, including synthesized drug candidates, food additives, and industrial chemicals.

Regarding the role of AChE in pharmacology and toxicology, many biochemical readouts, including spectrophotometric, colorimetric, radiometric, fluorometric, and electro-chemical, have been used to measure the activity of cholinesterase (Holas et al. 2012; Miao et al. 2010). The Ellman method is regarded as the golden method for determining AChE activity (Ellman et al. 1961). This highly regarded assay still has certain limitations, such as its reaction with AChE reactivators (e.g., oximes) as well as interference from hemoglobin in the blood (Sinko et al. 2007). Recently, a fluorescent assay has been developed using whole blood and cultured human neuroblastoma cells (SH-SY5Y) in which AChE activity was determined by measuring the fluorescence of resorufin, which is produced from coupled enzyme reactions involving acetylcholine, horseradish peroxidase, choline oxidase, and Amplex Red (10-acetyl-3,7-dihydroxyphenoxazine) (Santillo and Liu 2015). With the growing number of chemicals in the environment, as well as the need for novel therapeutics, developing AChE inhibition assays that are suitable to qHTS platforms will greatly add value to human health.

While the previously mentioned fluorescent method using Amplex Red was developed in a homogenous format using

SH-SY5Y cells, an enzyme-based assay using eel AChE was also optimized into a 1536-well format. In the Tox21 program, both assays were used to screen 1368 compounds, which included a library of pharmacologically active compounds (Library of Pharmacological Active Compounds, LOPAC) and 88 additional compounds, at multiple concentrations in a qHTS format (Li et al. 2017a). Each assay exhibited exceptional performance characteristics, including assay signal window and reproducibility. A group of inhibitors were identified from this study, including known (e.g., physostigmine and neostigmine bromide) and novel AChE inhibitors (e.g., chelerythrine chloride and cilostazol). As a result, this screening method developed for AChE was determined to be a useful tool for profiling inhibitors of this enzyme.

Some organophosphorus pesticides are not active AChE inhibitors in their parent form and require bioactivation in order to be effective (Sultatos 1994). A high-throughput AChE assay, in a 1536-well format, using liver microsomes was developed to provide an accurate estimation of metabolism using an *in vitro* method. In order to validate this assay, a group of organophosphorus pesticide compounds, containing both parental compounds and their active metabolites, was screened for AChE inhibition activity (Li et al. 2019). The assay utilized recombinant human AChE protein with human or rat liver microsomes; the Ellman colorimetric or fluorescent method was then used to measure AChE activity. Once the assay was completed, the reproducibility was evaluated, and each compound was ranked in the order of potency. Large potency differences between some parent compounds and their metabolites were observed in the assay with microsome addition. Many parental organophosphorus pesticides, such as chlorpyrifos, tebufos, and chlorethoxyfos, only showed the inhibitory effects on AChE after addition of the metabolic component into the reaction, signifying the need of bioactivation to occur in order to become potent AChE inhibitors. Together, these data demonstrated the promising ability to profile AChE inhibitors using metabolic simulation; further studies will be vital to acquire the full extent of safety assessment for each chemical. Cell- and enzyme-based AChE assays would increase the library of AChE inhibitors, having a significant impact on both the pharmaceutical and toxicology fields.

**Mitochondrial Toxicant Identification** Mitochondria, the intracellular powerhouse, generate 95% of cellular energy in the form of ATP through oxidative phosphorylation (Wallace et al. 1997). Mitochondrial membrane potential (MMP), the electric potential across the inner mitochondrial membrane, is generated by the mitochondrial electron transport chain through a series of redox reactions (Chen 1988). MMP is a key parameter for assessing mitochondrial function, cell health, and apoptosis. Several

cationic lipophilic fluorescent dyes are routinely used to evaluate MMP changes, including rhodamine 123 (R123) (Chen 1988), chloromethyl tetramethyl rosamine (Macho et al. 1996), tetramethylrhodamine methyl and ethyl esters (TMRM and TMRE) (Farkas et al. 1989), 3,3'-diehexiloxadicyanin iodide (DiOC6(3)) (Farkas et al. 1989), and 5,5',6,6'-tetrachloro-1,1',3,3'-tetraethylbenzimidazolcarbocyanin iodide (JC-1) (Salvioli et al. 1997).

Mitochondrial membrane potential indicator (m-MPI), a water-soluble derivative of JC-1 with improved signal to background performance, was developed by Codex Biosolutions to determine the MMP of certain chemicals. Using m-MPI, a homogenous cell-based assay was developed, optimized, and miniaturized into a 1536-well plate for assessing changes in MMP to determine mitochondrial toxicity (Sakamuru et al. 2012). In healthy cells, m-MPI accumulates in mitochondria as red fluorescent aggregates (emission at 590 nm); conversely, after mitochondrial toxicant treatment, the cells depolarize and become less healthy maintaining m-MPI in the cytoplasm as green fluorescent monomers (emission at 540 nm). The calculation of the ratio of red/green channel readings is then used to assess the mitochondrial function of the cells (Sakamuru et al. 2016). Using the m-MPI assay, the chemicals from the LOPAC, NTP, and Tox21 10 K compound collections were screened for mitochondrial toxicity by evaluating the effect of chemical compounds on changes of MMP in HepG2 cells (Attene-Ramos et al. 2015; Attene-Ramos et al. 2013; Sakamuru et al. 2012). The screening for mitochondrial toxicants from the NTP collection resulted in about 5% of the compounds having a potential decrease in MMP, while the selected active ones were further clustered based on structural similarity (Attene-Ramos et al. 2013). Some of these compounds were selected for confirmation and mechanistic studies based on potency, efficacy, and structural diversity by selecting at least one representative compound from each cluster. This study demonstrated the effectiveness of Tox21's strategy for evaluating the toxicological properties of a chemical collection.

In a separate study, the compounds identified as MMP inhibitors from the initial Tox21 10 K compound library screen were further profiled to identify the structural features associated with MMP changes (Attene-Ramos et al. 2015). For this approach, a multiplexed qHTS (measuring two endpoints: MMP and intracellular ATP) method was combined with structure-based clustering analysis. After the primary screening, about 11% of the compounds from the Tox21 10 K compound collection showed a decrease in MMP, among which several triarylmethane dyes and organotin compounds were identified to be potent. The cluster analysis from this study displayed that different categories of compounds, including flavonoids, chlorinated

organic insecticides, parabens, and thiazolidinedione-based drugs, are capable of decreasing MMP. The most potent MMP toxicants from the Tox21 primary screen were further tested with a tier-based approach that evaluated the mechanistic characterization of chemicals affecting mitochondrial function, which can potentially reduce animal use for toxicological testing (Xia et al. 2018). Based on the follow-up m-MPI assay, performed in HepG2 cells and rat hepatocytes, a group of compounds were selected for further testing in assays which had an effect on reactive oxygen species (ROS) production, p53 signaling pathway modulation, Nrf2/ARE pathway modulation, cellular respiration (i.e., mitochondrial oxygen consumption), cellular Parkin translocation, as well as larval development and ATP content in the nematode *Caenorhabditis elegans*. From this study, a group of known mitochondrial complex inhibitors, uncouplers, and a few not well-characterized mitochondrial toxicants (e.g., lasalocid, picoxystrobin, pinacyanol, and triclocarban) were identified.

### 2.3 Tox21 Data Analysis

Tox21 data analysis for raw data processing as well as concentration–response curve fitting and classification follows a standardized qHTS data analysis strategy that has been developed at NCATS (Inglese et al. 2006). The raw plate reads for each concentration point are initially normalized to the positive control compound (agonist mode: 100%; antagonist mode: –100%) and negative control (DMSO; 0% for both agonist and antagonist modes). Percent activity is then calculated as equal to  $((V_{\text{compound}} - V_{\text{DMSO}}) / (V_{\text{positive}} - V_{\text{DMSO}})) \times 100$ , where  $V_{\text{compound}}$  denotes the compound well values,  $V_{\text{positive}}$  denotes the median value of the positive control wells, and  $V_{\text{DMSO}}$  denotes the median values of the DMSO wells. The values are then corrected using two compound-free control plates (DMSO-only plates) placed before the compound plate stack. Concentration–response curves for each compound are fitted to a four-parameter Hill equation yielding concentrations of half-maximal activity ( $AC_{50}$ ) and maximal response (efficacy) values (Wang et al. 2010). Concentration–response curves are then designated as classes 1–4 based on efficacy, quality of fit, and the number of data points observed above background activity. Each curve class is converted to a curve rank such that more potent and efficacious compounds with higher quality curves are assigned a higher rank (5–9) and inactive compounds are assigned curve rank 0 (Huang 2016). These curve ranks are numerical measures of each compound's activity. Since the Tox21 screens are run in triplicate, the assay performances from three independent runs are measured by reproducibility scores. Three types of reproducibility calls (match, mismatch, and inconclusive) are

made based on the concordance of the replicate assay runs (Huang et al. 2011). The active compounds are selected and consequently cherry-picked for secondary follow-up studies. Lastly, as previously mentioned, all Tox21 screening data is released to public domains such as PubChem, a database for chemical compounds which includes bioactivity data alongside their respective names and general information (<http://pubchem.ncbi.nlm.nih.gov>).

### 3 Usage of Tox21 Data and Future Directions

The vast amount of data generated from high-throughput screenings are of valuable resources for many scientific areas, including data mining and predictive modeling studies. The high-quality concentration–response data generated so far, as a part of the Tox21 collaboration, including a broad array of phenotypic-, target-, and pathway-specific assays, provide datasets which can be used in quantitative structure–activity relationship (QSAR) studies to build robust computer models. In 2014, the Tox21 data challenge utilized this immense amount of data by asking participants to predict the effect of compounds on cellular signaling pathways and targets using chemical structure information. The challenge generated several high-quality models, demonstrating that computational approaches can provide meaningful predictions in the toxicology field (Huang et al. 2016a). By combining the structural information of the compounds with the Tox21 screening data, predictive models for 72 *in vivo* toxicity endpoints were built with a cluster-based approach, which suggests that primary screening data not only serves as *in vitro* signatures for predicting *in vivo* toxicity but also helps to prioritize compounds for further toxicological evaluation (Huang et al. 2016b). Predictive models for human-adverse drug effects have also been built using the Tox21 screening data with or without compound structure data, as well as a combination of structure and screening data with or without drug target annotations and animal toxicity endpoints (Huang et al. 2018), which validated that further addition of drug-target annotations to the current dataset resulted in improved model performances. Therefore, these predictive computational models combining screening data alongside structural features will facilitate a faster approach for assessing interference of compounds on various targets and/or endpoints.

The Tox21 program has been an instrumental asset to prioritizing environmental chemicals as toxic or safe. However, throughout the process, new challenges have arisen due to the results from these previous methods. A main biological issue discovered was the lack of metabolically competent systems within the assays, meaning that only the parent compound of a chemical was being

assessed, as well as an inability to determine if certain chemicals were still available once the initial metabolic process of the body was complete (Thomas et al. 2018). Due to these difficulties, Tox21 plans to use more physiologically relevant systems, including the use of liver microsomes and cells already comprising certain metabolizing enzymes. Another challenge that Tox21 is attempting to overcome is the issue of covering every pathway involved in a complex organism. Moving forward, new technologies will be used that can provide information that represents the global transcriptome, including global gene expression. Throughout the history of Tox21, it has become clear that this program is not only necessary for the identification of toxic chemicals but is a revolving, ever-changing entity which strives to improve and expand upon the knowledge of toxicity testing in the future.

**Acknowledgements** This work was supported in part by the Intramural Research Program of the National Center for Advancing Translational Sciences (NCATS) at the National Institutes of Health (NIH). The views expressed in this article are those of the authors and do not necessarily reflect the statements, opinions, views, conclusions, or policies of the NCATS, the NIH, or the US Government.

### References

- Ademuyiwa O, Ugbaja RN, Rotimi SO, Abam E, Okediran BS, Dosumu OA, Onunkwor BO (2007) Erythrocyte acetylcholinesterase activity as a surrogate indicator of lead-induced neurotoxicity in occupational lead exposure in Abeokuta, Nigeria. *Environ Toxicol Pharmacol* 24(2):183–188. <https://doi.org/10.1016/j.etap.2007.05.002>
- Attene-Ramos MS, Huang R, Michael S, Witt KL, Richard A, Tice RR, Simeonov A, Austin CP, Xia M (2015) Profiling of the Tox21 chemical collection for mitochondrial function to identify compounds that acutely decrease mitochondrial membrane potential. *Environ Health Perspect* 123(1):49–56. <https://doi.org/10.1289/ehp.1408642>
- Attene-Ramos MS, Huang RL, Sakamuru S, Witt KL, Beeson GC, Shou L, Schnellmann RG, Beeson CC, Tice RR, Austin CP, Xia MH (2013) Systematic study of mitochondria! toxicity of environmental chemicals using quantitative high throughput screening. *Chem Res Toxicol* 26(9):1323–1332. <https://doi.org/10.1021/tx4001754>
- Bi K, Nishihara K, Machleidt T, Hermanson S, Wang J, Sakamuru S, Huang R, Xia M (2015) Identification of known drugs targeting the endoplasmic reticulum stress response. *Anal Bioanal Chem* 407(18):5343–5351. <https://doi.org/10.1007/s00216-015-8694-2>
- Bond M, Rogers G, Peters J, Anderson R, Hoyle M, Miners A, Moxham T, Davis S, Thokala P, Wailoo A, Jeffreys M, Hyde C (2012) The effectiveness and cost-effectiveness of donepezil, galantamine, rivastigmine and memantine for the treatment of Alzheimer's disease (review of Technology Appraisal No. 111): a systematic review and economic model. *Health Technol Assess* 16(21):1–470. <https://doi.org/10.3310/hta16210>
- Chang C, Lee SO, Yeh S, Chang TM (2014) Androgen receptor (AR) differential roles in hormone-related tumors including prostate, bladder, kidney, lung, breast and liver. *Oncogene* 33(25):3225–3234. <https://doi.org/10.1038/ncr.2013.274>

- Chen LB (1988) Mitochondrial membrane potential in living cells. *Annu Rev Cell Biol* 4:155–181. <https://doi.org/10.1146/annurev.cb.04.110188.001103>
- Chen S, Hsieh JH, Huang R, Sakamuru S, Hsin LY, Xia M, Shockley KR, Auerbach S, Kanaya N, Lu H, Svoboda D, Witt KL, Merrick BA, Teng CT, Tice RR (2015) Cell-based high-throughput screening for aromatase inhibitors in the Tox21 10 K library. *Toxicol Sci* 147(2):446–457. <https://doi.org/10.1093/toxsci/kfv141>
- Chen Y, Sakamuru S, Huang R, Reese DH, Xia M (2016) Identification of compounds that modulate retinol signaling using a cell-based qHTS assay. *Toxicol Vitro* 32:287–296. <https://doi.org/10.1016/j.tiv.2016.01.011>
- Colovic MB, Krstic DZ, Lazarevic-Pasti TD, Bondzic AM, Vasic VM (2013) Acetylcholinesterase inhibitors: pharmacology and toxicology. *Curr Neuropharmacol* 11(3):315–335. <https://doi.org/10.2174/1570159X11311030006>
- Culig Z, Klocker H, Bartsch G, Hobisch A (2002) Androgen receptors in prostate cancer. *Endocr Relat Cancer* 9(3):155–170
- Ellman GL, Courtney KD, Andres V Jr, Feather-Stone RM (1961) A new and rapid colorimetric determination of acetylcholinesterase activity. *Biochem Pharmacol* 7:88–95
- Farkas DL, Wei MD, Febroriello P, Carson JH, Loew LM (1989) Simultaneous imaging of cell and mitochondrial membrane potentials. *Biophys J* 56(6):1053–1069. [https://doi.org/10.1016/S0006-3495\(89\)82754-7](https://doi.org/10.1016/S0006-3495(89)82754-7)
- FDA's Predictive Toxicology Roadmap (2017)
- Fernandez HL, Moreno RD, Inestrosa NC (1996) Tetrameric (G4) acetylcholinesterase: structure, localization, and physiological regulation. *J Neurochem* 66(4):1335–1346
- Fox JT, Sakamuru S, Huang R, Teneva N, Simmons SO, Xia M, Tice RR, Austin CP, Myung K (2012) High-throughput genotoxicity assay identifies antioxidants as inducers of DNA damage response and cell death. *Proc Natl Acad Sci USA* 109(14):5423–5428. <https://doi.org/10.1073/pnas.1114278109>
- Fradet A, Bouchet M, Delliaux C, Gervais M, Kan C, Benetollo C, Pantano F, Vargas G, Bouazza L, Croset M, Bala Y, Leroy X, Rosol TJ, Rieusset J, Bellahcene A, Castronovo V, Aubin JE, Clezardin P, Duterque-Coquillaud M, Bonnelye E (2016) Estrogen related receptor alpha in castration-resistant prostate cancer cells promotes tumor progression in bone. *Oncotarget* 7(47):77071–77086. <https://doi.org/10.18632/oncotarget.12787>
- Freitas J, Miller N, Mengeling BJ, Xia M, Huang R, Houck K, Rietjens IM, Furlow JD, Murk AJ (2014) Identification of thyroid hormone receptor active compounds using a quantitative high-throughput screening platform. *Curr Chem Genom Transl Med* 8:36–46. <https://doi.org/10.2174/2213988501408010036>
- Gao J, Xie W (2010) Pregnane X receptor and constitutive androstane receptor at the crossroads of drug metabolism and energy metabolism. *Drug Metab Dispos* 38(12):2091–2095. <https://doi.org/10.1124/dmd.110.035568>
- Giacobini E (2000) Cholinesterase inhibitors stabilize Alzheimer's disease. *Ann N Y Acad Sci* 920:321–327
- Gibb S (2008) Toxicity testing in the 21st century: a vision and a strategy. *Reprod Toxicol* 25(1):136–138. <https://doi.org/10.1016/j.reprotox.2007.10.013>
- Giguere V (1999) Orphan nuclear receptors: from gene to function. *Endocr Rev* 20(5):689–725. <https://doi.org/10.1210/edrv.20.5.0378>
- Gonzalez TL, Rae JM, Colacino JA (2019) Implications of Environmental estrogen and anti-androgen exposure on human health: a focus on the relationship between estrogenicity and breast cancer. *Toxicology*. <https://doi.org/10.1016/j.tox.2019.03.014>
- Greaves P, Williams A, Eve M (2004) First dose of potential new medicines to humans: how animals help. *Nat Rev Drug Discov* 3(3):226–236. <https://doi.org/10.1038/nrd1329>
- Guo J, Tang Q, Wang Q, Sun W, Pu Z, Wang J, Bao Y (2019) Pifithrin-alpha enhancing anticancer effect of topotecan on p53-expressing cancer cells. *Eur J Pharm Sci* 128:61–72. <https://doi.org/10.1016/j.ejps.2018.11.024>
- Hancock MK, Xia M, Frey ES, Sakamuru S, Bi K (2009) HTS-compatible beta-lactamase transcriptional reporter gene assay for interrogating the heat shock response pathway. *Curr Chem Genomics* 3:1–6. <https://doi.org/10.2174/1875397300903010001>
- He G, Tsutsumi T, Zhao B, Baston DS, Zhao J, Heath-Pagliuso S, Denison MS (2011) Third-generation Ah receptor-responsive luciferase reporter plasmids: amplification of dioxin-responsive elements dramatically increases CALUX bioassay sensitivity and responsiveness. *Toxicol Sci* 123(2):511–522. <https://doi.org/10.1093/toxsci/kfr189>
- Hedrich WD, Xiao J, Heyward S, Zhang Y, Zhang J, Baer MR, Hassan HE, Wang H (2016) Activation of the constitutive androstane receptor increases the therapeutic index of CHOP in lymphoma treatment. *Mol Cancer Ther* 15(3):392–401. <https://doi.org/10.1158/1535-7163.MCT-15-0667>
- Holas O, Musilek K, Pohanka M, Kuca K (2012) The progress in the cholinesterase quantification methods. *Expert Opin Drug Discov* 7(12):1207–1223. <https://doi.org/10.1517/17460441.2012.729037>
- Hsu CW, Hsieh JH, Huang R, Pijnenburg D, Khuc T, Hamm J, Zhao J, Lynch C, van Beuningen R, Chang X, Houtman R, Xia M (2016a) Differential modulation of FXR activity by chlorophacinone and ivermectin analogs. *Toxicol Appl Pharmacol* 313:138–148. <https://doi.org/10.1016/j.taap.2016.10.017>
- Hsu CW, Huang R, Khuc T, Shou D, Bullock J, Grooby S, Griffin S, Zou C, Little A, Astley H, Xia M (2016b) Identification of approved and investigational drugs that inhibit hypoxia-inducible factor-1 signaling. *Oncotarget* 7(7):8172–8183. <https://doi.org/10.18632/oncotarget.6995>
- Hsu CW, Shou D, Huang R, Khuc T, Dai S, Zheng W, Klumpp-Thomas C, Xia M (2016c) Identification of HDAC inhibitors using a cell-based HDAC I/II assay. *J Biomol Screen* 21(6):643–652. <https://doi.org/10.1177/1087057116629381>
- Hsu CW, Zhao J, Xia M (2016d) Transactivation and coactivator recruitment assays for measuring farnesoid X receptor activity. *Methods Mol Biol* 1473:43–53. [https://doi.org/10.1007/978-1-4939-6346-1\\_5](https://doi.org/10.1007/978-1-4939-6346-1_5)
- Hsu CW, Huang R, Attene-Ramos M, Austin CP, Simeonov A, Xia M (2017) Advances in high-throughput screening technology for toxicology. *Int J Risk Assess Manag* 20(1–3):109–135. <https://doi.org/10.1504/ijram.2017.082562>
- Hsu CW, Zhao J, Huang R, Hsieh JH, Hamm J, Chang X, Houck K, Xia M (2014) Quantitative high-throughput profiling of environmental chemicals and drugs that modulate farnesoid X receptor. *Sci Rep* 4:6437. <https://doi.org/10.1038/srep06437>
- Huang R, Sakamuru S, Martin MT, Reif DM, Judson RS, Houck KA, Casey W, Hsieh JH, Shockley KR, Ceger P, Fostel J, Witt KL, Tong W, Rotroff DM, Zhao T, Shinn P, Simeonov A, Dix DJ, Austin CP, Kavlock RJ, Tice RR, Xia M (2014) Profiling of the Tox21 10 K compound library for agonists and antagonists of the estrogen receptor alpha signaling pathway. *Sci Rep* 4:5664. <https://doi.org/10.1038/srep05664>
- Huang R, Southall N, Cho MH, Xia M, Ingles J, Austin CP (2008) Characterization of diversity in toxicity mechanism using in vitro cytotoxicity assays in quantitative high throughput screening. *Chem Res Toxicol* 21(3):659–667. <https://doi.org/10.1021/tx700365e>
- Huang R, Xia M, Cho MH, Sakamuru S, Shinn P, Houck KA, Dix DJ, Judson RS, Witt KL, Kavlock RJ, Tice RR, Austin CP (2011) Chemical genomics profiling of environmental chemical modulation of human nuclear receptors. *Environ Health Perspect* 119(8):1142–1148. <https://doi.org/10.1289/ehp.1002952>

- Huang RL (2016) A quantitative high-throughput screening data analysis pipeline for activity profiling. In: High-throughput screening assays in toxicology, vol 1473, pp 111–122. [https://doi.org/10.1007/978-1-4939-6346-1\\_12](https://doi.org/10.1007/978-1-4939-6346-1_12)
- Huang R, Xia M, Nguyen D-T, Zhao T, Sakamuru S, Zhao J, Shahane SA, Rossoshek A, Simeonov A (2016a) Tox21Challenge to build predictive models of nuclear receptor and stress response pathways as mediated by exposure to environmental chemicals and drugs. *Front Environ Sci* 3 (85). <https://doi.org/10.3389/fenvs.2015.00085>
- Huang R, Xia M, Sakamuru S, Zhao J, Shahane SA, Attene-Ramos M, Zhao T, Austin CP, Simeonov A (2016b) Modelling the Tox21 10 K chemical profiles for in vivo toxicity prediction and mechanism characterization. *Nat Commun* 7:10425. <https://doi.org/10.1038/ncomms10425>
- Huang R, Xia M, Sakamuru S, Zhao J, Lynch C, Zhao T, Zhu H, Austin CP, Simeonov A (2018) Expanding biological space coverage enhances the prediction of drug adverse effects in human using in vitro activity profiles. *Sci Rep* 8(1):3783. <https://doi.org/10.1038/s41598-018-22046-w>
- Inglese J, Auld DS, Jadhav A, Johnson RL, Simeonov A, Yasgar A, Zheng W, Austin CP (2006) Quantitative high-throughput screening: a titration-based approach that efficiently identifies biological activities in large chemical libraries. *Proc Natl Acad Sci USA* 103 (31):11473–11478. <https://doi.org/10.1073/pnas.0604348103>
- Jiang J, Hui CC (2008) Hedgehog signaling in development and cancer. *Dev Cell* 15(6):801–812. <https://doi.org/10.1016/j.devcel.2008.11.010>
- Johnson JA, Johnson DA, Kraft AD, Calkins MJ, Jakel RJ, Vargas MR, Chen PC (2008) The Nrf2-ARE pathway: an indicator and modulator of oxidative stress in neurodegeneration. *Ann NY Acad Sci* 1147:61–69. <https://doi.org/10.1196/annals.1427.036>
- Judson RS, Magpantay FM, Chickarmane V, Haskell C, Tania N, Taylor J, Xia M, Huang R, Rotroff DM, Filer DL, Houck KA, Martin MT, Sipes N, Richard AM, Mansouri K, Setzer RW, Knudsen TB, Crofton KM, Thomas RS (2015) Integrated model of chemical perturbations of a biological pathway using 18 in vitro high-throughput screening assays for the estrogen receptor. *Toxicol Sci* 148(1):137–154. <https://doi.org/10.1093/toxsci/kfv168>
- Kang JJ, Fang HW (1997) Polycyclic aromatic hydrocarbons inhibit the activity of acetylcholinesterase purified from electric eel. *Biochem Biophys Res Commun* 238(2):367–369. <https://doi.org/10.1006/bbrc.1997.7293>
- Khuc T, Hsu CW, Sakamuru S, Xia M (2016) Using beta-lactamase and nanoluciferase reporter gene assays to identify inhibitors of the HIF-1 signaling pathway. *Methods Mol Biol* 1473:23–31. [https://doi.org/10.1007/978-1-4939-6346-1\\_3](https://doi.org/10.1007/978-1-4939-6346-1_3)
- Leone TC, Lehman JJ, Finck BN, Schaeffer PJ, Wende AR, Boudina S, Courtois M, Wozniak DF, Sambandam N, Bernal-Mizrachi C, Chen Z, Holloszy JO, Medeiros DM, Schmidt RE, Saffitz JE, Abel ED, Semenkovich CF, Kelly DP (2005) PGC-1alpha deficiency causes multi-system energy metabolic derangements: muscle dysfunction, abnormal weight control and hepatic steatosis. *PLoS Biol* 3(4):e101. <https://doi.org/10.1371/journal.pbio.0030101>
- Li S, Huang R, Solomon S, Liu Y, Zhao B, Santillo MF, Xia M (2017a) Identification of acetylcholinesterase inhibitors using homogenous cell-based assays in quantitative high-throughput screening platforms. *Biotechnol J* 12(5). <https://doi.org/10.1002/biot.201600715>
- Li S, Zhao J, Huang R, Steiner T, Bourner M, Mitchell M, Thompson DC, Zhao B, Xia M (2017b) Development and application of human renal proximal tubule epithelial cells for assessment of compound toxicity. *Curr Chem Genom Transl Med* 11:19–30. <https://doi.org/10.2174/2213988501711010019>
- Li S, Zhao J, Huang R, Santillo MF, Houck KA, Xia M (2019) Use of high-throughput enzyme-based assay with xenobiotic metabolic capability to evaluate the inhibition of acetylcholinesterase activity by organophosphorous pesticides. *Toxicol Vitr* 56:93–100. <https://doi.org/10.1016/j.tiv.2019.01.002>
- Lin J, Wu PH, Tarr PT, Lindenberg KS, St-Pierre J, Zhang CY, Mootha VK, Jager S, Vianna CR, Reznick RM, Cui L, Manieri M, Donovan MX, Wu Z, Cooper MP, Fan MC, Rohas LM, Zavacki AM, Cinti S, Shulman GI, Lowell BB, Krainc D, Spiegelman BM (2004) Defects in adaptive energy metabolism with CNS-linked hyperactivity in PGC-1alpha null mice. *Cell* 119 (1):121–135. <https://doi.org/10.1016/j.cell.2004.09.013>
- Lionetto MG, Caricato R, Calisi A, Giordano ME, Schettino T (2013) Acetylcholinesterase as a biomarker in environmental and occupational medicine: new insights and future perspectives. *Biomed Res Int* 2013:321213. <https://doi.org/10.1155/2013/321213>
- Luo J, Sladek R, Carrier J, Bader JA, Richard D, Giguere V (2003) Reduced fat mass in mice lacking orphan nuclear receptor estrogen-related receptor alpha. *Mol Cell Biol* 23(22):7947–7956
- Lynch C, Mackowiak B, Huang R, Li L, Heyward S, Sakamuru S, Wang H, Xia M (2019a) Identification of modulators that activate the constitutive androstane receptor from the Tox21 10 K compound library. *Toxicol Sci* 167(1):282–292. <https://doi.org/10.1093/toxsci/kfy242>
- Lynch C, Zhao J, Sakamuru S, Zhang L, Huang R, Witt KL, Merrick BA, Teng CT, Xia M (2019b) Identification of compounds that inhibit estrogen-related receptor alpha signaling using high-throughput screening assays. *Molecules* 24(5). <https://doi.org/10.3390/molecules24050841>
- Lynch C, Pan Y, Li L, Heyward S, Moeller T, Swaan PW, Wang H (2014) Activation of the constitutive androstane receptor inhibits gluconeogenesis without affecting lipogenesis or fatty acid synthesis in human hepatocytes. *Toxicol Appl Pharmacol* 279(1):33–42. <https://doi.org/10.1016/j.taap.2014.05.009>
- Lynch C, Pan YM, Li LH, Ferguson SS, Xia MH, Swaan PW, Wang HB (2013) Identification of novel activators of constitutive androstane receptor from FDA-approved drugs by integrated computational and biological approaches. *Pharm Res Dordr* 30 (2):489–501. <https://doi.org/10.1007/s11095-012-0895-1>
- Lynch C, Sakamuru S, Huang R, Stavreva DA, Varticovski L, Hager GL, Judson RS, Houck KA, Kleinstreuer NC, Casey W, Paules RS, Simeonov A, Xia M (2017) Identifying environmental chemicals as agonists of the androgen receptor by using a quantitative high-throughput screening platform. *Toxicology* 385:48–58. <https://doi.org/10.1016/j.tox.2017.05.001>
- Lynch C, Zhao J, Huang R, Xiao J, Li L, Heyward S, Xia M, Wang H (2015) Quantitative high-throughput identification of drugs as modulators of human constitutive androstane receptor. *Sci Rep* 5:10405. <https://doi.org/10.1038/srep10405>
- Lynch C, Zhao J, Wang H, Xia M (2016) Quantitative high-throughput luciferase screening in identifying CAR modulators. *Methods Mol Biol* 1473:33–42. [https://doi.org/10.1007/978-1-4939-6346-1\\_4](https://doi.org/10.1007/978-1-4939-6346-1_4)
- Lynch C, Zhao JH, Huang RL, Kanaya N, Bernal L, Hsieh JH, Auerbach SS, Witt KL, Merrick BA, Chen SA, Teng CT, Xia MH (2018) Identification of estrogen-related receptor alpha agonists in the Tox21 compound library. *Endocrinology* 159(2):744–753. <https://doi.org/10.1210/en.2017-00658>
- Macho A, Decaudin D, Castedo M, Hirsch T, Susin SA, Zamzami N, Kroemer G (1996) Chloromethyl-X-Rosamine is an aldehyde-fixable potential-sensitive fluorochrome for the detection of early apoptosis. *Cytometry* 25(4):333–340. [https://doi.org/10.1002/\(SICI\)1097-0320\(19961201\)25:4<333::AID-CYTO4%3e3.0.CO;2-E](https://doi.org/10.1002/(SICI)1097-0320(19961201)25:4<333::AID-CYTO4%3e3.0.CO;2-E)
- Massoulié J, Pezzementi L, Bon S, Krejci E, Vallette FM (1993) Molecular and cellular biology of cholinesterases. *Prog Neurobiol* 41(1):31–91
- Matsushima H, Mori T, Ito F, Yamamoto T, Akiyama M, Kokabu T, Yoriki K, Umemura S, Akashi K, Kitawaki J (2016) Anti-tumor effect of estrogen-related receptor alpha knockdown on uterine

- endometrial cancer. *Oncotarget* 7(23):34131–34148. <https://doi.org/10.18632/oncotarget.9151>
- Miao Y, He N, Zhu JJ (2010) History and new developments of assays for cholinesterase activity and inhibition. *Chem Rev* 110(9):5216–5234. <https://doi.org/10.1021/cr900214c>
- Miller SC, Huang R, Sakamuru S, Shukla SJ, Attene-Ramos MS, Shinn P, Van Leer D, Leister W, Austin CP, Xia M (2010) Identification of known drugs that act as inhibitors of NF-kappaB signaling and their mechanism of action. *Biochem Pharmacol* 79(9):1272–1280. <https://doi.org/10.1016/j.bcp.2009.12.021>
- Mooser G, Sigman DS (1974) Ligand binding properties of acetylcholinesterase determined with fluorescent probes. *Biochemistry* 13(11):2299–2307
- Nachmansohn D, Wilson IB (1951) The enzymic hydrolysis and synthesis of acetylcholine. *Adv Enzymol Relat Subj Biochem* 12:259–339
- Nishihara K, Huang R, Zhao J, Shahane SA, Witt KL, Smith-Roe SL, Tice RR, Takeda S, Xia M (2016) Identification of genotoxic compounds using isogenic DNA repair deficient DT40 cell lines on a quantitative high throughput screening platform. *Mutagenesis* 31(1):69–81. <https://doi.org/10.1093/mutage/gev055>
- NRC NRC (1984). In: Toxicity testing: strategies to determine needs and priorities. The National Academies Collection: Reports funded by National Institutes of Health. Washington (DC). <https://doi.org/10.17226/317>
- Park S, Chang CY, Safi R, Liu X, Baldi R, Jasper JS, Anderson GR, Liu T, Rathmell JC, Dewhirst MW, Wood KC, Locasale JW, McDonnell DP (2016) ERRalpha-regulated lactate metabolism contributes to resistance to targeted therapies in breast cancer. *Cell Rep* 15(2):323–335. <https://doi.org/10.1016/j.celrep.2016.03.026>
- Pihlajamaa P, Sahu B, Janne OA (2015) Determinants of receptor- and tissue-specific actions in androgen signaling. *Endocr Rev* 36(4):357–384. <https://doi.org/10.1210/er.2015-1034>
- Qatanani M, Moore DD (2005) CAR, the continuously advancing receptor, in drug metabolism and disease. *Curr Drug Metab* 6(4):329–339
- Quinn DM (1987) Acetylcholinesterase: enzyme structure, reaction dynamics, and virtual transition states. *Chem Rev* 87(5):955–979. <https://doi.org/10.1021/cr00081a005>
- Reddy PM, Philip GH (1994) In vivo inhibition of AChE and ATPase activities in the tissues of freshwater fish, *Cyprinus carpio* exposed to technical grade cypermethrin. *Bull Environ Contam Toxicol* 52(4):619–626
- Rotroff DM, Martin MT, Dix DJ, Filer DL, Houck KA, Knudsen TB, Sipes NS, Reif DM, Xia M, Huang R, Judson RS (2014) Predictive endocrine testing in the 21st century using in vitro assays of estrogen receptor signaling responses. *Environ Sci Technol* 48(15):8706–8716. <https://doi.org/10.1021/es502676e>
- Sakamuru S, Attene-Ramos MS, Xia M (2016) Mitochondrial membrane potential assay. *Methods Mol Biol* 1473:17–22. [https://doi.org/10.1007/978-1-4939-6346-1\\_2](https://doi.org/10.1007/978-1-4939-6346-1_2)
- Sakamuru S, Li X, Attene-Ramos MS, Huang R, Lu J, Shou L, Shen M, Tice RR, Austin CP, Xia M (2012) Application of a homogenous membrane potential assay to assess mitochondrial function. *Physiol Genomics* 44(9):495–503. <https://doi.org/10.1152/physiolgenomics.00161.2011>
- Salvioli S, Ardizzoni A, Franceschi C, Cossarizza A (1997) JC-1, but not DiOC(6)(3) or rhodamine 123, is a reliable fluorescent probe to assess Delta Psi changes in intact cells: implications for studies on mitochondrial functionality during apoptosis. *FEBS Lett* 411(1):77–82. [https://doi.org/10.1016/S0014-5793\(97\)00669-8](https://doi.org/10.1016/S0014-5793(97)00669-8)
- Santillo MF, Liu Y (2015) A fluorescence assay for measuring acetylcholinesterase activity in rat blood and a human neuroblastoma cell line (SH-SY5Y). *J Pharmacol Toxicol Methods* 76:15–22. <https://doi.org/10.1016/j.vascn.2015.07.002>
- Shukla SJ, Huang R, Austin CP, Xia M (2010) The future of toxicity testing: a focus on in vitro methods using a quantitative high-throughput screening platform. *Drug Discov Today* 15(23–24):997–1007. <https://doi.org/10.1016/j.drudis.2010.07.007>
- Shukla SJ, Huang R, Simmons SO, Tice RR, Witt KL, Vanleer D, Ramabhadran R, Austin CP, Xia M (2012) Profiling environmental chemicals for activity in the antioxidant response element signaling pathway using a high throughput screening approach. *Environ Health Perspect* 120(8):1150–1156. <https://doi.org/10.1289/ehp.1104709>
- Shukla SJ, Sakamuru S, Huang R, Moeller TA, Shinn P, Vanleer D, Auld DS, Austin CP, Xia M (2011) Identification of clinically used drugs that activate pregnane X receptors. *Drug Metab Dispos* 39(1):151–159. <https://doi.org/10.1124/dmd.110.035105>
- Sinko G, Calic M, Bosak A, Kovarik Z (2007) Limitation of the Ellman method: cholinesterase activity measurement in the presence of oximes. *Anal Biochem* 370(2):223–227. <https://doi.org/10.1016/j.ab.2007.07.023>
- Skakkebaek A, Bojesen A, Kristensen MK, Cohen A, Hougaard DM, Hertz JM, Fedder J, Laurberg P, Wallentin M, Ostergaard JR, Pedersen AD, Gravholt CH (2014) Neuropsychology and brain morphology in Klinefelter syndrome—the impact of genetics. *Andrology* 2(4):632–640. <https://doi.org/10.1111/j.2047-2927.2014.00229.x>
- Soreq H, Seidman S (2001) Acetylcholinesterase—new roles for an old actor. *Nat Rev Neurosci* 2(4):294–302. <https://doi.org/10.1038/35067589>
- Sultatos LG (1994) Mammalian toxicology of organophosphorus pesticides. *J Toxicol Environ Health* 43(3):271–289. <https://doi.org/10.1080/15287399409531921>
- Tanaka F, Katsuno M, Banno H, Suzuki K, Adachi H, Sobue G (2012) Current status of treatment of spinal and bulbar muscular atrophy. *Neural Plast* 2012:369284. <https://doi.org/10.1155/2012/369284>
- Taylor P, Lappi S (1975) Interaction of fluorescence probes with acetylcholinesterase. The site and specificity of propidium binding. *Biochemistry* 14(9):1989–1997
- Taylor P, Radic Z (1994) The cholinesterases: from genes to proteins. *Annu Rev Pharmacol Toxicol* 34:281–320. <https://doi.org/10.1146/annurev.pa.34.040194.001433>
- Teng CT, Beames B, Alex Merrick B, Martin N, Romeo C, Jetten AM (2014) Development of a stable cell line with an intact PGC-1alpha/ERRalpha axis for screening environmental chemicals. *Biochem Biophys Res Commun* 444(2):177–181. <https://doi.org/10.1016/j.bbrc.2014.01.033>
- Teng CT, Hsieh JH, Zhao J, Huang R, Xia M, Martin N, Gao X, Dixon D, Auerbach SS, Witt KL, Merrick BA (2017) Development of novel cell lines for high-throughput screening to detect estrogen-related receptor alpha modulators. *SLAS Discov* 22(6):720–731. <https://doi.org/10.1177/2472555216689772>
- Thomas RS, Paules RS, Simeonov A, Fitzpatrick SC, Crofton KM, Casey WM, Mendrick DL (2018) The US federal Tox21 program: a strategic and operational plan for continued leadership. *Altex* 35(2):163–168. <https://doi.org/10.14573/altex.1803011>
- Wallace KB, Eells JT, Madeira VM, Cortopassi G, Jones DP (1997) Mitochondria-mediated cell injury. Symposium overview. *Fundam Appl Toxicol* 38(1):23–37
- Wang R, Tang XC (2005) Neuroprotective effects of huperzine A. A natural cholinesterase inhibitor for the treatment of Alzheimer's disease. *Neurosignals* 14(1–2):71–82. <https://doi.org/10.1159/000085387>
- Wang Y, Jadhav A, Southal N, Huang R, Nguyen DT (2010) A grid algorithm for high throughput fitting of dose-response curve data. *Curr Chem Genomics* 4:57–66. <https://doi.org/10.2174/1875397301004010057>
- Watkins PB, Zimmerman HJ, Knapp MJ, Gracon SI, Lewis KW (1994) Hepatotoxic effects of tacrine administration in patients with Alzheimer's disease. *JAMA* 271(13):992–998



- Wilson IB, Quan C (1958) Acetylcholinesterase studies on molecular complementarity. *Arch Biochem Biophys* 73(1):131–143
- Witt KL, Hsieh JH, Smith-Roe SL, Xia M, Huang R, Zhao J, Auerbach SS, Hur J, Tice RR (2017) Assessment of the DNA damaging potential of environmental chemicals using a quantitative high-throughput screening approach to measure p53 activation. *Environ Mol Mutagen* 58(7):494–507. <https://doi.org/10.1002/em.22112>
- Xia M, Huang R, Shi Q, Boyd WA, Zhao J, Sun N, Rice JR, Dunlap PE, Hackstadt AJ, Bridge MF, Smith MV, Dai S, Zheng W, Chu PH, Gerhold D, Witt KL, DeVito M, Freedman JH, Austin CP, Houck KA, Thomas RS, Paules RS, Tice RR, Simeonov A (2018) Comprehensive analyses and prioritization of Tox21 10 K chemicals affecting mitochondrial function by in-depth mechanistic studies. *Environ Health Perspect* 126(7):077010. <https://doi.org/10.1289/EHP2589>
- Xie HQ, Xu HM, Fu HL, Hu Q, Tian WJ, Pei XH, Zhao B (2013) AhR-mediated effects of dioxin on neuronal acetylcholinesterase expression in vitro. *Environ Health Perspect* 121(5):613–618. <https://doi.org/10.1289/ehp.1206066>
- Yamamoto Y, Moore R, Goldsworthy TL, Negishi M, Maronpot RR (2004) The orphan nuclear receptor constitutive active/androstane receptor is essential for liver tumor promotion by phenobarbital in mice. *Cancer Res* 64(20):7197–7200. <https://doi.org/10.1158/0008-5472.CAN-04-1459>
- Zhao JH, Shukla SJ, Xia MH (2016) Cell-based assay for identifying the modulators of antioxidant response element signaling pathway. In: *High-throughput screening assays in toxicology*, vol 1473, pp 55–62. [https://doi.org/10.1007/978-1-4939-6346-1\\_6](https://doi.org/10.1007/978-1-4939-6346-1_6)
- Zurlo J, Rudacille D, Goldberg AM (1994) *Animals and alternatives in testing: history, science, and ethics*. Mary Ann Liebert, Inc. Accessed 04 Feb 2019

# Mixture Modelling and Effect-Directed Analysis for Identification of Chemicals, Mixtures and Effects of Concern

Peta A. Neale and Beate I. Escher

## Abstract

The complex mixtures of organic pollutants detected in environmental matrices means that chemical analysis alone does not provide a full picture of the chemical burden. Instead, bioassays, which detect the effects of all active chemicals in a sample, are proposed as complementary tools for environmental monitoring. This chapter outlines relevant mixture toxicity modelling concepts and demonstrates how the bioanalytical equivalent concentration approach (BEQ) can be used to evaluate the effects of environmental mixtures. Using iceberg modelling, BEQ from bioanalysis and BEQ from chemical analysis can be compared to determine how much of the effect can be explained by detected chemicals, with examples of iceberg modelling in water and sediment discussed. In the case of contamination hotspots, effect-directed analysis can be applied to identify unknown bioactive chemicals using a combination of fractionation, bioanalysis and chemical analysis with structural identification. Finally, effect-based trigger values derived by reading across from existing chemical guideline values were proposed to assess whether the effects of chemical mixtures in water are acceptable or unacceptable. This chapter highlights the importance of using bioassays in parallel to chemical analysis for environmental monitoring to gain a better understanding of the overall chemical burden.

## Keywords

Bioassay • Chemical analysis • Concentration addition • Effect-based trigger values • Iceberg modelling

## 1 Introduction

The aquatic environment contains numerous organic pollutants, such as pesticides, pharmaceuticals and industrial compounds, with chemicals detected in different environmental matrices, including water, sediment and biota (Kadokami et al. 2013; Loos et al. 2013; Scott et al. 2018). Water quality monitoring typically relies on targeted chemical analysis, which provides concentrations of known chemicals in a sample and allows comparison of detected concentrations with available guideline values for priority chemicals. However, chemical analysis alone cannot provide a complete picture of the chemical burden in water as it cannot detect unknown chemicals or account for the mixture effects that occur between the many chemicals in a sample (Wernersson et al. 2015). Chemicals are often present at low concentrations (pg/L to µg/L range) in water and may be below analytical detection limits, but the mixture effects of many chemicals at low concentrations can still result in an observable effect (e.g. “something from nothing” effect) (Silva et al. 2002).

Owing to the limitations associated with chemical analysis, bioanalysis is proposed as a complementary tool for environmental monitoring. Bioassays, which are also known as effect-based methods or bioanalytical tools, provide information about the mixture effects of all chemicals in a sample and are risk-scaled, with potent chemicals having a greater effect in the bioassay (Escher and Leusch 2012). Test batteries of in vitro bioassays indicative of different stages of cellular toxicity pathways, including xenobiotic metabolism, receptor-mediated effects, adaptive stress responses and cell viability, as well as early-life stage in vivo assays indicative

---

P. A. Neale  
Australian Rivers Institute, School of Environment and Science,  
Griffith University, Southport, QLD 4222, Australia  
e-mail: [p.neale@griffith.edu.au](mailto:p.neale@griffith.edu.au)

B. I. Escher (✉)  
UFZ – Helmholtz Centre for Environmental Research, 04318  
Leipzig, Germany  
e-mail: [beate.escher@ufz.de](mailto:beate.escher@ufz.de)

B. I. Escher  
Eberhard Karls University Tübingen, Environmental Toxicology,  
Center for Applied Geoscience, 72074 Tübingen, Germany

of apical effects, have been proposed for water quality monitoring (Fig. 1) (Neale et al. 2017a). This combination of bioassays is recommended in order to capture modes of action commonly detected in water and to prevent overlooking any unexpected effects. While bioassays detect the mixture effects of chemicals in a sample, they cannot provide information about which chemicals are contributing to the effect, though some assays, such as those indicative of receptor-mediated effects, are highly specific to certain classes of chemicals, for example natural and synthetic estrogens in the activation of the estrogen receptor (ER) assay. Consequently, both bioanalysis and chemical analysis are required to gain a comprehensive understanding of the chemical burden in a sample and subsequent mixture effects.

This chapter will outline relevant mixture toxicity modelling concepts and how chemical analysis and bioanalysis can be applied to evaluate environmental mixtures and identify causative chemicals. It will primarily focus on water samples, reflecting much of the research in this area to date, though some examples for sediment will also be discussed.

## 2 Mixture Toxicity Modelling

Mixture toxicity concepts can be classified based on chemical mode of action and chemical interaction. Assuming that the chemicals in a mixture do not interact, the mixture toxicity of chemicals that share a common mode of action can be described by the model of concentration addition (CA), while the model of independent action (IA) is used to predict the mixture toxicity of dissimilarly acting chemicals (Backhaus and Faust 2012). The effect concentration

predicted by CA ( $EC_{y,CA}$ ) is calculated using Eq. 1, where  $p_i$  is the fraction of each chemical  $i$  in the mixture and  $EC_{y,i}$  is the effect concentration at any effect level  $y$  for chemical  $i$ . IA predicted effect ( $E_{IA}$ ) is determined using Eq. 2, where  $E_i$  is the effect of each chemical in the mixture.

$$EC_{y,CA} = \frac{1}{\sum_{i=1}^n \frac{p_i}{EC_{y,i}}} \quad (1)$$

$$E_{IA} = 1 - \prod_{i=1}^n (1 - E_i) \quad (2)$$

Chemicals that interact at the toxicokinetic or toxicodynamic level can be described by synergism, where the mixture components have a greater effect than expected based on CA, or antagonism, where the mixture components show less effect than IA. While synergism and antagonism are observed in some binary mixtures, these interactions are not likely to be relevant in environmental samples containing many chemicals at low concentrations (Cedergreen 2014). Instead, CA is considered a conservative model to evaluate the mixture toxicity of dissimilarly acting compounds (Backhaus et al. 2000) and is suitable to predict the toxicity of chemical mixtures in assays indicative of receptor-mediated effects (Kortenkamp 2007; Tang and Escher 2014), adaptive stress responses (Escher et al. 2013) and apical effects (Tang et al. 2013b; Altenburger et al. 2018). The effect of chemical mixtures that act in a concentration additive manner can be translated to bioanalytical equivalent concentrations (BEQ) (Sect. 2.1) or toxic units (TU) (Sect. 2.2).

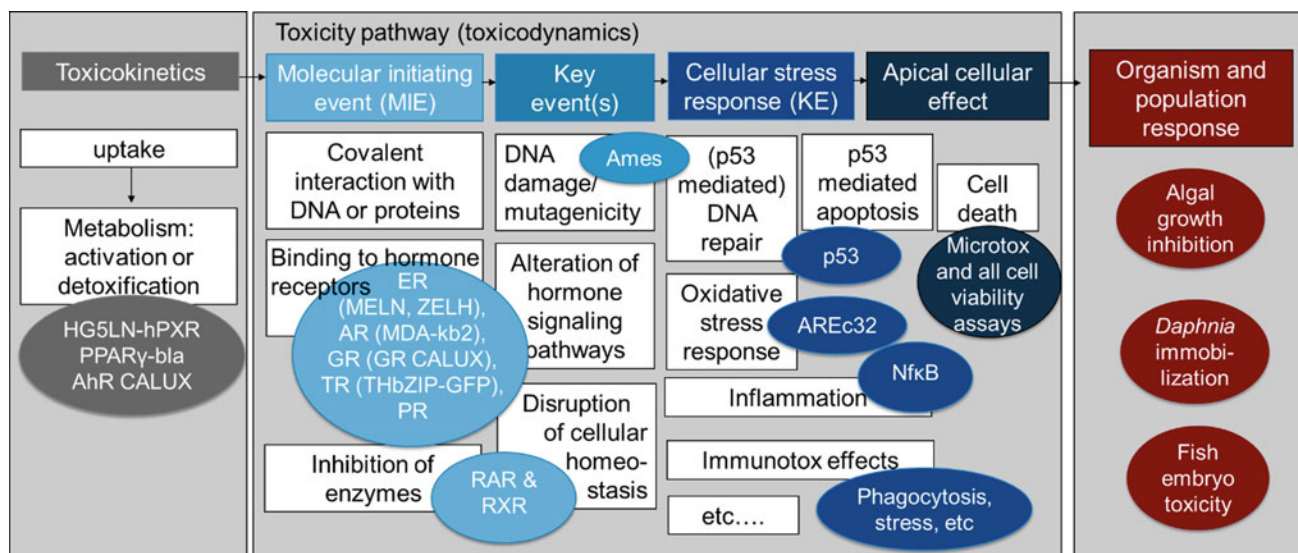


**Fig. 1** Proposed bioassay test battery covering assays indicative of different stages of the cellular toxicity pathway and apical effects in whole organisms. Reprinted from Neale et al. (2017a). Copyright 2017, with permission from Elsevier

## 2.1 Bioanalytical Equivalent Concentrations

The BEQ from bioanalysis ( $BEQ_{bio}$ ) relates the effect of a complex chemical mixture ( $EC_y$  (sample)) to the effect elicited by the assay reference compound ( $EC_y$  (ref)) (Fig. 2). This approach was initially applied to receptor-mediated effects, such as estradiol equivalent concentrations (EEQ) for assays indicative of estrogenic activity (Murk et al. 2002; Rutishauser et al. 2004), but is now applied more widely to assays indicative of xenobiotic metabolism, adaptive stress responses and non-specific toxicity (Escher et al. 2008, 2012; Neale et al. 2015). The BEQ from chemical analysis ( $BEQ_{chem}$ ) is calculated using the molar concentration of each detected chemical  $i$  and its relative effect potency ( $REP_i$ ) in the assay (Fig. 2).  $REP_i$  is determined based on the effect of the reference compound and the effect of the detected chemical  $i$ , with only experimental  $EC_y$  ( $i$ ) data used (Eq. 3).

$$REP_i = \frac{EC_y(\text{ref})}{EC_y(i)} \quad (3)$$

$BEQ_{bio}$  and  $BEQ_{chem}$  can be compared to determine the contribution of detected chemicals to the observed effect using an approach termed iceberg modelling (Eq. 4). Iceberg modelling has been applied to different environmental samples, including water, sediment and biota, with examples provided in Sect. 3.  $BEQ_{bio}$  and  $BEQ_{chem}$  can be used in mass balance models to understand how much of the effect is

explained by detected chemicals (e.g. how much of the iceberg is visible) and how much of the effect is due to undetected chemicals ( $BEQ_{unknown}$ ) (Fig. 2). The BEQ approach was also used to differentiate the effect of micropollutants and disinfection by-products in drinking water by comparing  $BEQ_{bio}$  before and after chlorination (Hebert et al. 2018).

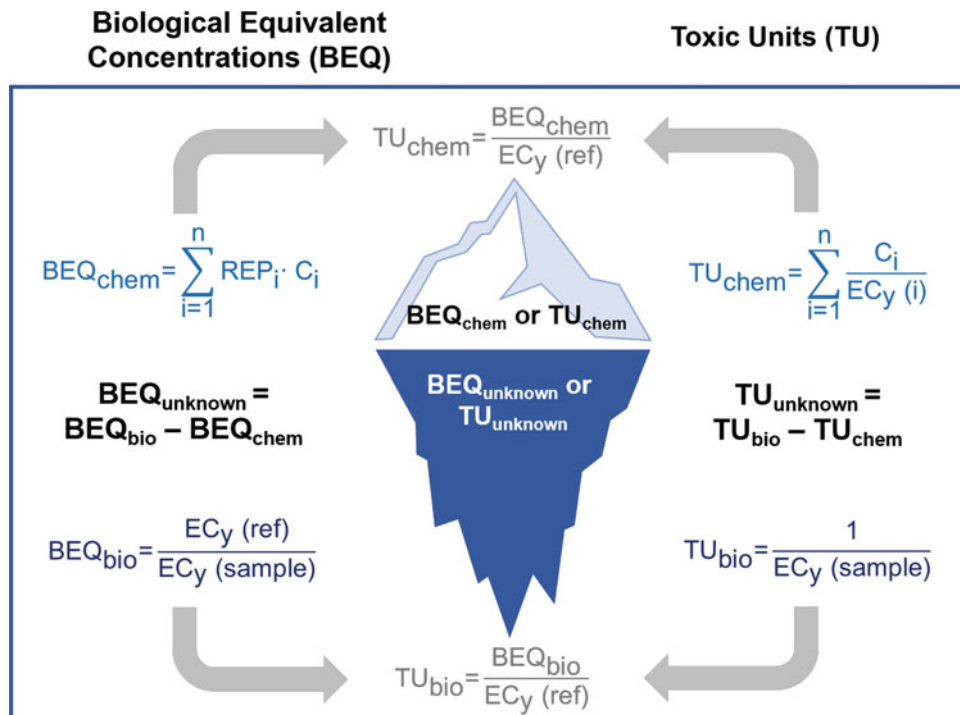
$$\% \text{ effect explained} = \frac{BEQ_{chem}}{BEQ_{bio}} \cdot 100\% \quad (4)$$

Iceberg modelling relies on experimental effect data for each detected chemical in order to calculate  $REP_i$  and the lack of available effect data is a limitation of this approach. However, US federal research collaborations Toxicity Forecaster (ToxCast) and Toxicology in the 21st Century (Tox21) have greatly increased the amount of available data, with effect data for over 9000 chemicals in up to 1192 assays in the iCSS ToxCast Dashboard (<https://actor.epa.gov/dashboard>). Several studies have also fingerprinted environmentally relevant chemicals in a range of bioassays (Leusch et al. 2014; Neale et al. 2017a).

## 2.2 Toxic Units

Effect data is also expressed in TU, particularly for in vivo assays. TU from chemical analysis ( $TU_{chem}$ ) are often used for chemical risk assessment (Kuzmanovic et al. 2015;

**Fig. 2** Bioanalytical equivalent concentration (BEQ) and toxic unit (TU) approaches for evaluating mixture toxicity, with equations linking BEQ and TU shown in grey. NB:  $C_i$ : concentration of chemical  $i$ ;  $EC_y$ : effect concentration; ref: reference compound;  $REP_i$ : relative effect potency



Beckers et al. 2018) and are calculated based on the detected chemical concentration and effect in a target organism (e.g. algae, daphnids, fish), with both experimental and Ecological Structure Activity Relationships (ECOSAR) predicted effect data used (Fig. 2). The TU are summed for each detected chemical to determine  $TU_{chem}$  and, like BEQ, CA is assumed. TU can also be calculated based on bioanalysis ( $TU_{bio}$ ) (Fig. 2) and several studies have compared  $TU_{chem}$  and  $TU_{bio}$  to determine which chemicals are contributing to the observed effect (Booij et al. 2014; Tousova et al. 2017; Guo et al. 2019).

As shown in Fig. 2, the BEQ and TU approaches are essentially equivalent, so both approaches can be used for in vitro and in vivo assays. The main difference is that only experimental EC values are used for  $BEQ_{chem}$ , while both experimental and predicted EC values are used to calculate  $TU_{chem}$ . Thus,  $TU_{chem}$  cannot be converted to  $BEQ_{chem}$  if predicted EC values are used. Owing to the inclusion of predicted data, a larger fraction of the effect may be explained using the TU approach compared to the BEQ approach. For example, between 0.84 and 20.6% of the effect in the 96 h fish embryo toxicity (FET) assay could be explained by detected chemicals in European surface waters using the TU approach with effect data for 90 chemicals predicted using the ECOSAR program (Tousova et al. 2017). In contrast, no more than 0.33% of the effect in the 48 h FET assay could be explained in the Danube River using the BEQ approach with experimental EC values for 19 detected chemicals (Neale et al. 2017a). These examples are not directly comparable as they represent different sampling sites, but help to illustrate the potential differences between BEQ and TU. It should be noted that the lower reliability of predicted data compared to experimental data is a limitation of the TU approach. Consequently, this chapter will primarily focus on the BEQ approach. It would also be possible to close data gaps in the BEQ approach using QSAR predictions, but to our knowledge there are no studies where predictive methods for effects were combined with a BEQ approach. The typically lower number of chemicals that are characterized for their effects is a limitation of the present application of the BEQ approach.

### 3 Iceberg Modelling Examples

Iceberg modelling using the BEQ approach has been applied to different environmental matrices to determine the contribution of detected chemicals to the observed effect. This section will focus on examples from the literature for water and sediment.

### 3.1 Water

Iceberg modelling has been applied to drinking water (Hebert et al. 2018; Shi et al. 2018), surface water (Neale et al. 2015; Conley et al. 2017), storm water (Tang et al. 2013a), wastewater and recycled water (Murk et al. 2002; Mehinto et al. 2015; Jia et al. 2016) and swimming pool water (Yeh et al. 2014). These studies have focused on a range of endpoints from different stages of cellular toxicity pathways (Fig. 3), though estrogenic activity is by far the most studied endpoint. In most cases, the effect in assays indicative of molecular initiating events, such as hormone receptor-mediated effects and photosystem II (PSII) inhibition, can be explained by the detected chemicals (e.g. Bengtson Nash et al. 2006; Jia et al. 2016; Conley et al. 2017). For example, over 100% of PSII inhibition in the Brisbane River can be explained by three herbicides, diuron, simazine and atrazine (Bengtson Nash et al. 2006), while simazine and atrazine also explain most of the PSII inhibition in samples from an advanced water treatment plant (Escher et al. 2011). Similarly, potent estrogenic hormones, such as estrone and  $17\beta$ -estradiol, typically explain most of the estrogenic activity in wastewater and surface water, with other weakly estrogenic compounds (e.g. bisphenol A, nonylphenol) only having a minor contribution to the effect (Rutishauser et al. 2004; Neale et al. 2015; Conley et al. 2017; Konig et al. 2017). In some studies only a small fraction of estrogenic activity could be explained (e.g. <5%), but this can be attributed to the presence of active compounds that are below the instrument limit of quantification but still contributed to the mixture effects in the sample (Escher et al. 2011).

Detected chemicals often only explain a small fraction of the effect in assays indicative of xenobiotic metabolism, adaptive stress responses and whole organism effects (Fig. 3). In many cases, <1% of the effect could be explained in the pregnane X receptor (PXR) (Creusot et al. 2010; Neale et al. 2017a), peroxisome proliferator-activated receptor ( $PPAR\gamma$ ) (Konig et al. 2017), oxidative stress response (Escher et al. 2013; Yeh et al. 2014; Neale et al. 2017b), p53 response (Neale et al. 2015) and FET assays (Neale et al. 2015). Unlike assays indicative of molecular initiating events, a wide variety of different chemicals can contribute to the effect in these assays.

Owing to low environmental concentrations, water samples need to be enriched prior to chemical analysis and bioanalysis, with solid-phase extraction (SPE) often applied to enrich water samples. Low recovery of some chemicals could mean that  $BEQ_{chem}$  underestimates the effect. However, recent studies have shown similar recovery of both individual

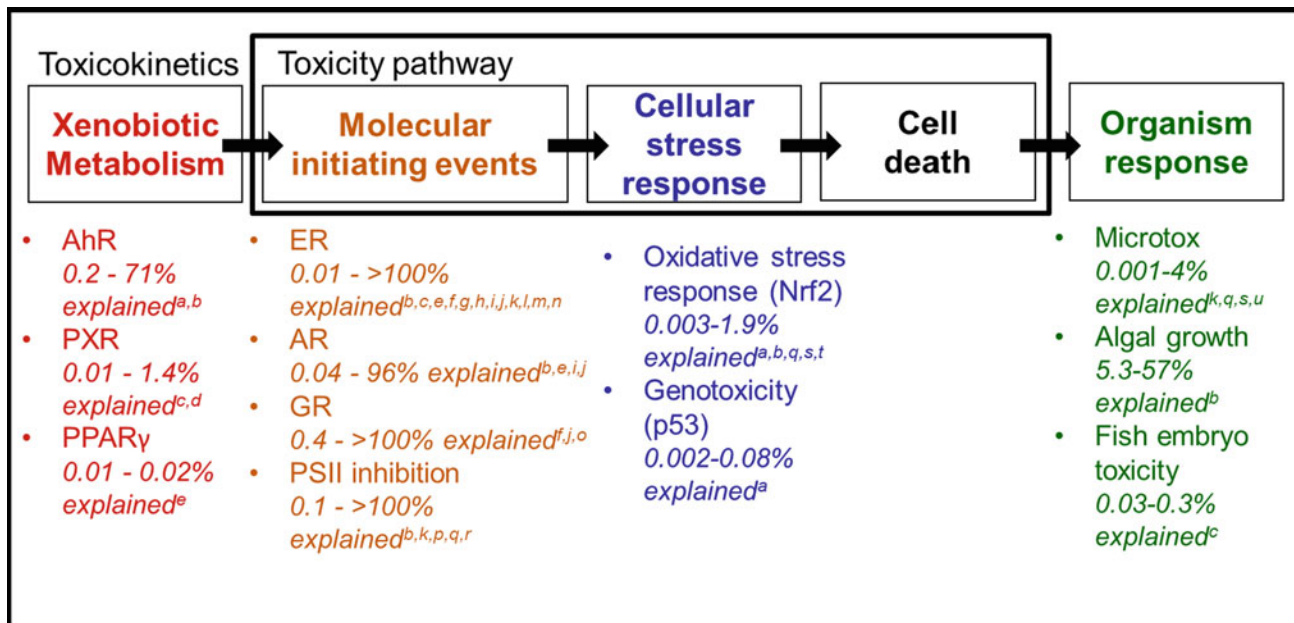


**Fig. 3** Examples of assays from the literature where iceberg modelling using the BEQ approach has been applied to determine the fraction of effect explained by detected chemicals. <sup>a</sup>Neale et al. (2015); <sup>b</sup>Neale et al. (2017b); <sup>c</sup>Neale et al. (2017a); <sup>d</sup>Creusot et al. (2010); <sup>e</sup>Konig et al. (2017); <sup>f</sup>Mehinto et al. (2015); <sup>g</sup>Fang et al. (2012); <sup>h</sup>Chou et al. (2015); <sup>i</sup>Conley et al. (2017); <sup>j</sup>Tousova et al. (2017); <sup>k</sup>Escher et al. (2011); <sup>l</sup>Murk et al. (2002); <sup>m</sup>Rutishauser et al. (2004); <sup>n</sup>Shi et al. (2018); <sup>o</sup>Jia

et al. (2016); <sup>p</sup>Bengtson Nash et al. (2006); <sup>q</sup>Tang et al. (2014); <sup>r</sup>Tang and Escher (2014); <sup>s</sup>Yeh et al. (2014); <sup>t</sup>Escher et al. (2013); <sup>u</sup>Tang et al. (2013b). NB: AhR: aryl hydrocarbon receptor (AhR); PXR: pregnane X receptor; PPAR $\gamma$ : peroxisome proliferator-activated receptor; ER: estrogen receptor; AR: androgen receptor; GR: glucocorticoid receptor; PSII: photosystem II

chemicals and biological effect by common SPE sorbents (Neale et al. 2018; Simon et al. 2019). Further, reverse recovery modelling was used to calculate  $BEQ_{chem}$  assuming 100% chemical recovery and showed good agreement with  $BEQ_{chem}$  from the literature, supporting the application of iceberg modelling for water extracts (Neale et al. 2018).

In addition to SPE, several studies have applied iceberg modelling to passive sampler extracts from surface water and wastewater (Vermeirssen et al. 2010; Creusot et al. 2014; Hamers et al. 2018; Novak et al. 2018; Tousova et al. 2019). Passive samplers absorb chemicals from the water phase over the deployment period and represent a time-integrated picture of the chemical mixture in water. Passive sampling showed similar trends to SPE extracts, with detected chemicals explaining the majority of estrogenic activity and PSII inhibition in wastewater (Vermeirssen et al. 2010; Escher et al. 2011), but <1% of PXR and oxidative stress response in river water (Creusot et al. 2014; Novak et al. 2018). Up to 10% of the aryl hydrocarbon receptor (AhR) response could be explained in wastewater effluent (Hamers et al. 2018). The fraction of effect explained is also affected by the type of passive sampler deployed, with polar samplers, such as polar organic chemical integrative sampler (POCIS) or Empore disks, more suitable for estrogenic compounds and non-polar samplers, such as semi-permeable membrane device (SPMD) or silicone

rubber, more appropriate for capturing hydrophobic contaminants. For example, a greater fraction of the effect in the activation of AhR assay could be explained by detected chemicals in SPMD extracts compared to POCIS extracts (Tousova et al. 2019). In contrast, a larger fraction of the estrogenic activity could be explained in Empore disk extracts compared to silicone rubber extracts (Novak et al. 2018). Therefore, the type of passive sampler will affect the chemical mixture extracted.

### 3.2 Sediment

Compared to water extracts, fewer studies have applied iceberg modelling to sediment extracts, with most focusing on AhR and estrogenic activity endpoints. For example, David et al. (2010) found that detected polycyclic aromatic hydrocarbons (PAH) explained between 63 and 121% of the effect in river and coastal sediment in the ethoxyresorufin-O-deethylase (EROD) assay after 4 h, but only 4–19% of the effect in the same assay after 24 h, suggesting undetected persistent contaminants were contributing to the effect. Further, up to 55% of the estrogenic activity in sediment from the Upper Danube River could be explained by detected chemicals (Grund et al. 2011), though  $BEQ_{unknown}$  was >94% for most of the sediment extracts. While most studies apply iceberg modelling to in vitro assays, Hu et al.

(2015) found that 54–125% of the effect in the 48 h *Daphnia magna* immobilization test could be explained by detected chemicals in sediment from an agriculturally impacted lake, with insecticides chlorpyrifos and cyfluthrin explaining most of the effect.

Exhaustive solvent extraction is commonly used to extract the total chemical mixture prior to bioanalysis. Creusot et al. (2016) used the iceberg modelling approach to assess effect recovery of spiked endocrine disrupting chemicals in artificial sediment using a range of solvents with pressurized liquid extraction. Extraction with 50:50 dichloromethane/methanol was optimal, with over 90% recovery of effects in assays indicative of activation of ER and activation of PXR. In addition to solvent extraction, the bioavailable chemical mixture in sediment can be analysed using passive sampling with polydimethylsiloxane (PDMS). Using an assay indicative of activation of AhR, Li et al. (2016) used iceberg modelling to evaluate the contribution of total and bioavailable PAHs to the effect in exhaustive solvent and PDMS extracts, respectively. Up to 41% of the effect could be explained by PAHs in the exhaustive solvent extract, while up to 71% could be explained in the PDMS extract, though the fraction explained varied greatly with different sampling sites.

#### 4 Iceberg Modelling Reveals Different Bioassay Categories

From the literature reviewed in Sect. 3, iceberg modelling indicates that bioassays generally fall into one of two categories: category 1 and category 2 bioassays (Escher et al. 2018) (Fig. 4). Category 1 bioassays detect the effect of defined mixtures where a small number of highly potent chemicals explain up to 100% of the effect. Category 1 bioassays are indicative of receptor-mediated effects, such as activation of hormonal receptors and PSII inhibition in green algae. In contrast, category 2 bioassays detect more integrative effects and include assays indicative of adaptive stress responses, most notably the oxidative stress response, and apical effects in whole organisms. These assays detect the mixture effects of mainly low potency chemicals, so the detected chemicals will only explain a small fraction of the effect. For example, <2% of the oxidative stress response was explained in wastewater effluent and surface water from small streams in Switzerland despite effect data available for 26 detected chemicals (Neale et al. 2017b). A wide range of chemicals can induce a response in category 2 bioassays and analysing more chemicals will not close the gap between the measured and predicted effect. This highlights the importance of using bioanalysis as well as chemical analysis for environmental monitoring.

It should be noted that not all assays will fit neatly into the two bioassay categories. For example, while detected

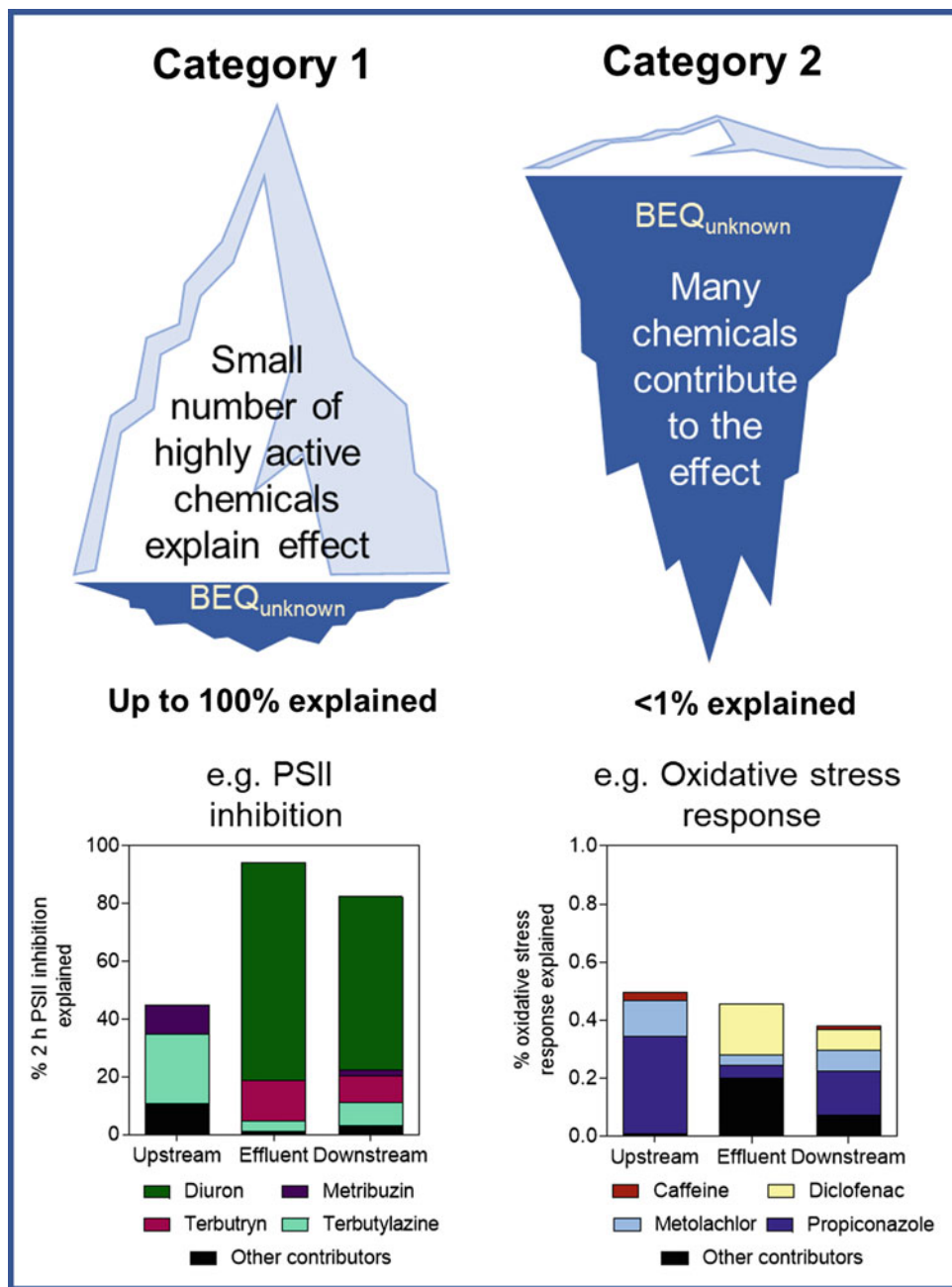
chemicals typically explained <1% of the effect in some xenobiotic metabolism assays (e.g. PXR and PPAR $\gamma$ ), a greater fraction of the effect could be explained in some cases for activation of AhR assays, particularly in sediment (David et al. 2010; Li et al. 2016) and biota (Jin et al. 2013, 2015a, b). Similarly, some compound classes will have a specific effect in whole organism assays indicative of apical effects, such as PSII inhibiting herbicides in algal growth assays and acetylcholinesterase (AChE) inhibitors in *D. magna* (Neale et al. 2017a).

#### 5 Identifying the Drivers of Toxicity Using Effect-Directed Analysis

Effect-directed analysis (EDA) is a tool that can be used to identify unknown chemicals that are driving toxicity in a contaminated site. After identification of a biologically active environmental extract, sample complexity is reduced by chromatographic fractionation, then additional bioanalysis is conducted to identify active fractions (Brack et al. 2016). These active fractions undergo chemical analysis and structural identification to identify the contributing chemicals, with the effect of the identified causative chemicals confirmed in the studied bioassay. As EDA aims to identify the chemicals that are driving the observed effect, it has primarily been applied to category 1 bioassays (e.g. assays indicative of receptor-mediated effects) in matrices including water, sediment and biota (Houtman et al. 2004; Weiss et al. 2009; Creusot et al. 2013; Sonavane et al. 2018). While iceberg modelling using the BEQ approach applies targeted chemical analysis to identify chemicals contributing to the effect, structural identification of unknown chemicals in active fractions in EDA can result in the discovery of new potent causative chemicals. For example, Muschket et al. (2018) found that 4-methyl-7-diethylaminocoumarin (C47), a compound used in consumer products, could explain the anti-androgenic activity in a polluted river. Further, two aromatic amines, 2,3- and 2,8-phenazinediamine, were found to explain up to 86% of the mutagenic activity in surface water receiving industrial wastewater effluent (Muz et al. 2017). EDA can also reveal the effects of contaminants masked by antagonists or non-specific toxicity (Brack et al. 2016).

EDA is not suitable for category 2 bioassays where a large number of chemicals contribute to the mixture effects. This was demonstrated by Hashmi et al. (2018) for an oxidative stress response assay, with the combined effect of the fractionated samples only able to explain 16% of the oxidative stress response detected in the unfractionated sample. While whole organism assays indicative of apical effects are often considered as category 2 bioassays, some assays sensitive to specific chemical modes of action are suitable for EDA. For example, insecticide methyl parathion

**Fig. 4** Category 1 bioassays include assays indicative of receptor-mediated effects and most of the effect is explained by known highly active chemicals. Category 2 bioassays include assays indicative of apical effects and adaptive stress responses and typically only a very small fraction of the effect can be explained. Photosystem II (PSII) inhibition and oxidative stress response data adapted from Neale et al. (2017b)



could explain 97% of the effect in *D. magna* in one fraction of river sediment, though the observed effect in other fractions could not be fully explained by detected chemicals (Brack et al. 1999).

## 6 Effect-Based Trigger Values for Environmental Mixtures

The chemical status of water is typically evaluated based on chemical guideline values for priority chemicals, but, as mentioned in Sect. 1, this approach does not consider

chemical mixture effects. While bioassays can detect the effects of complex chemical mixtures, the combination of high sample enrichment and increasingly sensitive bioassays means that effects can be detected in clean samples. For bioassays to be used for water quality monitoring, it is important to be able to differentiate between an acceptable effect in water and an unacceptable effect. Consequently, effect-based trigger values (EBTs) have been developed for drinking water (Brand et al. 2013; Escher et al. 2015), surface water (van der Oost et al. 2017; Escher et al. 2018) and wastewater effluent (Jarosova et al. 2014). EBTs are assay-specific and the comparison of an EBT with an effect



detected in a water sample can indicate whether the sample is compliant or not, with an exceedance of an EBT indicating further investigation, such as chemical analysis, is warranted.

Most studies initially focused on hormone-receptor mediated effects (e.g. category 1 bioassays), but more recently EBTs have been derived for assays indicative of xenobiotic metabolism and adaptive stress responses and apical effects in whole organisms (e.g. category 2 bioassays). Several approaches have been applied to derive EBTs, but one simple method to calculate EBTs is to convert existing guideline values to BEQ using the chemical concentration from the guidelines and its  $REP_1$ . This approach was applied to derive EBTs for drinking water using the Australian Guidelines for Water Recycling (Escher et al. 2015) and for surface water using average annual Environmental Quality Standards (AA-EQS) from the European Union Water Framework Directive (Escher et al. 2018), with 32 preliminary EBTs derived for surface water. In the case of category 2 assays, where a large fraction of the effect is not explained by known chemicals, an additional mixture factor was included. Reading across from existing guideline values does have some limitations, including the lack of effect data for some guideline chemicals and the lack of guideline values for potent chemicals in some important environmental endpoints such as glucocorticoid activity. However, the approach can be applied to any bioassay and represents an important step forward towards regulatory acceptance of bioassays.

## 7 Conclusions

The complementary use of bioassays and chemical analysis represents a valuable approach to evaluate the effects of environmental mixtures and determine the contribution of detected chemicals to the observed effect. Both BEQ and TU approaches have been applied to describe the mixture effects in environmental samples, but the two approaches are interchangeable, provided only experimental effect data is used to derive  $TU_{chem}$ . Iceberg modelling has shown that most of the mixture effect can be explained by detected chemicals for category 1 bioassays (e.g. assays indicative hormone receptor-mediated effects), with EDA a suitable approach to detect unknown active chemicals in these assays. While the lack of single chemical effect data is a limitation for some less-studied bioassays, detecting more chemicals will not close the BEQ mass balance for category 2 bioassays as a wide range of low potency chemicals contribute to the effect. This highlights the importance of a combined chemical analysis and bioanalysis approach as it provides a better picture of the chemical burden. Chemical mixtures are currently not considered when evaluating the chemical status of water in a regulatory context, but EBTs

that read across from existing chemical guideline values represent a step forward. EBTs for some category 1 bioassays are already quite advanced, though further work is still required to develop robust EBTs for category 2 bioassays.

## References

- Altenburger R, Scholze M, Busch W, Escher BI, Jakobs G, Krauss M, Kruger J, Neale PA, Ait-Aissa S, Almeida AC, Seiler TB, Brion F, Hilscherova K, Hollert H, Novak J, Schlichting R, Serra H, Shao Y, Tindall A, Tolefsen KE, Umbuzeiro G, Williams TD, Kortenkamp A (2018) Mixture effects in samples of multiple contaminants—an inter-laboratory study with manifold bioassays. *Environ Int* 114:95–106. <https://doi.org/10.1016/j.envint.2018.02.013>
- Backhaus T, Faust M (2012) Predictive environmental risk assessment of chemical mixtures: a conceptual framework. *Environ Sci Technol* 46(5):2564–2573. <https://doi.org/10.1021/es2034125>
- Backhaus T, Altenburger R, Boedeker W, Faust M, Scholze M, Grimme LH (2000) Predictability of the toxicity of a multiple mixture of dissimilarly acting chemicals to *Vibrio fischeri*. *Environ Toxicol Chem* 19(9):2348–2356. <https://doi.org/10.1002/etc.5620190927>
- Beckers LM, Busch W, Krauss M, Schulze T, Brack W (2018) Characterization and risk assessment of seasonal and weather dynamics in organic pollutant mixtures from discharge of a separate sewer system. *Water Res* 135:122–133. <https://doi.org/10.1016/j.watres.2018.02.002>
- Bengtson Nash SM, Goddard J, Muller JF (2006) Phytotoxicity of surface waters of the Thames and Brisbane River Estuaries: a combined chemical analysis and bioassay approach for the comparison of two systems. *Biosens Bioelectron* 21(11):2086–2093. <https://doi.org/10.1016/j.bios.2005.10.016>
- Booij P, Vethaak AD, Leonards PEG, Sjollem SB, Kool J, de Voogt P, Lamoree MH (2014) Identification of photosynthesis inhibitors of pelagic marine algae using 96-well plate microfractionation for enhanced throughput in effect-directed analysis. *Environ Sci Technol* 48(14):8003–8011. <https://doi.org/10.1021/es405428t>
- Brack W, Altenburger R, Ensenbach U, Moder M, Segner H, Schuurmann G (1999) Bioassay-directed identification of organic toxicants in river sediment in the industrial region of Bitterfeld (Germany)—a contribution to hazard assessment. *Arch Environ Contam Toxicol* 37(2):164–174. <https://doi.org/10.1007/s002449900502>
- Brack W, Ait-Aissa S, Burgess RM, Busch W, Creusot N, Di Paolo C, Escher BI, Hewitt LM, Hilscherova K, Hollender J, Hollert H, Jonker W, Kool J, Lamoree M, Muschket M, Neumann S, Rostkowski P, Ruttkies C, Schollee J, Schymanski EL, Schulze T, Seiler TB, Tindall AJ, Umbuzeiro GD, Vrana B, Krauss M (2016) Effect-directed analysis supporting monitoring of aquatic environments—an in-depth overview. *Sci Total Environ* 544:1073–1118. <https://doi.org/10.1016/j.scitotenv.2015.11.102>
- Brand W, de Jongh CM, van der Linden SC, Mennes W, Puijker LM, van Leeuwen CJ, van Wezel AP, Schriks M, Heringa MB (2013) Trigger values for investigation of hormonal activity in drinking water and its sources using CALUX bioassays. *Environ Int* 55:109–118. <https://doi.org/10.1016/j.envint.2013.02.003>
- Cedergreen N (2014) Quantifying synergy: a systematic review of mixture toxicity studies within environmental toxicology. *Plos One* 9(5). <https://doi.org/10.1371/journal.pone.0096580>
- Chou PH, Lin YL, Liu TC, Chen KY (2015) Exploring potential contributors to endocrine disrupting activities in Taiwan's surface

- waters using yeast assays and chemical analysis. *Chemosphere* 138:814–820. <https://doi.org/10.1016/j.chemosphere.2015.08.016>
- Conley JM, Evans N, Cardon MC, Rosenblum L, Iwanowicz LR, Hartig PC, Schenck KM, Bradley PM, Wilson VS (2017) Occurrence and *in vitro* bioactivity of estrogen, androgen, and glucocorticoid compounds in a nationwide screen of United States stream waters. *Environ Sci Technol* 51(9):4781–4791. <https://doi.org/10.1021/acs.est.6b06515>
- Creusot N, Kinani S, Balaguer P, Tapie N, LeMenach K, Maillot-Marechal E, Porcher JM, Budzinski H, Ait-Aissa S (2010) Evaluation of an hPXR reporter gene assay for the detection of aquatic emerging pollutants: screening of chemicals and application to water samples. *Anal Bioanal Chem* 396(2):569–583. <https://doi.org/10.1007/s00216-009-3310-y>
- Creusot N, Budzinski H, Balaguer P, Kinani S, Porcher JM, Ait-Aissa S (2013) Effect-directed analysis of endocrine-disrupting compounds in multi-contaminated sediment: identification of novel ligands of estrogen and pregnane X receptors. *Anal Bioanal Chem* 405(8):2553–2566. <https://doi.org/10.1007/s00216-013-6708-5>
- Creusot N, Ait-Aissa S, Tapie N, Pardon P, Brion F, Sanchez W, Thybaud E, Porcher JM, Budzinski H (2014) Identification of synthetic steroids in river water downstream from pharmaceutical manufacture discharges based on a bioanalytical approach and passive sampling. *Environ Sci Technol* 48(7):3649–3657. <https://doi.org/10.1021/es405313r>
- Creusot N, Devier MH, Budzinski H, Ait-Aissa S (2016) Evaluation of an extraction method for a mixture of endocrine disruptors in sediment using chemical and *in vitro* biological analyses. *Environ Sci Pollut Res* 23(11):10349–10360. <https://doi.org/10.1007/s11356-016-6062-1>
- David A, Gomez E, Ait-Aissa S, Rosain D, Casellas C, Fenet H (2010) Impact of urban wastewater discharges on the sediments of a small mediterranean river and associated coastal environment: assessment of estrogenic and dioxin-like activities. *Arch Environ Contam Toxicol* 58(3):562–575. <https://doi.org/10.1007/s00244-010-9475-8>
- Escher BI, Leusch FDL (2012) Bioanalytical tools in water quality assessment. IWA Publishing, London
- Escher BI, Bramaz N, Mueller JF, Quayle P, Rutishauser S, Vermeirssen ELM (2008) Toxic equivalent concentrations (TEQs) for baseline toxicity and specific modes of action as a tool to improve interpretation of ecotoxicity testing of environmental samples. *J Environ Monit* 10(5):612–621. <https://doi.org/10.1039/b800949j>
- Escher BI, Lawrence M, Macova M, Mueller JF, Poussade Y, Robillot C, Roux A, Gernjak W (2011) Evaluation of contaminant removal of reverse osmosis and advanced oxidation in full-scale operation by combining passive sampling with chemical analysis and bioanalytical tools. *Environ Sci Technol* 45(12):5387–5394. <https://doi.org/10.1021/es201153k>
- Escher BI, Dutt M, Maylin E, Tang JYM, Toze S, Wolf CR, Lang M (2012) Water quality assessment using the AREc32 reporter gene assay indicative of the oxidative stress response pathway. *J Environ Monit* 14(11):2877–2885. <https://doi.org/10.1039/c2em30506b>
- Escher BI, van Daele C, Dutt M, Tang JYM, Altenburger R (2013) Most oxidative stress response in water samples comes from unknown chemicals: the need for effect-based water quality trigger values. *Environ Sci Technol* 47(13):7002–7011. <https://doi.org/10.1021/es304793h>
- Escher BI, Neale PA, Leusch FDL (2015) Effect-based trigger values for *in vitro* bioassays: reading across from existing water quality guideline values. *Water Res* 81:137–148. <https://doi.org/10.1016/j.watres.2015.05.049>
- Escher BI, Ait-Aissa S, Behnisch PA, Brack W, Brion F, Brouwer A, Buchinger S, Crawford SE, Du Pasquier D, Hamers T, Hettwer K, Hilscherova K, Hollert H, Kase R, Kienle C, Tindall AJ, Tuerk J, van der Oost R, Vermeirssen E, Neale PA (2018) Effect-based trigger values for *in vitro* and *in vivo* bioassays performed on surface water extracts supporting the environmental quality standards (EQS) of the European Water Framework Directive. *Sci Total Environ* 628–629:748–765. <https://doi.org/10.1016/j.scitotenv.2018.01.340>
- Fang YX, Ying GG, Zhao JL, Chen F, Liu S, Zhang LJ, Yang B (2012) Assessment of hormonal activities and genotoxicity of industrial effluents using *in vitro* bioassays combined with chemical analysis. *Environ Toxicol Chem* 31(6):1273–1282. <https://doi.org/10.1002/etc.1811>
- Grund S, Higley E, Schonenberger R, Suter MJF, Giesy JP, Braunbeck T, Hecker M, Hollert H (2011) The endocrine disrupting potential of sediments from the Upper Danube River (Germany) as revealed by *in vitro* bioassays and chemical analysis. *Environ Sci Pollut Res* 18(3):446–460. <https://doi.org/10.1007/s11356-010-0390-3>
- Guo J, Deng DY, Wang YT, Yu HX, Shi W (2019) Extended suspect screening strategy to identify characteristic toxicants in the discharge of a chemical industrial park based on toxicity to *Daphnia magna*. *Sci Total Environ* 650:10–17. <https://doi.org/10.1016/j.scitotenv.2018.08.215>
- Hamers T, Legradi J, Zwart N, Smedes F, de Weert J, van den Brandhof EJ, van de Meent D, de Zwart D (2018) Time-integrative passive sampling combined with TOxicity Profiling (TIPTOP): an effect-based strategy for cost-effective chemical water quality assessment. *Environ Toxicol Pharmacol* 64:48–59. <https://doi.org/10.1016/j.etap.2018.09.005>
- Hashmi MAK, Escher BI, Krauss M, Teodorovic I, Brack W (2018) Effect-directed analysis (EDA) of Danube River water sample receiving untreated municipal wastewater from Novi Sad, Serbia. *Sci Total Environ* 624:1072–1081. <https://doi.org/10.1016/j.scitotenv.2017.12.187>
- Hebert A, Feliars C, Lecarpentier C, Neale PA, Schlichting R, Thibert S, Escher BI (2018) Bioanalytical assessment of adaptive stress responses in drinking water: A predictive tool to differentiate between micropollutants and disinfection by-products. *Water Res* 132:340–349. <https://doi.org/10.1016/j.watres.2017.12.078>
- Houtman CJ, Van Oostveen AM, Brouwer A, Lamoree MH, Legler J (2004) Identification of estrogenic compounds in fish bile using bioassay-directed fractionation. *Environ Sci Technol* 38(23):6415–6423. <https://doi.org/10.1021/es049750p>
- Hu XX, Shi W, Yu NY, Jiang X, Wang SH, Giesy JP, Zhang XW, Wei S, Yu HX (2015) Bioassay-directed identification of organic toxicants in water and sediment of Tai Lake, China. *Water Res* 73:231–241. <https://doi.org/10.1016/j.watres.2015.01.033>
- Jarosova B, Blaha L, Giesy JP, Hilscherova K (2014) What level of estrogenic activity determined by *in vitro* assays in municipal waters can be considered as safe? *Environ Int* 64:98–109. <https://doi.org/10.1016/j.envint.2013.12.009>
- Jia A, Wu SM, Daniels KD, Snyder SA (2016) Balancing the budget: accounting for glucocorticoid bioactivity and fate during water treatment. *Environ Sci Technol* 50(6):2870–2880. <https://doi.org/10.1021/acs.est.5b04893>
- Jin L, Gaus C, van Mourik L, Escher BI (2013) Applicability of passive sampling to bioanalytical screening of bioaccumulative chemicals in marine wildlife. *Environ Sci Technol* 47(14):7982–7988. <https://doi.org/10.1021/es401014b>
- Jin L, Escher BI, Limpus CJ, Gaus C (2015a) Coupling passive sampling with *in vitro* bioassays and chemical analysis to understand combined effects of bioaccumulative chemicals in blood of marine turtles. *Chemosphere* 138:292–299. <https://doi.org/10.1016/j.chemosphere.2015.05.055>
- Jin L, Gaus C, Escher BI (2015b) Adaptive stress response pathways induced by environmental mixtures of bioaccumulative chemicals in dugongs. *Environ Sci Technol* 49(11):6963–6973. <https://doi.org/10.1021/acs.est.5b00947>

- Kadokami K, Li XH, Pan SY, Ueda N, Hamada K, Jinya D, Iwamura T (2013) Screening analysis of hundreds of sediment pollutants and evaluation of their effects on benthic organisms in Dokai Bay, Japan. *Chemosphere* 90(2):721–728. <https://doi.org/10.1016/j.chemosphere.2012.09.055>
- Konig M, Escher BI, Neale PA, Krauss M, Hilscherova K, Novak J, Teodorovic I, Schulze T, Seidensticker S, Hashmi MAK, Ahlheim J, Brack W (2017) Impact of untreated wastewater on a major European river evaluated with a combination of in vitro bioassays and chemical analysis. *Environ Pollut* 220:1220–1230. <https://doi.org/10.1016/j.envpol.2016.11.011>
- Kortenkamp A (2007) Ten years of mixing cocktails: a review of combination effects of endocrine-disrupting chemicals. *Environ Health Perspect* 115:98–105. <https://doi.org/10.1289/ehp.9357>
- Kuzmanovic M, Ginebreda A, Petrovic M, Barcelo D (2015) Risk assessment based prioritization of 200 organic micropollutants in 4 Iberian rivers. *Sci Total Environ* 503:289–299. <https://doi.org/10.1016/j.scitotenv.2014.06.056>
- Leusch FDL, Khan SJ, Laingam S, Prochazka E, Frosio S, Trinh T, Chapman HF, Humpage A (2014) Assessment of the application of bioanalytical tools as surrogate measure of chemical contaminants in recycled water. *Water Res* 49:300–315. <https://doi.org/10.1016/j.watres.2013.11.030>
- Li JY, Su L, Wei FH, Yang JH, Jin L, Zhang XW (2016) Bioavailability-based assessment of aryl hydrocarbon receptor-mediated activity in Lake Tai Basin from Eastern China. *Sci Total Environ* 544:987–994. <https://doi.org/10.1016/j.scitotenv.2015.12.041>
- Loos R, Carvalho R, Antonio DC, Cornero S, Locoro G, Tavazzi S, Paracchini B, Ghiani M, Lettieri T, Blaha L, Jarosova B, Voorspoels S, Servaes K, Haglund P, Fick J, Lindberg RH, Schwesig D, Gawlik BM (2013) EU-wide monitoring survey on emerging polar organic contaminants in wastewater treatment plant effluents. *Water Res* 47(17):6475–6487. <https://doi.org/10.1016/j.watres.2013.08.024>
- Mehinto AC, Jia A, Snyder SA, Jayasinghe BS, Denslow ND, Crago J, Schlenk D, Menzie C, Westerheide SD, Leusch FDL, Maruya KA (2015) Interlaboratory comparison of in vitro bioassays for screening of endocrine active chemicals in recycled water. *Water Res* 83:303–309. <https://doi.org/10.1016/j.watres.2015.06.050>
- Murk AJ, Legler J, van Lipzig MMH, Meerman JHN, Belfroid AC, Spenklink A, van der Burg B, Rijs GBJ, Vethaak D (2002) Detection of estrogenic potency in wastewater and surface water with three in vitro bioassays. *Environ Toxicol Chem* 21(1):16–23. <https://doi.org/10.1002/etc.5620210103>
- Muschket M, Di Paolo C, Tindall AJ, Touak G, Phan A, Krauss M, Kirchner K, Seiler TB, Hollert H, Brack W (2018) Identification of unknown antiandrogenic compounds in surface waters by effect-directed analysis (EDA) using a parallel fractionation approach. *Environ Sci Technol* 52(1):288–297. <https://doi.org/10.1021/acs.est.7b04994>
- Muz M, Dann JP, Jager F, Brack W, Krauss M (2017) Identification of mutagenic aromatic amines in river samples with industrial wastewater impact. *Environ Sci Technol* 51(8):4681–4688. <https://doi.org/10.1021/acs.est.7b00426>
- Neale PA, Ait-Aissa S, Brack W, Creusot N, Denison MS, Deutschmann B, Hilscherova K, Hollert H, Krauss M, Novak J, Schulze T, Seiler TB, Serra H, Shao Y, Escher BI (2015) Linking in vitro effects and detected organic micropollutants in surface water using mixture-toxicity modeling. *Environ Sci Technol* 49(24):14614–14624. <https://doi.org/10.1021/acs.est.5b04083>
- Neale PA, Altenburger R, Ait-Aissa S, Brion F, Busch W, Umbuzero GD, Denison MS, Du Pasquier D, Hilscherova K, Hollert H, Morales DA, Novak J, Schlichting R, Seiler TB, Serra H, Shao Y, Tindall AJ, Tollefsen KE, Williams TD, Escher BI (2017a) Development of a bioanalytical test battery for water quality monitoring: Fingerprinting identified micropollutants and their contribution to effects in surface water. *Water Res* 123:734–750. <https://doi.org/10.1016/j.watres.2017.07.016>
- Neale PA, Munz NA, Ait-Aissa S, Altenburger R, Brion F, Busch W, Escher BI, Hilscherova K, Kienle C, Novak J, Seiler TB, Shao Y, Stamm C, Hollender J (2017b) Integrating chemical analysis and bioanalysis to evaluate the contribution of wastewater effluent on the micropollutant burden in small streams. *Sci Total Environ* 576:785–795. <https://doi.org/10.1016/j.scitotenv.2016.10.141>
- Neale PA, Brack W, Ait-Aissa S, Busch W, Hollender J, Krauss M, Maillot-Marechal E, Munz NA, Schlichting R, Schulze T, Vogler B, Escher BI (2018) Solid-phase extraction as sample preparation of water samples for cell-based and other in vitro bioassays. *Environmental Science-Processes & Impacts* 20(3):493–504. <https://doi.org/10.1039/c7em00555e>
- Novak J, Vrana B, Rusina T, Okonski K, Grabic R, Neale PA, Escher BI, Macova M, Ait-Aissa S, Creusot N, Allan I, Hilscherova K (2018) Effect-based monitoring of the Danube River using mobile passive sampling. *Sci Total Environ* 636:1608–1619. <https://doi.org/10.1016/j.scitotenv.2018.02.201>
- Rutishauser BV, Pesonen M, Escher BI, Ackermann GE, Aerni HR, Suter MJF, Eggen RIL (2004) Comparative analysis of estrogenic activity in sewage treatment plant effluents involving three in vitro assays and chemical analysis of steroids. *Environ Toxicol Chem* 23(4):857–864. <https://doi.org/10.1897/03-286>
- Scott PD, Coleman HM, Khan S, Lim R, McDonald JA, Mondon J, Neale PA, Prochazka E, Tremblay LA, Warne MS, Leusch FDL (2018) Histopathology, vitellogenin and chemical body burden in mosquitofish (*Gambusia holbrooki*) sampled from six river sites receiving a gradient of stressors. *Sci Total Environ* 616:1638–1648. <https://doi.org/10.1016/j.scitotenv.2017.10.148>
- Shi P, Zhou SC, Xiao HX, Qiu JF, Li AM, Zhou Q, Pan Y, Hollert H (2018) Toxicological and chemical insights into representative source and drinking water in eastern China. *Environ Pollut* 233:35–44. <https://doi.org/10.1016/j.envpol.2017.10.033>
- Silva E, Rajapakse N, Kortenkamp A (2002) Something from “nothing”—Eight weak estrogenic chemicals combined at concentrations below NOECs produce significant mixture effects. *Environ Sci Technol* 36(8):1751–1756. <https://doi.org/10.1021/es0101227>
- Simon E, Schifferli A, Bucher TB, Olbrich D, Werner I, Vermeirssen ELM (2019) Solid-phase extraction of estrogens and herbicides from environmental waters for bioassay analysis—effects of sample volume on recoveries. *Analytical and Bioanalytical Chemistry*. <https://doi.org/10.1007/s00216-019-01628-1>
- Sonavane M, Schollee JE, Hidas AO, Creusot N, Brion F, Suter MJF, Hollender J, Ait-Aissa S (2018) An integrative approach combining passive sampling, bioassays, and effect-directed analysis to assess the impact of wastewater effluent. *Environ Toxicol Chem* 37(8):2079–2088. <https://doi.org/10.1002/etc.4155>
- Tang JYM, Escher BI (2014) Realistic environmental mixtures of micropollutants in surface, drinking, and recycled water: herbicides dominate the mixture toxicity towards algae. *Environ Toxicol Chem* 33(6):1427–1436. <https://doi.org/10.1002/etc.2580>
- Tang JYM, Aryal R, Deletic A, Gernjak W, Glenn E, McCarthy D, Esther BI (2013a) Toxicity characterization of urban stormwater with bioanalytical tools. *Water Res* 47(15):5594–5606. <https://doi.org/10.1016/j.watres.2013.06.037>
- Tang JYM, McCarty S, Glenn E, Neale PA, Warne MSJ, Escher BI (2013b) Mixture effects of organic micropollutants present in water: towards the development of effect-based water quality trigger values for baseline toxicity. *Water Res* 47(10):3300–3314. <https://doi.org/10.1016/j.watres.2013.03.011>
- Tang JYM, Buseti F, Charrois JWA, Escher BI (2014) Which chemicals drive biological effects in wastewater and recycled water? *Water Res* 60:289–299. <https://doi.org/10.1016/j.watres.2014.04.043>

- Tousova Z, Oswald P, Slobodnik J, Blaha L, Muz M, Hu M, Brack W, Krauss M, Di Paolo C, Tarcai Z, Seiler TB, Hollert H, Koprivica S, Ahel M, Schollee JE, Hollender J, Suter MJF, Hidasi AO, Schirmer K, Sonavane M, Ait-Aissa S, Creusot N, Brion F, Froment J, Almeida AC, Thomas K, Tollefsen KE, Tufi S, Ouyang XY, Leonards P, Lamoree M, Torrens VO, Kolkman A, Schriks M, Spirhanzlova P, Tindall A, Schulze T (2017) European demonstration program on the effect-based and chemical identification and monitoring of organic pollutants in European surface waters. *Sci Total Environ* 601:1849–1868. <https://doi.org/10.1016/j.scitotenv.2017.06.032>
- Tousova Z, Vrana B, Smutna M, Novak J, Klucarova V, Grabic R, Slobodnik J, Giesy JP, Hilscherova K (2019) Analytical and bioanalytical assessments of organic micropollutants in the Bosna River using a combination of passive sampling, bioassays and multi-residue analysis. *Sci Total Environ* 650:1599–1612. <https://doi.org/10.1016/j.scitotenv.2018.08.336>
- van der Oost R, Sileno G, Suarez-Munoz M, Nguyen MT, Besselink H, Brouwer A (2017) SIMONI (smart integrated monitoring) as a novel bioanalytical strategy for water quality assessment: Part I—model design and effect-based trigger values. *Environ Toxicol Chem* 36(9):2385–2399. <https://doi.org/10.1002/etc.3836>
- Vermeirssen ELM, Hollender J, Bramaz N, van der Voet J, Escher BI (2010) Linking toxicity in algal and bacterial assays with chemical analysis in passive samplers deployed in 21 treated sewage effluents. *Environ Toxicol Chem* 29(11):2575–2582. <https://doi.org/10.1002/etc.311>
- Weiss JM, Hamers T, Thomas KV, van der Linden S, Leonards PEG, Lamoree MH (2009) Masking effect of anti-androgens on androgenic activity in European river sediment unveiled by effect-directed analysis. *Anal Bioanal Chem* 394(5):1385–1397. <https://doi.org/10.1007/s00216-009-2807-8>
- Wernersson AS, Carere M, Maggi C, Tusil P, Soldan P, James A, Sanchez W, Dulio V, Broeg K, Reifferscheid G, Buchinger S, Maas H, Van Der Grinten E, O'Toole S, Ausili A, Manfra L, Marziali L, Polesello S, Lacchetti I, Mancini L, Lilja K, Linderoth M, Lundeberg T, Fjallborg B, Porsbring T, Larsson DGJ, Bengtsson-Palme J, Forlin L, Kienle C, Kunz P, Vermeirssen E, Werner I, Robinson CD, Lyons B, Katsiadaki I, Whalley C, den Haan K, Messiaen M, Clayton H, Lettieri T, Carvalho RN, Gawlik BM, Hollert H, Di Paolo C, Brack W, Kammann U, Kase R (2015) The European technical report on aquatic effect-based monitoring tools under the water framework directive. *Environmental Sciences Europe* 27:1–11. <https://doi.org/10.1186/s12302-015-0039-4>
- Yeh RYL, Farre MJ, Stalter D, Tang JYM, Molendijk J, Esther BI (2014) Bioanalytical and chemical evaluation of disinfection by-products in swimming pool water. *Water Res* 59:172–184. <https://doi.org/10.1016/j.watres.2014.04.002>

# Mining Population Exposure and Community Health via Wastewater-Based Epidemiology

Phil M. Choi, Kevin V. Thomas, Jake W. O'Brien, and Jochen F. Mueller

## Abstract

An individual's excreta contains chemical information that reflects the chemicals one has consumed or been exposed to. Wastewater-based epidemiology (WBE) is the discipline concerned with mining the chemical information from municipal wastewater. WBE, also known as wastewater epidemiology, sewer epidemiology, urban water fingerprinting or sewage chemical information monitoring (SCIM), has been applied in populations around the globe to mainly measure chemical consumption and exposure patterns. In particular, WBE studies have added to our knowledge of illicit and licit drug consumption patterns, and shows increasing potential as a tool for measuring aspects of public health and socioeconomics. This chapter presents readers with an overview of key methodologies, advances and perspectives in adapting WBE as a tool for better understanding relationships between biochemical consumption and exposure behaviour with public health and socioeconomics.

## 1 Wastewater-Based Epidemiology

### 1.1 Brief History and Overview

Anthropogenic chemicals, such as pharmaceuticals and drugs, have been quantified in aquatic environments for a few decades, and wastewater treatment plants (WWTPs) were identified as sources of discharge of anthropogenic chemicals into the environment. These wastewater analysis studies viewed anthropogenic chemicals as potential environmental contaminants that had to be managed by increasing their removal in water treatment processes and

limit their release into the environment. However, the mid-2000s saw a number of wastewater analysis studies which (i) normalised chemical concentrations in wastewater influent by the size of the population served by the WWTP, and (ii) incorporated excretion factors to back-calculate the consumption of a parent chemical from its metabolite. This revealed the per capita load or consumption for said chemical within the catchment. This ushered in the era of wastewater-based epidemiology (WBE), where per capita use or excretion of a chemical could be deduced to inform population chemical consumption or exposure behaviour.

### 1.2 How Wastewater-Based Epidemiology Works

The modern WBE community has converged upon methodological consensus to foster accurate and reproducible quantification of chemicals. Wastewater entering the WWTP is often sampled as high frequency flow- (preferred) or time-proportionally composited samples over a 24-hour period (Ort et al. 2010). The use of autosamplers allows automated collection and refrigeration of multiple consecutive composite samples, and allows different compositing periods depending on the research or monitoring aims. A temporal analysis can be achieved by analysing samples from different time points. This can be useful in measuring the effect of interventions, special events or the passing of time on biomarker loads. Similarly, normalised results from different communities can be compared to study spatial differences. Once sampled, wastewater is usually preserved with additives such as hydrochloric acid or sodium metabisulphite to minimise chemical transformation prior to freezing if there is a delay between sampling and analysis (Chen et al. 2012). Depending on the concentration of the analyte(s) of interest in the sample and the analytical detection limit, samples may be concentrated using techniques such as liquid-liquid or solid-phase extraction (SPE) (Kasprzyk-Hordern et al. 2008). WBE typically relies on liquid chromatography coupled to

P. M. Choi (✉) · K. V. Thomas · J. W. O'Brien · J. F. Mueller  
Queensland Alliance for Environmental Health Sciences, The  
University of Queensland, Brisbane, QLD 4102, Australia  
e-mail: [p.choi@uq.edu.au](mailto:p.choi@uq.edu.au)

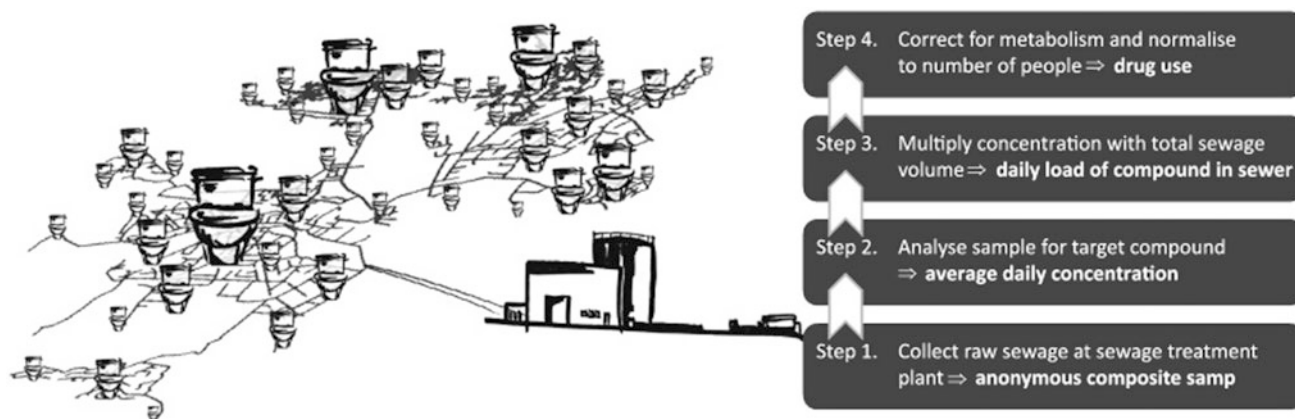


**Fig. 1** Key steps in wastewater-based epidemiology. Reprinted from *Science of the Total Environment*, vol. 432, Thomas et al., Comparing illicit drug use in 19 European cities through sewage analysis, 432–439, Copyright (2012), with permission from Elsevier

tandem mass spectrometry (LC-MS/MS) for chemical analysis. While non-target high-resolution mass spectrometry (HRMS) is being increasingly embraced by WBE studies, triple quadrupole mass spectrometers remain popular as they provide sensitive targeted quantification. Once quantified, concentrations of a chemical of interest can be converted into daily load by multiplying by the flow of wastewater during the sampling period (Fig. 1). Dividing this by the number of people served by the WWTP results in load per capita per day. With information on the proportion of a drug excreted after ingestion, some biomarkers (e.g. drugs) can be expressed in terms of mass or number of doses ingested per capita per day (Rousis et al. 2017; O'Brien et al. 2015).

Chemical consumption or exposure may be determined by measuring the parent chemical compound or a metabolite. It is preferable to measure a human-specific metabolite as metabolism/transformation of chemicals within the sewer may occur, and in some cases agricultural wastewater is connected to the domestic wastewater network. In many cases, however, metabolites are often excreted in lower quantities than the parent compound, hindering quantification. Parent biomarkers can be considered indicators of consumption in scenarios where entry into the sewer by routes other than human excretion (e.g. dumping, trade waste input) can be ruled out or deemed negligible. The stability of a chemical is also an important consideration. Sewer systems contain a considerable diversity of microbial life which can transform a chemical between the time it enters the sewer system and the time it is sampled and preserved (McCall et al. 2016). There is a growing awareness of stability as a potential confounding factor. Stability studies using real sewers, experimental sewers and laboratory-scale sewer reactors have been used to document the extent of potential in sewer transformation, particularly for biomarkers frequently used in the WBE repertoire (Gao et al. 2019; Li et al. 2018).

### 1.3 Advantages and disadvantages

WBE has a number of characteristics that make it well suited as an alternative or complementary tool for measuring chemical consumption or exposure behaviour. High population coverage is one of the advantages of WBE. In developed countries, most households are connected to a sewer line, making it possible to obtain wastewater samples representing entire populations. This encourages spatial comparisons between different populations served by different WWTPs at a relatively small cost compared to traditional survey methods. Indeed, WBE studies comparing chemical consumption and exposure measures involving tens of different communities or countries are becoming increasingly common (Banta-Green 2009; Du et al. 2017; Gao et al. 2016; Ort et al. 2014; O'Brien 2017; SCORE 2018). Traditional survey methods may suffer from low response or compliance rates, particularly when addressing potentially sensitive information such as illicit behaviour, or involving lengthy study periods. This is aptly illustrated in a study in Lier, Belgium, where licit and illicit drug use was measured using an online survey and WBE methods in parallel (van Wel et al. 2016). While the response rate to the survey was 1% over the 12-week study period, the WBE study revealed detailed information on drug consumption patterns, such as differences in use between weekends and week-to-week variation. Indeed, many WBE studies have revealed the nature of yearly (van Nuijs et al. 2018; Lai et al. 2015, 2016a, b; Mackie et al. 2019; Bade et al. 2018), inter-week (e.g. weekdays vs weekends) (Lai et al. 2015, 2016; van Nuijs et al. 2009; Lai et al. 2013a; Salvatore et al. 2015; Kankaanpaa et al. 2014; Lai et al. 2016; Tschärke et al. 2016; van Nuijs et al. 2011; Boogaerts et al. 2016; Lai et al. 2017) and even within-day variations (Lai et al. 2013b) in drug consumption. In Australia, the National Wastewater Drug Monitoring Program publishes a quarterly WBE study, and the percentage of the Australian population covered in

each edition has ranged between 51 and 61%. Crucially, self-reporting bias is not a concern for WBE. Surveys and studies with self-reporting components are prone to bias from self-presentation concerns, and the magnitude of this bias increases with the sensitivity of the question asked (Krumpal 2013). This makes WBE a useful tool to measure consumption or exposure patterns which individuals may be oblivious to, such as consumption of artificial sweeteners (Subedi and Kannan 2014), exposure to flame retardants (O'Brien et al. 2015) or excretion of metabolites of illness (Ryu et al. 2015).

Naturally, there are a number of limitations and considerations for implementing or interpreting WBE studies. Wastewater is a form of pooled urine, and does not contain information about the distribution of a biomarker excreted by individuals. In other words, excretion of a biomarker in high quantities by a minority and in low quantities by a majority may give the same result in a WBE study. Consequently, strictly speaking, WBE studies report the 'load' or 'burden' of a biomarker in a population. These figures may be converted to prevalence, dose or frequency when assumptions for this conversion are acceptable, or for harmonisation with other measures of chemical consumption. Similarly, WBE is inherently unable to identify specific individuals in a catchment who contribute to loads of a biomarker. Consequently, WBE measures 'loads' of potentially sensitive biomarkers such as biomarkers of illicit drug use or disease. The positive side to this limitation is that anonymity is preserved (Hall et al. 2012).

A key distinguishing feature separating WBE from simple wastewater analysis lies in how WBE reports chemical loads or exposures on a per capita (i.e. population normalised) basis. Although this allows comparison with other sources of data (e.g. surveys) which report chemical consumption in units such as doses per person, it relies on accurate counts of the population served by a WWTP during the sampling period. There are a number of ways to obtain population data. Confident WWTP catchment population counts can be obtained by using census-derived population figures (O'Brien et al. 2019). Where this is unavailable, population may be ascertained using proxies of population, such as the number of mobile phones in a catchment (Thomas et al. 2017). Alternatively, chemicals excreted at approximately uniform rates by individuals can be measured as proxies of population size. Examples of such population biomarkers include ammonium, creatinine, 5-hydroxyindole acetic acid or even mitochondrial DNA (Chen et al. 2014; Been et al. 2014; Yang et al. 2015). Loads of the former two can be affected by factors not related to population size such as industrial discharges, degradation of organic matter in the sewer or consumption of bodybuilding supplements. Hydrochemical parameters of wastewater, such as chemical oxygen demand or phosphorus, make poor population proxies for similar reasons (Rico et al. 2017). Chemicals consumed homogeneously among different

populations may also be used as population biomarkers. A notable example is acesulfame, whose loads correlated extremely well with population size ( $R^2 = 0.995$ ) in Australian wastewater samples (O'Brien et al. 2014). Other biomarkers such as caffeine have been suggested for Valencia in Spain (Rico et al. 2017). However, anthropogenic population biomarkers should be calibrated regularly as they may be prone to changes over time, and consumption rates may differ between different cultures (Gao et al. 2016). Interpreting WBE results for their implications on population behaviour and health effects relies on pre-existing information regarding the absorption, distribution, metabolism and excretion (ADME) studies of a biomarker. This is paramount, particularly for quantitative interpretation where results hinge upon excretion factors. Ideally, excretion factors should be calculated using a large number of subjects whose demographics are reasonably representative of the wastewater catchment being studied.

To date, the focus of WBE has been largely limited to small molecule biomarkers which are water-soluble and are excreted primarily through urine. There are more ADME studies on (hydrophilic) chemicals excreted primarily through urine than hydrophobic, faecally excreted chemicals. Although some WBE studies feature methods for sampling biomarkers bound to solid particulate matter (SPM), such studies have been primarily used to determine the extent to which urine-excreted, mildly hydrophobic chemicals bind to SPM (Baker et al. 2012; Asimakopoulos et al. 2017).

Using techniques such as these, WBE has been successfully applied in measuring per capita consumption of illicit and licit recreational drugs, pharmaceuticals and personal care products, industrial chemicals and markers of stress. In the following sections, we briefly summarise the measurement of these different classes of chemicals from wastewater, with a focus on how WBE has contributed to public health and socioeconomic trend analysis.

---

## 2 Wastewater-Based Epidemiology for Public Health

### 2.1 Useful Wastewater-Based Epidemiology Biomarkers

#### 2.1.1 Recreational Drugs

Illicit and licit recreational drug use is an important aspect of public health, as consumption of certain recreational drugs is associated with undesirable consequences at an individual and societal level. Since its inception, WBE has played an important role in monitoring recreational drug use in various communities and understanding temporal and spatial variations in their use. Cocaine was among the first WBE

biomarkers to be implemented. It can be measured as the parent metabolite or as its metabolite, benzoylecgonine, which is more stable than cocaine in wastewater (Chen et al. 2012). Co-consumption with alcohol can decrease urinary excretion of benzoylecgonine, but this can be accounted for by measuring cocaethylene, a biomarker of co-consumption of cocaine and ethanol (Harris et al. 2003). Alcohol consumption can be measured through ethyl sulphate and ethyl glucuronide, both metabolites of ethanol (Reid et al. 2011). In addition to cocaine, methamphetamine and MDMA (3,4-methylenedioxyamphetamine) were the first biomarkers to be used in WBE (Zuccato et al. 2008). Methamphetamine metabolises to amphetamine, which is a drug in its own right. Consequently, methamphetamine is usually measured as the parent drug. Similarly, MDMA is generally measured as the parent drug as it also metabolises to another drug, MDA (3,4-methylenedioxyamphetamine) (Khan and Nicell 2011). Heroin consumption results in excretion of its major metabolite, morphine, as well as a minor metabolite, 6-monoacetylmorphine (MAM). As morphine and codeine consumption also results in morphine excretion, monitoring heroin consumption through morphine is problematic unless accurate morphine and codeine prescription or consumption data is available (Boleda et al. 2009). Although MAM excretion is unique to heroin consumption, care must be taken when interpreting its loads as it has low stability in sewer conditions (McCall et al. 2016).

Similar challenges are encountered when measuring cannabis consumption through its primary metabolites hydroxy-(THC-OH) or carboxy-tetrahydrocannabinol (THC-COOH). Owing to the hydrophobic nature of these metabolites, care must be taken to account for its sorption onto SPM in wastewater (Choi et al. 2018).

WBE has also been used to measure licit drugs which are abused illicitly, such as the synthetic opioid methadone (Baker and Kasprzyk-Hordern 2011) and ketamine (Castiglioni et al. 2015). New psychoactive substances (NPS), also known as ‘designer drugs’, have also been measured. Although such efforts rely on existing knowledge of emerging NPS through sources such as police raids (Castiglioni 2016), wastewater is a viable method for measuring population consumption of these difficult-to-regulate drugs (Gracia-Lor et al. 2017; Bade et al. 2017).

WBE has been used extensively to measure tobacco consumption. Nicotine, an alkaloid in tobacco, is metabolised to cotinine, and cotinine is metabolised to trans-hydroxycotinine. All the four chemicals, especially hydroxycotinine and cotinine, are used as WBE biomarkers for tobacco consumption. Alternatively, the tobacco alkaloids anabasine and anatabine can be measured. While these are present in wastewater at much lower concentrations, they have

the advantage of not being excreted after application of nicotine replacement therapies (Zheng et al. 2019).

Many WBE studies have measured caffeine consumption by measuring caffeine or its metabolites, paraxanthine and 1,7-dimethyluric acid. Other metabolites of caffeine such as 1-methylxanthine and 7-methylxanthine have been proposed, but lack stability in wastewater (Senta et al. 2015).

### 2.1.2 Pharmaceuticals and Personal Care Products

A wide variety of pharmaceuticals and personal care products (PPCPs) have been measured through WBE, and per capita loads of a PPCP can be used as proxies of burden of specific illnesses, conditions or lifestyle characteristics in the population. Theoretically, prescription or sales volumes for pharmaceuticals and sales data for personal care products can be used to achieve accurate relationships between air pollution and pharmaceuticals. In the case of pharmaceuticals, this practice forms the basis of pharmacoepidemiology, a field in its own right. Unfortunately, prescription or sales data in most countries are not easily accessible, and may only cover small subsets of a population. Sales figures are even more difficult to arrive at for pharmaceuticals available over-the-counter. In this respect, WBE is a useful method of monitoring population PPCP use, as it can distinguish the day at which a product is used. Hundreds of different PPCPs have been measured in WBE to date (Choi et al. 2018). As with many other WBE biomarkers, properties that make PPCPs more amenable to WBE include: (i) excretion primarily through urine, (ii) a concentration in wastewater within the quantification range of the analytical method, (iii) well-established excretion factor and (iv) stability in sewer systems. It should be noted that availability of individual PPCPs may differ from jurisdiction to jurisdiction. Consequently, relationships found between a pharmaceutical measured with WBE and public health or socioeconomic phenomena may be affected by availability.

A subset of personal care products is considered endocrine-disrupting chemicals (EDCs) due to their potential to disrupt endocrine (hormonal) systems. Personal care products (e.g. cosmetics), food (e.g. bisphenols) and interaction with the anthropogenic environment (e.g. pesticides) are important routes of EDC ingestion. EDC exposure is typically measured using biomonitoring studies of urine or serum, which makes it costly to conduct studies on a large number of people due to the sheer number of individuals that must be sampled (Archer et al. 2017). Various WBE studies have measured EDCs, and WBE may be a useful alternative or complementary method for assessing exposure to EDCs (Lopardo et al. 2018).



### 2.1.3 Biomarkers of Industrial Chemicals

Exposure to industrial chemicals of concern has traditionally been measured using human biomonitoring samples on matrices such as serum or urine. As with the EDCs, WBE offers an effective alternative monitoring method. A number of pesticides, organophosphate esters, surfactants and similar chemicals have been measured using WBE (Rousis et al. 2017; O'Brien et al. 2015; Asimakopoulos et al. 2017; Gracia-Lor et al. 2012; Been et al. 2017). Many of these chemicals are poorly metabolised, and the ingested chemicals are often excreted unchanged. Therefore, it is difficult to distinguish between exposure, ingestion and input from sources other than human excreta. Although WBE cannot determine the magnitude of exposure to industrial chemicals in individuals, it nevertheless provides an effective method for monitoring, comparing and assessing population exposure.

### 2.1.4 Endogenous Markers of Stress

#### Prostaglandin F<sub>2α</sub>

8-iso prostaglandin F<sub>2α</sub> (8-iso-PGF<sub>2α</sub>) is a urinary marker of oxidative stress, and one of two endogenous (as opposed to exogenous) biomarkers of stress has been published in WBE studies. Formed from the oxidation of arachidonic acid, urinary 8-iso-PGF<sub>2α</sub> is used as a measure of systemic lipid oxidative stress in clinical and metabolomics studies. In addition, the factors influencing its excretion, including various diseases, BMI, age, smoking behaviour, sex and even ethnicity have been thoroughly documented. A conceptual paper by Daughton (2012) discussed the theoretical challenges and potential possibilities in using 8-iso-PGF<sub>2α</sub> (and other related biomarkers) in WBE. In 2015, Ryu and colleagues published a method for quantifying 8-iso-PGF<sub>2α</sub> for WBE. A major hurdle in measuring 8-iso-PGF<sub>2α</sub> in wastewater was its relatively low excretion loads (500–5000 ng/person/day). Owing to the low concentration of 8-iso-PGF<sub>2α</sub> in wastewater and interfering matrix effects in samples concentrated using traditional SPE methods, samples had to be concentrated 1000-fold using an immunoaffinity sorbent. While relatively time and resource-intensive, it is currently the only published method for measuring 8-iso-PGF<sub>2α</sub> from wastewater. In 2016, Ryu and colleagues used this method to show that loads of 8-iso-PGF<sub>2α</sub> in wastewater from 11 European cities correlated with the tobacco biomarker hydroxycotinine and not with the alcohol consumption biomarker ethyl sulphate. This study highlighted tobacco consumption as a major driver of lipid oxidative stress at a population level. The same study also observed that while there was no short-term temporal variation, baseline 8-iso-PGF<sub>2α</sub> levels differed considerably from city to city. This implies that direct spatial comparison of 8-iso-PGF<sub>2α</sub> levels in different cities may not be meaningful until more is

understood about the causes of differences in loads between cities. Nevertheless, the ability to measure a population's oxidative stress immensely broadens avenues where WBE could be utilised to understand the aspects of public health. Long-term temporal analyses could be used to see how population oxidative stress burden changes over time in response to public health interventions such as changes to medical care or smoking policy/taxes.

#### Methyl Imidazole Acetic Acid

A WBE study of wastewater from seven different Australian catchments found that loads of the antihistamines, fexofenadine and cetirizine, were significantly correlated to loads of 1,4-methylimidazole acetic acid (MIAA), an endogenous marker of histamine turnover (Choi et al. 2018). This study was also unique in that it presented an endogenous marker of illness that could be quantified using standard analytical methods without any additional sample preparation steps as with 8-iso-PGF<sub>2α</sub>. The study also reinforces the notion that antihistamines, as well as MIAA, may be suitable indicators of allergic histamine burden.

### 2.1.5 Potential Future Biomarkers

#### Food and Diet Biomarkers

Information about an individuals' short-term food consumption and dietary status can be gained by urinalysis. Several biomarkers of food and diet have been proposed for application in WBE, including biomarkers of consumption of vitamins, wholegrains, fruits and meats (Choi et al. 2018; Thomas and Reid 2011), although no research has been published in this niche. Unlike traditional WBE markers, interpretation of food and diet markers in a WBE study will have several important considerations unique to food and diet biomarkers. Most of the proposed food and diet biomarkers are excreted in the urine unmetabolised. We can therefore expect the biomarkers to enter the sewer system by routes other than human excreta, such as through food processing, food scraps in the home or from industrial waste (e.g. restaurants, food processing factories). For example, wastewater generated by industrial sources contained levels of the soy consumption marker genistein at concentrations up to two orders of magnitude higher than concentrations in WWTP influent (Lundgren and Novak 2009). Quantitative comparisons of food markers will be difficult as levels of the parent food biomarker in food products will vary considerably depending on the cultivar of food components, seasonality, freshness of the food, preparation methods and other similar factors (Gibbons et al. 2017). In short, more research is required to assess the suitability of food and diet biomarkers in wastewater.

## Proteins and Peptides

Urine contains a subset of proteins and peptides (henceforth proteins) found in serum, which reflects pathophysiological conditions experienced by an individual. Proteins measured in urine, many of which are validated for clinical settings, often reflect specific pathophysiological conditions such as glomerular diseases, prostate and bladder cancers, diabetes or coronary artery disease (Albalat et al. 2011; Hortin and Sviridov 2007). The nature of the conditions reported by urinary protein biomarkers therefore have little direct overlap with small molecules measured in urine, which are often byproducts of metabolism or metabolites reflecting food, drug or environmental contaminant intake (Bouatra et al. 2013). Accordingly, a number of proteins have been suggested as biomarkers for WBE, such as monocyte chemoattractant protein-1, a marker of renal disease, and gelsolin, a marker of cellular injury (Daughton 2018). While the prospect of measuring proteins in wastewater is an attractive one, a method capable of measuring specific proteins in influent or effluent wastewater is not available in the current literature. Methodological advances are required to access this as of yet untouched source of public health information from wastewater.

## Biologicals

Wastewater contains an abundance of microbial life, which could be studied to learn more about the health of the population contributing to the wastewater. A small proportion of the taxonomic groups of the wastewater microbiome reflects the microbiome of the population contributing to wastewater (McLellan et al. 2010). In fact, in a study of wastewater influent from 71 US cities, 16S rRNA (ribosomal RNA) sequencing results were able to estimate the obesity of a population with 81–89% accuracy (Newton et al. 2015). The health surveillance potential of wastewater extends also to viruses. Viruses of modern public health concern such as norovirus and poliovirus can be surveilled in wastewater. By comparing clinical and wastewater strains of virus, new strains can be monitored and the epidemiology of a virus is assessed (Tebbens et al. 2017; Lun et al. 2018). Wastewater is also a medium for monitoring a multitude of antibiotic resistance genes, with some antibiotic resistance genes showing seasonal trends or changing in response to measures of antibiotic consumption (Laht et al. 2014; Caucci 2016). However, differences in selecting, measuring and reporting antibiotic resistance genes impede cross-comparisons between studies, and standardised approaches are required for (Laht et al. 2014) comparisons in future WBE efforts.

## 2.2 Comparison with Other Sources of Data

Comparing WBE studies with parallel data sources is an important step in establishing its relevance as a public health monitoring tool. Several WBE studies of drug consumption have reported their findings in conjunction with epidemiological or survey data (Andrés-Costa et al. 2016). Below, we briefly discuss such studies and the extent to which WBE agrees with the existing methods of epidemiological information.

Roadside drug tests (RDTs) allow law enforcement authorities to measure the prevalence of drug use in a population. Bade and colleagues measured methamphetamine, 3,4-methylenedioxyamphetamine (MDMA) and cannabis (as tetrahydrocannabinol, THC) in wastewater from four wastewater treatment plants in Adelaide (Bade et al. 2018). Between 2011 and 2016, seven consecutive daily composite wastewater samples were collected every two months. RDTs were carried out as roadblocks on arterial roads within and in the vicinity of the WWTP catchments. Drivers of randomly selected cars were tested. In addition to a presumptive roadside test, oral swabs were collected from each driver for confirmatory laboratory analysis. The number of positive tests per drug per month was provided by the state police authority. The authors found significant Spearman correlations between the per capita load of drug and percentage of positive drugs tests for methamphetamine ( $R = 0.772$ ) and MDMA ( $R = 0.768$ ). Seasonal fluctuations in methamphetamine and MDMA levels matched well, and both data sources attested similar rates of increase and decrease in methamphetamine and MDMA consumption, respectively, over the study period. Agreement between WBE and RDT data for cannabis was robust during the first half of the sampling period, after which WBE and RDT trends diverged. A change in the time of day the RDT was conducted was suggested as an explanation, as THC levels in the oral cavity diminish relatively rapidly following cannabis use. Overall, however, the study shows that methamphetamine, MDMA, and, to a lesser extent, cannabis use measured by WBE reflects risk-taking behaviour (i.e. driving under the influence of drugs) among the population and reinforces the relevance of WBE to public health monitoring.

Opioid use is a problem in many communities. Intervention initiatives such as opioid substitution therapy or syringe distribution can provide quantitative proxies of opioid consumption with which to examine WBE data. In 2015, Been et al. published a WBE study focussing on methadone and heroin use in a catchment of Lausanne (population = 226,000), Switzerland (Been et al. 2015).

Methadone and its metabolite, 2-ethylidene 1,5-dimethyl-3,3-diphenylpyrrolidine (EDDP), were measured as proxies of methadone consumption. Heroin consumption was determined through its exclusive metabolite 6-monoacetylmorphine (MAM) and non-specific metabolite morphine, which can also be excreted following consumption of morphine and other opioids. Twenty-eight composite wastewater samples collected between October 2013 and July 2014 were analysed by SPE-LC-MS/MS. External measures of methadone and heroin data were based on multiple estimates and sources. Methadone data was obtained in the form of mass of methadone supplied to pharmacies and the number of patients undergoing methadone therapy in Canton Vaud (Lausanne is the biggest city in Canton Vaud, and accounts for a third of its population). Heroin use was calculated using the number of syringes distributed by pharmacies and dedicated facilities within the catchment, and a number of assumptions regarding the dose and syringe use, which added uncertainty into calculations. Methadone consumption measured using WBE ( $19.1 \pm 3.1$  (SD) g/day) was similar to estimates from sales and prescription data ( $15.0 \pm 0.5$  (SD) g/day), especially considering the poor geographical specificity of the sales data. Interestingly, WBE was also able to illustrate the extent of variation in daily loads of methadone and EDDP, which was as high as one order of magnitude. In contrast, agreement was poor for comparisons with MAM. This was attributable to the low stability of MAM in wastewater samples, and the consumption of opioids other than heroin contributing to morphine loads in wastewater. Use of stable and specific biomarkers is an important consideration for a WBE study and can profoundly affect comparison with other sources of data.

Smoking is the highest risk factor for all-cause Disability Adjusted Life Years (DALYs) in many developed countries, and remains among the top 10 risk factors for developing countries (Reitsma et al. 2017). Accordingly, many governments are vested in reducing and monitoring tobacco consumption, and estimates for smoking behaviour may be freely available for many countries. In a temporal study spanning from 2010 to 2017 involving seven consecutive daily composite samples every two months, Mackie and colleagues measured the tobacco consumption markers nicotine, cotinine and hydroxycotinine using direct injection LC-MS/MS. When compared with national, state and consultancy-derived estimates, WBE estimates of numbers of cigarettes smoked per capita were on average 29% higher than survey and sales data (Mackie et al. 2019). Importantly, the long-term decreasing trend in number of cigarettes smoked as measured by WBE (3% per year) was consistent with survey and sales data (4–5% per year). It must be acknowledged that the results from this study may not have been replicable had the tobacco consumption levels in the

specific catchment studied differed considerably to the national estimates of smoking. Comparisons with external sources of data are most meaningful when performed with catchment-specific data.

At least one study aimed to combine WBE with survey data from the WWTP catchment. In an aforementioned study, van Wel and colleagues aimed to address this issue in a WBE study of illicit drug, alcohol and tobacco consumption. During the 12-week study period, residents of the WWTP were asked to fill in an online survey through which they could report their drug use. Correlation between WBE and survey data for the illicit drugs, alcohol and tobacco use was poor, and this was attributed to the paltry (1%) survey response rate (Van Wel et al. 2016a, b).

WBE agreement with the external data sources largely depends on the scale of the external data used, which can range from national scale estimates in the case of the nicotine metabolites, or dispensing volumes in the case of methadone in Lausanne. Overall, however, WBE agrees well with parallel data from external sources. Comparative studies will be more meaningful if well coordinated with external data sources in terms of the population and timeframe for which wastewater was sampled. These same lessons should be carried over into WBE triangulation studies in order to find more accurate and relevant associations.

## 2.3 Data Sources for Triangulation

New relationships between WBE data and other phenomena can be established by triangulating with other data that is not directly related to the WBE biomarker in question. This approach differs from WBE studies that compare results with other data, whose aim is to show the congruence between consumption or exposure patterns measured by WBE and an equivalent method. The following is a discussion of WBE studies which feature triangulation with the external data sources with the primary purpose of understanding public health phenomena, as opposed to simply comparing wastewater measurements using external sources.

### 2.3.1 Events

Numerous WBE studies have sampled wastewater generated around and during the time of special events such as music festivals and bodybuilding events, typically for the purpose of identifying recreational drug use. One early example of such a study examined 13 illicit drugs in daily wastewater composite samples from a six-day music festival in 2010, the same music festival again in 2011 and from a nearby urban catchment in 2010. Conveniently, the music festival grounds had their own dedicated WWTP, allowing population size and demographics to be determined through ticket sales. Of the 13 drugs analysed, the study identified MDMA as the

only substance whose per capita consumption by festival participants exceeded consumption by the nearby urban catchment (Lai et al. 2013c). The authors attributed this to the relatively wide age demographic attending the festival compared with other music festivals.

In contrast, most of the other studies find higher illicit drug consumption during special events. This was almost consistently the case in a temporal study by Lai and co-workers, who analysed illicit drugs in daily composite wastewater samples from an urban WWTP catchment in Australia. Samples ( $n = 311$ ) were mostly collected consecutively between June 2010 and June 2011. De facto catchment population was estimated with a Bayesian model that used the mass loads of eight PPCPs in wastewater influent. This allowed the authors to account for population flux during the sampling period on a per sample (i.e. per day) basis. Having consecutive daily sampling revealed a consistent, repeating weekly pattern in drug consumption, where per capita consumption of cocaine, MDMA and methamphetamine was

significantly higher on weekends than weekdays (Lai et al. 2015). Importantly, per capita loads of cocaine more than doubled during New Year's Eve and New Year's Day compared with other equivalent days in each respective month (Fig. 2a). These same events also coincided with a several-fold increase in MDMA consumption (Fig. 2b). In contrast, methamphetamine loads increased only slightly relative to other days. For all three drugs, consumption was higher on weekends than weekdays ( $p < 0.0001$ ). These results provide detailed illustration of the day-to-day variation in illicit drug consumption (i.e. public health burden from drug consumption). In other words, WBE can provide an objective insight into the public health burden that can be expected from different special events.

In a study of two WWTPs in Western Kentucky, USA, Foppe et al. sampled 24-hour, time-composited samples for seven consecutive days around Independence Day and for seven consecutive days during periods without special events (Foppe et al. 2018). For one of the WWTPs, samples

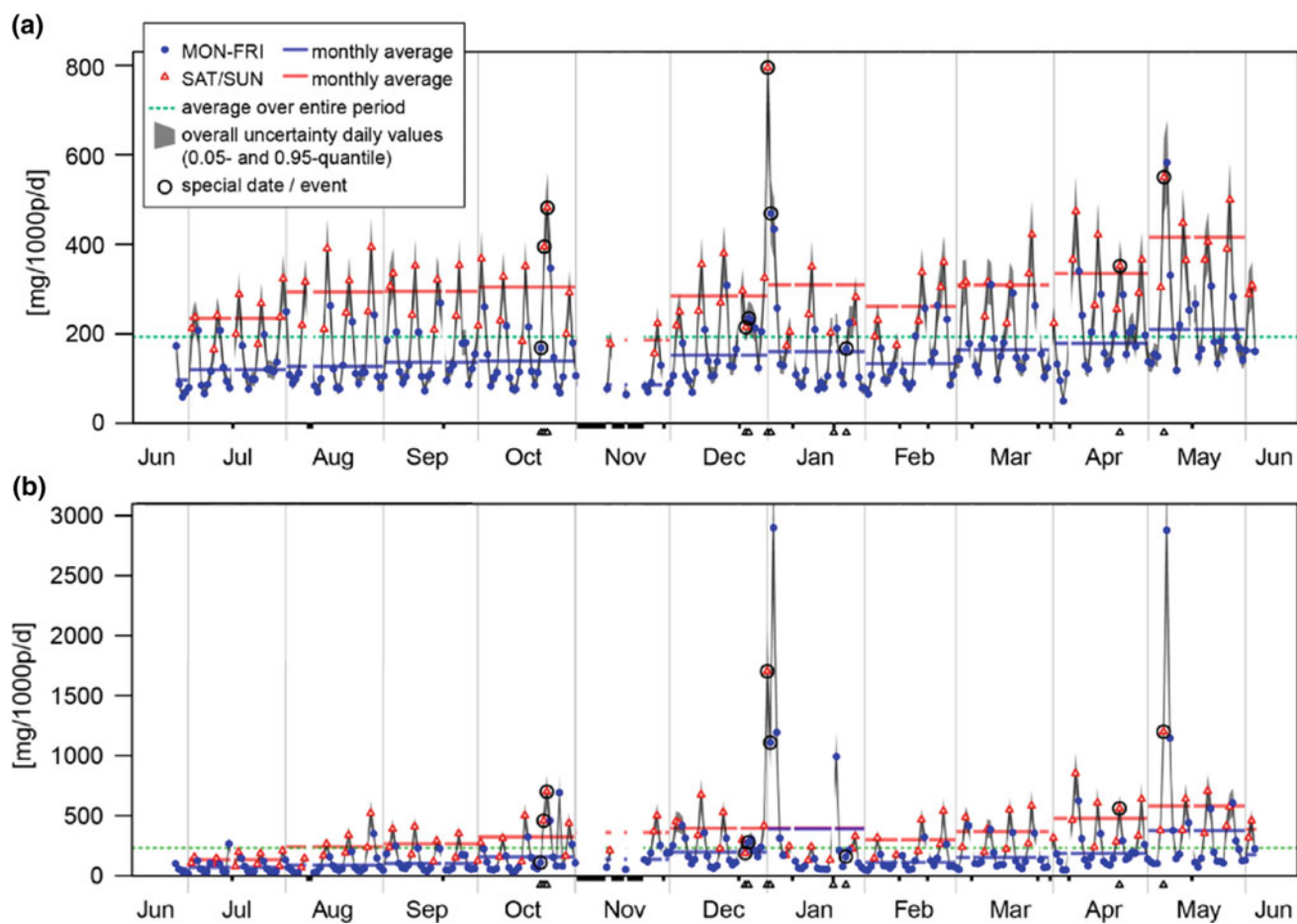


**Fig. 2** Estimated population-normalized (mg/day/1000 capita) consumption of **a** cocaine and **b** MDMA using normalisation to de facto population. Black bars and triangles represent missing days and special

event days, respectively. Reprinted (adapted) with permission from (Lai et al.). Copyright (2015) American Chemical Society

were also taken around the week of a solar eclipse. Ten recreational drugs were analysed from these samples using SPE followed by LC-MS/MS. For both WWTPs, per capita consumption of amphetamine, methamphetamine, cocaine, morphine and methadone was higher during Independence Day compared to the preceding and following days. Consumption of the same suite of drugs and also tetrahydrocannabinol (THC) was significantly higher in WWTP<sub>B</sub> during the time of the eclipse compared to the preceding and following days. Interestingly, when comparing the weekly sum of consumption rates of 'event' weeks to 'normal' weeks, differences ranged from negligible to minor. This suggests that the increased consumption during the special event day was offset by decreased consumption during the event week. WBE studies focussing on events can inform on drug consumption patterns during special events in an objective way that would be difficult to ascertain using traditional survey methods due to the illicit nature of the drugs consumed. Results from studies such as these can inform public health and law enforcement agencies on what to expect during special events, and provide a basis to help organise assistance or interventions.

Special events are ideal scenarios to measure doping substance use. Amateur athletes participating in sporting events are not always tested for performance enhancing drugs (PEDs) and doping substances to the same standard as professional athletes. In a study of three WWTP catchments, each holding a different sporting event, Causanilles and colleagues detected increases in the doping substances ephedrine, nor-ephedrine, methylhexanamine and 2,4-dinitrophenol (a weight loss substance) in the days preceding but not during an amateur bodybuilding event (Causanilles et al. 2018). This was presumably due to athletes avoiding consuming the substances on the day of the event. Similarly, a spike in per capita loads of 2,4-dinitrophenol was registered during a 2-day bodybuilding event attended by over 100 amateur athletes and 8000 visitors. In addition to compromising integrity in sports, doping can lead to detrimental effects on the health of the affected individuals and is a matter of public health concern. The consumption of 2,4-dinitrophenol in both events is of particular concern due to its acute toxicity which has led to several confirmed deaths (Kamour 2015). Doping control was not used in either of the events in this study, which demonstrates WBE can be used to determine the extent of doping during sporting events.

In conclusion, WBE can be used to study chemical consumption and excretion behaviours associated with a special event, whether it may be a festival, cultural event or a public health intervention. Accurate knowledge of the population at the time of the event as well as appropriate sampling practise can strengthen the findings from these events.

### 2.3.2 Environmental

#### Temperature

Changes in ambient temperature contribute directly and indirectly to an individual's health, and changes in temperature even lead to mortality (Basu 2009; Gasparrini et al. 2015). Although most individuals can readily sense and respond to ambient temperature, the effects of changes in ambient temperature on a population scale are difficult to document using traditional survey-based methods. A temporal WBE study of a metropolitan Australian catchment spanning 475 days set out to find associations between temperature, humidity and rainfall with loads of a selection of eight PPCPs (Phung et al. 2017). A time-series regression analysis showed that a 1 °C increase in average temperature was associated with a 1.2% decrease (compared to mean) in loads of the antihypertensive atenolol, which reflected a greater incidence of cardiovascular irregularities in cooler times. A 1 °C increase was also associated with a 0.84% decrease in loads of caffeine and 1.9% increase in loads of acesulfame, and this likely reflects reduced consumption of popular caffeine-rich beverages (tea and coffee) and increased consumption of soft drinks in hotter weather. Loads of the non-steroidal anti-inflammatory drug (NSAID) naproxen increased 0.64% with a 1 °C rise, which was surmised to reflect increased incidence and exacerbation of arthritis in hotter, more humid climes. However, contrary results have been reported for other NSAIDs. A wastewater analysis study set in a French catchment measured 25 drugs from daily composite samples between 21 March and 11 June 2016. In this study, the highest weekly loads of the NSAIDs ketoprofen, ibuprofen and diclofenac coincided with the two coldest weeks (5–11 °C) during the sampling period (Thiebault et al. 2019). Higher loads of morphine and codeine also coincided, although to a lesser extent, with the cold snaps, suggesting that colder weather causes increased consumption of NSAIDs and analgesics. The cold snaps also coincided with lower loads of the stimulants (cocaine, benzoylecgonine, cocaethylene, ecstasy and amphetamine), suggesting reduced recreational use of these stimulants in colder weather. Together, these two studies are a good example of how freely and publically available weather measurements can be used to provide insights into how a population responds to changes in the environment. It also highlights the extent to which temperature influences the consumption of specific chemicals, which may be useful for public health management.

Relationship between temperature and chemical exposure has also been examined in a study of 36 WWTPs, which accounted for 48% of the Australian population during two

days in August of 2016. O'Malley and colleagues measured loads of seven organic UV filters as proxies of sunscreen use. Total per capita UV filter load correlated with maximum daily temperature ( $R^2 = 0.195$ ), latitude ( $R^2 = 0.203$ ) and daily global solar exposure ( $R^2 = 0.149$ ) (O'Malley et al. 2019). The focus of this study was on establishing a national baseline for per capita UV filter use to inform environmental studies. Nevertheless, it identifies populations living closer to the equator as having greater exposure to UV filters, which may have endocrine disrupting properties. Future WBE studies triangulating with temperature could be used to determine and perhaps even quantify the role of temperature on public health and chemical exposure burdens.

### Pollen

Individuals' response to environmental cues can be detected in wastewater. A WBE study set in Oslo measured PPCPs using passive samplers. The authors found that per capita loads of the antihistamine cetirizine peaked 2–3-fold above baseline levels during the pollen season (Harman et al. 2011). Although cetirizine appeared to be a suitable proxy of pollen in this study, differences in availability of different antihistamines may result in different antihistamines correlating with pollen in different countries. Antihistamines such as cetirizine are available over-the-counter in most jurisdictions, and monitoring sales or prescription data would be poorly suited to understanding population response to pollen. Measuring other biomarkers related to allergic burden, such as other antihistamines (fexofenadine, diphenhydramine) and MIAA and perhaps even pharmaceuticals used for chronic obstructive pulmonary disease (e.g. salbutamol, terbutaline) or anti-inflammatories (e.g. ibuprofen) may be useful in understanding the full extent of pollen on population pharmaceutical consumption behaviour.

### Air Pollution

Air pollution exacerbates and predisposes to negative health outcomes such as asthma (Braman 2006). A study in Milan, Italy aimed to document the relationship between air pollution metrics and salbutamol, a short-acting beta2 agonist used to relieve bronchoconstriction, a hallmark symptom of asthma. The authors collected consecutive 24-hour composite wastewater samples from a WWTP serving the majority of Milan for 89 consecutive days. Wastewater samples were concentrated using an SPE method in order to measure salbutamol, which had minimum, median and maximum wastewater concentrations of 2.95, 5.85 and 9.97 ng/L, respectively. Despite this relatively narrow window of salbutamol concentrations, the authors found significant concentrations between daily per capita doses of salbutamol and levels of particulate matter. A log-linear

Poisson model found that the correlations between PM2.5 and PM10 levels were slightly higher with 7 or 8 days of lag, suggesting a culminative effect of air pollution on salbutamol consumption by individuals. However, salbutamol is a prescription drug. The delay likely reflects in large part the time taken for the exposure to manifest in individuals and cause them to present to a doctor to obtain a prescription. Although WBE is limited by population-level resolution, it can be used to determine the time at which the population actually consumed the prescribed pharmaceutical. This may make it more useful for finding associations with short-lived events such as onsets of smog or thunderstorm asthma.

### 2.3.3 Socioeconomic

#### Urbanicity: Oregon

Previous epidemiological studies have shown that illicit drug use is influenced by the degree of urbanicity of a population. This was affirmed using WBE in a 2009 publication by Banta-Green et al. (Banta-Green 2009). The authors measured benzoylecgonine (cocaine biomarker), methamphetamine and MDMA in wastewater from 96 WWTPs collectively covering 65% of the population of the state of Oregon (United States). Each WWTP provides one 24-hour composite sample. Each WWTP was designated as 'urban', 'large rural city/town' or 'small rural town' based on rural-urban commuting area (RUCA) codes derived from census information. Benzoylecgonine and MDMA loads were highest in urban areas, whereas methamphetamine loads were not significantly different by urbanicity. This study showed that WBE could replicate established epidemiological findings regarding drug use in urban versus rural areas in the United States. This was despite basing drug loads on measurements from one convenience sample per WWTP. Although other WBE studies have also identified urbanicity as a factor for differences in drug consumption patterns (Du et al. 2017; Boogaerts et al. 2016; Castiglioni et al. 2015), linking WBE results to sociodemographic metrics makes findings more immediate and relevant to a transdisciplinary and public health focussed audience.

Additionally, it was the first study to link WBE results to a sociodemographic factor, asserting its relevance in sociodemographic aspects of public health.

#### Economic: Greece

Financial information may be triangulated with WBE to see how chemical consumption or exposure changes or differs with the financial wellbeing of a population. When drug and pharmaceutical incurs financial cost to the individual, it is inevitable that socioeconomic differences will influence

consumption behaviour. A WBE study in Athens, Greece was able to determine the extent to which the Greek economic downturn and subsequent austerity measures affected illicit drug and PPCP consumption between 2010 and 2014 (Thomaidis et al. 2016). During the study period, Greece saw economic hardships which manifested as a 20% drop in GDP, a doubling of its unemployment rate and cuts to public health spending including cuts to drug expenditure, and more. The WBE study was conducted as five-sampling campaigns between 2010 and 2014, with each campaign consisting of 7–11 consecutive daily samples. Wastewater samples were concentrated using SPE and 148 substances were quantified by LC-MS/MS. The study found a 14-fold increase in per capita doses of antidepressants and benzodiazepines, which are collectively used to treat depression, anxiety, insomnia and seizures. Doses of antipsychotics increased 35-fold. Pharmaceuticals used to treat stress-induced or stress-exacerbated conditions such as atenolol (hypertension) and gastric ulcer drugs also increased (Fig. 3). Per capita loads of

certain illicit drugs, namely ecstasy, methamphetamine and methadone rose 2.2, 4.5 and 6.8-fold, respectively. This reflected the relatively low cost of street methamphetamine and the proliferation of methadone administration clinics, while no such trends could be established for cocaine, heroin, amphetamine and tetrahydrocannabinol (cannabis). There was a decrease in per capita doses of most antibiotics and most NSAIDs which could be explained by cuts in public health spending. Total number of doses of six benzodiazepines and antidepressants rose 10-fold over the sampling period. This study used broad, large-scale measures of socioeconomics and operated under a very unique scenario involving immense changes to the financial environment. Consequently, the degree to which methodological aspects or findings from this study can be replicated in other WBE studies, or the extent to which the findings can inform similar situations is unclear. Nevertheless, the study convincingly shows how dire socioeconomic changes led to increases in biomarkers of mental, physical and social distress.

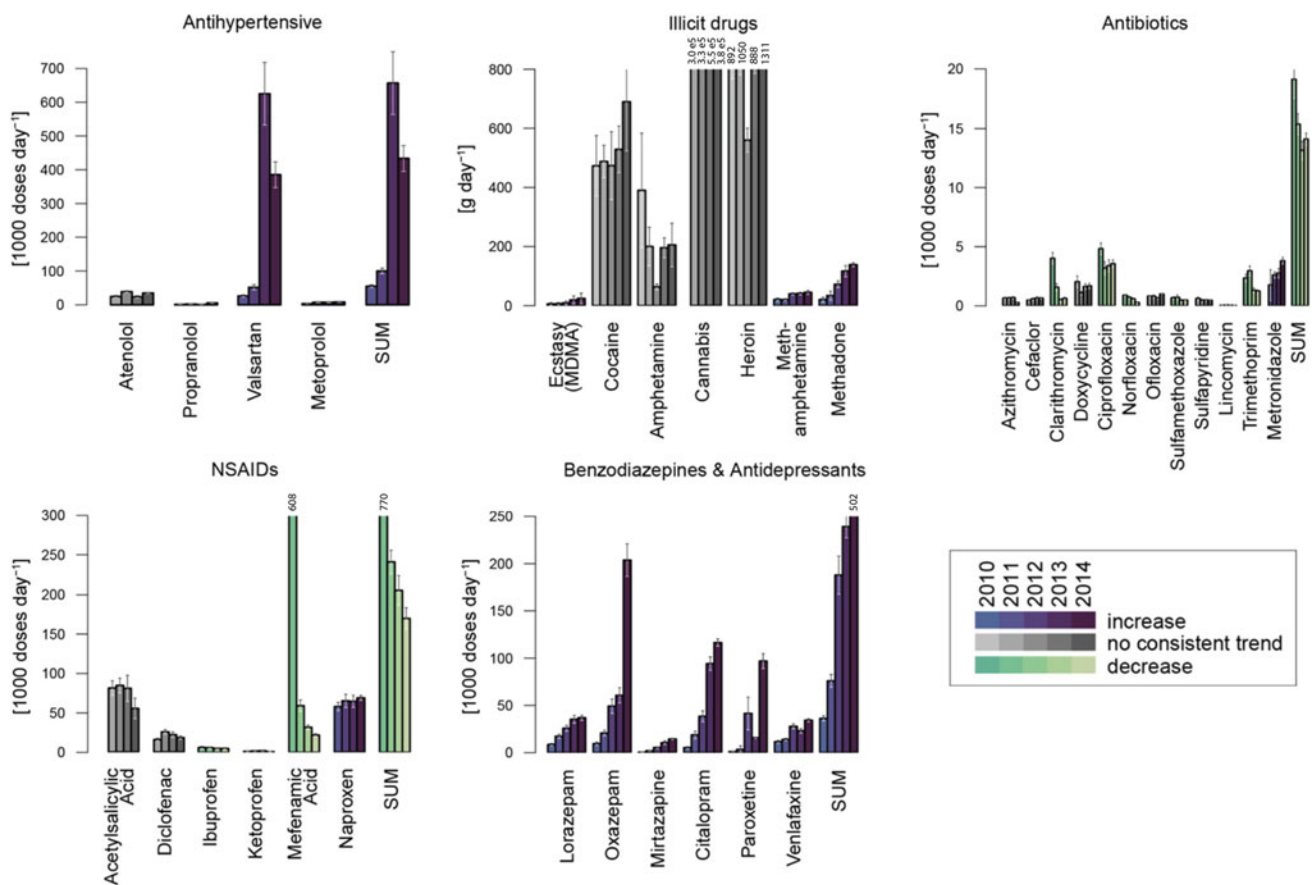


**Fig. 3** Estimated use of selected pharmaceuticals (1000 doses per day) and illicit drugs (g per day) over 2010–2014. Error bars represent variability of daily values within each annual sampling campaign

Reprinted (adapted) with permission from Thomaidis et al. Copyright (2016) American Chemical Society

## Housing Price and Density: Beijing

WBE has also been used to examine the relationship between housing price and PPCP use. A study involving eight WWTP catchments covering most of the population of Beijing, China, was able to establish an association between housing price and per capita loads of PPCPs. In this study, Zhang et al. sampled one 24-hour time composite wastewater sample per WWTP between November 2016 and January 2017. A panel of 17 PPCPs (propranolol, carbamazepine, N,N-dimethyl-meta-toluamide, sulpiride, metoprolol, caffeine, diclofenac, indomethacin, ketoprofen, mefenamic acid, bezafibrate, clofibrac acid, gemfibrozil, trimethoprim, nalidixic acid, chloramphenicol and acetaminophen) were measured using SPE-LC-MS/MS. Per capita loads of the panel of PPCPs correlated with catchment average housing price ( $R = 0.92$ ) and population density ( $R = 0.93$ ). Increased consumption of PPCPs among those living in more expensive areas was suggested as an explanation. However, this study had some limitations compared to other WBE triangulation studies. Only one sample was taken per catchment over a wide sampling window, which likely contributed towards unrepresentative sampling (Humphries et al. 2016). Population size was also determined using ammonia loads, a technique known to be better suited for measuring population fluctuations over time rather than between different catchments (Been et al. 2014). While this study revealed that variation in PPCP consumption behaviour can be attributed to socioeconomic measures, it must be noted that more synchronised sampling and more reliable population measurements would likely lead to more realistic findings.

### 2.3.4 Potential Future Sources of Data for Triangulation

Current best practise WBE methodologies have proven useful for accurately measuring chemicals excreted by individuals. Recent progress in WBE triangulation studies demonstrate that considerable insights into population health can be gained using existing WBE biomarkers. This is not to discount efforts in adopting other biomarkers for use in WBE. Rather, it is to stress that the success of future WBE triangulation studies which inform on public health will be proportional to the quality, novelty and public health relevance of the data used for triangulation. It is therefore imperative to look towards validated, well-curated, current and relevant sources of information for triangulation studies.

Where available, national census data is an attractive source of data for triangulation. Most nations conduct some form of census, which often record sociodemographic information about individuals. In countries such as Australia, census data are well curated, quality assured and validated by a census post enumeration survey (Harding et al. 2017).

Following the census, sociodemographic information about residents of specific geographic locations are made available. The sociodemographic characteristics of a WWTP catchment can be determined by mapping geographically grouped census data onto WWTP catchment maps using georeferencing software as further explained elsewhere (O'Brien et al. 2019). In addition to providing accurate population of a WWTP, these approaches can be used to determine the extent to which sociodemographic factors (e.g. occupation, housing characteristics) associate with or influence chemical consumption or exposure patterns. The aforementioned 2009 study by Banta-Green et al. incorporating RUCA into WBE can be considered a pioneering step into this approach, since the RUCA was devised using census-derived data. However, censuses can provide more specific descriptors than urbanicity. Incorporating aspects of the census into WBE studies could prove fruitful for identifying sociodemographic disparities which can be actioned upon by public health or government interests.

In the burgeoning field known as digital epidemiology (Salathé 2018), the internet has proven to be fertile grounds from which to reap information about the health and well-being of individuals. Good examples abound. A digital epidemiology study by Bakker et al. found Google search instances of 'chicken pox' in several countries between 2010 and 2016 had good agreement with clinical chicken pox cases (Bakker et al. 2016). Search data could also be used to model future outbreaks and immunisation events manifested as declines in searches. Social media platforms have also been identified as platforms ripe with public health information. Twitter has been identified as a resource from which to monitor prescription medication abuse (Sarker et al. 2016; Chary et al. 2017) and illicit drug use (Kazemi et al. 2017), as well as health outcomes such as pregnancies, heart and birth defects (Klein et al. 2018). Although the software required to process the vast amounts of data often implicated in digital epidemiology studies is easily accessible, meaningful, high-quality datasets but generally not publicly accessible (Salathé 2018). For example, privacy restrictions commonly prevent researchers from dividing the dataset by demographics, which limits the extent to which results can be generalised to different demographic ranges (Kazemi et al. 2017). Any future triangulation with WBE will also need to consider the location (i.e. WWTP catchment) in which data points correspond to. Therefore the WBE community should be mindful of approaching digital WBE with good hypotheses and experimental plans in hand. Nevertheless, identifying similar keywords or activities which associate with chemical consumption or exposure as measurable by WBE could provide a simple way to assess chemical consumption or exposure in near real-time. This is quite appropriate, particularly given that social media platforms often shape or motivate substance use such as alcohol



consumption (Moreno et al. 2009). Alternatively, a combination of digital epidemiology and non-targeted WBE could be used to unveil chemical signatures corresponding to specific internet use patterns in a population scale metabolomics study.

## 2.4 Future Directions

Moving forward, future WBE studies that explore aspects of public health should employ suitable wastewater sampling practise, sufficient sample sizes for the research question being asked (including minimal gaps in triangulation data) and, wherever possible, robust statistics in order to reduce the uncertainty and ambiguity in the putative relationships found.

As the WBE field develops the main sources of uncertainty, such as flow and population, biomarker stability and biomarker excretion factors will need to be better understood and in some cases reduced if studies are to have sufficient power to reflect small changes in communities. Many of the studies performed to date have generally been pilots employing spatial analysis and we envisage that more longitudinal studies will be performed that will not only investigate changes in the weighted biomarker load over time but investigate those factors that influence biomarker change and use WBE, for example, as an intervention assessment tool. Understanding sampling power will be the key in such studies.

Humans are continually exposed to multiple chemicals from different environmental sources and pathways, both intentionally and unintentionally. The exposome paradigm acknowledges this complexity and seeks methods to measure all environmental exposures and the related biological responses over the life course. It is clear that integrating the exposome paradigm into WBE will improve exposure assessments. Non-target analysis employing HRMS has been established over recent years as one of the key approaches for tackling this complexity. When coupled to smart study design, time-trend screening and case-control type studies, it may not only allow for improved exposure assessments but also allow for novel wastewater biomarker discovery.

Metagenomic analysis in WBE has to date been rarely applied but offers clear opportunities in understanding the genetic material contained in wastewater. Current sampling procedures may need optimisation to achieve this goal and realise the benefits that such an approach may have in future public health assessments. Chemical and biological sensors may also have a role to play in terms of monitoring a multiplex of biomarkers in real time.

In many countries, a wealth of data that can be defined by a sewer catchment area is already available. This enables integration of biomarker data with available socioeconomic, pharmaceutical, biomonitoring, exposure, climatic and other data. One can envisage an approach that would focus on understanding the collective functioning of systems, in terms of their dynamic relationships, feedback loops, interactions and dependencies. In order to facilitate such an ambition, there is an important role for including wastewater in systematic sampling and archiving programs that allow retrospective analysis. In the age of 'big data', global collaboration and the sharing of data through open/social platforms may revolutionise the way WBE and associated data are processed in order to achieve significant outcomes. The Sewage analysis COre group Europe (SCORE) Network is already working towards a platform for storing its illicit drug biomarker data from extensive global surveys. Its further development may serve as a springboard to bring together data from other similar surveys, such as the Global Sewage Surveillance Project (focused on antimicrobial resistance) and the Human Health Repository in the USA.

Finally, and by far the most critical aspect to the success of the future direction of WBE is the need to establish national frameworks for WBE to encourage, support and formalise the crucial role that WWTP operators play in supporting this growing and exciting area of interdisciplinary science.

---

## References

- Albalat A, Mischak H, Mullen W (2011) Clinical application of urinary proteomics/peptidomics. *Expert Rev Proteomics* 8(5):615–629
- Andrés-Costa MJ, Escrivá Ú, Andreu V, Picó Y (2016) Estimation of alcohol consumption during “Fallas” festivity in the wastewater of Valencia city (Spain) using ethyl sulfate as a biomarker. *Sci Total Environ* 541:616–622
- Archer E, Petrie B, Kasprzyk-Hordern B, Wolfaardt GM (2017) The fate of pharmaceuticals and personal care products (PPCPs), endocrine disrupting contaminants (EDCs), metabolites and illicit drugs in a WWTW and environmental waters. *Chemosphere* 174:437–446
- Asimakopoulos AG, Kannan P, Higgins S, Kannan K (2017) Determination of 89 drugs and other micropollutants in unfiltered wastewater and freshwater by LC-MS/MS: an alternative sample preparation approach. *Anal Bioanal Chem* 409(26):6205–6225
- Bade R et al (2017) Liquid chromatography-tandem mass spectrometry determination of synthetic cathinones and phenethylamines in influent wastewater of eight European cities. *Chemosphere* 168:1032–1041
- Bade R et al (2018) Investigating the correlation between wastewater analysis and roadside drug testing in South Australia. *Drug Alcohol Depend* 187:123–126
- Baker DR, Kasprzyk-Hordern B (2011) Multi-residue determination of the sorption of illicit drugs and pharmaceuticals to wastewater suspended particulate matter using pressurised liquid extraction,

- solid phase extraction and liquid chromatography coupled with tandem mass spectrometry. *J Chromatogr A* 1218(44):7901–7913
- Baker DR, Očenášková V, Kvicalova M, Kasprzyk-Hordern B (2012) Drugs of abuse in wastewater and suspended particulate matter—further developments in sewage epidemiology. *Environ Int* 48:28–38
- Bakker KM, Martinez-Bakker ME, Helm B, Stevenson TJ (2016) Digital epidemiology reveals global childhood disease seasonality and the effects of immunization. *Proc Natl Acad Sci* 113(24):6689
- Banta-Green CJ et al (2009) The spatial epidemiology of cocaine, methamphetamine and 3,4-methylenedioxymethamphetamine (MDMA) use: a demonstration using a population measure of community drug load derived from municipal wastewater. *Environ Int* 35(11):1874–1880
- Basu R (2009) High ambient temperature and mortality: a review of epidemiologic studies from 2001 to 2008. *Environ Health* 8(1):40
- Been F et al (2014) Population normalization with ammonium in wastewater-based epidemiology: application to illicit drug monitoring. *Environ Sci Technol* 48(14):8162–8169
- Been F et al (2015) Data triangulation in the context of opioids monitoring via wastewater analyses. *Drug Alcohol Depend* 151:203–210
- Been F, Bastiaansen M, Yin Lai F, van Nuijs ALN, Covaci A (2017) liquid chromatography-tandem mass spectrometry analysis of biomarkers of exposure to phosphorus flame retardants in wastewater to monitor community-wide exposure. *Anal Chem* 89(18):10045–10053
- Boleda MR, Galceran MT, Ventura F (2009) Monitoring of opiates, cannabinoids and their metabolites in wastewater, surface water and finished water in Catalonia Spain. *Water Res* 43(4):1126–1136
- Boogaerts T, Covaci A, Kinyua J, Neels H, van Nuijs ALN (2016) Spatial and temporal trends in alcohol consumption in Belgian cities: a wastewater-based approach. *Drug Alcohol Depend* 160:170–176
- Bouatra S et al (2013) The human urine metabolome. *PLoS ONE* 8(9):e73076
- Braman SS (2006) The global burden of asthma. *Chest* 130(1, Supplement):4S–12S
- Castiglioni S (2016) Assessing illicit drugs in wastewater: advances in wastewater-based drug epidemiology (Publications Office)
- Castiglioni S, Borsotti A, Senta I, Zuccato E (2015) Wastewater analysis to monitor spatial and temporal patterns of use of two synthetic recreational drugs, ketamine and mephedrone Italy. *Environ Sci Technol* 49(9):5563–5570
- Cauci S et al (2016) Seasonality of antibiotic prescriptions for outpatients and resistance genes in sewers and wastewater treatment plant outflow. *FEMS Microbiol Ecol* 92(5):fiw060
- Causanilles A et al (2018) Wastewater-based tracing of doping use by the general population and amateur athletes. *Anal Bioanal Chem* 410(6):1793–1803
- Chary M et al (2017) Epidemiology from Tweets: estimating misuse of prescription opioids in the USA from social media. *J Med Toxicol* 13(4):278–286
- Chen C, Kostakis C, Irvine RJ, Felgate PD, White JM (2012) Evaluation of pre-analysis loss of dependent drugs in wastewater: stability and binding assessments. *Drug Test Anal* 5(8):716–721
- Chen C et al (2014) Towards finding a population biomarker for wastewater epidemiology studies. *Sci Total Environ* 487:621–628
- Choi PM et al (2018a) Wastewater-based epidemiology biomarkers: past, present and future. *TrAC Trends Anal Chem* 105:453–469
- Choi PM et al (2018b) Population histamine burden assessed using wastewater-based epidemiology: the association of 1, 4-methylimidazole acetic acid and fexofenadine. *Environ Int* 120:172–180
- Daughton CG (2012) Using biomarkers in sewage to monitor community-wide human health: Isoprostanes as conceptual prototype. *Sci Total Environ* 424:16–38
- Daughton CG (2018) Monitoring wastewater for assessing community health: sewage chemical-information mining (SCIM). *Sci Total Environ* 619–620:748–764
- Du P et al (2017) Estimating heroin abuse in major Chinese cities through wastewater-based epidemiology. *Sci Total Environ* 605–606:158–165
- Foppe KS, Hammond-Weinberger DR, Subedi B (2018) Estimation of the consumption of illicit drugs during special events in two communities in Western Kentucky, USA using sewage epidemiology. *Sci Total Environ* 633:249–256
- Gao J et al (2016) Measuring selected PPCPs in wastewater to estimate the population in different cities in China. *Sci Total Environ* 568:164–170
- Gao J et al (2019) Systematic evaluation of biomarker stability in pilot scale sewer pipes. *Water Res* 151:447–455
- Gasparrini A et al (2015) Mortality risk attributable to high and low ambient temperature: a multicountry observational study. *Lancet* 386(9991):369–375
- Gibbons H et al (2017) Demonstration of the utility of biomarkers for dietary intake assessment; proline betaine as an example. *Mol Nutr Food Res* 61(10):1700037
- Gracia-Lor E, Martinez M, Sancho JV, Penuela G, Hernandez F (2012) Multi-class determination of personal care products and pharmaceuticals in environmental and wastewater samples by ultra-high performance liquid-chromatography-tandem mass spectrometry. *Talanta* 99:1011–1023
- Gracia-Lor E et al (2017) Measuring biomarkers in wastewater as a new source of epidemiological information: current state and future perspectives. *Environ Int* 99:131–150
- Hall W et al (2012) An analysis of ethical issues in using wastewater analysis to monitor illicit drug use. *Addiction* 107(10):1767–1773
- Harding S JPL, McDonald O, Morrison P, Trewin D, Voss A (2017) Report on the Quality of 2016 Census Data. (Independent Assurance Panel)
- Harman C, Reid M, Thomas KV (2011) In situ calibration of a passive sampling device for selected illicit drugs and their metabolites in wastewater, and subsequent year-long assessment of community drug usage. *Environ Sci Technol* 45(13):5676–5682
- Harris DS, Everhart ET, Mendelson J, Jones RT (2003) The pharmacology of cocaethylene in humans following cocaine and ethanol administration. *Drug Alcohol Depend* 72(2):169–182
- Hortin GL, Sviridov D (2007) Diagnostic potential for urinary proteomics. *Pharmacogenomics* 8(3):237–255
- Humphries MA et al (2016) Evaluation of monitoring schemes for wastewater-based epidemiology to identify drug use trends using cocaine, methamphetamine, MDMA and methadone. *Environ Sci Technol* 50(9):4760–4768
- Kamour A et al (2015) Increasing frequency of severe clinical toxicity after use of 2, 4-dinitrophenol in the UK: a report from the National Poisons Information Service. *BMJ* 350:g1133
- Kankaanpää A, Ariniemi K, Heinonen M, Kuoppasalmi K, Gunnar T (2014) Use of illicit stimulant drugs in Finland: a wastewater study in ten major cities. *Sci Total Environ* 487:696–702
- Kasprzyk-Hordern B, Dinsdale RM, Guwy AJ (2008) Multiresidue methods for the analysis of pharmaceuticals, personal care products and illicit drugs in surface water and wastewater by solid-phase extraction and ultra performance liquid chromatography-electrospray tandem mass spectrometry. *Anal Bioanal Chem* 391(4):1293–1308
- Kazemi DM, Borsari B, Levine MJ, Dooley B (2017) Systematic review of surveillance by social media platforms for illicit drug use. *J Public Health* 39(4):763–776
- Khan U, Nicell JA (2011) Refined sewer epidemiology mass balances and their application to heroin, cocaine and ecstasy. *Environ Int* 37(7):1236–1252

- Klein AZ, Sarker A, Cai H, Weissenbacher D, Gonzalez-Hernandez G (2018) Social media mining for birth defects research: a rule-based, bootstrapping approach to collecting data for rare health-related events on Twitter. *J Biomed Inf* 87:68–78
- Krumpal I (2013) Determinants of social desirability bias in sensitive surveys: a literature review. *Qual Quant* 47(4):2025–2047
- Laht M et al (2014) Abundances of tetracycline, sulphonamide and beta-lactam antibiotic resistance genes in conventional wastewater treatment plants (WWTPs) with different waste load. *PLoS ONE* 9(8):e103705
- Lai FY et al (2013a) Estimating daily and diurnal variations of illicit drug use in Hong Kong: a pilot study of using wastewater analysis in an Asian metropolitan city. *233(1-3):126–132*
- Lai FY et al (2013b) Estimating daily and diurnal variations of illicit drug use in Hong Kong: a pilot study of using wastewater analysis in an Asian metropolitan city. *Forensic Sci Int* 233(1):126–132
- Lai FY et al (2013c) Using quantitative wastewater analysis to measure daily usage of conventional and emerging illicit drugs at an annual music festival. *Drug Alcohol Rev* 32(6):594–602
- Lai FY et al (2015) Systematic and day-to-day effects of chemical-derived population estimates on wastewater-based drug epidemiology. *Environ Sci Technol* 49(2):999–1008
- Lai FY, O'Brien J, Thai PK, Hall WD, Mueller J (2016) Trends in methamphetamine residues in wastewater in metropolitan and regional cities in South East Queensland, 2009–2015. *Med J Aust* 204:151–152
- Lai FY et al (2016a) Cocaine, MDMA and methamphetamine residues in wastewater: consumption trends (2009–2015) in South East Queensland, Australia. *Sci Total Environ* 568:803–809
- Lai FY et al (2016b) Spatial variations in the consumption of illicit stimulant drugs across Australia: a nationwide application of wastewater-based epidemiology. *Sci Total Environ* 568:810–818
- Lai FY, Wilkins C, Thai P, Mueller JF (2017) An exploratory wastewater analysis study of drug use in Auckland, New Zealand. *Drug Alcohol Rev*
- Li J et al (2018) Stability of illicit drugs as biomarkers in Sewers: from lab to reality. *Environ Sci Technol* 52(3):1561–1570
- Lopardo L, Adams D, Cummins A, Kasprzyk-Hordern B (2018) Verifying community-wide exposure to endocrine disruptors in personal care products—in quest for metabolic biomarkers of exposure via in vitro studies and wastewater-based epidemiology. *Water Res* 143:117–126
- Lun JH et al (2018) Emerging recombinant noroviruses identified by clinical and waste water screening. *Emerg Microbes Infect* 7(1):50
- Lundgren MS, Novak PJ (2009) Quantification of phytoestrogens in industrial waste streams. *Environ Toxicol Chem* 28(11):2318–2323
- Mackie RS et al (2019) Trends in nicotine consumption between 2010 and 2017 in an Australian city using the wastewater-based epidemiology approach. *Environ Int* 125:184–190
- McCall A-K et al (2016) Critical review on the stability of illicit drugs in sewers and wastewater samples. *Water Res* 88:933–947
- McLellan SL, Huse SM, Mueller-Spitz SR, Andreishcheva EN, Sogin ML (2010) Diversity and population structure of sewage-derived microorganisms in wastewater treatment plant influent. *Environ Microbiol* 12(2):378–392
- Moreno MA, Briner LR, Williams A, Walker L, Christakis DA, Joah J (2009) Real use or “real cool”: adolescents speak out about displayed alcohol references on social networking websites. *45(4):420–422*
- Newton RJ et al (2015) Sewage reflects the microbiomes of human populations. *MBio* 6(2):e02574–e02614
- O'Brien JW et al (2014) A model to estimate the population contributing to the wastewater using samples collected on census day. *Environ Sci Technol* 48(1):517–525
- O'Brien JW et al (2015) Wastewater analysis of census day samples to investigate per capita input of organophosphorus flame retardants and plasticizers into wastewater. *Chemosphere* 138:328–334
- O'Brien JW et al (2017) National wastewater drug monitoring program—report 1. (The University of Queensland & University of South Australia, Australian Criminal Intelligence Commission (ACIC)), p 64
- O'Brien JW et al (2019) A national wastewater monitoring program for a better understanding of public health: a case study using the Australian census. *Environ Int* 122:400–411
- O'Malley E, O'Brien JW, Tscharke B, Thomas KV, Mueller JFJSOTTE (2019) Per capita loads of organic UV filters in Australian wastewater influent. *662:134–140*
- Ort C, Lawrence MG, Reungoat J, Mueller JF (2010) Sampling for PPCPs in wastewater systems: comparison of different sampling modes and optimization strategies. *Environ Sci Technol* 44(16):6289–6296
- Ort C et al (2014) Spatial differences and temporal changes in illicit drug use in Europe quantified by wastewater analysis. *Addiction* 109(8):1338–1352
- Phung D et al (2017) Can wastewater-based epidemiology be used to evaluate the health impact of temperature?—An exploratory study in an Australian population. *Environ Res* 156:113–119
- Reid MJ, Langford KH, Mørland J, Thomas KV (2011) Analysis and interpretation of specific ethanol metabolites, ethyl sulfate, and ethyl glucuronide in sewage effluent for the quantitative measurement of regional alcohol consumption. *Alcohol Clin Exper Res* 35(9):1593–1599
- Reitsma MB et al (2017) Smoking prevalence and attributable disease burden in 195 countries and territories, 1990–2015: a systematic analysis from the global burden of disease study 2015. *Lancet* 389(10082):1885–1906
- Rico M, Andrés-Costa MJ, Picó Y (2017) Estimating population size in wastewater-based epidemiology. Valencia metropolitan area as a case study. *J Hazard Mater* 323:9
- Rousis NI, Zuccato E, Castiglioni S (2017) Wastewater-based epidemiology to assess human exposure to pyrethroid pesticides. *Environ Int* 99(Supplement C):213–220
- Ryu Y, Reid MJ, Thomas KV (2015) Liquid chromatography-high resolution mass spectrometry with immunoaffinity clean-up for the determination of the oxidative stress biomarker 8-iso-prostaglandin F2alpha in wastewater. *J Chromatogr A* 1409:146–151
- Salathé M (2018) Digital epidemiology: what is it, and where is it going? *Life Sci Soc Policy* 14(1):1
- Salvatore S et al (2015) Wastewater-based epidemiology of stimulant drugs: functional data analysis compared to traditional statistical methods. *PLoS ONE* 10(9):e0138669
- Sarker A et al (2016) Social media mining for toxicovigilance: automatic monitoring of prescription medication abuse from Twitter. *Drug Saf* 39(3):231–240
- SCORE (2018) Wastewater monitoring data 2011–2017 Sewage analysis CORE group Europe. In: COST Action ES1307
- Senta I, Gracia-Lor E, Borsotti A, Zuccato E, Castiglioni S (2015) Wastewater analysis to monitor use of caffeine and nicotine and evaluation of their metabolites as biomarkers for population size assessment. *Water Res* 74:23–33
- Subedi B, Kannan K (2014) Fate of artificial sweeteners in wastewater treatment plants in New York State, U.S.A. *Environ Sci Technol* 48(23):13668–13674
- Tebbens RJD, Zimmermann M, Pallansch MA, Thompson KM (2017) Insights from a systematic search for information on designs, costs, and effectiveness of poliovirus environmental surveillance systems. *Food Environ Virol* 9(4):361–382
- Thiebault T, Fougère L, Destandau E, Réty M, Jacob J (2019) Impact of meteorological and social events on human-excreted contaminant

- loads in raw wastewater: from daily to weekly dynamics. *Chemosphere* 230:107–116
- Thomaidis NS et al (2016) Reflection of socioeconomic changes in wastewater: licit and illicit drug use patterns. *Environ Sci Technol* 50(18):10065–10072
- Thomas KV, Reid MJ (2011) What else can the analysis of sewage for urinary biomarkers reveal about communities? *Environ Sci Technol* 45(18):7611–7612
- Thomas KV, Amador A, Baz-Lomba JA, Reid M (2017) Use of mobile device data to better estimate dynamic population size for wastewater-based epidemiology. *Environ Sci Technol*
- Tscharke BJ, Chen C, Gerber JP, White JM (2016) Temporal trends in drug use in Adelaide, South Australia by wastewater analysis. *Sci Total Environ* 565:384–391
- van Nuijs AL et al (2009) Spatial and temporal variations in the occurrence of cocaine and benzoylecgonine in waste-and surface water from Belgium and removal during wastewater treatment. *Water Res* 43(5):1341–1349
- van Nuijs ALN et al (2011) A one year investigation of the occurrence of illicit drugs in wastewater from Brussels Belgium. *J Environ Monit* 13(4):1008–1016
- van Nuijs ALN et al (2018) Multi-year inter-laboratory exercises for the analysis of illicit drugs and metabolites in wastewater: development of a quality control system. *TrAC Trends Anal Chem* 103:34–43
- van Wel JHP et al (2016a) A comparison between wastewater-based drug data and an illicit drug use survey in a selected community. *Int J Drug Policy* 34:20–26
- van Wel JHP et al (2016b) Investigation of agreement between wastewater-based epidemiology and survey data on alcohol and nicotine use in a community. *Drug Alcohol Depend* 162:170–175
- Van Wel J et al (2016) A comparison between wastewater-based drug data and an illicit drug use survey in a selected community. 34:20–26
- Yang Z et al (2015) A novel DNA biosensor using a ferrocenyl intercalator applied to the potential detection of human population biomarkers in wastewater. *Environ Sci Technol* 49(9):5609–5617
- Zheng Q et al (2019) Uncertainties in estimating alcohol and tobacco consumption by wastewater-based epidemiology. *Curr Opin Environ Sci Health* 9:13–18
- Zuccato E, Chiabrando C, Castiglioni S, Bagnati R, Fanelli R (2008) Estimating community drug abuse by wastewater analysis. *Environ Health Perspect* 116(8):1027–1032

# Mechanistically Modeling Human Exposure to Persistent Organic Pollutants

Frank Wania, Li Li, and Michael S. McLachlan

## Abstract

Mechanistic modeling approaches simulate human exposure by describing the processes that are responsible for delivering contaminants to the human body. Starting with environmental concentrations, emissions, or production volumes, these approaches yield metrics of internal human exposure, either for individuals or for a generic representative of a population. These models are particularly useful for quantifying exposure to persistent organic pollutants (POPs), whose long residence time in the human body implies that past exposures influence current contaminant levels and thus need to be considered. Mechanistic models allow for the reconstruction of past exposures without relying on back-extrapolations with empirical surrogate parameters; consequently, they can account for lag periods between emissions and exposure as well as for shifts in the main exposure route over time. Such shifts can occur as a result of changes in chemical use and emission scenario, exposure factors, or the environment. However, because mechanistic models require an in-depth understanding of the relevant processes including the ability to numerically parameterize them, they have so far been applied to only a limited number of data-rich POPs. When used in simulations involving a large number of hypothetical property combinations, these models facilitate the comparison of the exposure potential of different substances and the identification of thresholds that separate chemicals with different dominant exposure routes. The motivations for mechanistic modeling of exposure to POPs are manifold, and include risk assessment and management, support of

biomonitoring and epidemiological investigations, and the identification of chemicals and human populations with high exposure potential.

## 1 Introduction

An important motivation for environmental chemistry is the estimation of human exposure to contaminants because it is that exposure that determines the possibility for detrimental effects. Exposure can be expressed as either an intake; the rate of a chemical crossing an outer exposure surface (e.g., a mouth) but without penetrating an absorption barrier (e.g., gastrointestinal and respiratory tract linings), or an uptake, which is the rate crossing an absorption barrier and entering the human circulatory system (Zartarian et al. 2005). Exposure can be quantified by measuring the occurrence of contaminants or their biotransformation products in the human body (e.g., in blood or urine). Human contaminant exposure is often also estimated by multiplying measured concentrations in exposure-relevant media (e.g., dietary items, drinking water, house dust, indoor air) with corresponding medium intake rates (e.g., rates of dietary intake, breathing, dust ingestion, etc.), followed by summing up the intake by various routes of exposure. More recently, there have also been efforts to simulate human exposure with models that mechanistically describe the processes that are responsible for delivering contaminants to the human body. The concentrations in the exposure-relevant media are not determined empirically, and are instead predicted in a deterministic way. This approach is particularly useful for studying exposure to persistent organic pollutants (POPs). This chapter reviews these mechanistic human exposure modeling efforts, with a particular focus on what motivates them.

An overarching characteristic of POPs is their long residence time in the human body. This slow elimination is the result of slow or non-existent biotransformation and

---

F. Wania (✉) · L. Li  
Department of Physical and Environmental Sciences,  
University of Toronto Scarborough, Toronto, Canada  
e-mail: [frank.wania@utoronto.ca](mailto:frank.wania@utoronto.ca)

M. S. McLachlan  
Department of Environmental Science and Analytical Chemistry,  
Stockholm University, Stockholm, Sweden

inefficient elimination by exhalation, urination, and fecal excretion. This long residence time creates a number of challenges when seeking to model internal exposure to POPs: Exposure is cumulative over time, meaning that, exposure that occurred in the (distant) past still influences current contaminant levels in the body. Simulating those concentrations, therefore, requires the reconstruction of past exposure. Furthermore, because of the inefficient elimination by other means, even slow biotransformation can influence levels in the human body. Unless the biotransformation is as slow as the other loss processes, simulating those levels requires quantitative knowledge of long biotransformation half-lives. Also, unusual elimination processes can become important, such as parturition and lactation for lipophilic POPs, or menstruation and blood donation for perfluorinated alkyl acids. On the other hand, the long residence time of POPs in the human body also simplifies other aspects of the simulation of contaminant exposure. In particular, a long residence time of POPs means that they can achieve equilibrium distribution between different tissues and the use of highly resolved physiologically based pharmacokinetic models to describe the kinetics of transport and distribution between tissues is often not required. Also, many uptake and elimination processes are of negligible importance, for example, exhalation for all but the most volatile POPs, or drinking water and urination for lipophilic POPs.

This review has four major parts. Firstly, we discuss the challenge of reconstructing past exposure to POPs and how the mechanistic modeling approach is addressing this. Next, we briefly address the challenge of obtaining long bio-transformation half-lives for POPs, followed by a presentation of the various characteristics of mechanistic exposure modeling with respect to the chemicals, regions and populations that were treated with this approach. Finally, we summarize the motivations for mechanistic modeling studies.

---

## 2 The Challenge of Addressing Past Exposure

### 2.1 The Two Approaches for Reconstructing Past Exposure

For POPs, defensibly characterizing past exposure is paramount, as their high persistence implies that the body burden reflects cumulative absorption of these compounds over a long period of time. In most cases, past exposure is however unknown or undocumented, because historical concentrations of POPs in different exposure-relevant media (e.g., food items, air, and drinking water) are unavailable. One reason is that the time period of exposure may predate the ability and/or interest in making measurements of such concentrations. For example, while it has been suggested that the inhalation of

contaminated indoor air was a prominent contributor to human exposure to PCBs in the 1950s (Li et al. 2018a), the issue of indoor air PCB contamination was not recognized until the 1980s (Williams et al. 1980). As such, modelers often need to resort to reconstructing past exposure in the absence of measured data.

There are two basic approaches to reconstruct past exposure. The first approach is to empirically extrapolate from the measured exposure at present to the past based on the observed temporal trend of a surrogate parameter. The second is to reconstruct past exposure through mechanistic modeling of the relevant processes. Notably, both approaches depend on the availability of historical data. Several factors determine how far into the past such information needs to reach (Gyalpo et al. 2015a; Quinn et al. 2012), including how fast a chemical can be eliminated from the human body and whether the emission of a chemical is increasing, decreasing, or leveling off during the period of interest. The time it takes for a chemical to be eliminated from the human body affects the influence of past exposure on the current human body burden, with slower removal leading to stronger effects. In other words, the human body has a “memory” of past exposure to a chemical that is not readily eliminated. Similarly, a decreasing temporal trend in emissions (typically occurs after production or new use of a chemical is banned, that is, during a “post-ban” period) usually means that past exposure was higher than today and is thus relatively more important to current exposure than it would be during time periods of increasing or constant emission. The reconstruction of past exposure, whether by simple extrapolation or by mechanistic modeling, is therefore required to reach further back in time the longer a chemical’s elimination half-life lasts in the human body and the stronger the temporal decline in human exposure.

### 2.2 Assumptions Made When Empirically Extrapolating Past Exposure from Surrogates

Common surrogate parameters used in the empirical back-extrapolation of exposure include estimates of emissions (Ritter et al. 2011; Wong et al. 2013, 2014), use (Bu et al. 2015), or concentrations in various abiotic environmental compartments such as indoor dust (Gyalpo et al. 2015b), air (Alcock et al. 2000; Wong et al. 2013), and freshwater (Alcock et al. 2000). Historical measurements of human body concentrations in scattered years have also been used as surrogate data (Lorber 2002). Underlying this extrapolation is the assumption that the time trends in the surrogate and human exposure are proportional. This is not always the case. For example, a time course in emission cannot serve as a surrogate for exposure if there is a time lag

between emissions and exposure. Peaks in contamination (and therefore exposure) in remote regions can be seriously delayed relative to peaks in emissions that occur in source regions (Gouin and Wania 2007). The time required for POPs to accumulate in a food chain can similarly result in a lag (Czub and McLachlan 2004b). In other words, emissions, environmental contamination and human exposure are not always correlated.

Underlying the use of a surrogate in exposure reconstruction is furthering the assumption that there has been no change in the relative importance of different exposure routes during the period of past exposure. However, changes in the relative importance can occur if there have been changes in (i) chemical use and emission scenarios, (ii) exposure factors, and (iii) the environment. The following paragraphs illustrate that assuming the constancy of these three factors may not always be valid.

### 2.2.1 Constancy of Chemical Use and Emission Scenarios

The first assumption is that the *use scenario* of a POP did not change in such a way that it would result in changes in the relative importance of different exposure routes. Of particular importance in this regard are changes that could result in differences in the relative rate of emission into the indoor and outdoor environment, as they would impact the relative importance of near-field (e.g., ingestion of indoor dust) and far-field (e.g., consumption of food with bioaccumulation-mediated contamination) exposure routes. For example, it is conceivable that in some jurisdictions DDT found initial use in agriculture that led to emissions outdoors, whereas later its use was restricted to use for public health purposes, which might include applications indoors (Ritter et al. 2010). In this case, scaling current exposure backward based on DDT sales figures may not be valid. Another example is PCBs, which are predominantly applied in ways that do not result in indoor emissions despite their initial use in many indoor applications (e.g., sealants, paints), but later predominantly used in applications that would not result in indoor emissions. Therefore, inhalation of PCB-contaminated indoor air contributed substantively to the exposure of earlier generations, for example, those living in the 1950s, whereas consumption of contaminated food became the dominant contributor for more recent generations (Li et al. 2018a). Again, scaling human exposure back in time based on PCB emissions to the outdoor environment would not be valid.

It is important to note that the assumption of the constancy of an *emission scenario* may be invalid even in situations where there was no change in the use scenario of a POP. This is due to the fact that the relative importance of different types of emissions vary over the different life stages of a chemical's life cycle (Li and Wania 2018). For example, chemicals present in products can produce emissions during

manufacturing, use and disposal. The emission scenario will therefore change over time, because after the ban of a POP, manufacturing will stop first and cessation of use will follow, whereas emissions associated with the disposal of waste containing the chemical can continue much longer. This may result in pronounced changes in the relative importance of near- and far-field exposure routes, particularly if a product containing the chemical is largely used indoors. An example is polybrominated diphenyl ethers (PBDEs), which are prevalent in consumer articles that are almost exclusively used indoors. There has been a transition from the dominance of indoor exposure routes when the chemicals were still used, to that of dietary exposure when use was phased out and waste disposal activities became the dominant contamination source (Li et al., submitted). In such a situation, we may expect inconsistent temporal trends of contamination in indoor and outdoor exposure media and in the importance of different exposure routes. The importance of indoor exposure during the use phase can hardly be captured by a simple empirical back-extrapolation of the current situation.

### 2.2.2 Constancy of Exposure Factors

The second assumption is that exposure factors for individuals belonging to different cohorts are constant; for instance, a 3-year-old in the 1950s and 2000s drank the same amount of milk each day. In other words, this assumption implies that intergenerational differences in exposure are entirely due to a change in the contamination of exposure media. While this assumption is often valid, it does not apply to situations where there have been major intergenerational shifts in human behavior, for example, in terms of diet. Examples include the intergenerational dietary transition of the indigenous population living in the Arctic from traditional food consisting of locally caught fish and marine mammals, to one dominated by food imported from the south (Quinn et al. 2012). Other examples of dietary transitions with obvious exposure implications for POPs are the increasing contribution of meat to the Chinese diet (Zhao et al. 2018), the decreasing amount of fish eaten in Northern Europe (Bonhommeau et al. 2013), and the change of the origin of food from locally produced to globally sourced (Undeman et al. 2018). One could also imagine other intergenerational changes in human behavior with exposure implications that are not related to diet, such as changes in the amount of time spent indoors versus outdoors or the frequency of hand contact with electronic devices (Yang et al. 2019).

### 2.2.3 Constancy of Environmental Behaviour

A third assumption is that there has been no change in the behaviour of the chemical in the environment and the food chain over time. Examples of why the environment may

have been different in the past include global climate change or large-scale urbanization (i.e., current human generations live in a more urban environment than previous generations). The extent of bioaccumulation of POPs in the food chain may have changed because of changes in agricultural cultivation methods (e.g., current cattle grow faster and thus may experience more growth dilution than cattle grown 30 years ago) or shifting trophic relationships (e.g., fish may feed at a different trophic level). Clearly, there are many reasons why caution is advisable when extrapolating exposure back in time based on surrogate parameters.

### 2.3 Mechanistic Reconstruction of Past Exposure

An alternative to the empirical approach is to mechanistically determine the temporal trend of exposure with process-based models. The scope of such an approach depends on the starting point of the simulation, namely whether the model is fed with time-variant estimates of

environmental concentrations, emissions, or production/consumption volumes (Fig. 1).

Mechanistic bioaccumulation models, which aim to characterize the enrichment of POPs in either humans or other organisms from the abiotic environment, start with estimates or measurements of concentrations in *environmental compartments* (e.g., air, water, soil, and sediments) (Czub and McLachlan 2004b). Through quantitative characterization of toxicokinetic processes such as absorption, distribution, metabolism (i.e., irreversible biotransformation), and excretion, bioaccumulation models calculate burdens and concentrations of POPs in different tissues or the whole bodies. A prominent example is the mechanistic, dynamic bioaccumulation model ACC-HUMAN which calculates the occurrence of POPs in organisms at different trophic levels of a food web based on inputs of time-dependent concentrations in the lower atmosphere, water, and soil (Czub and McLachlan 2004b). Note that mechanistic bioaccumulation models differ from empirical human exposure models (Trudel et al. 2008, 2011), which calculate human exposure from concentrations in *exposure*

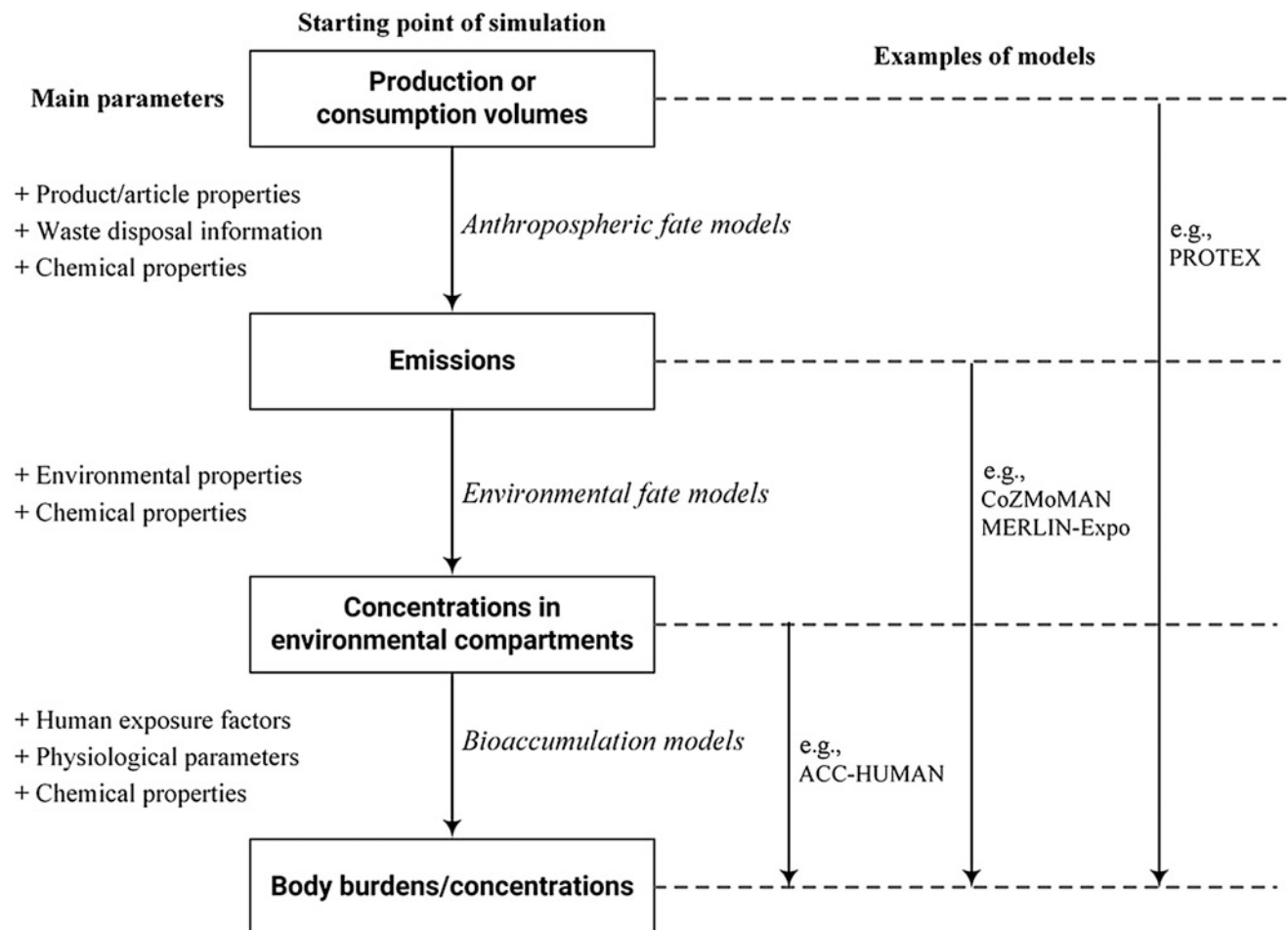


**Fig. 1** Scope and starting points of mechanistic human exposure models



*media* (food, dust, indoor air, etc.) and medium ingestion rates (food consumption rate, dust ingestion rate, inhalation rate, etc.).

Mechanistic bioaccumulation models can be coupled with environmental fate models describing chemical processes in the physical environment; in this case, the starting point of the simulation is the estimate of *emissions*. Such a model combination creates an emission-to-dose relationship. For example, the CoZMoMAN model (Breivik et al. 2010), which aims to quantify bioaccumulation-mediated human exposure to POPs, is a combination of a dynamic environmental fate and transport model, namely CoZMo-POP (Wania et al. 2006), and the ACC-HUMAN model (Czub and McLachlan 2004b). The CoZMo-POP module calculates time-dependent concentrations of POPs in up to 19 compartments of a coastal environment or the drainage basin of a large lake, which serve as inputs to the ACC-HUMAN module. Recently, the European Union has also developed a similar dynamic model “library” named MERLIN-Expo, which assembles an array of environmental fate and transport models and bioaccumulation models, aiming to create exposure-based risk assessments for prioritized chemicals (Ciffroy et al. 2016; Suciu et al. 2016). Another example is INTEGRA, which is an integrated external and internal exposure modeling platform (Sarigiannis et al. 2016).

The starting point of the simulation can even be extended to the estimates of *production or consumption volumes* if a module describing the chemical stocks and flows in the anthroposphere (human socioeconomic system) is incorporated, such as the PROduction-To-EXposure (PROTEX) model (Li et al. 2018a, b). By doing so, a production-to-exposure continuum can be established, which enables simultaneous modeling of the journey of a chemical in the anthroposphere, environment, and biosphere. A simulation starts with production volumes if a chemical is manufactured in the modeled region and otherwise, it starts with consumption volumes if a chemical is imported.

The advantages of the mechanistic approach are obvious. It does not rely on the assumption that emissions, environmental contamination and human exposure are correlated. Instead, it builds on an understanding of contaminant processes in the anthroposphere, the physical environment, in food-webs, and/or in the human body. Factors that can result in a lag between emissions and exposure or cause a shift in the main exposure pathway over time can be accounted for. Compared to observational data, it is less likely to suffer from sampling biases and measurement uncertainties. Additionally, the mechanistic approach can provide physical, chemical, or biological insights into individual processes in the system, and by extension, elucidate the relevant factors that have the largest influence on these processes.

The cost of the mechanistic approach is obvious as well. It is considerably more complex, requiring knowledge of the relevant processes, and the ability to numerically describe and parameterize them. For example, we are only gradually developing the ability for mechanistic modeling of the bioaccumulation of ionic POPs, such as PFOS (Ng and Hungerbühler 2014). Therefore, an empirical approach relying on surrogates can be preferable in those situations where it is clear that a correlation in the time trends of internal and external exposure exists.

---

### 3 The Challenge of Obtaining Reliable Biotransformation Half-Lives

Because of their slow elimination from organisms by exhalation, urination, and fecal egestion, the rate of biotransformation is often required when we are seeking to simulate the concentration of POPs in higher organisms. Only when the rate of biotransformation is slower than the rate of elimination by fecal egestion and shedding of skin (desquamation), which results in an elimination half-life on the order of 15–20 years (Rohde et al. 1999; Geusau et al. 2001), is it not necessary to know the biotransformation half-life accurately. Biotransformation half-lives on the order of 1–15 years are challenging to derive empirically. In particular, they cannot easily be derived from longitudinal studies (i.e., by measuring the decline in the concentration in an individual over time), because such studies would need to last at least one half-life, that is, multiple years, which is rarely feasible. Furthermore, such a decline will be confounded by ongoing exposure during the elimination period (Bartell 2012; Gyalpo et al. 2015a). Opportunistic longitudinal investigations in severely exposed individuals or populations (e.g., because of deliberate poisoning or occupational/accidental exposure) have the advantage in the sense that ongoing exposure may be negligible compared to the initial exposure (Chen et al. 1982; Brown Jr et al. 1989; Wolff et al. 1992; Masuda 2001; Thuresson et al. 2005). However, biotransformation kinetics may be concentration dependent, that is, it may occur at a different rate in severely contaminated individuals than in those with average concentration levels. A further complication arises from other factors that may confound elimination rates derived from rates of decline in longitudinal studies. Notably, the amount of lipid in a person (quantifiable through the body mass index or BMI) and the rate and direction of change in that lipid amount can have profound implications for the observed rate of elimination of POPs from the human body (Wolff et al. 2007).

There have been different responses to the challenge of performing mechanistic exposure modeling for POPs with

long elimination half-lives. Some studies simply choose to focus their modeling on POPs that are not biotransformed to any significant extent. In this case, modeling can be performed assuming no biotransformation. This may explain the prevalence of studies focused on polychlorinated biphenyl congener 153 (PCB-153) (see Sect. 4.1), which is hardly biotransformed by humans or any other organism. Other studies make the determination of the biotransformation half-life the very objective of the modeling effort. In particular, cross-sectional biomonitoring data that quantifies the rate of concentration decline in (a subsection of) a human population repeatedly sampled over time can be used to derive the intrinsic rate of elimination (and biotransformation) applicable to that population, as long as the exposure during the time of biomonitoring is reconstructed (Ritter et al. 2011; Wong et al. 2013).

However, despite the stated challenges, there have been studies that report half-lives of elimination in humans that can be used in exposure simulations. These are either determined directly (e.g., Bühler et al. (1988)), extrapolated from elimination observed in other organisms (e.g., Geyer et al. (2004)), or estimated using quantitative structure–activity relationships (QSARs, e.g., Papa et al. (2018)).

## 4 Characteristics of Mechanistic Human Exposure Modeling

### 4.1 The Pollutants that Have Been the Subject of Mechanistic Human Exposure Modeling

We can distinguish between simulations of human exposure to real contaminants and simulations that obtain model results for a large number of hypothetical property combinations, for example, the combination of equilibrium partition coefficients ( $K_{OW}$ ,  $K_{OA}$ , and/or  $K_{AW}$ ). The motivation between those approaches is largely complementary. The simulation of real contaminants is often aimed at understanding various aspects of the exposure to those specific contaminants, such as the dominant exposure route, the observed time trends, or variability in exposure. If multiple real chemicals (possibly belonging to a group of related compounds, such as different PCB congeners) are simulated, these studies can also shed some light on the differences in exposure caused by chemical properties. Those differences are in turn the primary focus of mechanistic human exposure modeling involving hypothetical chemical property combinations. An intriguing feature of such approaches is that they allow for the graphical display of model simulation results as a function of chemical properties. A commonly adopted approach is to rely on two key equilibrium partition coefficients to define a “chemical partitioning space” (Czub et al. 2008; Undeman et al. 2010; Li et al. 2019), although a

variety of chemical attributes can be used, including molecular size and transformation rates (McLachlan et al. 2010). A graphical representation facilitates the comparison of the exposure potential of different substances as well as the identification of important property thresholds, such as those that separate chemicals with different dominant exposure routes. If sufficiently comprehensive, such graphs can make at least some simulations for real contaminants obsolete, as a model result can often be obtained by locating a substance within the hypothetical property space and reading the simulation results for the hypothetical chemical with the same or similar properties as the real contaminant.

Table 1 summarizes the real contaminants that have been the subject of mechanistic modeling of human exposure. This list includes the polychlorinated biphenyls (PCBs), polychlorinated dibenzo-*p*-dioxins and -furans (PCDD/Fs), short-chain chlorinated paraffins (SCCPs), and polybrominated diphenyl ethers (PBDEs). This table indicates that PCB congeners feature prominently in such studies. This is easily explained by the fact that much of the information that is required for conducting such modeling is readily available for PCBs. This includes (i) emission information that is global in scope, historical in perspective, and resolved at the congener level, and (ii) congener-specific data on partitioning and degradation properties. It also extends to (iii) the availability of a large body of measured concentration data, including data from the past, that can serve in model evaluation, and (iv) a sufficient mechanistic understanding of the processes that lead to exposure to a substance group. The lack of such an understanding may explain the scarcity of mechanistic human exposure modeling for substances with properties that deviate considerably from those of classical POPs, such as the perfluorinated acids.

Studies in which past exposure is not reconstructed mechanistically, but estimated through extrapolation based on a surrogate parameter, have treated a more diverse set of substances, including PCDD/Fs, PCBs, PBDEs, selected organochlorine pesticides (OCPs) with a focus on DDT and its metabolite DDE, as well as perfluorooctane sulfonate (PFOS) (Table 2).

Mechanistic human exposure simulations using a large number of hypothetical property combinations are compiled in Table 3. Virtually all of these studies relied on a two-dimensional chemical partitioning space using either  $\log K_{OW}$  and  $\log K_{OA}$  or  $\log K_{OA}$  and  $\log K_{AW}$ , and accordingly provide graphical representations of simulation results. Model results of interest can be those indicating problematic chemical attributes, such as the high potential for bioaccumulation. These studies often take a comparative approach, such as the comparison of different food webs (Kelly et al. 2007) or human populations with different diets (Undeman et al. 2010; Zhao et al. 2015). Binnington et al. (2014) compared the same hypothetical person eating different

**Table 1** Real chemicals involved in mechanistic human exposure modeling studies

Compound group	Specific compound	Region and context	References
PCBs	28, 52, 101, 118, 138, 153, 180	Sweden	Breivik et al. (2010)
	118, 138, 153, 180	Norway	Nøst et al. (2013, 2015)
	118, 138, 153, 180	Canadian Arctic	Binnington et al. (2016b)
	138, 153	Canadian Arctic	Binnington et al. (2016a)
	118, 138, 153, 180	USA	Wood et al. (2016a)
	28, 153	Sweden	Li et al. (2018a)
	153	USA	Wood et al. (2016b), Dzierlenga et al. (2019)
	153	Sweden	Quinn et al. (2012), Quinn and Wania (2012)
	153	Various global populations	McLachlan et al. (2018), Undeman et al. (2018)
	153	China	Zhao et al. (2018)
153	Norway	Nøst et al. (2019)	
PCBs, PCDD/Fs	77, 126, 167, 169, 180 2,3,7,8-TCDD 1,2,3,7,8-PCDD 1,2,3,4,7,8-HCDD	Venice lagoon	Giubilato et al. (2016)
Phthalates	DBP, DEHP	The Netherlands	Franco et al. (2007)
SCCPs	37 formula groups	Nordic region	Krogseth et al. (2013)
Bisphenol A		Norway	Arp et al. (2017)
		European Union	Sarigiannis et al. (2016)
PBDEs	47, 99, 153, 209	Ontario, Canada	Li et al. (submitted)

**Table 2** Real chemicals involved in studies using a human toxicokinetic model with empirically estimated exposure data

Compound group	Specific compound	Region and context	References
PCDD/Fs	TEQ dose based on fractional contribution of 17 PCDD/F congeners	USA	Lorber (2002)
PCBs	101	United Kingdom	Alcock et al. (2000)
	52, 153	United Kingdom	Ritter et al. (2011)
	74, 99, 118, 138, 146, 153, 156, 170, 180, 187	Australia	Bu et al. (2015)
PBDEs	47, 99, 100, 153	North America	Wong et al. (2013)
	47, 99, 100, 153	Australia	Gyalpo et al. (2015b)
OCPs	<i>p,p'</i> -DDE, <i>p,p'</i> -DDT	Sweden	Ritter et al. (2009)
	HCB, $\beta$ -HCH, <i>p,p'</i> -DDE, <i>p,p'</i> -DDT, trans-nonachlor	Australia	Bu et al. (2015)
	DDT, DDE	South Africa	Gyalpo et al. (2012)
PFOS	PFOS	USA	Egeghy and Lorber (2011)
	PFOS	USA	Wong et al. (2014)
	PFOS, PFOA	USA, Australia	Gomis et al. (2017)

diets, based on varying compliance with food consumption advisories. Another use of simulations involving the chemical partitioning space is the identification of dominant exposure routes. For example, Zhang et al. (2014) identified the relative importance of different near-field routes (inhalation of indoor air, non-dietary ingestion, dermal permeation) for human exposure; Undeman et al. (2010) compared the relative importance of different far-field routes (drinking water, inhalation of outdoor air, and consumption of different types of food) to human exposure. Li et al. (2019) expanded these analyses to “aggregate” human exposure by coherently integrating near- and far-field routes. Many of these studies include scenarios in which the hypothetical chemicals are degraded at various rates, either in the physical environment and/or the organisms within the considered food webs.

## 4.2 The Regions and Populations that Have Been the Subject of Mechanistic Human Exposure Simulations

Table 1 also provides information on the geographical scope of the mechanistic modeling of human exposure to POPs. Most of the studies have a national scale and the countries

that are represented are in North America (USA, Canada) and Northern Europe (Sweden, Norway). The study by Zhao et al. (2018) on China is a notable exception. To some extent this reflects the availability of human biomonitoring data for the populations in those countries, for example as a result of national biomonitoring programs such as that available from national biomonitoring programs like the National Health and Nutrition Examination Survey (NHANES) in the USA, the Canadian Health Measures Survey (CHMS) and the Northern Contaminants Program (NCP) in Canada or as a result of specific studies on selected subpopulations (Nøst et al. 2013, 2019). Such data is often required to evaluate the model results.

If environmental fate is part of the exposure calculation, the models tend to be regional or national in scale, because POPs have by definition a fairly large spatial scale and cannot be adequately described with local scale models. For example, Breivik et al. (2010), Nøst et al. (2013), and Wood et al. (2016a) relied on the CoZMo-POP model parameterized for Sweden, Norway and the USA, respectively. A global-scale environmental fate model simulation becomes necessary when human exposure is not caused/dominated by regional emissions, but by transport from elsewhere [e.g., via long-range transport in environmental media (Binnington et al. 2016a, b) or via

**Table 3** Mechanistic human exposure modeling studies involving hypothetical chemicals

Study reference	Context	Chemical parameters being varied
Czub and McLachlan (2004a)	Identifying contaminants with high bioaccumulation potential in humans through diet	$K_{OW}$ , $K_{OA}$
Kelly et al. (2007)	Identifying contaminants with high biomagnification in different food webs, including humans	$K_{OW}$ , $K_{OA}$
Czub et al. (2008)	Identifying contaminants with high potential to reach Arctic and bioaccumulate in Arctic human populations	$K_{OA}$ , $K_{AW}$
Undeman et al. (2010)	Comparing different global human population in their exposure susceptibility to bioaccumulating contaminants	$K_{OW}$ , $K_{OA}$ , two categories of degradability
McLachlan et al. (2010)	Comparing different chemicals in terms of bioaccumulation	$K_{OA}$ , $K_{AW}$ , biotransformation rates in fish and mammals
Binnington et al. (2014)	Effectiveness of food consumption advisories	$K_{OW}$ , $K_{OA}$ , human biodegradation half-lives
Zhang et al. (2014)	Relative importance of near-field exposure routes, indoor intake fraction, unit emission-based human concentrations	$K_{OW}$ , $K_{OA}$ , molecular mass, degradation half-life in indoor compartments, whole body human biotransformation half-life
Zhao et al. (2015)	Differences in importance of different dietary exposure routes between Chinese and Western populations	$K_{OW}$ , $K_{OA}$
Li et al. (2019)	Importance of different exposure routes of chemicals emitted to indoor air	$K_{OA}$ , $K_{AW}$ , degradation half-lives in air and in outdoor surface media, biotransformation half-lives in higher organisms

international trade in food (Ng and von Goetz 2016), or if the scope of the exposure estimation is global in scale (McLachlan et al. 2018; Undeman et al. 2018).

### 4.3 Individual Modeling Versus Population Modeling

The simulation can be performed for either an individual or a group of people. Oftentimes, models characterize an “average” or a generic person that possesses typical anthropometric and physiological characteristics (e.g., the body weight, lipid content, skin surface, etc.), average exposure factors (e.g., food consumption and dust ingestion rates), and/or standardized living environments representative of the entire population in a region. That is, while the models ostensibly simulate a single individual, the modeled exposure essentially aims to represent the entire population. Currently, population-specific models have been available for Swedes (Breivik et al. 2010; Li et al. 2018a), Norwegians (Nøst et al. 2013), Americans (Wood et al. 2016a), Chinese (Zhao et al. 2018), Arctic indigenous people (Binnington et al. 2016b), and Canadians (Li et al., submitted). Undeman et al. (2018) and McLachlan et al. (2018) also compared various populations around the world based on their diverse diets and living environments.

In the meantime, the models can also be parameterized using individual-specific inputs, and repeatedly run to generate exposure estimates at an individual level. For example, Nøst et al. (2013) simulated the concentrations of PCB-153 in the bodies of 53 men from Northern Norway based on individual-specific information on the year of birth and fish consumption rate. Following that, Nøst et al. (2015) further simulated the concentrations of four PCB congeners in more than 500 pregnant and postmenopausal women based on individual-specific information on the year of birth, duration of breastfeeding, and dietary consumption of different food items. Wood et al. (2016a) quantified the lifetime exposure to four PCB congeners (118, 138, 153, and 180) of 6128 individuals participating in the NHANES biomonitoring program, using individual-specific information on diet, year of birth, age at sampling, body mass index, sex, and reproductive behavior. The performance of individual-specific modeling can usually be evaluated using (i) the coefficient of determination ( $R^2$ ), that is, the extent to which the interindividual variability is explained by the model, and (ii) the difference between modeled and observed body concentrations, such as the number of individuals falling within one order of magnitude in difference, or the root mean square error (RMSE). While a number of models are quite successful in producing estimates that are close to measurements in magnitude, their capacity in explaining the interindividual variability is often less satisfactory (Binnington et al. 2016b; Nøst et al. 2015;

Wood et al. 2016a). In Wood et al. (2016a), 62% of the modeled PCB-153 concentrations are within a factor of 3 of corresponding measured ones while 89% fall within one order of magnitude of measurements; however, the  $R^2$  of this model is only 0.11. This implies that the currently available model inputs generally support reproducing human exposure; however, some key parameters may still be missing or need to be refined to discriminate the exposure between two specific individuals.

Nevertheless, an advantage of these models is that they can provide mechanistic insights into the possible causes of interindividual variability in the human body burden. For instance, Wood et al. (2016a) indicate that the dietary lipid intake is the main contributor, followed by the sampling age to the interindividual variability in their modeled human concentrations, whereas the influence of the consumption of fish and dairy products is negligible. This result is partially supported by findings in a parallel statistical analysis, which indicates that the age at sampling is on average responsible for 30% of the variance in the observed body concentrations of NHANES participants (Wood et al. 2016a).

---

## 5 Motivations for Mechanistically Modeling Human Exposure to POPs

Non-steady-state models of the internal exposure of humans to POPs and other environmental contaminants have been used for a diverse range of objectives.

### 5.1 Risk Assessment

The primary objective in the development of integrated mechanistic models of human exposure is often a comprehensive risk assessment. The CoZMoMAN, INTEGRA, and MERLIN-Expo models were all developed to allow a differentiated assessment of various routes of human exposure while simultaneously enabling the comparison of combined exposure with metrics of effect based on internal exposure (Breivik et al. 2010; Ciffroy et al. 2016; Suci et al. 2016; Sarigiannis et al. 2016). These models allow a seamless evaluation of the link between contaminant emissions and effect, whereby exposure information that is more proximate to the human (e.g., concentrations in exposure media) can be readily incorporated into the assessment thanks to the mechanistic nature of the models. Techniques for the prediction of emissions at all stages of a chemical's lifecycle from production through usage to disposal are further expanding the domain of exposure assessment, more closely linking it to chemical lifecycle assessment and facilitating contaminant assessment in the context of a circular economy (Li and Wania 2016; Breivik et al. 2012).

Another approach to bridging human exposure and health outcomes is to combine a model of external exposure with reverse dosimetry. The internal exposure corresponding to a health outcome is translated into an equivalent external exposure using a pharmacokinetic model, and this is compared with the predicted external exposure (Moreau et al. 2017; Wetmore et al. 2011).

Integrated mechanistic models offer other benefits for risk assessment. For instance, they facilitate a comprehensive evaluation of the uncertainty in the exposure assessment. An integrated uncertainty assessment module is part of the MERLIN-Expo tool (Ciffroy et al. 2016). As they incorporate chemical accumulation through food webs, these models can also be tailored for combined human and environmental risk assessment (Ciffroy et al. 2016).

## 5.2 Confirming a Comprehensive, Quantitative Understanding of Human Exposure to a Chemical or Group of Chemicals

Mechanistic human exposure models are used to assess the completeness of our understanding of the processes and variables governing human exposure. They play an important role in identifying weaknesses in this understanding, thereby indicating directions for new research.

To date, many of the applications of this kind have focused on PCBs. PCBs were used to evaluate the first non-steady-state bioaccumulation model that included both the environment and humans. Relatively good agreement between modeled and observed concentrations in various organisms in southern Sweden was found, providing confidence in the understanding of human exposure to this substance group (Czub and McLachlan 2004b). Later work expanded the scope of the model to include environmental fate, and model evaluation with PCBs identified time trends in historical emissions as a critical knowledge gap (Breivik et al. 2010). That gap was later addressed in studies showing that measured longitudinal and cross-sectional time trends in human exposure to PCBs agreed relatively well with modeled time trends (Li et al. 2018a; Nøst et al. 2013, 2019). More recently, a global scale evaluation was conducted for PCB-153, showing good agreement between modeled and measured concentration in humans in many regions but pointing out assumptions about food sourcing and insufficient knowledge of exposure pathways in Africa as weaknesses (McLachlan et al. 2018).

Other chemicals have also been assessed. Polychlorinated dibenzo-*p*-dioxins and dibenzofurans as well as PCBs were modeled in the Venice Lagoon, whereby historical concentration scenarios in water were reconstructed from sediment cores and used to model concentrations in the aquatic food

web and the local population. Appreciable agreement was found between modeled and measured concentrations (Giubilato et al. 2016). Franco et al. (2007) studied human exposure to phthalates, found that the modeled concentrations in humans were far less than the observed concentrations, and attributed this to the lack of consumer exposure pathways in the models used. Short-chained chlorinated paraffins (SCCPs) were the subject of a study involving a comparison of concentrations in many media, and a multitude of knowledge deficits were identified including the composition of the SCCP mixture emitted, biotransformation rate constants, and inconsistency in the available measurements (Krogseth et al. 2013).

## 5.3 Identifying Relevant Exposure Routes

Since mechanistic human exposure models can link multi-route exposure to multimedia contamination resulting from multi-source emissions, an application of mechanistic human exposure models is the evaluation of the relative importance of different exposure routes. For instance, Arp et al. (2017) compared measured bisphenol A concentrations in humans and the environment with modeled concentrations and concluded that far-field emissions from the waste sector are likely insignificant for human exposure.

Considerable work has been done evaluating the relative importance of near- and/or far-field exposure routes. For example, a simulation using the PROTEX model (Li et al. 2018a) shows that near-field exposure routes made notable contributions to overall human exposure to some PCB congeners, challenging the widely held belief that the general population takes up PCBs predominantly with food contaminated through bioaccumulation in agricultural and aquatic food chains. This belief has been widely held because it is consistent with the detection of PCBs in food since the 1970s when instrumental analysis of PCBs in biological samples first became possible. The mechanistic modeling approach revealed that inhalation of PCB-contaminated indoor air contributed substantively to the exposure of earlier generations, such as that those living in the 1950s. Discounting the importance of indoor inhalation exposure was largely due to the absence of measurements in indoor air back in the 1950s. When indoor contamination of PCBs was recognized for the first time in the 1980s, levels indoors were already so much lower that the near-field environment had become a minor contributor to human exposure.

Even when the model performance is unsatisfactory, the mechanistic approach can aid in the identification of the weakest part in a model that hinders us from depicting the historical exposure. For instance, while the mechanistic

model in Binnington et al. (2016b) succeeded in reproducing the geometric mean of the exposure of Canadian indigenous populations, it failed to explain the considerable variability in the exposure at the individual level. Such a failure was ascribed mainly to the variance in reported intake rates of traditional food rather than the interindividual variance in the individual demographic input parameters as commonly assumed. This finding underscores the importance of accurate food consumption reporting in modeling human exposure to POPs.

#### 5.4 Designing and Evaluating the Effectiveness of Management Strategies

Mechanistic human exposure models can be used to evaluate strategies to manage or ameliorate human exposure to chemicals. One management strategy aimed at reducing exposure of infants to PCBs during critical stages of development is fish advisories. These are recommendations issued by responsible authorities that specify upper limits for consumption of certain fish for women of childbearing age. Human exposure simulations were used to demonstrate that this strategy has little influence on the exposure of the fetus or the newborn child to PCBs (Binnington et al. 2014).

Management strategy development can also be supported by mechanistic human exposure models. The mechanistic approach opens opportunities to conduct mechanistically sound “what-if” scenario calculations with policy relevance. For instance, model simulations played an integral role in a cost–benefit analysis of having indigenous Arctic Canadian women of childbearing age substitute traditional foods in order to increase nutrient intake (Binnington et al. 2016a). In another study, mechanistic human exposure models were employed to explore what factors could influence the future development of human exposure to PCBs in China, leading to a recommendation that environmental managers in China should go beyond setting national emission goals in order to reduce future exposure (Zhao et al. 2018).

#### 5.5 Supporting Biomonitoring/Epidemiology

The interpretation of biomonitoring data is an important application of mechanistic human exposure models. Models can provide physical, chemical, and biological insights into individual processes, and by extension, elucidate the relevant factors that have the largest influence on these processes. Internal exposure to a given contaminant is dependent on a myriad of factors that are age- and/or time-dependent. A sound evaluation of biomonitoring data, whether cross-sectional or longitudinal, is thus often dependent on unraveling the influence of these factors. Mechanistic human

exposure models have demonstrated a delay between peak emissions of PCBs and peak exposure of infants to PCBs and shown how this is influenced by the mother’s reproductive history (Quinn et al. 2012). Furthermore, they have been used to explore the differences in age dependence between cross-sectional and longitudinal studies, demonstrating that the time trend in contaminant emissions during the two decades prior to collection of the samples is a key factor determining the age-dependency of internal exposure to persistent chemicals (Quinn and Wania 2012). Even more complex interactions can be addressed. Recently, a model was used to unravel the different influences of age, exposure route, and biotransformation on the time trend of polybrominated diphenyl ether (PBDE) concentrations in humans, showing how the time trend of external exposure changed as the dominant exposure pathway shifted from near-field to far-field as a result of faster contaminant dissipation in the indoor environment, and how the impact of this transition on internal exposure was further modulated by differences in biotransformation rates between PBDE congeners (Li et al., submitted). For this reason, mechanistic models are valuable for recognizing and eliminating potential confounding factors frequently occurring in observation-based studies. A successful example is the use of the CoZMoMAN model to disentangle confounding effects between birth cohort, sampling period (i.e., cross-sections), and the age at sampling in environmental epidemiological studies, and to use this knowledge to inform future study designs (Nøst et al. 2013).

The influence of specific variables on human biomonitoring data can also be studied. Body mass index (BMI) is a variable influencing pharmacokinetics of lipophilic contaminants in humans. Mechanistic human exposure models have been used to show that either positive or negative associations between BMI and internal exposure to PCBs can be expected, depending on whether emissions have been historically increasing or decreasing (Wood et al. 2016b). In direct support of an epidemiological study, mechanistic human exposure models demonstrated that an observed correlation between type 2 diabetes and serum levels of PCB-153 was not significantly confounded by BMI (Dzierlenga et al. 2019).

#### 5.6 Identifying Chemicals Likely to Give High Exposure

Mechanistic human exposure models have been used to explore the chemical property space that leads to high human exposure. Much of this work has been done with simulations of hypothetical chemicals. The first application of this kind was the use of the ACC-HUMAN model to demonstrate that bioaccumulation of persistent chemicals

leading to human exposure is governed by both  $K_{OW}$  and  $K_{OA}$ , the former determining bioaccumulation in water-breathing organisms and the latter determining bioaccumulation in air-breathing organisms (e.g., livestock) (Czub and McLachlan 2004a). Further empirical evidence was later provided to support this conclusion (Kelly et al. 2007). In a second step, the scope of the model was expanded to include chemical fate and long-range transport, and the chemical partitioning space resulting in high exposure of indigenous Arctic people to persistent chemicals emitted in the mid-latitudes was determined (Czub et al. 2008). Chemicals subject to metabolism were later added to the chemical property space, whereby the influence of biotransformation in fish and in mammals was contrasted (McLachlan et al. 2010). More recently, the chemical properties leading to high exposure via the indoor environment have been studied (Zhang et al. 2014). A model including both the indoor environment and the outdoor environment was used to explore the influence of chemical properties on the relative importance of near-field versus far-field exposure and of individual exposure routes (Li et al. 2019).

In addition to these conceptual studies, mechanistic human exposure models can be used for chemical prioritization (Arnot and Mackay 2008; Arnot et al. 2012). Notably, data on chemical release, biotransformation and toxicity collected under the REACH regulation in work sponsored by the European Food Safety Authority (EFSA) has been used with model-based simulations of human exposure to identify emerging chemical risks in the food chain (Oltmanns et al. 2018).

## 5.7 Identifying Exposed Populations

Human exposure simulations of hypothetical chemicals have also been used to identify highly exposed populations. A regional fate model linked to a human bioaccumulation model was parameterized for different climatic regions and humans living on a diet of locally sourced food, and the internal exposure of humans living in these environments was compared for hypothetical chemicals. The simulations showed that differences in exposure were considerable and that these were largely determined by differences in the structure of the food web that the humans were feeding on (Undeman et al. 2010).

Models can also be used to identify populations that are highly exposed to specific chemicals. For instance, a global scale fate model was linked with a human bioaccumulation model and run with a historical emissions scenario to identify the population in the world that is most exposed to PCB-153 (Undeman et al. 2018).

## 5.8 Understanding and Anticipating the Impact of Change (Dietary Transition, Climate Change)

Mechanistic human exposure models are valuable for understanding and anticipating how changing conditions will impact human exposure in the future. One example is dietary transitions. Indigenous Arctic Canadians are undergoing a transition from a traditional diet based on marine mammals to a diet similar to that in southern Canada. Mechanistic human exposure models were used to show how this dietary transition would influence human exposure while accounting for other important variables such as age and changing emissions (Quinn et al. 2012; Binnington et al. 2016b).

Mechanistic human exposure models also have the potential for studying the influence of climate change on human exposure to environmental contaminants (Armitage et al. 2011).

## References

- Alcock RE, Sweetman AJ, Juan C-Y, Jones KC (2000) A generic model of human lifetime exposure to persistent organic contaminants: development and application to PCB-101. *Environ Pollut* 110(2):253–265
- Armitage JM, Quinn CL, Wania F (2011) Global climate change and contaminants—an overview of opportunities and priorities for modelling the potential implications for long-term human exposure to organic compounds in the Arctic. *J Environ Monit* 13(6):1532–1546
- Arnot JA, Brown TN, Wania F, Breivik K, McLachlan MS (2012) Prioritizing chemicals and data requirements for screening-level exposure and risk assessment. *Environ Health Perspect* 120(11):1565–1570
- Arnot JA, Mackay D (2008) Policies for chemical hazard and risk priority setting: can persistence, bioaccumulation, toxicity, and quantity information be combined? *Environ Sci Technol* 42(13):4648–4654
- Arp HPH, Morin NAO, Hale SE, Okkenhaug G, Breivik K, Sparrevik M (2017) The mass flow and proposed management of bisphenol A in selected Norwegian waste streams. *Waste Manag* 60:775–785
- Bühler F, Schmid P, Schlatter C (1988) Kinetics of PCB elimination in man. *Chemosphere* 17(9):1717–1726
- Bartell SM (2012) Bias in half-life estimates using log concentration regression in the presence of background exposures, and potential solutions. *J Expo Sci Environ Epidemiol* 22(3):299
- Binnington MJ, Curren MS, Chan HM, Wania F (2016a) Balancing the benefits and costs of traditional food substitution by indigenous Arctic women of childbearing age: Impacts on persistent organic pollutant, mercury, and nutrient intakes. *Environ Int* 94:554–566
- Binnington MJ, Curren MS, Quinn CL, Armitage JM, Arnot JA, Chan HM, Wania F (2016b) Mechanistic polychlorinated biphenyl exposure modeling of mothers in the Canadian Arctic: the challenge of reliably establishing dietary composition. *Environ Int* 92:256–268



- Binnington MJ, Quinn CL, McLachlan MS, Wania F (2014) Evaluating the effectiveness of fish consumption advisories: modeling prenatal, postnatal, and childhood exposures to persistent organic pollutants. *Environ Health Perspect* 122(2):178–186
- Bonhommeau S, Dubroca L, Le Pape O, Barde J, Kaplan DM, Chassot E, Nieblas A-E (2013) Eating up the world's food web and the human trophic level. *Proc Natl Acad Sci USA* 110(51):20617–20620
- Breivik K, Arnot JA, Brown TN, McLachlan MS, Wania F (2012) Screening organic chemicals in commerce for emissions in the context of environmental and human exposure. *J Environ Monit* 14(8):2028–2037
- Breivik K, Czub G, McLachlan MS, Wania F (2010) Towards an understanding of the link between environmental emissions and human body burdens of PCBs using CoZMoMAN. *Environ Int* 36(1):85–91
- Brown J Jr, Lawton R, Ross M, Feingold J, Wagner R, Hamilton S (1989) Persistence of PCB congeners in capacitor workers and Yusho patients. *Chemosphere* 19(1–6):829–834
- Bu Q, MacLeod M, Wong F, Toms L-ML, Mueller JF, Yu G (2015) Historical intake and elimination of polychlorinated biphenyls and organochlorine pesticides by the Australian population reconstructed from biomonitoring data. *Environ Int* 74:82–88
- Chen P, Luo M, Wong C, Chen C (1982) Comparative rates of elimination of some individual polychlorinated biphenyls from the blood of PCB-poisoned patients in Taiwan. *Food Chem Toxicol* 20(4):417–425
- Ciffroy P, Alfonso B, Altenpohl A, Banjac Z, Bierkens J, Brochot C, Critto A, De Wilde T, Fait G, Fierens T (2016) Modelling the exposure to chemicals for risk assessment: a comprehensive library of multimedia and PBPK models for integration, prediction, uncertainty and sensitivity analysis—the MERLIN-Expo tool. *Sci Total Environ* 568:770–784
- Czub G, McLachlan MS (2004a) Bioaccumulation potential of persistent organic chemicals in humans. *Environ Sci Technol* 38(8):2406–2412
- Czub G, McLachlan MS (2004b) A food chain model to predict the levels of lipophilic organic contaminants in humans. *Environ Toxicol Chem* 23(10):2356–2366
- Czub G, Wania F, McLachlan MS (2008) Combining long-range transport and bioaccumulation considerations to identify potential arctic contaminants. *Environ Sci Technol* 42(10):3704–3709
- Dzierlenga MW, Yoon M, Wania F, Ward PL, Armitage JM, Wood SA, Clewell HJ, Longnecker MP (2019) Quantitative bias analysis of the association of type 2 diabetes mellitus with 2,2',4,4',5,5'-hexachlorobiphenyl (PCB-153). *Environ Int* 125:291–299
- Egeghy PP, Lorber M (2011) An assessment of the exposure of Americans to perfluorooctane sulfonate: a comparison of estimated intake with values inferred from NHANES data. *J Expo Sci Environ Epidemiol* 21(2):150
- Franco A, Prevedouros K, Alli R, Cousins IT (2007) Comparison and analysis of different approaches for estimating the human exposure to phthalate esters. *Environ Int* 33(3):283–291
- Geusau A, Tschachler E, Meixner M, Pöpke O, Stingl G, McLachlan M (2001) Cutaneous elimination of 2, 3, 7, 8-tetrachlorodibenzo-p-dioxin. *Br J Dermatol* 145(6):938–943
- Geyer HJ, Schramm K-W, Darnerud PO, Aune M, Feicht EA, Fried KW, Henkelmann B, Lenoir D, Schmid P, McDonald TA (2004) Terminal elimination half-lives of the brominated flame retardants TBBPA, HBCD, and lower brominated PBDEs in humans. *Organohalogen Compd* 66(2004):3820–3825
- Giubilato E, Radomyski A, Critto A, Ciffroy P, Brochot C, Pizzol L, Marcomini A (2016) Modelling ecological and human exposure to POPs in Venice lagoon. Part I—application of MERLIN-Expo tool for integrated exposure assessment. *Sci Total Environ* 565:961–976
- Gomis MI, Vestergren R, MacLeod M, Mueller JF, Cousins IT (2017) Historical human exposure to perfluoroalkyl acids in the United States and Australia reconstructed from biomonitoring data using population-based pharmacokinetic modelling. *Environ Int* 108:92–102
- Gouin T, Wania F (2007) Time trends of Arctic contamination in relation to emission history and chemical persistence and partitioning properties. *Environ Sci Technol* 41(17):5986–5992
- Gyalpo T, Fritsche L, Bouwman H, Bornman R, Scheringer M, Hungerbühler K (2012) Estimation of human body concentrations of DDT from indoor residual spraying for malaria control. *Environ Pollut* 169:235–241
- Gyalpo T, Scheringer M, Hungerbühler K (2015a) Recommendations for evaluating temporal trends of persistent organic pollutants in breast milk. *Environ Health Perspect* 124(7):881–885
- Gyalpo T, Toms L-M, Mueller JF, Harden FA, Scheringer M, Hungerbühler K (2015b) Insights into PBDE uptake, body burden, and elimination gained from Australian age-concentration trends observed shortly after peak exposure. *Environ Health Perspect* 123(10):978–984
- Kelly BC, Ikononou MG, Blair JD, Morin AE, Gobas FA (2007) Food web-specific biomagnification of persistent organic pollutants. *Science* 317(5835):236–239
- Krogseth IS, Breivik K, Arnot JA, Wania F, Borgen AR, Schlabach M (2013) Evaluating the environmental fate of short-chain chlorinated paraffins (SCCPs) in the Nordic environment using a dynamic multimedia model. *Environ Sci Processes Impact* 15(12):2240–2251
- Li L, Arnot JA, Wania F (2018a) Revisiting the contributions of far- and near-field routes to aggregate human exposure to polychlorinated biphenyls (PCBs). *Environ Sci Technol* 52(12):6974–6984
- Li L, Arnot JA, Wania F (2018b) Towards a systematic understanding of the dynamic fate of polychlorinated biphenyls in indoor, urban and rural environments. *Environ Int* 117:57–68
- Li L, Arnot JA, Wania F (2019) How are humans exposed to organic chemicals released to indoor air? *Environ Sci Technol* (In revision)
- Li L, Hoang C, Arnot JA, Wania F (Submitted) Clarifying temporal trend variability in human biomonitoring of polybrominated diphenyl ethers through mechanistic modeling
- Li L, Wania F (2016) Tracking chemicals in products around the world: introduction of a dynamic substance flow analysis model and application to PCBs. *Environ Int* 94:674–686
- Li L, Wania F (2018) Occurrence of single- and double-peaked emission profiles of synthetic chemicals. *Environ Sci Technol* 52(8):4684–4693
- Lorber M (2002) A pharmacokinetic model for estimating exposure of Americans to dioxin-like compounds in the past, present, and future. *Sci Total Environ* 288(1):81–95
- Masuda Y (2001) Fate of PCDF/PCB congeners and change of clinical symptoms in patients with Yusho PCB poisoning for 30 years. *Chemosphere* 43(4–7):925–930
- McLachlan MS, Czub G, MacLeod M, Arnot JA (2010) Bioaccumulation of organic contaminants in humans: a multimedia perspective and the importance of biotransformation. *Environ Sci Technol* 45(1):197–202
- McLachlan MS, Undeman E, Zhao F, MacLeod M (2018) Predicting global scale exposure of humans to PCB 153 from historical emissions. *Environ Sci Process Impacts* 20(5):747–756
- Moreau M, Leonard J, Phillips KA, Campbell J, Pendse SN, Nicolas C, Phillips M, Yoon M, Tan Y-M, Smith S, Pudukodu H, Isaacs K, Clewell H (2017) Using exposure prediction tools to link exposure and dosimetry for risk-based decisions: a case study with phthalates. *Chemosphere* 184:1194–1201

- Nøst TH, Berg V, Hanssen L, Rylander C, Gaudreau E, Dumas P, Breivik K, Sandanger TM (2019) Time trends of persistent organic pollutants in 30 year olds sampled in 1986, 1994, 2001 and 2007 in Northern Norway: measurements, mechanistic modeling and a comparison of study designs. *Environ Res* 172:684–692
- Nøst TH, Breivik K, Fuskevåg O-M, Nieboer E, Odland JØ, Sandanger TM (2013) Persistent organic pollutants in Norwegian men from 1979 to 2007: intraindividual changes, age–period–cohort effects, and model predictions. *Environ Health Perspect* 121(11–12):1292–1298
- Nøst TH, Breivik K, Wania F, Rylander C, Odland JØ, Sandanger TM (2015) Estimating time-varying PCB exposures using person-specific predictions to supplement measured values: a comparison of observed and predicted values in two cohorts of Norwegian women. *Environ Health Perspect* 124(3):299–305
- Ng CA, Hungerbühler K (2014) Bioaccumulation of perfluorinated alkyl acids: observations and models. *Environ Sci Technol* 48(9):4637–4648
- Ng CA, von Goetz N (2016) The global food system as a transport pathway for hazardous chemicals: the missing link between emissions and exposure. *Environ Health Perspect* 125(1):1–7
- Oltmanns J, Licht O, Bitsch A, Bohlen M-L, Escher S, Silano V, MacLeod M, Serafimova R, Kass G, Merten C (2018) Development of a novel scoring system for identifying emerging chemical risks in the food chain. *Environ Sci Processes Impact* 20(2):340–353
- Papa E, Sangion A, Arnot JA, Gramatica P (2018) Development of human biotransformation QSARs and application for PBT assessment refinement. *Food Chem Toxicol* 112:535–543
- Quinn CL, Armitage JM, Breivik K, Wania F (2012) A methodology for evaluating the influence of diets and intergenerational dietary transitions on historic and future human exposure to persistent organic pollutants in the Arctic. *Environ Int* 49:83–91
- Quinn CL, Wania F (2012) Understanding differences in the body burden–age relationships of bioaccumulating contaminants based on population cross sections versus individuals. *Environ Health Perspect* 120(4):554–559
- Ritter R, Scheringer M, MacLeod M, Hungerbühler K (2010) Assessment of nonoccupational exposure to DDT in the tropics and the north: relevance of uptake via inhalation from indoor residual spraying. *Environ Health Perspect* 119(5):707–712
- Ritter R, Scheringer M, MacLeod M, Moeckel C, Jones KC, Hungerbühler K (2011) Intrinsic human elimination half-lives of polychlorinated biphenyls derived from the temporal evolution of cross-sectional biomonitoring data from the United Kingdom. *Environ Health Perspect* 119(2):225–231
- Ritter R, Scheringer M, MacLeod M, Schenker U, Hungerbühler K (2009) A multi-individual pharmacokinetic model framework for interpreting time trends of persistent chemicals in human populations: application to a postban situation. *Environ Health Perspect* 117(8):1280–1286
- Rohde S, Moser GA, Päpke O, McLachlan MS (1999) Clearance of PCDD/Fs via the gastrointestinal tract in occupationally exposed persons. *Chemosphere* 38(14):3397–3410
- Sarigiannis DA, Karakitsios SP, Handakas E, Simou K, Solomou E, Gotti A (2016) Integrated exposure and risk characterization of bisphenol-A in Europe. *Food Chem Toxicol* 98:134–147
- Suciu N, Tediosi A, Ciffroy P, Altenpohl A, Brochot C, Verdonck F, Ferrari F, Giubilato E, Capri E, Fàit G (2016) Potential for MERLIN-Expo, an advanced tool for higher tier exposure assessment, within the EU chemical legislative frameworks. *Sci Total Environ* 562:474–479
- Thuresson K, Höglund P, Hagmar L, Sjödin A, Bergman Å, Jakobsson K (2005) Apparent half-lives of hepta- to decabrominated diphenyl ethers in human serum as determined in occupationally exposed workers. *Environ Health Perspect* 114(2):176–181
- Trudel D, Horowitz L, Wormuth M, Scheringer M, Cousins IT, Hungerbühler K (2008) Estimating consumer exposure to PFOS and PFOA. *Risk Anal* 28(2):251–269
- Trudel D, Scheringer M, von Goetz N, Hungerbühler K (2011) Total consumer exposure to polybrominated diphenyl ethers in North America and Europe. *Environ Sci Technol* 45(6):2391–2397
- Undeman E, Brown TN, McLachlan MS, Wania F (2018) Who in the world is most exposed to polychlorinated biphenyls? Using models to identify highly exposed populations. *Environ Res Lett* 13(6):064036
- Undeman E, Brown TN, Wania F, McLachlan MS (2010) Susceptibility of human populations to environmental exposure to organic contaminants. *Environ Sci Technol* 44(16):6249–6255
- Wania F, Breivik K, Persson NJ, McLachlan MS (2006) CoZMo-POP 2–A fugacity-based dynamic multi-compartmental mass balance model of the fate of persistent organic pollutants. *Environ Model Softw* 21(6):868–884
- Wetmore BA, Wambaugh JF, Ferguson SS, Sochaski MA, Rotroff DM, Freeman K, Clewell HJ III, Dix DJ, Andersen ME, Houck KA (2011) Integration of dosimetry, exposure, and high-throughput screening data in chemical toxicity assessment. *Toxicol Sci* 125(1):157–174
- Williams DT, LeBel GL, Furmanczyk T (1980) Polychlorinated biphenyl contamination of laboratory air. *Chemosphere* 9(1):45–50
- Wolff MS, Anderson HA, Britton JA, Rothman N (2007) Pharmacokinetic variability and modern epidemiology—the example of dichlorodiphenyltrichloroethane, body mass index, and birth cohort. *Cancer Epidemiol Biomark Prev* 16(10):1925–1930
- Wolff MS, Fischbein A, Selikoff IJ (1992) Changes in PCB serum concentrations among capacitor manufacturing workers. *Environ Res* 59(1):202–216
- Wong F, Cousins IT, MacLeod M (2013) Bounding uncertainties in intrinsic human elimination half-lives and intake of polybrominated diphenyl ethers in the North American population. *Environ Int* 59:168–174
- Wong F, MacLeod M, Mueller JF, Cousins IT (2014) Enhanced elimination of perfluorooctane sulfonic acid by menstruating women: Evidence from population-based pharmacokinetic modeling. *Environ Sci Technol* 48(15):8807–8814
- Wood SA, Armitage JM, Binnington MJ, Wania F (2016a) Deterministic modeling of the exposure of individual participants in the National Health and Nutrition Examination Survey (NHANES) to polychlorinated biphenyls. *Environ Sci Process Impact* 18(9):1157–1168
- Wood SA, Xu F, Armitage JM, Wania F (2016b) Unravelling the relationship between body mass index and polychlorinated biphenyl concentrations using a mechanistic model. *Environ Sci Technol* 50(18):10055–10064
- Yang C, Harris SA, Jantunen LM, Siddique S, Kubwabo C, Tsirlin D, Latifovic L, Fraser B, St-Jean M, De La Campa R (2019) Are cell phones an indicator of personal exposure to organophosphate flame retardants and plasticizers? *Environ Int* 122:104–116
- Zartarian V, Bahadori T, McKone T (2005) Adoption of an official ISEA glossary. *J Expo Anal Environ Epidemiol* 15(1):1–5
- Zhang X, Arnot JA, Wania F (2014) Model for screening-level assessment of near-field human exposure to neutral organic chemicals released indoors. *Environ Sci Technol* 48(20):12312–12319
- Zhao S, Breivik K, Jones KC, Sweetman AJ (2018) Modeling the time-variant dietary exposure of PCBs in China over the period 1930 to 2100. *Environ Sci Technol* 52(13):7371–7379
- Zhao S, Price O, Liu Z, Jones KC, Sweetman AJ (2015) Applicability of western chemical dietary exposure models to the Chinese population. *Environ Res* 140:165–176

# **Solutions for Mitigating Hazardous Exposures**

# The Development and Challenges of Oxidative Abatement for Contaminants of Emerging Concern

Stanisław Waclawek, Miroslav Černík, and Dionysios D. Dionysiou

## Abstract

For several years now, many substances that are known for saving the lives of billions of people, have paradoxically appeared as a new group of very dangerous contaminants. These compounds (for example, pharmaceuticals, pesticides, their metabolites, etc.) often have chronic and acute dangerous effects on humankind and other living beings. The presence of these pollutants is being documented and novel systems are being developed for their treatment every day. In this chapter, we review the literature from approximately the past 10 years, illustrating the decontamination of these chemicals by advanced oxidation processes (AOPs). A range of methods including novel catalytic systems for hydroxyl radical production as well as computation methods for prediction of CEC removal rate constants and their transformations are discussed. Furthermore, many (bio)transformation (by)products possess different (lower/higher) toxicological fingerprints, which can now also be assessed by advanced modelling. Moreover, many of these AOPs are limited commercially by their high capital and operating costs. All of these issues are addressed in this book chapter.

## Keywords

AOP • Oxidation • Remediation • Pollutants of emerging concern • Micropollutants

## Abbreviation List

2,4-D	2,4-dichlorophenoxyacetic acid
ACR	Acridine
AOPs	Advanced Oxidation Processes
AST	Activated Sludge Treatment
ATZ	Atrazine
BE	Benzocaine
BHT	Butylated Hydroxytoluene
BPA	Bisphenol A
BZ8	Dioxybenzone
CAF	Caffeine
CBZ	Carbamazepine
CD-polymers	Cyclodextrin polymers
CECs	Contaminants of Emerging Concern
CFD	Computational Fluid Dynamics
CIP	Ciprofloxacin
CPI	Controlled Periodic Illumination
DCF	Diclofenac
DO	Dissolved Oxygen
DOM	Dissolved Organic Matter
E1	Estrone
E2	17- $\beta$ -Estradiol
EDCs	Endocrine disruptors
EE/O	Electrical energy per order for degradation
EE2	17- $\alpha$ -ethinylestradiol
EEME	Mestranol
EU	European Union
GBZ	Gemfibrozil
GCN	Graphitic Carbon Nitride
HCNNSs	Hollow Carbon Nitride Nanospheres
HCT	Hydrochlorothiazide
IBP	Ibuprofen
ISCO	In Situ Chemical Oxidation
I-TEF	International-Toxicity Equivalency Factor
LDH	Lactate Dehydrogenase
LDPE	Low-Density Polyethylene
LFER	Linear Free Energy Relationship
MTT	Methyl-thiazolyl blue tetrazolium reduction

S. Waclawek · M. Černík  
Centre for Nanomaterials, Advanced Technologies and  
Innovation, Technical University of Liberec, Studentská 1402/2,  
461 17 Liberec 1, Czech Republic

D. D. Dionysiou (✉)  
Environmental Engineering and Science Program,  
Department of Chemical and Environmental Engineering,  
705 Engineering Research Center, University of Cincinnati,  
Cincinnati, OH 45221-0012, USA  
e-mail: [dionysios.d.dionysiou@uc.edu](mailto:dionysios.d.dionysiou@uc.edu)

NP4EO	Nonylphenol ethoxylate
NPX	Naproxen
O <sub>3</sub> -MB	Ozonated microbubbles
ODZ	Oxadiazon
OSTP	Office of Science and Technology Policy
P4	Progesterone
PCDD/Fs	Polychlorinated dibenzo-p-dioxins and dibenzofurans
PDNN	Prednisolone
PPCPs	Pharmaceuticals and Personal Care Products
PVA	Polyvinyl Alcohol
ROS	Reactive Oxygen Species
TRI	Triallate
QC	Quantum Chemical Computations
QSARs/QSPR	Quantitative Structure–Activity(Property) Relationships
SMX	Sulfamethoxazole
SQX	Sulfaquinoxaline
TBA	Terbuthylazine
TF	Task Force on emerging contaminants
TMP	Trimethoprim
TPs	Transformation Products
TCS	Triclosan
TST	Transition State Theory
UV	Ultraviolet light
W/WWTP	Water and Wastewater Treatment Plant
YAS	Yeast Androgen Screen
YES	Yeast Estrogen Screen

## 1 Pollutants of Emerging Concern

Amongst all resources, Water is one of the most important resources for society, with several groups such as municipalities, agriculture and industry requiring large amounts of uncontaminated water to function Crutzen and Waclawek 2014). Worldwide chemical production and water abstraction is growing even faster than the human population (Ertl et al. 2017; Waclawek et al. 2018). This has resulted in the large-scale contamination of water systems, with several new contaminants appearing that escaped consideration or detection in the last few decades. This is partially due to the lack of sensitivity in analytical techniques at the time. These substances are called contaminants/pollutants of emerging concern (CECs) and/or micropollutants. Kümmerer (2011) postulated the exclusive use of the term micropollutants; however, the term CECs is still widely used in the scientific society (Gou et al. 2014; Bu et al. 2018) and in legal terminology. Most of these compounds have

properties that can hamper the functioning of hormones (by mimicking their effects) in people/animals and most of them have not been fully evaluated for the risks they may pose to the environment (plants, microorganisms, fish, wildlife) or to humankind. Some of these substances are endocrine active and are often not acutely toxic at the levels normally found in the environment; however, in the long run, they can affect organisms (Vandenberg et al. 2012). Additionally, since most of these substances appear at low concentrations, many of them raise toxicological concerns, especially when they are part of complex mixtures (Schwarzenbach et al. 2006; Kümmerer et al. 2019). Furthermore, the worldwide spread of these compounds can cause an increase in antibiotic-resistant microbes (Carvalho and Santos 2016). Water and wastewater treatment plants (W/WWTPs) are not equipped for the efficient decontamination of CECs and conventional treatment types, with activated sludge processes and filtration often proving ineffective in the treatment of most CECs entering WWTPs (von Gunten 2018; Krzeminski et al. 2019). As a consequence, these substances are emitted back into the environment in concentrations from ng/L (for example, carbamazepine, CBZ) up to mg/L (for example, acesulfame) (Salimi et al. 2017).

Although the concepts of ‘caring for the environment’ and eco living are gaining popularity in modern society, the main output of such behaviour often relies on documenting tragic cases such as plastic ingestion by animals or movie-making [The Devil We Know (2018, Director: Stephanie Soechtig, co-Director: Jeremy Seifert)]. These actions, although very useful, should be supplemented by investigating the long-term effects of microplastics or micropollutants/CECs and how to effectively degrade them. Such activities are also useful for both policymakers and conservation efforts (Avery-Gomm et al. 2018).

As stated by the law of the European Union (fEU) there are two classifications for pollutants: (1) priority substances, ‘presenting a significant risk to or via the aquatic environment’ (EU Water Framework Directive 2000), and (2) CECs, depending on the presence or absence of legislation. According to this directive, CECs include steroids and hormones, pharmaceuticals and personal care products (PPCPs), some pesticides, household and industrial chemicals, metals, industrial additives, surfactants. The EU Water Framework Directive (2000) was updated in 2013 (EU 2013), which places attention on CECs monitoring, for which legislation still did not exist. This was followed in 2015 by the establishment of a watch list of ten compounds/groups of compounds (a total of 17 substances), which have to be monitored in surface water within the EU (European Commission 2015). Therefore, the position of the European Commission on these compounds is clear (Barbosa et al. 2016; Tiedeken et al. 2017; Gorito et al. 2017).

As for the situation in the United States of America, US Congress in 2017–2018 requested that the OSTP (Office of Science and Technology Policy) develop a coordinated cross-agency plan for tackling several critical research gaps connected to CECs (United States. Congress. Senate. Committee on Appropriations 2018). The Task Force on Emerging Contaminants (TF) was established on 8 May 2018 and provided a report to the OSTP (TF (Task Force on Emerging Contaminants) 2018) in which CECs were defined as ‘newly identified or re-emerging manufactured or naturally occurring physical, chemical, biological, or radiological materials that may be harmful to humans under certain exposure scenarios and do not have an applicable regulatory health standard’. Moreover, the Federal Safe Drinking Water Act (1974, passed by Congress) identified several critical research gaps highlighted by TF in the areas of contaminant identification, exposure characterisation and human health impacts.

After reviewing the experience gained from these two regions (EU and USA) and screening management strategies for mitigating the risk associated with CECs, two steps were proposed for preventing the release of these compounds into the environment: 1) regulation of the maximum allowable concentrations, which could lead to a reduction in the release of known hazardous substances, and 2) the creation of strategies based on the preventative principle for minimizing the occurrence of CECs (Bieber et al. 2016).

For further information on the fate, occurrence, health effects, effective mitigation options and remediation of emerging pollutants, see several of the recently published review papers (Van Wezel et al. 2017; Salimi et al. 2017; Teodosiu et al. 2018; Rahman et al. 2018; Kümmerer et al. 2019).

Although the previously mentioned prevention of CEC pollution seems to be the best option for keeping the environment clean, many CECs are already present in the environment and novel treatment systems need to be continuously created for their removal. Novel, ‘green’ and sustainable treatments are continuously being developed for the specific and successful removal of pollutants *in/ex situ* (Kümmerer et al. 2019). Advanced oxidation processes (AOPs) can be considered (with some exceptions) as one of the greener and more effective alternatives for CEC treatment. Although some of them have been used in water/wastewater treatment for more than 100 years (von Sonntag and von Gunten 2012), numerous challenges related to the oxidative removal of CECs remain, such as better control of process efficiency and a lack of understanding of product formation (especially toxic ones), among others (von Gunten 2018). New developments, prediction of the kinetics of CEC removal, toxicity of the byproducts, consideration of the energy demands and the economics of

advanced oxidation techniques are discussed in this book chapter.

---

## 2 Recent Advances in AOPs for CECs Treatment

AOPs rely on the generation of very reactive hydroxyl radicals ( $\cdot\text{OH}$ ) that are able to transform complex substances into often smaller products and ideally into  $\text{CO}_2$  and water. Even though many methods for the generation of  $\cdot\text{OH}$  from various precursors have been reported, they differ in their application and viability. When discussing AOP reactions with CECs, we should consider several aspects. Firstly, CECs chiefly occur in natural matrices at low or very low concentrations and most studies focusing on CEC removal discuss the decontamination of emerging pollutants at high or very high concentrations (not really found in ‘real’ matrices). Secondly, most experiments are conducted in deionised spiked water and the effect of the naturally occurring water matrix is sometimes omitted. However, water matrix constituents can enormously influence the decontamination efficiency of single CECs by AOPs, having neutral (very rare), promoting (e.g. generation of reactive oxygen species (ROS) more suitable for removal of CEC, additional catalysts) or inhibiting (creation of radicals less reactive than hydroxyl radicals, scavenging effects, decrease in the specific surface area of catalysts) effects (Lado Ribeiro et al. 2019).

This section provides a chronological list of the advances (from over the past 10 years) in AOPs used for the treatment of CECs. Different homogeneous and heterogeneous approaches for CECs removal, including various modified  $\text{TiO}_2$  and Fenton processes as well as catalytic ozonation, are also discussed. Furthermore, some recently reported innovative ways for generation of  $\cdot\text{OH}$  (e.g. UV/chlorine and UV/permanganate) and the conjoined utilisation of AOPs (in example: sono-Fenton) are mentioned. This section is divided into several subsections concerning these systems. Although vacuum ultraviolet methods (VUV, UV radiation < 200 nm) are not reviewed herein, they have been the subject of several recent research works (Bagheri and Mohseni 2015; Wu et al. 2019b).

### 2.1 UV/ $\text{TiO}_2$

Photocatalytic material can absorb light, which brings it to a higher energy level and provides the obtained energy to a reactant (e.g. CECs or water) allowing the reaction to occur. For photocatalytic applications, semiconducting materials with the proper band requirements (energy band gap) are often used. The most commonly used semiconductor for environmental applications with the appropriate band structure is titanium dioxide anatase ( $\text{TiO}_2$ ), which forms a

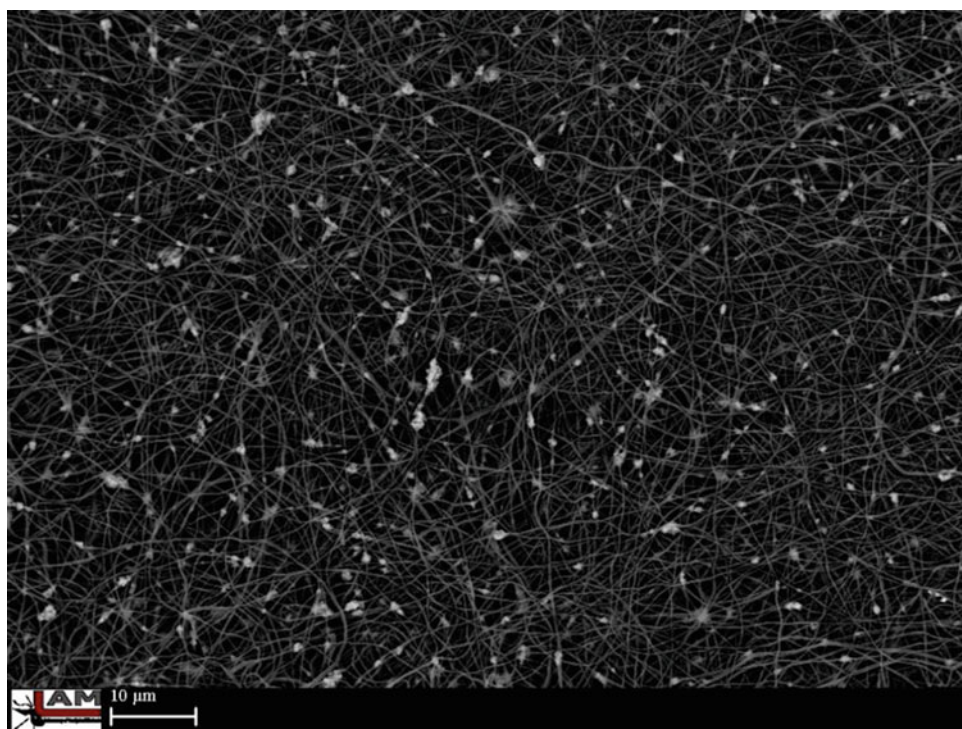
system extensively used for the production of OH or direct oxidation/reduction of contaminants (including CECs, Pelaez et al. 2012; Koltsakidou et al. 2019) when combined with UV light. There are several ways of introducing semiconductors into the reaction mixture (in suspension or on support), with subsequent positive or negative consequences, depending on many factors. Unlike a suspension, for example, an immobilized catalyst typically does not require an additional filtration procedure, which can generate extra costs and be less environmentally friendly due to, e.g. a potential release of nanoparticles to the environment. On the other hand, Plantard and Goetz (2012) compared several different stabilisers and determined that TiO<sub>2</sub> suspended in a solution had an enhanced capability to harvest radiation, and the alveolar structure considerably improved the efficiency in comparison to 2D commercial photocatalytic media. However, many stabilisers have been used for TiO<sub>2</sub> immobilisation, e.g. formation of thick TiO<sub>2</sub> films on volcanic mesoporous stones used in a packed bed reactor for CEC [triclosan (TCS)] photocatalytic removal from an aqueous solution. These films have good mechanical stability and exceptional photocatalytic activity (Martínez et al. 2014).

Another way of enhancing the use of photocatalytic semiconductors is to combine them with a magnetic material allowing for their (even) easier separation. Iron–TiO<sub>2</sub> composites have been presented as being very useful for the decontamination of CECs, including endocrine disruptors

(EDCs), PPCPs, and pesticides. Some of the preparation techniques for iron-based-TiO<sub>2</sub> nanomaterials were described in previous studies (Ren et al. 2013). Also Murgolo et al. (2017) investigated the combination of TiO<sub>2</sub> with iron, but in their work, the TiO<sub>2</sub> film was placed on a mesh composed of stainless steel (nanoTiO<sub>2</sub>-SS) using the metal organic chemical vapor deposition method. This composite was tested for the photocatalytic removal of a CEC mixture. Particularly, the removal rates of trimethoprim (TMP) and warfarin attained using this catalyst were found to be two-fold and ca. 1.6 times faster for CBZ, gemfibrozil (GBZ) and metoprolol than those observed using Degussa P25 TiO<sub>2</sub>. In another work, magnetic titanium dioxide was synthesised with SiO<sub>2</sub> and the resulting composite (Fe<sub>3</sub>O<sub>4</sub>/SiO<sub>2</sub>/TiO<sub>2</sub> particles) was used for photodegradation of norfloxacin, ciprofloxacin (CIP) and ibuprofen (IBP). These particles displayed extraordinary photocatalytic removal of recalcitrant CECs, with no significant loss of efficiency after five uses.

A non-magnetic type of TiO<sub>2</sub> modification was recently proposed by Li et al. (2018), who introduced a sol-gel synthesis method altered by acetic acid (used for hydroxylation of the TiO<sub>2</sub> surface) for a H-functionalised TiO<sub>2</sub>/kaolinite composite. According to the authors, the functionalized surface can allow the physical adsorption of uncharged carboxylic groups of CIP and enhance its degradation rate constants (2.6 and 1.6 times higher in

**Fig. 1** A SEM image showing TiO<sub>2</sub> immobilised on biopolymeric (gum karaya mixed with polyvinyl alcohol) nanofibers that were developed at the Technical University of Liberec. The white spots represent TiO<sub>2</sub> particles



comparison to those of  $\text{TiO}_2$  and  $\text{TiO}_2/\text{kaolinite}$ , respectively) (Li et al. 2018).

Another type of stabilisation/immobilisation of  $\text{TiO}_2$  is by nano/microfibers (Fig. 1). Modified nanofibers diminish the agglomeration of individual particles, make  $\text{TiO}_2$  more reusable and can reduce the recombination of photoexcited charge carriers and thus improve light absorbance as stated by Lin et al. (2019). The authors used  $\text{TiO}_2$  nanofibers wrapped in nanosheets of boron nitride (created by the electrospinning technique) for the removal of IBF. This method is also capable of removing the byproducts that appear as a result of IBF degradation. Kudlek et al. immobilised  $\text{TiO}_2$  on biopolymeric nanofibers and used it for photocatalytic oxidation of two CECs (bisphenol A, BPA and diclofenac, DCF) (Kudlek et al. 2017).

Other organic compounds more frequently used for environmental purposes are cyclodextrins and cyclodextrin polymers (CD-polymers) (Řezanka et al. 2015; Alsaiee et al. 2016). These uses comprise the stabilization of various nanoparticles including  $\text{TiO}_2$  (Agócs et al. 2016). Although stabilization with a CD-polymer enhanced  $\text{TiO}_2$  colloid stability and showed synergistic effects for decontamination of a model dye, IBF remediation displayed an opposite effect varying on the structure of the guest–host complex. Another example of the creation of a uniform organic coating that can enhance the photocatalytic activity of  $\text{TiO}_2$  is a polyvinyl alcohol (PVA) combined with  $\text{TiO}_2$ , which was further immobilised on metal meshes for the removal of nonylphenol ethoxylate (NP4EO) in spiked water (da Trindade et al. 2018). Moreover, the tests were performed in a wastewater matrix without losing substantial PVA/ $\text{TiO}_2$  photocatalytic activity (NP4EO degradation reached 91%).

As mentioned above, in parallel to the stabilisation of  $\text{TiO}_2$ , ongoing research focuses on making it more accessible to UV radiation. For this reason, a floating photocatalyst on the water surface (due to a lower density in comparison to water) has been developed. Moreover, several contaminants that can also float on the water surface, e.g. various oily films, can be more accessible to the catalyst and therefore more easily degraded.  $\text{TiO}_2$  can be deposited on an LDPE filament support printed on a 3D printer (Martín de Vidales et al. 2019) or immobilised in porous reticulated  $\text{ZrO}_2$  3D foams (Martín-Sómer et al. 2019) for the removal of CECs. Photocatalysts in foam used for the treatment of spiked water have shown lower efficacy than a catalyst in suspension; however, they could not be seen while treating a real effluent taken from a WWTP (Martín-Sómer et al. 2019).

Another problem of photocatalysts is to overcome issues related to low photonic efficiency. This can be achieved to some extent, for example, by controlled periodic illumination (CPI) (Liang et al. 2019). A UV-LED/ $\text{TiO}_2$  (CPI controlled) process was successfully used for the decontamination of 18 PPCP substances with reducing

energy requirements and no negative effects on the treatment performance (Liang et al. 2019). Also Biancullu et al. (2019) tested the removal of TMP, azithromycin, sulfamethoxazole (SMX) and ofloxacin from spiked wastewater by a  $\text{TiO}_2$ -photocatalytic treatment using UVA-LEDs (without CPI control). The best conditions were determined for the treatment (1 g/L of catalyst, 4 LEDs symmetrically distributed and 1-hour treatment).

The combination of a photocatalyst with hydrogen peroxide for the degradation of CECs has been shown several times recently (Moreira et al. 2018; Jiménez-Tototzintle et al. 2018). For example, Jiménez-Tototzintle et al. (2018) compared UVA/ $\text{TiO}_2$  (in suspension), UVA/ $\text{TiO}_2$ -immobilised, and UVA/ $\text{TiO}_2$ -immobilised +  $\text{H}_2\text{O}_2$  for the removal of a CEC mix (BPA, acetamiprid and imazalil). The combination of hydrogen peroxide and immobilised  $\text{TiO}_2$  treatment was found to be the most effective for CEC removal. Similar conclusions were created by Moreira et al. (2018), who used a comparable treatment for the removal of SMX, CBZ, and DCF). The influence of individual  $\text{H}_2\text{O}_2$  processes will be discussed in the next section.

## 2.2 UV/ $\text{H}_2\text{O}_2$ , Fenton and Modified-Fenton Processes

The oxidation of substances by  $\text{H}_2\text{O}_2$  and  $\text{Fe}^{2+}$  (ferrous iron) is known as ‘Fenton chemistry’, which was first explained by H.J.H. Fenton who studied it during the oxidative treatment of tartaric acid by hydrogen peroxide in the presence of  $\text{Fe}^{2+}$  (Fenton 1894). Notwithstanding many controversies and derivatives of this reaction (Barbusinski 2009), it is considered one of the most vital techniques in water and wastewater treatment. CECs can be removed in the so-called classical Fenton process (requiring a low pH) (Anis and Haydar 2019) and a modified-Fenton’s reagent, which is a very popular method in *in situ* chemical oxidation (ISCO) (Tsitonaki et al. 2010) often due to lower costs, non-inhibited bioremediation, etc. Another way of splitting  $\text{H}_2\text{O}_2$  is by UV light (quantum yield of 1.0), which can cleave the O-O bond and produce two molecules with unpaired electron–radicals. This process is very efficient in the sense of radical production, since two radicals are produced from one molecule of hydrogen peroxide, but it is often less energy efficient in comparison to, e.g.  $\text{H}_2\text{O}_2/\text{O}_3$  due to the high cost of the UV light generation (Lee and von Gunten 2016).

Nonetheless, the use of UV/ $\text{H}_2\text{O}_2$  for the decontamination of CECs has been extensively reported, e.g. 40 pharmaceuticals comprising metformin, venlafaxine, paroxetine, pindolol, and sotalol (Giannakis et al. 2017a), nine CECs i.e. 2,4-dichlorophenoxyacetic acid (2,4-D) and CBZ (Shu et al. 2016), TCS (Huang et al. 2018b) and BPA (Pérez-Moya



et al. 2017). Pharmaceuticals have a large range of reaction rate constants where  $\cdot\text{OH}$ , e.g. metformin, cyclophosphamide and ifosfamide react slowly, while ketoprofen, prednisolone (PDNN), pindolol, DCF (depending on the pH value:  $6.0\text{--}9.1 \cdot 10^9 \text{ M}^{-1} \text{ s}^{-1}$ ), TCS (depending on the pH value:  $4.4\text{--}7.0 \cdot 10^9 \text{ M}^{-1} \text{ s}^{-1}$ ) react rapidly (Wols et al. 2013; Huang et al. 2018b). Overall, the pH value has an important role in UV/H<sub>2</sub>O<sub>2</sub> processes for CEC decontamination by influencing the ionic state of the CECs ( $\text{pK}_a$  based) and scavenging  $\cdot\text{OH}$  at high pH values. Kinetic models can predict the removal of CECs during UV/H<sub>2</sub>O<sub>2</sub> treatment with high accuracy (Wols et al. 2014): however, this topic will be covered more in the next section (mechanistic predictions of reaction kinetics).

It has been reported many times that the addition of iron to the UV/H<sub>2</sub>O<sub>2</sub> system can create extra pathways advantageous for the degradation of CECs, e.g. iohexol (Giannakis et al. 2017b), paracetamol (Audino et al. 2019) and BPA (Pérez-Moya et al. 2017). This process, when the synergistic effect uses both—UV and iron activated H<sub>2</sub>O<sub>2</sub>, is called photo-Fenton. One precursor study focused on the photo-Fenton removal of a large group of 32 selected CECs (corrosion inhibitors, biocides/pesticides and pharmaceuticals) from an effluent taken from a WWTP (with AST). Both dissolved organic matter (DOM) and contaminants in low concentrations were kept for testing the environmental significance of such a treatment. Photo-Fenton remediation (UV<sub>254</sub>, 50 and 5 mg/L of H<sub>2</sub>O<sub>2</sub> and Fe<sup>2+</sup>, respectively) provided the best results (the rate of CEC removal reached around 98%). However, in contrast to the solar photo-Fenton process at a circumneutral pH for the removal of 45 CECs (Soriano-Molina et al. 2019), photo-Fenton performed with simulated sunlight was less efficient (De la Cruz et al. 2012).

Hydrogen peroxide in combination with electrolysis, known as electro-Fenton, based on the simultaneous production of H<sub>2</sub>O<sub>2</sub> and regeneration of Fe<sup>2+</sup>, has successfully been used for the removal of CECs (BPA, TCS and IBF) (Yuan et al. 2013). Another arrangement used is a combination of ultrasound and a Fenton reagent, known as sono-Fenton. This has very recently been proposed as an effective remedial option for CECs (Serna-Galvis et al. 2019).

The Fenton process can also be modified heterogeneously. Zero-valent iron or other magnetic particles have been reported for the activation of hydrogen peroxide (Xiang et al. 2016). One example has recently been reported by Palma et al. (2018), who synthesised hybrid magnetic nanoparticles based on compost-derived substances for this purpose. These synthesised magnetite nanoparticles were easily extracted after treatment and reused in the heterogeneous photodegradation of caffeine (CAF).

Attempts to upscale the hydrogen peroxide treatment process have also recently been reported, either by the

creation of a filter-type electro-Fenton device for the degradation of DCF (Plakas et al. 2016) or by the combination of UVC/H<sub>2</sub>O<sub>2</sub> with AST (sulfolane degradation efficiency of >81% in less than 24 h could be achieved in this system) (Sundaram et al. 2014; Khan et al. 2019). The use of UVC/H<sub>2</sub>O<sub>2</sub> after AST is advantageous because UVC/H<sub>2</sub>O<sub>2</sub> can perform dual roles in this composition, serving as an oxidant and as a disinfectant (Sundaram et al. 2014; Khan et al. 2019).

### 2.3 Ozone and Ozone-Based Processes

Ozone is probably the oldest known oxidant that can be utilised in water and wastewater treatment. It is an inorganic bent molecule (with C<sub>2v</sub> symmetry, which is comparable to the molecule of water) with the chemical formula O<sub>3</sub> (von Sonntag and von Gunten 2012). It is a pale blue gas with a distinctively pungent smell (the Greek word *ozein* means 'smell'). However, there is an interesting hypothesis that ozone is actually odourless, and what can be smelt originates from, e.g. skin oxidation (von Sonntag and von Gunten 2012). Ozone has been commercially used for the decontamination of water/wastewater from toxic substances for more than 120 years (first in 1906 for disinfection purposes in the city of Nice, France) (Rice et al. 1981). The oxidation of CECs during ozonation can occur through ozone (a very selective oxidant) or  $\cdot\text{OH}$ , or a combination of both (von Sonntag and von Gunten 2012). When comparing the oxidants usually used for water/wastewater treatment, ozone can be more reactive with humic-like compounds, while  $\cdot\text{OH}$  favourably reacts with protein-like ones (Chen et al. 2017). The oxidation pathway during ozonation can be verified by calculating the ratio of concentrations of ozone and  $\cdot\text{OH}$ . The degree of CECs oxidation by ozone and  $\cdot\text{OH}$  can be given by the kinetic calculations that were discussed in the review of von Gunten (2003). Generally, the spectrum of second-order reaction rate constants for the oxidative reactions of ozone varies between  $10^{-1} \text{ M}^{-1} \text{ s}^{-1}$  and about  $10^{10} \text{ M}^{-1} \text{ s}^{-1}$ . Many databases are freely accessible for obtaining the  $k$  values (see e.g. <http://kinetics.nist.gov/solution/>) and new articles are continuously being created in which the new  $k$  values are reported. Ozone-based processes are used extensively for the removal of CECs; as ozone is known to mainly react with activated aromatic systems, double bonds and deprotonated amines. Jin et al. (2012) selected 24 CECs with different structures and purposes of use including EDCs, PPCP and their  $k(\text{O}_3)$  and  $k(\cdot\text{OH})$  values were found during laboratory tests (at a neutral pH and at 20 °C). More recently, 12 xenobiotics (pesticides and pharmaceuticals) were selected for the creation of a database that compiles the literature outputs of experimental ozonation approaches under bench-scale and *in situ* conditions (Mathon et al.

2017). Further examples of ozone reactions with CECs were given by Liu et al. (2016), who studied the decontamination of forty various trace-level CECs in wastewater. The potential of online fluorescence measurements for quantitating the effects of ozonation on CECs in WWTP effluents was shown therein. Also Singh et al. (2015b) focused on researching the conversion of 41 target CECs in effluent (secondary-treated municipal wastewater) at a pilot scale, with two O<sub>3</sub> doses (2.8 and 4.4 mg/L). Generally, the removal efficacy of CECs could either increase or be retained at a higher dose of ozone. The higher dose of ozone was enough to transform 21 of the 31 detected CECs by over 80% (Singh et al. 2015b). Despite all these efforts, knowledge about compounds that contain nitrogen such as sulfaquinoxaline (SQX) and the related reaction mechanisms with ozone is still not complete (de Vera et al. 2017). The degradation of SQX by ozone was carefully performed by Urbano et al. (2017) at three pH values (3, 7 and 11). Ozonation was successful in the removal of SQX and as for the toxicity, samples ozonated at pH 3 and 7 were not or only slightly toxic to the luminescent bacteria; however, ·OH (the major oxidant at a pH of 11) was responsible for the generation of toxic by-products (Urbano et al. 2017). A very detailed research on the ozone oxidative treatment of SMX (including a systematic investigation of the product formation, reaction stoichiometry and reaction mechanisms) was performed by Willach et al. (2017). It was determined that ca. 3 mol of O<sub>3</sub> were spent per 1 mol of SMX removed. Oxidative removal of SMX can lead to 6 major transformation products (TPs) and some of their structures (taken from different studies) may be approximated by compound-specific stable isotope analysis.

One of the main disadvantages of oxidation (not exclusively but also by ozone) can be connected to the formation of often-toxic by-products that are further recalcitrant during the ongoing oxidation. Recently, experimental studies on catalytic ozonation with attempts to predict the reaction rates of catalysed ozone with CECs have attracted considerable attention (Guo et al. 2018c). Tasca et al. (2018) studied the successful degradation of terbuthylazine (TBA) and its metabolite desethylTBA. Both homogeneous and heterogeneous catalysts can enhance ozone transformation to hydroxyl radicals and thus increase the reaction rate for ozone-resistant CECs. An enormous number of varieties of solid catalysts are being developed for improving the ozone mineralization of CECs. For example, Kolosov et al. (2018) successfully tested the calcium-silicate minerals wollastonite, zeolite, Polonite®, TiO<sub>2</sub>-Al<sub>2</sub>O<sub>3</sub> (8%/92%) and AL-1010S (based on Al<sub>2</sub>O<sub>3</sub>) for the catalytic ozonation of wastewater for enhanced degradation of IBP, GBZ, naproxen [NPX, for TiO<sub>2</sub> reactions with NPX alone please see (Hernández-Colorado et al. 2017)] and

atrazine (ATZ). The results confirmed that polonite, zeolite and wollastonite did not promote CEC degradation; however, TiO<sub>2</sub> on an Al<sub>2</sub>O<sub>3</sub> support and AL-1010S improved the removal efficiency. Furthermore, the possible reuse of the catalysts was shown over four consecutive runs of six hours of usage in a continuous flow ozonation approach (Kolosov et al. 2018). In their next study (Kolosov and Yargeau 2019), they determined that catalytic ozonation is more useful for the oxidation of CECs in complicated matrices (such as effluents from WWTP).

Recently, Restivo et al. (2013) studied the application of a sophisticated catalyst based on carbon nanofibers developed on a surface of cordierite monoliths for CEC removal by ozone. Although there were some oxidation marks on the catalyst, it can be considered as stable in the long run. As expected, catalytic reactions were better for the degradation of by-products but did not enhance the decontamination of the parent compounds. Enormous interest was given to the improvement of catalytic ozonation systems by solar light with attractive results for the removal of both biological and chemical contaminants (Gomes et al. 2017).

In addition, there are a few methods for the enhancement of ozonation by increasing the dissolution of the ozone in water. This can be achieved in several ways, one of which is the method of ozonated microbubbles (O<sub>3</sub>-MB), which is becoming popular in efficient remediation and disinfection applications. Microbubbles rise slowly because of their very large ratio of surface to volume and therefore have higher stability in comparison to macro bubbles (Azuma et al. 2019). Furthermore, a high interior pressure can be produced by surface tension, initiating gas dissolution in the surrounding water, causing MB shrinkage and collapse. These properties led scientists to apply this treatment for the removal of 39 pharmaceuticals and authors compared the results with the results of ozone alone and in combination with UV, H<sub>2</sub>O<sub>2</sub>, or both. The obtained data suggests that ozone-microbubble-based treatments can significantly enhance decontamination rates (by 8–34%) compared to ozone alone, and degradation efficiencies of >90% were observed for 33 compounds. Introducing an ozone-microbubble treatment was vital in improving the degradation of acetaminophen glucuronide, bicalutamide, famciclovir and sulphiride (>96%). Further addition of UV and/or hydrogen peroxide to the O<sub>3</sub>-MB system, increased *k* by 2.9–5.5 times in comparison to O<sub>3</sub> and O<sub>3</sub>-MB used alone. Moreover, MB treatment increased O<sub>3</sub> consumption up to 2.8 times in comparison to ozone treatment alone (Azuma et al. 2019). Another method for improving the dissolution of ozone is sonication due to the enhanced mass transfer of O<sub>3</sub> in the treated medium because of the company of ultrasonic pressure waves. Yargeau and Danylo (2015)

used this technique for the remediation of popular CEC-IBF. They determined by-products (4-acetylbenzoic acid, 4-ethylbenzaldehyde, 4-isobutylacetophenone, oxalic acid and oxo-IBP) in the reaction solution. They also found that the removal of organic matter was highest when ozonation was combined with sonication, which can suggest that this AOPs possesses other reaction mechanisms that could lead to further abatement of the created by-products.

## 2.4 Other Novel Oxidation Processes Based Fully or Partially on Hydroxyl Radicals

Several sophisticated techniques have been developed recently, from which a combination of AOPs mentioned in the previous sections was revealed to have synergistic effects. As an example, one of the oldest known *in situ* oxidants—permanganate was recently combined with UV<sub>254</sub>, causing the efficient removal of CECs (nalidixic acid and GBZ), which are resistant to permanganate oxidation alone. Mn(V) peroxide and ·OH generated in the process of activating permanganate by UV were mainly responsible for the degradation improvement (Guo et al. 2018b). Another combination of a conventionally used oxidant (chlorine) with UV, has been studied by several researchers recently (Wang et al. 2017; Gao et al. 2017; Duan et al. 2018). Both of these processes (UV/permanganate and UV/chlorine) are novel AOPs that produce diverse reactive species, i.e. ·OH and reactive chlorine/manganese species, and can be used for effective removal of metronidazole, diethyltoluamide and CAF (Wu et al. 2017).

Peroxydisulfate and peroxymonosulfate are two other oxidants that when catalysed are considered to be AOPs by some researchers (Brienza and Katsoyiannis 2017; Wacławek et al. 2017; Miklos et al. 2018). This statement could be interpreted as slightly controversial because the main radical species in this system are sulphate radicals ( $\text{SO}_4^{\cdot-}$ ); however, in various matrices (e.g. possessing high pH) they can lead to the formation of hydroxyl radicals and other ROS (e.g. singlet oxygen), that can be further utilised for the degradation of CECs (Minh et al. 2019). They are also used in combination with UV for the removal of CECs such as artificial sweeteners (acesulfame and sucralose) (Fu et al. 2019). Although many studies have been performed to determine the reaction rates between sulphate radicals and CECs (Ranjbar-Mohammadi and Bahrami 2016; Liu et al. 2018; Rodríguez-Chueca et al. 2018; Deniere et al. 2018; Nihemaiti et al. 2018; Metheniti et al. 2018; Kim et al. 2019; Gómez Bernal et al. 2019), they will be discussed in this chapter only in combination with hydroxyl radical precursors. What is worth mentioning is that the combination of persulfates with ozone gained popularity several years ago. Due to the catalytic behaviour of ozone towards

peroxymonosulfate/peroxydisulfate, this combination is very effective for the removal of several CECs, mainly those slowly reacting with ozone (Deniere et al. 2018; Wu et al. 2019a).

Furthermore, constant developments in the field of nanomaterials are continuously contributing to AOPs by providing novel heterogeneous catalysts with various desired properties (Boyd et al. 2013; Yang et al. 2017; Rizzo et al. 2019b). For example, ZnO is the second most known photocatalyst used for remediation of organic pollutants (after  $\text{TiO}_2$ ) and its new derivatives are unceasingly being synthesised, e.g. magnetic ZnO with the structure  $\text{Fe}_x\text{Zn}_{1-x}\text{O}$  ( $x = 0.01, 0.03, 0.05$ ). These particles were used for BPA remediation with 99% being removed within 90 min by synergistic adsorption and photocatalytic removal (Dhiman et al. 2017). On the other hand, the creation of non-metal catalysts, especially based on nanocarbons, has gained considerable attention within the last years. For example, hollow carbon nitride nanospheres (HCNNSs) having a small particle size and a thin shell (200 and 40 nm, respectively) were successfully fabricated by a silica-nanocasting approach. HCNNSs in smaller sizes were found to possess exceptional visible-light photocatalytic efficiency for the removal of CECs (e.g. levofloxacin), when compared to bulk  $\text{g-C}_3\text{N}_4$  and larger sized HCNNSs (Yang et al. 2019). Another carbon-based photocatalyst investigated for the removal of CECs is graphitic carbon nitride (GCN), which can be synthesised by a facile thermal treatment with the use of dicyandiamide as a precursor. The efficiency of GCN in the removal of the target CECs was extraordinary higher than commercial photocatalysts  $\text{TiO}_2\text{-P25}$ . Most of the CECs were degraded in <10 min to concentrations below the quantification limit, from which CBZ was removed as the first and fluoxetine as the last compound (Moreira et al. 2019).

New homogeneous catalysis inventions are being put out to the scientific world continuously. For example, Rizzo et al. investigated the decontamination efficiency of three target CECs (CBZ, DCF and SMX) with UV activated peracetic acid. In contrast to heterogeneous GCN photocatalysis, CBZ was found to be the most recalcitrant (Rizzo et al. 2019a). Similarly, Molinari et al. investigated UV/decatungstate anions for the remediation of atenolol, levofloxacin and TMP (Molinari et al. 2017).

Electrolysis is one of the oldest methods for the creation of ROS, e.g. hydroxyl radicals or hydrogen peroxide. Its application in the electro-degradation of CECs is still often being reported, e.g. acetamiprid removal on Yb-doped  $\text{PbO}_2$  electrodes, which has shown a superior ability to generate ROS in comparison to bare  $\text{PbO}_2$  electrodes (Yao et al. 2019). Furthermore, a combination of photodegradation and electrolysis, dubbed photoelectrochemical degradation, was found to be even more effective for CEC remediation. For

example, nanocrystalline  $\text{WO}_3$  can absorb electromagnetic visible radiation (up to 470 nm) thus generating hydroxyl radicals through valence band injection, which initiates the degradation of CECs, e.g. atenolol and CBZ. A substantial acceleration in oxidation kinetics (as much as 4–5 times) can occur after the additional use of potential bias (1.5 voltage) that is instrumental in enhancing charge separation within thin films and for maximising the transfer rate of holes to the solution (Longobucco et al. 2017).  $\text{WO}_3$  can also be used with  $\text{TiO}_2$  as an electrode material. This electrode showed improved sunlight-collecting properties and enhanced separation of photogenerated charge carriers, which resulted in higher removal of 17- $\alpha$ -ethinylestradiol (EE2) from an aqueous solution (Oliveira et al. 2015). Gupta et al. examined the photoelectrochemical degradation of hydrochlorothiazide (HCT) by  $\text{SnO}_2$  nanotubes decorated by CdSe quantum dots (Gupta et al. 2017). A comparative study of the efficacies of electrochemical, photocatalytic and photoelectrochemical treatments showed that the combined processes presented a synergism for HCT and organic mass removal.

Another very effective oxidative method for CEC removal is the plasma-based water treatment technique. Plasma interacting with water forms ROS that can further react with CECs. High electric field conditions, plasma-driven chemical reactions, large density gradients and fluid dynamic effects occur in this multi-phase area. This area is also the source function for longer living reactive species that eventually purify the water. This method covers several AOPs at the same time without the necessity for traditional chemicals, making it potentially more facile. The primary barrier for implementation of plasma-based techniques for water and wastewater treatment is upscaling. Approaches to upscaling along with its performance data and the pathways from a laboratory demonstration of plasma-based systems to pilot testing and eventually guiding the technology to practical applications were explained in the work of Foster (2017), Foster et al. (2018).

### 3 Mechanistic Predictions of Reaction Kinetics

The removal of CECs by oxidative techniques is controlled by the kinetics of the reaction. There are two ways of determining kinetic rates ( $k$ ); i.e. experiment based or estimation based. The most popular method for the determination of kinetics is by conducting experiments in which we follow the analyte concentration over time. However, the experiments are very time consuming for the determination of a single  $k$  value. As mentioned in Tentscher et al. (2019), ‘If only a fraction of the about 100,000 commercially available chemicals can be found in water treatment systems

(especially wastewater and water reuse), it will be almost impossible to determine reaction kinetics, mechanisms and TPs experimentally’. Thus, researchers are searching for tools for the facilitation of these processes, e.g. expansion of quantum chemical computation (QC). With high precision, QC can now be considered as an alternative to the experimental approach and many researchers are at least supplementing their experimental studies with QC. By having an input structure, QC finds energetic minima on the potential energy surface. The  $k$  for the reactions of CECs with oxidising reagent can be further acquired by *ab initio* computations or by quantitative structure–activity(property) relationships (QSARs/QSPR) (von Gunten 2018) with various quantum chemical descriptors (Fig. 2). Quantum chemical descriptors are considered as an alternative to sigma and sigma\*-values (which can be difficult to find for many CECs) in QSAR applications (Lee et al. 2015). The most important descriptors for calculating  $k$  were found to be the orbital eigenvalue of the highest occupied molecular orbital ( $E_{\text{HOMO}}$ ) (Tentscher et al. 2019). However, Borhani et al. (2016) found the descriptor—BEHe1 (highest eigenvalue n. 1 of the Burden matrix/weighted by atomic Sanderson electronegativities) to be the most important for the forecasting of the  $\cdot\text{OH}$  rate constant with CECs, playing a very similar role to  $E_{\text{HOMO}}$ . The descriptor—ESpm05x was found to be the next most important parameter belonging to the edge adjacency indices type of descriptors by which important information on structural bond specifications can be encoded (Borhani et al. 2016). Other molecular descriptors relevant for AOP reactions with CECs include electron affinity, the number of ring atoms, the number of halogen atoms, the oxygen to carbon ratio, the weakly polar component of the solvent accessible surface area (Sudhakaran et al. 2012); double bond equivalence (Li et al. 2019) and the ionisation potential (Sudhakaran and Amy 2013).

Good correlations of QSAR/QSPR can often be found between  $k$  for the reactions of closely related substances (e.g. that possess the same functional group) and substituent descriptor variables (e.g. Hammett sigma constants; Lee and von Gunten 2012). Furthermore, QSAR/QSPR can be either embedded in a knowledge-based process model, wherein they can be used to forecast a model parameter, which can be applied in a hybrid model to predict the rate of removal and/or other parameters of various systems (Vries et al. 2013). The applicability domain of these models is often determined using the Williams plot (Jin et al. 2014).

The rate constants were predicted by QSAR/QSPR models for the reactions between CECs and hydroxyl radicals (Borhani et al. 2016; Gupta and Basant 2017a; Ortiz et al. 2017), chlorine, chlorine dioxide, ferrate (Lee and von Gunten 2012), ozone (Sudhakaran et al. 2012; Lee and von Gunten 2012; Jin et al. 2015), Fenton processes (Jia et al. 2015), tetra-amido macrocyclic ligand/ $\text{H}_2\text{O}_2$  (Su et al. 2018),

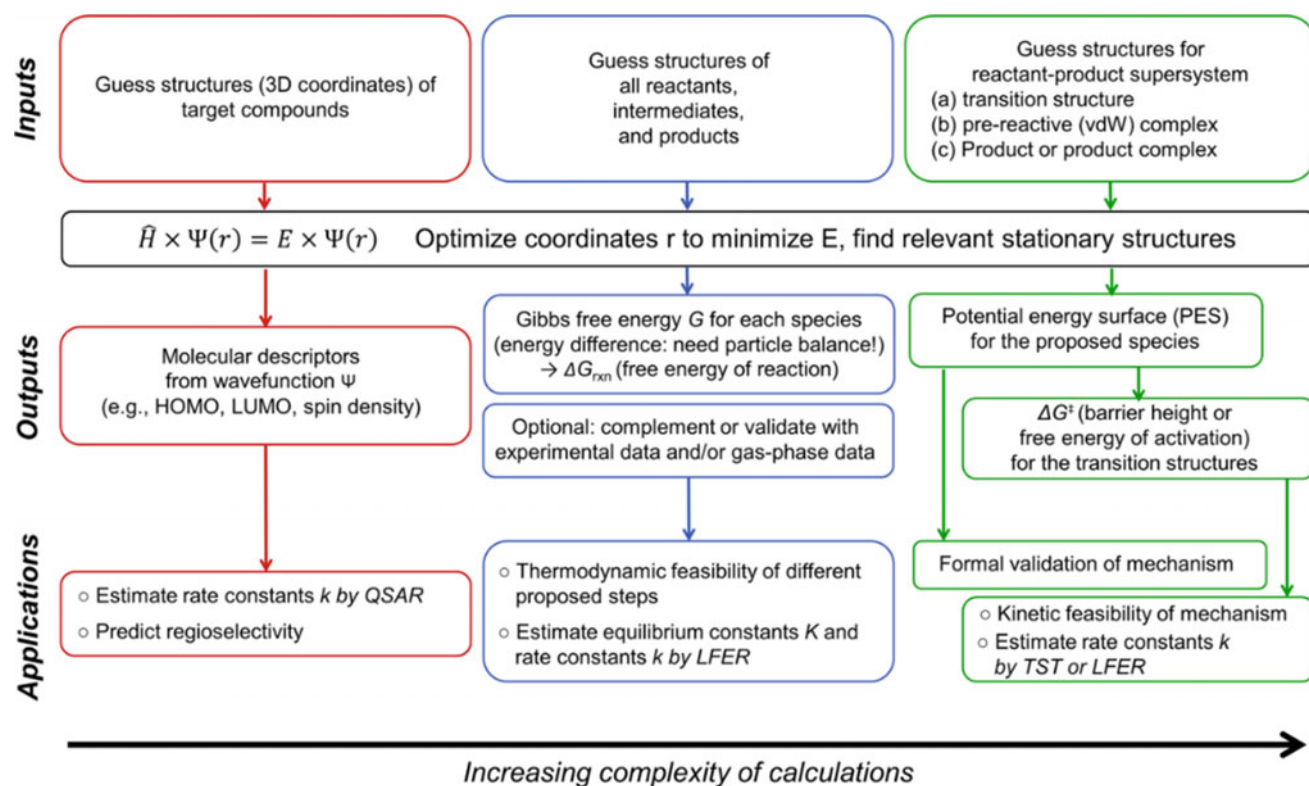


**Fig. 2** Diagram showing the calculations of several complexities for finding the relevant quantum chemical parameters of various applications (Tentscher et al. 2019). TST—transition state theory, LFER—

linear free energy relationship Reprinted with the kind permission of ACS (Tentscher et al. 2019)

peroxone (Cheng et al. 2018) and electro-peroxone (Li et al. 2019).

QSAR/QSPR can be also successfully used for modelling sulphate radical reaction rate constants with CECs (Xiao et al. 2015; Cvetnić et al. 2019). The models were submitted for validation (internal and external, using a set of additional 17 CECs) (Cvetnić et al. 2019). Three variable models predicting hydroxyl and sulphate radical reaction rate constants were characterised with high accuracy ( $R^2 = 0.876$  and  $R^2 = 0.832$ , respectively).

Modelling of  $k$  of CECs and hydroxyl radicals reactions was also presented on pH- and temperature-dependent QSPR models that were decision tree boost based (Gupta and Basant 2017b). Moreover, QC could be employed even for purposes such as determining the effects of bromide (Heeb et al. 2014) or dissolved oxygen (DO) on the radical oxidation of CECs. The importance of DO was confirmed experimentally (Lee et al. 2012) on the oxidation of CECs, and further provided a theoretical approach for studying the effects that could be caused by wastewater components on the decontamination of CECs in AOPs (Zhang et al. 2018).

Very recently, Cheng et al. (2018) modified the traditional QSAR modelling method focused on the physical and chemical properties of ligands, which could be causatively

connected to biological and chemical reactions and determined that the 3D-QSAR model can be more precise than the 2D model for predicting the physical and chemical parameters.

Even though it is known that the descriptors used (ionisation, bond dissociation energies and orbital energies) are typically not sufficiently mechanism specific to differentiate between various reaction channels, the regioselectivity (different reactive sites) could be depicted. Wave functions from the Schrodinger's equation possess descriptors for forecasting the sites that are most vulnerable to oxidation reactions in target compounds. Although forecasting of TPs generated from CECs through oxidative treatment is still challenging, QC can allow for (qualitative) assumptions on the forms of substances undergoing a studied reaction type (Tentscher et al. 2019). QC data can give information on the types of TPs that could be generated, and whether they are connected to the potential energy surface (Tentscher et al. 2019). This information can be utilised to reveal the probability of the formation/type of TPs. For example, Zhang et al. (2017) presented an *in silico* model for revealing mechanisms of CEC oxidation (by ozone). SMX was chosen as a model compound. A model can be created by knowing and following well-known patterns of ozonation and

secondary transformation reactions created experimentally for by-products. For an evaluation of the thermodynamic feasibility of reaction pathways, DFT calculations were employed and SMX oxidation products were forecasted by calculating Gibbs free energies. Moreover, the conducted experiments confirmed the formation of forecasted products. A similar case was studied by Psutka et al. (2018) who used QC as support for forecasting the products of TMP analysis [by differential mobility spectrometry coupled with tandem MS methods], a CEC in the environment, formed in the electro-Fenton system. Both the data obtained during the experiments and supporting QC showed that methoxy-containing phenyl ring hydroxylated and methylene-hydroxylated TPs are generated (Lecours et al. 2018; Psutka et al. 2018).

Some researchers not only focus their efforts on the modelling of oxidant/contaminant reactivity, but also on the modelling of their movement in space and time, often with the aim of evaluating a reactor of a special type. One such work (Hofman-Caris et al. 2012) introduced two models, wherein the authors combined the process kinetic parameters with computational fluid dynamics (CFD) (Hofman-Caris et al. 2012). Both models were used in pilot reactors, and a decent agreement was reported among the experimental and forecasted data. Similarly, Wols and Hofman-Caris (2012) applied the Lagrangian and Eulerian modelling methods with different levels of difficulty. The Eulerian method can be used to calculate compound concentrations on a fixed computational mesh and is most frequently utilised for forecasting the removal of compounds in UV/H<sub>2</sub>O<sub>2</sub> treatments, whereas the Lagrangian method can calculate the concentrations of compounds along the tracks of individual particles. For a pilot-scale flow-through reactor and a collimated beam, both techniques resulted in a comparable prediction of degradation (Wols and Hofman-Caris 2012). CFD models can be used for simulating the work of VUV/UV photoreactors used for W/WWT. Besides the creation of such a model (Bagheri and Mohseni 2014) evaluated it experimentally.

---

#### 4 Transformation Products and Toxicological Consequences

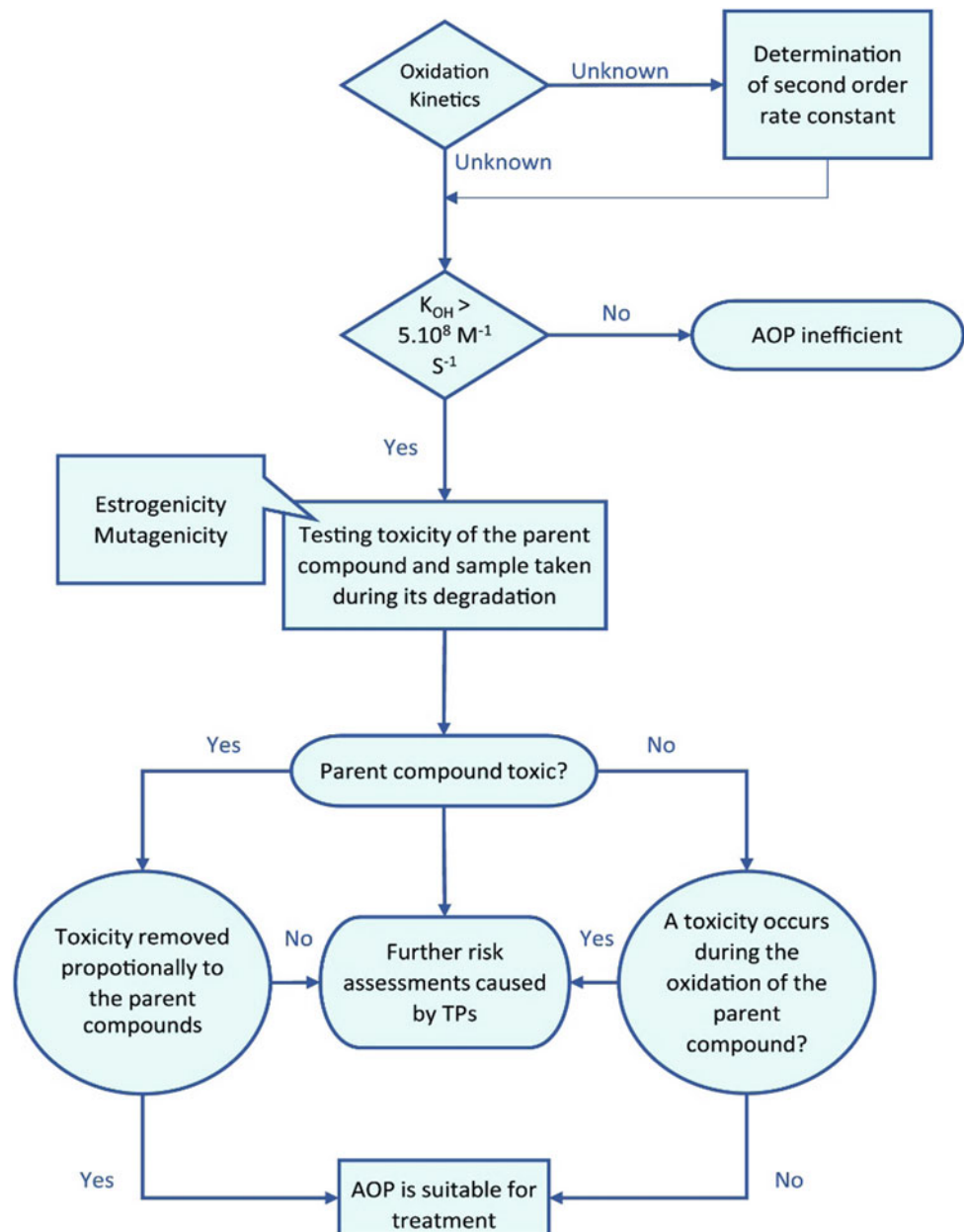
Interest in understanding the environmental relevance of TPs generated from CECs via abiotic and biotic processes has recently increased significantly. Studies published so far have elucidated numerous aspects of TPs including (i) the creation of appropriate analytical methods for the identification and quantification of TPs (Singh et al. 2015a), (ii) TP

formation pathways during various processes including biodegradation, chemical oxidation and photolysis, (iii) strategies for predicting transformation pathways and (iv) assessments regarding their toxicological relevance (Fig. 3). In relation to the QC methods discussed above, in silico toxicological prediction models have the potential for application as screening devices for the assessment of the bioactivity of TPs (Lee and von Gunten 2016). These methods were described as being fairly useful for the complex screening of undesirable chemical effects including CECs, while their application in the toxicological assessment of by-products is still limited (Lee and von Gunten 2016). Nonetheless, prediction and determination of transformation pathways in wastewater (or even cleaner matrices) can be very complicated, e.g. compounds possessing nitrogen derived from the degradation of several species can react with other fragments with the subsequent formation of several other compounds, e.g. secondary amines, pyridines, carbamate derivatives and diazoles, that can have estrogenic properties (Alvarez-Corena et al. 2016). In order to evaluate the relevance of TPs in the aquatic environment, appropriate and standardised analytical approaches and assessment protocols are needed to address the selection, identification and quantification of TPs, their role in natural water systems and engineered treatment processes, and their toxicological relevance (Drewes and Letzel 2016).

The biotoxicity of TPs by-products can be systematically evaluated using the sensibility of bio-luminescent bacteria (*Aliivibrio fischeri*; most often by a Microtox® *in vitro* testing system), which is a very useful tool for assessing the effectiveness of AOPs (Dudziak 2015; Ge et al. 2016; da Costa et al. 2019). Dudziak et al. (2018) studied selected indicator organisms (bacteria, crustacea, aquatic plants) from different taxonomic groups in order to assess the toxicity of CECs. Moreover, lactate dehydrogenase (LDH), thiazolyl blue tetrazolium reduction (MTT), yeast estrogen screen (YES) and yeast androgen screen (YAS), zebrafish embryo toxicity (*Danio rerio*) (Espíndola et al. 2019), (*Daphnia magna*, *Selenastrum capricornutum*) (Murgolo et al. 2017) and quantitative toxicogenomic-based assays can be used to determine potential estrogenic activity, cellular metabolic activity, cell viability and generally understood toxicity of CECs (Gou et al. 2014; Moreira et al. 2016; Westlund et al. 2018b; Espíndola et al. 2019). On the other hand, the international toxicity equivalency factor (I-TEF) can be used to express the toxicity of dioxins, furans and PCBs, which are sometimes formed in the AOPs (Solá-Gutiérrez et al. 2019).

One of the major concerns of AOPs is that treatments can cause an increase in toxicity due to more the toxic products

**Fig. 3** Contaminants toxicity assessment for AOP systems  
Reprinted with the kind permission of Elsevier (Sharma et al. 2018)



of oxidation processes. Even techniques that use ‘green’ reagents, e.g. UV, UV/TiO<sub>2</sub>, H<sub>2</sub>O<sub>2</sub>, O<sub>3</sub>, UV/H<sub>2</sub>O<sub>2</sub>, and UV/O<sub>3</sub>, can cause an increase in the toxicity of a processed solution, particularly ones having oxidation by-products of ACR, DCF, CBZ, TRI, TCS and 17-β-Estradiol (E2) (Kudlek et al. 2018 and Table 1). Some toxic by-products, e.g. polychlorinated dibenzo-p-dioxins and dibenzofurans (PCDD/Fs) (Solá-Gutiérrez et al. 2019), 2,4-dichlorophenol (Gou et al. 2014) determined by oxidation of TCS are extremely dangerous and persistent (Hrabák et al. 2016) and are sometimes used as a poison (e.g. PCDD/Fs was used

during an attempted poisoning of the ex-president of Ukraine—Viktor Yushchenko) (Sorg et al. 2009). On the other hand, BPA oxidation can result in a wide spectrum of stress responses, and several determined by-products possessing the phenolic or quinone group (e.g. hydroquinone, 1,4-benzoquinone) were determined and probably added to the transit toxicity displayed as membrane and DNA stress during decontamination (Gou et al. 2014). Oxidation of IBF can lead to a change in its toxicity profile from mostly membrane stress to membrane, protein and DNA stresses (Gou et al. 2014).

**Table 1** Toxicity of CECs (based on Microtox® test) in aqueous solution before and after the AOPs treatment (Non-toxic 0–25%, low toxicity 25–50%, moderate toxicity 50–75%, high toxicity 75–100%) Data taken from Kudlek et al. (2018)

	Toxic effect (%)						
	Blank	UV	H <sub>2</sub> O <sub>2</sub>	O <sub>3</sub>	UV/TiO <sub>2</sub>	UV/H <sub>2</sub> O <sub>2</sub>	UV/O <sub>3</sub>
CBZ	9.1	76.7	76.3	80.4	82.4	76.4	89.4
BE	0.0	24.3	11.3	16.8	25.7	22.4	20.7
DCF	3.2	1.2	0.0	25.0	0.2	3.7	75.6
IBP	4.0	0.2	0.0	10.0	0.1	1.7	58.0
ACR	28.7	79.8	79.2	86.4	84.1	80.7	99.3
BZ8	25.4	0.0	36.4	29.3	0.0	25.7	24.6
TRI	17.0	89.4	57.0	51.9	80.1	89.7	96.3
TCS	95.7	78.4	96.4	99.9	74.2	75.4	98.3
ODZ	0.0	63.8	23.7	63.8	53.4	54.1	64.4
E2	0.0	15.0	14.0	26.0	10.0	12.0	36.0
EE2	42.0	63.9	51.6	75.6	52.4	80.3	86.4
EEME	3.0	36.2	16.0	28.0	35.7	24.4	53.5
P4	17.5	42.9	36.8	57.7	40.4	21.4	64.0
BHT	0.0	36.0	28.0	40.0	10.0	20.0	59.0
CAF	0.3	0.3	0.9	0.8	0.3	1.0	1.0

In addition, ozonation of CECs in certain wastewaters can generate undesirable TPs (e.g. aldehydes, N-nitrosodime thylamine and bromate) or genotoxicity/cytotoxicity (Lee and von Gunten 2016; Westlund et al. 2018b), e.g. DCF and BPA after O<sub>3</sub> and O<sub>3</sub>/H<sub>2</sub>O<sub>2</sub> (Kudlek and Dudziak 2018). Another recent example was provided by Westlund et al. (2018a), who conducted two yeast-based bioassays for assessment of the endocrine activity potential of TPs generated throughout oxidation by the ozone of a pesticide mixture (ATZ, 2,4-D, propiconazole, tebuconazole, myclobutanil, climbazole, irgarol, dicamba, mecoprop, diuron and terbutryn). They showed that after oxidation the initial anti-androgenic activity was eliminated, whereas the estrogenic activity stayed as undetected and the androgenic activity increased by up to 60% compared to a blank. Shu et al. (2016) showed that UV/H<sub>2</sub>O<sub>2</sub> is not effective for the removal of acute estrogenic activity; however, it can minimise the estrogenic effects of reused water in chronic exposures. Moreover, the cytotoxicity of DCFs and TCS was not removed during the simultaneous elimination of the compounds (Huang et al. 2018b). Another example of CEC oxidation (BPA, E2 and EE2) by several UV processes (UV, UV/O<sub>3</sub>, UV/TiO<sub>2</sub>) and the subsequent evaluation of by-product toxicity was conducted by Dudziak et al. (2018). The toxicity of wastewater was assessed with the help of selected indicator organisms (bacteria, crustacea, aquatic plants) from different taxonomic groups and after the oxidation process, the wastewater was found to be toxic to one or more groups of indicator organisms. This work also emphasised the influence of an oxidised environmental matrix on the observed toxicity (Dudziak et al. 2018). Moreover, emerging oxidation techniques such as

UV/chlorine require many toxicological tests in order to confirm process safety. For example, a CEC—PDNN was degraded by UV/chlorine and the toxicity of the resulting matrix was comprehensively evaluated. Based on the performance of two toxicological tests, the post-treatment solution demonstrated much higher toxicity than PDNN itself, and an extended time of reaction was required to attain PDNN detoxification (Yin et al. 2018).

Regardless of all of these examples, most of the AOP-based remedial actions report reduction of the generally understood toxicity. Just to mention a few, H<sub>2</sub>O<sub>2</sub>-based processes can remove the toxicity of carbendazim, mono carbomethoxy guanidine, benzimidazole isocyanate, and 2-aminobenzimidazole (da Costa et al. 2019), azithromycin, NPX, atenolol, metformin, bezafibrate, IBF, TMP, CBZ, SMX, oxytetracycline and DCF (Espíndola et al. 2019, considerable reduction of the toxicity on zebrafish embryos), and 80% of the initial estrogenic activity of E1, E2, and EE2 (Cédât et al. 2016). Ozone-based processes can be used for the removal of CBZ, isoproturon, clarithromycin, norfluoxetine, fluoxetine, E2, EE2 and fluoroquinolones (in this case only antibacterial tests were performed) (Feng et al. 2018) without the formation of any products with estrogenic effects (Moreira et al. 2016). UV/chlorine can reduce estrogenic activity in spiked with E2 effluent samples (Li et al. 2016), completely reduce the toxicity (based on the luminescent bacterial assay) of dodecyl benzyl dimethyl ammonium chloride, partially reduce the toxicity (*lemna minor*) of climbazole (Cai et al. 2019) and partially reduce the biotoxicity of CIP (Deng et al. 2019), whereas an innovative UV/NO<sub>3</sub><sup>-</sup>/HCO<sub>3</sub><sup>-</sup> system can significantly reduce the



cytotoxicity of BPA (Huang et al. 2018a). Moreover,  $\cdot\text{OH}$  reactions with tris(2-chloroethyl) phosphate have resulted in lower toxicity when tested by the apoptosis of *Escherichia coli* (Chen et al. 2019).

## 5 Socioeconomic Considerations of Energy Demands and Technical and Economic Feasibility

Many studies have been performed over the past 10 years on various pilot/full-scale technologies of water and wastewater treatments for their economic and technical viability. Many of them, such as tight membrane filtration as employed in nanofiltration and reverse osmosis, were often determined to be very cost-intensive, which leaves the door open for, e.g. solar-driven AOPs (especially in some geographical areas that are highly irradiated by sun throughout the year) (Capocelli et al. 2019; Rizzo et al. 2019b). It is generally considered important to perform a cost assessment when introducing a new treatment system onto the market, and it is most often expressed as the electrical energy per order (EE/O) value, i.e. the quantity of electrical energy needed to reduce contaminant's concentration by one order of

magnitude, i.e. 90% (Bu et al. 2018). The EE/O value can be obtained for a specific AOP and relies on several aspects, i.e. its physical and chemical characteristics (e.g. reaction rate constants), the molecular structure of the pollutant, its concentration range (only if  $>1$  mg/L), process capacity, water matrix and process parameters not related to energy (for example, the dose of the catalyst or oxidant) (Miklos et al. 2018).

From the conventional AOPs, ozonation is known to be very cost-efficient and can be applied at a lower cost/power use than, for example, reverse osmosis, making the removal of CECs feasible, mainly in places where reverse osmosis treatments are not possible (Chen et al. 2017; Fig. 4).

On the contrary to  $\text{UV}/\text{H}_2\text{O}_2$ ,  $\text{O}_3/\text{H}_2\text{O}_2$  leads to undesirable and potentially toxic by-products (e.g. bromate). However, the energy consumption represented as the EE/O for the removal of CECs (90% removal) is usually around 4–20 times lower for the  $\text{O}_3/\text{H}_2\text{O}_2$  process compared to  $\text{UV}/\text{H}_2\text{O}_2$  (Katsoyiannis et al. 2011). The main cost of the  $\text{UV}/\text{H}_2\text{O}_2$  process is for the procurement of chemicals (Cédât et al. 2016); the energy required for this process could be reduced by improving the UV reactor geometry, by optimising the water matrix, by selecting the appropriate CECs (Hofman-Caris et al. 2017) and by the addition of

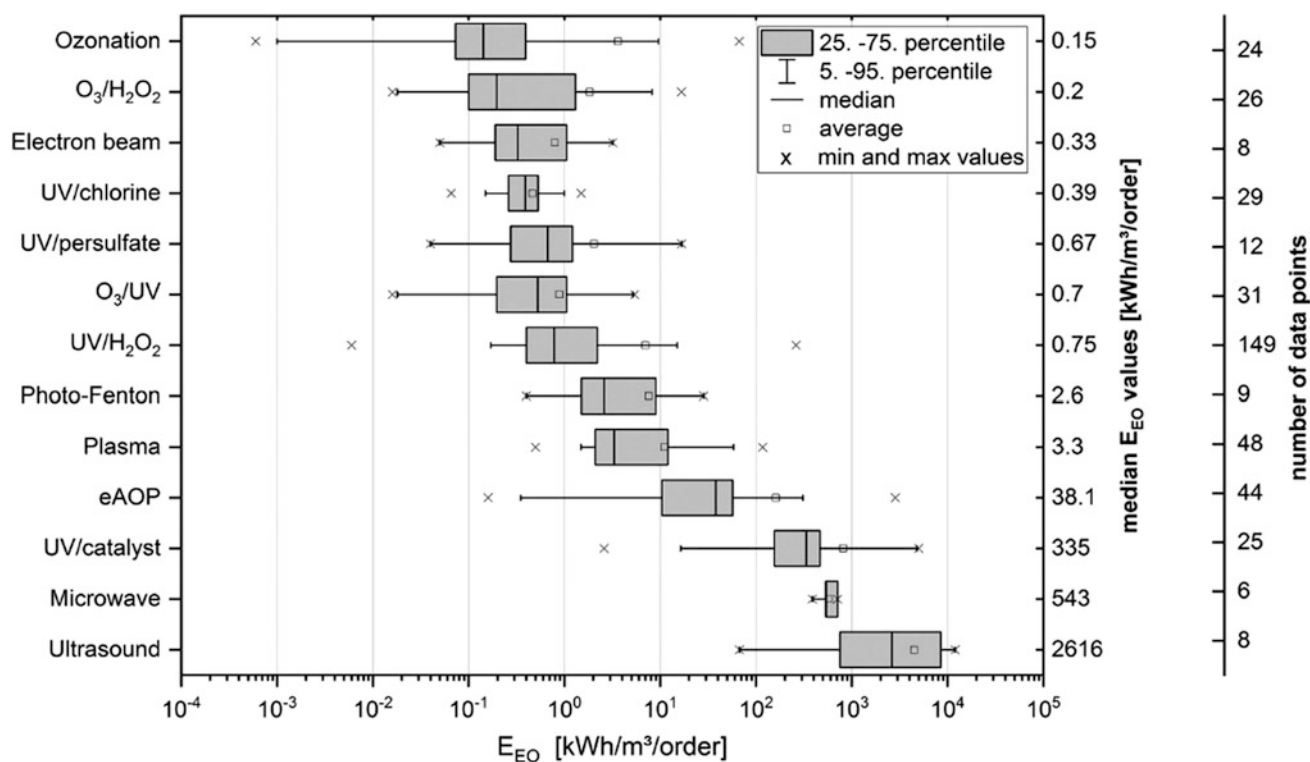


**Fig. 4** Summary of the published EE/O values of various AOPs. For data from ozone and UV-based processes, only compounds that are persistent to direct  $\text{O}_3$  and/or UV are presented. Median values and the

number of data points are presented respectively on the second and third y-axis (Miklos et al. 2018) Reprinted with the kind permission of Elsevier (Miklos et al. 2018)

H<sub>2</sub>O<sub>2</sub> to a system already irradiated by UV (Matafonova and Batoev 2017). Nonetheless, the O<sub>3</sub>/H<sub>2</sub>O<sub>2</sub> process is often used for water with lower and UV/H<sub>2</sub>O<sub>2</sub> with higher bromide concentrations (von Gunten 2018).

A study by Autin et al. (2013a) determined that although both UV-based methods (UV/TiO<sub>2</sub> and UV/H<sub>2</sub>O<sub>2</sub>) are very similar in the terms of EE/O (4.9 and 4.7 kWh/m<sup>3</sup>, respectively), the occurrence of DOM influenced the EE/O by 16% for UV/H<sub>2</sub>O<sub>2</sub> and 31% for UV/TiO<sub>2</sub>. More importantly, no change in EE/O was observed in the UV/H<sub>2</sub>O<sub>2</sub> system when carbonate ions were added, whereas there was a 5.4 times increase for the UV/TiO<sub>2</sub> process. Similar EE/O values were reported for modified and conventional TiO<sub>2</sub> for the removal of a CEC mixture (Murgolo et al. 2017). This may lead to difficulties when upscaling TiO<sub>2</sub> processes in W/WWTPs as discussed by von Gunten (2018).

One way of further improving UV/H<sub>2</sub>O<sub>2</sub> performance and cost-effectiveness is by electro-generation of H<sub>2</sub>O<sub>2</sub> (Mousset et al. 2016). In general, the EE/O of the electrochemical oxidation of CECs with boron diamond doped electrodes can range from 39.3 to 331.8 kWh/m<sup>3</sup> (Lanzarini-Lopes et al. 2017). Simultaneous electroproduction of H<sub>2</sub>O<sub>2</sub> and application of UV irradiation to enhance ozone reactions is called the E-peroxone process. This technique can decrease the consumption of energy that is needed to decontaminate chloramphenicol (by an order of magnitude) by 10–53% compared to the ozonation process alone. In comparison, the UV/O<sub>3</sub> system consumes ca. 4–10 times more energy than traditional O<sub>3</sub> treatment. It has been reported that an E-peroxone system offers a practical, effective and energy-efficient option for CEC removal and control of bromate in WWTPs (Yao et al. 2018). This theme was further reviewed by Wang et al. (2018).

Interestingly, it was determined by Zhang et al. (2016) and Guo et al. (2018a) that UV/PDS and UV/chlorine processes are less energy demanding than UV/H<sub>2</sub>O<sub>2</sub> for the degradation of sulphonamides (UV/PDS) and 16 PPCPs (UV/chlorine). Furthermore, UV/chlorine can save 3.5–93.5% and 19.1–98.1% of EE/O for PPCP removal in spiked clean aqueous and wastewater solutions, respectively (Guo et al. 2018a). However, it should be mentioned that by optimising the UV and oxidant addition, the UV/H<sub>2</sub>O<sub>2</sub> treatment can be optimised to attain higher efficiencies in comparison to the UV/PDS treatment in spiked wastewater.

Many researchers have wondered about the benefits of UV/LEDs for use in AOPs. The progress of UV-LEDs systems has been noteworthy in the past 10 years; however, the energy efficiency remains low (i.e., in the order of one to a few percents). On the whole, it is not yet clear at what extent UV/LEDs will contribute to water/wastewater treatment over the next few decades. Nevertheless, some authors have

predicted that such technologies will contribute and this may happen (enhancement of UV/H<sub>2</sub>O<sub>2</sub> and UV/TiO<sub>2</sub> processes) faster than what we expect (Autin et al. 2013b), but some LED parameters need to be improved (Autin et al. 2013b).

Another technique that has upscaling issues due to high-energy demands, among other things, is the gas-phase pulsed corona discharge, which has been examined for the elimination of CECs in several studies. The studied concentrations were as low as those found in WWTP effluents (around 5 µg/L) and a decrease of up to 97% in CBZ concentrations was obtained at a mere 0.3 kWh/m<sup>3</sup> of EE/O, and more than 99.9% was decontaminated at 1 kWh/m<sup>3</sup> (Ajo et al. 2016). Even higher EE/O was reported by Wardenier et al. (2019), who researched a continuous-flow pulsed dielectric barrier discharge reactor with a falling water film. A synthetic CEC mixture was used and under optimal conditions, EE/O was in the range of 2.4–4.2 kWh/m<sup>3</sup>, which is still approximately 2× lower than the economically practical AOPs energy cost (5 kWh/m<sup>3</sup>).

---

## 6 Conclusions and Future Prospects

Contaminants of emerging concern are gathering the attention of researchers and lawmakers due to the increased risk of their widespread use, toxicity and the toxicity of their metabolites. New analytical techniques have led to an eye-opening moment for humanity, in which many of us now realise that insufficient water and wastewater treatment can cause, in the worst case, the self-destruction of humanity and maybe the entire planet. In the last ten years, many researchers have devoted their time to studying the occurrence, fate, ecotoxicology and decontamination of CECs and the products of their (bio)degradation. Their removal by advanced oxidation processes is perhaps the most studied topic in this field. AOPs are generally very effective in the removal of CECs and the transformation products/by-products often generated in these processes. Development of novel materials for catalytic activation of commonly used oxidants can be considered as an interesting option, since many conventional AOPs do not remove the daughter products generated by them. Several countries have completely forbidden the use of AOPs in W/WWTPs for this reason. Moreover, as the remediation of CECs by AOPs are governed by the reaction kinetics and generated by-products, the development of *in silico* prediction models of the kinetics and mechanisms of reactions may not only verify the data gained in experiments but also provide precise forecasts in the future (not only assessing the chemical but also the biological properties).

Finally, in order to make AOPs more practical and applicable, chemical and environmental engineers, water scientists and microbiologists, and researchers from other related fields should work together in order to combine the existing (mainly biological) processes in wastewater treatment plants with AOPs for their synergistic treatment of contaminants present even at such low concentrations.

**Acknowledgements** This review was supported by the Ministry of Education, Youth and Sports in the framework of the targeted support of the OPR & DI project ‘Extension of CxI facilities’ (CZ.1.05/2.1.00/19.0386). The authors would also like to acknowledge the assistance provided by the Research Infrastructure NanoEnviCz, supported by the Ministry of Education, Youth and Sports of the Czech Republic under Project No. LM2015073. This work was also supported by the Ministry of Education, Youth and Sports of the Czech Republic and the European Union—European Structural and Investment Funds in the framework of the Operational Programme Research, Development and Education—project ‘Hybrid Materials for Hierarchical Structures’ (HyHi, Reg. No. CZ.02.1.01/0.0/0.0/16\_019/0000843). D. D. Dionysiou also acknowledges support from the University of Cincinnati through a UNESCO co-Chair Professor position on ‘Water Access and Sustainability’ and the Herman Schneider Professorship in the College of Engineering and Applied Sciences.

## References

- Agócs TZ, Puskás I, Varga E et al (2016) Stabilization of nanosized titanium dioxide by cyclodextrin polymers and its photocatalytic effect on the degradation of wastewater pollutants. *Beilstein J Org Chem* 12:2873–2882. <https://doi.org/10.3762/bjoc.12.286>
- Ajo P, Krzymyk E, Preis S et al (2016) Pulsed corona discharge oxidation of aqueous carbamazepine micropollutant. *Environ Technol* 37:2072–2081. <https://doi.org/10.1080/09593330.2016.1141236>
- Alsbaiee A, Smith BJ, Xiao L et al (2016) Rapid removal of organic micropollutants from water by a porous  $\beta$ -cyclodextrin polymer. *Nature* 529:190–194. <https://doi.org/10.1038/nature16185>
- Alvarez-Corena JR, Bergendahl JA, Hart FL (2016) Photocatalytic oxidation of five contaminants of emerging concern by UV/TiO<sub>2</sub>: identification of intermediates and degradation pathways. *Environ Eng Sci* 33:140–147. <https://doi.org/10.1089/ees.2015.0388>
- Anis M, Haydar S (2019) Oxidative degradation of acetaminophen by continuous flow classical Fenton process. *Desalin Water Treat* 139:166–173. <https://doi.org/10.5004/dwt.2019.23278>
- Audino F, Toro Santamaria J, del Valle Mendoza L et al (2019) Removal of paracetamol using effective advanced oxidation processes. *Int J Environ Res Public Health* 16:505. <https://doi.org/10.3390/ijerph16030505>
- Autin O, Hart J, Jarvis P et al (2013a) Comparison of UV/TiO<sub>2</sub> and UV/H<sub>2</sub>O<sub>2</sub> processes in an annular photoreactor for removal of micropollutants: influence of water parameters on metaldehyde removal, quantum yields and energy consumption. *Appl Catal B Environ* 138–139:268–275. <https://doi.org/10.1016/j.apcatb.2013.02.045>
- Autin O, Romelot C, Rust L et al (2013b) Evaluation of a UV-light emitting diodes unit for the removal of micropollutants in water for low energy advanced oxidation processes. *Chemosphere* 92:745–751. <https://doi.org/10.1016/J.CHEMOSPHERE.2013.04.028>
- Avery-Gomm S, Borrelle SB, Provencher JF (2018) Linking plastic ingestion research with marine wildlife conservation. *Sci Total Environ* 637–638:1492–1495
- Azuma T, Otomo K, Kunitou M et al (2019) Removal of pharmaceuticals in water by introduction of ozonated microbubbles. *Sep Purif Technol* 212:483–489. <https://doi.org/10.1016/j.seppur.2018.11.059>
- Bagheri M, Mohseni M (2015) A study of enhanced performance of VUV/UV process for the degradation of micropollutants from contaminated water. *J Hazard Mater* 294:1–8. <https://doi.org/10.1016/j.jhazmat.2015.03.036>
- Bagheri M, Mohseni M (2014) Computational fluid dynamics (CFD) modeling of VUV/UV photoreactors for water treatment. *Chem Eng J* 256:51–60. <https://doi.org/10.1016/J.CEJ.2014.06.068>
- Barbosa MO, Moreira NFF, Ribeiro AR et al (2016) Occurrence and removal of organic micropollutants: an overview of the watch list of EU decision 2015/495. *Water Res* 94:257–279
- Barbusinski K (2009) Fenton reaction—Controversy concerning the chemistry. *Ecol Chem Eng S/Chemia i Inz Ekol S* 16:347–358
- Biancullo F, Moreira NFF, Ribeiro AR et al (2019) Heterogeneous photocatalysis using UVA-LEDs for the removal of antibiotics and antibiotic resistant bacteria from urban wastewater treatment plant effluents. *Chem Eng J* 367:304–313. <https://doi.org/10.1016/J.CEJ.2019.02.012>
- Bieber S, Rauch-Williams T, Drewes JE (2016) An assessment of international management strategies for CECs in water. In: *ACS Symposium Series*, pp 11–22
- Borhani TNG, Saniedanesh M, Bagheri M, Lim JS (2016) QSPR prediction of the hydroxyl radical rate constant of water contaminants. *Water Res* 98:344–353. <https://doi.org/10.1016/J.WATRES.2016.04.038>
- Boyd GR, Tuccillo ME, Sandvig A et al (2013) Nanomaterials: removal processes and beneficial applications in treatment. *J Am Water Works Assoc* 105:E699–E708. <https://doi.org/10.5942/jawwa.2013.105.0154>
- Brienza M, Katsoyiannis IA (2017) Sulfate radical technologies as tertiary treatment for the removal of emerging contaminants from wastewater. *Sustain* 9:1604. <https://doi.org/10.3390/su9091604>
- Bu L, Zhou S, Zhu S et al (2018) Insight into carbamazepine degradation by UV/monochloramine: reaction mechanism, oxidation products, and DBPs formation. *Water Res* 146:288–297. <https://doi.org/10.1016/J.WATRES.2018.09.036>
- Cai W-W, Peng T, Zhang J-N et al (2019) Degradation of climbazole by UV/chlorine process: kinetics, transformation pathway and toxicity evaluation. *Chemosphere* 219:243–249. <https://doi.org/10.1016/J.CHEMOSPHERE.2018.12.023>
- Capocelli M, Prisciandaro M, Piemonte V, Barba D (2019) A technical-economical approach to promote the water treatment & reuse processes. *J Clean Prod* 207:85–96. <https://doi.org/10.1016/j.jclepro.2018.09.135>
- Carvalho IT, Santos L (2016) Antibiotics in the aquatic environments: a review of the European scenario. *Environ Int* 94:736–757
- Cédât B, de Brauer C, Métivier H et al (2016) Are UV photolysis and UV/H<sub>2</sub>O<sub>2</sub> process efficient to treat estrogens in waters? Chemical and biological assessment at pilot scale. *Water Res* 100:357–366. <https://doi.org/10.1016/j.watres.2016.05.040>
- Chen Y, Ye J, Chen Y et al (2019) Degradation kinetics, mechanism and toxicology of tris(2-chloroethyl) phosphate with 185 nm vacuum ultraviolet. *Chem Eng J* 356:98–106. <https://doi.org/10.1016/J.CEJ.2018.09.007>
- Chen Z, Li M, Wen Q, Ren N (2017) Evolution of molecular weight and fluorescence of effluent organic matter (EfOM) during oxidation processes revealed by advanced spectrographic and chromatographic tools. *Water Res* 124:566–575. <https://doi.org/10.1016/J.WATRES.2017.08.006>
- Cheng Z, Yang B, Chen Q et al (2018) 2D-QSAR and 3D-QSAR simulations for the reaction rate constants of organic compounds in ozonone-hydrogen peroxide oxidation. *Chemosphere* 212:828–836. <https://doi.org/10.1016/J.CHEMOSPHERE.2018.08.097>

- Crutzen PJ, Waclawek S (2014) Atmospheric chemistry and climate in the anthropocene/Chemia Atmosferyczna I Klimat W Antropocenie. *Chem Didact Ecol Metrol* 19:9–28. <https://doi.org/10.1515/cdem-2014-0001>
- Cvetnić M, Novak Stankov M, Kovačić M et al (2019) Key structural features promoting radical driven degradation of emerging contaminants in water. *Environ Int* 124:38–48. <https://doi.org/10.1016/j.envint.2018.12.043>
- da Costa EP, Bottrel SEC, Starling MCV et al (2019) Degradation of carbendazim in water via photo-fenton in raceway pond reactor: assessment of acute toxicity and transformation products. *Environ Sci Pollut Res* 26:4324–4336. <https://doi.org/10.1007/s11356-018-2130-z>
- da Trindade CM, da Silva SW, Bortolozzi JP et al (2018) Synthesis and characterization of TiO<sub>2</sub> films onto AISI 304 metallic meshes and their application in the decomposition of the endocrine-disrupting alkylphenolic chemicals. *Appl Surf Sci* 457:644–654. <https://doi.org/10.1016/j.apsusc.2018.06.287>
- De la Cruz N, Giménez J, Esplugas S et al (2012) Degradation of 32 emergent contaminants by UV and neutral photo-fenton in domestic wastewater effluent previously treated by activated sludge. *Water Res* 46:1947–1957. <https://doi.org/10.1016/j.watres.2012.01.014>
- de Vera GA, Gernjak W, Weinberg H et al (2017) Kinetics and mechanisms of nitrate and ammonium formation during ozonation of dissolved organic nitrogen. *Water Res* 108:451–461. <https://doi.org/10.1016/j.watres.2016.10.021>
- Deng J, Wu G, Yuan S et al (2019) Ciprofloxacin degradation in UV/chlorine advanced oxidation process: influencing factors, mechanisms and degradation pathways. *J Photochem Photobiol A Chem* 371:151–158. <https://doi.org/10.1016/j.jphotochem.2018.10.043>
- Deniere E, Van Hulle S, Van Langenhove H, Demeestere K (2018) Advanced oxidation of pharmaceuticals by the ozone-activated peroxymonosulfate process: the role of different oxidative species. *J Hazard Mater* 360:204–213. <https://doi.org/10.1016/j.jhazmat.2018.07.071>
- Dhiman P, Naushad M, Batoo KM et al (2017) Nano Fe<sub>x</sub>Zn<sub>1-x</sub>O as a tuneable and efficient photocatalyst for solar powered degradation of bisphenol A from aqueous environment. *J Clean Prod* 165:1542–1556. <https://doi.org/10.1016/j.jclepro.2017.07.245>
- Drewes JE, Letzel T (2016) Chemicals of emerging concern and their transformation products in the aqueous environment. In: ACS Symposium Series, pp 3–9
- Duan X, Sanan T, de la Cruz A et al (2018) Susceptibility of the algal toxin microcystin-LR to UV/chlorine process: comparison with chlorination. *Environ Sci Technol* 52:8252–8262. <https://doi.org/10.1021/acs.est.8b00034>
- Dudziak M (2015) Microtox as a tool to evaluate unfavourable phenomenon occurrences during micropollutants decompositions in AOPs. *ACEE Arch Civ Eng Environ* 8:85–90
- Dudziak M, Kudlek E, Burdzik-Niemiec E (2018) Decomposition of micropollutants and changes in the toxicity of water matrices subjected to various oxidation processes. *Desalin Water Treat* 117:181–187. <https://doi.org/10.5004/dwt.2018.22233>
- Ertl G, Zielńska M, Rajfur M, Waclawek M (2017) Elementary steps in heterogeneous catalysis: the basis for environmental chemistry. *Chem Didact Ecol Metrol* 22:11–41. <https://doi.org/10.1515/cdem-2017-0001>
- Espíndola JC, Cristóvão RO, Araújo SRF et al (2019) An innovative photoreactor, FluHelix, to promote UVC/H<sub>2</sub>O<sub>2</sub> photochemical reactions: tertiary treatment of an urban wastewater. *Sci Total Environ* 667:197–207. <https://doi.org/10.1016/j.scitotenv.2019.02.335>
- EU (2013) Directive 2013/39/EU of the European Parliament and of the Council of 12 August 2013. *Off J Eur Union L* 226/1-L 226/17
- EU Water Framework Directive (2000) Directive 2000/60/EC of the European Parliament and of the Council of 23 October 2000 establishing a framework for community action in the field of water policy. *Off J Eur Parliam L* 327:1–82. <https://doi.org/10.1039/ap9842100196>
- European Commission (2015) Commission Implementing Decision (EU) 2015/495 of 20 March 2015 establishing a watch list of substances for Union-wide monitoring in the field of water policy pursuant to Directive 2008/105/EC of the European Parliament and of the Council Off J Eur Union L78/40:20–30. [http://eur-lex.europa.eu/pri/en/oj/dat/2003/l\\_285/l\\_28520031101en00330037.pdf](http://eur-lex.europa.eu/pri/en/oj/dat/2003/l_285/l_28520031101en00330037.pdf)
- Feng M, Wang Z, Dionysiou DD, Sharma VK (2018) Metal-mediated oxidation of fluoroquinolone antibiotics in water: a review on kinetics, transformation products, and toxicity assessment. *J Hazard Mater* 344:1136–1154. <https://doi.org/10.1016/j.jhazmat.2017.08.067>
- Fenton HJH (1894) LXXIII—Oxidation of tartaric acid in presence of iron. *J Chem Soc Trans* 65:899–910. <https://doi.org/10.1039/CT8946500899>
- Foster JE (2017) Plasma-based water purification: challenges and prospects for the future. *Phys Plasmas* 24:055501. <https://doi.org/10.1063/1.4977921>
- Foster JE, Mujovic S, Groele J, Blankson IM (2018) Towards high throughput plasma based water purifiers: design considerations and the pathway towards practical application. *J Phys D Appl Phys* 51:293001. <https://doi.org/10.1088/1361-6463/aac816>
- Fu Y, Wu G, Geng J et al (2019) Kinetics and modeling of artificial sweeteners degradation in wastewater by the UV/persulfate process. *Water Res* 150:12–20. <https://doi.org/10.1016/j.watres.2018.11.051>
- Gao Z-C, Lin Y-L, Xu B et al (2017) Degradation of acrylamide by the UV/chlorine advanced oxidation process. *Chemosphere* 187:268–276. <https://doi.org/10.1016/j.chemosphere.2017.08.085>
- Ge L, Na G, Chen C-E et al (2016) Aqueous photochemical degradation of hydroxylated PAHs: kinetics, pathways, and multivariate effects of main water constituents. *Sci Total Environ* 547:166–172. <https://doi.org/10.1016/j.scitotenv.2015.12.143>
- Giannakis S, Hendaoui I, Jovic M et al (2017a) Solar photo-Fenton and UV/H<sub>2</sub>O<sub>2</sub> processes against the antidepressant Venlafaxine in urban wastewaters and human urine. Intermediates formation and biodegradability assessment. *Chem Eng J* 308:492–504. <https://doi.org/10.1016/j.cej.2016.09.084>
- Giannakis S, Jovic M, Gasilova N et al (2017b) Iohexol degradation in wastewater and urine by UV-based advanced oxidation processes (AOPs): process modeling and by-products identification. *J Environ Manage* 195:174–185. <https://doi.org/10.1016/j.jenvman.2016.07.004>
- Gomes J, Costa R, Quinta-Ferreira RM, Martins RC (2017) Application of ozonation for pharmaceuticals and personal care products removal from water. *Sci Total Environ* 586:265–283. <https://doi.org/10.1016/j.scitotenv.2017.01.216>
- Gómez Bernal H, Benito P, Rodríguez-Castellón E et al (2019) Synthesis of isopropyl levulinate from furfural: insights on a cascade production perspective. *Appl Catal A Gen* 575:111–119. <https://doi.org/10.1016/j.apcata.2019.02.018>
- Gorito AM, Ribeiro AR, Almeida CMR, Silva AMT (2017) A review on the application of constructed wetlands for the removal of priority substances and contaminants of emerging concern listed in recently launched EU legislation. *Environ Pollut* 227:428–443
- Gou N, Yuan S, Lan J et al (2014) A quantitative toxicogenomics assay reveals the evolution and nature of toxicity during the transformation of environmental pollutants. *Environ Sci Technol* 48:8855–8863. <https://doi.org/10.1021/es501222t>
- Guo K, Wu Z, Yan S et al (2018a) Comparison of the UV/chlorine and UV/H<sub>2</sub>O<sub>2</sub> processes in the degradation of PPCPs in simulated

- drinking water and wastewater: kinetics, radical mechanism and energy requirements. *Water Res* 147:184–194. <https://doi.org/10.1016/J.WATRES.2018.08.048>
- Guo K, Zhang J, Li A et al (2018b) Ultraviolet irradiation of permanganate enhanced the oxidation of micropollutants by producing HO• and reactive manganese species. *Environ Sci Technol Lett* 5:750–756. <https://doi.org/10.1021/acs.estlett.8b00402>
- Guo Y, Wang H, Wang B et al (2018c) Prediction of micropollutant abatement during homogeneous catalytic ozonation by a chemical kinetic model. *Water Res* 142:383–395. <https://doi.org/10.1016/J.WATRES.2018.06.019>
- Gupta S, Basant N (2017a) Modeling the aqueous phase reactivity of hydroxyl radical towards diverse organic micropollutants: an aid to water decontamination processes. *Chemosphere* 185:1164–1172. <https://doi.org/10.1016/J.CHEMOSPHERE.2017.07.057>
- Gupta S, Basant N (2017b) Modeling the pH and temperature dependence of aqueous phase hydroxyl radical reaction rate constants of organic micropollutants using QSPR approach. *Environ Sci Pollut Res* 24:24936–24946. <https://doi.org/10.1007/s11356-017-0161-5>
- Gupta VK, Fakhri A, Azad M, Agarwal S (2017) Synthesis of CdSe quantum dots decorated SnO<sub>2</sub> nanotubes as anode for photo-assisted electrochemical degradation of hydrochlorothiazide: kinetic process. *J Colloid Interface Sci* 508:575–582. <https://doi.org/10.1016/J.JCIS.2017.08.083>
- Heeb MB, Criquet J, Zimmermann-Steffens SG, von Gunten U (2014) Oxidative treatment of bromide-containing waters: formation of bromine and its reactions with inorganic and organic compounds—A critical review. *Water Res* 48:15–42. <https://doi.org/10.1016/J.WATRES.2013.08.030>
- Hernández-Colorado PP, Pinto S, Morales-Mejia JC et al (2017) Photocatalytic oxidation of aqueous naproxen with a horizontally placed solar CPC slurry reactor. *Desalin Water Treat* 67:159–167. <https://doi.org/10.5004/dwt.2017.20382>
- Hofman-Caris CHM, Harmsen DJH, Van Remmen AM et al (2017) Optimization of UV/H<sub>2</sub>O<sub>2</sub> processes for the removal of organic micropollutants from drinking water: effect of reactor geometry and water pretreatment on EEO values. *Water Sci Technol Water Supply* 17:508–518. <https://doi.org/10.2166/ws.2016.160>
- Hofman-Caris CHMHM, Harmsen DJH, Beerendonk EF et al (2012) Prediction of advanced oxidation performance in pilot UV/H<sub>2</sub>O<sub>2</sub> reactor systems with MP- and LP-UV lamps. *Ozone Sci Eng* 34:120–124. <https://doi.org/10.1080/01919512.2011.650598>
- Hrabák P, Homolková M, Waclawek S, Černík M (2016) Chemical degradation of PCDD/F in contaminated sediment. *Ecol Chem Eng S* 23:473–482. <https://doi.org/10.1515/eces-2016-0034>
- Huang Y, Kong M, Westerman D et al (2018a) Effects of HCO<sub>3</sub><sup>-</sup> on degradation of toxic contaminants of emerging concern by UV/NO<sub>3</sub><sup>-</sup>. *Environ Sci Technol* 52:12697–12707. <https://doi.org/10.1021/acs.est.8b04383>
- Huang Y, Liu Y, Kong M et al (2018b) Efficient degradation of cytotoxic contaminants of emerging concern by UV/H<sub>2</sub>O<sub>2</sub>. *Environ Sci Water Res Technol* 4:1272–1281. <https://doi.org/10.1039/c8ew00290h>
- Jia L, Shen Z, Guo W et al (2015) QSAR models for oxidative degradation of organic pollutants in the Fenton process. *J Taiwan Inst Chem Eng* 46:140–147. <https://doi.org/10.1016/J.JTICE.2014.09.014>
- Jiménez-Tototzintle M, Ferreira IJ, da Silva Duque S et al (2018) Removal of contaminants of emerging concern (CECs) and antibiotic resistant bacteria in urban wastewater using UVA/TiO<sub>2</sub>/H<sub>2</sub>O<sub>2</sub> photocatalysis. *Chemosphere* 210:449–457. <https://doi.org/10.1016/J.CHEMOSPHERE.2018.07.036>
- Jin X, Peldszus S, Huck PM (2012) Reaction kinetics of selected micropollutants in ozonation and advanced oxidation processes. *Water Res* 46:6519–6530. <https://doi.org/10.1016/J.WATRES.2012.09.026>
- Jin X, Peldszus S, Huck PM (2015) Predicting the reaction rate constants of micropollutants with hydroxyl radicals in water using QSPR modeling. *Chemosphere* 138:1–9. <https://doi.org/10.1016/J.CHEMOSPHERE.2015.05.034>
- Jin X, Peldszus S, Sparkes DI (2014) Modeling ozone reaction rate constants of micropollutants using quantitative structure-property relationships. *Ozone Sci Eng* 36:289–302. <https://doi.org/10.1080/01919512.2014.910444>
- Katsoyiannis IA, Canonica S, von Gunten U (2011) Efficiency and energy requirements for the transformation of organic micropollutants by ozone, O<sub>3</sub>/H<sub>2</sub>O<sub>2</sub> and UV/H<sub>2</sub>O<sub>2</sub>. *Water Res* 45:3811–3822. <https://doi.org/10.1016/j.watres.2011.04.038>
- Khan MF, Yu L, Achari G, Tay JH (2019) Degradation of sulfolane in aqueous media by integrating activated sludge and advanced oxidation process. *Chemosphere* 222:1–8. <https://doi.org/10.1016/J.CHEMOSPHERE.2019.01.097>
- Kim T-H, Lee S-H, Kim HY et al (2019) Decomposition of perfluorooctane sulfonate (PFOS) using a hybrid process with electron beam and chemical oxidants. *Chem Eng J* 361:1363–1370. <https://doi.org/10.1016/j.cej.2018.10.195>
- Kolosov P, Peyot M-L, Yargeau V (2018) Novel materials for catalytic ozonation of wastewater for disinfection and removal of micropollutants. *Sci Total Environ* 644:1207–1218. <https://doi.org/10.1016/J.SCITOTENV.2018.07.022>
- Kolosov P, Yargeau V (2019) Impact of catalyst load, chemical oxygen demand and nitrite on disinfection and removal of contaminants during catalytic ozonation of wastewater. *Sci Total Environ* 651:2139–2147. <https://doi.org/10.1016/J.SCITOTENV.2018.09.394>
- Koltsakidou A, Terzopoulou Z, Kyzas G et al (2019) Biobased poly(ethylene furanoate) polyester/TiO<sub>2</sub> supported nanocomposites as effective photocatalysts for anti-inflammatory/analgesic drugs. *Molecules* 24:564. <https://doi.org/10.3390/molecules24030564>
- Krzeminski P, Tomei MC, Karaolia P et al (2019) Performance of secondary wastewater treatment methods for the removal of contaminants of emerging concern implicated in crop uptake and antibiotic resistance spread: a review. *Sci Total Environ* 648:1052–1081
- Kudlek E, Dudziak M (2018) Toxicity and degradation pathways of selected micropollutants in water solutions during the O<sub>3</sub> and O<sub>3</sub>/H<sub>2</sub>O<sub>2</sub> process. *Desalin Water Treat* 117:88–100. <https://doi.org/10.5004/dwt.2018.22096>
- Kudlek E, Kudlek Edyta (2018) Decomposition of contaminants of emerging concern in advanced oxidation processes. *Water* 10:955. <https://doi.org/10.3390/w10070955>
- Kudlek E, Silvestri D, Waclawek S et al (2017) TiO<sub>2</sub> immobilised on biopolymer nanofibers for the removal of bisphenol A and diclofenac from water. *Ecol Chem Eng S* 24:417–429. <https://doi.org/10.1515/eces-2017-0028>
- Kümmerer K (2011) Emerging contaminants versus micro-pollutants. *CLEAN—Soil Air Water* 39:889–890. <https://doi.org/10.1002/clen.201110002>
- Kümmerer K, Dionysiou DD, Olsson O, Fatta-Kassinos D (2019) Reducing aquatic micropollutants—Increasing the focus on input prevention and integrated emission management. *Sci Total Environ* 652:836–850. <https://doi.org/10.1016/j.scitotenv.2018.10.1219>
- Lado Ribeiro AR, Moreira NFF, Li Puma G, Silva AMT (2019) Impact of water matrix on the removal of micropollutants by advanced oxidation technologies. *Chem Eng J* 363:155–173. <https://doi.org/10.1016/j.cej.2019.01.080>
- Lanzarini-Lopes M, Garcia-Segura S, Hristovski K, Westerhoff P (2017) Electrical energy per order and current efficiency for electrochemical oxidation of p-chlorobenzoic acid with

- boron-doped diamond anode. *Chemosphere* 188:304–311. <https://doi.org/10.1016/J.CHEMOSPHERE.2017.08.145>
- Lecours M-A, Eysseric E, Yargeau V et al (2018) Electrochemistry-high resolution mass spectrometry to study oxidation products of trimethoprim. *Environmets* 5:18. <https://doi.org/10.3390/environmets5010018>
- Lee H, Park SH, Kim BH et al (2012) Contribution of dissolved oxygen to methylene blue decomposition by hybrid advanced oxidation processes system. *Int J Photoenergy* 2012:1–6. <https://doi.org/10.1155/2012/305989>
- Lee M, Zimmermann-Steffens SG, Arey JS et al (2015) Development of prediction models for the reactivity of organic compounds with ozone in aqueous solution by quantum chemical calculations: the role of delocalized and localized molecular orbitals. *Environ Sci Technol* 49:9925–9935. <https://doi.org/10.1021/acs.est.5b00902>
- Lee Y, von Gunten U (2016) Advances in predicting organic contaminant abatement during ozonation of municipal wastewater effluent: reaction kinetics, transformation products, and changes of biological effects. *Environ Sci Water Res Technol* 2:421–442. <https://doi.org/10.1039/C6EW00025H>
- Lee Y, von Gunten U (2012) Quantitative structure–activity relationships (QSARs) for the transformation of organic micropollutants during oxidative water treatment. *Water Res* 46:6177–6195. <https://doi.org/10.1016/J.WATRES.2012.06.006>
- Li C, Sun Z, Dong X et al (2018) Acetic acid functionalized TiO<sub>2</sub>/kaolinite composite photocatalysts with enhanced photocatalytic performance through regulating interfacial charge transfer. *J Catal* 367:126–138. <https://doi.org/10.1016/j.jcat.2018.09.001>
- Li M, Xu B, Liungai Z et al (2016) The removal of estrogenic activity with UV/chlorine technology and identification of novel estrogenic disinfection by-products. *J Hazard Mater* 307:119–126. <https://doi.org/10.1016/J.JHAZMAT.2016.01.003>
- Li X, Wang B, Wang Y et al (2019) Synergy effect of E-peroxone process in the degradation of structurally diverse pharmaceuticals: a QSAR analysis. *Chem Eng J* 360:1111–1118. <https://doi.org/10.1016/J.CEJ.2018.10.191>
- Liang R, Van Leuwen JC, Bragg LM et al (2019) Utilizing UV-LED pulse width modulation on TiO<sub>2</sub> advanced oxidation processes to enhance the decomposition efficiency of pharmaceutical micropollutants. *Chem Eng J* 361:439–449. <https://doi.org/10.1016/j.cej.2018.12.065>
- Lin L, Jiang W, Bechelany M et al (2019) Adsorption and photocatalytic oxidation of ibuprofen using nanocomposites of TiO<sub>2</sub> nanofibers combined with BN nanosheets: degradation products and mechanisms. *Chemosphere* 220:921–929. <https://doi.org/10.1016/j.chemosphere.2018.12.184>
- Liu C, Li P, Tang X, Korshin GV (2016) Ozonation effects on emerging micropollutants and effluent organic matter in wastewater: characterization using changes of three-dimensional HP-SEC and EEM fluorescence data. *Environ Sci Pollut Res* 23:20567–20579. <https://doi.org/10.1007/s11356-016-7287-8>
- Liu Z, Zhao C, Wang P et al (2018) Removal of carbamazepine in water by electro-activated carbon fiber-peroxydisulfate: comparison, optimization, recycle, and mechanism study. *Chem Eng J* 343:28–36. <https://doi.org/10.1016/j.cej.2018.02.114>
- Longobucco G, Pasti L, Molinari A et al (2017) Photoelectrochemical mineralization of emerging contaminants at porous WO<sub>3</sub> interfaces. *Appl Catal B Environ* 204:273–282. <https://doi.org/10.1016/J.APCATB.2016.11.007>
- Martín-Sómer M, Pablos C, de Diego A et al (2019) Novel macroporous 3D photocatalytic foams for simultaneous wastewater disinfection and removal of contaminants of emerging concern. *Chem Eng J* 366:449–459. <https://doi.org/10.1016/j.cej.2019.02.102>
- Martín de Vidales MJ, Nieto-Márquez A, Morcuende D et al (2019) 3D printed floating photocatalysts for wastewater treatment. *Catal Today* 328:157–163. <https://doi.org/10.1016/j.cattod.2019.01.074>
- Martínez S, Morales-Mejía JC, Hernández PP et al (2014) Solar photocatalytic oxidation of triclosan with tio<sub>2</sub> immobilized on volcanic porous stones on a CPC pilot scale reactor. *Energy Procedia* 57:3014–3020. <https://doi.org/10.1016/J.EGYPRO.2014.10.337>
- Matafonova G, Batoev V (2017) Comparison of energy requirements for removal of organic micropollutants from lake water and wastewater effluents by direct UV and UV/H<sub>2</sub>O<sub>2</sub> using excilamp. *Desalin Water Treat* 85:92–102. <https://doi.org/10.5004/dwt.2017.21245>
- Mathon B, Coquery M, Miegé C et al (2017) Removal efficiencies and kinetic rate constants of xenobiotics by ozonation in tertiary treatment. *Water Sci Technol* 75:2737–2746. <https://doi.org/10.2166/wst.2017.114>
- Metheniti ME, Frontistis Z, Ribeiro RS et al (2018) Degradation of propyl paraben by activated persulfate using iron-containing magnetic carbon xerogels: investigation of water matrix and process synergy effects. *Environ Sci Pollut Res* 25:34801–34810. <https://doi.org/10.1007/s11356-017-0178-9>
- Miklos DB, Remy C, Jekel M et al (2018) Evaluation of advanced oxidation processes for water and wastewater treatment—A critical review. *Water Res* 139:118–131. <https://doi.org/10.1016/J.WATRES.2018.03.042>
- Do Minh T, Neibi MC, Srivastava V et al (2019) Gingerbread ingredient-derived carbons-assembled CNT foam for the efficient peroxymonosulfate-mediated degradation of emerging pharmaceutical contaminants. *Appl Catal B Environ* 244:367–384. <https://doi.org/10.1016/j.apcatb.2018.11.064>
- Molinari A, Sarti E, Marchetti N, Pasti L (2017) Degradation of emerging concern contaminants in water by heterogeneous photocatalysis with Na<sub>4</sub>W<sub>10</sub>O<sub>32</sub>. *Appl Catal B Environ* 203:9–17. <https://doi.org/10.1016/j.apcatb.2016.09.031>
- Moreira NFF, Narciso-da-Rocha C, Polo-López MI et al (2018) Solar treatment (H<sub>2</sub>O<sub>2</sub>, TiO<sub>2</sub>-P25 and GO-TiO<sub>2</sub> photocatalysis, photo-Fenton) of organic micropollutants, human pathogen indicators, antibiotic resistant bacteria and related genes in urban wastewater. *Water Res* 135:195–206. <https://doi.org/10.1016/J.WATRES.2018.01.064>
- Moreira NFF, Sampaio MJ, Ribeiro AR et al (2019) Metal-free g-C<sub>3</sub>N<sub>4</sub> photocatalysis of organic micropollutants in urban wastewater under visible light. *Appl Catal B Environ* 248:184–192. <https://doi.org/10.1016/J.APCATB.2019.02.001>
- Moreira NFF, Sousa JM, Macedo G et al (2016) Photocatalytic ozonation of urban wastewater and surface water using immobilized TiO<sub>2</sub> with LEDs: micropollutants, antibiotic resistance genes and estrogenic activity. *Water Res* 94:10–22. <https://doi.org/10.1016/J.WATRES.2016.02.003>
- Moussé E, Wang Z, Lefebvre O (2016) Electro-Fenton for control and removal of micropollutants—process optimization and energy efficiency. *Water Sci Technol* 74:2068–2074. <https://doi.org/10.2166/wst.2016.353>
- Murgolo S, Yargeau V, Gerbasi R et al (2017) A new supported TiO<sub>2</sub> film deposited on stainless steel for the photocatalytic degradation of contaminants of emerging concern. *Chem Eng J* 318:103–111. <https://doi.org/10.1016/j.cej.2016.05.125>
- Nihemaiti M, Miklos DB, Hübner U et al (2018) Removal of trace organic chemicals in wastewater effluent by UV/H<sub>2</sub>O<sub>2</sub> and UV/PDS. *Water Res* 145:487–497. <https://doi.org/10.1016/J.WATRES.2018.08.052>
- Oliveira HG, Ferreira LH, Bertazzoli R, Longo C (2015) Remediation of 17- $\alpha$ -ethinylestradiol aqueous solution by photocatalysis and electrochemically-assisted photocatalysis using TiO<sub>2</sub> and TiO<sub>2</sub>/

- WO<sub>3</sub> electrodes irradiated by a solar simulator. *Water Res* 72:305–314. <https://doi.org/10.1016/J.WATRES.2014.08.042>
- Ortiz EV, Bennardi DO, Babelo DE et al (2017) The conformation-independent QSPR approach for predicting the oxidation rate constant of water micropollutants. *Environ Sci Pollut Res* 24:27366–27375. <https://doi.org/10.1007/s11356-017-0315-5>
- Palma D, Bianco Prevot A, Brigante M et al (2018) New insights on the photodegradation of caffeine in the presence of bio-based substances-magnetic iron oxide hybrid nanomaterials. *Mater (Basel)* 11:1084. <https://doi.org/10.3390/ma11071084>
- Pelaez M, Nolan NT, Pillai SC et al (2012) A review on the visible light active titanium dioxide photocatalysts for environmental applications. *Appl Catal B Environ* 125:331–349
- Pérez-Moya M, Kaisto T, Navarro M, del Valle LJ (2017) Study of the degradation performance (TOC, BOD, and toxicity) of bisphenol A by the photo-Fenton process. *Environ Sci Pollut Res* 24:6241–6251. <https://doi.org/10.1007/s11356-016-7386-6>
- Plakas KV, Sklari SD, Yiankakis DA et al (2016) Removal of organic micropollutants from drinking water by a novel electro-Fenton filter: pilot-scale studies. *Water Res* 91:183–194. <https://doi.org/10.1016/J.WATRES.2016.01.013>
- Plantard G, Goetz V (2012) Experimental and numerical studies of a solar photocatalytic process in a dynamic mode applied to three catalyst media. *Chem Eng Process Process Intensif* 62:129–136. <https://doi.org/10.1016/J.CEP.2012.08.002>
- Psutka JM, Dion-Fortier A, Dieckmann T et al (2018) Identifying Fenton-reacted trimethoprim transformation products using differential mobility spectrometry. *Anal Chem* 90:5352–5357. <https://doi.org/10.1021/acs.analchem.8b00484>
- Rahman SM, Eckelman MJ, Onnis-Hayden A, Gu AZ (2018) Comparative life cycle assessment of advanced wastewater treatment processes for removal of chemicals of emerging concern 52:11346–11358. <https://doi.org/10.1021/acs.est.8b00036>
- Ranjbar-Mohammadi M, Bahrani SH (2016) Electrospun curcumin loaded poly( $\epsilon$ -caprolactone)/gum tragacanth nanofibers for biomedical application. *Int J Biol Macromol* 84:448–456. <https://doi.org/10.1016/j.ijbiomac.2015.12.024>
- Ren B, Han C, Al Anazi AH et al (2013) Iron-based nanomaterials for the treatment of emerging environmental contaminants. *ACS Symp Ser* 1150:135–146. <https://doi.org/10.1021/bk-2013-1150.ch008>
- Restivo J, Órfão JJM, Pereira MFR et al (2013) Catalytic ozonation of organic micropollutants using carbon nanofibers supported on monoliths. *Chem Eng J* 230:115–123. <https://doi.org/10.1016/j.cej.2013.06.064>
- Řezanka M, Langton MJ, Beer PD (2015) Anion recognition in water by a rotaxane containing a secondary rim functionalised cyclodextrin stoppered axle. *Chem Commun* 51:4499–4502. <https://doi.org/10.1039/C5CC00171D>
- Rice RG, Robson CM, Miller GW, Hill AG (1981) Uses of ozone in drinking water treatment. *J Am Water Work Assoc* 73:44–57. <https://doi.org/10.2307/41270552>
- Rizzo L, Agovino T, Nahim-Granados S et al (2019a) Tertiary treatment of urban wastewater by solar and UV-C driven advanced oxidation with peracetic acid: effect on contaminants of emerging concern and antibiotic resistance. *Water Res* 149:272–281. <https://doi.org/10.1016/J.WATRES.2018.11.031>
- Rizzo L, Malato S, Antakyali D et al (2019b) Consolidated vs new advanced treatment methods for the removal of contaminants of emerging concern from urban wastewater. *Sci Total Environ* 655:986–1008. <https://doi.org/10.1016/J.SCITOTENV.2018.11.265>
- Rodríguez-Chueca J, Laski E, García-Cañibano C et al (2018) Micropollutants removal by full-scale UV-C/sulfate radical based advanced oxidation processes. *Sci Total Environ* 630:1216–1225. <https://doi.org/10.1016/J.SCITOTENV.2018.02.279>
- Salimi M, Esrafil A, Gholami M et al (2017) Contaminants of emerging concern: a review of new approach in AOP technologies. *Environ Monit Assess* 189:414. <https://doi.org/10.1007/s10661-017-6097-x>
- Schwarzenbach RP, Escher BI, Fenner K et al (2006) The challenge of micropollutants in aquatic systems. *Science* 313:1072–1077
- Serna-Galvis EA, Botero-Coy AM, Martínez-Pachón D et al (2019) Degradation of seventeen contaminants of emerging concern in municipal wastewater effluents by sonochemical advanced oxidation processes. *Water Res* 154:349–360. <https://doi.org/10.1016/J.WATRES.2019.01.045>
- Sharma A, Ahmad J, Flora SJS (2018) Application of advanced oxidation processes and toxicity assessment of transformation products. *Environ Res* 167:223–233. <https://doi.org/10.1016/J.ENVRES.2018.07.010>
- Shu Z, Singh A, Klammerth N, et al (2016) Application of the UV/H<sub>2</sub>O<sub>2</sub> advanced oxidation process for municipal reuse water: bench- and pilot-scale studies. In: *Water Pollution XIII*. WP, pp 233–244
- Singh RR, Lester Y, Linden KG et al (2015a) Application of metabolite profiling tools and time-of-flight mass spectrometry in the identification of transformation products of iopromide and iopamidol during advanced oxidation. *Environ Sci Technol* 49:2983–2990. <https://doi.org/10.1021/es505469h>
- Singh S, Seth R, Tabe S, Yang P (2015b) Oxidation of emerging contaminants during pilot-scale ozonation of secondary treated municipal effluent. *Ozone Sci Eng* 37:323–329. <https://doi.org/10.1080/01919512.2014.998755>
- Solá-Gutiérrez C, Schröder S, San Román MF, Ortiz I (2019) PCDD/Fs traceability during triclosan electrochemical oxidation. *J Hazard Mater* 369:584–592. <https://doi.org/10.1016/J.JHAZMAT.2019.02.066>
- Sorg O, Zennegg M, Schmid P et al (2009) 2,3,7,8-tetrachlorodibenzo-p-dioxin (TCDD) poisoning in Victor Yushchenko: identification and measurement of TCDD metabolites. *Lancet* 374:1179–1185. [https://doi.org/10.1016/S0140-6736\(09\)60912-0](https://doi.org/10.1016/S0140-6736(09)60912-0)
- Soriano-Molina P, Plaza-Bolaños P, Lorenzo A et al (2019) Assessment of solar raceway pond reactors for removal of contaminants of emerging concern by photo-Fenton at circumneutral pH from very different municipal wastewater effluents. *Chem Eng J* 366:141–149. <https://doi.org/10.1016/j.cej.2019.02.074>
- Su H, Yu C, Zhou Y et al (2018) Quantitative structure–activity relationship for the oxidation of aromatic organic contaminants in water by TAML/H<sub>2</sub>O<sub>2</sub>. *Water Res* 140:354–363. <https://doi.org/10.1016/J.WATRES.2018.04.062>
- Sudhakaran S, Amy GL (2013) QSAR models for oxidation of organic micropollutants in water based on ozone and hydroxyl radical rate constants and their chemical classification. *Water Res* 47:1111–1122. <https://doi.org/10.1016/J.WATRES.2012.11.033>
- Sudhakaran S, Calvin J, Amy GL (2012) QSAR models for the removal of organic micropollutants in four different river water matrices. *Chemosphere* 87:144–150. <https://doi.org/10.1016/J.CHEMOSPHERE.2011.12.006>
- Sundaram V, Emerick RW, Shumaker SE (2014) Advanced treatment process for pharmaceuticals, endocrine disruptors, and flame retardants removal. *Water Environ Res* 86:111–122. <https://doi.org/10.2175/106143013X13807328849053>
- Tasca AL, Puccini M, Fletcher A (2018) Terbutylazine and desethyl-terbutylazine: recent occurrence, mobility and removal techniques.

- Chemosphere 202:94–104. <https://doi.org/10.1016/J.CHEMOSPHERE.2018.03.091>
- Tentscher PR, Lee M, von Gunten U (2019) Micropollutant oxidation studied by quantum chemical computations: methodology and applications to thermodynamics, kinetics, and reaction mechanisms. *Acc Chem Res* 52:605–614. <https://doi.org/10.1021/acs.accounts.8b00610>
- Teodosiu C, Gilca AF, Barjoveanu G, Fiore S (2018) Emerging pollutants removal through advanced drinking water treatment: a review on processes and environmental performances assessment. *J Clean Prod* 197:1210–1221
- TF (Task force on emerging contaminants) (2018) Plan for addressing critical research gaps related to emerging contaminants in drinking water
- Tiedeken EJ, Tahar A, McHugh B, Rowan NJ (2017) Monitoring, sources, receptors, and control measures for three European Union watch list substances of emerging concern in receiving waters—A 20 year systematic review. *Sci Total Environ* 574:1140–1163
- Tsitonaki A, Petri B, Crimi M et al (2010) In situ chemical oxidation of contaminated soil and groundwater using persulfate: a review. *Crit Rev Environ Sci Technol* 40:55–91. <https://doi.org/10.1080/10643380802039303>
- United States. Congress. Senate. Committee on Appropriations (2018) Departments of commerce and justice, science, and related agencies appropriations bill
- Urbano VR, Maniero MG, Pérez-Moya M, Guimarães JR (2017) Influence of pH and ozone dose on sulfaquinoxaline ozonation. *J Environ Manage* 195:224–231. <https://doi.org/10.1016/J.JENVMAN.2016.08.019>
- Van Wezel AP, Ter Laak TL, Fischer A et al (2017) Mitigation options for chemicals of emerging concern in surface waters operationalising solutions-focused risk assessment. *Environ Sci Water Res Technol* 3:403–414. <https://doi.org/10.1039/c7ew00077d>
- Vandenberg LN, Colborn T, Hayes TB et al (2012) Hormones and endocrine-disrupting chemicals: low-dose effects and nonmonotonic dose responses. *Endocr Rev* 33:378–455. <https://doi.org/10.1210/er.2011-1050>
- von Gunten U (2018) Oxidation processes in water treatment: are we on track? *Environ Sci Technol* 52:5062–5075. <https://doi.org/10.1021/acs.est.8b00586>
- von Gunten U (2003) Ozonation of drinking water: part I. Oxidation kinetics and product formation. *Water Res* 37:1443–1467. [https://doi.org/10.1016/S0043-1354\(02\)00457-8](https://doi.org/10.1016/S0043-1354(02)00457-8)
- von Sonntag C, von Gunten U (2012) Chemistry of ozone in water and wastewater treatment
- Vries D, Wols BA, de Voogt P (2013) Removal efficiency calculated beforehand: QSAR enabled predictions for nanofiltration and advanced oxidation. *Water Sci Technol Water Supply* 13:1425–1436. <https://doi.org/10.2166/ws.2013.109>
- Waclawek S, Lutze HV, Grübel K et al (2017) Chemistry of persulfates in water and wastewater treatment: a review. *Chem Eng J* 330:44–62. <https://doi.org/10.1016/j.cej.2017.07.132>
- Waclawek S, Padil VVT, Černík M (2018) Major advances and challenges in heterogeneous catalysis for environmental applications: a review. *Ecol Chem Eng S* 25:9–34. <https://doi.org/10.1515/ECES-2018-0001>
- Wang A-Q, Xu B, Zhang T-Y et al (2017) Effect of UV irradiation and UV/chlorine processes on trichloronitromethane formation during chlorination of ronidazole. *CLEAN—Soil Air Water* 45:1600163. <https://doi.org/10.1002/clen.201600163>
- Wang Y, Yu G, Deng S et al (2018) The electro-peroxone process for the abatement of emerging contaminants: mechanisms, recent advances, and prospects. *Chemosphere* 208:640–654. <https://doi.org/10.1016/J.CHEMOSPHERE.2018.05.095>
- Wardenier N, Vanraes P, Nikiforov A et al (2019) Removal of micropollutants from water in a continuous-flow electrical discharge reactor. *J Hazard Mater* 362:238–245. <https://doi.org/10.1016/J.JHAZMAT.2018.08.095>
- Westlund P, Isazadeh S, Therrien A, Yargeau V (2018a) Endocrine activities of pesticides during ozonation of waters. *Bull Environ Contam Toxicol* 100:112–119. <https://doi.org/10.1007/s00128-017-2254-8>
- Westlund P, Isazadeh S, Yargeau V (2018b) Investigating the androgenic activity of ozonation transformation products of testosterone and androstenedione. *J Hazard Mater* 342:492–498. <https://doi.org/10.1016/J.JHAZMAT.2017.08.032>
- Willach S, Lutze HV, Eckey K et al (2017) Degradation of sulfamethoxazole using ozone and chlorine dioxide—Compound-specific stable isotope analysis, transformation product analysis and mechanistic aspects. *Water Res* 122:280–289. <https://doi.org/10.1016/J.WATRES.2017.06.001>
- Wols BA, Harmsen DJH, Beerendonk EF, Hofman-Caris CHM (2014) Predicting pharmaceutical degradation by UV (LP)/H<sub>2</sub>O<sub>2</sub> processes: a kinetic model. *Chem Eng J* 255:334–343. <https://doi.org/10.1016/j.cej.2014.05.088>
- Wols BA, Hofman-Caris CHM (2012) Modelling micropollutant degradation in UV/H<sub>2</sub>O<sub>2</sub> systems: Lagrangian versus Eulerian method. *Chem Eng J* 210:289–297. <https://doi.org/10.1016/j.cej.2012.08.088>
- Wols BA, Hofman-Caris CHM, Harmsen DJH, Beerendonk EF (2013) Degradation of 40 selected pharmaceuticals by UV/H<sub>2</sub>O<sub>2</sub>. *Water Res* 47:5876–5888. <https://doi.org/10.1016/J.WATRES.2013.07.008>
- Wu G, Qin W, Sun L et al (2019a) Role of peroxymonosulfate on enhancing ozonation for micropollutant degradation: performance evaluation, mechanism insight and kinetics study. *Chem Eng J* 360:115–123. <https://doi.org/10.1016/J.CEJ.2018.11.183>
- Wu Y, Deng L, Bu L et al (2019b) Degradation of diethyl phthalate (DEP) by vacuum ultraviolet process: influencing factors, oxidation products, and toxicity assessment. *Environ Sci Pollut Res* 26:5435–5444. <https://doi.org/10.1007/s11356-018-3914-x>
- Wu Z, Guo K, Fang J et al (2017) Factors affecting the roles of reactive species in the degradation of micropollutants by the UV/chlorine process. *Water Res* 126:351–360. <https://doi.org/10.1016/J.WATRES.2017.09.028>
- Xiang W, Zhang B, Zhou T et al (2016) An insight in magnetic field enhanced zero-valent iron/H<sub>2</sub>O<sub>2</sub> Fenton-like systems: critical role and evolution of the pristine iron oxides layer. *Sci Rep* 6:24094. <https://doi.org/10.1038/srep24094>
- Xiao R, Ye T, Wei Z et al (2015) Quantitative structure-activity relationship (QSAR) for the oxidation of trace organic contaminants by sulfate radical. *Environ Sci Technol* 49:13394–13402. <https://doi.org/10.1021/acs.est.5b03078>
- Yang Y, Hu A, Wang X et al (2019) Nanopore enriched hollow carbon nitride nanospheres with extremely high visible-light photocatalytic activity in the degradation of aqueous contaminants of emerging concern. *Catal Sci Technol* 9:355–365. <https://doi.org/10.1039/C8CY02073F>
- Yang Y, Ok YS, Kim K-H et al (2017) Occurrences and removal of pharmaceuticals and personal care products (PPCPs) in drinking water and water/sewage treatment plants: a review. *Sci Total Environ* 596–597:303–320. <https://doi.org/10.1016/J.SCITOTENV.2017.04.102>
- Yao W, Ur Rehman SW, Wang H et al (2018) Pilot-scale evaluation of micropollutant abatements by conventional ozonation, UV/O<sub>3</sub>, and



- an electro-peroxone process. *Water Res* 138:106–117. <https://doi.org/10.1016/j.watres.2018.03.044>
- Yao Y, Teng G, Yang Y et al (2019) Electrochemical oxidation of acetamiprid using Yb-doped PbO<sub>2</sub> electrodes: electrode characterization, influencing factors and degradation pathways. *Sep Purif Technol* 211:456–466. <https://doi.org/10.1016/j.seppur.2018.10.021>
- Yargeau V, Danylo F (2015) Removal and transformation products of ibuprofen obtained during ozone- and ultrasound-based oxidative treatment. *Water Sci Technol* 72:491–500. <https://doi.org/10.2166/wst.2015.234>
- Yin K, He Q, Liu C et al (2018) Prednisolone degradation by UV/chlorine process: influence factors, transformation products and mechanism. *Chemosphere* 212:56–66. <https://doi.org/10.1016/J.CHEMOSPHERE.2018.08.032>
- Yuan S, Gou N, Alshwabkeh AN, Gu AZ (2013) Efficient degradation of contaminants of emerging concerns by a new electro-Fenton process with Ti/MMO cathode. *Chemosphere* 93:2796–2804. <https://doi.org/10.1016/J.CHEMOSPHERE.2013.09.051>
- Zhang R, Wang X, Zhou L et al (2018) The impact of dissolved oxygen on sulfate radical-induced oxidation of organic micro-pollutants: a theoretical study. *Water Res* 135:144–154. <https://doi.org/10.1016/J.WATRES.2018.02.028>
- Zhang R, Yang Y, Huang C-H et al (2016) Kinetics and modeling of sulfonamide antibiotic degradation in wastewater and human urine by UV/H<sub>2</sub>O<sub>2</sub> and UV/PDS. *Water Res* 103:283–292. <https://doi.org/10.1016/J.WATRES.2016.07.037>
- Zhang S, Yu G, Chen J et al (2017) Elucidating ozonation mechanisms of organic micropollutants based on DFT calculations: taking sulfamethoxazole as a case. *Environ Pollut* 220:971–980. <https://doi.org/10.1016/J.ENVPOL.2016.10.076>

# Biochar for Water and Soil Remediation: Production, Characterization, and Application

Hao Zheng, Chenchen Zhang, Bingjie Liu, Guocheng Liu, Man Zhao, Gongdi Xu, Xianxiang Luo, Fengmin Li, and Baoshan Xing

## Abstract

Water and soil pollution has caused serious global concerns due to their detrimental effect on ecological security and health risks. Remediation of the contaminated water and soil to rehabilitate their ecological functions is urgently needed to ensure sustainable food production and water supply. As a novel multifunctional carbonaceous material, biochar (BC), recognized for its potential roles in carbon sequestration, waste biomass management, bioenergy production, soil improvement, greenhouse gas emission reduction, and crop productivity enhancement, is highly recommended as an amendment for water and soil remediation. This chapter summarizes the feedstock and technologies for BC production, formation, and characterization, systematically reviews the current research findings on the roles of BC in removing inorganic contaminants (e.g., heavy metals, oxyanions) and organic contaminants (e.g., pesticides, antibiotics) from water, and extensively discusses BC application in remediation of soil contaminated with

metals and organic pollutants. The stability of BC and its priming effects on native soil organic matter when used in soil carbon sequestration is also reviewed, as are the limitations and risks associated with applying it to environmental remediation. Additionally, existing knowledge gaps and future directions regarding water and soil remediation are identified. This information will be useful for the development and application of BC-based technologies in water and soil remediation.

## Keywords

Biochar • Pyrolysis • Sorption • Soil remediation • Carbon sequestration

## 1 Introduction

Water and soil pollution by inorganic (e.g., heavy metals (HMs)) and organic contaminants (e.g., pesticides, and antibiotics), two primary global environmental issues, has significantly increased over the last decades (Wang et al. 2019; Vilela et al. 2018; Kuppusamy et al. 2016; Panasiuk et al. 2015; MEP 2014; Sun et al. 2018; Gong et al. 2016). The pollution has substantially decreased sustainable supplies of water and deteriorate soil for food production, and has largely threatened global food security for the growing population, likely to increase to 9 billion by roughly the middle of this century (Godfray et al. 2010). Water and soil pollution also presents harm to ecological security and health risks to humans. As such, meeting the goals of food security and human health is a major challenge, and has attracted significant global attention from both government regulatory agencies and the general public (Vilela et al. 2018; MEP 2014; Gong et al. 2016). Remediation of the contaminated water and soil to rehabilitate their ecological functions and to ensure sustainable water supply and food production is urgently needed, which has provided strong incentives to develop alternative, cost-effective, and environmental-friendly

H. Zheng (✉) · C. Zhang · B. Liu · M. Zhao · X. Luo · F. Li  
Key Laboratory of Marine Environment and Ecology, Institute of Coastal Environmental Pollution Control, Ministry of Education, Institute for Advanced Ocean Study, Ocean University of China, Qingdao, 266100, China  
e-mail: zhenghao2013@ouc.edu.cn

H. Zheng · X. Luo · F. Li  
Laboratory for Marine Ecology and Environmental Science, Qingdao National Laboratory for Marine Science and Technology, Qingdao, 266237, China

C. Zhang · M. Zhao · G. Xu  
College of Ecology and Environment, Hainan Tropical Ocean University, Sanya, 572022, China

G. Liu  
College of Resource and Environment, Qingdao Agricultural University, Qingdao, 266109, China

B. Xing (✉)  
Stockbridge School of Agriculture, University of Massachusetts, Amherst, MA 01003, USA  
e-mail: bx@umass.edu

technologies for remediating the contaminants in water and soil (Song et al. 2017; Sarwar et al. 2017; Wu et al. 2019b; Yang et al. 2019). Conversion of biomass into biochar (BC) provides a promising approach for this endeavor.

BC is a solid carbonaceous material which is produced from heating biomass in the absence of or with limited air to above 250 °C. It was originally intended for application in carbon (C) sequestration and soil improvement, but has now expanded to environmental management (Lehmann and Joseph 2015; IBI 2012). BC has a long history in soil application (Glaser et al. 2001; Lehmann 2009). The history of BC is associated with the discovery of “Terra Preta di indio” (also called Amazonian Dark Earths) in Amazonia, where the dark earth soils (accounting for ~10% of Amazonia) were created via intentional addition of BC using the technique of slash-and-char (Lehmann 2009). The dark earth soils have sustained high fertilities for hundreds to thousands of years (Glaser et al. 2001). This discovery inspired scientists to purposefully manufacture BC with modern artificial techniques in order to rebuild the ancient agricultural miracle in Amazonia. The feedstock of BC includes various biomasses, especially waste and low-value biomass such as agricultural straw, livestock manure, wood chips, and sawdust (Cao et al. 2009; Keiluweit et al. 2010; Zimmerman 2010; Wang et al. 2015b; Yang and Jiang 2014; Liu and Zhang 2009). Thus, BC production may achieve the target of resource utilization of this waste biomass, a value-added process. Moreover, by-products such as bio-oil and syngas can be captured and used as bioenergy during BC production (Liu et al. 2017). BC, similar to activated C (AC), possesses a large specific surface area, porous structure abundant surface functional groups, and can be used as sorbent or passivator for removal or immobilization of inorganic and organic pollutants from water or soil (Tan et al. 2016b; Zheng et al. 2013c, 2019a; Liu et al. 2018b; Yuan et al. 2019; O’Connor et al. 2018). Because of these benefits, such as improving soil quality, abating climate change, mitigating greenhouse gas (GHG) (e.g., CO<sub>2</sub>, CH<sub>4</sub>, and N<sub>2</sub>O) emissions, remediating water and soil pollution, managing and utilizing waste biomass, and generating bioenergy (e.g., bio-oil, syngas), BC technology has attracted public interest over the past decade (Sohi 2012; Abiven et al. 2014; Marris 2006; Woolf et al. 2010; Lehmann 2007). Recently, growing studies have recommended BC as a management tool for linking environmental management and bioenergy production beyond soil improvement and C sequestration (Woolf et al. 2010; Yuan et al. 2019; Xiao et al. 2018; O’Connor et al. 2018).

Publications including “BC” in the topic and title have remarkably increased from 2005 to 2019 (Fig. 1). Among these studies, the numbers of publications containing “water

& BC” and “soil & BC” in the topic (accounting for 40.0 and 59.4% of the total publications) and title (accounting for 5.76 and 34.6% of the total publications) also showed notably increasing trends. The growing interest in BC research has highlighted the promising prospect of BC application in water and soil remediation. These studies have extensively showed that BC can be used in different aspects of water and soil remediation for various contaminants. In addition, BC properties are dependent on feedstock and heating conditions, affecting its performance in remediation. A good understanding of BC properties from different feedstock using different thermal treatments is critical for ensuring its successful application in water or soil remediation. This chapter reviews the feedstock and technologies for BC production, formation process and characterization in the first section, presents a systematic analysis of current research findings on the roles of BC in removing inorganic contaminants (HMs, oxyanions) and organic contaminants from water in the second section, and summarizes BC application in the remediation of contaminated soil and BC-based C sequestration in the third section. Finally, the limitations of BC application for environmental remediation are discussed and future perspectives are proposed.

---

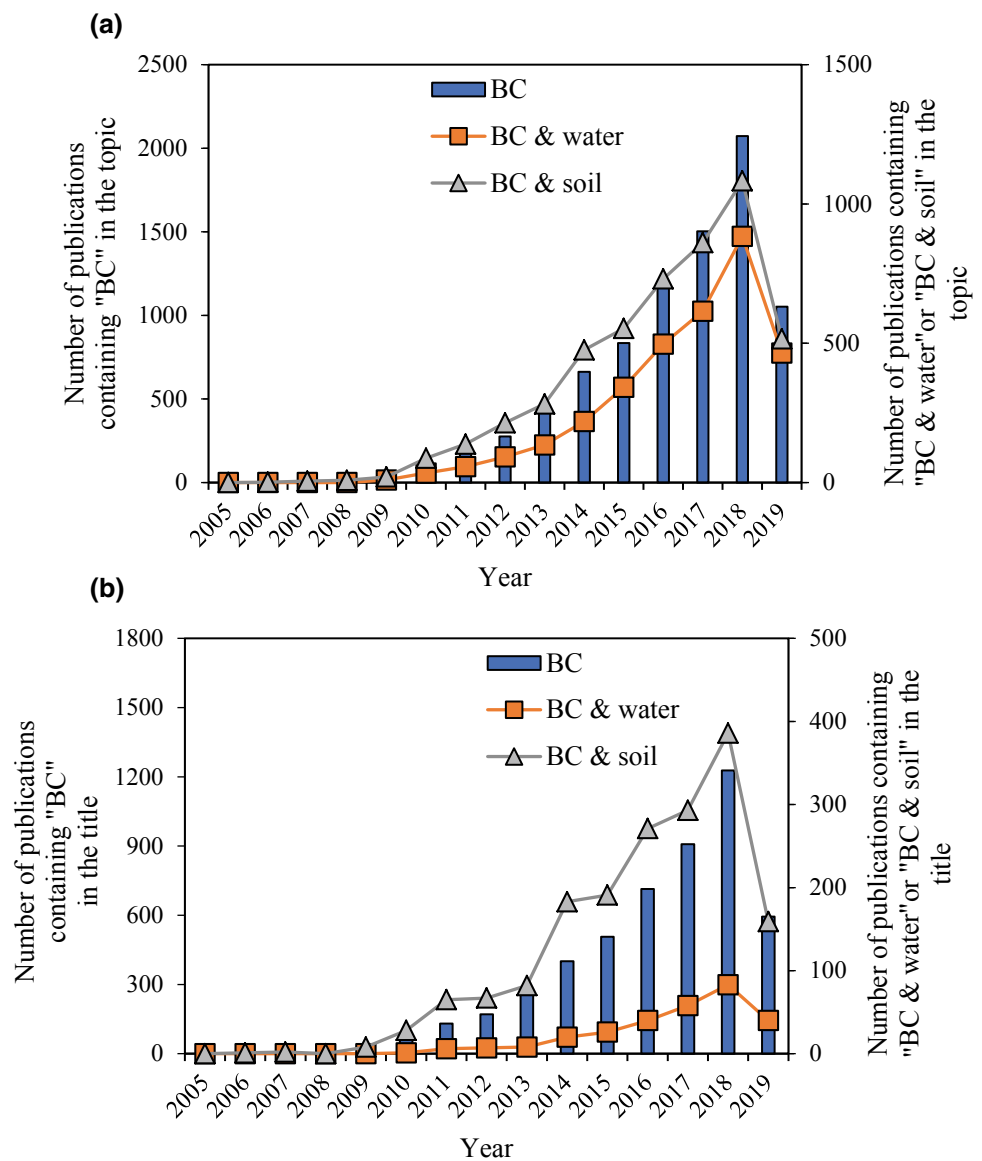
## 2 Production, Formation, and Characterization of BC

### 2.1 BC Production

#### 2.1.1 Feedstock for BC Production

The type of parent feedstock is one of the key factors controlling BC physicochemical characteristics because of the difference in chemical and structural compositions of biomass, generally containing cellulose, hemicellulose, lignin, and minerals (Li et al. 2016b; Manyà 2012). The waste biomass reported as BC’s feedstock include agricultural waste (e.g., straw, livestock manure) (Cao et al. 2009; Keiluweit et al. 2010; Liu and Zhang 2009), forest residuals (e.g., wood chips, sawdust) (Zimmerman 2010; Wang et al. 2015b; Yang and Jiang 2014), industrial by-products (e.g., sugarcane bagasse, sewage sludge, waste paper, and furfural residue) (Liu et al. 2018a; Nie et al. 2018; Chen et al. 2018d; Gao et al. 2019), and residuals of algae and seaweed (Choi et al. 2014; De Bhowmick et al. 2018). Among these biomass wastes, agricultural waste (e.g., straw and animal manure) and forestry residues (e.g., bark, chips, sawdust) are two commonly used feedstock. The high moisture content in animal manure (e.g., swine manure) usually limits its employment in BC production using pyrolysis technology. Low moisture of 5–20% is advisable for BC production

**Fig. 1** Number of publications in scientific journals searched from ISI Web of Knowledge (<http://apps.webofknowledge.com>) with the terms “BC”, “BC & water”, and “BC & soil” contained in the topic (a) and title (b) between 2005 and 2019, respectively. The data were collected on May 23, 2019



using pyrolysis due to its economic feasibility (Tripathi et al. 2016). Industrial byproducts show low calorific values alongside difficulty and considerable cost in handling, transport and storage. Using them as feedstock to produce BC is a potential means of achieving the goal of recycling organic waste and mitigating the environmental problems that waste produces (Liu et al. 2018a; Nie et al. 2018; Chen et al. 2018d; Gao et al. 2019). Interest in the pyrolysis of algae to produce valuable biofuels and BC has increased in past years (Boakye et al. 2019; Son et al. 2018; De Bhowmick et al. 2018; Yu et al. 2017; Bird et al. 2011, 2012). The properties of algae-derived BC are similar to those produced from animal manure, which has a higher level of ash content, higher pH value, and lower surface area and C content compared to those of the lignocellulose-derived BC (Son et al. 2018; Bird et al. 2012). However, literature regarding

the algal production and application of BC remains very limited at the time of writing, which largely impedes the development of any algae-based BC technology. As a result, more studies are needed to produce and utilize BC from a diverse type of algae biomass. It is a big challenge to produce BC from various potential biomasses with different characteristics for specific purposes. As such, selecting appropriate feedstock for BC production is critical to ensure its successful application in soil or water remediation. In principle, any biomass resources can be used as feedstock to produce BC, although the yield of BC, bio-oil, and syngas varies greatly (Yu et al. 2017; Manyà 2012). From the perspective of management and resource utilization of solid waste, use of waste biomass for BC production is practical and highly recommended. Moreover, the application of waste feedstock does not result in competition with food and

energy crops for arable land, whose sustainability has been seriously threatened by its degradation and reduction (Koch et al. 2012; Lambin and Meyfroidt 2011). Therefore, the reasonable selection and sustainable supply of biomass is a critical precondition for BC production and application, which should be carefully considered as those in bioenergy production.

### 2.1.2 Technologies for BC Production

BC is rarely the sole product of biomass, and is usually a co- or byproduct of bioenergy production from biomass materials (Liu et al. 2015b; Meyer et al. 2011). Consequently, numerous thermochemical technologies for bioenergy production can be used for BC production. The summary of thermochemical technologies is given in Table 1, including slow pyrolysis, fast pyrolysis, flash pyrolysis, microwave pyrolysis, and gasification. It is well known that the yields and properties of the BC, bio-oil, and syngas are controlled by parameters such as temperature, heating rate, and residence time (Tan et al. 2016b; Zheng et al. 2013b; Liu et al. 2015a; Karunanayake et al. 2017). For example, slow pyrolysis, a conventional technology with a slow heating rate (approximately  $1\text{--}10\text{ }^{\circ}\text{C min}^{-1}$ ) and long duration time (hours to days), is commonly used in BC production due to the maximum BC yield and less organic contaminants like polycyclic aromatic hydrocarbons (PAHs) compared to other processes (e.g., fast pyrolysis and gasification) (Zheng et al. 2013b; Hale et al. 2012). Flash pyrolysis could be an interesting option for BC production because of the much shorter reaction time (less than 30 min) than conventional slow pyrolysis (hours to days). Microwave pyrolysis is a promising alternative to conventional pyrolysis for BC and biofuel production because of its fast heating rate, selective, volumetric, and uniform heating (Dong et al. 2018; Li et al. 2016b). Many studies have been well reviewed on development of microwave pyrolysis techniques for production of bio-oil and syngas (Macquarrie et al. 2012; Motasemi and Afzal 2013). Recently, Li et al. (2016b) provided a review of BC production and characterization using microwave pyrolysis of biomass. BC derived from microwave pyrolysis generally has higher yield (e.g., up to 60.9%) and higher surface area than that from conventional pyrolysis (Li et al. 2016b; Mamaeva et al. 2016). Additionally, drying biomass may not be an essential pretreatment during microwave pyrolysis, because water content in biomass can increase the heating rate of biomass in the microwave reactor (Macquarrie et al. 2012). Still, the technical and economic assessments of BC production using microwave pyrolysis from various biomasses are needed in the future. Last but not least, more attention should be paid to the balance between energy input and output for an environmentally or economically sustainable BC production using the technologies in Table 1.

## 2.2 BC Formation from Pyrolysis

In order to effectively regulate the morphology, porosity, and functionality of the resulting BC for different applications, it is necessary to fully understand the conversion process of biomass during BC formation (Liu et al. 2017). The decomposition of biomass components (e.g., cellulose, hemicellulose, lignin, alkali, and alkaline earth metallic elements) under charring starts at different temperatures (Mohan et al. 2006; Liu et al. 2017; Zheng et al. 2018a). Hemicellulose is the first to decompose at about  $200\text{--}260\text{ }^{\circ}\text{C}$ , producing many volatile compound, and few tars and chars. With pyrolytic temperature increasing to  $240\text{--}350\text{ }^{\circ}\text{C}$ , cellulose starts to break down to produce anhydrocellulose and levoglucosan. Lignin is relatively stable compared to hemicelluloses and cellulose, and usually decomposes at  $280\text{--}500\text{ }^{\circ}\text{C}$ , with a maximum rate of decay being observed at  $350\text{--}450\text{ }^{\circ}\text{C}$ . Formation of BC from overall decomposition of biomass in slow pyrolysis is depicted in Fig. 2, showing three stages of reactions varied with increasing heating temperature during biomass pyrolysis (Lian and Xing 2017). Briefly, for the first stage of pyrolysis, the mass loss is mainly contributed to conversion of the most unstable fractions by rearrangement or fragmentation including dehydration, bond breakage, appearance of free radicals, and formation of carbonyl and carboxyl groups. In this stage, hemicellulose has the most severe mass loss compared to cellulose and lignin. At the second stage, the maximum weight loss is observed during the pyrolysis process as temperature continuously increases with the bond between the monomer units of biopolymers undergoing depolymerization and leading to the decrease of polymerization degree in chains until the produced molecules become volatile. The anhydrosugars can be degraded by dehydration and fission reactions that are promoted by acidic or basic catalysts. In this process, hemicellulose still has the highest rate of mass loss, while cellulose and lignin start to degrade, and the production of BC and ash increases (Liu et al. 2017). At the third stage, a large amount of the original elements including oxygen (O), hydrogen (H), nitrogen (N), and sulfur (S) are eliminated, and carbon (C) is likely to be the majority substance remaining as a residual solid. The residual solid decomposes at a very slow rate and benzene rings are condensed into polycyclic structures, forming BC with more graphitic structure (Liu et al. 2017).

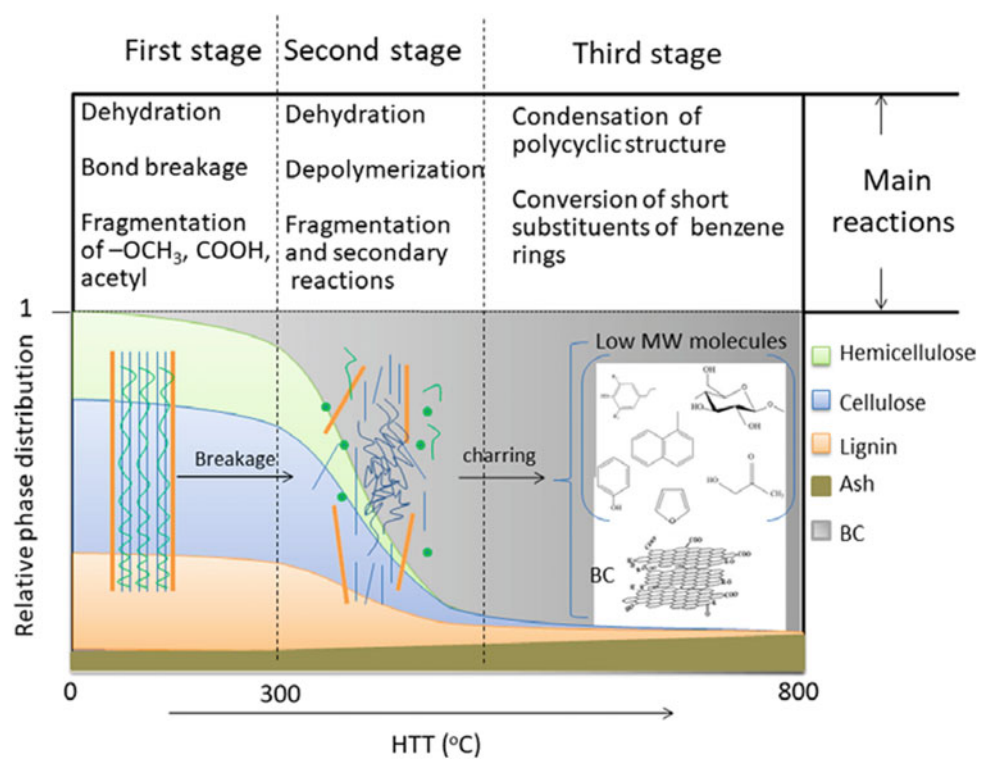
## 2.3 BC Characteristics

BC originating from different biomasses using different technologies may show distinct characteristics (Manyà 2012; Xiao et al. 2018), which may directly and indirectly affect its functionality in environmental remediations (Yuan et al.

**Table 1** Comparison of thermal technologies used to produce BC

Technology	Heating temperature (°C)	Heating rate	Residence time	BC yield (%)	Bio-oil yield (%)	Syngas yield (%)	Major intended product	Reference
Slow pyrolysis	300–800	1–10 °C min <sup>-1</sup>	Hours to days	15–40	20–55	20–35	BC	Tan et al. (2016b), Zheng et al. (2013b), Liu et al. (2015a)
Fast pyrolysis	400–1000	>300 °C min <sup>-1</sup>	0.5–60 s	10–30	50–70	5–15	Bio-oil	Karunanayake et al. (2017), Liu et al. (2015a)
Flash pyrolysis	400–1000	~ 1000 °C min <sup>-1</sup>	<30 min	30–40	0–10	60–70	Syngas and BC	Liu et al. (2015a), Manyà (2012), Meyer et al. (2011)
Microwave pyrolysis	550–700	0.1–1000 °C s <sup>-1</sup>	900–1200 s	~ 34	~ 42	~ 24	Bio-oil	Dong et al. (2018), Li et al. (2016b)
Gasification	500–1800	50–100 °C s <sup>-1</sup>	10–20 s	0–10	0–10	90–100	Syngas	Cheah et al. (2014), Kambo and Dutta (2015)

**Fig. 2** Three stages of reactions varied with increasing heating temperature during biomass pyrolysis for biochar production. This figure is cited from Lian and Xing (2017), with permission from the publisher



2019; Sun et al. 2018; Dai et al. 2019; Peiris et al. 2017). Determining BC’s characteristics is not only important for developing engineered remediation solutions, but also for understanding its behavior, fate, and risk in the environment.

**2.3.1 Elemental Composition**

BC is mainly composed of C, H, O, N, and mineral elements, all originate from biomass feedstock (Zheng et al. 2013b; Liu et al. 2018a; Liu et al. 2017; Xu et al. 2017). These elements are the fundamental building blocks of BCs, and the roles of these multiple elements endow BC with unique structures and functions (Xiao et al. 2018). These

elements in biomass also substantially affect the reactions of dehydration, demethylation, and decarboxylation during pyrolysis (Keiluweit et al. 2010), forming different species and products (Liu et al. 2017) and contributing to the diversity of BCs (Xiao et al. 2018; Liu et al. 2015a). Clearly, C, H, O, and N are the most common elements and have different mass percentages, whereas other elements such as Si, N, P, S, and Fe showed a wide range of mass percentages in different BCs (Xiao et al. 2018; El-Naggar et al. 2019; Zhang et al. 2019). BC’s elemental compositions are largely dependent on the nature of biomass feedstock and pyrolytic temperature, which has been well reviewed by many

researchers (Xiao et al. 2018; Xu et al. 2017; Liu et al. 2017; Lian and Xing 2017; Liu et al. 2019; El-Naggar et al. 2019). It is worth noting that the bulk organic C (OC) can be used to grade BC into three classes, i.e., class 1 BC (OC content  $\geq 60\%$ ), class 2 BC ( $30\% \leq$  OC content  $< 60\%$ ), and class 3 BC ( $10\% \leq$  OC content  $< 30\%$ ) (IBI 2012). Selecting BC for a specific application is largely dependent on these elemental compositions. For example, BC with a high content of stable C that was produced from high temperature (e.g.,  $\geq 500$  °C) is recommended as a promising material for C sequestration (Zimmerman 2010; Singh et al. 2012), while BC containing high levels of O has the ability of complexation with metal ions (Yang et al. 2019; O'Connor et al. 2018). For total N, its content increases and then slightly decreases with increasing pyrolysis temperature (Zheng et al. 2013b), and peptide-N bonds in biomass transform to N-heteroaromatic C compounds with form of pyrrole-N, amide-N, and pyridine-N (Liu et al. 2019; Zheng et al. 2013b; Liu et al. 2017). Compared with the bulk elemental content, the surficial elemental composition and contents of BC are more critical factors affecting its properties and interaction with contaminants in environmental remediation. Lian and Xing (2017) proposed that 300–400 °C can be considered as the temperature boundary to estimate the changes of bulk and surficial O/C ratios for the plant-derived BC. Moreover, the surficial elemental compositions may determine surface functional groups, charge, and hydrophilicity or hydrophobicity of BC, greatly influencing BC's reactivity and functionality in environmental remediation (Pignatello et al. 2017). For instance, complexation with O-containing functional groups (e.g.,  $-\text{COOH}$ , alcoholic-OH, or phenolic-OH groups) is involved in HM sorption by BC (Wang et al. 2015d; Lu et al. 2012). Additionally, various inorganic elements such as Si, N, P, S, and Fe in BC are also feedstock- and temperature-dependent (Zheng et al. 2013b; Xu et al. 2017; Xiao et al. 2014). They also markedly affect the corresponding role, function, and application of BC (Xiao et al. 2018; Xu et al. 2017; El-Naggar et al. 2019). Although these inorganic elements in BC received less attention in the past, research on them is increasing recently (Xu et al. 2017). Inorganic elements such as P, K, Ca, and Mg may directly supply nutrients to plants in soil (Zheng et al. 2013b; Liu et al. 2019), contribute to removal or immobilization of pollutants such as HMs and organic contaminants in water or soil (Zheng et al. 2013c; Wang et al. 2015d; Cao et al. 2009, 2011), or enhance BC's C retention and stability for C sequestration (Xiao et al. 2014; Guo and Chen 2014).

### 2.3.2 Surface Properties

The surface of BC, highly variable due to its heterogeneous composition (Zheng et al. 2013b; Liu et al. 2017, 2018a; Xu et al. 2017), is the main interface where many chemical and

biological interactions occur (Zhu et al. 2017; Pignatello et al. 2017). As such, determining BC's surface chemistry and reactivity is critical for designing environmental remediation solutions using suitable BC. General surface properties include surface functional groups, charge, hydrophilicity and hydrophobicity, surface area and pore structure, and surface free radicals. Among these, surface functional groups play critical roles in the properties and applications of BCs as functional materials such as adsorbent (Yang et al. 2019; Li et al. 2018a), catalyst (Mian and Liu 2018), soil conditioner (Zheng et al. 2018b; Al-Wabel et al. 2018), and C sequestration agent (Woolf et al. 2010; Lehmann 2007). Typically, the polyaromatic rings are rimmed with heteroatomic groups (e.g., O, N, P, S, and Cl) including keto, quinone, lactone, pyrone, ether, hydroxyl, carboxyl, and various types of amines (Pignatello et al. 2017). These functional groups can be classified into different types according to the heteroatom, such as O-containing functional groups, N-containing functional groups, and S-containing functional groups (Yang et al. 2019). The species and contents of these surface functional groups are controlled by feedstock and pyrolytic conditions (Zheng et al. 2013c; Sun et al. 2011; Liu et al. 2018a). BC produced at low temperature with low degree of carbonization and aromaticity contains more surface functional groups (e.g.,  $-\text{COOH}$  and  $-\text{C}=\text{O}$ ) that may promote adsorption for certain contaminants (Yang et al. 2019; Chen et al. 2015). On the contrary, BC prepared at high temperatures tends to have fewer of these groups because of elimination of the heteroatoms such as O, N, and S during charring (Liu et al. 2017). Among these groups, O-containing functional groups (e.g.,  $-\text{OH}$ ,  $-\text{COOH}$ ,  $-\text{C}=\text{O}$ , and  $-\text{C}-\text{O}$ ), which is extensively studied so far, are the most important in regulating surface reactions, surface behavior, hydrophilicity, electrical, and catalytic properties of BCs (Pignatello et al. 2017; Teixidó et al. 2011). For example, quinone groups have been proved to participate in the redox behavior of BC (Kluepfel et al. 2014; Yang et al. 2016b; Yuan et al. 2017), while the carboxyl and hydroxyl groups are responsible for the negative charges of BC (Yuan et al. 2011). In order to enhance the functionality and quantity of O-containing functional groups, surface oxidation is a highly recommended and easiest technique (Yang et al. 2019). Conventionally, a single or a mixture of inorganic acids (e.g.,  $\text{HNO}_3$ ,  $\text{H}_2\text{SO}_4$ ,  $\text{H}_3\text{PO}_4$ ) or an oxidizing agent (e.g.,  $\text{H}_2\text{O}_2$ ,  $\text{KMnO}_4$ , and  $\text{NaOCl}$ ) is usually used to introduce O to BC's surface (Rajapaksha et al. 2016). During these modification processes, it is critical to optimize the dosage of these agents and reaction conditions (e.g., reaction time and temperature) for regulating the desired functional structures on a given BC. Relative to O-containing groups, other groups like N-containing functional groups (e.g.,  $-\text{NH}_2$ ,  $-\text{NH}$ ,  $-\text{C}=\text{N}$ , and  $-\text{C}-\text{N}$ ) in BC are much less examined (Liu et al. 2019). More work is still needed to clarify the

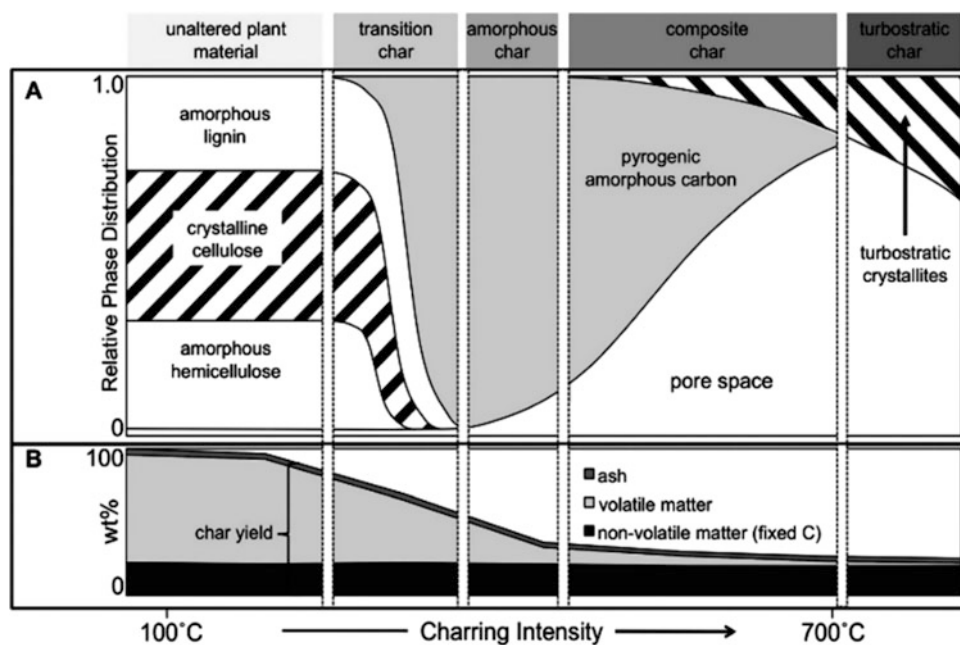
transformation and functionality of these hetero-elements and related functional groups in BC. As a type of carbonaceous functional materials, surface area and pore structure are also very important features. They have been extensively studied in various BCs produced from different feedstock at various conditions (Jagiello et al. 2019; Sigmund et al. 2017). In fact, BC directly produced from heating biomass without any activation treatment often possesses lower surface area in the range of 2.72–542 m<sup>2</sup> g<sup>-1</sup> (Zheng et al. 2013b; Thompson et al. 2016) than AC in the range of 568–2060 m<sup>2</sup> g<sup>-1</sup> (Chiu and Ng 2012; Plaza et al. 2012). Generally, with increasing pyrolytic temperature from 300 to 500 °C, the surface area of BC gradually increases due to the removal of –OH, aliphatic C–O, and ester C=O groups from outer surfaces of plant feedstock and complete destruction of aliphatic alkyl and ester C=O groups shielding the aromatic core, then a decrease in surface area can be observed above 500 °C, at which BC structural deformation occurs (Chen et al. 2008; Zheng et al. 2013c). These changes in BC's surface area and pore structure would have significant influences on its adsorptive behavior with contaminants in water or soil.

### 2.3.3 Phase Structure

The abovementioned elements build BC via forming massive chemical bonds during biomass charring (Chen et al. 2015; Keiluweit et al. 2010). As a solid material, BC contains organic phase presented as aliphatic C, aromatic C, and functionalized C (Kasozzi et al. 2010; Keiluweit et al. 2010) and inorganic phase such as carbonate and bicarbonate (Ji et al. 2011; Yuan et al. 2011; Yao et al. 2012). Heterogeneous BC can be viewed as an aggregation of both organic

and mineral phases (Xiao et al. 2018). These different phases endow BC with unique structures and functions. Organic phase in BC may be classified into different categories according to different perspectives. For example, according to C molecular structure, OC in BC could be classified into aliphatic and aromatic phase (Zheng et al. 2013c; Keiluweit et al. 2010). According to the classical dual-mode sorption model (Xing and Pignatello 1997), which has been successfully used to assess the contribution of partitioning and adsorption in sorption of organic compounds on chars (Chen et al. 2008; Zheng et al. 2013c; Lian et al. 2011), BC can be considered as an organic partitioning phase with rubbery state and a surface adsorption phase with glassy state. On the basis of particle size, we can sort BC into bulk BC (0.04–20 mm) and nano-BC with size smaller than 100 nm (Lian et al. 2019; Liu et al. 2018a; Chen et al. 2018b). A widely accepted phase model showing phase transitions during BC formation was reported by Keiluweit et al. (2010). As shown in Fig. 3, four different chemical phases and physical states were identified: (1) transition char with amorphous centers amidst a largely intact crystalline matrix that derived from volatile dissociation at 100–200 °C; (2) amorphous char composed of small, heat-resistant aliphatic and (hetero)aromatic elements formed at 200–350 °C; (3) composite char with turbostratic crystallites embedded in a low-density amorphous phase generated at 350–500 °C; and (4) turbostratic char with disordered graphitic crystallites formed above 500 °C. Still, more efforts are needed to quantify these different organic phases in various BCs and investigate their roles in BC's application, thereby establishing the structure–function relationships. Compared to the C phase, the formation and role of mineral phase in BC has received

**Fig. 3** Organic phase of the BC produced at different pyrolysis temperatures. Schematic representation of the four proposed char categories and their individual phases. This figure is cited from Keiluweit et al. (2010), with permission from the publisher





less attention. This is probably attributed to the wide application of plant-derived BC that contains limited mineral components (Keiluweit et al. 2010; Ahmed et al. 2018; Fang et al. 2013), and pretreatments which are often employed to remove the mineral fraction from the original BC before its application (Xu et al. 2017; Chen et al. 2008; Zheng et al. 2013c). However, with increasing production and characterization of BC from more feedstock for different applications, the viewpoint that mineral fractions could influence the properties and functionalities of BC is gradually being recognized (Liu et al. 2019; Xu et al. 2017). Recently, Xu et al. (2017) reviewed the physicochemical properties and indispensable roles of BC-inherited mineral phase in its environmental and agronomic applications. However, more studies are required to fill the knowledge gaps of the formation, properties, and roles of mineral components in BC and its application.

### 3 Application of BC in Polluted Water Remediation

Water pollution via contaminants (e.g., HMs, pesticides, PAHs and antibiotics) poses a serious threat to both environmental functions and human health, and has continued to attract significant global attention from both government regulatory agencies and the general public as a result (Wu and Wu 2019; Vilela et al. 2018; Panasiuk et al. 2015). Sorption, an essential interfacial process controlling the fate and risk of pollutants in the environment, using sorbents (e.g., ACs, carbon nanotubes (CNTs)), has been shown to be one of the powerful, simple, and economical approaches (Zheng et al. 2013c; Wang et al. 2015d; Yang and Xing 2010). A number of studies have demonstrated that BC can be used as a low-cost adsorbent for wastewater treatment, particularly with respect to treating HMs and some organic pollutants (e.g., PAHs, pesticides, and antibiotics) (Dai et al. 2019; Li et al. 2018a; Peiris et al. 2017; Tan et al. 2015, 2016b; Wang et al. 2015d; Zheng et al. 2013c, 2019a), and even some pathogenic microorganisms (Mohanty et al. 2014; Mohanty and Boehm 2014). According to the available literatures on the topic of BC application in wastewater treatment reviewed by Tan et al. (2015), approximately 46% of the studies investigated the removal ability of BC for HMs, 39% for organic pollutants, 13% for nitrate ( $\text{NO}_3^-$ ) and phosphate ( $\text{PO}_4^{3-}$ ), and 2% for other pollutants. In some cases, BC was proven to be a superior alternative adsorbent to AC (Thompson et al. 2016). Additionally, besides sorption, organic contaminants in waters may degrade with the help of electron transfer (Oh et al. 2013; Fu et al. 2014) or persistent-free radicals (PFRs) derived from BC (Pan et al. 2019).

### 3.1 Sorption of HMs by BC

#### 3.1.1 Overview of Different HM Sorption by BC

Numerous studies have used BC materials to capture HMs in water and established the relationship between the adsorption characteristic/mechanisms for HMs and the physicochemical properties of BCs (Yang et al. 2019; Tan et al. 2015; Wang et al. 2015d). Moreover, the engineered BC sorbents with desirable properties have been developed through diverse methods for improving pristine BC's adsorption performance (Thines et al. 2017; Rajapaksha et al. 2016). The summary of HMs sorbed by various BCs is shown in Table 2.

The commonly studied HMs sorbed by BCs include lead (Pb), cadmium (Cd), copper (Cu), zinc (Zn), nickel (Ni), and mercury (Hg). Taking Pb as an example, lots of studies have reported that BC displays superior sorption capacity for Pb, and its sorption on BC is largely influenced not only by pyrolytic temperature but also by feedstock (Table 2). For instance, Cao et al. (2009) evaluated the ability of dairy-manure-derived BCs at low temperature of 200 and 350 °C to sorb Pb. The two BCs effectively removed Pb from water, and the lower temperature one showed higher sorption capacity ( $133 \text{ mg g}^{-1}$ ) than the higher temperature one ( $93.6 \text{ mg g}^{-1}$ ). BCs derived from pig and cow manure at the higher temperatures (400 and 600 °C), also have greater sorption capacity for Pb (up to 213–219  $\text{mg g}^{-1}$ ), and pyrolysis at 600 °C is optimally produces BC as an effective sorbent for Pb (Kołodziejńska et al. 2012). Pb sorption by BC also varies with its feedstock. The BC from digested manure at 400–600 °C had a great sorption capacity of 128–248  $\text{mg g}^{-1}$  toward Pb (Liang et al. 2017; Inyang et al. 2012a). Sewage sludge is also promising feedstock for BC used as a sorbent for Pb removal due to its high mineral content (Gao et al. 2019; Lu et al. 2012). However, the plant-derived BC generally shows lower sorption capacity for Pb than the manure or sewage sludge-derived BC. For example, the adsorption amount of Pb by the BCs from rice husks (Liu and Zhang 2009), green waste (Park et al. 2013), and pine wood (Wang et al. 2015b) was only 2.40, 6.53, and 2.35  $\text{mg g}^{-1}$ , respectively. Our early research investigated Pb sorption by a batch of BCs produced from peanut shell and Chinese medicine material residue at temperatures of 300–600 °C. We found that the BC produced at medium temperature of 350–400 °C had maximum adsorption capacity of 52.8  $\text{mg g}^{-1}$  and 82.5  $\text{mg g}^{-1}$ , respectively (Wang et al. 2015d). Modification of BC using different methods (e.g., coating with metal oxides, acid/base treatment, and chemical oxidation sorption) may enhance BC's sorption capacity for Pb (Thines et al. 2017; Rajapaksha et al. 2016; Wang et al. 2015b). For instance, covering  $\text{MnO}_x$  ultrafine particles on BC increased Pb sorption

**Table 2** Summary of HMs adsorbed on BCs and the proposed mechanisms

HMs	Feedstock	Pyrolysis temperature (°C)	Adsorption capacity (mg g <sup>-1</sup> )	Proposed mechanisms	Reference
Pb	Dairy-manure	200	133	Precipitation	Cao et al. (2009)
	Rice husk	300	2.40	Complexation	Liu and Zhang (2009)
	Sludge	550	30.9	Metal–ligand complexation, surface precipitation	Lu et al. (2012)
	Digested dairy waste	600	248	Surface precipitation	Inyang et al. (2012b)
	Digested whole sugar beet	600	197	Surface precipitation	Inyang et al. (2012b)
	Pig manure	400–600	213–219	External mass transfer, intra-particle diffusion	Kołodzyńska et al. (2012)
	Green waste	300	6.53	Precipitation	Park et al. (2013)
	Peanut shells	300–600	41.2–43.6	Complexation, Pb <sup>2+</sup> – $\pi$ interaction, precipitation	Wang et al. (2015c)
	Medicine material residues	300–600	40.7–91.7	Complexation, Pb <sup>2+</sup> – $\pi$ interaction, precipitation	Wang et al. (2015c)
	Pinewood	600	2.35	Precipitation	Wang et al. (2015b)
	Banana peels	600	247	Complexation, ion exchange, precipitation	Ahmad et al. (2018)
	Cauliflower leaves	600	178	Complexation, ion exchange, precipitation	Ahmad et al. (2018)
	Cauliflower leaves	600	178	Complexation, ion exchange, precipitation	Ahmad et al. (2018)
	Wheat straw	600	120	Ion exchange, precipitation	Cao et al. (2018)
	Sludge	600	181	Electrostatic interaction, surface complexation, ion exchange	Chen et al. (2018d)
	Tobacco stem	300–700	186–399	Surface interactions, complexation, Pb <sup>2+</sup> – $\pi$ interaction	Zhou et al. (2018)
Sewage sludge	400	210	Complexation, physical adsorption	Ifthikar et al. (2018)	
Cu	Dairy manure	350	54.4	Surface precipitation, complexation, cation– $\pi$ bonding	Xu et al. (2013)
	Sawdust	500	17	Complexation, ion exchange, chelation, precipitation	Yang and Jiang (2014)
	Tobacco stem	300–700	182–350	Surface interactions, complexation, $\pi$ interaction	Zhou et al. (2018)
	Forestry wood waste	650	57.4	Physical adsorption, complexation	Sun et al. (2019b)
Zn	Dairy manure	200–350	31.6	Surface precipitation, complexation, cation– $\pi$ bonding	Xu et al. (2013)
	Dairy manure	350	32.8	Surface precipitation, complexation, cation– $\pi$ bonding	Xu et al. (2013)
	Rice straw	600	38.6	Ion exchange	Park et al. (2017b)
	Cornstalk	800	110	Precipitation, physical adsorption	Yang et al. (2018a)
Cd	Dairy manure	200	31.9	Surface precipitation, complexation, cation– $\pi$ bonding	Xu et al. (2013)
	Sewage sludge	900	50	Cation exchange, surface precipitation	Chen et al. (2014a)
	Cellulose powder	700	369	Complexation, surface precipitation, pore-filling	Chen et al. (2018c)
	Banana peels	600	121	Complexation, ion exchange, precipitation	Ahmad et al. (2018)
	Cauliflower leaves	600	73.8	Complexation, ion exchange, precipitation	Ahmad et al. (2018)
	Oak bark	450	7.40	Complexation, ion exchange, precipitation	Ahmad et al. (2018)
	Pig manure	300–700	78.1–79.4	Complexation, cation– $\pi$ bonding, precipitation, ion exchange	Wang et al. (2018b)
	Bamboo	300–700	74.4–75.3	Complexation, cation– $\pi$ bonding, precipitation, ion exchange	Wang et al. (2018b)
	Rice straw	700	128	Complexation, precipitation, cation– $\pi$ bonding, ion exchange	Gao et al. (2019)
Sewage sludge	700	57.9	Complexation, precipitation, cation– $\pi$ bonding, ion exchange	Gao et al. (2019)	

(continued)

**Table 2** (continued)

HMs	Feedstock	Pyrolysis temperature (°C)	Adsorption capacity (mg g <sup>-1</sup> )	Proposed mechanisms	Reference
Ni	Residues of biogas production	400	27.9	Physical adsorption, surface precipitation	Bogusz et al. (2017)
	Residues of biogas production	600	34.8	Physical adsorption, surface precipitation	Bogusz et al. (2017)
	Wheat straw	600	17.7	Physical adsorption, surface precipitation	Bogusz et al. (2017)
Hg	Corn straw	500	3.23	Complexation, precipitation	Tan et al. (2016a)
	Corn straw	500	5.71	Complexation, precipitation	Tan et al. (2016a)
	Corn straw	500	4.26	Complexation	Ifthikar et al. (2018)
	Sewage sludge	400	594	Complexation	Ifthikar et al. (2018)

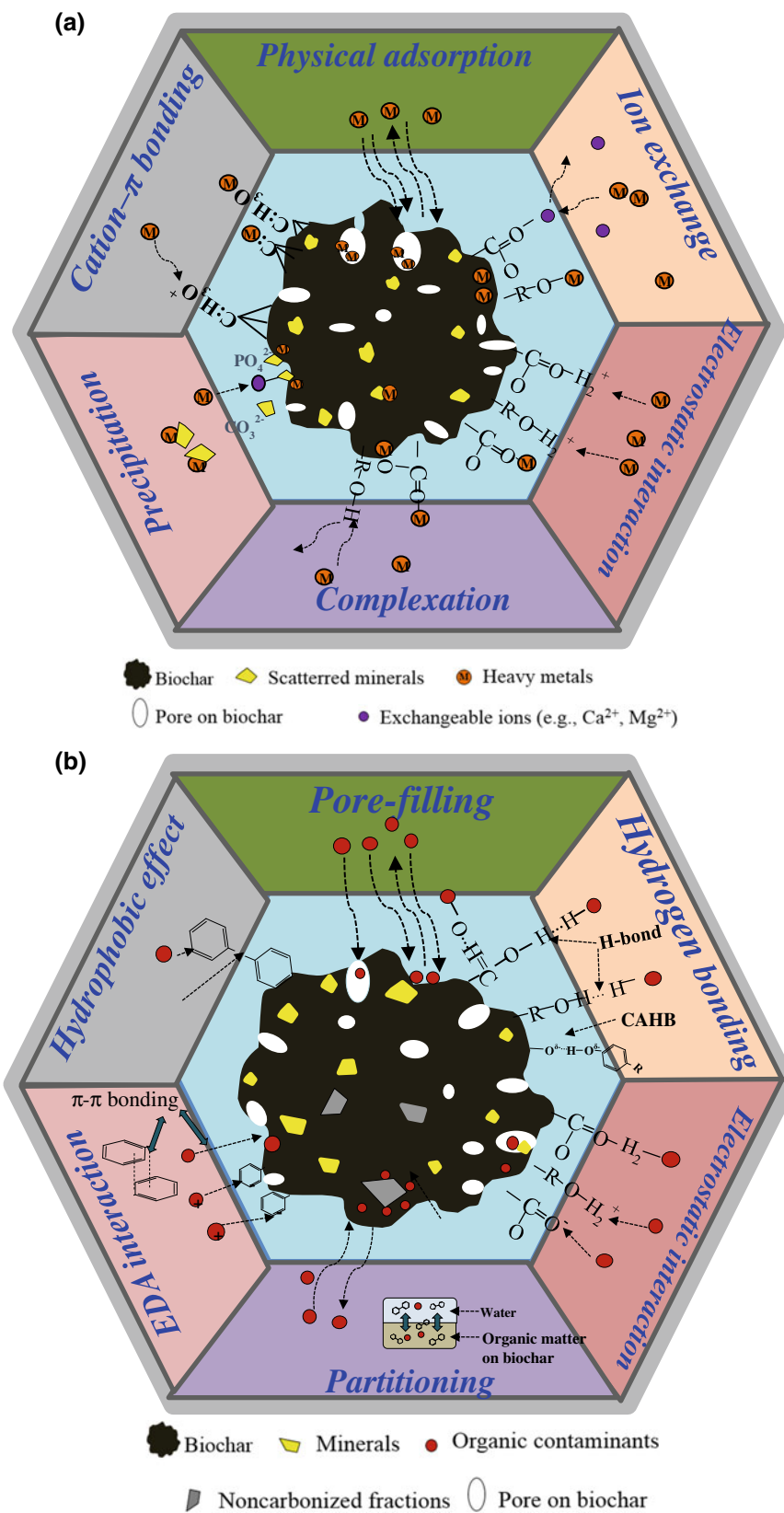
capacity from 71.1 to 153 mg g<sup>-1</sup> (Wang et al. 2015a). Similarly, amorphous MnO<sub>2</sub>-modified BC derived from aerobically composted swine manure displayed higher Pb sorption (268 mg g<sup>-1</sup>) than untreated BC (128 mg g<sup>-1</sup>) (Liang et al. 2017). Up to date, superior adsorption performance of modified BCs or BC-based nanocomposites for Pb has been widely reported for many engineered BCs, such as MgO-N-BCs (476–893 mg g<sup>-1</sup>) (Ling et al. 2017), nanoscale zero-valent iron (nZVI) BC (181 mg g<sup>-1</sup>) (Chen et al. 2018d), carboxymethyl chitosan-BC (210 mg g<sup>-1</sup>) (Ifthikar et al. 2018), and MnFe<sub>2</sub>O<sub>4</sub>-BC (179–349 mg g<sup>-1</sup>) (Jung et al. 2018). Recently, ball-milling, which may introduce high mineral content, O-containing functional groups, and unsaturated C bonds to BC surface, was proposed as a novel method to increase BC's sorption capacity for HMs like Pb (Li et al. 2018b; Lyu et al. 2018). For other HM (e.g., Cd, Zn), similar findings were also reported (Table 2). Overall, extensive studies have demonstrated BC's capability to serve as a green environmental sorbent for removal of HMs from water. However, not all BCs are suitable for HM removal because of the diversity of BC's properties in terms of elemental composition, surface properties, and phase structure, as discussed in Sect. 3.2.3 (BC characteristics). Consequently, more efforts should be made to design engineered or smart BC with high sorption capacity for different HMs and further to elucidate the binding mechanisms.

### 3.1.2 Mechanisms for HM Sorption by BC

The key features endowing BC with high removal efficiencies of HMs include the large specific surface area, porous structure, surface functional groups, and inherent minerals (Tan et al. 2015, 2016b). The heterogeneity of BC characteristics means that multiple mechanisms jointly contribute to the sorption of HMs by BC in water. A number of mechanisms may control the removal of HMs from aqueous solutions by BC, including (1) physical adsorption, (2) ion exchange, (3) electrostatic interaction, (4) complexation, (5) precipitation, and (6) cation  $-\pi$  bonding. These mechanisms proposed for the interaction of BC with HMs are

summarized in Fig. 4a. BC with a high surface area and pore volume will favor the adsorption of metallic ions due to physical adsorption (Kołodziejńska et al. 2012; Liu and Zhang 2009; Wang et al. 2015d). Liu and Zhang (2009) reported that Pb removal from water using the pinewood and rice husk BCs was mainly controlled by intra-particle diffusion. Similarly, our group presented a process pattern for Pb adsorption on the BCs from peanut shells and Chinese medicine material residue at 300–600 °C (Wang et al. 2015d). This process involves three stages: (i) Pb from solution quickly reaches to BC surface via crossing the boundary layer; (ii) Pb is adsorbed onto the external sites of BC; and (iii) Pb diffuses through the pores and reacts with the internal surfaces of BC. As a result, an increase in micro-pores and the surface area of BC may promote the physical adsorption of HMs onto BCs (Tan et al. 2015; Mohan et al. 2014). Additionally, physical adsorption, while common, is unlikely to serve as the predominant adsorption mechanism for HMs due to the presence of other strong interactions like complexation and precipitation (Yang et al. 2019). Ion exchange is one of the major mechanisms responsible for HM adsorption by carbonaceous adsorbents like BC and AC (Yang et al. 2019; Yang and Jiang 2014; Cao et al. 2018; Gao et al. 2019). The sorption efficiency resulted from ion exchange is closely related to the target metal species, exchangeable cations and surface functional groups in BC. Lu et al. (2012) detected significant release of divalent alkaline earth cations (e.g., Ca<sup>2+</sup> and Mg<sup>2+</sup>) after Pb sorption on a sewage sludge BC, confirming the occurrence of ion exchange between Pb and the BC. Cation exchange capacity (CEC) would be an important indicator for predicting adsorption capacity of HMs by BC via predominant ion exchange (Lee et al. 2010). Electrostatic interaction between HMs and BC is mainly determined by the point of zero charge (PZC) of BC and the solution pH (Wang et al. 2015d; Yang et al. 2019; Ahmad et al. 2018). When solution pH > PZC, the electrostatic attraction occurs between negatively charged BC and metal cations, favoring the adsorption, while when pH < PZC, the electrostatic repulsion

**Fig. 4** Schematic illustrations of sorption mechanisms of HM (a) and organic contaminants (b) onto BCs



occurs between the positively charged BC and metal cations, hindering the adsorption performance. Surface complexation (inner and outer sphere) takes place between HMs and surface functional groups (e.g.,  $-\text{COOH}$  and  $-\text{OH}$ ) of BC (Inyang et al. 2012a; Wang et al. 2015d), playing a predominant role in the sorption (Yang et al. 2019; Tan et al. 2015; Mohan et al. 2014). Lu et al. (2012) observed dramatic decrease of Pb sorption by the sludge-derived BC when the free  $-\text{COOH}$  groups were chemically blocked by  $\text{CH}_3\text{OH}$ , confirming the complexation of surface  $-\text{COOH}$  in BC with Pb. They also estimated that the complexation interaction accounted for 38.2–42.3% of the total sorption varying with pH, whereas the coprecipitation or complex on mineral surfaces accounted for 57.7–61.8%. Precipitation may occur between HMs and minerals retained in BC during BC charring or modification, resulting in the formation of solid products on either the surface of BC or the solution itself, with both contributing to the removal of HMs (Wang et al. 2015d). The formation of HM precipitations is closely related to the species and phases of minerals in BC (Jiang et al. 2018; Wang et al. 2015d; Inyang et al. 2012a; Cao et al. 2009). For example, a study reported that Pb was precipitated as  $\text{Pb}_9(\text{PO}_4)_6$  on the dairy-manure-derived BC prepared at 200 °C, while as  $\text{Pb}_3(\text{CO}_3)_2(\text{OH})_2$  on the BC prepared at 350 °C (Cao et al. 2009). Other forms of Pb precipitates, such as  $\text{Pb}(\text{OH})_2$ ,  $\text{PbCO}_3$ ,  $\beta\text{-Pb}_9(\text{PO}_4)_6$ ,  $\text{Pb}_5(\text{PO}_4)_3\text{Cl}$ , and  $\text{Pb}_3(\text{CO}_3)_2(\text{OH})_2$ , have also been reported in Pb removal by BCs (Wang et al. 2015d; Cao et al. 2009; Lu et al. 2012). BC containing high amounts of graphitic C can serve as  $\pi$ -donor (Zheng et al. 2013c; Keiluweit et al. 2010), allowing them to serve as adsorption sites for positively charged hydrated metal cations in aqueous solution (Chen et al. 2018c; Zhou et al. 2018; Song et al. 2014). This cation  $-\pi$  interaction serves as one of the primary mechanisms for Cd adsorption by BC, which has been well reported by researchers (Chen et al. 2018c; Zhou et al. 2018; Song et al. 2014).

### 3.1.3 Factors Influencing Adsorption of HMs on BC

The adsorption process and characteristics of HM onto BCs is likely controlled by the properties and dosage of BC, environmental conditions (e.g., pH and temperature), and co-existed substances (e.g., alkali metal/alkaline earth metal ions, organic contaminants) in water (Uchimiya 2014; Tan et al. 2015). The properties of BC, as described in Sect. 3.2, would have conspicuous influence on the sorption efficiency toward HMs by determining the contributions of the above-mentioned sorption mechanisms (Fig. 4a). The relationships between BC properties and HM sorption have been well reviewed by Mohan et al. (2014), Tan et al. (2015), and Lian

and Xing (2017). The solution pH is one of the most critical parameters affecting the adsorption process (Tan et al. 2015). The pH affects both the charge of BC surface and the degree of ionization and speciation of HMs in a solution. The deprotonation of the O-containing functional groups occurs at solution  $\text{pH} > \text{p}K_a$  of O-containing functional groups, while their protonation occurs at solution  $\text{pH} < \text{p}K_a$  (Chen et al. 2015). Park et al. (2017a) reported the negatively charged surfaces of BC resulted from the deprotonated O-containing functional groups (e.g.,  $-\text{O}^-$  and  $-\text{COO}^-$ ) favored the adsorption of Cd through electrostatic attraction as pH increased from 3.5 to 8. For very low pH (<3.5), the excessive protonation of O-containing functional groups in BC may cause the competition for the binding sites between  $\text{H}^+$  and Cd ions. Similar pH-dependent patterns of HM sorption by BC have been extensively reported (Liu and Zhang 2009; Yang and Jiang 2014; Wang et al. 2015a, d; Gao et al. 2019; Uchimiya 2014). The interaction temperature is generally considered an important factor of adsorption at liquid–solid interfaces. Studies have shown that sorption of HMs by BC is an endothermic process, in which adsorption capacity increases with increasing environmental temperature (Liu and Zhang 2009; Yang and Jiang 2014). For example, a study reported by Liu and Zhang (2009) demonstrated that the adsorption capacity of Pb on two BCs from pinewood and rice husk at 300 °C increased with increasing solution temperature from 25 °C to 45 °C. The higher temperature favouring Pb ion adsorption onto BCs implies that the adsorption was an endothermic process, and is primarily the result of the energy provided by the higher temperature allowing Pb ions to more easily reach and adsorb onto the interior structure of BC. Alkali metals (e.g., Na and K) and alkaline earth metals (e.g., Ca and Mg) are ubiquitous in natural environments, which are usually considered to compete with HM ions for the active sites of adsorbents. In fact, numerous studies have reported that the removal efficiency of HM ions (e.g., Pb, Cd and Cu) decreases in various BCs when the ionic strength of the solution increases (Yang and Jiang 2014; Wang et al. 2015a; Kołodyńska et al. 2012). Additionally, the co-existing organic contaminants (e.g., atrazine, simazine, and phenanthrene) may also decrease HM sorption by BC due to the competition for the active sites (Cao et al. 2009; Chen et al. 2011a). However, most of these findings were based on simulated or artificial wastewater, which cannot fully reflect the actual situation in the environment. Many complex pollutants and ions usually coexist in actual wastewater, and the environmental conditions greatly vary; this would in turn cause sorption performance to vary. As such, further studies are required to consider more realistic conditions to elaborate on interactions between BC and HMs.

## 3.2 Removal of Organic Pollutants by BC

Reported organic pollutants in water include PAHs, PBCs, pesticides, antibiotics, phthalic acid esters (PAEs), perfluoroalkyl acids (PFOAs), disinfection by-products, volatile organic compounds (VOCs), and natural organic matter (NOM) (Vilela et al. 2018; Panasiuk et al. 2015; Dai et al. 2019; Peiris et al. 2017; Inyang and Dickenson 2015). The multifunctional BC with low cost and easy availability which may remove organic pollutants from water via sorption and degradation (Chen and Chen 2009; Zheng et al. 2013c; Kluepfel et al. 2014; Rajapaksha et al. 2014b) has provided a promising option.

### 3.2.1 Overview of Different Organic Contaminant Sorption by BC

In the past few years, studying the adsorption of organic pollutants by BC has become one of the research hotspots in the field of environmental science. A large number of studies have shown that BC has a strong affinity and high capacity for the uptake of organic pollutants due to characteristics such as its well-developed pore structure and rich O-containing functional groups (Ahmed et al. 2018; Zhang and Gao 2013; Rajapaksha et al. 2016; Chen et al. 2008; Kasozi et al. 2010; Lattao et al. 2014; Teixidó et al. 2011; Peiris et al. 2017). Many contaminants sorbed by BC have extensively been demonstrated, some of which are summarized in Table 3. Increasing concern regarding organic contaminants has been focused on PAHs, PCBs, pesticides, PAEs, and antibiotics. The results from these studies showed that BC can be used as a low-cost adsorbent for removal of organic pollutants from wastewater, thus reducing their environmental risks. For example, our previous study showed that the maximum sorption capacities of the giant-reed-derived BC at 300–600 °C for sulfamethoxazole was in the range of 1.93–4.99 mg g<sup>-1</sup> (Zheng et al. 2013c), larger than the reported literature values on soils, minerals, sediments, and other plant-derived BCs (Yao et al. 2012). Teixidó et al. (2011) also reported the successful application of hardwood-litter-derived BC for sulfamethazine sorption. Wang et al. (2017b) investigated the sorption of naphthalene and three hydroxyl-substituted naphthalene substitutes, i.e., 1-naphthol, 4-nitro-1-naphthol, and 1-naphthalenemethanol, onto two corn-straw-derived BCs and demonstrated that BCs are good sorbents for these polar and ionizable pollutants. Similar results were also reported by Chen and Chen (2009), who found that the maximum 1-naphthol and naphthalene sorption was observed on the orange-peel-derived BCs at 700 °C. Compared to these ionizable organic compounds (IOCs), BC shows higher affinity and capacity for hydrophobic organic compounds (HOCs). For example, Wang et al. (2016b) successfully used the BCs derived from

maize straw, wood dust, and swine manure at 250–600 °C to adsorb four HOCs, including acetochlor, dibutyl phthalate, 17 $\alpha$ -ethynyl estradiol, and phenanthrene. Pesticides are one type of the organic pollutants which were extensively investigated for their sorption by BCs (Table 3). For example, Yang et al. (2004) reported that a wheat-residue-derived BC can be used to sorb ionizable pesticides such as diuron, bromoxynil, and ametrine, and the sorption was greatly influenced by solution pHs. This is also why BC can be used as soil amendments to remediate the pesticide-contaminated soil (Varjani et al. 2019; Liu et al. 2018c). NOM in wastewaters may affect water quality due to the formation of carcinogenic disinfection by-products and promotion of microbial regrowth, especially pathogenic bacteria in the water distribution system (Lin et al. 2012). BC has been used for removing NOM such as catechol (Kasozi et al. 2010), humic acids, and tannic acids (Jung et al. 2015) from waters via sorption. For the small molecule catechol, the sorption capacity of BC increased as the pyrolytic temperature from 250 to 650 °C, with pine < oak < grass and coarse < fine particle size, and greater sorption occurred on the higher temperatures BCs with nanopores (Kasozi et al. 2010). Although lots of studies have proved that BC can be used as an alternative to AC for sorption of organic contaminants, some studies showed that BC was not better than AC for adsorption of some organic pollutants. For example, Gomez-Eyles et al. (2013) observed that ACs consistently removed more organic contaminants including PCBs, PAHs, dichlorodiphenyltrichloroethanes, and metabolites (DDXs) from water than the BCs at environmentally relevant concentrations tested, probably due to the lower surface area for the BCs. Obviously, the BC with lower sorption capacity has limited application to environment remediation. As a result, growing attention has recently focused on the modification of BC with novel structures and high surface properties in order to enhance its sorption capacity and affinity (Mian and Liu 2018; Tan et al. 2016b; Rajapaksha et al. 2016). Several works of literature have accurately summarized and evaluated BC modification methods, corresponding mechanisms, and their benefits for organic contaminant removal from wastewater (Thines et al. 2017; Tan et al. 2016b; Rajapaksha et al. 2016; Liu et al. 2015a). The modification methods include chemical modifications, physical modifications, impregnation with mineral sorbents, and magnetic modifications, which aim to improve BC's surface properties, including surface area, surface charge, functional groups, and pore volume and distribution, as well as inorganic and organic phase structure. For example, Reguyal et al. (2017) synthesized a strong magnetic BC by controlling the formation of nano-sized Fe<sub>3</sub>O<sub>4</sub> on a pine sawdust BC via oxidative hydrolysis of FeCl<sub>2</sub>, and successfully used it to remove sulfamethoxazole via

**Table 3** Summary of organic pollutants adsorbed on BCs and the mechanisms

Organic pollutants	Feedstock	Pyrolysis temperature (°C)	Adsorption capacity (mg g <sup>-1</sup> )	$K_d$ (L g <sup>-1</sup> )	Proposed mechanisms	References
<b>PAHs</b>						
Naphthalene	Pine needle	200–700	0.33–137	0.27–1.09	Partitioning, pore-filling	Chen et al. (2008)
Naphthalene	Orange peel	250–700	1.92–80.8	0.05–1.47	Partitioning, pore-filling, partition	Chen and Chen (2009)
Phenanthrene	Poultry litter	250–400	46.7–61.8	159–282	H-bonding, hydrophobic effect, pore-filling, $\pi$ - $\pi$ EDA interaction	Sun et al. (2011)
Phenanthrene	Wheat straw	400	6.92	120	H-bonding, hydrophobic effect, pore-filling, $\pi$ - $\pi$ interaction	Sun et al. (2011)
Phenanthrene	Rice straw	450–600	NR	1.32–2.34	Hydrophobic effect, H-bonding, $\pi$ - $\pi$ interactions	Sun et al. (2013)
1-Naphthol	Orange peel	300	44.2	0.11	Pore-filling, partition	Chen et al. (2012b)
1-Naphthol	Pine needle	300	15.0	0.10	Pore-filling, partition	Chen et al. (2012b)
1-Naphthol	Sugar cane bagasse	300	19.6	0.24	Pore-filling, partition	Chen et al. (2012b)
Phenanthrene	Rice straw	450	NR	9.55	$\pi$ - $\pi$ EDA interaction, pore-filling	Jin et al. (2017)
Phenanthrene	Maize straw	450	NR	7.76	$\pi$ - $\pi$ EDA interaction, pore-filling	Jin et al. (2017)
Phenanthrene	Swine manure	450	NR	9.12	$\pi$ - $\pi$ EDA interaction, pore-filling	Jin et al. (2017)
<b>PCBs</b>						
2,4,4'-CB	Wheat straw	350–550	NR	41.7–77.6	$\pi$ - $\pi$ EDA interaction, H-bonding, complexation, van der Waals interaction	Wang et al. (2013a)
2,4,4'-CB	Pine needle	350–550	NR	7.59–10.7	$\pi$ - $\pi$ EDA interaction, H-bonding, complexation, van der Waals interaction	Wang et al. (2013a)
<b>Pesticides</b>						
Carbaryl	Pig manure	350–700	2.23–2.28	0.45–4.57	Pore-filling, hydrophobic effect, $\pi$ - $\pi$ EDA interaction, partition	Zhang et al. (2013c)
Atrazine	Pig manure	350–700	0.04–0.16	0.08–0.32	Pore-filling, hydrophobic effect, $\pi$ - $\pi$ EDA interaction, H-bonding, partition	Zhang et al. (2013c)
Atrazine	Pig manure (treated with acid)	350–700	0.34–0.64	0.68–1.29	Pore-filling, hydrophobic effect, $\pi$ - $\pi$ EDA interaction, H-bonding, partition	Zhang et al. (2013c)
Atrazine	Corn straw	NR	346	NR	H-bonding, $\pi$ - $\pi$ EDA interaction, electrostatic attraction	Yang et al. (2017)
<b>PAEs</b>						
DEP	Wood waste	700	NR	132	Hydrophobic effect, H-bonding, $\pi$ - $\pi$ EDA interaction	Sun et al. (2012)
DEP	Grass	700	NR	218	Hydrophobic effect, H-bonding, $\pi$ - $\pi$ EDA interaction	Sun et al. (2012)
DBP	Wood waste	700	NR	696	Hydrophobic effect, H-bonding, $\pi$ - $\pi$ EDA interaction	Sun et al. (2012)
DBP	Grass	700	NR	330	Hydrophobic effect, H-bonding, $\pi$ - $\pi$ EDA interaction	Sun et al. (2012)
DBP	Soybean straw	450	NR	10.1	H-bonding, $\pi$ - $\pi$ EDA interaction, hydrophobic effect	Jin et al. (2014)

(continued)

**Table 3** (continued)

Organic pollutants	Feedstock	Pyrolysis temperature (°C)	Adsorption capacity (mg g <sup>-1</sup> )	$K_d$ (L g <sup>-1</sup> )	Proposed mechanisms	References
DBP	Rice straw	450	NR	9.76	H-bonding, $\pi$ - $\pi$ EDA interaction, hydrophobic effect	Jin et al. (2014)
DBP	Cotton straw	450	NR	9.35	H-bonding, $\pi$ - $\pi$ EDA interaction, hydrophobic effect	Jin et al. (2014)
DEP	Maize straw	450	NR	47.9	H-bonding, $\pi$ - $\pi$ EDA interaction, van der Waals force, pore-filling	Jing et al. (2018)
DEP	Wheat straw	450	NR	35.5	H-bonding, $\pi$ - $\pi$ EDA interaction, van der Waals force, pore-filling	Jing et al. (2018)
DEP	Corn cob	650	NR	10.0	H-bonding, $\pi$ - $\pi$ EDA interaction, van der Waals force, pore-filling	Jing et al. (2018)
DEP	Wheat straw	650	NR	15.5	H-bonding, $\pi$ - $\pi$ EDA interaction, van der Waals force, pore-filling	Jing et al. (2018)
<b>Antibiotics</b>						
Sulfamethazine	Hardwood litter	600	NR	NR	$\pi$ - $\pi$ EDA interaction, (-)CAHB	Teixidó et al. (2011)
Sulfamethoxazole	Giant reed	300–600	1.93–4.99	0.48–0.95	Pore-filling, partitioning, $\pi$ - $\pi$ EDA interaction, hydrophobic interaction	Zheng et al. (2013c)
Tetracycline	Rice husk	450–500	10.3	NR	$\pi$ - $\pi$ EDA interaction, H-bonding, external/surface/pore diffusion	Jing et al. (2014)
Tetracycline	Rice husk	450–500	18.5	NR	$\pi$ - $\pi$ EDA interaction, H-bonding, external/surface/pore diffusion	Jing et al. (2014)
Sulfamethazine	Tea waste	300–700	2.43–7.12	18.0–1080	$\pi$ - $\pi$ EDA interaction, cation- $\pi$ interaction, cation exchange, (-)CAHB	Rajapaksha et al. (2014b)
Sulfamethazine	Tea waste (steam activation)	300–700	2.79–33.8	62–2454	$\pi$ - $\pi$ EDA interaction, cation- $\pi$ interaction, cation exchange, (-)CAHB	Rajapaksha et al. (2014b)
Sulfamethazine	<i>Sicyos angulatus</i> L.	300–700	15.7–20.6	45.0–893	$\pi$ - $\pi$ EDA, H-bonding, hydrophobic effect, electrostatic interaction	Rajapaksha et al. (2015)
Sulfamethazine	Rice straw	600	31.4	0.815	H-bonding, $\pi$ - $\pi$ EDA interaction, partitioning	Zhang et al. (2016a)
Norfloxacin	Cornstalks	500	7.25	900	Electrostatic interaction, $\pi$ - $\pi$ EDA interaction, pore-filling	Wang et al. (2017a)
Norfloxacin	Reed stalks	500	3.51	2802	Electrostatic interaction, $\pi$ - $\pi$ EDA interaction, pore-filling	Wang et al. (2017a)
Norfloxacin	Willow branch	500	6.26	834	Electrostatic interaction, $\pi$ - $\pi$ EDA interaction, pore-filling	Wang et al. (2017a)

$K_d$ : Sorption coefficient; NR: Not reported

sorption. The hierarchically porous BC foams consisting of micro-, meso-, and macropores with high surface area (1370 m<sup>2</sup> g<sup>-1</sup>) were fabricated by heating biomass mixed with NaHCO<sub>3</sub> by Yang et al. (2017), who proposed a green novel method for producing modified BC adsorbents with high removal efficiency for atrazine (97.9 mg g<sup>-1</sup>). Overall, these studies highlight the promising prospects of engineered BC applied for organic contaminant removal. However, the negative effects should be carefully considered during the engineered BC production and application, such as the

negative effect of modification on BC-C stability and potential contaminants released from the physical/chemical activation processes and from the engineered BC during its application.

### 3.2.2 Mechanisms for Organic Pollutant Sorption by BC

A number of mechanisms may play roles in controlling the sorption of organic contaminants by BC, including (1) pore-filling, (2) electrostatic interaction, (3) hydrophobic



effect, (4) H-bonding, (5) electron donor–acceptor (EDA) interaction, and (6) partitioning. These interactions are shown in Fig. 4b. The contribution of these interaction mechanisms to the overall sorption is a function of both the surface and bulk properties of BC and a characteristic of organic contaminants. BC is a porous adsorbent that is typically composed of micropores, mesopores, and macropores (Jagiello et al. 2019; Sigmund et al. 2017). Thus, pore-filling is one of the dominant sorption mechanisms for those organic molecules which can access into BC's pores (Yang et al. 2017; Ji et al. 2011; Nguyen et al. 2007). Pore features of BCs and the molecular size of organic pollutants both control the contribution of pore-filling in sorption (Xiao and Pignatello 2015; Lattao et al. 2014; Li et al. 2013; Nguyen et al. 2007). Electrostatic interaction has been utilized to interpret adsorption of dissociated chemicals (e.g., antibiotics) and BCs with PZC of  $\sim 2$ , generally carrying negative charges over the pH range of 2–12 and positive charge at  $\text{pH} < 2$  (Chen et al. 2015; Zheng et al. 2013c). Hence, electrostatic repulsion between the dissociated species of organic chemicals and negatively charged BCs could result in an adsorption decrease (Zheng et al. 2013c; Liu et al. 2018b), while electrostatic attraction may increase adsorption (Xu et al. 2011; Qiu et al. 2009b). However, it is difficult to evaluate the contribution of electrostatic interaction to the overall sorption, because the dissociation of organic chemicals is always accompanied by the decrease of hydrophobic effect and H-bonding interaction of organic chemicals (Yang and Xing 2010). The surface of fresh BC (particularly produced at high temperature) with low surface oxidation is generally hydrophobic, and the aromatic C component can provide sites for sorption of HOCs or neutral molecule via hydrophobic effect (Zhu and Pignatello 2005; Sun et al. 2019b). For instance, Chen et al. (2011b) reported that hydrophobic interaction occurred between the C-F chains of perfluorooctane sulfonate (PFOS), one class of contaminants of emerging concerns, and hydrophobic sites on the maize straw- and willow-derived BCs. BC with numerous O-containing functional groups has a high potential for H-bonding accepting or donating with organic sorbates containing electronegative elements (Yang et al. 2019; Xiao et al. 2018; Lian and Xing 2017). For example, Sun et al. (2011) confirmed that the H-bonding interaction played a key role for bisphenol A (BPA) and 17 $\alpha$ -ethinyl estradiol sorption onto the hydrothermal BCs due to the higher abundance of O-containing functional groups, while H-bonding was minimal in phenanthrene sorption onto the thermal BCs with lower content of functional groups. Moreover, an exceptionally strong H-bonding that can form between a favorably orientated donor–acceptor pair having closely similar proton affinity (or pKa), known as negative charge-assisted hydrogen bonds [(-)CAHB] (Ni and Pignatello 2018), is usually overlooked in BC adsorption

(Inyang and Dickenson 2015). Teixidó et al. (2011) confirmed the existence of this special H-bonding between negative sulfamethazine and negative BCs at alkaline pH. EDA interaction with bond energy of 4–167  $\text{kJ mol}^{-1}$ , an important type of noncovalent-specific interaction involving aromatic  $\pi$ -systems, is now well accepted and proven to be a critical force for adsorption of planar aromatic compounds on graphene-like BC surfaces (Zhu et al. 2005; Teixidó et al. 2011; Rajapaksha et al. 2014b; Zheng et al. 2013c). Additionally, the effects of pH on EDA interactions cannot be ignored. At acidic solution, Teixidó et al. (2011) observed that the  $\pi$ – $\pi$  EDA interaction of the protonated aniline ring with the  $\pi$ -electron-rich graphene surface of BC, referred to as  $\pi^+$ – $\pi$  EDA, which was dominated instead of experiencing electrostatic cation exchange. Recently, Zhao et al. (2017) demonstrated the important role of cation  $-\pi$  interaction in ciprofloxacin (a model fluoroquinolone antibiotic) sorption on graphite (a model pyrogenic carbonaceous material), which has been confirmed in sorption of HMs to BCs (Fig. 4a). They also successfully identified the relative contribution of hydrophobic effect,  $\pi$ – $\pi$  EDA interaction, and cation  $-\pi$  interactions to the overall adsorption using sequential competition experiments. BC is heterogeneous, a mixture of non-carbonized phase and carbonized phase (Keiluweit et al. 2010; Chen et al. 2015; Liu et al. 2018a), thus partitioning in non-carbonized phase and adsorption with carbonized phase both contribute to the overall sorption of organic compounds on chars (Chen et al. 2008; Cao et al. 2009). This interaction has well been demonstrated for lots of organic contaminants sorbed on a variety of BCs (Table 3). Generally, partition is predominant in sorption of organic pollutants (e.g., antibiotics) to low-temperature BC, whereas adsorption was predominant for high-temperature BC (Zheng et al. 2013c). For moderate-temperature BCs (e.g., 300–400  $^{\circ}\text{C}$ ), both adsorption and partition cofunction. For example, Chen et al. (2008) verified that sorption mechanisms of BCs for naphthalene, nitrobenzene, and *m*-dinitrobenzene from water are evolved from partitioning dominant to adsorption dominant with increasing pyrolytic temperatures from 200 to 700  $^{\circ}\text{C}$ . Moreover, the partitioning presented with linear isotherm is non-concentration dependent (Zheng et al. 2013c), and its contribution can be easily estimated by the dual-mode model (Zheng et al. 2013c; Chen et al. 2008; Lian et al. 2011).

### 3.2.3 Degradation of Organic Contaminants by BCs

BC is commonly considered to control the fate and transport of organic contaminants via sorption in the environment. However, in recent years, BC has been shown to act as an electron transfer mediator for the reduction of organic contaminants (Oh et al. 2013; Fu et al. 2014; Fang et al. 2015b). For example, Oh et al. (2013) found that two BCs from

poultry litter and wastewater biosolids promoted the reductive reactions of nitro herbicides and explosives by dithiothreitol, probably resulted from graphene moieties, surface functional groups, and redox-active metals in the BCs. Ding and Xu (2016) reported that 1-trichloro-2,2-di(4-chlorophenyl)ethane (DDT) and its metabolites 1,1-dichloro-2,2-bis(4-chlorophenyl)-ethane (DDD) were degraded through surface intermediates of sulfide and BC, acting as both nucleophiles and bases. However, the nature of these surface intermediates is not clearly shown in this study, and requires further discernment. Similar results were also observed on other carbonaceous material such as AC (Chen et al. 2014b), graphene oxide (GO), and CNT (Fu et al. 2014). Studies have shown that BCs can donate, accept, or transfer electrons in their surrounding environments, either abiotically or via biological pathways (Yuan et al. 2017; Pignatello et al. 2017; Mian and Liu 2018), thus promoting degradation of organic contaminants. Two types of redox-active structures in BCs may be involved in the catalytic degradation, i.e., quinones and polycondensed aromatic structures as electron acceptor, and phenolic species as electron donor (Kluepfel et al. 2014). The activity and reactivity of pyrogenic carbonaceous matter (e.g., BC and AC) toward organic compounds involved reactions mediated or catalyzed by these materials were well reviewed by Pignatello et al. (2017). Further efforts are needed to better understand what chemical structures facilitate BC-mediated degradation of organic pollutants.

The PFRs in BC may also be responsible for the transformation of organic contaminants sorbed on BC (Yang et al. 2016b; Fang et al. 2015a). These radicals may induce the generation of reactive oxygen species (ROS), thus promoting the degradation of organic contaminants in water. Pan et al. extensively studied the generation of PFRs in BC and its roles in water remediation (Liao et al. 2014; Yang et al. 2016b; Pan et al. 2019). They found that BC could activate  $O_2$ ,  $H_2O_2$ , and persulfate to produce ROS such as  $\cdot OH$  and sulfate radical ( $SO_4^{\cdot -}$ ) to degrade organic contaminants. According to loading metals ( $Fe^{3+}$ ,  $Cu^{2+}$ ,  $Ni^{2+}$ , and  $Zn^{2+}$ ) and phenolic compounds (hydroquinone, catechol, and phenol) in biomass, Fang et al. (2015a) proposed novel methods to manipulate PFR concentration and type in BC for contaminant degradation. Recently, Wang et al. (2019a) found that the PFRs contained in BC acted as the electron donor involved in sulfamethoxazole degradation in the BC-induced  $Fe^{3+}$  reduction for persulfate activation system. As such, the degradation of organic pollutants from PFR in BC could be a common process and should not be ignored. These deeper understandings of redox reactions and PFRs

induced by BC will help in developing in situ bioremediation technologies for water or soil that are environmentally compatible.

### 3.3 Removal of Oxyanion Contaminants in Water by BC

Besides the aforementioned contaminants such as HMs, pesticides, antibiotics, and PAHs, inorganic oxyanions are also frequently detected in widespread surface and groundwater (Zheng et al. 2019b; Zhang and Gao 2013; Mizuta et al. 2004). The inorganic oxyanions include  $NO_3^-$ ,  $PO_4^{3-}$ , arsenate ( $AsO_4^{3-}$ ), arsenite ( $AsO_3^{3-}$ ), chromate ( $CrO_4^{2-}$ ), and perchlorate ( $ClO_4^-$ ), which seriously threaten water quality and safety due to their high solubility, mobility, and toxicity even in very low concentrations (Kumar et al. 2014). The removal of inorganic oxyanions is often a challenging task due to their various properties, such as solubility, ionic radius, hydration energy and bulk diffusion, especially when compared to other aquatic pollutants (e.g., metals, organic pollutants). Sorption is one preferred approach due to its low cost, high efficiency, simple operation, and environmental-friendly nature. However, pristine BC has a low removal capacity for oxyanions because of electrostatic repulsion between the anions and the negatively charged BC. For example, in our early study (Zheng et al. 2013b), we found no significant  $NO_3^-$  sorption on low-temperature BC ( $\leq 400^\circ C$ ), while only a small amount of  $NO_3^-$  (0.17–0.53  $mg\ g^{-1}$ ) was sorbed by the high-temperature BCs (500–600  $^\circ C$ ), which is related to the  $NO_3^-$  species being repelled by negatively charged BC surface. For  $PO_4^{3-}$ , all the BCs produced at 300–600  $^\circ C$  showed no sorption, owing to the high amount of  $PO_4^{3-}$  released from the BCs, as well as the electrostatic repulsion. However, more recent results on the sorption of the oxyanion by BC seem more promising. For example, Fang et al. (2013) reported that the wood-derived BCs produced at 500–700  $^\circ C$  with low polarity and high aromaticity displayed a superior  $ClO_4^-$  adsorption capacity, since these high-temperature BCs provided a hydrophobic microenvironment to accommodate weakly hydrated  $ClO_4^-$  and facilitated the H-bonds for  $ClO_4^-$  binding to functional groups by the large  $\pi$  subunit of their aromatic substrate. Yao et al. (2011) observed that the sugar beet tailing-derived BC had a high removal ability for  $PO_4^{3-}$  with a removal rate around 73%, likely due to the large amount of colloidal and nano-sized periclase ( $MgO$ ) on its surface. Similarly, Yao et al. (2013) reported that the maximum  $PO_4^{3-}$  sorption capacity by a BC prepared from

Mg-enriched tomato tissues was greater than  $100 \text{ mg g}^{-1}$ , much higher than those reported in other studies (Soenne et al. 2014; Zheng et al. 2013b; Chen et al. 2011a). Still, limited studies are available for any general conclusion on the sorption of oxyanion by the untreated BC, which should be paid more attention in the future.

To enhance sorption of these oxyanion contaminants, engineered or modified BCs using physical or chemical modification are highly recommended (Chen et al. 2011a; Zhang et al. 2013b; Zhang and Gao 2013; Wang et al. 2019b; Tan et al. 2016b; Rajapaksha et al. 2016; Yang et al. 2019). For example, Chen et al. (2011a) synthesized a novel magnetic BC by charring the chemical coprecipitation of  $\text{Fe}^{3+}/\text{Fe}^{2+}$  on orange peel powders, and the sorption capacity to  $\text{PO}_4^{3-}$  increased from  $0.48 \text{ mg g}^{-1}$  to  $1.24 \text{ mg g}^{-1}$ . Zhang and Gao (2013) reported that the sorption capacity of BC-AIOOH nanocomposite for  $\text{AsO}_4^{3-}$  was  $17.4 \text{ mg kg}^{-1}$ , much higher than other adsorbents such as  $\text{Al}_2\text{O}_3$  and activated  $\text{Al}_2\text{O}_3$ . For selecting the modification method, a basic guide is to introduce a metal or metals into a BC either in elemental, oxide/hydroxide or layered double hydroxide (LDH) form from the known reactivity of oxyanions with ions or oxides of metals like La, Al, Ca, Fe, Mg, etc. (Kumar et al. 2014). Recently, Li et al. (2018a) reviewed the sorption of oxyanion contaminants from aqueous solution by the metal oxide-BC composites prepared by different carbothermal treatments, including chemical activation (e.g.,  $\text{MgCl}_2$ ,  $\text{ZnCl}_2$ , and  $\text{FeCl}_3$ ), elemental metal support (e.g.,  $\text{Cu}^0$  and  $\text{Fe}^0$ ), single metal oxide/hydroxide modification (e.g., oxides/hydroxides of La, Al), and binary metal oxide/hydroxide functionalization (e.g., Ca-Mg-BC composite). The sorption mechanisms of these metal oxide-BC composites toward the oxyanion contaminants involve surface complexation, electrostatic interactions, ion exchange, chemical reduction, chemical oxidation, and precipitation (Li et al. 2018a). For a given modified BC, it should be noted that these mechanisms contribute differently for the specific oxyanion, and are largely affected by the properties of the modified BC. Moreover, aside from production cost which must be minimized, the environmental risks such as potential toxicity resulted from the incorporated metals should be carefully examined.

### 3.4 BC as Amendment for Soil Remediation

Global food security will still be a worldwide challenge for the next 50 years and beyond (Godfray et al. 2010). Healthy soil is essential for sustainably providing food, maintaining ecosystem biodiversity, and mitigating the climate change (Koch et al. 2012, 2013). However, soil contamination with xenobiotic compounds such as HMs and organic pollutants (e.g., PAHs, polychlorinated biphenyls (PCBs), pesticides,

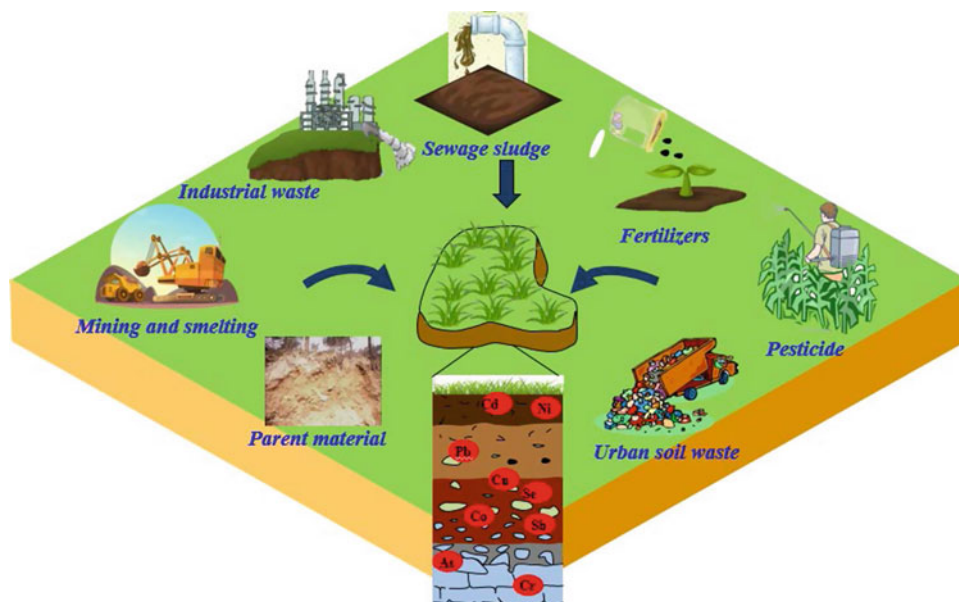
phthalic acid esters (PAEs), and antibiotics) not only leads to gradually declining soil quality and severe economic constraints, but also threatens ecosystem functions and public health. Soil contamination is becoming a global issue, and the problem is especially severe in China (MEP 2014). Research and practice on various techniques such as washing with extractants, chemical oxidation/reduction, and bioremediation for these polluted soils have been performed due to growing awareness about the harmful effects of HM and organic pollutants (Sun et al. 2018; Gong et al. 2016; Wang et al. 2018a; Morillo and Villaverde 2017). As a multi-beneficial amendment, BC has been recognized as a promising solution for these problematic soils (Kuppusamy et al. 2016; Sun et al. 2018; Gong et al. 2016). Application of BC in soil not only may remediate the contaminants, but also has some potential benefits with respect to soil fertility improvement (Zheng et al. 2013b, 2018b; Wang et al. 2017d), waste management (Liao et al. 2013), C sequestration (Zheng et al. 2018c; Luo et al. 2016), and bioenergy production (Zheng et al. 2017).

## 3.5 Remediation of HMs in Soils by BC

### 3.5.1 Soil Contamination with HMs

Soil pollution by HMs has become a global issue, especially for developing countries (Yang et al. 2018b; Zhang et al. 2018). According to a 6-year national soil quality survey issued by the former Chinese Ministry of Environment Protection (MEP 2014), approximately 19.4% of the nation's agricultural land (26 million out of 135 million ha) has been contaminated by HM(loid)s and organic chemicals. Particularly, the over-standard rates (GB15618-1995) of Cd, Hg, As, Pb, and Cr in the sampled soils were 7.0%, 1.6%, 2.7%, 1.5%, and 1.1%, respectively. Recently, several researchers reviewed soil HM pollution in China (Zhang et al. 2018; Yang et al. 2018b). For example, according to the collected data of Pb, As, Cd, Cr, and Hg concentration in soils of 402 industrial sites and 1041 agricultural sites in China via document retrieval, Yang et al. (2018b) concluded that Cd, Pb, and As presented more serious pollution and associated risks in the soils, and that those in southeast China were more severely affected than those in northwest China. HMs in soils are primarily the result of anthropogenic human activities, such as sewage irrigation, sludge application, and mining and smelting operations for metallic ores (Fig. 5). It is estimated that approximately more than 30,000 tons of Cr and 800,000 tons of Pb have been released into the environment globally, with the majority of this accumulating in soil (Yang et al. 2018b). Unlike organic contaminants, HMs cannot be degraded by microorganisms, and both persist and continuously accumulate in soil as a result, posing a serious risk to plants, human beings, and animals

**Fig. 5** Major sources of HMs in soil from anthropogenic human activities and natural mineralization of rocks and minerals



via direct exposure or the food chain (Yuan et al. 2019; Sarwar et al. 2017). Moreover, soil contamination always results in the diminishing availability of arable lands, aggravating the contradiction between increasing population and demand for arable lands. The government of China has taken a variety of approaches to solve the serious soil pollution, such as a national action plan “Soil Ten Chapter”. Consequently, there is growing demand for the remediation of HM-polluted soils (Sun et al. 2018; Song et al. 2017; Yuan et al. 2019).

A variety of physical, chemical, and biological techniques can be used to remediate metal contaminated soil (Song et al. 2017; Sarwar et al. 2017). The remediation technologies generally can be divided into in situ and ex situ remediation. Compared to the costly and expensive ex situ remediation, in situ remediation has several advantages such as lower cost, less ecological disruption, and easier operation (Sarwar et al. 2017; Song et al. 2017). The in situ remediation technologies include physical, chemical, biological, and combined methods, which have been reviewed by Song et al. (2017). Recently, using BC for in situ remediation of contaminated soil has been recommended (Kołodziejńska et al. 2012; Rajapaksha et al. 2014b; Cao et al. 2009), because of BC’s porous structure and large surface area, high mineral content, and the associated benefits for soil improvement (Yuan et al. 2019; Xiao et al. 2018).

### 3.5.2 Remediation of Soils Contaminated with HMs by BC

A growing number of studies have reported great potential for BC amendment in the immobilization and reduction of mobility and availability of HMs in the contaminated soils using laboratory and field trials, which are summarized in

Table 4. Most of these studies documented that positive effect of BC on remediating HM-contaminated soils. For example, Uchimiya et al. (2010) reported significant immobilization of Cu, Cd, Ni, and Pb by the broiler-litter-derived BCs at 350 and 700 °C in soil respectively, mainly due to adsorption and precipitation of the metals with BCs. A study used dairy-manure-derived BC to remediate the Pb-contaminated soil, and showed that the released P contained in BC (~2%) reacted with Pb to form insoluble  $Pb_5(PO_4)_3(OH)$ , and thus decreased  $CaCl_2$  extracted and toxicity characteristic leaching procedure (TCLP) concentrations of Pb by 57% and 89%, respectively (Cao et al. 2011). In addition, a commercial AC as a comparison was included in this study, but the AC was ineffective for immobilizing Pb, with only 13–25% reduction of Pb in  $CaCl_2$  extract and 12–18% reduction in the TCLP extract. This is mainly attributed to the much lower ash content of the AC (0.8% for AC vs 52% for BC). These results suggested that the mineral component in BC significantly contribute to HM immobilization in soil. Similar to the BC from animal manure waste, the BC from plant biomass can also passive HMs in soil (Table 4). For instance, Zheng et al. (2012) incorporated the BCs from different parts of rice plants (straw, husk, and bran) in a historically multi-metal contaminated soil, and they found that the BCs significantly decreased pore water concentrations of Cd and Zn, thus decreasing rice shoot concentrations of Cd and Zn by up to 98 and 83% respectively. Besides the combined effect of increasing pH and sorption of HMs by complexation and precipitation with BCs, the increased capacity of iron plaque for retaining HMs (e.g., Pb, Cd) is considered as the main mechanism for reducing their accumulation in rice shoots (Zheng et al. 2012). Consequentially, the enhanced

immobilization of HMs by BC addition can reduce the toxicity of HMs and their uptake and accumulation in plants (Ahmad et al. 2012; Fellet et al. 2011; Houben et al. 2013; Li et al. 2016a; Wang et al. 2018c; Zheng et al. 2012).

A few studies reported no and even negative effects (Table 4). For instance, Namgay et al. (2010) conducted a pot experiment to investigate the influence of BC on the availability of As, Cu, Pb, and Zn in a sandy soil grown with maize. They observed that BC addition increased the concentrations of extractable As and Zn in soil, while Cu concentration did not change and Pb concentration decreased. As a result, the BC treatment decreased the concentration of As and Cu in the maize shoot, whereas increased Pb and Zn concentrations in the shoots. Houben and Sonnet (2015) reported that the concentrations of Cd, Pb, and Zn in roots and shoots of both *Agrostis capillaris* L. and *Lupinus albus* L. were not significantly reduced by BC from miscanthus straw. This was mainly attributed to the remobilization of metals in the rhizosphere soil as a result of organic acids (e.g., malic acid, citric acid) in root exudates, which counteracted the liming effect of BC for metal immobilization. This study also addressed the significance of pH changes in rhizosphere soils amended with BC. Moreover, reversible sorption of HMs on BC via specific interactions (e.g., ion exchange and electrostatic interaction) may result in remobilization of the bonded metals into soil, weakening the positive contribution of BC in HM remediation (Melo et al. 2016). These studies suggested that one type of BC may not be appropriate for all cases of HM-contaminated soils. Therefore, more research is warranted to investigate BCs' effectiveness in HM remediation in soil under different conditions.

Most of these remediation studies are conducted under laboratory conditions, which are typically simplified and carefully managed without any disturbance (Cao et al. 2011; Park et al. 2011; Uchimiya et al. 2010; Wang et al. 2018). BC application in the remediation of polluted land has not been well-studied in the field due to various environmental factors, such as dry-wet cycling, freeze-thawing cycling, rainfall, and temperature. According to a document retrieval, O'Connor et al. (2018) only found that 29 publications were related to the in situ field applications of BC in remediation of HM-contaminated soil. These studies reported inconsistent results (i.e., beneficial, neutral, or adverse effects), likely due to the large variety of soil types, BC properties, and field conditions. For example, Bian et al. (2016) conducted a field experiment in a Cd-contaminated rice paddy field to evaluate the effect of wheat straw BC and other stabilizers (i.e., calcium hydroxide and silicon slag) on Cd mobility and rice uptake. They found that the BC decreased Cd extractability by up to 43% and Cd rice uptake by up to 61%, being the most

effective on Cd immobilization. Moreno-Jiménez et al. (2016) demonstrated that a holm oak chip-derived BC reduced Cd and Pb in grain, whereas As concentration slightly increased in a field plot experiment. To practically apply BC as a promising passivator for soil remediation, more field trials using carefully selected or designed BC are necessary.

The positive effect of BC on heavy metal remediation is primarily dependent on BC's strong adsorption capacity resulted from the abovementioned sorption mechanisms (Sect. 3.1.2), and BC's liming effect due to its inherent minerals (Xu et al. 2017; Cao et al. 2011; Uchimiya et al. 2010). Apart from these mechanisms, the application of BC may improve soil properties, such as soil aggregate stability, WHC, CEC, soil organic matter (SOM), and nutrient content, and thus increase the plant biomass. The increased biomass may lead to a "dilution effect" of HMs in plant (Beesley et al. 2010; Park et al. 2011; Yasmin et al. 2017), which is also one of the reasons responsible for the decreased concentration of HMs in plants. In addition, the formation of iron plaque around plant roots in flooded conditions would contribute to the reduced uptake of HMs. Zheng et al. (2012) first observed that the increased formation of iron plaque following BC addition, which can retain Pb via sorption, is the main mechanism for reducing Pb accumulation in rice shoots in the BC-amended soil under flooded conditions. Similar findings were also reported by Qiao et al. (2018a). They co-applied BC and nZVI to a paddy soil to remediate Cd and As pollution. They demonstrated that the mixture of nZVI and BC addition reduced the mobility and bioavailability of both Cd and As in the soil, and the co-application showed synergistic effects relative to the BC or nZVI alone. The main reasons for this positive effect are the enhanced formation of iron plaque as a result of the increased amorphous Fe oxides in soil, the strong adsorption capacity of BC, and the increased soil pH. This study provides a good choice for remediating Cd and As co-contaminated soil using the mixture of nZVI and BC. Moreover, this study also highlights the significance of designing engineered BC or BC composite with specific properties to the target HMs in soil. A variety of physical and chemical methods can be used to enhance BC's effectiveness in HM remediation, which have been reviewed by Wang et al. (2019b), Tan et al. (2016b), and Rajapaksha et al. (2016). The HMs immobilized by BC in soil by these mechanisms would unavoidably undergo a series of processes such as plant uptake, leaching, volatilization, redox reaction, and/or methylation/demethylation (Yuan et al. 2019). These processes will determine the final fate of HMs during soil remediation, which should be carefully considered in future studies.

**Table 4** Application of BC in remediating soils contaminated by HMs

HMs	Feedstock	Pyrolysis temperature (°C)	Dosage	Study scale	Performance of BC	Proposed mechanism	References
Pb	Broiler litter	350	5, 10, 20%	Lab	Enhanced immobilization and retention of Pb	Adsorption, liming effect	Uchimiya et al. (2010)
	Dairy manure	450	2.5%	Lab	Decreased TCLP concentration in soil by 70–89%	Adsorption	Cao et al. (2011)
	Green waste	550	5%	Lab	Increased immobilization by 36.8%	Adsorption	Park et al. (2011)
	Chicken manure	550	1, 5, 15%	Lab	Decreased exchangeable Pb by 9.6–42.2%	Adsorption	Park et al. (2011)
	Wheat straw	350–550	10, 20, 40 t ha <sup>-1</sup>	Field	Decreased Pb uptake in rice by 16.7–79.6%	Adsorption	Bian et al. (2014)
	Canola straw	400	5%	Lab	Enhanced the adsorption capacity for Pb by 44%	Adsorption, liming effect	Jiang et al. (2014)
	Soybean straw	400	5%	Lab	Enhanced the adsorption capacity for Pb by 37.3%	Adsorption, liming effect	Jiang et al. (2014)
	Peanut straw	400	5%	Lab	Enhanced the adsorption capacity for Pb by 60.8%	Adsorption, liming effect	Jiang et al. (2014)
	Bamboo	500	5%	Lab	Decreased TCLP-extractable Pb	Adsorption	Wang et al. (2018c)
	Walnut shell	500	5%	Lab	Decreased TCLP-extractable Pb	Adsorption	Wang et al. (2018c)
	Sugarcane bagasse	450	1.5, 2.25, 3.0 t ha <sup>-1</sup>	Field	Decreased Cd bioavailability by 5.3–8.4%	Adsorption, precipitation	Nie et al. (2018)
Cd	Broiler litter manure	350	5, 10, 20%	Lab	Enhanced Cd immobilization	Adsorption, liming effect	Uchimiya et al. (2010)
	Green waste	550	5%	Lab	Immobilized Cd by 30.3% for the spiked soil	Adsorption	Park et al. (2011)
	Rice straw	500	5%	Lab	Decreased rice shoot concentrations of Cd by 98%	Adsorption	Zheng et al. (2012)
	Wheat straw	350–550	10, 20, 40 t ha <sup>-1</sup>	Field	Decreased extractable Cd by 28.3–70.9%	Surface precipitation	Bian et al. (2014)
	Wheat straw	450	10, 20, 40 t ha <sup>-1</sup>	Field	Decreased total Cd concentrations in paddy soil by 7.5–23.3%	Abundant functional groups and improve soil microstructure	Cui et al. (2016b)
	Corn straw	300	5%	Lab	Decreased CaCl <sub>2</sub> extractable Cd by 53.6%	O-containing groups of biochar provide oxygenated binding sites	Li et al. (2016a)
	Sugarcane bagasse	450	1.5, 2.25, 3 t ha <sup>-1</sup>	Field	Decreased bioavailability of Cd by 2.7–5.6%	Adsorption	Nie et al. (2018)
	Rice straw	500	5%	Lab	Decreased Cd concentration in plant	Adsorption	Wang et al. (2018c)
	Walnut shell	500	5%	Lab	Decreased Cd in roots by 77%	Adsorption	Wang et al. (2018c)
	Bamboo	500	1%	Lab	Decreased exchangeable Cd in soil by 12.5%	Adsorption	Wu et al. (2019a)
	S-modified bamboo	500	1%	Lab	Decreased exchangeable Cd in soil by 29.7%	Adsorption	Wu et al. (2019a)

(continued)

**Table 4** (continued)

HMs	Feedstock	Pyrolysis temperature (°C)	Dosage	Study scale	Performance of BC	Proposed mechanism	References
Cu	Broiler litter manure	350	5, 10, 20%	Lab	Enhanced Cu immobilization	Adsorption, precipitation	Uchimiya et al. (2010)
	Green waste	550	1, 5, 15%	Lab	Decreased exchangeable Cu by 1.4% – 20.5%	Adsorption	Park et al. (2011)
	Chicken manure	550	1, 5, 15%	Lab	Decreased exchangeable Cu by 3.5–11.7%	NR	Park et al. (2011)
	Rice hull	500	10%	Lab	Decreased uptake of Cu in lettuce by 28%	NR	Kim et al. (2015)
	Corn straw	300	5%	Lab	Decreased available Cu by 66.8%	Adsorption	Li et al. (2016a)
	Sugarcane bagasse	450	1.5, 2.25, 3.0 t ha <sup>-1</sup>	Field	Decreased bioavailability of Cu by 3.4–6.0%	Adsorption	Nie et al. (2018)
	Rice straw	500	5%	Lab	Reduced Cu uptake in roots by 35%	Adsorption	Wang et al. (2018c)
	Walnut shell	500	5%	Lab	Reduced Cu uptake in roots by 26%	Adsorption	Wang et al. (2018c)
Zn	Sydney blue gum	550	1.5%	Lab	No effect on Zn uptake by plant	NR	Namgay et al. (2010)
	Miscanthus straw	600	5%	Lab	No effect on Zn uptake by plant	Remobilization of metals in soil resulted from root exudates	Houben and Sonnet (2015)
	Hardwood	600	0.5, 1, 2%	Field	Reduced extracted Zn by 83–98%	Adsorption	Shen et al. (2016)
	Rice straw	500	124, 270 t ha <sup>-1</sup>	Field	Decreased recommended concentration in wheat grains by 16.7–18.7%	Precipitation, adsorption	Wu et al. (2018)
Ni	Hardwood	600	0.5%, 1%, 2%	Field	Reduced extracted Ni by 83–98%	Adsorption	Shen et al. (2016)
	Broiler litter manure	350	5%, 10%, 20%	Lab	Enhanced immobilization	Adsorption and precipitation	Uchimiya et al. (2010)
	Broiler litter manure	700	5, 10, 20%	Lab	Enhanced immobilization	Adsorption and precipitation	Uchimiya et al. (2010)
	Rice husk	550	2.5%	Lab	Decreased Ni uptake by plant by 65.2%	Liming effect	Boostani et al. (2019)
	Licorice root pulp	350	2.5%	Lab	Decreased Ni uptake by plant by 67.2%	Liming effect	Boostani et al. (2019)
As	Activated wood	550	0.5, 1.5%	Field	Decreased the concentration of As in maize shoots significantly	Adsorption	Namgay et al. (2010)
	Sydney blue gum	550	1.5%	Lab	Increased the concentration of available As in soil	NR	Namgay et al. (2010)
	Wheat straw	200	1, 2, 5%	Lab	Decreased the bioavailability of As	Regulated iron leaching which contributed to arsenic immobilization	Zhu et al. (2019)

NR: Not reported

### 3.5.3 Factors Affecting HM Remediation in Soil Using BC

The effectiveness of BC in remediating HMs in soil is governed by the properties and dosage of BC, species and concentrations of HMs, soil properties (e.g., pH, SOM), plant types, and climate conditions. It is well known that the feedstock and pyrolytic temperature are two main factors that greatly influence BC's characteristics, such as surface area, O-containing groups, and inherent minerals (Xiao et al. 2018; Lian and Xing 2017). As such, these varied properties would determine BC's effectiveness in amending HM-contaminated soil via mediating the interactions between BC and HMs (Fig. 4a). A large number of BCs prepared from different biomasses have been reported to display positive performance in reducing the availability and mobility of HMs in soils, such as wheat straw (Bian et al. 2013; Cui et al. 2016b), woody waste (Cui et al. 2016a; Shen et al. 2016), industrial by-product (Nie et al. 2018), and sewage sludge (Zhang et al. 2016e). For example, Zheng et al. (2015) reported that the rice-straw-derived BC had a greater potential in reducing the accumulation in rice than the bean-stalk-derived BC, mainly due to the higher ash content and higher pH. Similarly, Igalavithana et al. (2017) reported that the BC from vegetable waste exhibited greater ability for Pb immobilization than the pine cone BC under field condition. Although various BCs produced at a wide range of pyrolytic temperatures (200–700 °C) have been used to remediate the HM-polluted soils (Table 4), the current understanding of the relationship between BCs' performance (particularly at field conditions) and the pyrolysis temperature and resultant physicochemical characteristics of BCs is largely limited.

The dosage of BC is one of the predominant factors in improving soil properties and remediation effects and also determines the cost of remediation project. In general, high dosage of BC application would favor immobilization of HMs in soil. Cui et al. (2011) undertook a 2-year field experiment with BC at 10–40 t ha<sup>-1</sup> into Cd-contaminated soil, and they found that the Cd enrichment in rice grains decreased with increasing BC dosages. Similarly, a 40 t ha<sup>-1</sup> BC addition showed greater reduction of Cd content in rice grain compared with a lower rate of 20 t ha<sup>-1</sup> (Bian et al. 2013). Lu et al. (2017) also reported that the higher dosage (5%) of bamboo and rice straw BCs favored the immobilization of Cd, Cu, Pb, and Zn and the decrease of their mobility and bioavailability in contaminated land than the lower dosage (1%). In the laboratory studies, BC is usually added by rate of BC weight per unit soil (w%) in pots, which is hard to compare with the rate of BC weight per ha soil (t ha<sup>-1</sup>), when the soil properties such as bulk density and depth of plough layer are not presented. Therefore, it is better to use the consistent unit (e.g., t ha<sup>-1</sup>) for BC application rate in both laboratory and field studies in future. It

should be noted that several studies applied BC at a relatively high rate (e.g., 124–270 t ha<sup>-1</sup>) (Wu et al. 2018), which is not practical. Such large amount of BC added into soil may increase the remediation cost and potential risk to soil ecosystem. Most of the studies used the moderate rates 10–40 t ha<sup>-1</sup>, which also may result in high economical burden for the remediation project because of the high cost of BC due to the immaturity commercial market. Only a small number of studies applied BC at low dosage rates of <5 t ha<sup>-1</sup>, showing promising results for BC application. Moreover, an optimum BC rate for the positive effect in terms of HM immobilization and economic feasibility has not been observed. As such, it is still necessary to decrease the rate of BC added in soil as less as possible. More studies are needed to establish the dosage-dependent positive effects of BCs when applied to soil at modest and practicable application rates (e.g., < 5 t ha<sup>-1</sup>) (Zhang et al. 2016e).

The mobility and availability of HMs in soil is also determined by a large number of soil conditions, including pH, SOM, redox potential, CEC, moisture, nutrient level, mineral composition, and temperature (Lahori et al. 2017). Among these factors, pH and SOM are the two most important factors, which also largely affect the effectiveness of BC on HM remediation. Soil pH is a key factor determining the forms and solubility of HMs in soil. As discussed above, BC may increase soil pH and thus immobilize HMs in soil due to its alkaline nature and high pH buffering capacity (Xu et al. 2017; Cao et al. 2011; Uchimiya et al. 2010). This effect is more profound for acidic soil (normally <5.5) (Dai et al. 2017) than alkaline soils, in which BC has little effect on soil pH, or even may decrease soil pH (Zheng et al. 2018b). A decrease in soil pH may increase availability of HMs, offsetting the BC's positive effect. Additionally, the pH buffering capacity of BC would decrease and even exhaust with time (Dai et al. 2017), thus the contribution of liming effect of BC on HM immobilization could unavoidably decrease or even vanish. SOM, carrying with negative charge with the presence of carboxyl and phenol groups, may effectively immobilize HMs by various interactions such as complexation, ion exchange, and electrostatic interaction. Generally, higher content of SOM results in better stabilization of HMs (O'Connor et al. 2018). Being carbonaceous, BC will inherently increase SOM content, which will be discussed in the following section, thus contributing to stabilization of HMs. BC may show different performances in HM-contaminated soil with different levels of SOM. For example, Uchimiya and Bannon (2013) observed that the BCs effectively stabilized Pb and Cu in a soil containing disproportionately high OC (31.6%), whereas the BCs mobilized Pb and Cu in sandy soils containing low OC (0.5–2.0%). They speculated that this negative effect was due to the depletion of dissolved OC by supernatant replacements leading to reduced solution-phase



complexation of Pb and Cu. However, no general relationship has been established between the content of SOM and HM remediation by BC. According to a meta-analysis, Chen et al. (2018a) demonstrated that BC is more prone to reducing HM availability in coarse or medium soils than fine-textured soil, but the mechanisms are not clear. The concentration of target metals in soil may also affect BC's efficacy. For instance, Zhang et al. (2017) observed that the addition of rice straw BC addition decreased the uptake of Cd by lettuce in a lightly Cd-polluted soil, but had either no effect or promoted Cd uptake in heavily Cd-polluted soils. The authors concluded that this unexpected negative result might be attributed to the BC's limited adsorption capacity, which was not enough to immobilize soil bioavailable Cd at the rate of 20 t ha<sup>-1</sup>. Thus, it is necessary to carefully evaluate the maximum adsorption capacity of BC and the interactions between BC and the target metals before applying BC as a passivator for remediating HMs in soil. The efficacy of BC will further depend on other soil conditions such as soil redox potential, CEC, moisture, and nutrient level, which received little attention in the past. The climatic factors including precipitation and temperature in the field studies should also be carefully considered. For example, greater rainfall may result in higher leaching potential, or the acceleration of BC aging through weathering (O'Connor et al. 2018), affecting BC's efficacy in soil remediation. Therefore, more investigations should be carried out in different climates and soil environments.

### 3.6 Remediation of Organic Pollutants in Soils Using BC

#### 3.6.1 Soil Contamination with Organic Pollutants

Agricultural soil has been severely polluted by various organic chemicals, such as PAHs, PCBs, pesticides, PAEs, antibiotics, and even petroleum hydrocarbons. These contaminants are usually the result of anthropogenic activities like the long-term application of pesticides, chemical fertilizer, livestock manure, plastic film, wastewater irrigation, sewage application, and oil exploitation (Sun et al. 2018; Morillo and Villaverde 2017). Soil has become one of the sinks for organic pollutants, and lots of these contaminants in soil are difficult to degrade under normal environmental conditions (Zhang et al. 2013a). For example, PAHs are primarily formed during the incomplete combustion or pyrolysis of organic matter (Zheng et al. 2018a), and the total emission of the 16 priority PAHs for China in 2003 contributed to over 20% of the global emissions (Zhang and Tao 2009). PAEs are a class of chemicals that are widely used as plasticizers in products like toys, cosmetics, food packaging, medical devices, and plastic films (He et al. 2015; Sun et al. 2019b). The extensive use of plastic films has resulted in widespread

PAE pollution in agricultural soils, with the highest levels of 3738 ± 5840 ng g<sup>-1</sup> among the studied organic contaminants in Chinese agricultural soils (Sun et al. 2018). China uses the largest amount of pesticides in the world, and more than 20 organochlorine pesticides were detected in the agricultural soils with an average concentration of 58.9 ± 51.5 ng g<sup>-1</sup> (Sun et al. 2018). Antibiotics can be introduced into soil through reclaimed water irrigation and sludge or manure-based fertilizer application, and their reported concentration (μg–mg per kg soil) varies greatly (Qiao et al. 2018b). The concentrations of these organic contaminants have increased over the decades, especially in industrialized regions of the world, and they will continue increasing due to ever-increasing anthropogenic emissions, if the efficient regulations are not adopted. Additionally, new organic contaminants which have yet to be detected or reported may already be present in soils due to the limitations of the analytical methods used and government regulations.

The continuous accumulation of the organic pollutants in agricultural soil may pose significant risks to the ecological functions of soils, plant growth, and eventually, human health. Some organic pollutants (e.g., PAHs, PCBs) recalcitrant degradation are even carcinogenic and mutagenic (Henner et al. 1999). PAHs could also serve as one of the selective stresses for enriching antibiotic resistance genes (ARGs) in soil (Chen et al. 2016). Numerous toxicological studies have demonstrated that some PAEs are endocrine disrupting chemicals (Sun et al. 2019a), and dimethyl phthalate (DMP), di-n-butyl phthalate (DBP), and di-n-octyl phthalate (DOP) have been classified as the priority control pollutants by United States and China. Antibiotics in soils may cause the occurrence of antibiotic resistance genes (ARGs), which is a global health crisis (Hao et al. 2015). Moreover, an increasing number of studies on plant uptake of antibiotics and ARGs have addressed the potential risk to human health through trophic transfers (Miller et al. 2016). As a result, it is imperative to decrease or eliminate these chemicals from soils. Sun et al. (2018) reviewed the remediation technologies for soil organic pollution according to different categories, including thermal treatment, vapor extraction technology, chemical oxidation and reduction, bioremediation, phytoremediation, and integrated remediation technologies. Among these methods, application of BC in chemical remediation, bioremediation, or phytoremediation has gained increasing interest due to the unique properties and the attached benefits (Yuan et al. 2019; Liu et al. 2018c; Kuppusamy et al. 2016).

#### 3.6.2 Remediation of Soils Contaminated with Different Organic Pollutants by BC

In the past 10 years, a growing number of studies reported that BC can be used for remediating organic pollutants in soil (Table 5). As a low-cost and environment-friendly carbonaceous adsorbent, BC may increase sorption of the

organic compounds by soil, thus largely reducing their mobility and bioavailability to crops and fauna. For example, Yu et al. (2009) investigated the effectiveness of two woody BCs produced at 450 and 850 °C in reducing the bioavailability of two soil-applied insecticides (chlorpyrifos and carbofuran) to spring onion (*Allium cepa*). They found that the uptake of pesticides by onion decreased markedly with increasing BC rate from 0.1 to 1%, and the high-temperature BC (850 °C) showed better performance than the lower temperature BC (450 °C). Hurtado et al. (2017) assessed the attenuation capacity of a woody BC to mitigate the lettuce uptake and translocation of 10 organic contaminants (i.e., BPA, caffeine, carbamazepine, clofibrac acid, furosemide, ibuprofen, methyl dihydrojasmonate, tris (2-chloroethyl)phosphate, triclosan, and tonalide) commonly found in reclaimed irrigation water. After 28 days of irrigation with the water containing these organic contaminants at 15 µg L<sup>-1</sup>, their average concentration in roots and leaves decreased by 20–76% in the BC-amended soil relative to the non-amended soil. A large number of BCs produced from different biomasses at different conditions have been reported to remediate the soils contaminated by PAHs, PCBs, pesticides, PAEs, and antibiotics (Table 5).

PAHs and PCBs are two commonly reported organic contaminants in soil, which have been early remediated using carbonaceous materials such as AC and charcoal (Gong et al. 2007; Liu and Yu 2006). Similarly, BC has also been shown to reduce the bioavailability of PAHs or PCBs due to its strong affinity and high capacity of PAHs sorption (Table 5). For example, Zhang et al. (2010) and Chen et al. (2012a) reported that BC addition enhanced soil sorption to PAHs (e.g., phenanthrene, naphthalene, and pyrene). The BC-enhanced sorption of PAHs in soil may decrease their leaching (Beesley et al. 2010; Oleszczuk et al. 2012), and reduce their uptake by plants (Khan et al. 2013; Brennan et al. 2014; Ni et al. 2018) or earthworms (Gomez-Eyles et al. 2010). Denyes et al. (2013) first compared the effects of in situ BC and AC amendments to a PCB-contaminated Brownfield soil, and found that the PCB concentrations in *Cucurbita pepo* root were reduced by 74, 72, and 64%, with the addition of granular AC and two BCs from manufacturers, respectively. This study implied that both BCs performed equally to the AC at decreasing PCB bioavailability. Moreover, BC can promote bioremediation of contaminated soil as carriers for functional microbes. For example, Chen et al. (2012a) loaded two PAH-degrading bacteria, *Pseudomonas putida* and an unidentified indigenous bacterium on four plant-derived BCs for bioremediation of soil with a long history of PAH contamination. They found that the BCs can promote bioremediation of contaminated soil as microbial carriers, because the BCs could pre-concentrate PAHs to a high concentration via sorption after being input into soil, and then significantly shorten the contact distance between

the pre-concentrated PAHs and the immobilized microorganisms. However, these findings were only obtained from a laboratory study, and the performance of these bacteria-loaded BCs should be tested in the field under actual environmental conditions in future. In addition, it should be noted that BC addition may also increase soil PAH content. For instance, Kusmierz et al. (2016) studied the persistence of PAHs in an acidic soil (loamy sand) applied with BC in a two and half year field trial. Unexpectedly, they observed that the BC addition increased the PAHs content from 0.24 mg g<sup>-1</sup> in control soil to 0.53-mg g<sup>-1</sup> and 1.31 mg g<sup>-1</sup> in the soil amended with BC at 30 and 45 t ha<sup>-1</sup>, respectively, which was resulted from the inherent PAHs formed during BC production (Keiluweit et al. 2012; Hale et al. 2012). As a result, the BC should be carefully selected and suitable strategies should be applied to produce BC with minimum contamination of PAHs and other pollutants (Buss et al. 2016).

In situ application of BC amendment for remediating the pesticide-contaminated soil is one of the hotspots over the past years, and lots of studies at laboratory and field scale were extensively reported (Table 5). The involved pesticides include chlorpyrifos, carbofuran, fipronil, atrazine, malathion, parathion, and diazinon. All these studies demonstrated that BC addition may increase their sorption by soils, and thus mitigating their mobility and plant uptake. Besides sorption, BC may affect pesticide transformation via affecting soil physicochemical properties (e.g., pH, WHC, and SOM), microbial activity and community composition, and enzyme activity (Zhu et al. 2017). For example, Ali et al. (2019) observed that four BC amendments reduced the accessible content of 21 different organochlorine pesticides, but increased the abundances of *Proteobacteria*, *firmicutes*, *Gemmatimonadetes*, and *Actinobacteria*. Further, Tang et al. (2017) compared the ability of BC and Fe-impregnated BC to reduce uptake of chlorpyrifos by Welsh onion from soil. They found that the Fe-BC was more effective in reducing the uptake of chlorpyrifos and its degradation product (3,5,6-trichloro-2-pyridinol) because of the improved sorption ability and increased plant root iron plaque. However, it should be noted that BC addition may have contrary effects on transformation of pesticides in soil. On the one hand, pesticide sorption on BC may increase its retention (Larsbo et al. 2013; Tang et al. 2017), and thus decrease the bioavailability to plants and soil microbes (Yu et al. 2009; Yang et al. 2010). This may well contribute to reduce pesticides residues in agricultural products from agricultural perspective. On the other hand, the decreased bioavailability of pesticide may reduce its efficiency for pest and disease control, which is undesirable for agricultural production. Moreover, the enhanced soil microbial activity induced by improvement of soil habitat in the BC-amended soil may accelerate the biodegradation of pesticides (Ali et al. 2019;

**Table 5** Application of BC in remediating soils contaminated by organic pollutants

Organic pollutants	Feedstock	Pyrolytic temperature (°C)	Dosage	Study scale	Performance of BC	Proposed mechanism	References
<b>PAHs</b>							
Phenanthrene	Sawdust	700	0.1, 0.5%	Lab	Increased $K_d$ value of soil from 47 to $2.1-3.4 \times 10^4 \text{ L kg}^{-1}$	Adsorption	Zhang et al. (2010)
2-, 3-, 4-, 5-ring PAHs	Hardwood	NR	13.3%	Lab	Reduced bioavailability of PAHs	Adsorption, microbial degradation	Beesley et al. (2010)
$\sum 5$ PAHs	Maize stover	600	10%	Lab	Reduced freely dissolved PAHs in sewage sludge by 57%	Pore-filling, aging effect	Oleszczuk et al. (2012)
$\sum 15$ PAHs	Pine needle	400	10%	Lab	Enhanced removal of PAHs in soil	Adsorption, pre-concentration, and biodegradation	Chen et al. (2012a)
$\sum 16$ PAHs	Sewage sludge	500	2, 5, 10%	Lab	Reduced bioaccumulation by 58.0–63.2%	Adsorption, dilution effect	Khan et al. (2013)
3-, 4- and 5-ring PAHs	Pine woodchip	450	3%	Lab	Reduced biota-soil accumulation factor by 25–33%	Adsorption, interactions with root exudates	Brennan et al. (2014)
$\sum 16$ PAHs	Corn straw	300	2%	Lab	Reduced rice uptake by 10–40%	Adsorption, microbial degradation	Ni et al. (2018)
$\sum 16$ PAHs	Bamboo	700	2%	Lab	Reduced rice uptake by 14–46%	Adsorption, microbial degradation	Ni et al. (2018)
<b>PCBs</b>							
Aroclors 1254, 1260	Wood waste	700	2.8, 11.1%	Lab	Reduced concentration in root of <i>Cucurbita pepo</i> by 58–77%	Adsorption	Denyes et al. (2012)
Aroclors 1254, 1260	Wood waste	700	2.8%	Field	Reduced the concentration in <i>Cucurbita pepo</i> by 72%	Adsorption	Denyes et al. (2013)
Aroclors 1254, 1260	Softwood	450	2.8%	Field	Reduced the concentration in <i>Cucurbita pepo</i> by 64%	Adsorption	Denyes et al. (2013)
Aroclor 1242 and 4 PCB congeners	Bamboo	820	2%	Lab	Enhanced PCB degradation	Adsorption, microbial degradation	Huang et al. (2018)
<b>Pesticide</b>							
Chlorpyrifos	Wood chips	850	1%	Lab	Decreased the residues in plant by 10%	Adsorption and reduced desorption	Yu et al. (2009)
Carbofuran	Wood chips	850	1%	Lab	Decreased the residues in plant by 25%	Adsorption and reduced desorption	Yu et al. (2009)
Chlorpyrifos	Cotton straws	850	1%	Lab	Increased half-life of chlorpyrifos by 161%; decreased plant uptake by 81%	Adsorption, microbial degradation	Yang et al. (2010)
Fipronil	Cotton straws	450	1%	Lab	Decreased plant uptake by 20%	Adsorption, microbial degradation	(Yang et al. 2010)

(continued)

**Table 5** (continued)

Organic pollutants	Feedstock	Pyrolytic temperature (°C)	Dosage	Study scale	Performance of BC	Proposed mechanism	References
Chlorpyrifos	Cotton straws	450	1%	Lab	Reduced plant uptake by 56%	Adsorption, microbial degradation	Yang et al. (2010)
Diuron	Poultry litter	550	10 t ha <sup>-1</sup>	Field	Increased sorption of diuron on soil by 5 times	Adsorption	Martin et al. (2012)
Diuron	Paper mill sludge	550	10 t ha <sup>-1</sup>	Field	Increased sorption of diuron on soil by 2 times	Adsorption	Martin et al. (2012)
Organochlorine pesticides	Sewage sludge	500	3%	Lab	Reduced the accessibility by 8–69%	Adsorption, altered soil microbial community structure	Ali et al. (2019)
Organochlorine pesticides	Peanut shells	500	3%	Lab	Reduced the accessibility by 11–75%	Adsorption, altered soil microbial community	Ali et al. (2019)
Organochlorine pesticides	Rice straw	500	3%	Lab	Reduced the accessibility of by 6–67%	Adsorption, altered soil microbial community	Ali et al. (2019)
Organochlorine pesticides	Soybean straw	500	3%	Lab	Reduced the accessibility by 14–86%	Adsorption, altered soil microbial community	Ali et al. (2019)
<b>PAEs</b>							
DEP	Rice straw	650	0.1, 0.5%	Lab	Increased sorption of DEP on low OC content soil by 2.7–4.1 times	Adsorption	Zhang et al. (2014)
DEHP	Bamboo sawdust	500	2%	Lab	Decreased plant uptake in low SOC soil, but no effect for high SOC soil	Adsorption, microbial degradation	He et al. (2016)
DEHP	Rice straw	500	2%	Lab	Decreased plant uptake in low SOC soil, but no effect for high SOC soil	Adsorption, microbial degradation	He et al. (2016)
DEP	Bamboo	820	0.5%	Lab	Increased soil sorption by nearly 98 times	Adsorption	Zhang et al. (2016d)
DBP	Dead pigs	650	1%	Lab	Reduced leaching loss by 88%	Adsorption	Qin et al. (2018)
DEHP	Dead pigs	650	0.5%	Lab	Decreased the half-lives of DEHP in low SOC soil, have no effect on high SOC soil; enhanced degradation for low SOC soil	Adsorption, microbial degradation	He et al. (2018)
<b>Antibiotic</b>							
Sulfamethazine	Hardwood litter	600	1, 2%	Lab	Increased soil sorption with increasing dose	Adsorption	Teixidó et al. (2013)
Sulfamethazine	Burcucumber	700	5%	Lab	Reduced plant uptake by 86%	Adsorption	Rajapaksha et al. (2014a)
Sulfamethazine	Burcucumber	300	2%	Lab	No effect on leaching	Not clear	Vithanage et al. (2014)
Sulfamethazine	Burcucumber	700	2%	Lab	Increased retention by 82–89%	Adsorption	Vithanage et al. (2014)

(continued)

**Table 5** (continued)

Organic pollutants	Feedstock	Pyrolytic temperature (°C)	Dosage	Study scale	Performance of BC	Proposed mechanism	References
Carbamazepine	wheat chaff	450	0.5%	Lab	Decreased plant uptake by 17%	Adsorption	Williams et al. (2015)
Carbamazepine	Oil mallee	450	0.5%	Lab	Decreased plant uptake by 32%	Adsorption	Williams et al. (2015)
Carbamazepine	Blue mallee	520	0.5%	Lab	Decreased plant uptake by 42%	Adsorption	Williams et al. (2015)
Carbamazepine	Wood waste	650	2.5, 5%	Lab	Decreased lettuce uptake	Adsorption	Hurtado et al. (2017)

NR: Not reported

Tang et al. 2017), which may reduce pesticides residues and increase its bioavailability to some certain microbes in soil. Overall, using BC in remediation of soil associated with pesticide is a complicated practice. In order to establish the feasible BC-based technology for remediating pesticide-contaminated soil, further work is needed to investigate the fate of pesticides in soil and its mechanism in different field circumstances.

Although many studies investigated the sorption of PAEs by BC in aqueous environments (Sun et al. 2019b; Jin et al. 2014; Jing et al. 2018), few studies used BC to removal or immobilize PAEs in soil (Table 5). For example, Zhang et al. (2014) conducted a laboratory study to evaluate the effect of bamboo BC addition on soil adsorption and desorption of diethyl phthalate (DEP), and found that the BC significantly enhanced soil's adsorption capacity, especially for the high-temperature BC (e.g., 600 °C). Later, Zhang et al. (2016c) revealed that the enhancement of the adsorption capacity was dependent on the soil organic carbon (SOC) levels and BC aging processes. The enhanced sorption of PAEs in soils by BC may dramatically decrease the leaching loss. Qin et al. (2018) demonstrated that application of dead pig-derived BC in a low SOC soil significantly reduced the leaching loss by up to 88% for DBP. However, its impact was insignificant for the high SOC soil, probably due to the high sorption contribution of SOM for DBP and coating of BC's sorption sites by humic substances in soil. BC also may promote degradation of PAEs in soil. He et al. (2018) reported that the half-life of di-(2-ethylhexyl) phthalate (DEHP) was shorter in the low SOC soil amended by a combination of BC and compost manure than in the soil that received only a single amendment. This was probably due to the improved microbial activity resulted from BC and compost. According to these studies, it is clearly showed that SOC content can strongly affect BC's efficacy on PAE remediation, and BC may show better performance in the low SOC soil. As such, the effect of soil properties of

remediation should be carefully considered alongside suitable BC selection.

Antibiotics, now frequently detected in soils, have resulted in negative effects on soil ecosystems such as the occurrence of ARGs, which has become one type of emerging concerns (Berendonk et al. 2015; Allen et al. 2010). It is imperative to control and remediate antibiotic and ARG contamination in soil. As for now, more efforts focus on reducing antibiotics in the environment via reduction promising results for and via proper treatment/disposal of animal effluents (Tasho and Cho 2016). While the remediation of antibiotics in water has been extensively studied, few studies have been reported on the topic of remediation for antibiotic-contaminated soil (Peiris et al. 2017; Teixidó et al. 2011; Lian et al. 2013), few studies have been reported on the topic of remediation for antibiotic-contaminated soil (Kumar et al. 2019; Vithanage et al. 2014). For example, Vithanage et al. (2014) reported BC produced at 700 °C may achieve up to 89 and 82% increase in sulfamethazine retention in sandy loam and loamy sand soils, respectively, due to the  $\pi$ - $\pi$  EDA interaction and electrostatic cation exchange between sulfamethazine and BC. Rajapaksha et al. (2014a) found that the application of a BC derived from an invasive plant, burcucumber (*Sicyos angulatus* L.) at 700 °C effectively reduced the sulfamethazine uptake of lettuce, which is attributed to adsorption of sulfamethazine onto the BC surface and reduction of its bioavailability. With concern for ARGs rising, several researchers recently attempted to use BC to control ARG contamination in soil. Ye et al. (2016) first reported that BC application significantly decreased the richness of sulfonamide-resistant endophytes and the abundance of *sul* genes in lettuce tissues, as well as uptake of sulfonamides. Duan et al. (2017) found that BC addition reduced the relative abundances of ARGs by 51.8%, 43.4%, and 44.1% in lettuce leaves, roots, and soil, respectively, due to bacterial community succession and reduction of Firmi-

cutes in the BC-amended soils. These studies highlight the potential of using BC to remediate antibiotic polluted soil which is abundant in ARB and ARGs. However, limited information is available in the field of antibiotics remediation using BC, and the underlying mechanisms are still not clear. Further studies that utilize a range of relevant and representative agricultural soils and a wide range of BCs with distinct properties are required to illuminate the specific interactions between antibiotics, ARGs and ARB with BCs.

### 3.6.3 Mechanisms for Remediation of Soils Contaminated with Organic Pollutants Using BC

As discussed above, a growing number of studies have demonstrated that BC could be a powerful strategy to deal with the organic pollution in soil (Varjani et al. 2019; Liu et al. 2018c; Xiong et al. 2017). Before the practical application of BC in remediation, it is necessary to know how BC works within polluted soil. According to the published studies, the mechanisms for remediating organic pollutant-contaminated soil using BC can be summarized as follows: (1) high sorption affinity and capacity of BCs for organic pollutants (Zheng et al. 2013c, 2019a; Vithanage et al. 2014; Bielska et al. 2018); (2) chemical degradation of the contaminants induced by electron transfer mediator or PFRs related with BCs (Oh et al. 2013; Fang et al. 2014; Yuan et al. 2017); and (3) biodegradation of organic contaminants resulted from the enhanced microbial activity and altered microbial community in soil (Zhu et al. 2017; Xin et al. 2014; García-Delgado et al. 2015; Xiong et al. 2017; Li et al. 2019a). Extensive studies have indicated that BC is a promising alternative to AC, and the sorption performance and underlying mechanisms are comprehensively summarized in Sect. 3.2. Teixidó et al. (2013) reported that the BCs produced from slow pyrolysis have larger surface area and porosity and higher content of C than those from fast pyrolysis, thus favoring sulfamethazine adsorption in soil. Thus, it is suitable to select high-temperature BC (e.g., >500 °C) with higher surface area and pore volumes for remediating the contaminated soil from the view of sorption. The sorption mechanisms of BC for organic chemicals in water are also suitable for its sorption in soil, but the contributions of different mechanisms will be controlled by soil properties (e.g., SOC, pH) and interactions between BC and soil. For example, Martin et al. (2012) found that soil freshly amended with BCs showed a 2–5-fold increase in sorption of diuron and atrazine, but BC aging in the soil over 32 months reduced the sorption capacity by 47–68% for diuron. This study highlighted that BC was likely to lose its sorption capability over time due to aging or weathering in soil. As a result, the aging of BC over time should be considered in its application in soil remediation. Degradation of the contaminants induced by electron transfer mediator or PFRs in BC

has been proven in aqueous solution (Pignatello et al. 2017; Fang et al. 2014; Yang et al. 2016b; Yuan et al. 2017). These interactions could also occur in the BC-amended soils contaminated with similar organic chemicals. Studies reported that BC can degrade diethyl phthalate (DEP) (Fang et al. 2015b), 1,1-trichloro-2,2-di(4-chlorophenyl)ethane (DDT) and its metabolites 1,1-dichloro-2,2-bis(4-chlorophenyl)ethane (DDD) (Ding and Xu 2016), and p-nitrophenol (Yang et al. 2016b), providing new insights for developing an alternative in situ remediation technique for rapidly decontaminating soils under environmentally relevant conditions. However, less information is available in this area, probably due to the difficulty in distinguishing the abiotic degradation from biodegradation. Moreover, interaction between SOM and PFRs may impair the roles of BC in chemical degradation of organic contaminants (Pan et al. 2019). More work should be conducted to enhance the capacity and roles of BC for degradation of soil organic pollutants in the future.

Biodegradation is a common process of dissipation and decomposition for most of organic pollutants in soils (Li et al. 2019a; Xiong et al. 2017), which is the core of bioremediation or phytoremediation techniques in soil remediation (Sun et al. 2018). BC may enhance biodegradation of organic contaminants (e.g., dichlobenil, atrazine, cyazofamid) in soil due to improvement of microbial abundance and activity resulted from direct and indirect influences (e.g., providing shelter and nutrients, changing soil pH, and aeration condition) (Qiu et al. 2009a; Zhang et al. 2005; Tang et al. 2019). For example, Huang et al. (2018) reported that BC addition substantially increased PCBs degradation, especially for the di- and tri-CBs, and the reduction of soil PCB could be mostly attributed to the microbial degradation, whereas the sorption of PCBs by BC only accounted for 0.7–1.4% of its dissipation in soil. Tong et al. (2014) observed that BC acted as a growth stimulant for iron(III)-reducing and dechlorinating bacteria, which consequently promoted pentachlorophenol biotransformation. Moreover, BC can also be used as carrier for functional bacteria to promote degradation of organic contaminants (e.g., PAHs, petroleum hydrocarbon) (Chen et al. 2012a; Zhang et al. 2016b; García-Delgado et al. 2015), which has been shown as an effective strategy for alleviating soil contamination. From the perspective of soil remediation, the nutrient-rich BC with high porosity should be selected in terms of biodegradation (Zhang et al. 2005; Qiu et al. 2009a; Zhu et al. 2017). However, the performance of BC on biodegradation of organic contaminants is not always consistent. Several studies have reported that BC application may significantly decrease the biodegradation of organic contaminants (e.g., PAHs, acetamiprid, 4-chloro-2-methylp-henoxyacetic acid) due to its super sorption capacity, which limited the availability of contaminants to microbes (Sigmund et al. 2018; Yu et al. 2011; Muter et al. 2014). But it

should be noted that the enhanced sorption will decrease their accessibility to plants and mobility in soil, which is also beneficial to soil remediation. Furthermore, BC incorporation in soil may stimulate plant growth, especially at root development (Zheng et al. 2018b; Wang et al. 2017d), probably enhancing the uptake and degradation of the pesticides due to rhizosphere effect such as the release of root exudates (Li et al. 2019b). How to make a balance between sorption and biodegradation is important in BC selection for soil remediation. Obviously, the effect of BC on biodegradation of organic contaminants involves different aspects, and the dominant aspect is determined by BC's functions in soil, which are still not clear. Therefore, future investigations should focus on the interactions between BC, microorganisms, organic contaminants, plants, and soils.

### 3.7 Sequestration of C in Soil Using BC

A healthy soil should contain a certain amount of SOC, which has profound effects for soil function, such as providing soil's CEC and WHC, stabilizing soil aggregates, supplying nutrient and energy to plants and microorganisms, and playing critical roles in the global C balance. Hence, it is very important to manage and maintain the quantity and quality of SOC in soil remediation (Al-Wabel et al. 2018). Incorporation of organic matters such as crop straw and livestock manure into soil to increase SOC or enhance C sequestration is traditional practice in agricultural production (Janzen 2015). However, these organic matters are ready to decompose to generate CO<sub>2</sub> in a few months and do not mitigate atmospheric CO<sub>2</sub> concentration in a long term. BC with high content of stable C offers the chance to turn biomass into a C-negative product that can be used as soil amendment to increase C sequestration (Marris 2006; Lehmann 2007). Application of BC for C sequestration also could remove CO<sub>2</sub> from the atmosphere due to biomass production via photosynthesis (Woolf et al. 2010). Beside C sequestration in soil, BC also may directly reduce GHG emissions in soil (Zheng et al. 2018c; Wang et al. 2013b), promote plant growth, and increase its biomass (Zheng et al. 2018b; Wang et al. 2017c). Moreover, BC production can be conducted at various scales ranging from domestic level or individual farm to large modern factory, which is suitable for a variety of socioeconomic situations in different countries (Woolf et al. 2010). As a promising strategy for mitigating climate change, BC has attracted increasing global attention (Marris 2006; Sohi 2012; Abiven et al. 2014; Lehmann 2007). The overall contribution of BC to the soil recalcitrant C pool depends on the balance between decomposition and sequestration of the C in both soil and BC (Zheng et al. 2018c; Leng et al. 2019a; Singh et al. 2014; Yang et al.

2016a), which is mainly affected by C stability of BC and interaction between BC and native SOM.

#### 3.7.1 Stability of BC

Stability of C in BC is the most important and essential feature to make BC as a promising C sequestration material (Singh et al. 2012; Lehmann 2007). Studies on this topic are the most attractive since BC was proposed (Leng et al. 2019a; Zimmerman 2010), and the heterogeneous nature of BC hinders the understanding of long-term stability of BC (Xiao et al. 2018). BC's stability is determined by content and structure of aromatic C formed during charring, including an amorphous phase (randomly organized aromatic rings) and a crystalline phase (condensed polyaromatic sheets) (Keiluweit et al. 2010; Nguyen et al. 2010; Singh et al. 2012). High aromaticity or high carbonization of BC means its high stability and is more likely to resist to biotic and abiotic degradations in soil. Thus aromaticity or carbonization degree and fixed C content are frequently used to evaluate BC stability (Leng et al. 2019b). BC covers the range of different C structures from slightly charred (more easily degradable) to highly condensed refractory graphitized C (Keiluweit et al. 2010; Guo and Chen 2014). The reported half-life time of BC varied, ranging from 10<sup>2</sup> to 10<sup>7</sup> years (Zimmerman 2010). Most of the C (>90%) in BC directly contributed to long-term C sequestration in soil (Zheng et al. 2018c). Besides the C phase, the inorganic phase also has an important effect on BC's C stability (Xiao et al. 2014; Guo and Chen 2014; Li et al. 2014). For example, Chen's group reported that protective interaction between C and Si within BC particles enhanced its C stability (Xiao et al. 2014; Guo and Chen 2014). Thus, loading the inorganic phase (e.g., triple superphosphate) to reduce C loss during pyrolysis can enhance BC stability in soil (Li et al. 2014).

#### 3.7.2 Priming Effects of BC on Native SOC

BC application in soil may affect stability of native SOC, which has been termed a 'priming effect' (Zheng et al. 2018c; Keith et al. 2011). BC-induced a priming effect will increase or decrease the C sequestration potential of BC itself. As such, predicting the BC-mediated priming effect on native SOC is critical to assessing its C abatement potential (Zimmerman et al. 2011). Extensive studies have reported a priming effect for different soils amended with different BCs (Wang et al. 2016a; Maestrini et al. 2015), including positive (Luo et al. 2011; Zimmerman et al. 2011), negative (Lu et al. 2014; Zheng et al. 2018c), and neutral priming (Cross and Sohi 2011). For example, Luo et al. (2011) demonstrated an early and rapid dynamics of positive priming effect following the application of BC to both low and high pH soils, whereas Zheng et al. (2018c) reported that two

cornstalk-derived BCs induced a negative priming effect in coastal wetland soil. Cross and Sohi (2011) found that although C mineralization was often higher in BC-amended soil resulted from rapid decomposition of a small labile component of BC, BC showed a neutral priming effect for the loss of native SOC. However, positive priming generally occurs over the short term, i.e., within few days to few months after BC application (Zimmerman et al. 2011; Zheng et al. 2018c). This is mainly attributed to the stimulated soil microbial activity or abundance following incorporation of BC, which contains a certain amount of labile OC and other nutrients like N and P (Zimmerman 2010; Singh et al. 2012; Zheng et al. 2013b).

Recently, a few studies started to investigate priming effect in soil–BC–plant systems (Keith et al. 2015; Whitman et al. 2014), in which rhizosphere priming is crucial for regulating soil C and N biogeochemical cycles (Huo et al. 2017). One field study showed that the application of BC into an agricultural field planted with maize (year 1) and grass (years 2 and 3) had little effect on SOM mineralization (Jones et al. 2012). However, another study reported that BC application in the presence of corn plants decreased SOM mineralization. The soils in these studies contained three C sources including soil, BC, and plant, largely limiting partition of each C source from others to determine the true priming effect. Moreover, they also did not consider the rhizosphere priming effect in soil amended with BC. Recently, a study was set out to evaluate the rhizosphere priming effect in three different soils amended with BC. The soybean (*Glycine max*) was labeled with an isotopically depleted  $\delta^{13}\text{C}$  signature to separate plant-derived  $\text{CO}_2\text{-C}$  from the total  $\text{CO}_2\text{-C}$ . They found that the soil type largely affected direction of the rhizosphere priming effect, and BC application may partially counteract the positive rhizosphere priming or reduce it further where it is already negative. This study confirmed the contribution of BC to long-term C storage in soil–BC–plant system. However, developing methods are still needed to partition the released  $\text{CO}_2$  from the source of SOM, BC, and plant, which is helpful to understand the interactive priming effects in soil–BC–plant system.

The priming effect of SOC in BC-amended soil is affected by several factors, including the recalcitrant nature of BC, interaction between BC surface (e.g., O-containing functional groups) and soil minerals, sorption of SOM on BC, and response of soil microbial community (bacteria and fungus) to BC application. These factors were reviewed by Ameloot et al. (2013) and Zhu et al. (2017), who comprehensively summarized the recent research progress on effects and mechanisms of biochar–microbe interactions in terms of soil improvement and pollution remediation. Several mechanisms have been proposed to explain negative priming effects: (1) substrate switching: the easily decomposed OC in BC,

particularly low-temperature BC, can be used preferentially by microbes as a C substrate, leading to decreased native SOM mineralization (Jones et al. 2011); (2) physical protection: BC may enhance stability of soil aggregates via intimate physicochemical associations between soil minerals and BC particles, physically protecting SOC decomposition by microbes (Zheng et al. 2018c); (3) stabilization: BC may sorb SOC via different mechanisms such as pore-filling and cation-bridging, lowering its availability to microbes (Kasozi et al. 2010); (4) N inhibition: BC may increase soil C/N ratio and shift the bacterial community toward low C turnover bacteria taxa (e.g., *Actinobacteria* and *Deltaproteobacteria*), slowing the rate of SOM mineralization (Zheng et al. 2018c); (5) accumulation of inorganic C: the increased pH in the BC-amended soil may be in favor of dissolving  $\text{CO}_2$  in soil aqueous phase (especially for alkaline soil), enhancing formation of soil inorganic C (e.g.,  $\text{CaCO}_3$ ,  $\text{MgCO}_3$ ) (Luo et al. 2016); and (6) inhibition of microbial growth: BC may inhibit soil microbial activity and abundance due to its inherent toxic compounds (e.g., PAHs, HMs) and PFRs (Wang et al. 2013b, 2015e). The positive priming is mainly ascribed to the stimulation of soil microbial activity by the labile C contained within the BC (Zimmerman et al. 2011; Luo et al. 2011), or abiotic release of  $\text{CO}_2$  from carbonates in BC (Jones et al. 2011; Bruun et al. 2013). Although these mechanisms have been shown by a large amount of laboratory and field studies, the contribution of each mechanism is not clearly estimated. Moreover, the roles of these mechanisms in field circumstances under extreme climatic conditions (e.g., drought and flood, freezing and thawing) are also not clear. Therefore, more efforts are warranted to further explore BC-mediated priming effect in field observations under extreme climatic conditions, and to investigate effect of soil contaminants regarding the potential of BC-based C sequestration.

---

#### 4 Limitations of BC Application for Environmental Remediation

Successful application of BC in environmental remediation is determined by unique BC characteristics, sustainable commercial production, economic feasibility, and low environmental risk. Selecting the suitable BC with multilevel structures (e.g., elemental composition, surface properties, and phase structure) for soil or water remediation is still difficult due to the complication production process of BC formation from various feedstock varying compositions and contents of constituents using different technologies. Thus, how to more precisely establish the link between the characteristics of BCs with their starting materials and charring conditions is a critical question that needs to be further elucidated. This will be in favor of designing BC or synthesizing BC-based materials with preferable properties for



specific purpose in remediation (Liu et al. 2015a; Xiao et al. 2018; Lian and Xing 2017). Moreover, a strong understanding of BC characteristics is also very beneficial for developing standard methods of BC production, characterization, and application.

For practical application of BC, another critical question confronting researchers is how to reduce BC application costs. Even extensive studies have shown that BC has a high potential to remediate contaminated soil or water, and its economic feasibility is still a challenge due to a high associated cost. According to a survey result of state of the BC industry by Jirka and Tomlinson (2015), the mean price of BC was US\$ 2869 ton<sup>-1</sup>, which was close to the price of AC, but higher than other soil amendments like compost (US\$ 40 ton<sup>-1</sup>). The high price of BC was mainly attributed to small-scale production using low-efficiency manufacturing facilities, as well as the high cost for waste biomass transport in long distance. However, it should be noted that BC's roles in soil remediation (e.g., nutrient retention, C sequestration) may sustain for several years or decades after one time of addition into soil (Wang et al. 2017c), with other economic benefits such as lowering the demand for inorganic fertilizers and enhancing water retention (Zheng et al. 2013a). These value-added benefits are usually ignored in the cost-benefit assessment during BC application in water or soil remediation. Several strategies can be used to reduce BC cost during its application: (1) using local waste biomass to produce BC to avoid its cost of long-distance transport and to achieve the environmental benefits in waste management; (2) developing diverse commercial equipment with suitable technology (e.g., slow pyrolysis, microwave pyrolysis, HTC) to sustainably produce BC, ensuring adequate supply of BC product on the market; (3) considering C offset credits of potential long-term C storage benefits in soil to make BC economically feasible, especially for the developing countries; (4) applying the minimum or optimum rate of BC in water or soil remediation to reduce the cost, because the excessive addition of in soil is not economically efficient, and even may result in environmental risk; and (5) choosing the appropriate method of BC application (e.g., topsoil incorporation, deep application, top-dressing) to ensure a BC's performance for a specific site conditions. Overall, more efforts should be made to assess the economic feasibility of BC in the entire system, including feedstock production, transportation, and preparation of feedstock, energy consumption or production of the pyrolysis process itself, storage, transportation, and application of BC product.

Apart from the abovementioned aspects, the environmental risks of BC during its application should be carefully considered, and the high environmental risk of BC in soil or water remediation would limit its practical application. Potential risk of BC involves release of inherent contaminants from BC, negative impacts to organisms (e.g., plants,

microbes), and facilitated transport and transformation of contaminants (Lian and Xing 2017). The reported contaminants in BC include PAHs, dioxins, volatile organic compounds (VOC), and HMs, which has been reviewed by Zheng et al. (2018a). To mitigate possible negative effects in environmental remediation, it is essential to manufacture BC without these contaminants. BC may have negative effects on soil/water biota, partially due to the inherent contaminants. For example, a significant correlation between the toxic effect to *D. magna* and the content of PAHs in BC was reported by Oleszczuk et al. (2013). Moreover, other properties of BC may also result in negative effects, such as high pH, soluble K<sup>+</sup>, Na<sup>+</sup> (Lian and Xing 2017), and nano-BC particles (Liu et al. 2018a). The colloidal or nano-BC particles may enhance transport of contaminants in water as vectors due to their high mobility in the environment and strong affinity to the contaminants (Liu et al. 2018a, 2019). Additionally, our previous study found that nano-BC was likely to aggregate with positively charged hematite to form stacked complexes of nano-biochar-hematite. This may hinder vertical transport of nano-BC particles in soil, thus weakening migration of soil contaminants sorbed on BC particles. However, limited information is available on co-transport of BC and contaminants in soil or water, which should receive more attention. Overall, the potential environmental risk of BC must be thoroughly addressed before its application in terms of inherent contaminants and the interaction between BC and contaminants and/or biota in soil and water.

---

## 5 Conclusions and Future Perspectives

A variety of biomass, particularly waste biomass with little to no value and different thermal treatments can be used for BC production, which can produce BCs with distinct characteristics in terms of elemental composition, surface properties and phase structure. These multilevel structures of BC have promising potentials for its application in remediation of water and soil. Application of BC in water and soil remediation may remove or immobilize HMs and organic contaminants (e.g., pesticides and antibiotics). The interactions responsible for HM removal from water using BC include physical adsorption, ion exchange, electrostatic interaction, complexation, precipitation, and cation- $\pi$  bonding. Sorption of organic contaminants by BC in water is mainly determined by pore-filling, electrostatic interaction, hydrophobic effect, H-bonding, EDA interaction, and partitioning. Moreover, organic pollutants could be degraded via electron transfer or PFRs of BC. These interactions between BC and pollutants in the water environment may also occur in soil, thus affecting BC's performance in soil remediation. The efficiency of BC in soil remediation depends on the

properties and dosage of BC, species and concentrations of contaminants, soil conditions, plant types, and climatic conditions. More field-scale studies are required to optimize BC's properties and performance targeting at contaminants in water and soil remediation. The Stability of C in BC makes it a promising C sequestration material, benefiting the improvement of soil properties (e.g., increasing SOC content) during soil remediation. In addition, priming effect of BC on native SOM should be carefully assessed, which may counteract the C sequestration potential of BC.

Although these studies have provided promising use for BC-based remediation technologies, most of them were mainly conducted in the laboratory, greenhouses or small plot experiments, and large-scale field trials in long term are still rare, limiting any practical large-scale application of BC in remediation. To make BC a viable method for environmental remediation, more efforts should be made to the following directions:

(1) BC production and characterization: Although extensive studies have been conducted on BC production and characterization, the relationships between BC properties and feedstock and thermal technologies are still not clear, largely limiting BC selection in the remediation. As such, more specific studies should be conducted to qualitatively and quantitatively characterize the properties of BC in terms of different levels (e.g., elements, surface, phase) thus to establish the relationships of “feedstock-production conditions-structure—application.” This will be critical for designing smart engineered BC for soil or water remediation. Meanwhile, the guidelines or standards should be developed for BC production and characterization in order to promote marketization of BC product and avoid potential environmental risk.

(2) BC modification and functionalization: BC can be modified or functionalized to be more specific to target contaminants. In future, more studies are needed to focus on the modification of BC using novel, feasible and eco-friendly approaches to produce smart BC for particular waters' or soils' need, which is essential in promoting effectively practical application of BC in water and soil remediation. Of these, surface modification and synthesis of BC-based nanocomposites are two key areas for enhancing BC's functionalization.

(3) Long-term investigation in large-scale field: Most of the studies using BC for water or soil remediation were conducted in laboratories, greenhouses, or small plot experiments. These results were mainly obtained under ideal conditions, which cannot fully reflect the practical situations of BC's application in the field. Moreover, BC would undoubtedly be subjected to physical, chemical, and biological aging, subsequently affecting BC's stability and functionality in water or soil. Therefore, more studies should

focus on the long-term effectiveness of BC use in water or soil remediation on a large field scale under different conditions, such as types of contaminants and climatic conditions (e.g., precipitation, temperature).

(4) Economical benefit analysis: For the practical application of BC, one critical question is how to reduce BC production and application costs. More efforts are needed to assess the economic feasibility of BC in the entire system at various scales ranging from domestic level or individual farm to large modern factory, which is suitable for a variety of socioeconomic situations in different countries. The cost for BC should be considered in terms of feedstock, production technique and reactor, transportation, and application of BC product. The reasonable and variability in BC price will be beneficial to the maturation of the BC market, thus ensuring successful and sustainable application of BC-based techniques in water or soil remediation.

(5) Environmental risk assessment: Studies have shown that BC has negative effects on plant, fauna, and microorganisms, can even threaten human health. Thus, the potential environmental risk of BC must be thoroughly examined and assessed before its application in terms of inherent contaminants, nano-BC particles, and the interaction between BC and contaminants and/or biota in soil and water.

**Acknowledgements** This study was supported by Shandong Key Research and Development Program-Science and Technology Innovation Project (2018CXGC0304), Shandong Province Natural Science Foundation (ZR2019MD017), and USDA NIFA McIntire-Stennis Program (MAS 00028).

## References

- Abiven S, Schmidt MWI, Lehmann J (2014) Biochar by design. *Nature Geosci* 7(5):326–327. <https://doi.org/10.1038/ngeo2154>
- Ahmad M, Soo Lee S, Yang JE, Ro H-M, Lee YH, Ok YS (2012) Effects of soil dilution and amendments (mussel shell, cow bone, and biochar) on Pb availability and phytotoxicity in military shooting range soil. *Ecotox Environ Safe* 79:225–231. <https://doi.org/10.1016/j.ecoenv.2012.01.003>
- Ahmad Z, Gao B, Mosa A, Yu H, Yin X, Bashir A, Ghozeisi H, Wang S (2018) Removal of Cu(II), Cd(II) and Pb(II) ions from aqueous solutions by biochars derived from potassium-rich biomass. *J Clean Prod* 180:437–449. <https://doi.org/10.1016/j.jclepro.2018.01.133>
- Ahmed MB, Zhou JL, Ngo HH, Johir MAH, Sornalingam K (2018) Sorptive removal of phenolic endocrine disruptors by functionalized biochar: competitive interaction mechanism, removal efficacy and application in wastewater. *Chem Eng J* 335:801–811. <https://doi.org/10.1016/j.cej.2017.11.041>
- Al-Wabel MI, Hussain Q, Usman ARA, Ahmad M, Abduljabbar A, Sallam AS, Ok YS (2018) Impact of biochar properties on soil conditions and agricultural sustainability: a review. *Land Degrad Dev* 29:2124–2161. <https://doi.org/10.1002/ldr.2829>

- Ali N, Khan S, Li Y, Zheng N, Yao H (2019) Influence of biochars on the accessibility of organochlorine pesticides and microbial community in contaminated soils. *Sci Total Environ* 647:551–560. <https://doi.org/10.1016/j.scitotenv.2018.07.425>
- Allen HK, Donato J, Wang HH, Cloud-Hansen KA, Davies J, Handelsman J (2010) Call of the wild: antibiotic resistance genes in natural environments. *Nat Rev Microbiol* 8:251–259. <https://doi.org/10.1038/nrmicro2312>
- Ameloot N, Graber ER, Verheijen FGA, De Neve S (2013) Interactions between biochar stability and soil organisms: review and research needs. *Eur J Soil Sci* 64:379–390. <https://doi.org/10.1111/ejss.12064>
- Beesley L, Moreno-Jimenez E, Gomez-Eyles JL (2010) Effects of biochar and greenwaste compost amendments on mobility, bioavailability and toxicity of inorganic and organic contaminants in a multi-element polluted soil. *Environ Pollut* 158:2282–2287. <https://doi.org/10.1016/j.envpol.2010.02.003>
- Berendonk TU, Manaia CM, Merlin C, Fatta-Kassinos D, Cytryn E, Walsh F, Burgmann H, Sorum H, Norstrom M, Pons M-N, Kreuzinger N, Huovinen P, Stefani S, Schwartz T, Kisand V, Baquero F, Martinez JL (2015) Tackling antibiotic resistance: the environmental framework. *Nat Rev Micro* 13:310–317. <https://doi.org/10.1038/nrmicro3439>
- Bian R, Chen D, Liu X, Cui L, Li L, Pan G, Xie D, Zheng J, Zhang X, Zheng J, Chang A (2013) Biochar soil amendment as a solution to prevent Cd-tainted rice from China: results from a cross-site field experiment. *Ecol Eng* 58:378–383. <https://doi.org/10.1016/j.ecoleng.2013.07.031>
- Bian R, Joseph S, Cui L, Pan G, Li L, Liu X, Zhang A, Rutledge H, Wong S, Chia C, Marjo C, Gong B, Munroe P, Donne S (2014) A three-year experiment confirms continuous immobilization of cadmium and lead in contaminated paddy field with biochar amendment. *J Hazard Mater* 272:121–128. <https://doi.org/10.1016/j.jhazmat.2014.03.017>
- Bian R, Li L, Bao D, Zheng J, Zhang X, Zheng J, Liu X, Cheng K, Pan G (2016) Cd immobilization in a contaminated rice paddy by inorganic stabilizers of calcium hydroxide and silicon slag and by organic stabilizer of biochar. *Environ Sci Pollut Res* 23:10028–10036. <https://doi.org/10.1007/s11356-016-6214-3>
- Bielska L, Skulcova L, Neuwirthova N, Cornelissen G, Hale SE (2018) Sorption, bioavailability and ecotoxic effects of hydrophobic organic compounds in biochar amended soils. *Sci Total Environ* 624:78–86. <https://doi.org/10.1016/j.scitotenv.2017.12.098>
- Bird MI, Wurster CM, De Paula Silva PH, Paul NA, De Nys R (2012) Algal biochar: effects and applications. *GCB Bioenergy* 4:61–69. <https://doi.org/10.1111/j.1757-1707.2011.01109.x>
- Bird MI, Wurster CM, Silva PH, Bass AM, de Nys R (2011) Algal biochar - production and properties. *Bioresour Technol* 102:1886–1891. <https://doi.org/10.1016/j.biortech.2010.07.106>
- Boakye P, Tran HN, Lee DS, Woo SH (2019) Effect of water washing pretreatment on property and adsorption capacity of macroalgae-derived biochar. *J Environ Manage* 233:165–174. <https://doi.org/10.1016/j.jenvman.2018.12.031>
- Bogusz A, Nowak K, Stefaniuk M, Dobrowolski R, Oleszczuk P (2017) Synthesis of biochar from residues after biogas production with respect to cadmium and nickel removal from wastewater. *J Environ Manage* 201:268–276. <https://doi.org/10.1016/j.jenvman.2017.06.019>
- Boostani HR, Najafi-Ghiri M, Mirsoleimani A (2019) The effect of biochars application on reducing the toxic effects of nickel and growth indices of spinach (*Spinacia oleracea* L.) in a calcareous soil. *Environ Sci Pollut Res* 26:1751–1760. <https://doi.org/10.1007/s11356-018-3760-x>
- Brennan A, Moreno Jimenez E, Albuquerque JA, Knapp CW, Switzer C (2014) Effects of biochar and activated carbon amendment on maize growth and the uptake and measured availability of polycyclic aromatic hydrocarbons (PAHs) and potentially toxic elements (PTEs). *Environ Pollut* 193:79–87. <https://doi.org/10.1016/j.envpol.2014.06.016>
- Bruun S, Clauson-Kaas S, Bobuľská L, Thomsen IK (2013) Carbon dioxide emissions from biochar in soil: role of clay, microorganisms and carbonates. *Eur J Soil Sci* 65:52–59. <https://doi.org/10.1111/ejss.12073>
- Buss W, Graham MC, MacKinnon G, Mašek O (2016) Strategies for producing biochars with minimum PAH contamination. *J Anal Appl Pyrolysis* 119:24–30. <https://doi.org/10.1016/j.jaap.2016.04.001>
- Cao X, Ma L, Gao B, Harris W (2009) Dairy-manure derived biochar effectively sorbs lead and atrazine. *Environ Sci Technol* 43:3285–3291. <https://doi.org/10.1021/es803092k>
- Cao X, Ma L, Liang Y, Gao B, Harris W (2011) Simultaneous immobilization of lead and atrazine in contaminated soils using dairy-manure biochar. *Environ Sci Technol* 45:4884–4889. <https://doi.org/10.1021/es103752u>
- Cao Y, Xiao W, Shen G, Ji G, Zhang Y, Gao C, Han L (2018) Carbonization and ball milling on the enhancement of Pb(II) adsorption by wheat straw: competitive effects of ion exchange and precipitation. *Bioresour Technol* 273:70–76. <https://doi.org/10.1016/j.biortech.2018.10.065>
- Cheah S, Malone SC, Feik CJ (2014) Speciation of sulfur in biochar produced from pyrolysis and gasification of oak and corn stover. *Environ Sci Technol* 48:8474–8480. <https://doi.org/10.1021/es500073r>
- Chen B, Chen Z (2009) Sorption of naphthalene and 1-naphthol by biochars of orange peels with different pyrolytic temperatures. *Chemosphere* 76:127–133. <https://doi.org/10.1016/j.chemosphere.2009.02.004>
- Chen B, Chen Z, Lv S (2011a) A novel magnetic biochar efficiently sorbs organic pollutants and phosphate. *Bioresour Technol* 102:716–723. <https://doi.org/10.1016/j.biortech.2010.08.067>
- Chen X, Xia X, Wang X, Qiao J, Chen H (2011b) A comparative study on sorption of perfluorooctane sulfonate (PFOS) by chars, ash and carbon nanotubes. *Chemosphere* 83:1313–1319. <https://doi.org/10.1016/j.chemosphere.2011.04.018>
- Chen B, He R, Yuan K, Chen E, Lin L, Chen X, Sha S, Zhong J, Lin L, Yang L, Yang Y, Wang X, Zou S, Luan T (2016) Polycyclic aromatic hydrocarbons (PAHs) enriching antibiotic resistance genes (ARGs) in the soils. *Environ Pollut* 220:1005–1013. <https://doi.org/10.1016/j.envpol.2016.11.047>
- Chen D, Liu X, Bian R, Cheng K, Zhang X, Zheng J, Joseph S, Crowley D, Pan G, Li L (2018a) Effects of biochar on availability and plant uptake of heavy metals—a meta-analysis. *J Environ Manage* 222:76–85. <https://doi.org/10.1016/j.jenvman.2018.05.004>
- Chen M, Alim N, Zhang Y, Xu N, Cao X (2018b) Contrasting effects of biochar nanoparticles on the retention and transport of phosphorus in acidic and alkaline soils. *Environ Pollut* 239:562–570. <https://doi.org/10.1016/j.envpol.2018.04.050>
- Chen Q, Zheng J, Zheng L, Dang Z, Zhang L (2018c) Classical theory and electron-scale view of exceptional Cd(II) adsorption onto mesoporous cellulose biochar via experimental analysis coupled with DFT calculations. *Chem Eng J* 350:1000–1009. <https://doi.org/10.1016/j.cej.2018.06.054>
- Chen Y, Ho SH, Wang D, Wei Z, Chang J, Ren N (2018d) Lead removal by a magnetic biochar derived from persulfate-ZVI treated sludge together with one-pot pyrolysis. *Bioresour Technol* 247:463–470. <https://doi.org/10.1016/j.biortech.2017.09.125>
- Chen B, Zhou D, Zhu L (2008) Transitional adsorption and partition of nonpolar and polar aromatic contaminants by biochars of pine needles with different pyrolytic temperatures. *Environ Sci Technol* 42:5137–5143
- Chen T, Zhang Y, Wang H, Lu W, Zhou Z, Zhang Y, Ren L (2014a) Influence of pyrolysis temperature on characteristics and heavy metal adsorptive performance of biochar derived from municipal

- sewage sludge. *Bioresour Technol* 164:47–54. <https://doi.org/10.1016/j.biortech.2014.04.048>
- Chen W, Li Y, Zhu D, Zheng S, Chen W (2014b) Dehydrochlorination of activated carbon-bound 1,1,2,2-tetrachloroethane: implications for carbonaceous material-based soil/sediment remediation. *Carbon* 78:578–588. <https://doi.org/10.1016/j.carbon.2014.07.041>
- Chen B, Yuan M, Qian L (2012a) Enhanced bioremediation of PAH-contaminated soil by immobilized bacteria with plant residue and biochar as carriers. *J Soils Sed* 12:1350–1359. <https://doi.org/10.1007/s11368-012-0554-5>
- Chen Z, Chen B, Zhou D, Chen W (2012b) Bisolute sorption and thermodynamic behavior of organic pollutants to biomass-derived biochars at two pyrolytic temperatures. *Environ Sci Technol* 46:12476–12483. <https://doi.org/10.1021/es303351e>
- Chen Z, Xiao X, Chen B, Zhu L (2015) Quantification of chemical states, dissociation constants and contents of oxygen-containing groups on the surface of biochars produced at different temperatures. *Environ Sci Technol* 49:309–317. <https://doi.org/10.1021/es5043468>
- Chiu KL, Ng DHL (2012) Synthesis and characterization of cotton-made activated carbon fiber and its adsorption of methylene blue in water treatment. *Biomass Bioenerg* 46:102–110. <https://doi.org/10.1016/j.biombioe.2012.09.023>
- Choia JH, Woob HC, Suha DJ (2014) Pyrolysis of seaweeds for bio-oil and bio-char production. *Chem Eng* 37:121–126. <https://doi.org/10.3303/CET1437021>
- Cross A, Sohi SP (2011) The priming potential of biochar products in relation to labile carbon contents and soil organic matter status. *Soil Biol Biochem* 43:2127–2134. <https://doi.org/10.1016/j.soilbio.2011.06.016>
- Cui H, Fan Y, Fang G, Zhang H, Su B, Zhou J (2016a) Leachability, availability and bioaccessibility of Cu and Cd in a contaminated soil treated with apatite, lime and charcoal: a five-year field experiment. *Ecotoxicol Environ Saf* 134:148–155. <https://doi.org/10.1016/j.ecoenv.2016.07.005>
- Cui L, Pan G, Li L, Bian R, Liu X, Yan J, Quan G, Ding C, Chen T, Liu Y, Liu Y, Yin C, Wei C, Yang Y, Hussain Q (2016b) Continuous immobilization of cadmium and lead in biochar amended contaminated paddy soil: a five-year field experiment. *Ecol Eng* 93:1–8. <https://doi.org/10.1016/j.ecoleng.2016.05.007>
- Cui L, Li L, Zhang A, Pan G, Bao D, Chang A (2011) Biochar amendment greatly reduces rice Cd uptake in a contaminated paddy soil: a two-year field experiment. *BioResources* 6:2605–2618
- Dai Y, Zhang N, Xing C, Cui Q, Sun Q (2019) The adsorption, regeneration and engineering applications of biochar for removal of organic pollutants: a review. *Chemosphere* 223:12–27. <https://doi.org/10.1016/j.chemosphere.2019.01.161>
- Dai Z, Zhang X, Tang C, Muhammad N, Wu JJ, Brookes PC, Xu J (2017) Potential role of biochars in decreasing soil acidification-A critical review. *Sci Total Environ* 581:601–611. <https://doi.org/10.1016/j.scitotenv.2016.12.169>
- De Bhowmick G, Sarmah AK, Sen R (2018) Production and characterization of a value added biochar mix using seaweed, rice husk and pine sawdust: a parametric study. *J Clean Prod* 200:641–656. <https://doi.org/10.1016/j.jclepro.2018.08.002>
- Denyes MJ, Langlois VS, Rutter A, Zeeb BA (2012) The use of biochar to reduce soil PCB bioavailability to *Cucurbita pepo* and *Eisenia fetida*. *Sci Total Environ* 437:76–82. <https://doi.org/10.1016/j.scitotenv.2012.07.081>
- Denyes MJ, Rutter A, Zeeb BA (2013) In situ application of activated carbon and biochar to PCB-contaminated soil and the effects of mixing regime. *Environ Pollut* 182:201–208. <https://doi.org/10.1016/j.envpol.2013.07.016>
- Ding K, Xu W (2016) Black carbon facilitated dechlorination of DDT and its metabolites by sulfide. *Environ Sci Technol* 50:12976–12983. <https://doi.org/10.1021/acs.est.6b03154>
- Dong Q, Li H, Niu M, Luo C, Zhang J, Qi B, Li X, Zhong W (2018) Microwave pyrolysis of moso bamboo for syngas production and bio-oil upgrading over bamboo-based biochar catalyst. *Bioresour Technol* 266:284–290. <https://doi.org/10.1016/j.biortech.2018.06.104>
- Duan M, Li H, Gu J, Tuo X, Sun W, Qian X, Wang X (2017) Effects of biochar on reducing the abundance of oxytetracycline, antibiotic resistance genes, and human pathogenic bacteria in soil and lettuce. *Environ Pollut* 224:787–795. <https://doi.org/10.1016/j.envpol.2017.01.021>
- El-Naggar A, Lee SS, Rinklebe J, Farooq M, Song H, Sarmah AK, Zimmerman AR, Ahmad M, Shaheen SM, Ok YS (2019) Biochar application to low fertility soils: a review of current status, and future prospects. *Geoderma* 337:536–554. <https://doi.org/10.1016/j.geoderma.2018.09.034>
- Fang G, Gao J, Liu C, Dionysiou DD, Wang Y, Zhou D (2014) Key role of persistent free radicals in hydrogen peroxide activation by biochar: implications to organic contaminant degradation. *Environ Sci Technol* 48:1902–1910. <https://doi.org/10.1021/es4048126>
- Fang G, Liu C, Gao J, Dionysiou DD, Zhou D (2015a) Manipulation of persistent free radicals in biochar to activate persulfate for contaminant degradation. *Environ Sci Technol* 49:5645–5653. <https://doi.org/10.1021/es5061512>
- Fang G, Zhu C, Dionysiou DD, Gao J, Zhou D (2015b) Mechanism of hydroxyl radical generation from biochar suspensions: implications to diethyl phthalate degradation. *Bioresour Technol* 176:210–217. <https://doi.org/10.1016/j.biortech.2014.11.032>
- Fang Q, Chen B, Lin Y, Guan Y (2013) Aromatic and hydrophobic surfaces of wood-derived biochar enhance perchlorate adsorption via hydrogen bonding to oxygen-containing organic groups. *Environ Sci Technol* 48:279–288. <https://doi.org/10.1021/es403711y>
- Fellet G, Marchiol L, Delle Vedove G, Peressotti A (2011) Application of biochar on mine tailings: effects and perspectives for land reclamation. *Chemosphere* 83:1262–1267. <https://doi.org/10.1016/j.chemosphere.2011.03.053>
- Fu H, Guo Y, Chen W, Gu C, Zhu D (2014) Reductive dechlorination of hexachloroethane by sulfide in aqueous solutions mediated by graphene oxide and carbon nanotubes. *Carbon* 72:74–81. <https://doi.org/10.1016/j.carbon.2014.01.053>
- Gao L, Deng J, Huang G, Li K, Cai K, Liu Y, Huang F (2019) Relative distribution of Cd<sup>2+</sup> adsorption mechanisms on biochars derived from rice straw and sewage sludge. *Bioresour Technol* 272:114–122. <https://doi.org/10.1016/j.biortech.2018.09.138>
- Garcia-Delgado C, Alfaro-Barta I, Eymar E (2015) Combination of biochar amendment and mycoremediation for polycyclic aromatic hydrocarbons immobilization and biodegradation in creosote-contaminated soil. *J Hazard Mater* 285:259–266. <https://doi.org/10.1016/j.jhazmat.2014.12.002>
- Glaser B, Haumaier L, Guggenberger G, Zech W (2001) The ‘Terra Preta’ phenomenon: a model for sustainable agriculture in the humid tropics. *Naturwissenschaften* 88:37–41. <https://doi.org/10.1007/s001140000193>
- Godfray HCJ, Beddington JR, Crute IR, Haddad L, Lawrence D, Muir JF, Pretty J, Robinson S, Thomas SM, Toulmin C (2010) Food security: the challenge of feeding 9 billion people. *Science* 327:812–818. <https://doi.org/10.1126/science.1185383>
- Gomez-Eyles JL, Sizmur T, Collins CD, Hodson ME (2010) Effects of biochar and the earthworm *Eisenia fetida* on the bioavailability of polycyclic aromatic hydrocarbons and potentially toxic elements. *Environ Pollut* 159:616–622. <https://doi.org/10.1016/j.envpol.2010.09.037>
- Gomez-Eyles JL, Yupanqui C, Beckingham B, Riedel G, Gilmour C, Ghosh U (2013) Evaluation of biochars and activated carbons for in situ remediation of sediments impacted with organics, mercury, and methylmercury. *Environ Sci Technol* 47:13721–13729. <https://doi.org/10.1021/es403712q>

- Gong Y, Tang J, Zhao D (2016) Application of iron sulfide particles for groundwater and soil remediation: a review. *Water Res* 89:309–320. <https://doi.org/10.1016/j.watres.2015.11.063>
- Gong Z, Alef K, Wilke B-M, Li P (2007) Activated carbon adsorption of PAHs from vegetable oil used in soil remediation. *J Hazard Mater* 143:372–378. <https://doi.org/10.1016/j.jhazmat.2006.09.037>
- Guo J, Chen B (2014) Insights on the molecular mechanism for the recalcitrance of biochars: interactive effects of carbon and silicon components. *Environ Sci Technol* 48:9103–9112. <https://doi.org/10.1021/es405647e>
- Hale SE, Lehmann J, Rutherford D, Zimmerman A, Bachmann RT, Shitumbanuma V, O'Toole A, Sundqvist KL, Arp HPH, Cornelissen G (2012) Quantifying the total and bioavailable PAHs and dioxins in biochars. *Environ Sci Technol* 46:2830–2838. <https://doi.org/10.1021/es203984k>
- Hao R, Zhao R, Qiu S, Wang L, Song H (2015) Antibiotics crisis in China. *Science* 348:1100–1101. <https://doi.org/10.1126/science.348.6239.1100-d>
- He L, Fan S, Muller K, Wang H, Che L, Xu S, Song Z, Yuan G, Rinklebe J, Tsang DCW, Ok YS, Bolan NS (2018) Comparative analysis biochar and compost-induced degradation of di-(2-ethylhexyl) phthalate in soils. *Sci Total Environ* 625:987–993. <https://doi.org/10.1016/j.scitotenv.2018.01.002>
- He L, Gielen G, Bolan NS, Zhang X, Qin H, Huang H, Wang H (2015) Contamination and remediation of phthalic acid esters in agricultural soils in China: a review. *Agron Sustain Dev* 35:519–534. <https://doi.org/10.1007/s13593-014-0270-1>
- He LZ, Fan SL, Muller K, Hu GT, Huang HG, Zhang XK, Lin XM, Che L, Wang HL (2016) Biochar reduces the bioavailability of di-(2-ethylhexyl) phthalate in soil. *Chemosphere* 142:24–27. <https://doi.org/10.1016/j.chemosphere.2015.05.064>
- Henner P, Schiavon M, Druelle V, Lichtfouse E (1999) Phytotoxicity of ancient gaswork soils. Effect of polycyclic aromatic hydrocarbons (PAHs) on plant germination. *Org Geochem* 30:963–969. [https://doi.org/10.1016/S0146-6380\(99\)00080-7](https://doi.org/10.1016/S0146-6380(99)00080-7)
- Houben D, Evrard L, Sonnet P (2013) Beneficial effects of biochar application to contaminated soils on the bioavailability of Cd, Pb and Zn and the biomass production of rapeseed (*Brassica napus* L.). *Biomass Bioenergy* 57:196–204. <https://doi.org/10.1016/j.biombioe.2013.07.019>
- Houben D, Sonnet P (2015) Impact of biochar and root-induced changes on metal dynamics in the rhizosphere of *Agrostis capillaris* and *Lupinus albus*. *Chemosphere* 139:644–651. <https://doi.org/10.1016/j.chemosphere.2014.12.036>
- Huang S, Bao J, Shan M, Qin H, Wang H, Yu X, Chen J, Xu Q (2018) Dynamic changes of polychlorinated biphenyls (PCBs) degradation and adsorption to biochar as affected by soil organic carbon content. *Chemosphere* 211:120–127. <https://doi.org/10.1016/j.chemosphere.2018.07.133>
- Huo C, Luo Y, Cheng W (2017) Rhizosphere priming effect: a meta-analysis. *Soil Biol Biochem* 111:78–84. <https://doi.org/10.1016/j.soilbio.2017.04.003>
- Hurtado C, Cañameras N, Domínguez C, Price GW, Comas J, Bayona JM (2017) Effect of soil biochar concentration on the mitigation of emerging organic contaminant uptake in lettuce. *J Hazard Mater* 323:386–393. <https://doi.org/10.1016/j.jhazmat.2016.04.046>
- IBI (2012) Guidelines for specifications of biochars for use in soils
- Ifthikar J, Jiao X, Ngambia A, Wang T, Khan A, Jawad A, Xue Q, Liu L, Chen Z (2018) Facile one-pot synthesis of sustainable carboxymethyl chitosan-sewage sludge biochar for effective heavy metal chelation and regeneration. *Bioresour Technol* 262:22–31. <https://doi.org/10.1016/j.biortech.2018.04.053>
- Igalavithana AD, Lee S-E, Lee YH, Tsang DCW, Rinklebe J, Kwon EE, Ok YS (2017) Heavy metal immobilization and microbial community abundance by vegetable waste and pine cone biochar of agricultural soils. *Chemosphere* 174:593–603. <https://doi.org/10.1016/j.chemosphere.2017.01.148>
- Inyang M, Dickenson E (2015) The potential role of biochar in the removal of organic and microbial contaminants from potable and reuse water: a review. *Chemosphere* 134:232–240. <https://doi.org/10.1016/j.chemosphere.2015.03.072>
- Inyang M, Gao B, Yao Y, Xue Y, Zimmerman AR, Pullammanappallil P, Cao X (2012a) Removal of heavy metals from aqueous solution by biochars derived from anaerobically digested biomass. *Bioresour Technol* 110:50–56. <https://doi.org/10.1016/j.biortech.2012.01.072>
- Inyang M, Gao B, Yao Y, Xue Y, Zimmerman AR, Pullammanappallil P, Cao X (2012b) Removal of heavy metals from aqueous solution by biochars derived from anaerobically digested biomass. *Bioresour Technol* 110:50–56. <https://doi.org/10.1016/j.biortech.2012.01.072>
- Jagiello J, Kenvin J, Celzard A, Fierro V (2019) Enhanced resolution of ultra micropore size determination of biochars and activated carbons by dual gas analysis using N<sub>2</sub> and CO<sub>2</sub> with 2D-NLDFT adsorption models. *Carbon* 144:206–215. <https://doi.org/10.1016/j.carbon.2018.12.028>
- Janzen HH (2015) Beyond carbon sequestration: soil as conduit of solar energy. *Eur J Soil Sci* 66:19–32. <https://doi.org/10.1111/ejss.12194>
- Ji L, Wan Y, Zheng S, Zhu D (2011) Adsorption of tetracycline and sulfamethoxazole on crop residue-derived ashes: implication for the relative importance of black carbon to soil sorption. *Environ Sci Technol* 45:5580–5586. <https://doi.org/10.1021/es200483b>
- Jiang B, Lin Y, Mbog JC (2018) Biochar derived from swine manure digestate and applied on the removals of heavy metals and antibiotics. *Bioresour Technol* 270:603–611. <https://doi.org/10.1016/j.biortech.2018.08.022>
- Jiang T, Xu R, Gu T, Jiang J (2014) Effect of crop-straw derived biochars on pb(II) adsorption in two variable charge soils. *J Integr Agric* 13:507–516. [https://doi.org/10.1016/S2095-3119\(13\)60706-6](https://doi.org/10.1016/S2095-3119(13)60706-6)
- Jin J, Sun K, Wang Z, Han L, Du P, Wang X, Xing B (2017) Effects of chemical oxidation on phenanthrene sorption by grass- and manure-derived biochars. *Sci Total Environ* 598:789–796. <https://doi.org/10.1016/j.scitotenv.2017.04.160>
- Jin J, Sun K, Wu F, Gao B, Wang Z, Kang M, Bai Y, Zhao Y, Liu X, Xing B (2014) Single-solute and bi-solute sorption of phenanthrene and dibutyl phthalate by plant- and manure-derived biochars. *Sci Total Environ* 473–474:308–316. <https://doi.org/10.1016/j.scitotenv.2013.12.033>
- Jing F, Sohi SP, Liu Y, Chen J (2018) Insight into mechanism of aged biochar for adsorption of PAEs: Reciprocal effects of ageing and coexisting Cd<sup>2+</sup>. *Environ Pollut* 242:1098–1107. <https://doi.org/10.1016/j.envpol.2018.07.124>
- Jing X, Wang Y, Liu W, Wang Y, Jiang H (2014) Enhanced adsorption performance of tetracycline in aqueous solutions by methanol-modified biochar. *Chem Eng J* 248:168–174. <https://doi.org/10.1016/j.cej.2014.03.006>
- Jirka S, Tomlinson T (2015) IBI. State of the Biochar Industry. accessed at. [http://www.biocharinternational.org/sites/default/files/State\\_of\\_the\\_Biochar\\_Industry.2013.pdf](http://www.biocharinternational.org/sites/default/files/State_of_the_Biochar_Industry.2013.pdf)
- Jones DL, Murphy DV, Khalid M, Ahmad W, Edwards-Jones G, DeLuca TH (2011) Short-term biochar-induced increase in soil CO<sub>2</sub> release is both biotically and abiotically mediated. *Soil Biol Biochem* 43:1723–1731. <https://doi.org/10.1016/j.soilbio.2011.04.018>
- Jones DL, Rousk J, Edwards-Jones G, DeLuca TH, Murphy DV (2012) Biochar-mediated changes in soil quality and plant growth in a three year field trial. *Soil Biol Biochem* 45:113–124. <https://doi.org/10.1016/j.soilbio.2011.10.012>
- Jung C, Phal N, Oh J, Chu KH, Jang M, Yoon Y (2015) Removal of humic and tannic acids by adsorption-coagulation combined

- systems with activated biochar. *J Hazard Mater* 300:808–814. <https://doi.org/10.1016/j.jhazmat.2015.08.025>
- Jung KW, Lee SY, Lee YJ (2018) Facile one-pot hydrothermal synthesis of cubic spinel-type manganese ferrite/biochar composites for environmental remediation of heavy metals from aqueous solutions. *Bioresour Technol* 261:1–9. <https://doi.org/10.1016/j.biortech.2018.04.003>
- Kambo HS, Dutta A (2015) A comparative review of biochar and hydrochar in terms of production, physico-chemical properties and applications. *Renew Sust Energ Rev* 45:359–378. <https://doi.org/10.1016/j.rser.2015.01.050>
- Karunanayake AG, Todd OA, Crowley ML, Ricchetti LB, Pittman CU, Anderson R, Mlsna TE (2017) Rapid removal of salicylic acid, 4-nitroaniline, benzoic acid and phthalic acid from wastewater using magnetized fast pyrolysis biochar from waste Douglas fir. *Chem Eng J* 319:75–88. <https://doi.org/10.1016/j.cej.2017.02.116>
- Kasozi G, Zimmerman A, Nkedi-Kizza P, Gao B (2010) Catechol and humic acid sorption onto a range of laboratory-produced black carbons (biochars). *Environ Sci Technol* 44:6189–6195. <https://doi.org/10.1021/es1014423>
- Keilueit M, Kleber M, Sparrow MA, Simoneit BRT, Prahlg FG (2012) Solvent-Extractable polycyclic aromatic hydrocarbons in biochar: influence of pyrolysis temperature and feedstock. *Environ Sci Technol* 46:9333–9341. <https://doi.org/10.1021/es302125k>
- Keilueit M, Nico PS, Johnson MG, Kleber M (2010) Dynamic molecular structure of plant biomass-derived black carbon (biochar). *Environ Sci Technol* 44:1247–1253. <https://doi.org/10.1021/es9031419>
- Keith A, Singh B, Dijkstra FA (2015) Biochar reduces the rhizosphere priming effect on soil organic carbon. *Soil Biol Biochem* 88. <https://doi.org/10.1016/j.soilbio.2015.06.007>
- Keith A, Singh B, Singh BP (2011) Interactive priming of biochar and labile organic matter mineralization in a smectite-rich soil. *Environ Sci Technol* 45:9611–9618. <https://doi.org/10.1021/es202186j>
- Khan S, Wang N, Reid BJ, Freddo A, Cai C (2013) Reduced bioaccumulation of PAHs by *Lactuca sativa* L. grown in contaminated soil amended with sewage sludge and sewage sludge derived biochar. *Environ Pollut* 175:64–68. <https://doi.org/10.1016/j.envpol.2012.12.014>
- Kim H-S, Kim K-R, Kim H-J, Yoon J-H, Yang JE, Ok YS, Owens G, Kim K-H (2015) Effect of biochar on heavy metal immobilization and uptake by lettuce (*Lactuca sativa* L.) in agricultural soil. *Environ Earth Sci* 74:1249–1259. <https://doi.org/10.1007/s12665-015-4116-1>
- Kluepfel L, Keilueit M, Kleber M, Sander M (2014) Redox properties of plant biomass-derived black carbon (biochar). *Environ Sci Technol* 48:5601–5611. <https://doi.org/10.1021/es500906d>
- Koch A, McBratney A, Adams M, Field D, Hill R, Crawford J, Minasny B, Lal R, Abbott L, O'Donnell A, Angers D, Baldock J, Barbier E, Binkley D, Parton W, Wall DH, Bird M, Bouma J, Chenu C, Flora CB, Goulding K, Grunwald S, Hempel J, Jastrow J, Lehmann J, Lorenz K, Morgan CL, Rice CW, Whitehead D, Young I, Zimmermann M (2013) Soil security: solving the global soil crisis. *Global Policy* 4:434–441. <https://doi.org/10.1111/1758-5899.12096>
- Koch A, McBratney A, Lal R (2012) Global soil week: put soil security on the global agenda. *Nature* 492:186. <https://doi.org/10.1038/492186d>
- Kołodziejka D, Wnętrzak R, Leahy JJ, Hayes MHB, Kwapiński W, Hubicki Z (2012) Kinetic and adsorptive characterization of biochar in metal ions removal. *Chem Eng J* 197:295–305. <https://doi.org/10.1016/j.cej.2012.05.025>
- Kumar E, Bhatnagar A, Hogland W, Marques M, Sillanpää M (2014) Interaction of inorganic anions with iron-mineral adsorbents in aqueous media—a review. *Adv Colloid Interfac* 203:11–21. <https://doi.org/10.1016/j.cis.2013.10.026>
- Kumar M, Jaiswal S, Sodhi KK, Shree P, Singh DK, Agrawal PK, Shukla P (2019) Antibiotics bioremediation: perspectives on its ecotoxicity and resistance. *Environ Int* 124:448–461. <https://doi.org/10.1016/j.envint.2018.12.065>
- Kuppusamy S, Thavamani P, Megharaj M, Venkateswarlu K, Naidu R (2016) Agronomic and remedial benefits and risks of applying biochar to soil: current knowledge and future research directions. *Environ Int* 87:1–12. <https://doi.org/10.1016/j.envint.2015.10.018>
- Kusmierz M, Oleszczuk P, Kraska P, Palys E, Andruszczak S (2016) Persistence of polycyclic aromatic hydrocarbons (PAHs) in biochar-amended soil. *Chemosphere* 146:272–279. <https://doi.org/10.1016/j.chemosphere.2015.12.010>
- Lahori AH, Guo X, Zhang Z, Li R, Mahar A, Awasthi MK, Shen F, Sial TA, Kumbhar F, Wang P, Jiang S (2017) Use of biochar as an amendment for remediation of heavy metal-contaminated soils: prospects and challenges. *Pedosphere* 27:991–1014. [https://doi.org/10.1016/S1002-0160\(17\)60490-9](https://doi.org/10.1016/S1002-0160(17)60490-9)
- Lambin EF, Meyfroidt P (2011) Global land use change, economic globalization, and the looming land scarcity. *P Natl Acad Sci USA* 108:3465–3472. <https://doi.org/10.1073/pnas.1100480108>
- Larsbo M, Löfstrand E, de Veer DvA, Ulén B (2013) Pesticide leaching from two Swedish topsoils of contrasting texture amended with biochar. *J Contam Hydrol* 147:73–81. <https://doi.org/10.1016/j.jconhyd.2013.01.003>
- Lattao C, Cao X, Mao J, Schmidt-Rohr K, Pignatello JJ (2014) Influence of molecular structure and adsorbent properties on sorption of organic compounds to a temperature series of wood chars. *Environ Sci Technol* 48:4790–4798. <https://doi.org/10.1021/es405096q>
- Lee JW, Kidder M, Evans BR, Paik S, Buchanan Iii AC, Garten CT, Brown RC (2010) Characterization of biochars produced from cornstovers for soil amendment. *Environ Sci Technol* 44:7970–7974. <https://doi.org/10.1021/es101337x>
- Lehmann J (2007) A handful of carbon. *Nature* 447:143. <https://doi.org/10.1038/447143a>
- Lehmann J (2009) Terra preta nova—Where to from here? In: Woods W, Teixeira V, Lehmann J, Steiner C, WinklerPrins A, Rebellato L (eds) Amazonian dark earths: Wim Sombroek's Vision. Springer, Netherlands, pp 473–486. [https://doi.org/10.1007/978-1-4020-9031-8\\_28](https://doi.org/10.1007/978-1-4020-9031-8_28)
- Lehmann J, Joseph S (2015) Biochar for environmental management: Science, technology and implementation, 2nd edn. Earthscan Publications Ltd., London, UK
- Leng L, Huang H, Li H, Li J, Zhou W (2019a) Biochar stability assessment methods: a review. *Sci Total Environ* 647:210–222. <https://doi.org/10.1016/j.scitotenv.2018.07.402>
- Leng L, Xu X, Wei L, Fan L, Huang H, Li J, Lu Q, Li J, Zhou W (2019b) Biochar stability assessment by incubation and modelling: methods, drawbacks and recommendations. *Sci Total Environ* 664:11–23. <https://doi.org/10.1016/j.scitotenv.2019.01.298>
- Li F, Cao X, Zhao L, Wang J, Ding Z (2014) Effects of mineral additives on biochar formation: carbon retention, stability, and properties. *Environ Sci Technol* 48:11211–11218. <https://doi.org/10.1021/es501885n>
- Li H, Ye X, Geng Z, Zhou H, Guo X, Zhang Y, Zhao H, Wang G (2016a) The influence of biochar type on long-term stabilization for Cd and Cu in contaminated paddy soils. *J Hazard Mater* 304:40–48. <https://doi.org/10.1016/j.jhazmat.2015.10.048>
- Li J, Dai J, Liu G, Zhang H, Gao Z, Fu J, He Y, Huang Y (2016b) Biochar from microwave pyrolysis of biomass: a review. *Biomass Bioenergy* 94:228–244. <https://doi.org/10.1016/j.biombioe.2016.09.010>

- Li R, Wang J, Gaston LA, Zhou B, Li M, Xiao R, Wang Q, Zhang Z, Huang H, Liang W, Huang H, Zhang X (2018a) An overview of carbothermal synthesis of metal–biochar composites for the removal of oxyanion contaminants from aqueous solution. *Carbon* 129:674–687. <https://doi.org/10.1016/j.carbon.2017.12.070>
- Li Y, Liu X, Zhang P, Wang X, Cao Y, Han L (2018b) Qualitative and quantitative correlation of physicochemical characteristics and lead sorption behaviors of crop residue-derived chars. *Bioresour Technol* 270:545–553. <https://doi.org/10.1016/j.biortech.2018.09.078>
- Li X, Li Y, Zhang X, Zhao X, Sun Y, Weng L, Li Y (2019a) Long-term effect of biochar amendment on the biodegradation of petroleum hydrocarbons in soil microbial fuel cells. *Sci Total Environ* 651:796–806. <https://doi.org/10.1016/j.scitotenv.2018.09.098>
- Li X, Song Y, Wang F, Bian Y, Jiang X (2019b) Combined effects of maize straw biochar and oxalic acid on the dissipation of polycyclic aromatic hydrocarbons and microbial community structures in soil: a mechanistic study. *J Hazard Mater* 364:325–331. <https://doi.org/10.1016/j.jhazmat.2018.10.041>
- Li X, Pignatello JJ, Wang Y, Xing B (2013) New insight into adsorption mechanism of ionizable compounds on carbon nanotubes. *Environ Sci Technol* 47:8334–8341. <https://doi.org/10.1021/es4011042>
- Lian F, Huang F, Chen W, Xing B, Zhu L (2011) Sorption of apolar and polar organic contaminants by waste tire rubber and its chars in single- and bi-solute systems. *Environ Pollut* 159:850–857. <https://doi.org/10.1016/j.envpol.2011.01.002>
- Lian F, Song Z, Liu Z, Zhu L, Xing B (2013) Mechanistic understanding of tetracycline sorption on waste tire powder and its chars as affected by  $\text{Cu}^{2+}$  and pH. *Environ Pollut* 178:264–270. <https://doi.org/10.1016/j.envpol.2013.03.014>
- Lian F, Xing B (2017) Black carbon (biochar) in water/soil environments: molecular structure, sorption, stability, and potential risk. *Environ Sci Technol* 51:13517–13532. <https://doi.org/10.1021/acs.est.7b02528>
- Lian F, Yu W, Wang Z, Xing B (2019) New insights into black carbon nanoparticle-induced dispersibility of goethite colloids and configuration-dependent sorption for phenanthrene. *Environ Sci Technol* 53:661–670. <https://doi.org/10.1021/acs.est.8b05066>
- Liang J, Li X, Yu Z, Zeng G, Luo Y, Jiang L, Yang Z, Qian Y, Wu H (2017) Amorphous  $\text{MnO}_2$  modified biochar derived from aerobically composted swine manure for adsorption of Pb(II) and Cd(II). *ACS Sustain Chem Eng* 5:5049–5058. <https://doi.org/10.1021/acssuschemeng.7b00434>
- Liao R, Gao B, Fang J (2013) Invasive plants as feedstock for biochar and bioenergy production. *Bioresour Technol* 140:439–442. <https://doi.org/10.1016/j.biortech.2013.04.117>
- Liao S, Pan B, Li H, Zhang D, Xing B (2014) Detecting free radicals in biochars and determining their ability to inhibit the germination and growth of corn, wheat and rice seedlings. *Environ Sci Technol* 48:8581–8587. <https://doi.org/10.1021/es404250a>
- Lin D, Tian X, Li T, Zhang Z, He X, Xing B (2012) Surface-bound humic acid increased  $\text{Mn}^{2+}$  sorption on carbon nanotubes. *Environ Pollut* 167:138–147. <https://doi.org/10.1016/j.envpol.2012.03.044>
- Ling L, Liu W, Zhang S, Jiang H (2017) Magnesium oxide embedded nitrogen self-doped biochar composites: fast and high-efficiency adsorption of heavy metals in an aqueous solution. *Environ Sci Technol* 51:10081–10089. <https://doi.org/10.1021/acs.est.7b02382>
- Liu G, Zheng H, Jiang Z, Zhao J, Wang Z, Pan B, Xing B (2018a) Formation and physicochemical characteristics of nano biochar: Insight into chemical and colloidal stability. *Environ Sci Technol* 52:10369–10379. <https://doi.org/10.1021/acs.est.8b01481>
- Liu G, Zheng H, Zhai X, Wang Z (2018b) Characteristics and mechanisms of microcrystalline-LR adsorption by giant reed-derived biochars: Role of minerals, pores, and functional groups. *J Clean Prod* 176:463–473. <https://doi.org/10.1016/j.jclepro.2017.12.156>
- Liu Y, Lonappan L, Brar SK, Yang S (2018c) Impact of biochar amendment in agricultural soils on the sorption, desorption, and degradation of pesticides: a review. *Sci Total Environ* 645:60–70. <https://doi.org/10.1016/j.scitotenv.2018.07.099>
- Liu L, Tan Z, Gong H, Huang Q (2019) Migration and transformation mechanisms of nutrient elements (N, P, K) within biochar in straw–biochar–soil–plant systems: a review. *ACS Sustain Chem Eng* 7:22–32. <https://doi.org/10.1021/acssuschemeng.8b04253>
- Liu W, Li W, Jiang H, Yu H (2017) Fates of chemical elements in biomass during its pyrolysis. *Chem Rev* 117:6367–6398. <https://doi.org/10.1021/acs.chemrev.6b00647>
- Liu W, Jiang H, Yu H (2015a) Development of biochar-based functional materials: toward a sustainable platform carbon material. *Chem Rev* 115:12251–12285. <https://doi.org/10.1021/acs.chemrev.5b00195>
- Liu W, Jiang H, Yu H (2015b) Thermochemical conversion of lignin to functional materials: a review and future directions. *Green Chem* 17:4888–4907. <https://doi.org/10.1039/c5gc01054c>
- Liu X, Yu G (2006) Combined effect of microwave and activated carbon on the remediation of polychlorinated biphenyl-contaminated soil. *Chemosphere* 63:228–235. <https://doi.org/10.1016/j.chemosphere.2005.08.030>
- Liu Z, Zhang F (2009) Removal of lead from water using biochars prepared from hydrothermal liquefaction of biomass. *J Hazard Mater* 167:933–939. <https://doi.org/10.1016/j.jhazmat.2009.01.085>
- Lu H, Zhang W, Yang Y, Huang X, Wang S, Qiu R (2012) Relative distribution of  $\text{Pb}^{2+}$  sorption mechanisms by sludge-derived biochar. *Water Res* 46:854–862. <https://doi.org/10.1016/j.watres.2011.11.058>
- Lu K, Yang X, Gielen G, Bolan N, Ok YS, Niazi NK, Xu S, Yuan G, Chen X, Zhang X, Liu D, Song Z, Liu X, Wang H (2017) Effect of bamboo and rice straw biochars on the mobility and redistribution of heavy metals (Cd, Cu, Pb and Zn) in contaminated soil. *J Environ Manage* 186:285–292. <https://doi.org/10.1016/j.jenvman.2016.05.068>
- Lu W, Ding W, Zhang J, Li Y, Luo J, Bolan N, Xie Z (2014) Biochar suppressed the decomposition of organic carbon in a cultivated sandy loam soil: a negative priming effect. *Soil Biol Biochem* 76:12–21. <https://doi.org/10.1016/j.soilbio.2014.04.029>
- Luo X, Wang L, Liu G, Wang X, Wang Z, Zheng H (2016) Effects of biochar on carbon mineralization of coastal wetland soils in the Yellow River Delta, China. *Ecol Eng* 94:329–336. <https://doi.org/10.1016/j.ecoleng.2016.06.004>
- Luo Y, Durenkamp M, De Nobili M, Lin Q, Brookes PC (2011) Short term soil priming effects and the mineralisation of biochar following its incorporation to soils of different pH. *Soil Biol Biochem* 43:2304–2314. <https://doi.org/10.1016/j.soilbio.2011.07.020>
- Lyu H, Gao B, He F, Zimmerman AR, Ding C, Huang H, Tang J (2018) Effects of ball milling on the physicochemical and sorptive properties of biochar: Experimental observations and governing mechanisms. *Environ Pollut* 233:54–63. <https://doi.org/10.1016/j.envpol.2017.10.037>
- Macquarrie DJ, Clark JH, Fitzpatrick E (2012) The microwave pyrolysis of biomass. *Biofuel Bioprod Bior* 6:549–560. <https://doi.org/10.1002/bbb.1344>
- Maestrini B, Nannipieri P, Abiven S (2015) A meta-analysis on pyrogenic organic matter induced priming effect. *GCB Bioenergy* 7:577–590. <https://doi.org/10.1111/gcbb.12194>
- Mamaeva A, Tahmasebi A, Tian L, Yu J (2016) Microwave-assisted catalytic pyrolysis of lignocellulosic biomass for production of phenolic-rich bio-oil. *Bioresour Technol* 211:382–389. <https://doi.org/10.1016/j.biortech.2016.03.120>
- Manya JJ (2012) Pyrolysis for biochar purposes: a review to establish current knowledge gaps and research needs. *Environ Sci Technol* 46:7939–7954. <https://doi.org/10.1021/es301029g>

- Marris E (2006) Black is the new green. *Nature* 442:624–626. <https://doi.org/10.1038/442624a>
- Martin SM, Kookana RS, Van Zwieten L, Krull E (2012) Marked changes in herbicide sorption–desorption upon ageing of biochars in soil. *J Hazard Mater* 231–232:70–78. <https://doi.org/10.1016/j.jhazmat.2012.06.040>
- Melo LCA, Puga AP, Coscione AR, Beesley L, Abreu CA, Camargo OA (2016) Sorption and desorption of cadmium and zinc in two tropical soils amended with sugarcane-straw-derived biochar. *J Soils Sed* 16:226–234. <https://doi.org/10.1007/s11368-015-1199-y>
- MEP (2014) National soil contamination survey report. Ministry of Environmental Protection, Beijing, China
- Meyer S, Glaser B, Quicker P (2011) Technical, economical, and climate-related aspects of biochar production technologies: a literature review. *Environ Sci Technol* 45:9473–9483. <https://doi.org/10.1021/es201792c>
- Mian MM, Liu G (2018) Recent progress in biochar-supported photocatalysts: synthesis, role of biochar, and applications. *RSC Adv* 8:14237–14248. <https://doi.org/10.1039/c8ra02258e>
- Miller EL, Nason SL, Karthikeyan KG, Pedersen JA (2016) Root uptake of pharmaceuticals and personal care product ingredients. *Environ Sci Technol* 50:525–541. <https://doi.org/10.1021/acs.est.5b01546>
- Mizuta K, Matsumoto T, Hatate Y, Nishihara K, Nakanishi T (2004) Removal of nitrate-nitrogen from drinking water using bamboo powder charcoal. *Bioresour Technol* 9:255–257
- Mohan D, Pittman CU, Steele PH (2006) Pyrolysis of wood/biomass for bio-oil: a critical review. *Energy Fuel* 20:848–889. <https://doi.org/10.1021/ef0502397>
- Mohan D, Sarswat A, Ok YS, Pittman Jr CU (2014) Organic and inorganic contaminants removal from water with biochar, a renewable, low cost and sustainable adsorbent—a critical review. *Bioresour Technol* 160:191–202. <https://doi.org/10.1016/j.biortech.2014.01.120>
- Mohanty S, Boehm AB (2014) *Escherichia coli* removal in biochar-augmented biofilter: effect of infiltration rate, initial bacterial concentration, biochar particle size and presence of compost. *Environ Sci Technol* 48:11535–11542. <https://doi.org/10.1021/es5033162>
- Mohanty SK, Cantrell KB, Nelson KL, Boehm AB (2014) Efficacy of biochar to remove *Escherichia coli* from stormwater under steady and intermittent flow. *Water Res* 61:288–296. <https://doi.org/10.1016/j.watres.2014.05.026>
- Moreno-Jiménez E, Fernández JM, Puschenreiter M, Williams PN, Plaza C (2016) Availability and transfer to grain of As, Cd, Cu, Ni, Pb and Zn in a barley agri-system: impact of biochar, organic and mineral fertilizers. *Agric Ecosyst Environ* 219:171–178. <https://doi.org/10.1016/j.agee.2015.12.001>
- Morillo E, Villaverde J (2017) Advanced technologies for the remediation of pesticide-contaminated soils. *Sci Total Environ* 586:576–597. <https://doi.org/10.1016/j.scitotenv.2017.02.020>
- Motasemi F, Afzal MT (2013) A review on the microwave-assisted pyrolysis technique. *Renew Sust Energ Rev* 28:317–330. <https://doi.org/10.1016/j.rser.2013.08.008>
- Muter O, Berzins A, Strikauska S, Pugajeva I, Bartkevics V, Dobele G, Truu J, Truu M, Steiner C (2014) The effects of woodchip- and straw-derived biochars on the persistence of the herbicide 4-chloro-2-methylphenoxyacetic acid (MCPA) in soils. *Ecotoxicol Environ Saf* 109:93–100. <https://doi.org/10.1016/j.ecoenv.2014.08.012>
- Namgay T, Singh B, Singh BP (2010) Influence of biochar application to soil on the availability of As, Cd, Cu, Pb, and Zn to maize (*Zea mays* L.). *Soil Res* 48:638–647. <https://doi.org/10.1071/SR10049>
- Nguyen BT, Lehmann J, Hockaday WC, Joseph S, Masiello CA (2010) Temperature sensitivity of black carbon decomposition and oxidation. *Environ Sci Technol*. <https://doi.org/10.1021/es903016y>
- Nguyen TH, Cho H-H, Poster DL, Ball WP (2007) Evidence for a pore-filling mechanism in the adsorption of aromatic hydrocarbons to a natural wood char. *Environ Sci Technol* 41:1212–1217. <https://doi.org/10.1021/es0617845>
- Ni J, Pignatello JJ (2018) Charge-assisted hydrogen bonding as a cohesive force in soil organic matter: water solubility enhancement by addition of simple carboxylic acids. *Environ Sci-Proc Imp* 20:1225–1233. <https://doi.org/10.1039/c8em00255j>
- Ni N, Wang F, Song Y, Bian Y, Shi R, Yang X, Gu C, Jiang X (2018) Mechanisms of biochar reducing the bioaccumulation of PAHs in rice from soil: Degradation stimulation vs immobilization. *Chemosphere* 196:288–296. <https://doi.org/10.1016/j.chemosphere.2017.12.192>
- Nie C, Yang X, Niazi NK, Xu X, Wen Y, Rinklebe J, Ok YS, Xu S, Wang H (2018) Impact of sugarcane bagasse-derived biochar on heavy metal availability and microbial activity: a field study. *Chemosphere* 200:274–282. <https://doi.org/10.1016/j.chemosphere.2018.02.134>
- O'Connor D, Peng T, Zhang J, Tsang DCW, Alessi DS, Shen Z, Bolan NS, Hou D (2018) Biochar application for the remediation of heavy metal polluted land: a review of in situ field trials. *Sci Total Environ* 619–620:815–826. <https://doi.org/10.1016/j.scitotenv.2017.11.132>
- Oh SY, Son JG, Chiu PC (2013) Biochar-mediated reductive transformation of nitro herbicides and explosives. *Environ Toxicol Chem* 32:501–508. <https://doi.org/10.1002/etc.2087>
- Oleszczuk P, Hale SE, Lehmann J, Cornelissen G (2012) Activated carbon and biochar amendments decrease pore-water concentrations of polycyclic aromatic hydrocarbons (PAHs) in sewage sludge. *Bioresour Technol* 111:84–91. <https://doi.org/10.1016/j.biortech.2012.02.030>
- Oleszczuk P, Joško I, Kuśmierz M (2013) Biochar properties regarding to contaminants content and ecotoxicological assessment. *J Hazard Mater* 260:375–382. <https://doi.org/10.1016/j.jhazmat.2013.05.044>
- Pan B, Li H, Lang D, Xing B (2019) Environmentally persistent free radicals: occurrence, formation mechanisms and implications. *Environ Pollut* 248:320–331. <https://doi.org/10.1016/j.envpol.2019.02.032>
- Panasniuk O, Hedström A, Marsalek J, Ashley RM, Viklander M (2015) Contamination of stormwater by wastewater: a review of detection methods. *J Environ Manage* 152:241–250. <https://doi.org/10.1016/j.jenvman.2015.01.050>
- Park CM, Han J, Chu KH, Al-Hamadani YAJ, Her N, Heo J, Yoon Y (2017a) Influence of solution pH, ionic strength, and humic acid on cadmium adsorption onto activated biochar: experiment and modeling. *J Ind Eng Chem* 48:186–193. <https://doi.org/10.1016/j.jiec.2016.12.038>
- Park JH, Wang JJ, Kim SH, Cho JS, Kang SW, Delaune RD, Han KJ, Seo DC (2017b) Recycling of rice straw through pyrolysis and its adsorption behaviors for Cu and Zn ions in aqueous solution. *Colloid Surface A* 533:330–337. <https://doi.org/10.1016/j.colsurfa.2017.08.041>
- Park JH, Choppala G, Lee SJ, Bolan N, Chung JW, Edraki M (2013) Comparative sorption of Pb and Cd by biochars and its implication for metal immobilization in soils. *Water Air Soil Pollut* 224:1711. <https://doi.org/10.1007/s11270-013-1711-1>
- Park JH, Choppala GK, Bolan NS, Chung JW, Chuasavathi T (2011) Biochar reduces the bioavailability and phytotoxicity of heavy metals. *Plant Soil* 348:439–451. <https://doi.org/10.1007/s11104-011-0948-y>
- Peiris C, Gunatilake SR, Milsna TE, Mohan D, Vithanage M (2017) Biochar based removal of antibiotic sulfonamides and tetracyclines in aquatic environments: a critical review. *Bioresour Technol* 246:150–159. <https://doi.org/10.1016/j.biortech.2017.07.150>
- Pignatello JJ, Mitch WA, Xu W (2017) Activity and reactivity of pyrogenic carbonaceous matter toward organic compounds. *Environ Sci Technol* 51:8893–8908. <https://doi.org/10.1021/acs.est.7b01088>



- Plaza MG, González AS, Pevida C, Pis JJ, Rubiera F (2012) Valorisation of spent coffee grounds as CO<sub>2</sub> adsorbents for postcombustion capture applications. *Appl Energ* 99:272–279. <https://doi.org/10.1016/j.apenergy.2012.05.028>
- Qiao J, Liu T, Wang X, Li F, Lv Y, Cui J, Zeng X, Yuan Y, Liu C (2018a) Simultaneous alleviation of cadmium and arsenic accumulation in rice by applying zero-valent iron and biochar to contaminated paddy soils. *Chemosphere* 195:260–271. <https://doi.org/10.1016/j.chemosphere.2017.12.081>
- Qiao M, Ying G, Singer AC, Zhu Y (2018b) Review of antibiotic resistance in China and its environment. *Environ Int* 110:160–172. <https://doi.org/10.1016/j.envint.2017.10.016>
- Qin P, Wang H, Yang X, He L, Müller K, Shaheen SM, Xu S, Rinklebe J, Tsang DCW, Ok YS, Bolan N, Song Z, Che L, Xu X (2018) Bamboo- and pig-derived biochars reduce leaching losses of dibutyl phthalate, cadmium, and lead from co-contaminated soils. *Chemosphere* 198:450–459. <https://doi.org/10.1016/j.chemosphere.2018.01.162>
- Qiu Y, Pang H, Zhou Z, Zhang P, Feng Y, Sheng GD (2009a) Competitive biodegradation of dichlobenil and atrazine coexisting in soil amended with a char and citrate. *Environ Pollut* 157:2964–2969. <https://doi.org/10.1016/j.envpol.2009.06.003>
- Qiu Y, Zheng Z, Zhou Z, Sheng GD (2009b) Effectiveness and mechanisms of dye adsorption on a straw-based biochar. *Bioresour Technol* 100:5348–5351. <https://doi.org/10.1016/j.biortech.2009.05.054>
- Rajapaksha AU, Chen SS, Tsang DC, Zhang M, Vithanage M, Mandal S, Gao B, Bolan NS, Ok YS (2016) Engineered/designer biochar for contaminant removal/immobilization from soil and water: potential and implication of biochar modification. *Chemosphere* 148:276–291. <https://doi.org/10.1016/j.chemosphere.2016.01.043>
- Rajapaksha AU, Vithanage M, Ahmad M, Seo DC, Cho JS, Lee SE, Lee SS, Ok YS (2015) Enhanced sulfamethazine removal by steam-activated invasive plant-derived biochar. *J Hazard Mater* 290:43–50. <https://doi.org/10.1016/j.jhazmat.2015.02.046>
- Rajapaksha AU, Vithanage M, Lim JE, Ahmed MBM, Zhang M, Lee SS, Ok YS (2014a) Invasive plant-derived biochar inhibits sulfamethazine uptake by lettuce in soil. *Chemosphere* 111:500–504. <https://doi.org/10.1016/j.chemosphere.2014.04.040>
- Rajapaksha AU, Vithanage M, Zhang M, Ahmad M, Mohan D, Chang SX, Ok YS (2014b) Pyrolysis condition affected sulfamethazine sorption by tea waste biochars. *Bioresour Technol* 166:303–308. <https://doi.org/10.1016/j.biortech.2014.05.029>
- Reguay F, Sarmah AK, Gao W (2017) Synthesis of magnetic biochar from pine sawdust via oxidative hydrolysis of FeCl<sub>2</sub> for the removal of sulfamethoxazole from aqueous solution. *J Hazard Mater* 321:868–878. <https://doi.org/10.1016/j.jhazmat.2016.10.006>
- Sarwar N, Imran M, Shaheen MR, Ishaque W, Kamran MA, Matloob A, Rehman A, Hussain S (2017) Phytoremediation strategies for soils contaminated with heavy metals: modifications and future perspectives. *Chemosphere* 171:710–721. <https://doi.org/10.1016/j.chemosphere.2016.12.116>
- Shen Z, Som AM, Wang F, Jin F, McMillan O, Al-Tabbaa A (2016) Long-term impact of biochar on the immobilisation of nickel (II) and zinc (II) and the revegetation of a contaminated site. *Sci Total Environ* 542:771–776. <https://doi.org/10.1016/j.scitotenv.2015.10.057>
- Sigmund G, Hüffer T, Hofmann T, Kah M (2017) Biochar total surface area and total pore volume determined by N<sub>2</sub> and CO<sub>2</sub> physisorption are strongly influenced by degassing temperature. *Sci Total Environ* 580:770–775. <https://doi.org/10.1016/j.scitotenv.2016.12.023>
- Sigmund G, Poyntner C, Pinar G, Kah M, Hofmann T (2018) Influence of compost and biochar on microbial communities and the sorption/degradation of PAHs and NSO-substituted PAHs in contaminated soils. *J Hazard Mater* 345:107–113. <https://doi.org/10.1016/j.jhazmat.2017.11.010>
- Singh BP, Cowie AL, Smernik RJ (2012) Biochar carbon stability in a clayey soil as a function of feedstock and pyrolysis temperature. *Environ Sci Technol* 46:11770–11778. <https://doi.org/10.1021/es302545b>
- Singh N, Abiven S, Maestrini B, Bird JA, Torn MS, Schmidt MWI (2014) Transformation and stabilization of pyrogenic organic matter in a temperate forest field experiment. *Glob Chang Biol* 20:1629–1642. <https://doi.org/10.1111/gcb.12459>
- Sohi SP (2012) Carbon storage with benefits. *Science* 338:1034–1035. <https://doi.org/10.1126/science.1225987>
- Soinne H, Hovi J, Tammeorg P, Turtola E (2014) Effect of biochar on phosphorus sorption and clay soil aggregate stability. *Geoderma* 219–220:162–167. <https://doi.org/10.1016/j.geoderma.2013.12.022>
- Son EB, Poo KM, Chang JS, Chae KJ (2018) Heavy metal removal from aqueous solutions using engineered magnetic biochars derived from waste marine macro-algal biomass. *Sci Total Environ* 615:161–168. <https://doi.org/10.1016/j.scitotenv.2017.09.171>
- Song B, Zeng G, Gong J, Liang J, Xu P, Liu Z, Zhang Y, Zhang C, Cheng M, Liu Y, Ye S, Yi H, Ren X (2017) Evaluation methods for assessing effectiveness of in situ remediation of soil and sediment contaminated with organic pollutants and heavy metals. *Environ Int* 105:43–55. <https://doi.org/10.1016/j.envint.2017.05.001>
- Song Z, Lian F, Yu Z, Zhu L, Xing B, Qiu W (2014) Synthesis and characterization of a novel MnOx-loaded biochar and its adsorption properties for Cu<sup>2+</sup> in aqueous solution. *Chem Eng J* 242:36–42. <https://doi.org/10.1016/j.ccej.2013.12.061>
- Sun C, Zhang G, Zheng H, Liu N, Shi M, Luo X, Chen L, Li F, Hu S (2019a) Fate of four phthalate esters with presence of *Karenia brevis*: uptake and biodegradation. *Aquat Toxicol* 206:81–90. <https://doi.org/10.1016/j.aquatox.2018.11.010>
- Sun Y, Yu IKM, Tsang DCW, Cao X, Lin D, Wang L, Graham NJD, Alessi DS, Komárek M, Ok YS, Feng Y, Li X (2019b) Multifunctional iron-biochar composites for the removal of potentially toxic elements, inherent cations, and hetero-chloride from hydraulic fracturing wastewater. *Environ Int* 124:521–532. <https://doi.org/10.1016/j.envint.2019.01.047>
- Sun J, Pan L, Tsang DCW, Zhan Y, Zhu L, Li X (2018) Organic contamination and remediation in the agricultural soils of China: a critical review. *Sci Total Environ* 615:724–740. <https://doi.org/10.1016/j.scitotenv.2017.09.271>
- Sun K, Jin J, Keiluweit M, Kleber M, Wang Z, Pan Z, Xing B (2012) Polar and aliphatic domains regulate sorption of phthalic acid esters (PAEs) to biochars. *Bioresour Technol* 118:120–127. <https://doi.org/10.1016/j.biortech.2012.05.008>
- Sun K, Kang M, Zhang Z, Jin J, Wang Z, Pan Z, Xu D, Wu F, Xing B (2013) Impact of deashing treatment on biochar structural properties and potential sorption mechanisms of phenanthrene. *Environ Sci Technol* 47:11473–11481. <https://doi.org/10.1021/es4026744>
- Sun K, Ro K, Guo M, Novak J, Mashayekhi H, Xing B (2011) Sorption of bisphenol A, 17 $\alpha$ -ethinyl estradiol and phenanthrene on thermally and hydrothermally produced biochars. *Bioresour Technol* 102:5757–5763. <https://doi.org/10.1016/j.biortech.2011.03.038>
- Tan G, Sun W, Xu Y, Wang H, Xu N (2016a) Sorption of mercury (II) and atrazine by biochar, modified biochars and biochar based activated carbon in aqueous solution. *Bioresour Technol* 211:727–735. <https://doi.org/10.1016/j.biortech.2016.03.147>
- Tan X, Liu Y, Gu Y, Xu Y, Zeng G, Hu X, Liu S, Wang X, Liu S, Li J (2016b) Biochar-based nano-composites for the decontamination of wastewater: A review. *Bioresour Technol* 212:318–333. <https://doi.org/10.1016/j.biortech.2016.04.093>
- Tan X, Liu Y, Zeng G, Wang X, Hu X, Gu Y, Yang Z (2015) Application of biochar for the removal of pollutants from aqueous solutions. *Chemosphere* 125:70–85. <https://doi.org/10.1016/j.chemosphere.2014.12.058>

- Tang F, Xu Z, Gao M, Li L, Li H, Cheng H, Zhang C, Tian G (2019) The dissipation of cyazofamid and its main metabolite in soil response oppositely to biochar application. *Chemosphere* 218:26–35. <https://doi.org/10.1016/j.chemosphere.2018.11.094>
- Tang X, Huang W, Guo J, Yang Y, Tao R, Feng X (2017) Use of Fe-impregnated biochar to efficiently sorb chlorpyrifos, reduce uptake by *Allium fistulosum* L., and enhance microbial community diversity. *J Agric Food Chem* 65:5238–5243. <https://doi.org/10.1021/acs.jafc.7b01300>
- Tasho RP, Cho JY (2016) Veterinary antibiotics in animal waste, its distribution in soil and uptake by plants: a review. *Sci Total Environ* 563–564:366–376. <https://doi.org/10.1016/j.scitotenv.2016.04.140>
- Teixidó M, Hurtado C, Pignatello JJ, Beltrán JL, Granados M, Peccia J (2013) Predicting contaminant adsorption in black carbon (biochar)-amended soil for the veterinary antimicrobial sulfamethazine. *Environ Sci Technol* 47:6197–6205. <https://doi.org/10.1021/es400911c>
- Teixidó M, Pignatello JJ, Beltrán JL, Granados M, Peccia J (2011) Speciation of the ionizable antibiotic sulfamethazine on black carbon (biochar). *Environ Sci Technol* 45:10020–10027. <https://doi.org/10.1021/es202487h>
- Thines KR, Abdullah EC, Mubarak NM, Ruthiraan M (2017) Synthesis of magnetic biochar from agricultural waste biomass to enhancing route for waste water and polymer application: a review. *Renew Sust Energ Rev* 67:257–276. <https://doi.org/10.1016/j.rser.2016.09.057>
- Thompson KA, Shimabuku KK, Kearns JP, Knappe DRU, Summers RS, Cook SM (2016) Environmental comparison of biochar and activated carbon for tertiary wastewater treatment. *Environ Sci Technol* 50:11253–11262. <https://doi.org/10.1021/acs.est.6b03239>
- Tong H, Hu M, Li FB, Liu CS, Chen MJ (2014) Biochar enhances the microbial and chemical transformation of pentachlorophenol in paddy soil. *Soil Biol Biochem* 70:142–150. <https://doi.org/10.1016/j.soilbio.2013.12.012>
- Tripathi M, Sahu JN, Ganesan P (2016) Effect of process parameters on production of biochar from biomass waste through pyrolysis: a review. *Renew Sust Energ Rev* 55:467–481. <https://doi.org/10.1016/j.rser.2015.10.122>
- Uchimiya M (2014) Influence of pH, ionic strength, and multidentate ligand on the interaction of Cd<sup>II</sup> with biochars. *ACS Sustain Chem Eng* 2:2019–2027. <https://doi.org/10.1021/sc5002269>
- Uchimiya M, Bannon DI (2013) Solubility of lead and copper in biochar-amended small arms range soils: influence of soil organic carbon and pH. *J Agric Food Chem* 61:7679–7688. <https://doi.org/10.1021/jf401481x>
- Uchimiya M, Lima I, Klasson K, Chang S, Wartelle L, Rodgers J (2010) Immobilization of heavy metal ions (Cu<sup>II</sup>, Cd<sup>II</sup>, Ni<sup>II</sup>, and Pb<sup>II</sup>) by broiler litter-derived biochars in water and soil. *J Agric Food Chem* 58:5538–5544. <https://doi.org/10.1021/jf9044217>
- Varjani S, Kumar G, Rene ER (2019) Developments in biochar application for pesticide remediation: current knowledge and future research directions. *J Environ Manage* 232:505–513. <https://doi.org/10.1016/j.jenvman.2018.11.043>
- Vilela CLS, Bassin JP, Peixoto RS (2018) Water contamination by endocrine disruptors: impacts, microbiological aspects and trends for environmental protection. *Environ Pollut* 235:546–559. <https://doi.org/10.1016/j.envpol.2017.12.098>
- Vithanage M, Rajapaksha AU, Tang X, Thiele-Bruhn S, Kim KH, Lee S-E, Ok YS (2014) Sorption and transport of sulfamethazine in agricultural soils amended with invasive-plant-derived biochar. *J Environ Manage* 141:95–103. <https://doi.org/10.1016/j.jenvman.2014.02.030>
- Wang B, Jiang Y, Li F, Yang D (2017a) Preparation of biochar by simultaneous carbonization, magnetization and activation for norfloxacin removal in water. *Bioresour Technol* 233:159–165. <https://doi.org/10.1016/j.biortech.2017.02.103>
- Wang F, Sun H, Ren X, Zhang K (2017b) Sorption of naphthalene and its hydroxyl substitutes onto biochars in single-solute and bi-solute systems with propranolol as the co-solute. *Chem Eng J* 326:281–291. <https://doi.org/10.1016/j.cej.2017.05.159>
- Wang H, Zheng H, Jiang Z, Dai Y, Liu G, Chen L, Luo X, Liu M, Wang Z (2017c) Efficacies of biochar and biochar-based amendment on vegetable yield and nitrogen utilization in four consecutive planting seasons. *Sci Total Environ* 593–594:124–133. <https://doi.org/10.1016/j.scitotenv.2017.03.096>
- Wang Z, Chen L, Sun F, Luo X, Wang H, Liu G, Xu Z, Jiang Z, Pan B, Zheng H (2017d) Effects of adding biochar on the properties and nitrogen bioavailability of an acidic soil. *Eur J Soil Sci* 68:559–572. <https://doi.org/10.1111/ejss.12436>
- Wang H, Gao B, Wang S, Fang J, Xue Y, Yang K (2015a) Removal of Pb(II), Cu(II), and Cd(II) from aqueous solutions by biochar derived from KMnO<sub>4</sub> treated hickory wood. *Bioresour Technol* 197:356–362. <https://doi.org/10.1016/j.biortech.2015.08.132>
- Wang S, Gao B, Li Y, Mosa A, Zimmerman AR, Ma LQ, Harris WG, Migliaccio KW (2015b) Manganese oxide-modified biochars: preparation, characterization, and sorption of arsenate and lead. *Bioresour Technol* 181:13–17. <https://doi.org/10.1016/j.biortech.2015.01.044>
- Wang Z, Liu G, Zheng H, Li F, Ngo HH, Guo W, Liu C, Chen L, Xing B (2015c) Investigating the mechanisms of biochar's removal of lead from solution. *Bioresour Technol* 177:308–317. <https://doi.org/10.1016/j.biortech.2014.11.077>
- Wang Z, Liu G, Zheng H, Li F, Ngo HH, Guo W, Liu C, Chen L, Xing B (2015d) Investigating the mechanisms of biochar's removal of lead from solution. *Bioresour Technol* 177:308–317. <https://doi.org/10.1016/j.biortech.2014.11.077>
- Wang Z, Zong H, Zheng H, Liu G, Chen L, Xing B (2015e) Reduced nitrification and abundance of ammonia-oxidizing bacteria in acidic soil amended with biochar. *Chemosphere* 138:576–583. <https://doi.org/10.1016/j.chemosphere.2015.06.084>
- Wang H, Guo W, Yin R, Du J, Wu Q, Luo H, Liu B, Sseguya F, Ren N (2019a) Biochar-induced Fe(III) reduction for persulfate activation in sulfamethoxazole degradation: insight into the electron transfer, radical oxidation and degradation pathways. *Chem Eng J* 362:561–569. <https://doi.org/10.1016/j.cej.2019.01.053>
- Wang S, Zhao M, Zhou M, Li YC, Wang J, Gao B, Sato S, Feng K, Yin W, Deshani Igalavithana A, Oleszczuk P, Wang X, Ok YS (2019b) Biochar-supported nZVI (nZVI/BC) for contaminant removal from soil and water: a critical review. *J Hazard Mater* 373:820–834. <https://doi.org/10.1016/j.jhazmat.2019.03.080>
- Wang J, Xiong Z, Kuzyakov Y (2016a) Biochar stability in soil: meta-analysis of decomposition and priming effects. *GCB Bioenergy* 8:512–523. <https://doi.org/10.1111/gcbb.12266>
- Wang Z, Han L, Sun K, Jin J, Ro KS, Libra JA, Liu X, Xing B (2016b) Sorption of four hydrophobic organic contaminants by biochars derived from maize straw, wood dust and swine manure at different pyrolytic temperatures. *Chemosphere* 144:285–291. <https://doi.org/10.1016/j.chemosphere.2015.08.042>
- Wang M, Zhu Y, Cheng L, Anderson B, Zhao X, Wang D, Ding A (2018a) Review on utilization of biochar for metal-contaminated soil and sediment remediation. *J Environ Sci-China* 63:156–173. <https://doi.org/10.1016/j.jes.2017.08.004>
- Wang R, Huang D, Liu Y, Zhang C, Lai C, Zeng G, Cheng M, Gong X, Wan J, Luo H (2018b) Investigating the adsorption behavior and the relative distribution of Cd<sup>2+</sup> sorption mechanisms on biochars by different feedstock. *Bioresour Technol* 261:265–271. <https://doi.org/10.1016/j.biortech.2018.04.032>
- Wang Y, Zhong B, Shafi M, Ma J, Guo J, Wu J, Ye Z, Liu D, Jin H (2018c) Effects of biochar on growth, and heavy metals accumulation of moso bamboo (*Phyllostachy pubescens*), soil physical properties, and heavy metals solubility in soil. *Chemosphere* 219:510–516. <https://doi.org/10.1016/j.chemosphere.2018.11.159>

- Wang Y, Wang L, Fang G, Herath HMSK, Wang Y, Cang L, Xie Z, Zhou D (2013a) Enhanced PCBs sorption on biochars as affected by environmental factors: humic acid and metal cations. *Environ Pollut* 172:86–93. <https://doi.org/10.1016/j.envpol.2012.08.007>
- Wang Z, Zheng H, Luo Y, Deng X, Herbert S, Xing B (2013b) Characterization and influence of biochars on nitrous oxide emission from agricultural soil. *Environ Pollut* 174:289–296. <https://doi.org/10.1016/j.envpol.2012.12.003>
- Whitman T, Enders A, Lehmann J (2014) Pyrogenic carbon additions to soil counteract positive priming of soil carbon mineralization by plants. *Soil Biol Biochem* 73:33–41. <https://doi.org/10.1016/j.soilbio.2014.02.009>
- Williams M, Martin S, Kookana RS (2015) Sorption and plant uptake of pharmaceuticals from an artificially contaminated soil amended with biochars. *Plant Soil* 395:75–86. <https://doi.org/10.1007/s11104-015-2421-9>
- Woolf D, Amonette JE, Street-Perrott FA, Lehmann J, Joseph S (2010) Sustainable biochar to mitigate global climate change. *Nat Commun* 1:56. <https://doi.org/10.1038/ncomms1053>
- Wu C, Shi L, Xue S, Li W, Jiang X, Rajendran M, Qian Z (2019a) Effect of sulfur-iron modified biochar on the available cadmium and bacterial community structure in contaminated soils. *Sci Total Environ* 647:1158–1168. <https://doi.org/10.1016/j.scitotenv.2018.08.087>
- Wu S, Vymazal J, Brix H (2019b) Critical review: biogeochemical networking of iron, is it important in constructed wetlands for wastewater treatment? *Environ Sci Technol*. <https://doi.org/10.1021/acs.est.8b07136>
- Wu P, Cui P, Fang G, Wang Y, Wang S, Zhou D, Zhang W, Wang Y (2018) Biochar decreased the bioavailability of Zn to rice and wheat grains: insights from microscopic to macroscopic scales. *Sci Total Environ* 621:160–167. <https://doi.org/10.1016/j.scitotenv.2017.11.236>
- Wu S, Wu H (2019) Incorporating biochar into wastewater eco-treatment systems: Popularity, reality, and complexity. *Environ Sci Technol*. <https://doi.org/10.1021/acs.est.9b01101>
- Xiao F, Pignatello JJ (2015) Interactions of triazine herbicides with biochar: steric and electronic effects. *Water Res* 80:179–188. <https://doi.org/10.1016/j.watres.2015.04.040>
- Xiao X, Chen B, Chen Z, Zhu L, Schnoor JL (2018) Insight into multiple and multilevel structures of biochars and their potential environmental applications: a critical review. *Environ Sci Technol* 52:5027–5047. <https://doi.org/10.1021/acs.est.7b06487>
- Xiao X, Chen B, Zhu L (2014) Transformation, morphology, and dissolution of silicon and carbon in rice straw-derived biochars under different pyrolytic temperatures. *Environ Sci Technol* 48:3411–3419. <https://doi.org/10.1021/es405676h>
- Xin J, Liu X, Liu W, Zheng X (2014) Effects of biochar–BDE-47 interactions on BDE-47 bioaccessibility and biodegradation by *Pseudomonas putida* TZ-1. *Ecotoxicol Environ Saf* 106:27–32. <https://doi.org/10.1016/j.ecoenv.2014.04.036>
- Xing B, Pignatello JJ (1997) Dual-mode sorption of low-polarity compounds in glassy poly(vinyl chloride) and soil organic matter. *Environ Sci Technol* 31:792–799. <https://doi.org/10.1021/es960481f>
- Xiong B, Zhang Y, Hou Y, Arp HPH, Reid BJ, Cai C (2017) Enhanced biodegradation of PAHs in historically contaminated soil by *M. gilvum* inoculated biochar. *Chemosphere* 182:316–324. <https://doi.org/10.1016/j.chemosphere.2017.05.020>
- Xu R, Xiao S, Yuan J, Zhao A (2011) Adsorption of methyl violet from aqueous solutions by the biochars derived from crop residues. *Bioresour Technol* 102:10293–10298. <https://doi.org/10.1016/j.biortech.2011.08.089>
- Xu X, Cao X, Zhao L, Wang H, Yu H, Gao B (2013) Removal of Cu, Zn, and Cd from aqueous solutions by the dairy manure-derived biochar. *Environ Sci Pollut Res Int* 20:358–368. <https://doi.org/10.1007/s11356-012-0873-5>
- Xu X, Zhao Y, Sima J, Zhao L, Mašek O, Cao X (2017) Indispensable role of biochar-inherent mineral constituents in its environmental applications: A review. *Bioresour Technol* 241:887–899. <https://doi.org/10.1016/j.biortech.2017.06.023>
- Yang F, Sun L, Zhang W, Zhang Y (2017) One-pot synthesis of porous carbon foam derived from corn straw: atrazine adsorption equilibrium and kinetics. *Environ Sci Nano* 4:625–635. <https://doi.org/10.1039/c6en00574h>
- Yang F, Zhang S, Sun Y, Cheng K, Li J, Tsang DCW (2018a) Fabrication and characterization of hydrophilic corn stalk biochar-supported nanoscale zero-valent iron composites for efficient metal removal. *Bioresour Technol* 265:490–497. <https://doi.org/10.1016/j.biortech.2018.06.029>
- Yang Q, Li Z, Lu X, Duan Q, Huang L, Bi J (2018b) A review of soil heavy metal pollution from industrial and agricultural regions in China: pollution and risk assessment. *Sci Total Environ* 642:690–700. <https://doi.org/10.1016/j.scitotenv.2018.06.068>
- Yang F, Zhao L, Gao B, Xu X, Cao X (2016a) The interfacial behavior between biochar and soil minerals and its effect on biochar stability. *Environ Sci Technol* 50:2264–2271. <https://doi.org/10.1021/acs.est.5b03656>
- Yang J, Pan B, Li H, Liao S, Zhang D, Wu M, Xing B (2016b) Degradation of p-nitrophenol on biochars: Role of persistent free radicals. *Environ Sci Technol* 694–700. <https://doi.org/10.1021/acs.est.5b04042>
- Yang G, Jiang H (2014) Amino modification of biochar for enhanced adsorption of copper ions from synthetic wastewater. *Water Res* 48:396–405. <https://doi.org/10.1016/j.watres.2013.09.050>
- Yang K, Xing B (2010) Adsorption of organic compounds by carbon nanomaterials in aqueous phase: polanyi theory and its application. *Chem Rev* 110:5989–6008. <https://doi.org/10.1021/cr100059s>
- Yang X, Wan Y, Zheng Y, He F, Yu Z, Huang J, Wang H, Ok YS, Jiang Y, Gao B (2019) Surface functional groups of carbon-based adsorbents and their roles in the removal of heavy metals from aqueous solutions: a critical review. *Chem Eng J* 366:608–621. <https://doi.org/10.1016/j.cej.2019.02.119>
- Yang X, Ying G, Peng P, Wang L, Zhao J, Zhang L, Yuan P, He H (2010) Influence of biochars on plant uptake and dissipation of two pesticides in an agricultural soil. *J Agric Food Chem* 58:7915–7921. <https://doi.org/10.1021/jf1011352>
- Yang Y, Chun Y, Sheng G, Huang M (2004) pH-dependence of pesticide adsorption by wheat-residue-derived black carbon. *Langmuir* 20:6736–6741. <https://doi.org/10.1021/la049363t>
- Yao Y, Gao B, Chen H, Jiang L, Inyang M, Zimmerman AR, Cao X, Yang L, Xue Y, Li H (2012) Adsorption of sulfamethoxazole on biochar and its impact on reclaimed water irrigation. *J Hazard Mater* 209–210:408–413. <https://doi.org/10.1016/j.jhazmat.2012.01.046>
- Yao Y, Gao B, Chen J, Yang L (2013) Engineered biochar reclaiming phosphate from aqueous solutions: mechanisms and potential application as a slow-release fertilizer. *Environ Sci Technol* 47:8700–8708. <https://doi.org/10.1021/es4012977>
- Yao Y, Gao B, Inyang M, Zimmerman AR, Cao X, Pullammanappallil P, Yang L (2011) Biochar derived from anaerobically digested sugar beet tailings: characterization and phosphate removal potential. *Bioresour Technol* 102:6273–6278. <https://doi.org/10.1016/j.biortech.2011.03.006>
- Yasmin KK, Ali B, Cui X, Feng Y, Yang X, Joseph Stoffella P (2017) Impact of different feedstocks derived biochar amendment with cadmium low uptake affinity cultivar of pak choi (*Brassica rapa* ssp. *chinensis* L.) on phytoavoidance of Cd to reduce potential dietary toxicity. *Ecotoxicol Environ Saf* 141:129–138. <https://doi.org/10.1016/j.ecoenv.2017.03.020>
- Ye M, Sun M, Feng Y, Wan J, Xie S, Tian D, Zhao Y, Wu J, Hu F, Li H, Jiang X (2016) Effect of biochar amendment on the control of soil sulfonamides, antibiotic-resistant bacteria, and gene enrichment

- in lettuce tissues. *J Hazard Mater* 309:219–227. <https://doi.org/10.1016/j.jhazmat.2015.10.074>
- Yu K, Lau B, Show P, Ong H, Ling T, Chen W, Ng EP, Chang J (2017) Recent developments on algal biochar production and characterization. *Bioresour Technol* 246:2–11. <https://doi.org/10.1016/j.biortech.2017.08.009>
- Yu X, Mu C, Gu C, Liu C, Liu X (2011) Impact of woodchip biochar amendment on the sorption and dissipation of pesticide acetamiprid in agricultural soils. *Chemosphere* 85:1284–1289. <https://doi.org/10.1016/j.chemosphere.2011.07.031>
- Yu X, Ying G, Kookana RS (2009) Reduced plant uptake of pesticides with biochar additions to soil. *Chemosphere* 76:665–671. <https://doi.org/10.1016/j.chemosphere.2009.04.001>
- Yuan J, Xu R, Zhang H (2011) The forms of alkalis in the biochar produced from crop residues at different temperatures. *Bioresour Technol* 102:3488–3497. <https://doi.org/10.1016/j.biortech.2010.11.018>
- Yuan P, Wang J, Pan Y, Shen B, Wu C (2019) Review of biochar for the management of contaminated soil: preparation, application and prospect. *Sci Total Environ* 659:473–490. <https://doi.org/10.1016/j.scitotenv.2018.12.400>
- Yuan Y, Bolan N, Prévosteau A, Vithanage M, Biswas JK, Ok YS, Wang H (2017) Applications of biochar in redox-mediated reactions. *Bioresour Technol* 246:271–281. <https://doi.org/10.1016/j.biortech.2017.06.154>
- Zhang C, Lai C, Zeng G, Huang D, Yang C, Wang Y, Zhou Y, Cheng M (2016a) Efficacy of carbonaceous nanocomposites for sorbing ionizable antibiotic sulfamethazine from aqueous solution. *Water Res* 95:103–112. <https://doi.org/10.1016/j.watres.2016.03.014>
- Zhang H, Tang J, Wang L, Liu J, Gurav RG, Sun K (2016b) A novel bioremediation strategy for petroleum hydrocarbon pollutants using salt tolerant *Corynebacterium variabile* HRJ4 and biochar. *J Environ Sci China* 47:7–13. <https://doi.org/10.1016/j.jes.2015.12.023>
- Zhang X, Sarmah AK, Bolan NS, He L, Lin X, Che L, Tang C, Wang H (2016c) Effect of aging process on adsorption of diethyl phthalate in soils amended with bamboo biochar. *Chemosphere* 142:28–34. <https://doi.org/10.1016/j.chemosphere.2015.05.037>
- Zhang X, Sarmah AK, Bolan NS, He L, Lin X, Che L, Tang C, Wang H (2016d) Effect of aging process on adsorption of diethyl phthalate in soils amended with bamboo biochar. *Chemosphere* 142:28–34. <https://doi.org/10.1016/j.chemosphere.2015.05.037>
- Zhang Y, Chen T, Liao Y, Reid BJ, Chi H, Hou Y, Cai C (2016e) Modest amendment of sewage sludge biochar to reduce the accumulation of cadmium into rice (*Oryza sativa* L.): a field study. *Environ Pollut* 216:819–825. <https://doi.org/10.1016/j.envpol.2016.06.053>
- Zhang H, Lin K, Wang H, Gan J (2010) Effect of *Pinus radiata* derived biochars on soil sorption and desorption of phenanthrene. *Environ Pollut* 158:2821–2825. <https://doi.org/10.1016/j.envpol.2010.06.025>
- Zhang H, Luo Y, Teng Y, Wan H (2013a) PCB contamination in soils of the Pearl River Delta, South China: levels, sources, and potential risks. *Environ Sci Pollut Res* 20:5150–5159. <https://doi.org/10.1007/s11356-013-1488-1>
- Zhang M, Gao B, Yao Y, Inyang M (2013b) Phosphate removal ability of biochar/MgAl-LDH ultra-fine composites prepared by liquid-phase deposition. *Chemosphere* 92:1042–1047. <https://doi.org/10.1016/j.chemosphere.2013.02.050>
- Zhang P, Sun H, Yu L, Sun T (2013c) Adsorption and catalytic hydrolysis of carbaryl and atrazine on pig manure-derived biochars: impact of structural properties of biochars. *J Hazard Mater* 244–245:217–224. <https://doi.org/10.1016/j.jhazmat.2012.11.046>
- Zhang M, Gao B (2013) Removal of arsenic, methylene blue, and phosphate by biochar/AlOOH nanocomposite. *Chem Eng J* 226:286–292. <https://doi.org/10.1016/j.cej.2013.04.077>
- Zhang P, Sheng G, Feng Y, Miller DM (2005) Role of wheat-residue-derived char in the biodegradation of benzonitrile in soil: nutritional stimulation versus adsorptive inhibition. *Environ Sci Technol* 39:5442–5448. <https://doi.org/10.1021/es0480670>
- Zhang R, Li Z, Liu X, Wang B, Zhou G, Huang X, Lin C, Wang A, Brooks M (2017) Immobilization and bioavailability of heavy metals in greenhouse soils amended with rice straw-derived biochar. *Ecol Eng* 98:183–188. <https://doi.org/10.1016/j.ecoleng.2016.10.057>
- Zhang X, He L, Sarmah AK, Lin K, Liu Y, Li J, Wang H (2014) Retention and release of diethyl phthalate in biochar-amended vegetable garden soils. *J Soils Sed* 14:1790–1799. <https://doi.org/10.1007/s11368-014-0929-x>
- Zhang X, Zha T, Guo X, Meng G, Zhou J (2018) Spatial distribution of metal pollution of soils of Chinese provincial capital cities. *Sci Total Environ* 643:1502–1513. <https://doi.org/10.1016/j.scitotenv.2018.06.177>
- Zhang Y, Tao S (2009) Global atmospheric emission inventory of polycyclic aromatic hydrocarbons (PAHs) for 2004. *Atmos Environ* 43:812–819. <https://doi.org/10.1016/j.atmosenv.2008.10.050>
- Zhang Z, Zhu Z, Shen B, Liu L (2019) Insights into biochar and hydrochar production and applications: a review. *Energy* 171:581–598. <https://doi.org/10.1016/j.energy.2019.01.035>
- Zhao Q, Zhang S, Zhang X, Lei L, Ma W, Ma C, Song L, Chen J, Pan B, Xing B (2017) Cation- $\pi$  Interaction: a key force for sorption of fluoroquinolone antibiotics on pyrogenic carbonaceous materials. *Environ Sci Technol* 51:13659–13667. <https://doi.org/10.1021/acs.est.7b02317>
- Zheng H, Liu B, Liu G, Cai Z, Zhang C (2018a) Potential toxic compounds in biochar: knowledge gaps between biochar research and safety. In: Tsang D, Ok YS (eds) *Biochar from a*. Elsevier
- Zheng H, Wang X, Chen L, Wang Z, Xia Y, Zhang Y, Wang H, Luo X, Xing B (2018b) Enhanced growth of halophyte plants in biochar-amended coastal soil: roles of nutrient availability and rhizosphere microbial modulation. *Plant, Cell Environ* 41:517–532. <https://doi.org/10.1111/pce.12944>
- Zheng H, Wang X, Luo X, Wang Z, Xing B (2018c) Biochar-induced negative carbon mineralization priming effects in a coastal wetland soil: Roles of soil aggregation and microbial modulation. *Sci Total Environ* 610–611:951–960. <https://doi.org/10.1016/j.scitotenv.2017.08.166>
- Zheng H, Sun C, Hou X, Wu M, Yao Y, Li F (2017) Pyrolysis of *Arundo donax* L. to produce pyrolytic vinegar and its effect on the growth of dinoflagellate *Karenia brevis*. *Bioresour Technol* 247:273–281. <https://doi.org/10.1016/j.biortech.2017.09.049>
- Zheng H, Wang Z, Deng X, Herbert S, Xing B (2013a) Impacts of adding biochar on nitrogen retention and bioavailability in agricultural soil. *Geoderma* 206:32–39. <https://doi.org/10.1016/j.geoderma.2013.04.018>
- Zheng H, Wang Z, Deng X, Zhao J, Luo Y, Novak J, Herbert S, Xing B (2013b) Characteristics and nutrient values of biochars produced from giant reed at different temperatures. *Bioresour Technol* 130:463–471. <https://doi.org/10.1016/j.biortech.2012.12.044>
- Zheng H, Wang Z, Zhao J, Herbert S, Xing B (2013c) Sorption of antibiotic sulfamethoxazole varies with biochars produced at different temperatures. *Environ Pollut* 181:60–67. <https://doi.org/10.1016/j.envpol.2013.05.056>
- Zheng H, Zhang Q, Liu G, Luo X, Li F, Zhang Y, Wang Z (2019a) Characteristics and mechanisms of chlorpyrifos and chlorpyrifos-methyl adsorption onto biochars: Influence of deashing and low molecular weight organic acid (LMWOA) aging and

- co-existence. *Sci Total Environ* 657:953–962. <https://doi.org/10.1016/j.scitotenv.2018.12.018>
- Zheng Y, Wang B, Wester AE, Chen J, He F, Chen H, Gao B (2019b) Reclaiming phosphorus from secondary treated municipal wastewater with engineered biochar. *Chem Eng J* 362:460–468. <https://doi.org/10.1016/j.cej.2019.01.036>
- Zheng R, Cai C, Liang J, Huang Q, Chen Z, Huang Y, Arp HPH, Sun G (2012) The effects of biochars from rice residue on the formation of iron plaque and the accumulation of Cd, Zn, Pb, As in rice (*Oryza sativa* L.) seedlings. *Chemosphere* 89:856–862. <https://doi.org/10.1016/j.chemosphere.2012.05.008>
- Zheng R, Chen Z, Cai C, Tie B, Liu X, Reid BJ, Huang Q, Lei M, Sun G, Baltrėnaitė E (2015) Mitigating heavy metal accumulation into rice (*Oryza sativa* L.) using biochar amendment—a field experiment in Hunan, China. *Environ Sci Pollut Res* 22:11097–11108. <https://doi.org/10.1007/s11356-015-4268-2>
- Zhou Z, Xu Z, Feng Q, Yao D, Yu J, Wang D, Lv S, Liu Y, Zhou N, Zhong M-e (2018) Effect of pyrolysis condition on the adsorption mechanism of lead, cadmium and copper on tobacco stem biochar. *J Clean Prod* 187:996–1005. <https://doi.org/10.1016/j.jclepro.2018.03.268>
- Zhu D, Kwon S, Pignatello JJ (2005) Adsorption of single-ring organic compounds to wood charcoals prepared under different thermochemical conditions. *Environ Sci Technol* 39:3990–3998. <https://doi.org/10.1021/es050129e>
- Zhu D, Pignatello JJ (2005) Characterization of aromatic compound sorptive interactions with black carbon (charcoal) assisted by graphite as a model. *Environ Sci Technol* 39:2033–2041. <https://doi.org/10.1021/es0491376>
- Zhu N, Qiao J, Yan T (2019) Arsenic immobilization through regulated ferrollysis in paddy field amendment with bismuth impregnated biochar. *Sci Total Environ* 648:993–1001. <https://doi.org/10.1016/j.scitotenv.2018.08.200>
- Zhu X, Chen B, Zhu L, Xing B (2017) Effects and mechanisms of biochar-microbe interactions in soil improvement and pollution remediation: a review. *Environ Pollut* 227:98–115. <https://doi.org/10.1016/j.envpol.2017.04.032>
- Zimmerman AR (2010) Abiotic and microbial oxidation of laboratory-produced black carbon (biochar). *Environ Sci Technol* 44:1295–1301. <https://doi.org/10.1021/es903140c>
- Zimmerman AR, Gao B, Ahn MY (2011) Positive and negative carbon mineralization priming effects among a variety of biochar-amended soils. *Soil Biol Biochem* 43(6):1169–1179. <https://doi.org/10.1016/j.soilbio.2011.02.005>

# Nanotechnology as a Key Enabler for Effective Environmental Remediation Technologies

Yi Jiang, Bo Peng, Zhishang Wan, Changwoo Kim, Wenlu Li, and John Fortner

## Abstract

**Overview** This chapter provides an overview and outlook of nanotechnology's enabling roles in developing effective environmental remediation processes. Nanotechnology has the potential to substantially improve environmental remediation technologies. Here, instead of an exhaustive review of all developments related to nano-enabled environmental remediation processes/technologies, we present a brief overview and then specific comparison(s) between the two most common application approaches—individual (free) nanoparticles and those systems with integrated nanomaterials/nanotechnology. Specifically, we review examples of metal oxide nanoparticles (as nano-adsorbents) and graphene oxide enabled membranes to illustrate key technological aspects regarding their application potential in environmental remediation. Lastly, we highlight three key steps to further advancing the material development, namely, establishing structure–property–function relationships, delineating the effects of environmental factors, and addressing potential risk issues.

## Keywords

Engineered nanomaterials • Adsorbent • Membrane • Environmental remediation

## 1 Introduction

Nanotechnology is the science, engineering, and technology conducted at the nanoscale, which is typically from about 1–100 nm. Nanotechnology holds a broad promise to fundamentally advance technological landscapes, from information technology to precision medicine, among others. Over the past two decades, with the launch of signature research initiatives such as the US National Nanotechnology Initiative (NNI), groundbreaking discoveries have been made at the nanoscale, including materials with specifically enhanced properties such as higher strength, lighter weight, increased control of the electromagnetic spectrum, greater chemical reactivity, etc. Discoveries at the nanoscale have also led to the improvement of environmental technologies, including contaminant detection, removal, and treatment processes that have remained difficult with conventional approaches. Broadly speaking, the environmental applications of nanotechnology fall into three categories: environmentally friendly and/or sustainable products (e.g., nanocatalysts for the production of solar fuels), remediation of contaminated environmental media, such as air, water, and soil, and sensors for detecting contaminants (Tratnyek and Johnson 2006). To date, a wide range of nanomaterials have been considered and evaluated, including metal (oxide) nanoparticles (e.g., Ag, Cu, TiO<sub>2</sub>, Fe<sup>0</sup>, Fe<sub>3</sub>O<sub>4</sub>, SiO<sub>2</sub>), carbon nanomaterials (e.g., fullerenes, carbon nanotubes, graphene), metal–organic frameworks (MOF), and multicomponent hybrid materials among others.

At the technology development/application level, the use of nanomaterials can be categorized via two application strategies: individual particles and incorporated systems (Fig. 1). The former describes nanomaterials applied as discrete, monodispersed particles (although aggregation of nanomaterials is usually always observed under typical environmental conditions), such as nanoscale adsorbents and/or catalysts. The later describes nanomaterials which are being incorporated/embedded into a surface or matrix.

Y. Jiang (✉) · B. Peng · Z. Wan  
Department of Civil and Environmental Engineering, The Hong Kong Polytechnic University, Kowloon, Hong Kong, China  
e-mail: [yijiang@polyu.edu.hk](mailto:yijiang@polyu.edu.hk)

C. Kim · W. Li · J. Fortner (✉)  
Department of Chemical and Environmental Engineering, Yale University, New Haven, CT, USA  
e-mail: [john.fortner@yale.edu](mailto:john.fortner@yale.edu)

Examples include membranes that have functional nanomaterials incorporated on or in a surface and/or matrix. For the use of individual particles, applications commonly mirror the spectrum of “non-nano” strategies for contaminant remediation, but with higher reactivity and specificity. Enhanced reactivity is often attributed to larger overall surface area, greater density of reactive surface sites, and/or higher intrinsic reactivity of the reactive surface sites. For the use of nanomaterials as part of the incorporated systems, unique features of nanomaterials are being integrated into the original system, e.g., the surface coating of antimicrobial nanomaterials on membrane surface to achieve effective antifouling. Use of nanomaterials allows for new or significantly improved functions of the original system.

In this chapter, we do not present an exhaustive, detailed review of the methods and developments of applications of nanotechnology for every environmental remediation process. Instead, we provide an overview which is centered on one core question—how the use of nanomaterials enables high-performance remediation processes. Toward this, we focus on individual (discrete) nanoparticle systems and nanomaterial-incorporated systems. The discussion is mainly based on our previous research, including the development and use of metal oxide nanoparticles as nano-adsorbents and graphene oxide as a performance enabler in water treatment membranes. Finally, we provide our thoughts on advancing nanotechnology applications in environmental remediation.

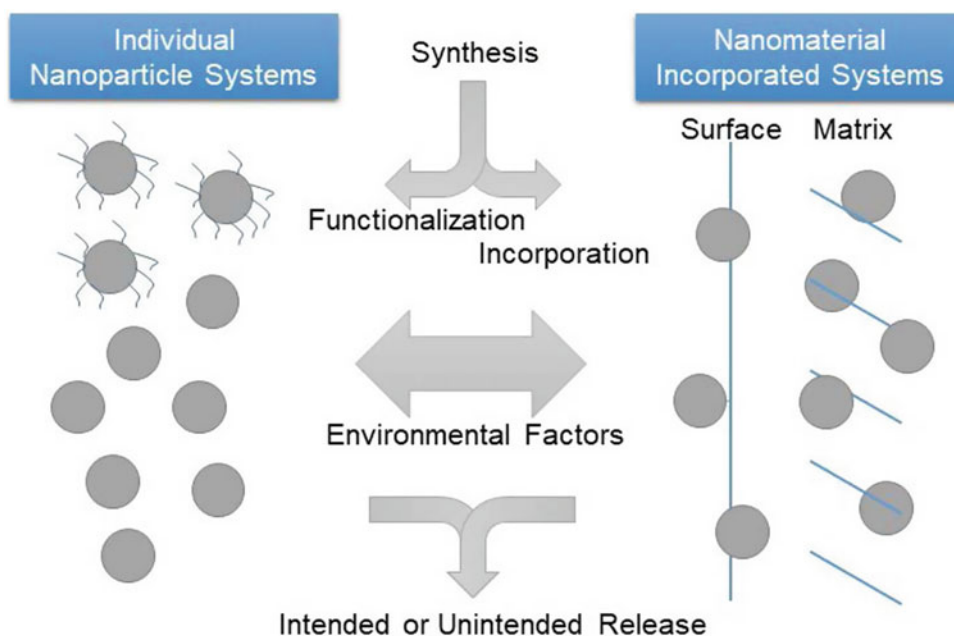
## 2 A Tale of Two Nanotechnology Applications in Environmental Remediation

### 2.1 Individual Nanoparticle Systems—Nano-Adsorbents

High-capacity sorbents, enabled by engineered nanomaterials (ENMs), have wide application potential in environmental remediation, including in situ groundwater remediation, and point-of-use drinking water treatment. Sorptive remediation technologies remove contaminants by sequestration and immobilization, and can be further combined with reactive technologies to achieve enhanced degradation of contaminants. Using ENMs for the adsorptive removal of contaminants is advantageous due to enhanced capacity, selectivity, reactivity, and kinetic control (Qu et al. 2013; Alvarez et al. 2018; Mauter et al. 2018). Nanoscale sorbents have been broadly proposed and evaluated, including metal oxides (e.g., iron (Madden et al. 2006) and manganese oxides (Camtakan et al. 2012)), nanocarbons (e.g., carbon nanotube (CNT) (Yang and Xing 2010) and graphene oxide (GO) (Gao et al. 2012)), and metal–organic frameworks (MOFs) (Wang et al. 2018), among others (Shannon et al. 2008; Alvarez et al. 2018).

Among these, metal oxide nanomaterials are effective and affordable adsorbents for the removal of heavy metals,

**Fig. 1** The two categories of nanomaterial applications in environmental remediation



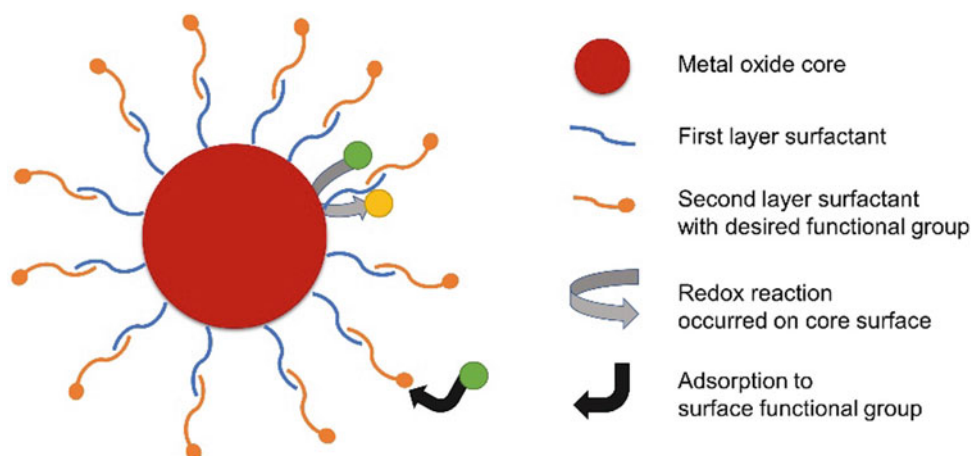
metalloids, and radionuclides, such as arsenic (As), chromium (Cr), uranium (U) (Yeap et al. 2014; Gómez-Pastora et al. 2014; Tang and Lo 2013; Qu et al. 2013; Kim et al. 2018a). Tunable size and surface structure/chemistry of metal oxide nanoparticles enable optimization of active (adsorption) sites to improve kinetics and capacities, while also allowing for selectivity (Auffan et al. 2008; Yang et al. 2008; Roduner 2006; Qu et al. 2013). For example, the functionalization of nanoparticles with specific surface coating (organic and/or inorganic) allows for extended surface area(s), enhanced selectivity, and high colloidal stability (Kim et al. 2018a; Davis et al. 1988; Moore and Shen 1983; Wang et al. 2015; Yavuz et al. 2006; Feng et al. 2012; Yantasee et al. 2007; Warner et al. 2010).

In our recent studies, a series of precisely engineered monodispersed metal oxide nanoparticles (i.e. manganese oxide (MO), iron oxide (IO), and manganese ferrite (MF)) were synthesized and systematically studied for the sorption of various contaminants (i.e. uranium, arsenic, and chromium) in water (Fig. 2) (Lee et al. 2015a, b; Li et al. 2016, 2017b; Kim et al. 2018a, b). Nanoparticles were synthesized via thermal decomposition routes to produce highly uniform metal oxide nanoparticles with a narrow size distribution. By varying reaction temperature, time, ratio of precursor(s) to surfactant, and concentrations of coating polymer(s), various sizes and compositions of nanoparticles can be precisely controlled. For aqueous applications, such nanoparticles can be phase transferred from organic solvent (s) into water by ligand encapsulation or exchange, effectively adding a second organic layer(s) or exchanging with a single organic layer(s), which allows for a broad spectrum of surface chemistries. As we have detailed in a number of reports, sorption capacities are dependent on the nature of nanomaterials (size and composition), surface coatings (structure and functional group), and water chemistry (pH and constituent) (Lee et al. 2015a, b; Li et al. 2016, 2017b; Kim et al. 2018a, b).

**(1) Core Composition:** The composition of nanoscale metal oxides was found to affect the mechanism(s) and thus the capacity of decontamination and separation (Lee et al. 2015a, b; Li et al. 2016, 2017b; Kim et al. 2018b). For example, through a combination of functional group binding and U(VI) reduction, engineered manganese oxide (MO) nanoparticles and iron oxide (IO) nanoparticles displayed similar uranium sorption capacity (both around 50% wt U/wt Mn or Fe, which is 100-fold higher than their commercially available analogues). Interestingly, a higher portion of U(VI) was reduced to U(IV) on the surface of IO nanoparticles (Lee et al. 2015a; Li et al. 2016, 2017b), indicating different binding (sorption) mechanisms for these two materials (i.e. surface redox and ligand associated). In addition, IO nanoparticles can be separated via low-field magnet field due to their superparamagnetic properties (Li et al. 2016). Further, as binary and/or ternary oxide analogues seemed more effective than mono-oxide analogues (Dui et al. 2013; Wang et al. 2011), the uranium sorption capacity of manganese ferrite (MF) nanoparticles was also systematically investigated (Lee et al. 2015b). Maximum sorption capacity of MF nanoparticles increased significantly (1666.7 mg U per g nanoparticle, ca. 160 wt% loading to the nanoparticle) under optimal conditions compared to MO or IO (Lee et al. 2015b). The enhancement was in part due to the enhanced reduction from U(VI) to U(IV) at the interface between the nanocrystal and uranium ion via partial redox reactions. Uranium sorption capacity for these was found to vary among MF nanoparticles with different manganese/iron ratios, with Fe-rich MF nanoparticles demonstrating superior sorption capacity than Mn-rich MF nanoparticles (Lee et al. 2015b; Kim et al. 2018b). This can be attributed to the decreased Fe(II) availability on Mn-rich MF nanoparticles due to the formation of  $Mn_2FeO$ , MnO, and  $Mn_3O_4$  (Lee et al. 2015b; Krycka et al. 2013; López-Ortega et al. 2012).

**(2) Size:** In addition to nanoparticle composition, the size was also found to influence sorption performance (Lee et al.

**Fig. 2** A schematic showing the structure and decontamination processes of the metal oxide nanoparticles as advanced adsorbents





2015a; Li et al. 2017b; Kim et al. 2018a). Nanoparticles with smaller size are normally considered to possess higher sorption capacities due to larger specific surface areas, which is, by in large, what we observed in our studies (Lee et al. 2015a; Li et al. 2017b). However, size might not be the only consideration when the nanoparticle surface is functionalized with ligands. For example, we observed similar arsenic and chromium sorption capacity among various sizes (i.e., 8, 12, 19, and 25 nm) of IO nanoparticles coated with cetyltrimethylammonium bromide (CTAB), which is due to higher CTAB loading (i.e., grafting density) on larger particles as a function of surface curvature dynamics (Kim et al. 2018a). As such, total sorption capacity is not exclusively dependent on particle size, as the surface area advantages of smaller particles may be negated when larger particles possess denser functional groups, underlining the importance of surface coating in determining sorption capacity (Kim et al. 2018a).

**(3) Surface Coatings:** Surface coating(s) properties should be taken into consideration when optimizing nanomaterial sorption performance (Lee et al. 2015a; Li et al. 2017b; Kim et al. 2018a; Li et al. 2016). For example, the uranium sorption capacity of polyethylene glycol (PEG) coated MO nanoparticles is inversely correlated to the molecular weight of the coatings (Lee et al. 2015a). PEG-200 coated nanoparticles exhibited the highest maximum sorption capacity of 227.3 mg/g compared to 142.9 mg/g for PEG-1 k and 119.0 mg/g for PEG-10 k coated MO nanoparticles, indicating that a thinner coating may allow for enhanced interfacial interactions/bindings (Lee et al. 2015a). Further, the surface coating structure and chemistry are also critical for optimized sorption performance. A bilayer coating structure of unsaturated–unsaturated carbon chains (e.g., oleic acid–oleyl phosphate) exhibited better sorption performance than those with an unsaturated–saturated carbon chain linkage (e.g., oleic acid–octadecyl phosphonic acid) (Kim et al. 2018a; Lee et al. 2015a, b), possibly due to enhanced colloidal/bilayer stability rising from additional hydrophobic and van der Waals interactions between unsaturated chains (Prakash et al. 2009). Second (outer) layer chain length also plays a role for these types of surface bilayers. Maximum uranium sorption capacity of IO nanoparticles decreased from 419 mg U/g Fe to 274 mg U/g Fe as a function of chain length, dropping from 18-carbon to 12-carbon chains, respectively (Li et al. 2017b). Lastly, the functional group(s) of surface coatings are important as they relate to charge and/or specific interactions between contaminants and coatings. For instance, positively charged CTAB coated MF nanoparticles displayed a uranium sorption capacity of 178.6 mg U/g nanoparticle while all the other MF nanoparticles with negatively charged coatings demonstrated a uranium sorption capacity at least two times greater than their CTAB counterparts (Lee et al. 2015b). Oleyl phosphate (OP) coated

MF nanoparticle demonstrated the highest sorption capacities (1666.7 mg U/g nanoparticle) (Lee et al. 2015b). Similar electrostatic interaction has also been observed for arsenic/chromium sorption using IO nanoparticles with various coatings (Li et al. 2017b). Additionally, both MO and MF nanoparticles with coatings containing phosphate based functional (head) groups (i.e. sodium monododecyl phosphate, octadecylphosphonic acid, and oleyl phosphate) exhibited better sorption capacity than those coatings without phosphate, e.g., 1666.7 mg U/g nanoparticle of oleyl phosphate coated MF nanoparticle versus 909.1 mg U/g nanoparticle of oleic acid coated MF nanoparticle (Lee et al. 2015a, b). These observations underscore the importance of the well-documented uranium–phosphate interactions underpinning binding processes (Sutton and Burastero 2004; Wang et al. 2006).

**(4) Water Chemistry:** Apart from nanomaterial properties, including surface coatings, water chemistry (pH and constituent, etc.) is a critical variable to consider for engineering sorption processes. Sorption capacity of various contaminants (e.g., uranium/chromium/arsenic) was found to be pH dependent (Lee et al. 2015a, b; Li et al. 2016, 2017b; Kim et al. 2018a, b), as it affects surface coating properties (e.g., charge) and target contaminant speciation/complexation. For example, higher uranium sorption was observed at a slightly acidic pH (pH = 5.8), possibly due to the formation of  $\text{UO}_2^{2+}$ ,  $\text{UO}_2(\text{OH})^+$ , and  $(\text{UO}_2)_3(\text{OH})_5^+$  at pH < 6, inducing more favorable electrostatic interaction between positively charged uranium species and negatively charged particles (Li et al. 2017b; Sutton and Burastero 2004; Zhao et al. 2014). Similarly, for both chromium and arsenic, the sorption was found to be higher at slightly acidic conditions due to the change of sorbate speciation and surface properties (Kim et al. 2018a). In addition to pH, ionic strength and type (e.g.,  $\text{Na}^+$  and  $\text{Ca}^{2+}$ , among others) may, in many cases, negatively influence the sorption process. The presence of ions can destabilize nanoparticles (thus inducing nanoparticle aggregation and reducing the surface area available for contaminants binding) and/or compete for available binding sites (Lee et al. 2015b; Prakash et al. 2009). As an illustration, uranium sorption capacity of MF nanoparticles decreased ca. 40% from 1250 to 714.3 mg U/g nanoparticle in typical groundwater with sodium/calcium composition of around 125 ppm (5.44 mM) sodium and 24 ppm (0.61 mM) calcium (Lee et al. 2015b).

## 2.2 Nanomaterial-Incorporated Systems— Graphene Oxide Enabled Membranes

A membrane is a selective barrier which allows certain feed components (e.g., water) to pass while rejecting others, which are often those with larger sizes (Zeman and Zydney 2017). Membrane separation is capable of removing a

broad-spectrum of contaminants from environmental media, including water and air. Current prevailing membranes are made of various synthetic polymers, and exhibit two main technical limits. Firstly, there exists an effective trade-off between permeability and selectivity—when permeability increases, the membrane selectivity usually decreases (Sadeghi et al. 2018). However, both high permeability and selectivity are desirable. Higher permeability decreases the amount of membrane area required to treat a given amount of liquid, thereby decreasing the capital cost of membrane units, while higher selectivity results in higher purity of produced water. Secondly, membrane surfaces/processes experience fouling, especially in wastewater treatment using membrane bioreactors, where irreversible bio-fouling leads to permeability reduction that cannot be restored (Shannon et al. 2008). These issues have, in many ways, limited the technological advantages (and advancement) of membrane separations by decreasing product water quality, increasing operational costs, and shortening service lifetime.

As discussed, engineered nanomaterials (ENMs) have received substantial attention for next generation membrane applications due to their high reactivity, tunable surface properties, and tailored structures (Mauter and Elimelech 2008; Mauter et al. 2018). By taking advantage of such properties, nanomaterial integration enables the (polymeric) membranes to have tunable internal and surface structure and chemistries, underpinning the potential for higher permeability, selectivity, and enhanced antifouling performance (Alvarez et al. 2018). Considering ultrafiltration nanocomposite membranes as an example, ENMs are incorporated or assembled mainly through two strategies—impregnation (as nanofillers) or surface coating (Fig. 3). To date, a wide range of nanomaterials have been studied for these two strategies,

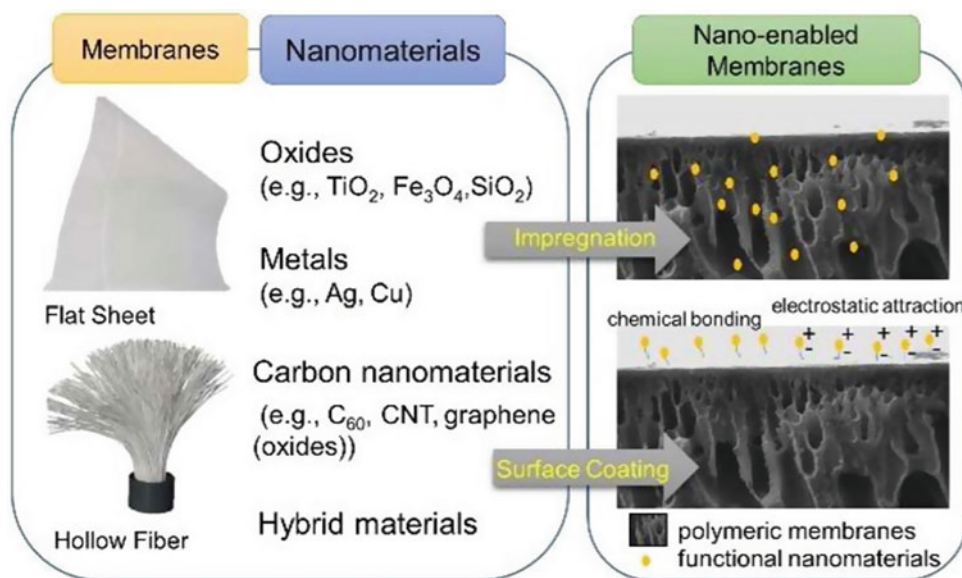
including metal (oxide) NPs (e.g., Ag (Zodrow et al. 2009), Cu (Ben-Sasson et al. 2016),  $\text{TiO}_2$  (Razmjou et al. 2011)), carbon nanomaterials (e.g.,  $\text{C}_{60}$  (Taurozzi et al. 2011), CNT (Sianipar et al. 2017), graphene (Jiang et al. 2016a)), metal-organic frameworks (MOF) (Sun et al. 2017), and hybrid materials (Yu et al. 2013).

Among these materials, graphene oxide (GO) can be easily fabricated with tunable size, surface chemistry, and shape at the commercial scale (Jiang et al. 2016a). GO partially remains as a one-atom-thick planar sheet with a  $\text{sp}^2$ -bonded carbon structure while being derivatized with oxygen functional groups both on the basal plane (e.g., hydroxyl and epoxy groups) and at the sheet edges (e.g., carboxyl and carbonyl, etc.). Due to its unique properties and relative ease of production, it has been extensively researched for membrane applications, from ultrafiltration (UF) to reverse osmosis (RO). Below, we discuss recent progress in the applications of GO with a focus on addressing the two main drawbacks of membranes—specifically the trade-off between permeability and selectivity, and fouling.

### (1) Achieving High Permeability and Selectivity

Mixed-matrix membranes (MMMs) commonly consist of a dispersed nanomaterial phase and a continuous polymer matrix, hoping to combine the high intrinsic permeability and separation properties of advanced nanomaterials with the robust processing and mechanical properties of polymers. Molecular sieving fillers with nanoscale size or nanosheet shapes (e.g., MOF nanoparticles or 2D nanosheets) were found to possibly improve both permeability and selectivity (Park et al. 2017). GO has been widely applied as nanofillers in synthesizing MMMs, including both UF and

**Fig. 3** Schematic illustration of current approaches to synthesizing nano-enabled ultrafiltration membranes for water and wastewater treatment



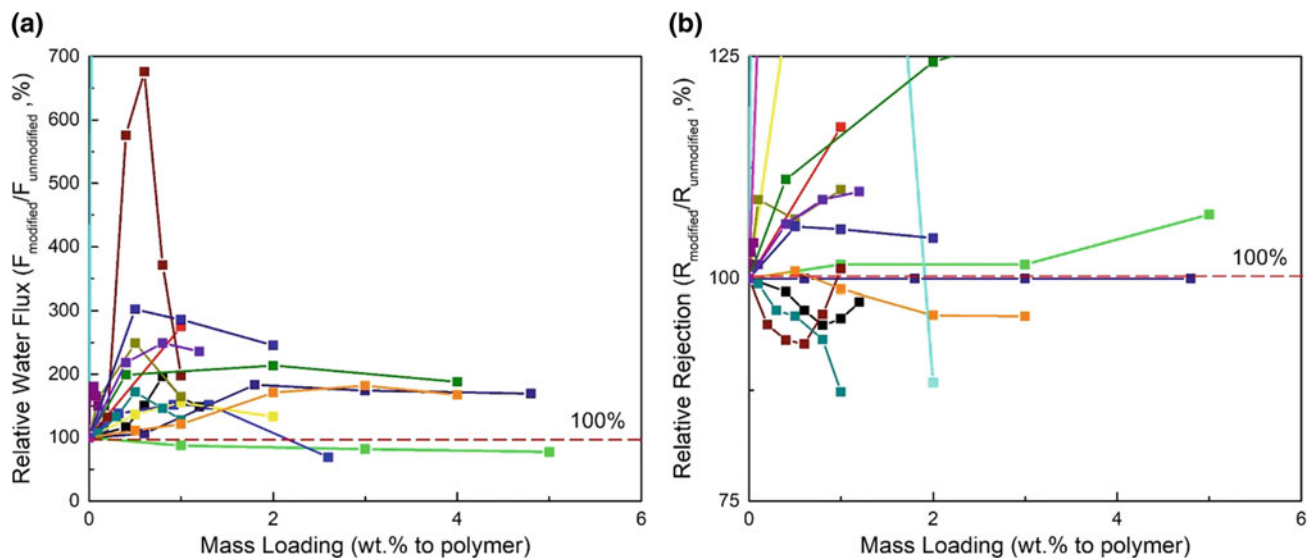


**Fig. 4** The change of water permeability (a) and rejection performance (b) of graphene-based MMMs compared to pristine membranes. Data was extracted from existing literature and processed (the permeability and rejection rate of pristine membranes were taken as

100%), with each line representing one study of the material variable. The Y-axis in (b) was adjusted to focus on the major changes/trends of most cases, and thus 4 cases with normalized rejection >125% (and up to 275%) were not shown with complete data sets in the figure

RO membranes. GO-enabled membranes can be easily synthesized by blending different amounts of GO in the membrane casting solutions (usually 0.1–6 wt% with respect to polymer) (Ganesh et al. 2013; Zhang et al. 2013; Crock et al. 2013; Wang et al. 2014).

We have summarized the existing literature regarding graphene-enabled MMMs, with most of the nanofillers as GO or its derivatives. As seen in Fig. 4, upon the incorporation of GO-based materials, the maximum water permeability can increase ca. 0.1–20 times compared with pristine membranes. For rejection (also selectivity, defined as the reciprocal of the sieving coefficient (Mehta and Zydney 2005)), it can increase at the same time (Zhang et al. 2013; Xu et al. 2014; Zinadini et al. 2014; Li et al. 2017a); or it can also decrease, showing inverse relationships between permeability and selectivity (Ma et al. 2017; Yu et al. 2013; Li et al. 2017a). Taken together, the data sets clearly shows that the mass loading and properties of nanomaterials have a large impact on membrane structure and resultant performance (Jiang et al. 2019b), and also the MMMs incorporated with GO can potentially have both high permeability and selectivity.

The impact and its extent of adding nanomaterials can be described as a function of both the properties of GO (or derivatives or hybrids) and its impacts on the membrane matrix upon incorporation. A number of studies have explained qualitatively the role of nanomaterials affecting membrane structure (e.g., surface chemistry, hydrophilicity,

charge, etc.) and performance (e.g., permeability, selectivity, mechanical strength, etc.). GO has a high density of hydrophilic functional groups, which as a result improves the hydrophilicity and porosity of the membrane, thus resulting in enhanced permeability (Ma et al. 2017; Zinadini et al. 2014; Crock et al. 2013; Jiang et al. 2019b). Furthermore, such change(s) can be due to dynamic phase inversion processes which are sensitive to the presence of the nanomaterials themselves—in other words, the addition of nanomaterials will change both the kinetics and thermodynamics of membrane formation. For example, our experimental results showed that changes in the shape of graphene oxide alone can result in varied performance. And such differences can be attributed to the (more) effective dispersion/stability of crumpled GO nanoparticles in solvent (NMP) as a result of shape effects, which lowers the tipping mass percentage after which the effect of viscosity increase outweighs that of hydrophilicity increase (Jiang et al. 2019b). With the increasing molecular understanding of membranes in recent years, key design factors to disrupt the permeability–selectivity trade-off have been recognized to potentially include thin(er) selective layers, highly tuned interactions between membrane and permeants/solutes of interest (e.g., electrostatic repulsion/attraction), and properly sized pores and its distribution (Park et al. 2017). However, the fundamental insight between (addition of) nanomaterials and those factors, and the pathways which would allow for predictive frameworks remain largely outstanding.

## (2) Fouling Control

For fouling control, surface hydrophilicity/charge and roughness are considered to be critical factors as they reduce favorable interactions and attachment of aqueous substances with a membrane surface. For example, the increase of hydrophilicity limits hydrophobic–hydrophobic interaction between solutes/bacteria and membrane surface. GO contains densely arranged hydrophilic functional groups, which increase membrane surface hydrophilicity (Ma et al. 2017; Zinadini et al. 2014; Crock et al. 2013). Therefore, the hydrophobic solutes are less prone to interact with the membrane surface. Moreover, enhanced surface hydrophilicity can mitigate protein adsorption because of the repulsion force(s) arising from hydrated layers on the surface which also preserves protein (tertiary) structure and thus reversible attachment (Xu et al. 2014). The incorporation of GO also reduces organic fouling by electrostatic repulsion for other foulants (e.g., humic acids, which are negatively charged at pH values from 6 to 9) (Igbigin et al. 2016; Zhang et al. 2018; Jiang et al. 2016a). Furthermore, as surface roughness increases, faster fouling typically happens, while smoother surfaces provide less adhesion sites (Elimielech et al. 1997). GO nanosheets have been shown to form much smoother surfaces (RMS roughness decreased from 37.2 nm to 8.8 nm) when coated to PES membranes, contributing to a higher water flux recovery of 70%, compared to 28% of the unmodified ones (Igbigin et al. 2016).

Interestingly, bio-fouling control using GO has been observed. GO can physically disrupt and chemically inactivate bacteria (i.e., via ROS), resulting in loss of cell integrity and proliferation (Liu et al. 2011; Tu et al. 2013). GO-enabled membranes have shown enhanced antimicrobial activity (against, e.g., *E. Coli.*, *M. smegmatis*, and *S. aureus*), with <35% viable CFU after contact/inactivation experiments, compared with that of control membranes (PSF, PVDF, PTFE, and nylon) (Zou et al. 2017; Li et al. 2013; Lu et al. 2017; Kaneda et al. 2019; Perreault et al. 2013). The properties of GO nanomaterials (e.g., alignment and shape) have a large impact on fouling control efficiency. The vertically aligned GO membranes showed stronger antimicrobial activity, reducing viable *E. coli* cell number by 72% for cells in contact with the membrane surface compared to nonaligned GO membranes (Lu et al. 2017, 2018). The orientation-dependent cell inactivation could be related to the density of exposed GO edges with preferential orientation for bacteria inactivation (Lu et al. 2017, 2018). Our previous studies also showed that through combining GO and nano-Ag, both contact and dissolution-based antimicrobial mechanisms can be leveraged to achieve even more effective fouling control (Jiang et al. 2015, 2016b).

## 3 Challenges and Opportunities

The highlighted examples clearly show that the application of nanotechnology can considerably improve the performance of traditional remediation processes such as adsorption/removal and membrane separations. Some of the highest adsorption capacities reported to date were observed with the advanced metal oxide nano-adsorbents. Regardless of the way(s) engineered nanomaterials are being used—individual nanoparticles or incorporated systems, advantages at the nanoscale including high surface area and reactivity can and will be leveraged to enhance or impart additional functions, which ultimately result in the removal of contaminants with enhanced capacity, selectivity, and kinetics.

For these technologies to reach their potential, there exists a significant degree of complexity based on the numerous variations of nanomaterial properties (e.g., size of graphene oxide, or molecular weights and functional groups of surface coating), and their combinations. A small variation in one nanomaterial property can potentially result in a substantial change of function/performance (e.g., the size of graphene oxide on its toxicity (Perreault et al. 2015)). In general, for both approaches, the underlying pathway(s)—how the change(s) is transmitted from nanomaterial to eventual performance—remain poorly characterized. Notably, understanding of the interactions between the nanomaterials and the surface/matrix in incorporated systems is still a challenging prospect. This further adds to the systematic complexity and will only increase with scale.

Additionally, environmental factors, including water chemistry, foulants, etc., will have a significant impact on performance, as they affect not only the structure and properties of nanomaterials/incorporated systems but also the properties of the contaminants (e.g., chemical speciation). Overall, the studies on the effects of environmental factors have been focused on those conducted in laboratories, which largely oversimplify real-world conditions.

Lastly, for both approaches, the release and potential risks of nanomaterials should be carefully considered. However, this issue is more serious for individual particles when they are applied, as they will have higher mobility compared to those incorporated into a system.

### 3.1 Establishing Structure–Property–Function Relationships for Better Material Design

Despite the large volume of literature on environmental applications of nanotechnology, as described in the previous section, generalized knowledge, i.e., *Structure–Property–Function* relationships that relate the nanoscale structural

variables, macroscale physical and chemical properties, and eventual functions, remains nascent. For example, for nano-enabled membrane separation, a systematic framework with more translatable data is needed to establish an understanding of material processing, material structure and properties, membrane applications, and their fundamental relationships (steps 1–3 in Fig. 5) (Jiang et al. 2016a). The establishment of such relationships will provide answers to a number of key questions—namely, which nanomaterial properties are desired so that the resultant MMMs can have both high permeability and selectivity? How can the nano-enabled antifouling functions be sustained? What scale-up strategies of production can be designed and optimized? And so on.

Also, high-order correlations regarding surface coating characteristics (e.g., molecular weight, charge, etc.) and fundamental aqueous behaviors (aggregation, sedimentation, deposition) and performance (e.g., adsorption capacity and mechanism(s)) will generate knowledge that informs better design of high-performance, highly selective, “smarter” nano-adsorbents. For instance, new surface coatings could give the exact mobility and affinity of nanomaterials used for groundwater remediation applications—allowing sufficient but not over delivery of the treatment to the contaminated volume of media. Such understanding also enables more sophisticated, multifunctional nanocomposites, such as catalyzing several different pollutant reactions on the same particle, interacting with both hydrophobic and hydrophilic pollutants, or pre-concentrating and degrading high-priority pollutants using photocatalytic reactions (the so-called “bait-hook-and destroy” strategy) (Karn et al. 2009; Alvarez et al. 2018).

The nature of such structure–property–function relationships remains challenging due to the fractal complexity of the studied systems (i.e., commonly with variables differing by a few orders of magnitude) and lack of abundant, translatable, and benchmarkable data. Toward these goals, the

disclosure and accessibility of research data will become necessary, in some form, if such relationships are to be established.

### 3.2 Delineating the Effects of Environmental Factors for Real Applications

There have yet to be many large-scale field applications or commercial products for nano-enabled environmental remediation. Among the examples to date, nanoscale zero-valent iron (nZVI) nanoparticles have been tested in a number of field applications for groundwater remediation, and for nano-enabled membranes, the incorporation of zeolite nanoparticles into polyamide layer has yielded a commercial thin-film nanocomposite membrane (LG NanoH2O Inc). In addition, novel composites that incorporate iron oxide nanoparticles in millimeter-sized polystyrene spheres are being used in meter-scale reactors to decontaminate tanning, electroplating, and mining wastewaters (Zhang et al. 2017).

For real-world applications, environmental factors are critical to consider as mentioned, in addition to the intrinsic material properties and functions. For example, the use of metal oxide nanoparticles for site remediation, usually has site-specific requirements that must be met in order for it to be effective. Compared to the common factors involved in bench-scale studies (e.g., pH, ionic strength, NOM), field applications are complicated by additional, macroscale geologic, hydrogeologic, and subsurface conditions, including soil properties, porosity, hydraulic conductivity, flow velocity, etc. (Karn et al. 2009). How bench-scale studies inform the application of nanoparticles in real environments remains unclear at this time. For instance, although being capable of producing fundamental insights, current methodologies to studying nanoparticle stability and mobility (e.g., stability studies using static and dynamic light

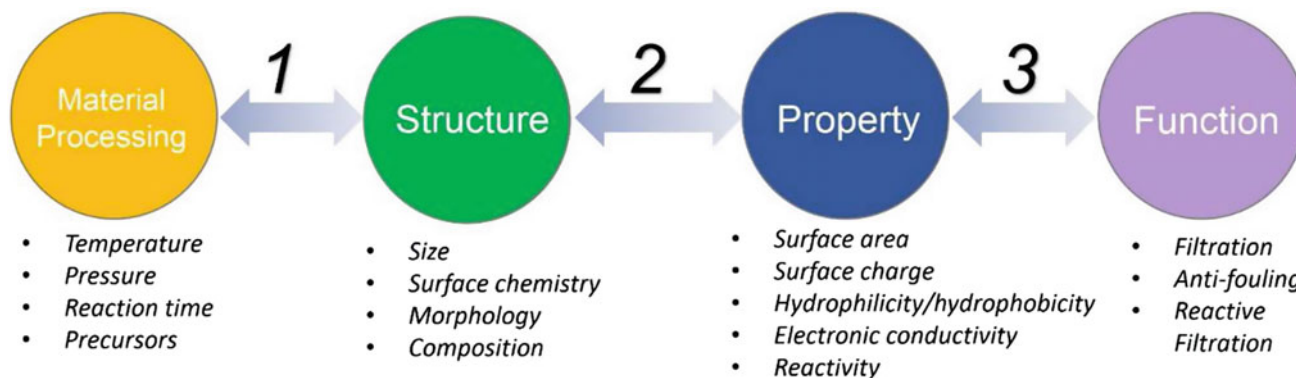


**Fig. 5** A need for a systematic thinking from material processing to membrane (and also similarly, to other nanotechnology) applications. Reproduced from Ref. Jiang et al. (2016a) with permission from The Royal Society of Chemistry

scattering, deposition studies using quartz crystal microbalance or column experiments) may fail to provide sufficient information to interpret their behaviors in real complex conditions. Also, the transformation of nanomaterials under field conditions is a concern and is currently being evaluated. Changes induced by environmental factors such as light, oxidants, and microorganisms will likely result in chemical or biological modifications/degradation of the functionalized surface or coating of the surface (Karn et al. 2009). Our current way of technology development has been mainly targeted at one specific contaminant, which neglects the fact that many contaminants coexist and typically need to be removed at the same time. Also, almost all types of membrane fouling occur simultaneously, so it will be beneficial to look into the effects of nanotechnology on the mitigation of more than one type of fouling for the same system. It is therefore suggested that tests under real environmental conditions (e.g., real wastewater, contaminated groundwater) should be conducted in addition to classic bench-scale analyses (i.e., synthetic conditions) to assess the potential for real-world application(s).

### 3.3 Addressing Potential Risk Issues to Achieve Sustainability

Understanding potential ecological and health risks associated with the use of engineered nanomaterials, including in environmental applications, has been a broad, active area of research. Regardless of the application/process type, there is potential for material release into the environment and subsequent ecosystems. Despite a considerable body of related research, quantifying real risk remains a largely outstanding concern (Westerhoff et al. 2018).

The release and exposure in real (or future) scenarios are still difficult to estimate for most nanomaterials, which is further complicated by their transformation and interactions (e.g., with other pollutants) in the environment over time. To understand and quantify potential risks, mobility, bioavailability, toxicity, and persistence of manufactured nanoparticles will need to be continuously studied. Engineered nanomaterials are usually made to have enhanced, sometimes unique physical, chemical, and toxicological properties, which could pose inherent risk(s). Moreover, other than the particles themselves, their surface coating and surface reactions (e.g., ROS produced by UV irradiation) could also exert effects. Furthermore, whereas the nanoparticles themselves may not possess toxic properties, the pollutants they could carry with them may. For instance, iron-based nanoparticles may bind with metal or metalloids, thus effectively acting as a pollutant vector.

Fundamentally linking knowledge obtained in laboratory settings with the real systems will become an important

research direction. The release and exposure for potentially high-concentration scenarios such as manufacturing should become a priority area of study. It also provides a venue to test new detection methods, apply precautionary/mitigation measures, consider epidemiological evaluations, and so forth (Jiang et al. 2019a).

To conclude, a number of recent studies suggest that the risks related to nanotechnology are likely to be low (at least lower than originally thought, at the current stage of material production and usage) as they relate to the environmental application. For the vast majority of exposure scenarios proposed, engineered nanomaterials are predicted to exist at low concentrations, often orders of magnitude lower than natural nanoparticles in natural waters. Further, it has been reported that current engineered barriers/treatment processes, such as water treatment facilities, can effectively intercept nanomaterial transmission into drinking water/food sources (Westerhoff et al. 2018). In a similar vein, continued research on real-world material exposure is needed to provide accurate guidance on use-risk trade-offs for both specific and broad applications, and ultimate technological sustainability.

### References

- Alvarez PJJ, Chan CK, Elimelech M, Halas NJ, Villagrán D (2018) Emerging opportunities for nanotechnology to enhance water security. *Nat Nanotechnol* 13(8):634–641.
- Auffan M, Rose J, Proux O, Borschneck D, Masion A, Chaurand P, Hazemann J-L, Chaneac C, Jolivet J-P, Wiesner MR (2008) Enhanced adsorption of arsenic onto maghemite nanoparticles: as (III) as a probe of the surface structure and heterogeneity. *Langmuir* 24(7):3215–3222
- Ben-Sasson M, Lu X, Nejati S, Jaramillo H, Elimelech M (2016) In situ surface functionalization of reverse osmosis membranes with biocidal copper nanoparticles. *Desalination* 388:1–8.
- Camtakan Z, Erenturk S, Yusan S (2012) Magnesium oxide nanoparticles: preparation, characterization, and uranium sorption properties. *Environ Prog Sustain Energy* 31(4):536–543
- Crock CA, Rogensues AR, Shan W, Tarabara VV (2013) Polymer nanocomposites with graphene-based hierarchical fillers as materials for multifunctional water treatment membranes. *Water Res* 47(12):3984–3996.
- Davis ME, Saldarriaga C, Montes C, Garces J, Crowder C (1988) A molecular sieve with eighteen-membered rings. *Nature* 331(6158):698–699.
- Dui J, Zhu G, Zhou S (2013) Facile and Economical Synthesis of Large Hollow Ferrites and Their Applications in Adsorption for As(V) and Cr(VI). *ACS Appl Mater Interfaces* 5(20):10081–10089.
- Elimelech M, Zhu X, Childress AE, Hong S (1997) Role of membrane surface morphology in colloidal fouling of cellulose acetate and composite aromatic polyamide reverse osmosis membranes. *J Membr Sci* 127(1):101–109
- Feng L, Cao M, Ma X, Zhu Y, Hu C (2012) Superparamagnetic high-surface-area Fe<sub>3</sub>O<sub>4</sub> nanoparticles as adsorbents for arsenic removal. *J Hazard Mater* 217:439–446
- Ganesh BM, Isloor AM, Ismail AF (2013) Enhanced hydrophilicity and salt rejection study of graphene oxide-polysulfone mixed matrix membrane. *Desalination* 313:199–207.

- Gao Y, Li Y, Zhang L, Huang H, Hu J, Shah SM, Su X (2012) Adsorption and removal of tetracycline antibiotics from aqueous solution by graphene oxide. *J Colloid Interface Sci* 368(1):540–546
- Gómez-Pastora J, Bringas E, Ortiz I (2014) Recent progress and future challenges on the use of high performance magnetic nano-adsorbents in environmental applications. *Chem Eng J* 256:187–204
- Igbinigun E, Fennell Y, Malaisamy R, Jones KL, Morris V (2016) Graphene oxide functionalized polyethersulfone membrane to reduce organic fouling. *J Membr Sci* 514:518–526.
- Jiang Y, Biswas P, Fortner JD (2016a) A review of recent developments in graphene-enabled membranes for water treatment. *Environ Sci Water Res Technol* 2(6):915–922.
- Jiang Y, Liu D, Cho M, Lee SS, Zhang F, Biswas P, Fortner JD (2016b) In situ photocatalytic synthesis of Ag nanoparticles (nAg) by crumpled graphene oxide composite membranes for filtration and disinfection applications. *Environ Sci Technol* 50(5):2514–2521
- Jiang Y, Quan X, Jiang G, Li X (2019a) Current prospective on environmental nanotechnology research in China. *Environ Sci Technol* 53(8):4001–4002.
- Jiang Y, Zeng Q, Biswas P, Fortner JD (2019b) Graphene oxides as nanofillers in polysulfone ultrafiltration membranes: shape matters. *J Membr Sci* 581:453–461.
- Jiang Y, Wang W-N, Liu D, Nie Y, Li W, Wu J, Zhang F, Biswas P, Fortner JD (2015) Engineered crumpled graphene oxide nanocomposite membrane assemblies for advanced water treatment processes. *Environ Sci Technol* 49(11):6846–6854
- Kaneda M, Lu X, Cheng W, Zhou X, Bernstein R, Zhang W, Kimura K, Elimelech M (2019) Photografting graphene oxide to inert membrane materials to impart antibacterial activity. *Environ Sci Technol Lett* 6(3):141–147.
- Karn B, Kuiken T, Otto M (2009) Nanotechnology and *in Situ* remediation: a review of the benefits and potential risks. *Environ Health Perspect* 117(12):1813–1831.
- Kim C, Lee SS, Lafferty BJ, Giammar DE, Fortner JD (2018a) Engineered superparamagnetic nanomaterials for arsenic(v) and chromium(vi) sorption and separation: quantifying the role of organic surface coatings. *Environ Sci Nano* 5(2):556–563.
- Kim C, Lee SS, Reinhart BJ, Cho M, Lafferty BJ, Li W, Fortner JD (2018b) Surface-optimized core-shell nanocomposites (Fe<sub>3</sub>O<sub>4</sub>@MnxFe<sub>y</sub>O<sub>4</sub>) for ultra-high uranium sorption and low-field separation in water. *Environ Sci Nano* 5(10):2252–2256.
- Krycka KL, Borchers JA, Salazar-Alvarez G, López-Ortega A, Estrader M, Estrade S, Winkler E, Zysler RD, Sort J, Peiró F (2013) Resolving material-specific structures within Fe<sub>3</sub>O<sub>4</sub>/γ-Mn<sub>2</sub>O<sub>3</sub> core/shell nanoparticles using anomalous small-angle X-ray scattering. *ACS Nano* 7(2):921–931
- Lee SS, Li W, Kim C, Cho M, Catalano JG, Lafferty BJ, Decuzzi P, Fortner JD (2015a) Engineered manganese oxide nanocrystals for enhanced uranyl sorption and separation. *Environ Sci Nano* 2(5):500–508.
- Lee SS, Li W, Kim C, Cho M, Lafferty BJ, Fortner JD (2015b) Surface functionalized manganese ferrite nanocrystals for enhanced uranium sorption and separation in water. *J Mater Chem A* 3(43):21930–21939.
- Li M, Shi J, Chen C, Li N, Xu Z, Li J, Lv H, Qian X, Jiao X (2017a) Optimized permeation and antifouling of PVDF hybrid ultrafiltration membranes: synergistic effect of dispersion and migration for fluorinated graphene oxide. *J Nanoparticle Res* 19(3).
- Li W, Troyer LD, Lee SS, Wu J, Kim C, Lafferty BJ, Catalano JG, Fortner JD (2017b) Engineering nanoscale iron oxides for uranyl sorption and separation: optimization of particle core size and bilayer surface coatings. *ACS Appl Mater Interfaces* 9(15):13163–13172.
- Li W, Mayo JT, Benoit DN, Troyer LD, Lewicka ZA, Lafferty BJ, Catalano JG, Lee SS, Colvin VL, Fortner JD (2016) Engineered superparamagnetic iron oxide nanoparticles for ultra-enhanced uranium separation and sensing. *J Mater Chem A* 4(39):15022–15029.
- Li Y, Yuan H, von dem Bussche A, Creighton M, Hurt RH, Kane AB, Gao H (2013) Graphene microsheets enter cells through spontaneous membrane penetration at edge asperities and corner sites. *Proc Natl Acad Sci USA* 110(30):12295–12300.
- Liu S, Zeng TH, Hofmann M, Burcombe E, Wei J, Jiang R, Kong J, Chen Y (2011) Antibacterial activity of graphite, graphite oxide, graphene oxide, and reduced graphene oxide: membrane and oxidative stress. *ACS Nano* 5(9):6971–6980.
- López-Ortega A, Estrader M, Salazar-Alvarez G, Estradé S, Golosovsky IV, Dumas RK, Keavney DJ, Vasilakaki M, Trohidou KN, Sort J (2012) Strongly exchange coupled inverse ferrimagnetic soft/hard, Mn<sub>x</sub>Fe<sub>3-x</sub>O<sub>4</sub>/Fe<sub>x</sub>Mn<sub>3-x</sub>O<sub>4</sub> core/shell heterostructured nanoparticles. *Nanoscale* 4(16):5138–5147
- Lu X, Feng X, Werber JR, Chu C, Zucker I, Kim JH, Osuji CO, Elimelech M (2017) Enhanced antibacterial activity through the controlled alignment of graphene oxide nanosheets. *Proc Natl Acad Sci USA* 114(46):E9793–E9801.
- Lu X, Feng X, Zhang X, Chukwu MN, Osuji CO, Elimelech M (2018) Fabrication of a desalination membrane with enhanced microbial resistance through vertical alignment of graphene oxide. *Environ Sci Technol Lett* 5(10):614–620.
- Ma J, Guo X, Ying Y, Liu D, Zhong C (2017) Composite ultrafiltration membrane tailored by MOF@GO with highly improved water purification performance. *Chem Eng J* 313:890–898.
- Madden AS, Hochella MF Jr, Luxton TP (2006) Insights for size-dependent reactivity of hematite nanomineral surfaces through Cu<sup>2+</sup> sorption. *Geochim Cosmochim Acta* 70(16):4095–4104
- Mauter MS, Elimelech M (2008) Environmental applications of carbon-based nanomaterials. *Environ Sci Technol* 42(16):5843–5859
- Mauter MS, Zucker I, Fo Perreault, Werber JR, Kim J-H, Elimelech M (2018) The role of nanotechnology in tackling global water challenges. *Nat Sustain* 1(4):166–175.
- Mehta A, Zydny AL (2005) Permeability and selectivity analysis for ultrafiltration membranes. *J Membr Sci* 249(1–2):245–249
- Moore PB, Shen J (1983) An X-ray structural study of cacoxenite, a mineral phosphate. *Nature* 306(5941):356–358.
- Park HB, Kamcev J, Robeson LM, Elimelech M, Freeman BD (2017) Maximizing the right stuff: the trade-off between membrane permeability and selectivity. *Science* 356(6343).
- Perreault F, De Faria AF, Nejati S, Elimelech M (2015) Antimicrobial properties of graphene oxide nanosheets: why size matters. *ACS Nano* 9(7):7226–7236
- Perreault F, Tousley ME, Elimelech M (2013) Thin-film composite polyamide membranes functionalized with biocidal graphene oxide nanosheets. *Environ Sci Technol Lett* 1(1):71–76.
- Prakash A, Zhu H, Jones CJ, Benoit DN, Ellsworth AZ, Bryant EL, Colvin VL (2009) Bilayers as phase transfer agents for nanocrystals prepared in nonpolar solvents. *ACS Nano* 3(8):2139–2146.
- Qu X, Brame J, Li Q, Alvarez PJJ (2013) Nanotechnology for a safe and sustainable water supply: enabling integrated water treatment and reuse. *Acc Chem Res* 46(3):834–843.
- Razmjou A, Mansouri J, Chen V (2011) The effects of mechanical and chemical modification of TiO<sub>2</sub> nanoparticles on the surface chemistry, structure and fouling performance of PES ultrafiltration membranes. *J Membr Sci* 378(1):73–84
- Roduner E (2006) Size matters: why nanomaterials are different. *Chem Soc Rev* 35(7):583–592
- Sadeghi I, Kaner P, Asatekin A (2018) Controlling and expanding the selectivity of filtration membranes. *Chem Mater* 30(21):7328–7354

- Shannon MA, Bohn PW, Elimelech M, Georgiadis JG, Marinas BJ, Mayes AM (2008) Science and technology for water purification in the coming decades. *Nature* 452(7185):301–310.
- Sianipar M, Kim SH, Khoiruddin K, Iskandar F, Wenten IG (2017) Functionalized carbon nanotube (CNT) membrane: progress and challenges. *RSC Adv* 7(81):51175–51198.
- Sun H, Tang B, Wu P (2017) Development of hybrid ultrafiltration membranes with improved water separation properties using modified superhydrophilic metal-organic framework nanoparticles. *ACS Appl Mater Interfaces* 9(25):21473–21484.
- Sutton M, Burastero SR (2004) Uranium(VI) solubility and speciation in simulated elemental human biological fluids. *Chem Res Toxicol* 17(11):1468–1480.
- Tang SC, Lo IM (2013) Magnetic nanoparticles: essential factors for sustainable environmental applications. *Water Res* 47(8):2613–2632
- Taurozzi JS, Crock CA, Tarabara VV (2011) C<sub>60</sub>-polysulfone nanocomposite membranes: entropic and enthalpic determinants of C<sub>60</sub> aggregation and its effects on membrane properties. *Desalination* 269(1–3):111–119.
- Tratnyek PG, Johnson RL (2006) Nanotechnologies for environmental cleanup. *Nano Today* 1(2):44–48.
- Tu Y, Lv M, Xiu P, Huynh T, Zhang M, Castelli M, Liu Z, Huang Q, Fan C, Fang H, Zhou R (2013) Destructive extraction of phospholipids from *Escherichia coli* membranes by graphene nanosheets. *Nat Nanotechnol* 8(8):594–601.
- Wang C-M, Lee L-W, Chang T-Y, Chen Y-C, Lin H-M, Lu K-L, Lii K-H (2015) Organic-inorganic hybrid zinc phosphate with 28-ring channels. *Chem A Eur J* 21(5):1878–1881.
- Wang D, Gilliland SE, Yi X, Logan K, Heitger DR, Lucas HR, Wang W-N (2018) Iron mesh-based metal organic framework filter for efficient arsenic removal. *Environ Sci Technol* 52(7):4275–4284.
- Wang L, Yang Z, Gao J, Xu K, Gu H, Zhang B, Zhang X, Xu B (2006) A biocompatible method of decorporation: bisphosphonate-modified magnetite nanoparticles to remove uranyl ions from blood. *J Am Chem Soc* 128(41):13358–13359
- Wang Y, Cheng R, Wen Z, Zhao L (2011) Synthesis and characterization of single-crystalline MnFe<sub>2</sub>O<sub>4</sub> ferrite nanocrystals and their possible application in water treatment. *Eur J Inorg Chem* 19:2942–2947.
- Wang Z, Teychene B, Chalew TE, Ajmani GS, Zhou T, Huang H, Wu X (2014) Aluminum-humic colloid formation during pre-coagulation for membrane water treatment: mechanisms and impacts. *Water Res* 61:171–180.
- Warner CL, Addleman RS, Cinson AD, Droubay TC, Engelhard MH, Nash MA, Yantasee W, Warner MG (2010) High-Performance, superparamagnetic, nanoparticle-based heavy metal sorbents for removal of contaminants from natural waters. *ChemSusChem* 3(6):749–757
- Westerhoff P, Atkinson A, Fortner J, Wong MS, Zimmerman J, Gardea-Torresdey J, Ranville J, Herckes P (2018) Low risk posed by engineered and incidental nanoparticles in drinking water. *Nat Nanotechnol* 13(8):661–669.
- Xu Z, Zhang J, Shan M, Li Y, Li B, Niu J, Zhou B, Qian X (2014) Organosilane-functionalized graphene oxide for enhanced antifouling and mechanical properties of polyvinylidene fluoride ultrafiltration membranes. *J Membr Sci* 458:1–13.
- Yang HG, Sun CH, Qiao SZ, Zou J, Liu G, Smith SC, Cheng HM, Lu GQ (2008) Anatase TiO<sub>2</sub> single crystals with a large percentage of reactive facets. *Nature* 453(7195):638
- Yang K, Xing B (2010) Adsorption of organic compounds by carbon nanomaterials in aqueous phase: polanyi theory and its application. *Chem Rev* 110(10):5989–6008.
- Yantasee W, Warner CL, Sangvanich T, Addleman RS, Carter TG, Wiacek RJ, Fryxell GE, Timchalk C, Warner MG (2007) Removal of heavy metals from aqueous systems with thiol functionalized superparamagnetic nanoparticles. *Environ Sci Technol* 41(14):5114–5119
- Yavuz CT, Mayo J, William WY, Prakash A, Falkner JC, Yean S, Cong L, Shipley HJ, Kan A, Tomson M (2006) Low-field magnetic separation of monodisperse Fe<sub>3</sub>O<sub>4</sub> nanocrystals. *Science* 314(5801):964–967
- Yeap SP, Leong SS, Ahmad AL, Ooi BS, Lim J (2014) On size fractionation of iron oxide nanoclusters by low magnetic field gradient. *J Phys Chem C* 118(41):24042–24054
- Yu L, Zhang Y, Zhang B, Liu J, Zhang H, Song C (2013) Preparation and characterization of HPEI-GO/PES ultrafiltration membrane with antifouling and antibacterial properties. *J Membr Sci* 447:452–462.
- Zeman LJ, Zydney AL (2017) Microfiltration and ultrafiltration: principles and applications. CRC Press
- Zhang J, Xu Z, Mai W, Min C, Zhou B, Shan M, Li Y, Yang C, Wang Z, Qian X (2013) Improved hydrophilicity, permeability, antifouling and mechanical performance of PVDF composite ultrafiltration membranes tailored by oxidized low-dimensional carbon nanomaterials. *J Mater Chem A* 1(9).
- Zhang W, Cheng W, Ziemann E, Be'er A, Lu X, Elimelech M, Bernstein R (2018) Functionalization of ultrafiltration membrane with polyampholyte hydrogel and graphene oxide to achieve dual antifouling and antibacterial properties. *J Membr Sci* 565:293–302.
- Zhang X, Cheng C, Qian J, Lu Z, Pan S, Pan B (2017) Highly efficient water decontamination by using sub-10 nm FeOOH confined within millimeter-sized mesoporous polystyrene beads. *Environ Sci Technol* 51(16):9210–9218.
- Zhao Y, Li J, Zhao L, Zhang S, Huang Y, Wu X, Wang X (2014) Synthesis of amidoxime-functionalized Fe<sub>3</sub>O<sub>4</sub>@ SiO<sub>2</sub> core-shell magnetic microspheres for highly efficient sorption of U (VI). *Chem Eng J* 235:275–283
- Zinadini S, Zinatizadeh AA, Rahimi M, Vatanpour V, Zangeneh H (2014) Preparation of a novel antifouling mixed matrix PES membrane by embedding graphene oxide nanoplates. *J Membr Sci* 453:292–301.
- Zodrow K, Brunet L, Mahendra S, Li D, Zhang A, Li Q, Alvarez PJ (2009) Polysulfone ultrafiltration membranes impregnated with silver nanoparticles show improved biofouling resistance and virus removal. *Water Res* 43(3):715–723.
- Zou F, Zhou H, Jeong DY, Kwon J, Eom SU, Park TJ, Hong SW, Lee J (2017) Wrinkled surface-mediated antibacterial activity of graphene oxide nanosheets. *ACS Appl Mater Interfaces* 9(2):1343–1351.



## Emerging Issues of Future Concern

# Disinfection: A Trade-Off Between Microbial and Chemical Risks

Nicholas Wawryk, Di Wu, Angela Zhou, Birget Moe, and Xing-Fang Li

## Abstract

While the disinfection of drinking water has largely eliminated the threat of waterborne diseases, it has resulted in an unintended consequence; the byproducts produced as a result of the disinfection process (DBPs). Every aspect of the water treatment process from source water acquisition to treated water distribution has an impact on this trade-off between microbial and chemical risk. Water utilities must consider how these variables interact within a complex system. Optimization of water treatment to balance microbial and chemical risks requires expertise from analytical chemists, toxicologists, engineers, and epidemiologists to characterize the classes of DBPs that are driving the toxicity associated with disinfected water beyond currently regulated DBPs. This chapter discusses how decisions made from source to tap affect water quality and the formation of DBPs using case studies from around the world.

## 1 Introduction

Water that is free from contamination is essential to human health and is defined as a basic human right by the World Health Organization (WHO 2017). However, the provision of safe drinking water continues to be a major public health concern throughout the world. Approximately 159 million

people still collect drinking water directly from untreated surface water sources that may be contaminated by sewage, pathogens, and industrial effluent (WHO and UNICEF 2017). Diarrheal diseases associated with poor water sanitation remain a leading cause of death in the developing world (WHO 2009). Fortunately, the majority of the world does not face these concerns because of drinking water disinfection, an essential practice to eliminate pathogenic microorganisms and prevent waterborne disease. The use of chlorine to disinfect municipal drinking waters has largely eliminated the threat of cholera, typhoid, and other waterborne disease outbreaks (Centers for Disease Control and Prevention 2019).

Disinfection practices eliminate the threat of waterborne pathogens, but constant monitoring and diligence is necessary to ensure that water treatment is effectively eliminating this risk. While the risk of waterborne pathogens is typically associated with developing countries, one of the most documented cases illustrating the causes and consequences of contaminated drinking water occurred in Walkerton, Ontario, Canada in 2000. By the end of the outbreak, the rural community located outside of Toronto would bury seven community members while thousands suffered from gastrointestinal illness. Researchers from the water disinfection community were shocked: How could an incident like this occur in a wealthy, technologically advanced nation?

The source of the issue arose from the three wells used by the community to obtain its drinking water and that were regularly treated with chlorine disinfection. At the beginning of May 2000, Walkerton experienced extreme rainfall that led to flooding around the wells, contaminating their primary source of drinking water. With proper chlorine disinfection and residual chlorine in the distribution system, this contamination would likely not have caused any adverse health effects to the people of Walkerton. However, improper measurement of residual chlorine levels and an uninstalled chlorine dosing meter on one of the wells prevented a corrective response, leading to significant microbial contamination throughout the entire distribution system of the town.

N. Wawryk · D. Wu · A. Zhou · B. Moe (✉) · X.-F. Li (✉)  
Division of Analytical and Environmental Toxicology,  
Department of Laboratory Medicine and Pathology,  
Faculty of Medicine and Dentistry, University of Alberta,  
Edmonton, AB T6G 2G3, Canada  
e-mail: [birget@ualberta.ca](mailto:birget@ualberta.ca)

X.-F. Li  
e-mail: [xingfang.li@ualberta.ca](mailto:xingfang.li@ualberta.ca)

B. Moe  
Alberta Centre for Toxicology, Department of Physiology  
and Pharmacology, Faculty of Medicine, University of Calgary,  
Calgary, AB T2N 4N1, Canada

On May 17, 2000, microbiological test results of water samples showed the presence of total coliforms and *Escherichia coli* in the water of the town's distribution system. The test results were ignored, and the contamination was not reported. Within days, the first person in the community had died, and by the end, several more fatalities were recorded. An estimated 2300 peoples suffered from gastrointestinal illness, in many cases severe. The following inquiry identified many contributing factors that led to the outbreak, including inadequate chlorination, organizational negligence, and negligence by operators and managers. This event showed that a community like Walkerton, which is in a developed country and has a well-established treatment facility for drinking water, is not immune to outbreaks when the water treatment process is not properly controlled, managed, or routinely monitored (Hrudey et al. 2014). The lesson learned is that drinking water safety is not a developing world issue but a global challenge.

By reducing the acute risk posed by microbials, the chlorination of drinking water remains one of the greatest public health achievements. However, the Walkerton case study shows that the threat of waterborne disease is constant, even in developed nations, and water treatment processes need to be constantly monitored and evaluated to ensure global drinking water quality. In addition to the acute risk of pathogens, water treatment must also deal with disinfection by-products (DBPs), which present a chronic health risk. To ensure safe drinking water, a delicate balance should exist between microbial (pathogens) and chemical (DBPs) risks, as illustrated in Fig. 1. This chapter will discuss some of the challenges affecting water treatment using case studies from around the world. Special attention will be paid to the

greatest chemical concern of water treatment, DBPs, and its influencing factors, including source water composition, water treatment processes, and water distribution systems.

## 2 A Historical Perspective: The Discovery and Regulation of Disinfection By-Products

Although the goal of disinfectant use is to kill harmful pathogens, one of the inevitable consequences is the production of DBPs. These compounds are formed as by-products of reactions between disinfectants and natural organic matter (NOM) present in the source water. DBPs were first identified in 1974 by analytical chemists, who found trihalomethanes (THMs) in finished drinking water (Rook 1974; Bellar and Lichtenberg 1974), a discovery aided by improvements in analytical instrumentation and sample preparation methods (Kristiana et al. 2012). Up until this time, it was assumed that drinking water treatment was sufficient to provide consistently safe water, as disinfection had led to the near eradication of major waterborne disease epidemics. In this context, Rook's discovery of THMs was truly revolutionary and showed how little was known concerning the chemistry of drinking water treatment.

The discovery of THMs was independently verified by U.S. Environmental Protection Agency (EPA) scientists, who incorrectly believed that the precursor responsible for their formation was ethanol, a compound with likely minimal occurrence in natural waters. The widespread use of chloroform (a type of THM) in consumer products at the time further complicated matters, and ultimately the landmark findings

**Fig. 1** Trade-off between acute microbial risk and chronic chemical risk. Used with permission, further usage requires ACS permission. <https://pubs.acs.org/doi/10.1021/acs.est.7b05440>. (Li and Mitch 2018)

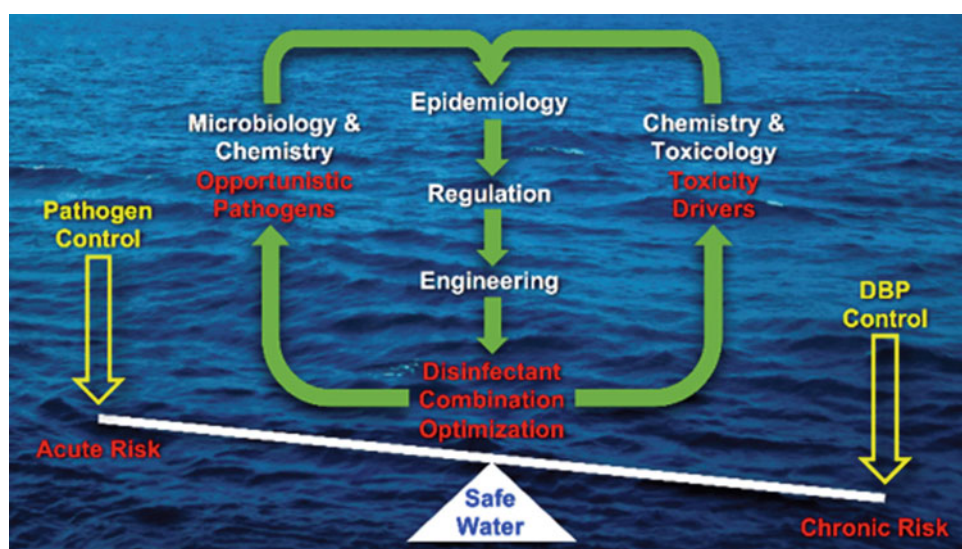


**Table 1** Current maximum containment levels (mg/L) for DBPs

DBP	U.S. (2006)	Canada (2017)	EU (1998)	People's Republic of China (2006)	WHO (2017)
THM4	0.08	0.1	0.1	1	1
Chloroform	–	–	–	0.06	0.3
Bromodichloromethane	–	–	–	0.06	0.06
Dibromochloromethane	–	–	–	0.1	0.1
Bromoform	–	–	–	0.1	0.1
HAA5	0.06	0.08	–	–	–
Monochloroacetic acid	–	–	–	–	0.02
Dichloroacetic acid	–	–	–	0.05	0.05
Trichloroacetic acid	–	–	–	0.1	0.2
Chloral hydrate	–	–	–	0.01	–
Bromate	0.01	0.01	0.01	0.01	0.01
Formaldehyde	–	–	–	0.9	–
Chlorite	1	1	–	0.7	0.7
Chlorate	–	1	–	0.7	0.7
Cyanogen chloride	–	–	–	0.07	–
Dichloroacetonitrile	–	–	–	–	0.02
Dibromoacetonitrile	–	–	–	–	0.07
2,4,6-Trichlorophenol	–	–	–	0.2	0.2
<i>N</i> -nitrosodimethylamine (NDMA)	–	0.00004	–	–	0.0001

were ignored by the agency. However, growing evidence suggested that NOM was the primary precursor for THMs and that THMs had widespread presence in chlorinated drinking water (Symons 1975). A rodent cancer bioassay study from the National Cancer Institute also found that chloroform exposure induced tumors in mice and rats (National Cancer Institute 1976). Typical to practices at the time, the bioassay performed was designed to reveal any carcinogenic effects and used very high treatment doses (Hrudey 2009). Therefore, the results provided very strong evidence for the formation of chloroform-induced tumors in mice and raised public fears over the safety of its use. Soon after, health concerns associated with chloroform and its parent class, THMs, resulted in the ban of chloroform in cosmetics and the adoption of the first drinking water guidelines addressing DBPs.

In 1978, Canada set a maximum containment level guideline of 350 µg/L for total THM4 (chloroform, bromodichloromethane, dibromochloromethane, and bromoform), becoming the first country to set a THM guideline (Hrudey 2009). The United States (U.S.) followed suit in 1979 with the Total Trihalomethane Rule that limited THM4 in U.S. drinking water to <100 µg/L (Federal Register 1998). This regulation significantly reduced the fraction of U.S. utilities with THM4 >100 µg/L from about 30% to 3% by 1988 (Mcguire 1988). Since then, guidelines and maximum allowable concentration regulations for many DBPs

have been regularly updated by several organizations. The current DBP regulations adopted by the U.S., Canada, the European Union (EU), China, and the WHO are found in Table 1.

## 2.1 Epidemiology and Unknown DBPs

After the initial finding on the carcinogenicity of chloroform, several epidemiological studies were initiated to determine whether consumption of disinfected drinking water increases excess cancer risk due to the now known presence of chemical by-products. Although insufficient evidence has been found to determine the carcinogenicity of individual DBPs, a consistent association between urinary bladder cancer and consumption of chlorinated water has been observed. A summary of these epidemiological studies, and more information on the risk assessment of DBPs, can be found in publications prepared by Dr. Steve Hrudey (Hrudey 2009; Hrudey et al. 2015). In general, although these findings are consistently found, the strength of association is typically weak. However, a small increase in risk coupled with the vast exposure to chlorinated drinking water could become a significant public health issue. In addition to the bladder cancer risk associated with treated drinking water, epidemiological studies have observed associations between consumption of chemically

treated water and adverse reproductive outcomes (Hrudey 2009). One of the initial concerns associated with disinfected water was spontaneous abortion, but this association has been dispelled (Savitz et al. 2006). While several reproductive health outcomes have been found to have no, low, or inconsistent association with disinfected drinking water, positive associations were found for impaired fetal growth, as measured by low birth weight and small body length or head circumference (Tardiff et al. 2006).

Since the mid-1970s, over 600 DBPs have been identified in treated drinking water (Richardson 2011), spurred by advancements in analytical instrumentation, as well as changes to water treatment inputs and water treatment technology. Gas chromatography (GC) has been in frequent use for the identification and quantification of volatile and semi-volatile DBPs since the identification of THMs. Although electron impact is the most common ionization source for GC, the use of softer ionization techniques such as chemical ionization may allow for the discovery of novel DBPs. For detection, the use of electron capture is standard for many U.S. EPA methods for DBPs. However, the use of mass spectrometry (MS) for detection is often preferred due to its increased selectivity, allowing for both targeted and non-targeted analysis. Additionally, the use of triple quadrupole-MS with multiple-reaction monitoring (MRM) allows for increased sensitivity and selectivity for targeted quantification. For example, this technique was used for the quantification of 14 nitrosamines at nanogram per liter levels in tap waters (Qian et al. 2015). Ionization sources for MS detection are varied, and are selected on the basis of the analytes of interest. Electrospray ionization (ESI) is a commonly applied ionization source; however, the less common atmospheric pressure chemical ionization (APCI) is useful for analysis of less polar DBPs. Because DBPs occur within a complex mixture of finished water, advances in the development of separation techniques have greatly improved the ability to identify novel DBPs within a complex matrix. The application of high-performance liquid chromatography (HPLC) has increased the characterization of the unknown total organic halide (TOX), as the technique is suitable for analysis of polar, high-molecular weight, and thermally labile DBPs. Currently, the most promising technique for the identification of unknown DBPs is the use of high-resolution mass spectrometry (HRMS), such as quadrupole-time-of-flight mass spectrometry (QTOF-MS), due to its ability to very accurately determine the mass of analytes. For more information on these analytical methods, a recent review from Yang and colleagues provides a comprehensive review on current DBP analysis and instrument trends (Yang et al. 2019).

While improvements in analytical chemistry have allowed for the identification of many new DBPs and DBP classes, the subset that has been quantified only constitutes about 30% of TOX in chlorinated waters, highlighting the importance of continuing to identify new DBPs of

toxicological importance (Krasner et al. 2006). A significant focus is still placed on the two most abundant classes of DBPs; THMs and haloacetic acids (HAA), mostly due to the corresponding focus on these compounds by regulations. However, mounting evidence is beginning to suggest that these two classes of DBPs are not sufficiently potent to account for the adverse human health effects associated with DBPs (Plewa et al. 2017; Bull et al. 2011). Understanding the chemistry of DBP formation and how that may change depending on the source water input, disinfection practice, and other water treatment system choices is the key to minimizing the exposure to DBPs in finished drinking water. With this information, water utilities can optimize water treatment to improve drinking water quality from source to tap.

---

### 3 DBP Challenges: Changing Source Water

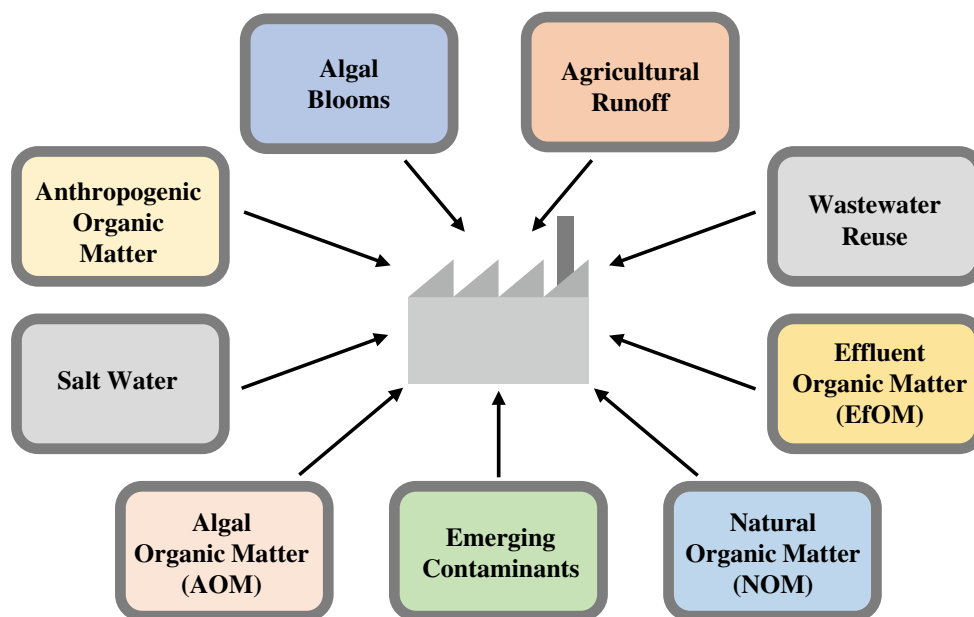
#### 3.1 Case Study: Cape Town, South Africa

After years of concern and warnings about water scarcity, the worst fears for many South Africans came true when severe droughts gripped the nation in 2015 and 2016, decimating their water supply (Ziervogel 2019). To counteract water loss, restrictions on personal water usage were increased in 2017 to a meager 87 L per person per day. Even with these additional measures in place, Cape Town was expected to reach “Day Zero” on April 12, 2018, the day on which all taps would be turned off. As a result, more severe water restrictions were announced to restrict personal water usage down to 50 L per person per day, and large-scale irrigation in agricultural areas was significantly reduced (Ziervogel 2019). Fortunately, the restriction measures, in combination with regional source water supplementation, use of small-scale desalination plants, and increased rains, prevented the arrival of “Day Zero” on April 12, pushing its portended arrival further into the future. In preparation, Cape Town is developing a revised water strategy, adopting new approaches to water management and governance that will increase their preparedness for the impacts of climate change and climate variability. With hotter, drier climates becoming more commonplace throughout many areas of the globe, some populations in sensitive areas, as witnessed in Cape Town, may be forced into a state of crisis management at the expense of long-term development planning.

#### 3.2 Source Water Composition

Globally, the quantity and quality of freshwater sources are in decline (Mekonnen and Hoekstra 2016), leading water utilities to switch or supplement their source water with

**Fig. 2** Complexity of source water composition for water treatment inputs



alternative water sources such as desalinated brackish water or treated wastewater. Additionally, human impact on water sources has led to the presence of emerging contaminants that have been difficult for water utilities to mitigate, as many of these contaminants are toxic or may transform during water treatment. Effluent organic matter (EfOM), algal organic matter (AOM), NOM, and anthropogenic organic material all contribute to the formation of DBPs, with the most productive precursors being the hydrophobic, acidic, and aromatic fractions of NOM. Hence, changing source water composition presents an important challenge for water treatment (Fig. 2), as the precursor pool for DBP formation can be significantly altered.

### 3.2.1 Alternative Source Water

In many areas, its demand for freshwater surpasses the availability due to rapid population growth and an increased occurrence of drought. The number of people that live in areas with severe water scarcity at least one month of the year is estimated at four billion, or 66% of the world population (Mekonnen and Hoekstra 2016). As a global issue, these people live in areas all around the world from Asia to the Americas. It is expected that meeting the demand for freshwater, both for drinking and water-intensive products, will be one of the most difficult challenges facing humanity this century (Mekonnen and Hoekstra 2016). Hence, the utilization of alternative water sources has become a logical approach to supplement current water supplies (Gude et al. 2010).

#### Seawater

While still costly and energy-prohibitive, saltwater desalination technologies have undergone dramatic improvements

in the last 50 years since their initial development, and their use has risen exponentially from that time. From 2007 to 2012, worldwide total installed desalination capacity rose from 47.6 to 74.8 million m<sup>3</sup>/d, a trend that is expected to continue (Bennett 2013). Utilities in California (U.S.), Australia, Singapore, China, and Saudi Arabia have all implemented desalination as part of their plan to overcome water scarcity (Gude 2016). However, the increasing demand for desalination technology has been accompanied by growing concern regarding the environmental impact of desalination plants, as they require large quantities of energy to function. This energy is often obtained via the use of fossil fuels, leading to increased greenhouse gas production (Gude 2016). Additionally, the waste produced by desalination may pose an environmental hazard due to increased salinity, temperature, and contaminants such as chlorine, copper, and anti-scalants (Roberts et al. 2010). The salinization of water resources is not limited to the use of desalination plants, as natural processes (e.g., seawater intrusion into aquifers) and anthropogenic forcing (e.g., agricultural runoff and wastewater contamination) can also affect salinity. Thus, salinization is a global issue that water treatment processes must also adjust to, regardless of the origin of their source water (Vengosh et al. 2014).

Like surface water sources, seawater sources also require chemical disinfection, but treatment processes require adaptation to prevent undesirable effects during water treatment due to compositional differences. Because seawater contains less total organic carbon (TOC), DBP formation is expected to be lower (Kim et al. 2015). However, seawater typically contains elevated levels of both bromide and iodide, 50,000–80,000 and 21–60 µg/L, respectively

(Kim et al. 2015). Total organic bromide (TOBr) and total organic iodide (TOI) have both been found to correlate with increased cytotoxicity and genotoxicity of disinfected water (Kim et al. 2015). In vitro studies have shown that halogenated DBPs follow a general toxicity order of  $I^- > Br^- > Cl^-$  (Plewa et al. 2008, 2014; Li et al. 2016), with iodinated DBPs (I-DBPs) more toxic than brominated DBPs (Br-DBPs), which in turn are much more toxic than chlorinated DBPs (Richardson et al. 2003, 2008; Hua et al. 2006; Chen and Westerhoff 2010; Ged and Boyer 2014; Ged et al. 2015). Elevated bromide concentrations can increase the formation of many classes of Br-DBPs, such as Br-THMs and Br-HAAs, as HOBr is a more efficient halogenating agent than HOCl (Ged and Boyer 2014; Westerhoff et al. 2004; Parker et al. 2014). Thus, caution needs to be taken when using source water with elevated bromide and iodide, such as seawater, as the formation of more toxic Br- and I-DBPs is a potential outcome. With increasing use of seawater desalination and the salinization of freshwater resources, further research is required to address how to control the formation of these Br- and I-DBPs in finished drinking water.

### Potable Water Reuse

Potable water reuse is another solution to concerns over both water scarcity and water quality deterioration. There are two main types of potable water reuse: (1) indirect, which uses an environmental water to buffer the water before treatment, or (2) direct reuse. While the majority of wastewater reuse plants are indirect potable reuse, a growing number of direct potable reuse facilities can be found (Richardson and Kimura 2017). Major water reuse facilities utilizing reclaimed water are in operation in 43 countries around the world (National Research Council 2012). China is also turning to water reuse as rapid development and historical misuse of water resources has left the country facing severe water stress and water contamination issues in many parts of the country. Increasing demand from industry and urban populations has also placed increased pressure on the current water supply (Zhao et al. 2017). In a country with increasing amounts of wastewater and many areas lacking proper wastewater treatment (Sun et al. 2016), potable water reuse has been identified as a potential solution for these water management issues.

One successful example of water reuse is the island nation of Singapore (Lee et al. 2016). Owing to limited options for a freshwater supply, the country was heavily dependent on neighboring countries to meet its water demand. Starting in 2003, the country's water utilities turned to water reuse to produce reclaimed drinking water, which they called NEWater. Having utilized water reuse to produce non-potable water for industrial uses since 1966, the country

now produces reclaimed water that conforms to drinking water guidelines meeting up to 30% of their total water demand. NEWater effectively closes Singapore's water loop, increasing resiliency and freeing up limited land area by reducing the need for significant water storage.

Like seawater, using treated wastewater as source water for water treatment has implications for DBP formation, as wastewater contains a set of precursors that are fundamentally different from NOM. The characteristic organic matter derived from wastewater impacted water is commonly defined as EfOM. EfOM has been shown to be a precursor source for carbonaceous DBPs such as THMs or HAAs (Krasner et al. 2009), although its lower aromaticity (less reactive compounds) in comparison to NOM should result in decreased THM production (Li and Mitch 2018). However, EfOM does contain higher organic nitrogen (Westerhoff et al. 2002), which can promote the formation of nitrogen containing DBPs (N-DBPs). N-DBPs have been shown to be more cytotoxic and genotoxic than their carbonaceous analogs in in vitro mammalian cell assays (Plewa et al. 2008; Bond et al. 2011; Krasner and 2009; Muellner et al. 2007). Thus, removal of DBP precursors from potable water reuse is a unique challenge for water utilities. While the removal of THM precursors is similar among treatment types, nitrification processes are required for potable water reuse to remove precursors for N-DBPs, including haloacetonitriles (HANs), *N*-nitrosodimethylamine (NDMA), and trihaloacetaldehyde (Krasner et al. 2009; Shah and Mitch 2012). Many potable water reuse plants also use reverse osmosis (RO), which is effective for removing many compounds, especially charged compounds and those larger than 200 Da in size.

### 3.2.2 Human Impacts on Source Water

The use of alternative water sources such as saltwater or wastewater illustrates the challenges associated with intentional changes in source water. However, it is important to recognize that challenges can arise in source water that has already been successfully used for drinking water treatment when unintentional human impacts influence source water composition.

### Nutrient Loading and Algal Blooms

Increased nutrient loading into source waters due to anthropogenic activities such as agricultural runoff and wastewater discharges has led to an increased occurrence of algal blooms, which in many cases have become annual events such as at Lake Erie in North America (Michalak et al. 2013). Lake Taihu in China also experiences annual phytoplankton blooms due to excessive nutrient loading caused by human inputs (Chen et al. 2003; Duan et al. 2009). During one particularly massive bloom of cyanobacteria in 2007, attempts to clear the bloom

unintentionally funneled it directly into the drinking water treatment plant of the city of Wuxi. This caused a public health emergency, leaving nearly two million people without clean drinking water (Qin et al. 2010; Guo 2007). Thus, algal bloom formation is a growing concern due to its association with mortality across a range of biota, economic impacts through ecological and human health costs, and the need for additional water treatment measures (Hoagland et al. 2002; Hoeger et al. 2005; Landsberg 2002). The human health concerns regarding algal blooms are typically due to the presence of microcystins produced by some species of *Microcystis* (Fu et al. 2015). In Lake Taihu and Lake Erie, *Microcystis* species have been shown to be the dominant species of algal blooms (Michalak et al. 2013; Deng et al. 2014), and significant concentrations of toxic microcystins, including MC-LR, have been found (Song et al. 2007; Sakai et al. 2013). The most successful strategy for prevention of algal blooms in source waters is to limit the presence of excessive nutrients, such as phosphorous, through regulatory policies preventing eutrophication (Ibelings et al. 2016). However, in situations where this is not possible or in response to an already present algal bloom, there are techniques that can be applied on site to control or mitigate bloom growth. These techniques include compartmentalization, removal of biomass through chemical or physical measures, and flushing or mixing (Stroom and Kardinaal 2016). Removal of blooms prior to arrival at the water intake is particularly important since algal cells cause physical issues with settling and clogged filters or membrane fouling (Fang et al. 2010a).

Algal-impacted source water provides an interesting example of the potential interactions between microorganisms and DBPs, as AOM present during water treatment has been shown to impact DBP formation. The formation of both THMs and HAAs has been reported from the chlorination of algal cells (Plummer and Edzwald 2001). Like wastewater-impacted water, AOM exhibits higher organic nitrogen content (Fang et al. 2010a). AOM also contains more hydrophilic and less aromatic carbon content and greater structural diversity when compared to NOM (Her et al. 2004). These differences in composition mean that AOM produces more N-DBPs, haloaldehydes (HALs), and less carbonaceous DBPs than chlorination of NOM (Fang et al. 2010a). In contrast, during chloramination, most DBPs were formed in smaller quantities in AOM than in NOM (Fang et al. 2010b). AOM adds an additional level of complexity in that the composition of algal proteins, carbohydrates, and lipids changes depending on the growth stage of the algae; meaning that DBP formation also depends on the algal growth stage (Fang et al. 2010a; Brown et al. 1993). As mentioned earlier, some species of algae also produce algal toxins, such as toxic variants of microcystins,

which have also been shown to be precursors to DBPs. Chlorination of the algal toxin MC-LR was shown to produce many different classes of DBPs, including THMs, HALs, and HANs (Chu et al. 2017).

### Emerging Contaminants

Owing to their low concentration in the environment, emerging contaminants (ECs) are often referred to as micropollutants or microconstituents. However, continuous improvement of analytical techniques has allowed for the detection of an increasing number of these contaminants in environmental waters (Richardson and Kimura 2017; Richardson and Ternes 2018). Disinfectants readily react with many ECs during treatment processes to form transformation products, classified as pollutant DBPs. Recent studies have found the formation of pollutant DBPs from pharmaceuticals (Negreira and Regueiro 2015; Carpinteiro et al. 2017), brominated flame retardants (Gao et al. 2016; Nika et al. 2017), surfactants (Gong et al. 2016), recreational drugs (Saleh et al. 2019; Mackie et al. 2017), and ultraviolet light (UV) filters (Trebse et al. 2016). In many cases, these transformation products have been shown to be more toxic or biologically active than the parent contaminant, emphasizing the importance of the removal of these precursors prior to treatment (Richardson and Ternes 2018).

ECs are a difficult issue for water treatment because of their large variation in chemical, biological, and physical properties that affect their ability to be removed during the treatment process. A number of studies have investigated the removal of micropollutants using oxidation strategies (Lee and von Gunten 2010). In general, ozonation can remove many pharmaceuticals (Ternes et al. 2003), whereas chlorine dioxide is not able to remove some of the most persistent pharmaceuticals such as ibuprofen (Huber et al. 2005). Advanced oxidation processes (AOPs) using combinations of UV, hydrogen peroxide ( $H_2O_2$ ), and ozone have been shown to remove many micropollutants such as pharmaceuticals and pesticides, with a high removal efficiency (Kim et al. 2009). The use of membrane-based techniques such as nanofiltration and RO is highly effective in the removal of many micropollutants, including X-ray contrast media, pharmaceuticals, and per- and polyfluoroalkyl substances (PFAS) (Snyder et al. 2007; Radjenović et al. 2008; Drewes et al. 2005; Kimura et al. 2003; Tang et al. 2006). Typically, a multi-barrier approach instead of a single engineering process is necessary to remove ECs because of their diversity. When considering what water treatment processes should be used, the cost of construction and maintenance is also an important factor. Richardson and Kimura summarize the cost of many water treatments in reference to EC removal (Richardson and Kimura 2017).



## 4 DBP Challenges: Changing Water Treatment

### 4.1 Case Study: *N*-Nitrosamines

In response to the initial regulations on THMs and HAAs, water utilities sought new technologies that would allow them to meet DBP guidelines while eliminating microbial risk. Because THMs and HAAs primarily form through reactions between chlorine and humic substances, chloramination limits the production of these DBPs. As a result, many utilities switched to chloramine as the primary disinfectant. In addition to low THM and HAA formation, chloramine was also found to be useful for maintaining a disinfectant residual in the distribution system (Seidel et al. 2005). However, while chloramine reduced the risk of regulated DBPs, this switch also had unintended consequences for many water utilities attempting to balance microbial and chemical risks. For example, although a potent antibacterial, chloramine use has been associated with increased levels of mycobacteria (Rhoads et al. 2017). More importantly, the switch to chloramine also leads to a significant trade-off in the chemical risk of DBPs produced.

In 1989, the *N*-nitrosamine, *N*-nitrosodimethylamine (NDMA), was first identified as a DBP after being detected in treated drinking water in Ohsweken, Ontario, Canada (Taguchi et al. 1994). While originally thought to have come from an anthropogenic source, further experiments confirmed that its presence was a direct result of the chloramine used in the water disinfection process, with formation requiring nitrogen derived from precursors in the source water, referred to as dissolved organic nitrogen (DON), or from the disinfectant itself (chloramine) (Bond et al. 2011). As such, chloramination has been shown to promote the formation of nitrosamines (Zhao et al. 2008; Schreiber and Mitch 2006).

Since the discovery of NDMA, a total of seven *N*-nitrosamines have been identified as DBPs and have been detected in several other locations, including California (U.S.), Alberta (Canada), Japan, China, and the U.K. The discovery of NDMA as a DBP was important, as the toxicity of *N*-nitrosamines at the time had been well documented due to their presence in foods, beverages, and consumer products (Scanlan and Issenberg 1975; Rostkowska et al. 1998). In vivo animal studies have shown that nitrosamines are potent carcinogens, inducing cancer in every major tissue in laboratory animals, and are suspected human carcinogens (International Agency for Research on Cancer 1978; Magee et al. 1967). While the nitrosamines themselves are not carcinogenic, they are bioactivated within the body, forming a hydroxyl radical which can methylate macromolecules such as DNA (Liteplo et al. 2002). N-DBPs, including *N*-

nitrosamines such as NDMA, are widely considered to be more genotoxic and cytotoxic than currently regulated DBPs. By switching from chlorination to chloramination, water utilities inadvertently caused the formation of new, highly toxic DBPs in finished water.

The history of *N*-nitrosamines provides an excellent example of how changes in drinking water practice can have unintended effects on the formation of DBPs. In order to meet the limits on THMs and HAAs, such as those set by the Stage 1 and 2 Disinfectants and Disinfection By-products Rules, utilities are switching from sole reliance on chlorine or chloramine disinfection to combinations of primary disinfectants (ozone, UV, or chlorine) with chloramines as secondary disinfectants (Seidel et al. 2005; Dotson 2019). In order to deal with changes to source water, new physical treatment processes are also being developed and have seen widespread use.

### 4.2 Alternative Treatment Methods

Alternative treatment methods are being employed to balance the chemical risks associated with traditional chemical treatment methods of chlorination and chloramination, as well as the physical treatment methods of coagulation, sedimentation, and filtration. Since THMs and HAAs are associated with the use of chlorine disinfection and are the focus of many DBP regulations, water utilities are experimenting with alternative treatment methods, both chemical and physical.

#### 4.2.1 Chemical Treatment Methods

While each disinfectant has benefits and drawbacks associated with its use (Table 2), all disinfection schemes form DBPs. Owing to the hazards associated with known DBP formation from traditionally used disinfectants, ozone and UV disinfection are becoming increasingly popular for use.

##### Ozone

A strong oxidant, ozone is capable of oxidizing most organic and inorganic chemicals and can be used as a primary disinfectant (von Gunten 2003a). It is produced on site at water treatment plants by passing oxygen or dry air through a high-voltage electric field (WHO 2017). Although a powerful disinfectant, care must be taken to monitor bromate in finished water, as ozone promotes bromate formation through oxidation of naturally occurring bromide (von Gunten 2003b). The formation of bromate depends on several factors: pH, concentration of bromide, concentration of ozone, and contact time (WHO 2017). Hence, bromate formation can be minimized by operating at lower pH (e.g., pH 6.5), using lower ozone doses with shorter contact time, and with the addition of ammonia which blocks bromate

**Table 2** Advantages and disadvantages of selected disinfection processes (Ireland Environmental Protection Agency 2011; WHO 2017; Washington State Department of Health 2019)

Disinfectant	Advantages	Disadvantages	Typical DBPs
Chlorine/hypochlorite	Deactivates most microorganisms Weak residual in distribution system	Ineffective against <i>Cryptosporidium</i> Associated with taste and odor issues	THMs, HAAs, HANs, chloral hydrate, chloropicrin, chlorophenols, <i>N</i> -chloramines, halofuranones, bromohydrins, chlorate, aldehydes, cyanoalkanoic acids, alkanolic acids, benzene, carboxylic acid, NDMA
Monochloramine	Long lasting disinfectant residual Reduced formation of THMs and many other chlorine DBPs Associated with fewer taste and odor issues	On-site production is necessary Less effective disinfectant which can require use of a stronger primary disinfectant	HANs, cyanogen chloride, organic chloramines, chloramino acids, chloral hydrate, halo ketones, nitrate, nitrite, chlorate, hydrazine, aldehydes, ketones, NDMA
Chlorine dioxide	More suitable for disinfection at higher pH Forms less regulated DBPs Associated with fewer taste and odor issues	On-site production is necessary More labor- and cost-intensive than chlorine	Chlorate and chlorite
Ozone	Highly powerful disinfectant Inactivates <i>Cryptosporidium</i> and <i>Giardia</i> Destruction of organic EC	On-site production is necessary More labor- and cost-intensive than chlorine No residual in distribution system	Bromate, bromoform, monobromoacetic acid, dibromoacetic acid, dibromoacetone, cyanogen bromide, chlorate, iodate, hydrogen peroxide, hypobromous acid, epoxides, ozonates, aldehyde, ketoacids, ketones, carboxylic acids
UV	Inactivates <i>Cryptosporidium</i> and <i>Giardia</i>	Weak viral inactivation No residual in distribution system	Aldehydes, carboxylic acids, nitrite

formation pathways by reacting with HOBr (von Gunten 2003; Pinkernell and von Gunten 2001). An important limitation of ozone is that it does not provide a residual disinfectant within the distribution system due to its short half-life (WHO 2017). Thus, a secondary disinfectant such as chlorine or chloramine must be added to maintain a disinfectant residual. Ozone use can also result in the formation of halonitromethanes (McCurry et al. 2016) and haloacetaldehydes (Shah et al. 2012) when coupled with chlorination or chloramination for secondary disinfection.

### UV Disinfection

The use of UV disinfection as an alternative to chemical disinfection dates back to the early 1900s. UV damages the nucleic acids of cells or viruses, preventing their

multiplication (Hijnen et al. 2006). Thus, UV treatment is broadly effective against pathogens and is particularly effective against *Cryptosporidium*, a pathogen highly resistant to chlorination (Hijnen et al. 2006). Unlike free chlorine or chloramine, UV disinfection does not produce halogenated DBPs during primary disinfection (Dotson and Rodriguez 2012). Although some DBPs such as aldehydes and carboxylic acids have been identified as products of UV disinfection, the concentration and identity of these non-halogenated DBPs have been of little concern (Liu et al. 2002; Dotson and Rodriguez 2012). It is important to note that turbidity and dissolved substances can inhibit UV disinfection (WHO 2017; Dotson and Rodriguez 2012), and that similar to ozone, a secondary disinfectant must be added to maintain disinfection residual in the distribution system

when used as a primary disinfectant. Although UV disinfection is not associated with formation of notable DBPs, the fragmented UV photolysis products of NOM can be DBP precursors when followed by chlorination or chloramination (Liu et al. 2006; Shah et al. 2011).

To avoid elevated formation of DBPs associated with individual disinfectants, the use of carefully optimized combinations of disinfectants may be able to provide water that is free from pathogens and has minimal chemical risk. For example, the use of a pre-oxidant, such as chlorine or ozone, with post-chloramination may be able to reduce the formation of NDMA (Shah and Mitch 2012). However, this still comes with a trade-off, as DBPs associated with the pre-oxidant will be produced. Because every water source is unique and regulations vary between regions, each water utility must consider their own situation when choosing which disinfectant(s) to use.

#### 4.2.2 Physical Treatment Methods

Traditional physical treatment methods used during water treatment processes can also increase the formation of DBPs (Ding et al. 2019). Coagulants, biological filtration, and adsorbents can all act as DBP precursors. Coagulants are used to promote aggregation or precipitate formation from the organic matter present in source water. However, many of these compounds and their monomers contain amide and amine groups that can react with disinfectants to form N-DBPs (Bolto and Gregory 2007; Krasner et al. 2013). Biofiltration has been shown to reduce the amount of DBP precursors (Liu et al. 2017), but more recent work has shown that this process can also increase the formation of N-DBPs under certain conditions due to the release of precursors from the biofilter, including biomass and cationic polymers (Chu et al. 2011, 2015). Activated carbon is commonly used to adsorb contaminants, including DBP precursors, but this process poorly removes DON and bromide ions, leading to increased formation of N-DBPs and Br-DBPs (Chiu et al. 2012; Symons et al. 1993a; Krasner et al. 2016; Zhang et al. 2017). Fullerene is another potential adsorbent for drinking water treatment that has been identified as a possible DBP precursor (Wang et al. 2012a; Alpatova et al. 2013). In response to the challenges affecting source water such as water reuse and desalination, many utilities have opted for the use of advanced physical treatments, including RO and granular activated carbon (GAC). Although costly, these methods have had demonstrated improvement in water quality.

#### Reverse Osmosis

RO works by using pressure to force water through a semi-permeable membrane which rejects dissolved matter based on size, charge, and physico-chemical interactions (Radjenović et al. 2008; Bellona and Drewes 2005). The

indirect potable water reuse system in the Orange County (California) Water District was one of the first systems to use RO. Since its inception in 1977, the advanced treatment plant has treated wastewater for the purpose of injecting it into aquifers to counteract seawater intrusion. Originally, the water flow was split between RO and GAC due to the high cost of RO. When the system was expanded in 2008, an integrated membrane system with RO and microfiltration was installed to treat the entire water flow (Marron et al. 2019). An AOP using UV and H<sub>2</sub>O<sub>2</sub> was later installed when NDMA and 1,4-dioxane were found in the treated water. Today, this updated system is called the Groundwater Replenishment System and currently treats 379,000 m<sup>3</sup>/d (Marron et al. 2019). This project is one of the longest running advanced treatment plants and has significant community support, leading to its use as a model for future multiple treatment systems around the world (Harris-Lovett et al. 2015).

While effective, there are some concerns regarding the use of RO that must be addressed prior to its implementation by a water utility. Because of its efficient removal of small molecules and charged particles, RO water may be missing nutritionally important ions. Ion-free water can also enhance the rate of unwanted mineral dissolution, such as dissolving iron oxide layers on the inside of pipes. However, the addition of essential ions into finished water may overcome some of these issues (Sedlak 2019). Another issue associated with RO and other membrane-based techniques that can impact the chemical risk of treated water is the ability of small, non-charged, and hydrophilic contaminants such as DBPs to pass through the membranes (Linge et al. 2013). If produced by disinfection upstream of RO treatment through pre-oxidation, many neutral and low molecular weight DBPs, such as di-HANs are poorly rejected by RO (Linge et al. 2013; Agus and Sedlak 2010). Although not as effective as RO, nanofiltration has been proposed as an alternative to RO treatment because it requires less pressure, and thus less energy. It also produces a smaller volume of brackish concentrate due to the ability of some monovalent salts to pass through (Bellona et al. 2012). Ozone and biologically activated carbon is another alternative treatment method as it requires less energy and capital cost compared to RO (Marron et al. 2019).

#### Granular Activated Carbon

Another advanced physical technique for water treatment systems is GAC. GAC has been used for many years to reduce NOM precursors for THMs and HAAs prior to disinfection (Chiu et al. 2012; Krasner et al. 2016; Knappe 2006; Summers et al. 2010). While effective for controlling the formation of regulated DBPs, the use of GAC can increase the ratio of DON:dissolved organic carbon

(DOC) and  $\text{Br}^-$ :DOC as the treatment preferentially removes DOC over DON and does not remove bromide (Chiu et al. 2012; Symons et al. 1993b; Summers et al. 1993). Therefore, the use of GAC may result in the increased formation of N-DBPs and Br-DBPs. Nonetheless, while these compounds are typically more cytotoxic and genotoxic compared to THMs and HAAs, a study has shown that the overall cytotoxicity and genotoxicity of GAC-treated waters was reduced by 32–83% in comparison to water treatment without GAC (Cuthbertson et al. 2019).

Increasing use of AOP for treatment is an important point of consideration for utilities that plan to use them in connection with advanced physical treatment methods such as RO or GAC. AOPs are often employed to reduce the concentration of NDMA, but many of the same compounds poorly removed by RO are also not removed to an appreciable extent using these treatments. For example, chloroform has a low reactivity with hydroxyl radicals and does not undergo direct photolysis, meaning that a much higher UV dose than would be cost effective would be necessary to remove it (Marron et al. 2019). Also, since AOPs typically lead to transformation products instead of complete mineralization, some products may be more toxic than the parent compounds. While these are important considerations that need to be studied, the toxicity-weighted concentration of DBPs is typically lower in recycled water produced using RO-UV/ $\text{H}_2\text{O}_2$  treatment than with conventional drinking water treatment (Zeng et al. 2016; Szczuka et al. 2017, 2019). However, incorporation of GAC may be a more functional alternative for utilities. Studies have shown that DBP precursors formed during pre-oxidation within the treatment plant are effectively removed by GAC (Bond et al. 2012; Kimura et al. 2013), sometimes more easily than the original precursor (Jiang et al. 2017).

---

## 5 DBP Challenges: Changing Distribution Systems

### 5.1 Case Study: The Netherlands

In the Netherlands, water used to produce drinking water is carefully selected (Smeets et al. 2009). The country has vast sandy aquifers that provide microbiologically safe ground water. Following World War II, natural replenishment of some of these aquifers could not support urbanization, and therefore some areas in the country were forced to use surface water sources to supplement their source water. This was initially treated with standard physical processes (coagulation, sedimentation, and filtration), as well as use of chlorine as a disinfectant. However, Rook's discovery of THMs led to the immediate abandonment of the use of chlorine disinfection whenever possible.

The improved physical treatments and optimization of chlorination conditions led to a reduction in required chlorine. Eventually, other treatment methods including ozonation with GAC or UV were optimized to replace chlorination. However, chlorine residual was still applied in certain situations to prevent bacterial growth in the country's water distribution system. With the ultimate goal of achieving a chemical-free treatment and distribution system, water utilities in the Netherlands shifted their focus from water treatment to the production of biostable water. A disinfectant residual was used in order to suppress regrowth of bacteria; however, it was predicted that if treated water was clean enough, utilities could effectively "starve" any bacteria present in the distribution system, preventing regrowth. Their goal of chemical-free water distribution was reached in 2008, having slowly reduced the amount of residual disinfectant present until no chlorine was required to be applied at all.

This unique approach to water distribution by the Netherlands relies on several key aspects. First and foremost, the chosen source water must be of high quality, and the strict protection of source water is necessary to achieve this. In order of preference, the source water should be (1) microbiologically safe ground water, (2) surface water with a soil passage, or (3) surface water utilizing multiple barriers for treatment. Next, a physical process treatment is used, and if it cannot be avoided, oxidation by ozone or peroxide. When considering the distribution system, it should not allow the entry of contamination and should be routinely monitored for failures. Finally, the water should be biologically stable and only biostable materials should be used to prevent microbial growth within the distribution system. Smeets and colleagues provide an in-depth explanation of the production and legal requirements of the water treatment process in the Netherlands (Smeets et al. 2009). While this approach significantly reduces the risks associated with DBPs, it also requires significant capital to build and maintain the physical treatment processes and distribution system. Nevertheless, the water distribution system used in the Netherlands is an excellent example of the careful optimization of conditions, both before and after treatment, to ensure safe, chemical-free drinking water. While chemical-free treatment and distribution may be a lofty goal for most utilities, overcoming challenges associated with residual disinfectant and aging infrastructure is a shared global challenge.

### 5.2 Chemical, Biological, and Physical Challenges in the Distribution System

The water distribution system is a complex network of pipes connecting the water treatment plant and the tap in your home. This network of pipes can act as an entry point for opportunistic pathogens into treated water. For this reason, it

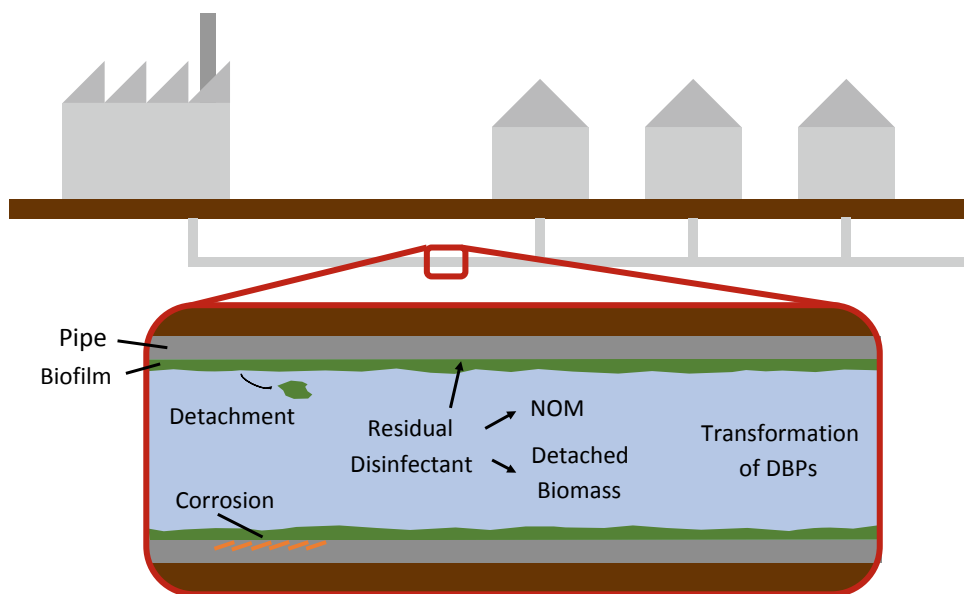
is important to monitor and optimize not only the treatment of water within the water treatment plant but also throughout the distribution system to ensure the finished water meets required guidelines and standards. Thus, the use of residual disinfectant is important to maintain water quality from treatment to tap. Although this ensures the microbial safety of finished water, it also makes monitoring the chemical safety of the water during distribution far more challenging. DBP concentrations in water distribution systems have exhibited both temporal and spatial variations, often associated with changes in water quality, residual disinfectant, or the physical structure of the distribution system (Fig. 3) (Wang et al. 2014; Zhao et al. 2006). This variation means that measurements taken at the water treatment plant may not be representative of the water that is being used and consumed by end users depending on their location in the distribution system. Nitrosamine concentrations were found to increase with distance from the water treatment plant, while halobenzoquinone (HBQ) DBPs were transformed to hydroxyl-HBQs throughout the distribution system (Wang et al. 2014; Zhao et al. 2006). THMs were also found to be highest at sampling sites further from the treatment plant, the opposite for HAAs which were found to be lowest. Thus, users of the same water treatment plant may be exposed to different DBPs depending on their distance from the plant, complicating the issue of ensuring drinking water with minimal chemical risk.

Another important consideration for the distribution system is the growth of biofilm, particularly in aging infrastructure. Biofilms are not only a problem in drinking water distribution systems but also in purified water supply systems used in laboratory and medical facilities. The term biofilm refers to the accumulation of microorganisms on a

surface and consists of many aggregated microbial cells within a matrix of biomolecules such as nucleic acids, polysaccharides, or lipids that together are known as extracellular polymeric substances (EPS). As expected, biofilms consume the residual disinfectant in the distribution system. To maintain the biostability of the finished water, utilities typically increase the necessary disinfectant dose. However, increasing the residual disinfectant dose also increases the formation of DBPs in the distribution system. Much of the biomass of biofilms is made up of EPS, which has a similar composition to AOM and EfOM DBP precursors (Bond et al. 2009; Wei et al. 2011; Sutherland 1985). High reactivity between chlorine and biofilm has been reported; however, non-specific reactions limit its penetration into biofilm (Chen and Stewart 1996). DBP formation from biofilm is still not well understood, but is an important consideration (Wei et al. 2011; Wang et al. 2012b, 2013).

Corrosion and the leaching of contaminants from drinking water distribution systems are affected by several factors, including the age of the distribution system, the type of materials used, and the quality and standing time of the water (WHO 2017; Liu et al. 2017). The materials used for distribution systems include two families: metallic and non-metallic materials. Corrosion of metallic pipes, such as galvanized steel, iron, or copper, can cause increased heavy metal (e.g., lead, cadmium, copper) concentrations in drinking water (WHO 2017; Liu et al. 2017). Among these heavy metals, lead is of particular concern because of its toxicity (Kim and Herrera 2010). Though lead water pipes have been banned for use in new construction, water utilities with aging infrastructure continue their utilization, often due to the costs associated with their replacement (Rabin 2008). Lead can leach from the pipe itself, as well as from lead

**Fig. 3** Challenges in the distribution system



solders and galvanized iron pipe plumbing (Liu et al. 2017). To reduce lead corrosion, the pH within the distribution system can be increased to 8.0–8.5 to directly prevent leaching, or treatment with orthophosphate or other phosphates can inhibit lead release by the formation of insoluble lead phosphate compounds which can also form an additional protective coating on the pipe to prevent further leaching (WHO 2017; Trueman et al. 2018). Non-metallic pipes are usually made of polyvinylchloride (PVC), chlorinated polyvinylchloride (CPVC), or polyethylene (PE). Unlike metallic pipes, non-metallic pipes are corrosion-resistant (Liu et al. 2017). However, PVC water pipes may still leach vinyl chloride and dialkyltins which are used as stabilizers in plastic (WHO 2017).

## 6 The Complexity of Ensuring Safe Drinking Water

Consistent production of safe drinking water is necessary for public health, and as seen from the previous sections of this chapter, it is not a simple task. Balancing chemical and microbial risks to ensure safe drinking water requires extensive research, optimization, and maintenance. The effects of failing to do so are highlighted in our final case study of Flint, Michigan. The Flint water crisis has received significant media attention that continues as the events are analyzed. This series of events has had a profound effect on the well-being of Flint citizens and highlights the complexity that water utilities face.

### 6.1 Case Study: Flint, Michigan, USA

In the 1960s, the city of Flint, Michigan switched to the Detroit Water and Sewage Department as the city's main provider of treated water (Masten and Davies 2017). The switch was made in part to ensure sufficient quantities of drinking water, as source water for Flint's Water Service Center was supplied by the Flint River, which was found to be difficult to treat. The Detroit water utility, on the other hand, collected water from the more stable and easily treatable source of Lake Huron. In the ensuing years, Flint's Water Service Center was maintained as a backup producer of drinking water, but its use was limited to only a few times each year. In 2013, as a cost-saving measure, the city of Flint decided to join the newly formed Karegnondi Water Authority which was constructing its own pipeline from Lake Huron. While construction was being completed, city officials decided to restore full-time operation of the city's Water Service Center, again utilizing source water from the Flint River. Under a tight timeline to complete the transition, inadequate preparation was put into the analysis of the

variables and risks associated with such significant changes in infrastructure and source water. As a result, several physical, chemical, and biological water quality issues were soon discovered. This included increased THM concentrations, corrosion of iron pipes leading to breaks, red water, lead leaching from pipes, and elevated bacteria levels (Del Toral 2015; Croft et al. 2015). The structural issues were due to the city's decision not to use a corrosion inhibitor as well as the use of ferric chloride as a coagulant which exasperated the corrosivity of the water toward the lead pipes (Del Toral 2015; Croft et al. 2015; Pieper et al. 2017). In the end, a public health emergency was declared, as the number of children with elevated blood levels increased by 6.6% in some areas of the city (Hanna-Attisha et al. 2016). These events and the intense negative publicity surrounding the issue forced Flint officials to make the switch back to the Detroit Water and Sewage Department in October 2015. However, lead levels remained elevated, and extra corrosion inhibitor was added in December 2015 (Allen et al. 2017). Even with these changes, many residents were reluctant to use their tap water. Concerns regarding the presence of skin rashes were a purported result of elevated DBP exposure, although this was ultimately proven not to be the case as it was soon found that the water did not have significantly different levels of DBPs compared to surrounding cities (Allen et al. 2017).

Although lead exposure was the driving force behind the intense media scrutiny of the city of Flint, chemical contamination was not the only threat to public health. In the aftermath of the crisis, information was soon released on several cases of Legionnaires' disease caused by *Legionella* bacteria. A total of 91 cases were diagnosed and 12 deaths were reported when source water was obtained from the Flint River (Michigan Department of Health and Human Services 2015a, b; Zahran et al. 2018). While the origin of this outbreak has not been identified, it is expected that one of the main drivers for this microbial growth was significant fluctuations in levels of free chlorine residual (Rosen et al. 2017). Residual chlorine is necessary to maintain the safety of the water throughout the distribution system. Many factors are associated with the loss of free chlorine, and it is unknown which factors were affected that led to the growth of *Legionella*. In addition, the presence of iron and high concentrations of assimilable organic carbon was also expected to have contributed to the biological growth and propagation of *Legionella* in the distribution system by lowering residual chlorine levels.

The case study of Flint highlights the importance of understanding the variables within a water system. The source water from the Flint River was considered difficult to treat due to high bacterial and carbon content, as well as significant seasonal variation in these chemical and biological parameters. Very few studies, including no pilot study,

were performed on the water from the Flint River before the switch to ensure that the water utility could provide safe drinking water with the proposed changes. Although the Flint River is no longer being used to provide drinking water, nearly irreparable damage has been done to the community and to the water system, shattering public trust in water management. Currently, all lead pipes in the Flint distribution system are being replaced at great cost. However, as observed in Madison, Wisconsin, simply replacing the pipes will not eliminate the lead problem immediately, leaving a legacy of poor water quality (Cantor 2006).

## 7 Perspectives

As water is essential to human life, every effort should be made to achieve drinking water that is as safe as possible. The primary goal of water treatment is to eliminate the microbial risk that poses a direct threat to human health. Nonetheless, there is a trade-off to the reduction of microbial risk. DBPs pose a chemical risk that forces water utilities to take measures to limit the production of DBPs. The complexity and variety of DBPs and their precursors mean that there are further compromises when it comes to reducing the production of certain DBPs. Regulations focus on THMs and HAAs, as these compounds are typically used as a representative measure of the total concentration of chlorinated DBPs. However, it remains unknown which DBPs are the toxicity drivers responsible for the human health effects associated with consumption of treated water (Federal Register 1998; Li and Mitch 2018). The assumption that THMs and HAAs should correlate with toxicity drivers in disinfected water seems reasonable; yet, the focus on THMs and HAAs may overlook the true toxicity drivers and drive water treatment optimization toward more toxic compounds, as observed in the case study of *N*-nitrosamines in Sect. 4.1. Therefore, collaborative efforts between DBP researchers in diverse fields such as chemistry and toxicology have been established to determine which DBPs are the toxicity drivers. This work has developed a set of quantitative cytotoxicity and genotoxicity data using Chinese hamster ovary (CHO) cells for over 100 regulated and unregulated DBPs (Wagner and Plewa 2017). Most importantly, this work has demonstrated that some unregulated DBPs, particularly N-DBPs as well as Br- and I-DBPs, are orders of magnitude more cytotoxic and genotoxic than many currently regulated DBPs (Wagner and Plewa 2017; Pals et al. 2013; Plewa et al. 2010). Regulations on DBPs have driven the optimization of water treatment, leading to a narrow focus on which DBPs to reduce. By identifying the toxicity drivers, regulations based on risk evidence may be developed to protect human health and would drive the optimization of water treatment to minimize the production of these toxic DBPs.

While animal studies are the gold standard in toxicology, only 24 DBPs have been evaluated for carcinogenicity by *in vivo* assays, with 22 inducing tumor formation (Richardson et al. 2007). These tests are quite time-consuming and expensive, limiting the number of compounds that can be tested. Therefore, alternative methods are often used to prioritize which of the large number of DBPs (more than 600 identified) should undergo *in vivo* testing. As mentioned earlier, quantitative *in vitro* cytotoxicity and genotoxicity assays based on CHO cells has generated a database of over 100 DBPs, which allows for the ranking of their toxicity (Wagner and Plewa 2017). To date, this is the largest *in vitro* toxicity data set of DBPs. However, CHO cells lack certain metabolic features that may be important for the activation of DBPs to mutagens (Li and Mitch 2018). For example, carcinogenicity of NDMA requires activation by metabolic enzymes (Beranek et al. 1983; Souliotis et al. 2002). Identification of the toxicity mode(s) of action, likely to be associated with specific end points (e.g. bladder cancer), can also help prioritize DBPs for confirmation with *in vivo* assays (Li and Mitch 2018).

In addition to measuring the toxicological potency of new DBPs, it is important to consider the relative concentration of these DBPs to determine DBP toxicity drivers. Therefore, DBP researchers are beginning to compare measured DBP concentrations weighted by metrics of toxic potency, such as CHO cytotoxicity. This method may provide better information to assess the DBP-associated safety of water as compared to simply looking at the total amount of DBPs (mass basis) in water without considering the toxicological potency (toxicity-weighted basis) of each DBP (Fig. 4). By using a toxicity-weighted measurement, researchers have shown that unregulated halogenated DBP classes, particularly HANs, may be greater contributors to the DBP-associated toxicity in conventional European drinking waters (Plewa et al. 2017), chlorinated or chloraminated high salinity groundwaters (Szczuka et al. 2017), and chloraminated potable reuse effluents (Zeng et al. 2016). When these toxicity-weighted measurements are used, toxicity results from single compound assays are generally assumed to be additive (Zeng et al. 2016; Szczuka et al. 2017). However, previous research has shown that this assumption is not always valid (Boorman et al. 1999; Narotsky et al. 2015). More research is needed to determine the potential for DBPs in mixtures to exhibit synergistic or antagonistic interactions.

In response to this new information, there is a need for water treatment practices to shift toward reducing toxicity drivers and not simply the regulated DBPs. As was discussed previously, efforts to reduce the formation of regulated THMs and HAAs at some utilities had implications for the formation of unregulated DBPs that are potentially a greater risk to human health. Therefore, in addition to the trade-off between chemical and microbial risks, water

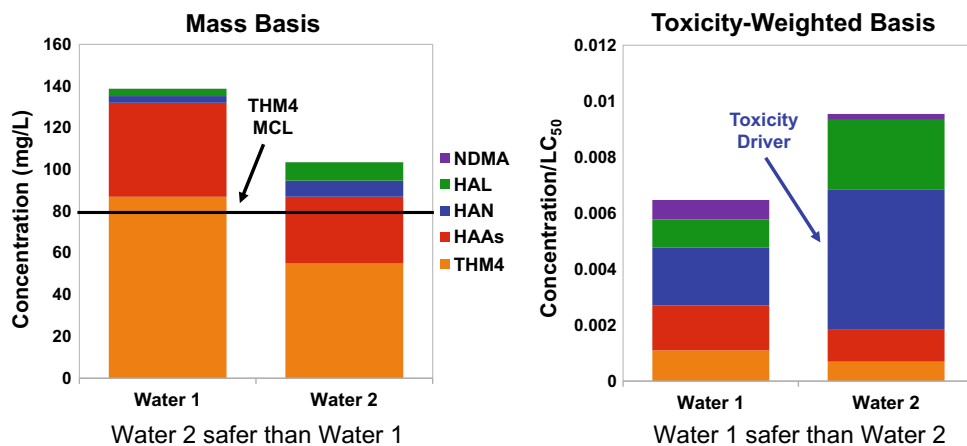


**Fig. 4** Evaluation of two water samples (Water 1 and Water 2) using the conventional mass basis approach (left) and emerging toxicity-weighted basis approach (right), illustrating how the incorporation of toxicological potency can strongly influence the assessment of

water safety. Used with permission, further usage requires ACS permission. <https://pubs.acs.org/doi/10.1021/acs.est.7b05440>. (Li and Mitch 2018)

utilities must also make difficult decisions that trade-off between different chemical risks. These decisions do not only apply to the details regarding the water treatment system and disinfectant choice but also to the selection of source water and decisions on infrastructure spending. Since each water treatment system is unique, the fundamental rule that governs these decisions is “know your system”. As discussed in the preceding case studies, there are many variables to water treatment, and therefore it is important to understand the importance of each and continuously monitor changes. DBPs are only one of the hazards to consider when talking about water quality management. Water utilities should seek to minimize DBP exposure to consumers; however, this should never come at the expense of effective disinfection to keep the microbial risk of untreated water at a minimum.

In certain situations, it may be more practical to lower DBP guidelines in order to ensure that microbial-free water is delivered to consumers. These types of decisions are potentially short-term, in response to emergencies and disasters, or the initial step to a long-term solution in areas with a lack of infrastructure and/or quality water sources. Climate change is expected to affect the number of and intensity of extreme water-related weather events (Levy et al. 2017). Heavy rainfall events can transport pathogens in the environment and can increase run-off into water sources, thereby increasing potential human exposure to waterborne pathogens. Additionally, water treatment plants may be overwhelmed, leading to contamination of drinking water pipes, overflow of sewage, or untreated waste being dumped into waterways. Changes in global climate can also reduce the availability of clean drinking water sources. Higher peak temperatures can lead to increased frequency of drought as well as sea level rise leading to salination of groundwater

sources. All of these changes to water treatment inputs require optimization and improvements in order to ensure safe drinking water. More extreme weather events will lead to an increased frequency of natural disasters and emergency scenarios. In these situations, the availability of clean drinking water is limited. People may move to an area with contaminated drinking water, or when sanitation is inadequate, it is highly likely that unprotected water sources around temporary settlements will become contaminated. Therefore, drinking water quality standards addressing factors such as odor, color, and DBPs should be flexible in order to prevent excessive restrictions on water use which can lead to more critical health effects.

Water treatment is necessary to provide safe drinking water that is free from pathogenic microorganisms. This chapter began with the story of Walkerton, highlighting the constant threat of waterborne disease and the need for constant monitoring and improvement from water treatment processes. In addition to the threat of pathogens, water utilities must also manage the threat of DBPs, an important chemical risk. To ensure safe drinking water, a delicate balance exists between the two. Every aspect of the water treatment process from source to tap has an impact on this trade-off between microbial and chemical risk. Changes to our environment driven by human activity have led to the use of alternative water sources that can contain differing sets of DBPs precursors. Owing to concerns over the adverse chronic health effects of chlorinated water, countries have regulated the maximum contaminant levels of DBPs. This in turn has driven the optimization of water treatment to reduce the concentration of these compounds, but has led to a trade-off between different chemical risks. Water utilities must also consider the distribution system as a potential source for contamination and reactor for transformation. All



these aspects come together to form a complex system with many variables that interact. DBP researchers are working to discover the toxicity drivers so that these systems can be optimized such that both the microbial and chemical risks are minimized.

## References

- Agus E, Sedlak DL (2010) *Water Res* 44(5):1616–1626
- Allen JM, Cuthbertson AA, Liberatore HK, Kimura SY, Mantha A, Edwards MA, Richardson SD (2017) *J Environ Sci* 58:271–284
- Alpatova AL, Baumann MJ, Davies SH, Masten SJ (2013) *Environ Chem Lett* 11(3):309–313
- Bellar TA, Lichtenberg JJ, Kroner RC (1974) *C J Am Water Work Assoc* 66(12):703–706
- Bellona C, Drewes EJ (2005) *Memb Sci* 249:227–234
- Bellona C, Heil D, Yu C, Fu P, Drewes JE (2012) *Sep Purif Technol* 85:69–76
- Bennett A (2013) *Filtr Sep* 50(3):32–39
- Beranek DT, Weis CC, Evans FE, Chetsanga CJ, Kadlubar FF (1983) *Biochem Biophys Res Commun* 110(2):625–631
- Bolto B, Gregory J (2007) *Water Res* 41(11):2301–2324
- Bond T, Henriot O, Goslan EH (2009) *Environ Sci Technol* 43(15):5982–5989
- Bond T, Huang J, Templeton MR, Graham N (2011) *Water Res* 45(15):4341–4354
- Bond T, Templeton MR, Graham N (2012) *J Hazard Mater* 235–236:1–16
- Boorman GA, Dellarco V, Dunnick JK, Chapin RE, Hauchman F, Gardner H, Cox M, Sills RC, Boorman GA, Dellarco V, Dunnick JK, Chapin RE, Hunter S, Hauchman F, Gardner H, Cox M, Sills RC (1999) *Environ Heal Perspect* 107:207–217
- Brown MR, Garland CD, Jeffrey SW, Jameson ID, Leroi JM (1993) *J Appl Phycol* 5(3):285–296
- Bull RJ, Reckhow DA, Li X, Humpage AR, Joll C, Hrudey SE (2011) *Toxicology* 286(1–3):1–19
- Canada Health (2017) Guidelines for Canadian drinking water quality—Summary table. Ontario, Ottawa
- Cantor AF (2006) *Am Water Work Assoc* 98(1):117–126
- Carpinteiro I, Rodil R, Quintana JB, Cela R (2017) *Water Res* 120:280–289
- Centers for Disease Control and Prevention (2019) History of drinking water treatment: a century of U.S. water chlorination and treatment: one of the ten greatest public health achievements of the 20th century. <https://www.cdc.gov/healthywater/drinking/history.html>. Accessed Mar 19, 2019
- Chen X, Stewart PS (1996) *Environ Sci Technol* 30(6):2078–2083
- Chen B, Westerhoff P (2010) *Water Res* 44(13):3755–3762
- Chen Y, Qin B, Teubner K, Dokulil MT (2003) *J Plankton Res* 25(4):445–453
- Chiu CA, Westerhoff P, Ghosh A (2012) *J Am Water Works Assoc* 104(7)
- Chu W, Gao N, Deng Y, Templeton MR, Yin D (2011) *Bioresour Technol* 102(24):11161–11166
- Chu W, Li C, Gao N, Templeton MR, Zhang Y (2015) *Chemosphere* 121:33–38
- Chu W, Yao D, Deng Y, Sui M, Gao N (2017) *J Hazard Mater* 327:153–160
- Croft HD, Walling D, Ambrose G (2015) City of Flint: water system questions & answers. Flint, MI
- Cuthbertson AA, Kimura SY, Liberatore HK, Summers RS, Knappe DRU, Stanford BD, Maness JC, Mulhern RE, Selbes M, Richardson SD (2019) *Environ Sci Technol* 53:5987–5999
- Del Toral MA (2015) High lead levels in flint. Michigan—Interim report, Chicago, IL
- Deng J, Qin B, Paerl HW, Zhang Y, Ma J, Chen Y (2014) *Freshw Biol* 59:1076–1085
- Ding S, Deng Y, Bond T, Fang C, Cao Z, Chu W (2019) *Water Res*
- Dotson A, Westerhoff P (2019) *Am Water Work Assoc* 101(9):101–115
- Dotson AD, Rodriguez CE, Linden KG (2012) *J Am Water Work Assoc* 104(5):318–324
- Drewes JE, Bellona C, Oedekoven M, Xu P, Kim TU, Amy G (2005) *Environ Prog* 24(4):400–409
- Duan H, Ma R, Xu X, Kong F, Zhang S, Kong W, Hao J, Shang L (2009) *Environ Sci Technol* 43(10):3522–3528
- European Union (1998) Council directive 98/83/EC of 3 November 1998 on the quality of water intended for human consumption
- Fang J, Ma J, Yang X, Shang C (2010a) *Water Res* 44(6):1934–1940
- Fang J, Yang X, Ma J, Shang C, Zhao Q (2010b) *Water Res* 44(20):5897–5906
- Federal Register (1998) 40 CFR parts 9, 141, 142. 63(241):69390–69476
- Fu KZ, Moe B, Li XF, Le XC (2015) *J Environ Sci (China)* 32:249–251
- Gao Y, Pang S, Jiang J, Zhou Y, Li J, Wang L-H, Lu X-T, Yuan L-P (2016) *Environ Sci Technol* 50:9608–9618
- Ged EC, Boyer TH (2014) *Desalination* 345:85–93
- Ged EC, Chadik PA, Boyer TH (2015) *J Environ Manage* 149:253–262
- Gong T, Zhang X, Li Y, Xian Q (2016) *Chemosphere* 149:70–75
- Gude VG (2016) *Water Res* 89:87–106
- Gude VG, Nirmalakhandan N, Deng S (2010) *Desalin Water Treat* 20:281–290
- Guo L (2007) *Sci New Ser* 317(5842):1166
- Hanna-Attisha M, Lachance J, Sadler RC, Schnepf AC (2016) *AJPH* 106(2):283–290
- Harris-Lovett SR, Binz C, Sedlak DL, Kiparsky M, Truffer B (2015) *Environ Sci Technol* 49(13):7552–7561
- Her N, Amy G, Park H, Song M (2004) *Water Res* 38:1427–1438
- Hijnen WAM, Beerendonk EF, Medema GJ (2006) *Water Res* 40:3–22
- Hoagland AP, Anderson DM, Kaoru Y, White AW (2002) *Estuaries* 25(4):819–837
- Hoeger SJ, Hitzfeld BC, Dietrich DR (2005) *Toxicol Appl Pharmacol* 203:231–242
- Hrudey SE (2009) *Water Res* 43:2057–2092
- Hrudey SE, Hrudey EJ (2014) Ensuring safe drinking water: learning from frontline experience with contamination. American Water Works Association, Denver
- Hrudey SE, Backer LC, Humpage AR, Krasner SW, Michaud DS, Moore LE, Singer PC, Stanford BD (2015) *J Toxicol Environ Heal Part B Crit Rev* 18(5):213–241
- Hua G, Reckhow DA, Kim J (2006) *Environ Sci Technol* 40(9):3050–3056
- Huber MM, Korhonen S, Termes TA, Von Gunten U (2005) *Water Res* 39(15):3607–3617
- Ibelings BW, Bormans M, Fastner J, Visser PM (2016) *Aquat Ecol* 50(3):595–605
- International Agency for Research on Cancer (1978) IARC monographs on the evaluation of the carcinogenic risk of chemicals to humans: some N-nitroso compounds
- Ireland Environmental Protection Agency (2011) Water treatment manual: disinfection. Wexford, Ireland
- Jiang J, Zhang X, Zhu X, Li Y (2017) *Environ Sci Technol* 51:3435–3444

- Kim EJ, Herrera JE (2010) *Environ Sci Technol* 44(16):6054–6061
- Kim I, Yamashita N, Tanaka H (2009) *J Hazard Mater* 166(2–3):1134–1140
- Kim D, Amy GL, Karanfil T (2015) *Water Res* 81:343–355
- Kimura K, Amy G, Drewes JE, Heberer T, Kim TU, Watanabe YJ (2003) *Memb Sci* 227(1–2):113–121
- Kimura SY, Komaki Y, Plewa MJ (2013) *Environ Sci Technol* 47:12382–12390
- Knappe DRU (2006) *Interface science and technology*. Elsevier, New York, pp 155–177
- Krasner SW (2009) *Philos Trans R Soc A Math Phys Eng Sci* 367:4077–4095
- Krasner SW, Weinberg HS, Richardson SD, Pastor SJ, Chinn R, Scilimenti MJ, Onstad GD, Thruston AD (2006) *Environ Sci Technol* 40(23):7175–7185
- Krasner SW, Westerhoff P, Chen B, Rittmann BE, Nam S-N, Amy G (2009) 43:2911–2918
- Krasner SW, Mitch WA, McCurry DL, Hanigan D, Westerhoff P (2013) *Water Res* 47(13):4433–4450
- Krasner SW, Lee TCF, Westerhoff P, Fischer N, Hanigan D, Karanfil T, Beita-Sandí W, Taylor-Edmonds L, Andrews RC (2016) *Environ Sci Technol* 50(17):9583–9591
- Kristiana I, Charrois JWA, Hrudey SE (2012) *Disinfection by-products*. In: Hrudey SE, Charrois JWA (eds) IWA Publishing, London, U.K., pp 11–39
- Landsberg JH (2002) *Rev Fish Sci* 10(2):113–390
- Lee H, Tan TP (2016) *Int J Water Resour Dev* 32(4):611–621
- Lee Y, von Gunten U (2010) *Water Res* 44(2):555–566
- Levy K, Woster AP, Goldstein RS, Carlton E (2017) *J Environ Sci Technol* 50(10):4905–4922
- Li X-F, Mitch WA (2018) *Environ Sci Technol* 52:1681–1689
- Li J, Moe B, Vemula S, Wang W, Li XF (2016) *Environ Sci Technol* 50(13):6744–6752
- Linge KL, Blythe JW, Busetti F, Blair P, Rodriguez C, Heitz A (2013) *Sep Purif Technol* 104:221–228
- Liteplo RG, Meek ME, Windle W (2002) *N-nitrosodimethylamine: concise international chemical assessment document 38*. Stuttgart, Germany
- Liu W, Andrews SA, Bolton JR, Kinden KG, Sharpless C, Stefan M (2002) *Water Supply* 2(5–6):515–521
- Liu W, Cheung L, Yang X, *ACS* (2006) 40:2033–2043
- Liu C, Olivares CI, Pinto AJ, Lauderdale CV, Brown J, Selbes M, Karanfil T (2017) *Water Res* 124:630–653
- Mackie AL, Park YR, Gagnon GA (2017) *Environ Sci Technol* 51:10711–10717
- Magee PN, Barnes JM (1967) *Advances in cancer research*. In: Haddow A, Weinhouse S (eds) Academic Press, pp 163–246
- Marron EL, Mitch WA, Gunten UV, Sedlak DL (2019) *Acc Chem Res* 52(3):615–622
- Masten SJ, Davies SH, Mcelmurry SP (2017) *J Am Water Work Assoc* 108(12):22–34
- McCurry DL, Quay AN, Mitch WA (2016) *Environ Sci Technol* 50(3):1209–1217
- Mcguire MJ, Meadow RG (1988) *J Am Water Work Assoc* 80(1):61–68
- Mekonnen MM, Hoekstra AY (2016) *Sci Adv* 2(2):1–7
- Michalak AM, Anderson EJ, Beletsky D, Boland S, Bosch NS, Bridgeman TB, Chaffin JD, Cho K, Confesor R, Daloglu I, DePinto JV, Evans MA, Fahnenstiel GL, He L, Ho JC, Jenkins L, Johengen TH, Kuo KC, LaPorte E, Liu X, McWilliams MR, Moore MR, Posselt DJ, Richards RP, Scavia D, Steiner AL, Verhamme E, Wright DM, Zagorski MA (2013) *Proc Natl Acad Sci* 110(16):6448–6452
- Michigan Department of Health and Human Services GCPHD (2015a) *Legionellosis outbreak-genesee county, June, 2014–November, 2015 summary analysis*
- Michigan Department of Health and Human Services GCPHD (2015b) *Legionellosis outbreak-genesee county, May, 2014–March, 2015 full analysis*
- Muellner MG, Wagner ED, Mccalla K, Richardson SD, Woo YT, Plewa M (2007) *J Environ Sci Technol* 41(2):645–651
- Narotsky MG, Klinefelter GR, Goldman JM, Deangelo AB, Best DS, Mcdonald A, Strader LF, Murr AS, Suarez JD, George MH, Hunter ES, Simmons JE (2015) *Environ Heal Perspect* 123(6):564–570
- National Research Council (2012) *Water reuse: potential for expanding the nation’s water supply through reuse of municipal wastewater*. The National Academies Press, Washington, DC
- National Cancer Institute (1976) *Carcinogenesis bioassay of chloroform*. Bethesda, MD
- Negreira N, Regueiro J (2015) *Water Res* 85:103–113
- Nika M-C, Bletsou AA, Koumaki E, Noutsopoulos C, Mamais D, Stasinakis AS, Thomaidis NS (2017) *J Hazard Mater* 323:400–413
- Pals J, Attene-Ramos MS, Xia M, Wagner ED, Plewa M (2013) *J Environ Sci Technol* 47(21):12514–12523
- Parker KM, Zeng T, Harkness J, Vengosh A, Mitch WA (2014) *Environ Sci Technol* 48(19):11161–11169
- People’s Republic of China (2006) *Standards for drinking water quality, GB5749-2006*. Beijing, China.
- Pieper KJ, Tang M, Edwards MA (2017) *Environ Sci Technol* 51:2007–2014
- Pinkernell U, von Gunten U (2001) *Environ Sci Technol* 35:2525–2531
- Plewa MJ, Wagner ED, Muellner MG, Hsu K-M, Richardson SD (2008) *Disinfection by-products in drinking water. Occur. Form. Health Eff. Control* 995(7):36–50
- Plewa MJ, Simmons JE, Richardson SD, Wagner ED (2010) *Environ Mol Mutagen* 51(8–9):871–878
- Plewa MJ, Simmons JE, Richardson SD, Wagner ED (2014) *Environ Mol Mutagen* 51:871–878
- Plewa MJ, Wagner ED, Richardson SD (2017) *J Environ Sci* 58:208–216
- Plummer JD, Edzwald JK (2001) *Environ Sci Technol* 35(18):3661–3668
- Qian Y, Wu M, Wang W, Chen B, Zheng H, Krasner SW, Hrudey SE, Li XF (2015) *Anal Chem* 87(2):1330–1336
- Qin B, Zhu G, Gao G, Zhang Y, Li W, Paerl HW, Carmichael WW (2010) *Env Manage* 45:105–112
- Rabin R (2008) *Am J Public Health* 98(9):1584–1592
- Radjenović J, Petrović M, Ventura F, Barceló D (2008) *Water Res* 42(14):3601–3610
- Rhoads WJ, Pruden A, Edwards MA (2017) *Environ Sci Technol* 51(12):7065–7075
- Richardson SD (2011) *Encyclopedia of environmental health*. In: Nriagu JO (ed). Elsevier Inc., pp 110–136
- Richardson SD, Kimura SY (2017) *Environ Technol Innov* 8:40–56
- Richardson SD, Ternes TA (2018) *Anal Chem* 90(1):398–428
- Richardson SD, Thruston AD, Rav-Acha C, Groisman L, Popilevsky I, Juraev O, Glezer V, McKague AB, Plewa MJ, Wagner ED (2003) *Environ Sci Technol* 37(17):3782–3793
- Richardson SD, Plewa MJ, Wagner ED, Schoeny R, Demarini DM (2007) *Mutat Res* 636:178–242
- Richardson SD, Fasano F, Ellington JJ, Crumley FG, Buettner KM, Evans JJ, Blount BC, Silva LK, Waite TIMJ, Luther GW, Mckague AB, Miltner RJ, Wagner ED, Plewa MJ (2008) *Environ Sci Technol* 42(22):8330–8338
- Roberts DA, Johnston EL, Knott NA (2010) *Water Res* 44(18):5117–5128

- Rook J (1974) *Water Treat Exam* 23:234–243
- Rosen MB, Pokhrel LR, Weir MH (2017) *Sci Total Environ* 590–591:843–852
- Rostkowska K, Zwierz K, Rozanski A, Moniuszko-Jakoniuk J, Roszczenko A (1998) *Pol J Environ Stud* 7:321–325
- Sakai H, Hao A, Iseri Y, Wang S, Kuba T, Zhang Z, Katayama H (2013) *Sci World J*
- Saleh NB, Apul O, Karanfil T (2019) *Environ Sci Technol* 53:1746–1747
- Savitz DA, Singer PC, Herring AH, Hartmann KE, Weinberg HS, Makarushka C (2006) *Am J Epidemiol* 164(11):1043–1051
- Scanlan RA, Issenberg P (1975) *CRC Crit Rev Food Sci Nutr* 5:357–402
- Schreiber IM, Mitch WA (2006) *Environ Sci Technol* 40(19):6007–6014
- Sedlak DL (2019) *Environ Sci Technol* 53:3999–4000
- Seidel CJ, McGuire MJ, Summers RS, Via S (2005) *J Am Water Work Assoc* 97(10):87–97
- Semiati R (2000) *Water Int* 25(1):54–65
- Shah AD, Mitch WA (2012) *Environ Sci Technol* 46(1):119–131
- Shah AD, Dotson AD, Linden KG, Mitch WA (2011) *Environ Sci Technol* 45:3657–3664
- Shah AD, Krasner SW, Lee CFT, von Gunten U, Mitch WA (2012) *Environ Sci Technol* 46(9):4809–4818
- Smeets PWMH, Medema GJ, van Dijk JC (2009) *Drink Water Eng Sci* 2:1–14
- Snyder SA, Adham S, Redding AM, Cannon FS, DeCarolis J, Oppenheimer J, Wert EC, Yoon Y (2007) *Desalination* 202(1–3):156–181
- Song L, Chen W, Peng L, Wan N, Gan N, Zhang X (2007) *Water Res* 41:2853–2864
- Souliotis VL, Henneman JR, Reed CD, Chhabra SK, Diwan BA, Anderson LM, Kyrtopoulos SA (2002) *Mutat Res Fundam Mol Mech Mutagen* 500(1–2):75–87
- Stikker A (2002) *Water Policy* 4:47–55
- Stroom JM, Kardinaal WEA (2016) *Aquat Ecol* 50(3):541–576
- Summers RS, Benz MA, Shukairy MH, Cummings L (1993) *J Am Water Work Assoc* 85(1):88–95
- Summers RS, Knappe DRU, Snoeyink VL (2010) *Water quality and treatment*. American Water Works Association McGraw-Hill, New York
- Sun Y, Chen Z, Wu G, Wu Q, Zhang F, Niu Z, Hu HY (2016) *J Clean Prod* 131:1–9
- Sutherland IW (1985) *Ann Rev Microbiol* 39:243–270
- Symons JM (1975) National organics reconnaissance survey. Preliminary assessment of suspected carcinogens in drinking water (Appendices). Washington, DC
- Symons JM, Krasner SW, Simms LA, Sclimenti M (1993a) *Am Water Work Assoc* 85(1):51–62
- Symons JM, Krasner SW, Simms LA, Sclimenti MJ (1993b) *J Am Water Work Assoc* 85(1):51–62
- Szczuka A, Parker KM, Harvey C, Hayes E, Vengosh A, Mitch WA (2017) *Water Res* 122:633–644
- Szczuka A, Berglund-Brown JP, Chen HK, Quay AN, Mitch WA (2019) *Environ Sci Technol* 53(6):3166–3176
- Taguchi V, Jenkins SDW, Wang DT, Palmentier JPPF, Reiner EJ (1994) *Can J Appl Spectrosc* 39(3):87–93
- Tang CY, Fu QS, Robertson AP, Criddle CS, Leckie JO (2006) *Environ Sci Technol* 40(23):7343–7349
- Tardiff RG, Carson ML, Ginevan ME (2006) *Regul Toxicol Pharmacol* 45(2):185–205
- Ternes TA, Stüber J, Herrmann N, McDowell D, Ried A, Kampmann M, Teiser B (2003) *Water Res* 37(8):1976–1982
- Trebe P, Polyakova OV, Baranova M, Kralj MB, Dolenc D, Sarakha M, Kutin A, Lebedev AT (2016) *Water Res* 101:95–102
- Trueman BF, Krkosek WH, Gagnon GA (2018) *Environ Sci Water Res* 4:505–512
- US Environmental Protection Agency (2006) *Fed Regist* 71:388–493
- Vengosh A (2014) *Salinization and saline environments*, 2nd edn. Elsevier Ltd
- von Gunten U (2003a) *Water Res* 37:1443–1467
- von Gunten U (2003b) *Water Res* 37:1469–1487
- Wagner ED, Plewa MJ (2017) *J Environ Sci* 58:64–76
- Wang C, Shang C, Ni M, Dai J, Jiang F (2012a) *Environ Sci Technol* 46(17):9398–9405
- Wang Z, Kim J, Seo Y (2012b) *Environ Sci Technol* 46(20):11361–11369
- Wang J, Liu X, Wai T, Xiao J, Chow AT, Keung P (2013) *Water Res* 47(8):2701–2709
- Wang W, Qian Y, Li J, Moe B, Huang R, Zhang H, Hrudey SE, Li XF (2014) *Anal Chem* 86(10):4982–4988
- Washington State Department of Health. Alternate Disinfectants. <https://www.doh.wa.gov/CommunityandEnvironment/DrinkingWater/Disinfection/DisinfectionByproducts/DisinfectantsandDisinfectionByproducts/AlternateDisinfectants>. Accessed May 27, 2019
- Wei Y, Liu Y, Zhang Y, Dai R, Liu X, Wu J, Zhang Q (2011) *Environ Sci Pollut Res* 18:46–50
- Westerhoff P, Mash H (2002) *J Water Supply Res Technol AQUA* 51(8):415–448
- Westerhoff P, Chao P, Mash H (2004) *Water Res* 38(6):1502–1513
- World Health Organization (2017) *Guidelines for drinking-water quality: incorporating the first addendum*, 4th edn. WHO Press, Geneva, Switzerland
- World Health Organization (2009) *Global health risks: mortality and burden of disease attributable to selected major risks*. WHO Press, Geneva, Switzerland
- World Health Organization, UNICEF (2017) *Main report progress on drinking water, sanitation and hygiene: 2017 update and SDG baselines*
- Yang M, Liberatore HK, Zhang X (2019) *Curr Opin Environ Sci Heal* 7:98–107
- Zahrn S, Mcelmurry SP, Kilgore PE, Mushinski D, Press J, Love NG, Sadler RC, Swanson MS (2018) *Proc Natl Acad Sci* 115(25):5835
- Zeng T, Plewa MJ, Mitch WA (2016) *Water Res* 101:176–186
- Zhang Y, Chu W, Yao D, Yin D (2017) *J Environ Sci* 58:322–330
- Zhao Y, Boyd J, Hrudey SE, Li X-F (2006) *Environ Sci Technol* 40(24):7636–7641
- Zhao Y-Y, Boyd JM, Woodbeck M, Andrews RC, Qin F, Hrudey SE, Li X-F (2008) *Environ Sci Technol* 42(13):4857–4862
- Zhao Z, Zuo J, Zillante G (2017) *J Clean Prod* 163:136–145
- Ziervogel G (2019) *Unpacking the Cape Town drought: lessons learned*

# Plastic and Microplastic Pollution: From Ocean Smog to Planetary Boundary Threats

Liang-Ying Liu, Lei Mai, and Eddy Y. Zeng

## Abstract

Plastics and microplastics (MPs) are emerging pollutants which have become a global environmental issue. They are abundant in oceanic and terrestrial environments, undergoing bioaccumulation and trophic transfer and potentially harming the entirety of mankind. Microplastics in the environment may be transferred to humans via different pathways, such as dietary intake and inhalation. This chapter summarizes the occurrences of MPs in seawaters, sediments, freshwaters, bivalves, and atmospheric fallouts. Generally, the spatial distribution of plastics and MPs in seawaters suggested that higher levels were found in areas which are closer to lands. Similarly, high levels of MPs in freshwaters, sediments, and aquatic organisms were associated with intensified human activities. The occurrences of MPs in bivalves from around the globe suggested a potential human exposure via dietary intake. Moreover, trophic transfer of MPs under controlled conditions suggested that MPs can be transferred to organisms at higher trophic levels. Plastics and MPs were found in atmospheric fallouts from urban, suburban, and remote mountain sites, suggesting the potential for long-range atmospheric transport of MPs. This chapter provides the reader with a snapshot of the plastic and MP pollution in the global oceans and planetary boundaries. Future studies are desirable for examining the exposure pathways, mechanisms of toxicity, and possible health effects.

## 1 Introduction

Plastic products have provided unprecedented socio-economic benefits. The global demand for plastics has been rising consistently. The United Nations Environment Programme (UNEP) estimated that the production of plastics would reach 2000 million tons by 2050 if no action was taken to avert the trends of production and usage of plastic products. Meanwhile, plastic waste has become another emerging global environmental issue. They are widespread in a variety of environmental compartments, including seawater, marine sediment, marine organisms, terrestrial freshwater, soil, and seafood among others. Historical lessons remind us that anthropogenically discharged pollutants will always find their way back to human bodies and pose potential adverse effects to human health, and plastic waste is no exception.

Large plastics debris discharged to the environment can be fragmented into smaller particles through physical, chemical, or biological processes, and those with aerodynamic diameters smaller than 5 mm are commonly defined as microplastics (MPs) (Andrady 2011; Cole et al. 2011; Duis and Coors 2016). Microplastic particles are also manufactured for use in facial cleansers, drilling fluids, and industrial abrasives (Cole et al. 2011; Fendall and Sewell 2009). Numerous studies have demonstrated the occurrences of MPs in edible seafood and freshwater organisms (e.g., fish and bivalves), table salts, atmospheric fallout, and indoor and outdoor air. Dietary ingestion and inhalation are two of the main exposure pathways. Microplastic pollution is by no means a micro issue; it is an issue not only with global oceans but also with the Earth's planetary boundary, threatening the entire mankind. It should be noted that MPs can be further degraded to nano-sized particles (thereby defined as nanoplastics) under multiple processes, such as UV photodegradation (Song et al. 2017), bio-fragmentation (Dawson et al. 2018), and mechanical abrasion (Lambert and

L.-Y. Liu · L. Mai · E. Y. Zeng (✉)  
Guangdong Key Laboratory of Environmental Pollution and Health, Jinan University, Guangzhou, 510632, China  
e-mail: eddyzeng@jnu.edu.cn

Wagner 2016). Therefore, MPs, and nanoplastics to a lesser extent, are also an important part of the plastic pollution.

This chapter consists of four parts. Firstly, the occurrences and abundances of plastics and MPs in marine (water and sediment) and freshwater (rivers and lakes) systems are summarized. Secondly, the occurrences of MPs in seafood (especially bivalves) and the current knowledge about trophic transfer are assimilated. Thirdly, available data on the occurrences of MPs in the atmosphere and the long-range atmospheric transport potential of MPs are discussed. Finally, a short section of nanoplastics in the environment is presented. The chapter is intended to provide the reader with a snapshot of the plastic and MP pollution in the global oceans and planetary boundaries.

## 2 Plastic and Microplastic Pollution in Global Oceans and Freshwater Systems

**State of plastic and microplastic pollution.** Plastics are synthetic polymers with a variety of beneficial properties to human daily life. Plastics can be made into different products, such as bags, bottles, and bowls among many others. The most commonly used plastic types are polyethylene (PE) (including low-density polyethylene and high-density polyethylene), polypropylene (PP), polyvinyl chloride (PVC), polystyrene (PS), and polyethylene terephthalate (PET). These five types of plastics account for 90% of the total plastic production. Unsupervised disposed plastic litters can be transported to areas far away from human settlements, such as oceans. Three scientific reports about plastic pollutions in marine waters were published in *Science* (Carpenter et al. 1972; Carpenter and Smith 1972; Jr et al. 1974) in the early 1970, and the concentrations of plastics in coastal water ranged from 0 to 14 pieces  $\text{m}^{-3}$  (Carpenter et al. 1972). More than 20 years later, Moore et al. (2001) conducted sampling of plastics from the surface water of the North Pacific Central Gyre (NPCG) using a manta trawl with 0.33 mm mesh. Strikingly large amounts of plastic debris were found in the NPCG area, with a number concentration of 334,000 pieces  $\text{km}^{-2}$  and a mass concentration of 5000 g  $\text{km}^{-2}$  (Moore et al. 2001). Later, the invasion of anthropogenic plastic debris to marine life was reported (Barnes 2002). Since then, plastic pollution has gained increasing concern from around the world. Unsupervised disposal of plastic litters has resulted in the widespread occurrences of plastics in various environmental compartments, including marine oceans, freshwater systems, aquatic organisms, and human feces. It is estimated that plastic litters consist of 10% of the total municipal waste. Approximately 50–80% of plastic wastes end up in marine water, marine sediment, and beaches. News media have reported many shockingly serious environmental accidents involving

plastics. One recent but not the last example is a young whale died with 88 lb of plastic debris in its stomach. Briefly, a dying curvier beaked whale in the Davao Gulf was brought back to a laboratory for a necropsy at the D’Bone Collector Museum. Eighty-eight pounds of plastics were pulled out of its stomach, including plastic bags, snack bags, and big tangles of nylon ropes. Undoubtedly, plastic pollution has become one of the most serious environmental problems around the world.

The name “microplastics” first appeared in scientific literature when Thompson et al. (2004) reported “*Lost at sea: Where is all the plastic?*” in a paper published in *Nature*. Since then, the number of publications on MPs has been growing rapidly, and MPs have become a hot topic in recent years. There are currently more than a thousand of scientific articles concerning MPs have been published worldwide, and the number is continuously rising (Fig. 1).

**Plastic and microplastic pollution in ocean waters.** Terrestrial and maritime human activities are two main input sources of plastics in the oceans (Auta et al. 2017; Ivar do Sul and Costa 2014). Plastics intensely accumulated in the oceans are largely exported from terrestrial anthropogenic discharges (Jambeck et al. 2015). Plastics transported to coastal waters can be further dissipated to the marine environment (including remote oceanic areas) under the effects of wind and ocean currents (Allen et al. 2019; Ivar Do Sul et al. 2014). Generally, plastics with density lower than seawater (e.g., polypropylene, polyethylene, and extruded polystyrene) can float on surface water, while those with density higher than seawater (e.g., polyvinyl chloride and polyethylene terephthalate) sink to the sediment. Therefore, plastics have been found widely in ocean waters and sediments around the globe (Auta et al. 2017). Plastics were prevalently found in the surface water of the global oceans,

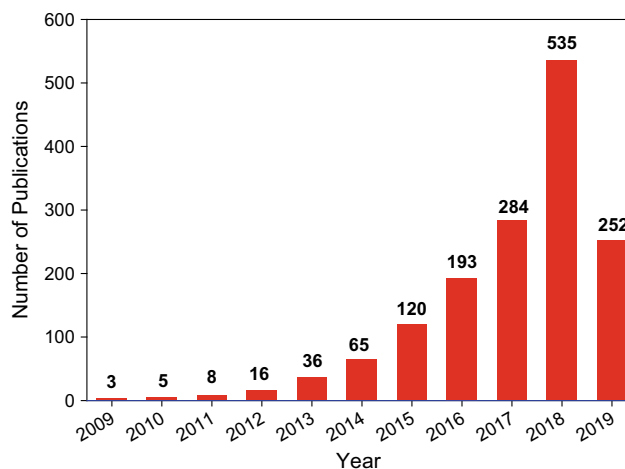


**Fig. 1** Number of publications on microplastics in the last 10 years by searching with the keywords “microplastics” and “environment” on the Web of Science (updated to April 30, 2019)

with an estimated loading ranging from 7000 to 250,000 tons (Cózar et al. 2014; Eriksen et al. 2014). Plastics have also been found in the Pacific Oceans (Eriksen et al. 2014; Goldstein et al. 2012), the North Atlantic Ocean (Barnes et al. 2009), and the Arctic Ocean which is supposed to be the dead end of floating plastic debris (Cózar et al. 2017). The Mediterranean Sea is a hotspot of plastic pollution because it is an inner sea surrounded by urbanized regions. A large number of publications reported the occurrence of plastics/MPs in the Mediterranean Sea (Collignon et al. 2012; Güven et al. 2017; Pedrotti et al. 2016; Suaria et al. 2016). Under the effects of ocean currents, these plastics may reach the North Atlantic Ocean through the Gibraltar Strait.

Here, data on plastic pollution in coastal and oceanic waters are summarized. Different sampling methods (Song et al. 2014; Tamminga et al. 2018) were applied to acquire the data on plastic particles. To maintain a consistent comparison of different datasets, only the results derived from the use of surface trawling nets as sampling devices are assimilated (Fig. 2). In general, the concentrations of plastics in oceanic waters varied widely as a function of distance from land to sampling sites. Higher concentrations were found in areas closer to human settlements (Pedrotti et al. 2016). The distribution patterns of plastics in marine surface

water may vary under the influences of wind and ocean currents, resulting in the accumulation of plastics in the ocean gyres (Morét-Ferguson et al. 2010). Cózar et al. (2014) demonstrated that the plastic concentrations in the five subtropical gyres were much higher than those in other oceanic areas.

Concentrations of MPs in coastal marine waters are generally higher than those in open oceans (Fig. 2). For example, in the surface water of the northern Gulf of Mexico, concentrations of MPs were 4.8–8.2 particles  $m^{-3}$  (Di Mauro et al. 2017), which were higher than those found in the Western Tropical Atlantic Ocean (0.015–0.04 particles  $m^{-3}$ ) (Ivar Do Sul et al. 2014). It was a surprise to observe that the concentrations of plastics in Baltic Sea decreased gradually from 0.3–2.1 particles  $m^{-3}$  in 2016 to 0.29 particles  $m^{-3}$  in 2017 and  $0.07 \pm 0.02$  particles  $m^{-3}$  in 2018 (Gewert et al. 2017; Setälä et al. 2016; Tamminga et al. 2018). This can be explained by the implementation of regulations and management measures for plastic wastes, as an international pact, “*Global Declaration for Solutions on Marine Litter*”, was signed by many countries in the world (PlasticsEurope 2017).

**Plastic and microplastic pollution in freshwaters.** Plastic pollution is undoubtedly correlated to anthropogenic activities. Understanding the occurrences of different plastic types

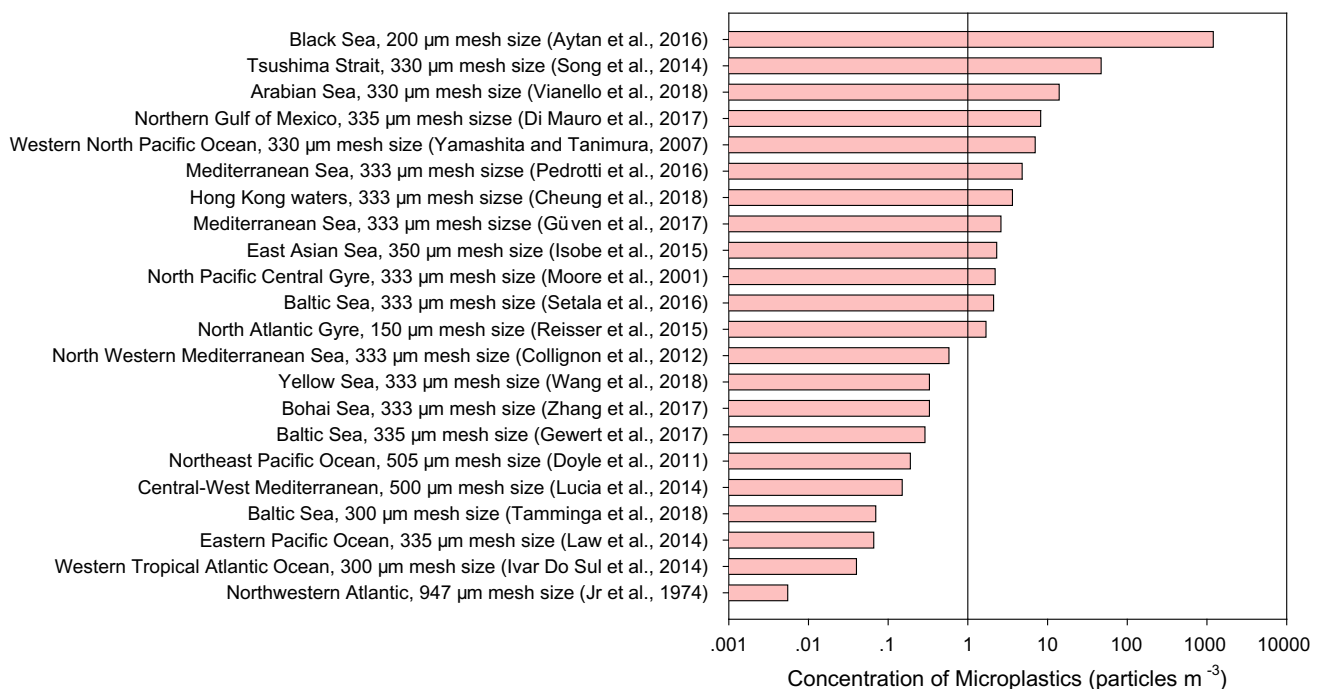


**Fig. 2** Concentrations (particles  $m^{-3}$ ) of microplastics in global seawaters. Values reported as particles  $km^{-2}$  by some studies are divided by the trawl height and converted to particles  $m^{-3}$ . Mean values are used for those reported as mean  $\pm$  standard deviations, whereas the upper values are adopted for those reported as a concentration range. Data are summarized from the literature (Aytan et al. 2016; Cheung

et al. 2018; Collignon et al. 2012; Di Mauro et al. 2017; Doyle et al. 2011; Güven et al. 2017; Gewert et al. 2017; Isobe et al. 2015; Ivar Do Sul et al. 2014; Jr et al. 1974; Kai et al. 2017; Law et al. 2014; Lucia et al. 2014; Moore et al. 2001; Pedrotti et al. 2016; Reisser et al. 2015; Setälä et al. 2016; Song et al. 2014; Tamminga et al. 2018; Vianello et al. 2018; Wang et al. 2018; Yamashita and Tanimura 2007)

in freshwater systems, such as rivers and lakes, is important for examining the transport and fate of plastics in the environment. Plastics in freshwater systems can be transported to coastal waters and undergo global cycling under the impacts of ocean currents. Riverine input is one of the most important pathways to transport terrestrial plastic wastes to the oceans. Based on the concept of Mismanaged Plastic Waste (Jambeck et al. 2015), the annual riverine flux of plastics was estimated to be 1.15–2.41 million tons (Lebreton et al. 2017) and 0.47–2.75 million tons (Schmidt et al. 2017), respectively. Under extreme weather conditions, for example, flood, the amount of plastics exported from rivers may increase due to resuspension of sedimentary plastics (Hurley et al. 2018). Apparently, field measurements of riverine plastic inputs, even for a selected number of rivers around the world, are urgently needed to validate the model estimates.

Microplastic pollution in riverine or estuarine waters has been prevalently reported. The concentrations of MPs varied in three orders of magnitude among different regions (Fig. 3), ranging from 0.028 particles  $m^{-3}$  in the Tamar Estuary (Sadri and Thompson 2014) to 817 particles  $m^{-3}$  in

the Coyote Creek (Moore et al. 2011), and were in the range of 0.17–0.74 particles  $m^{-3}$  in the surface waters of four rivers in Chile (Rech et al. 2015). The concentrations of MPs also varied in one order of magnitude within Illinois River in the United States, with the mean concentration in downstream areas ( $18 \pm 11$  particles  $m^{-3}$ ) 10 times higher than that in upstream areas ( $1.94 \pm 0.81$  particles  $m^{-3}$ ) (McCormick et al. 2014), indicating preferable accumulation of MPs in the downstream areas of a river. The mean concentration of MPs in the Geneva part (0.29 particles  $m^{-3}$ ) of Rhone River was twice that (0.13 particles  $m^{-3}$ ) in the Chancy part (Faure et al. 2015). As the Rhone River flows through different cities in Switzerland, the spatial difference in MP concentrations was probably attributable to the difference in the intensities of regional anthropogenic activities.

The correlation between MP concentrations in Japanese rivers and regional population density and urbanization was analyzed to illustrate the influences of regional anthropogenic activities on the spatial distribution patterns of MPs (Kataoka et al. 2019). The results suggested that both population density and urbanization were positively and significantly correlated with MP concentrations in river water

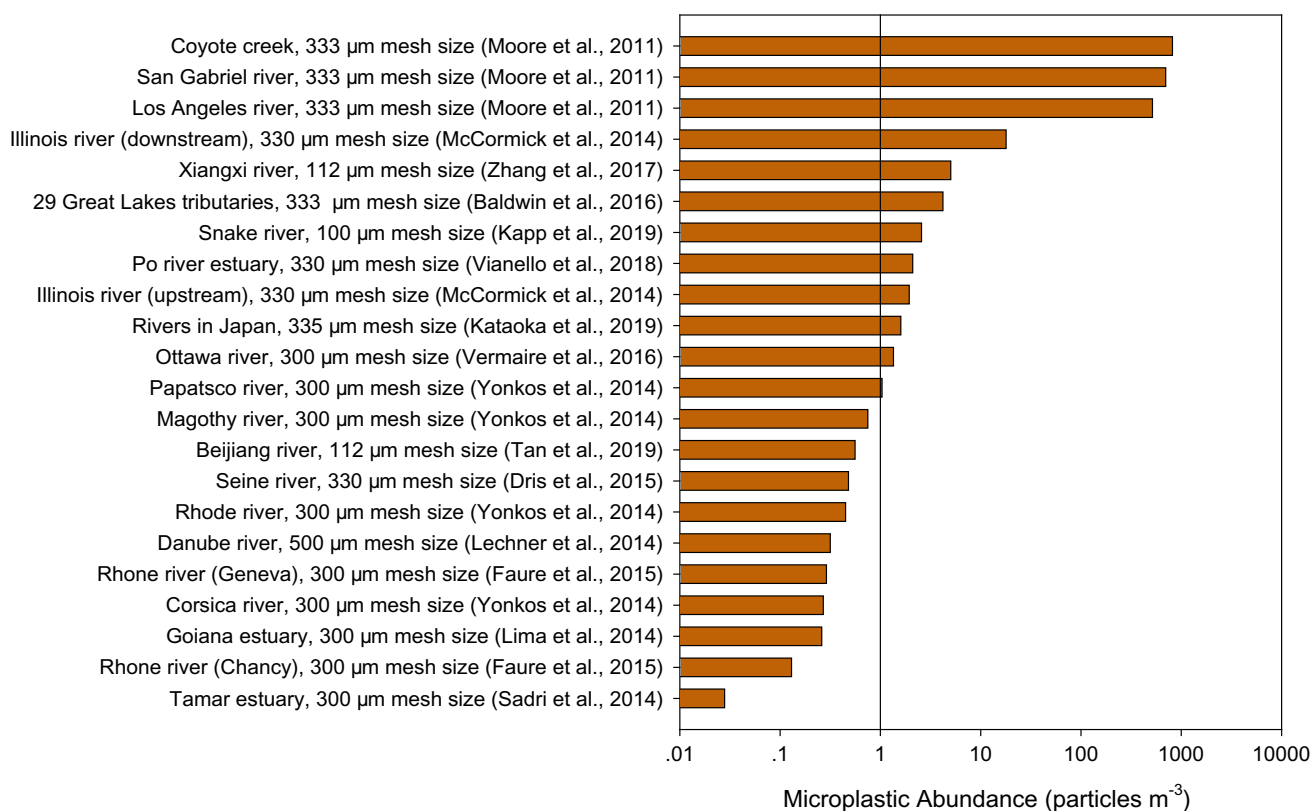


**Fig. 3** Concentrations (particles  $m^{-3}$ ) of microplastics in freshwaters around the globe. Values reported as particles  $km^{-2}$  by some studies are divided by the trawl height and converted to particles  $m^{-3}$ . Mean values are used for those reported as mean  $\pm$  standard deviations, whereas the upper values are adopted for those reported as a concentration range.

Data are summarized from the literature (Dris et al. 2015; Faure et al. 2015; Kapp and Yeatman 2018; Kataoka et al. 2019; Lechner et al. 2014; Lima et al. 2014; Sadri and Thompson 2014; Tan et al. 2019; Vermaire et al. 2017; Vianello et al. 2018; Yonkos et al. 2014; Zhang et al. 2017)

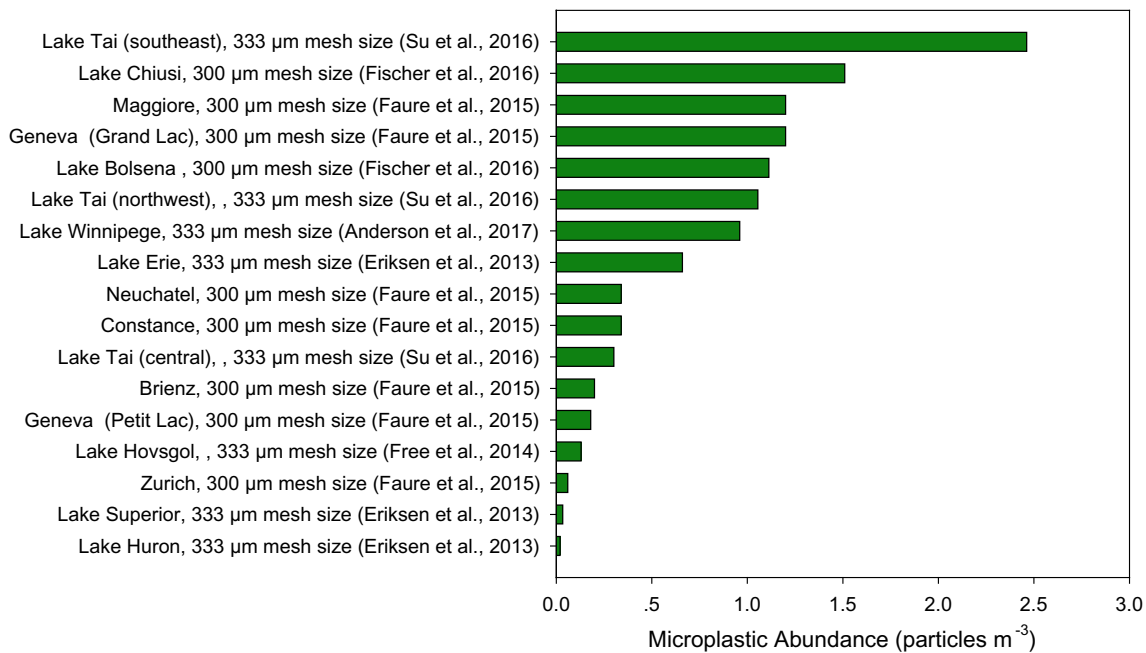


**Fig. 4** Concentrations (particles m<sup>-3</sup>) of microplastics in lake surface water. Values reported as particles km<sup>-2</sup> by some studies are divided by the trawl height and converted to particles m<sup>-3</sup>. Mean values are used for studies reported as mean ± standard deviations, whereas the upper

values are adopted for those reported as a concentration range. Data are summarized from the literature (Anderson et al. 2017; Eriksen et al. 2013; Faure et al. 2015; Fischer et al. 2016; Su et al. 2016)

(Kataoka et al. 2019). This finding was also corroborated by a field measurement of MPs in waters of 29 Great Lakes tributaries (Baldwin et al. 2016). These results have confirmed the effects of anthropogenic activities in river catchments on the spatial distribution patterns of riverine MPs. Besides regional anthropogenic activity, other factors such as climate conditions may also impact the spatial distribution of MPs. For example, the concentration of MPs in the Venoge River was 64 particles m<sup>-3</sup> in the wet weather season, 10 times higher than that (6.5 particles m<sup>-3</sup>) in the dry weather season (Faure et al. 2015).

Freshwater lakes are generally drinking water sources for local residents, but they also receive plastic waste generated from human activities. The concentrations of MPs in lake surface water varied greatly (Fig. 4), with the mean values ranging from 0.02 particles m<sup>-3</sup> in Lake Huron of North America (Eriksen et al. 2013) to 2.46 particles m<sup>-3</sup> in Lake Tai of China (Su et al. 2016). Su et al. (2016) found that MP concentrations were lower in the lake center than those close to residential areas, further demonstrating the importance of human activities to microplastic pollution in the environment. Faure et al. (2015) collected water samples from both rivers and lakes in Switzerland, and obtained MP concentrations of 7 ± 0.2 and 0.5 ± 0.67 particles m<sup>-3</sup> in river and lake waters, respectively.

A summary of the current literature (Fig. 5) suggested that MP concentrations were lower in lake waters than those

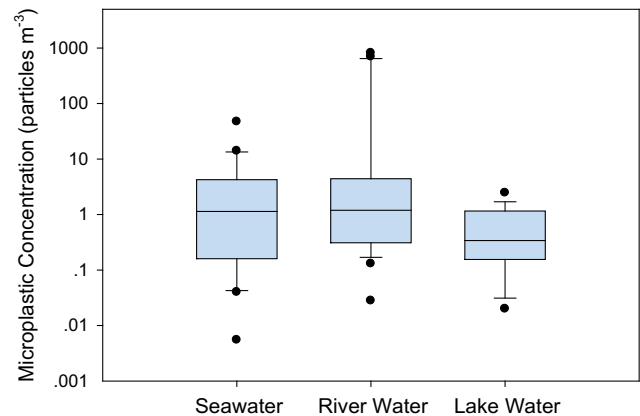


**Fig. 5** Comparison of microplastic concentrations (particles m<sup>-3</sup>) in surface waters of seas/oceans, rivers, and lakes. Median, 25th, and 75th percentiles are presented in the boxplots

in seawaters and river waters. Comparable (*t*-test; *p* > 0.05) concentrations of MPs were found in seawaters and river waters, indicating little dilution effects between seawaters and river waters. Seawater receives pollutants not only from rivers but also from coastal discharge. Coastal seas are considered as a sink of land-based plastic wastes because of long-term accumulation (Browne et al. 2011). However, dilution effects have been observed in lakes. For example, the average MP concentration in the surface water of 29 tributaries of the Great Lakes (3.8 particles m<sup>-3</sup>) (Baldwin



et al. 2016) was much greater than that in Lake Erie (0.66 particles  $m^{-3}$ ), a receiving waterbody (Eriksen et al. 2013). This dilution effect was likely to result from the limited accumulation ability of lake water and low discharge from the tributaries.

**Plastic and microplastic pollution in sediment.** Sediment serves as a reservoir for anthropogenic pollutants, including plastics. Plastics have been found in beach and bottom sediment (Lo et al. 2018; Vaughan et al. 2017; Zobkov and Esiukova 2017), and even in deep-sea sediment (van Cauwenberghe et al. 2013). Plastics in beach sediment are directly exposed to UV light, which facilitates the fragmentation of plastics in to smaller particles (Song et al. 2017). Microplastic pollution in beach sediment was reported as early as in the 1970s, and became the main focus of plastic research soon after (Gregory 1978). Numerous studies suggested that beach areas with intensified human activities were highly contaminated with plastic wastes (Abu-Hilal and Al-Najjar 2009; Browne et al. 2011; Jang et al. 2014; Lo et al. 2018; Lozoya et al. 2016). For example, high abundance of plastic particles (100,000 particles  $m^{-2}$ ) was found in New Zealand beaches, which were supposed to primarily derive from local plastic industries and harbor transports (Gregory 1978). Owing to the complex nature of interactions between beaches and seawater, it is difficult to track the sources of plastic debris found in beach sediment.

Similarly, sediment has also become an important sink of MPs. In St. Lawrence River sediment, the median concentration of MPs was 52 particles  $m^{-2}$ , with the most frequently observed particle sizes in the range of 0.5–1.0 mm (Castañeda et al. 2014). A mean abundance of 253 particles  $m^{-2}$  was reported in the estuarine sediment of Vembanad

Lake in India (Sruthy and Ramasamy 2017). If a sediment sampling area is not measured, MP concentrations are reported in particles per kilogram dry weight sediment. In a UK urban lake, the maximum concentrations of sediment MPs reached 250–300 particles  $kg^{-1}$  (Vaughan et al. 2017). In the Lagoon of Venice (Italy), abundances of sediment MPs ranged from 670 to 2170 particles  $kg^{-1}$  (Vianello et al. 2013).

Various techniques have been used to sample and analyze MPs in sediment. Therefore, it is a challenge to compare the concentrations of MPs reported by different studies. The units used have also been inconsistent among different studies, for example, particles  $m^{-2}$  and particles  $kg^{-1}$ . Some MP data in particles per kg dry weight sediment are depicted in Fig. 6. Slightly (but not significantly) higher ( $t$ -test;  $p > 0.05$ ) sediment MP concentrations were found in Asia than in Europe. Extremely low MP concentrations occurred in sediment of North Sea islands of Norderney (1.3–2.3 particles  $kg^{-1}$ ) (Dekiff et al. 2014). Graca et al. (2017) reported that MP abundance in sediment of an urbanized bay (53 particles  $kg^{-1}$ ) was higher than that in open sea beach (25 particles  $kg^{-1}$ ), consistent with increased MP abundances by anthropogenic events. One order of magnitude difference in the concentrations of MPs ( $1100 \pm 983$  and  $108 \pm 55$  particles  $m^{-2}$ ) was found between the northern and southern shores of Lake Garda (Imhof et al. 2013). In short, direct comparison of sediment MP concentrations through different studies is quite challenging, as different methods for sampling, extraction, and analysis have been used. Standardization of existing (and future) sampling and analytical protocols is a critical step toward better research on MPs.

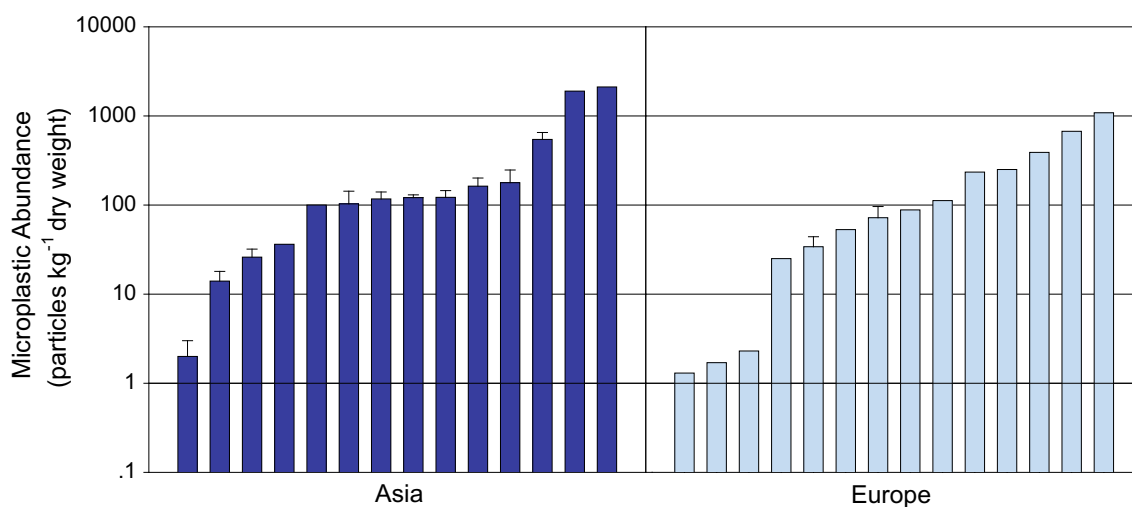


**Fig. 6** Comparison of microplastic abundances (particles  $kg^{-1}$  dry weight sediment) measured in freshwater sediments (including lakeshore/riverbank and bottom sediments) from Asia and Europe

### 3 Microplastics in Food

**Microplastics in bivalves.** Microplastics in both marine and freshwater systems can be ingested by aquatic organisms and undergo trophic transfer through the food chain. Bivalves are particularly of health concern because they accumulate and retain MP particles due to the lack of intact gastrointestinal tracts. Consumption of MPs-contaminated bivalves poses potential health risks to humans. Numerous studies reported the occurrences of MPs in bivalves from around the globe. Li et al. (2015) investigated MP pollution in nine commercial bivalves from a fishery market in China. The average number of MPs in these bivalves ranged from 2.1 to 10.5 items  $g^{-1}$  (Li et al. 2015). The abundance of MPs, obtained in mussels (*Mytilus edulis*) from 22 sites along the 12,400-mile coastlines of China, was significantly higher in areas with higher human impacts (3.3 items  $g^{-1}$ ) than that (1.6 items  $g^{-1}$ ) with less human impacts (Li et al. 2016). The number of MP particles in mussels along the coast of China (0.9–4.6 items  $g^{-1}$ ) (Li et al. 2016) was lower than that in commercial bivalves (2.1–10.5 items  $g^{-1}$ ) (Li et al. 2015).

The average abundance of MPs detected in *M. edulis* from Germany and in *Crassostrea gigas* from France was 0.36 and 0.47 items  $g^{-1}$ , respectively (Van Cauwenberghe and Janssen 2014). The abundance of MPs in mussels (*M. edulis*) from Belgium ranged from 0.26 to 0.51 items  $g^{-1}$  (De Witte et al. 2014). The occurrences of MPs in mussels (*M. edulis*) and lugworms (*Arenicola marina*) living in

natural habitats located along the French-Belgium-Dutch coastline were  $0.2 \pm 0.3$  and  $1.2 \pm 2.8$  items  $g^{-1}$ , respectively (Van Cauwenberghe et al. 2015). These concentrations were similar to those found in wild mussels along the Chinese coastline (0.9–4.6 items  $g^{-1}$ ) (Li et al. 2016).

The spatial distribution of MPs in bivalves (Fig. 7) suggested that the concentrations of MPs in bivalves from China were higher than those from the United Kingdom, Belgium, Baltic Sea, and North Sea. This was a preliminary assessment of the spatial distributions of MPs in bivalves from around the world. The types and sizes of MPs and the bivalve species were not taken into consideration. Nevertheless, this assessment did confirm the positive correlation between the abundances of MPs in bivalves and environmental pollution. The abundances of MPs in mussels and water sampled simultaneously were positively correlated ( $p < 0.05$ ) with each other (Qu et al. 2018). Apparently, the occurrence of MPs in bivalves is reflective of the state of contamination in the surrounding environment. Therefore, mussel was proposed as a global bioindicator of coastal MP pollution (Li et al. 2019).

**Trophic transfer of microplastics.** The trophic transfer of MPs and associated contaminants in aquatic systems has considerable implications for human health, especially if consumption of seafood and/or aquatic products is frequent (Carbery et al. 2018). Increasing attention has been paid to the trophic transfer of MPs recently amid the widespread occurrence and ubiquity of MPs in the environment. Two

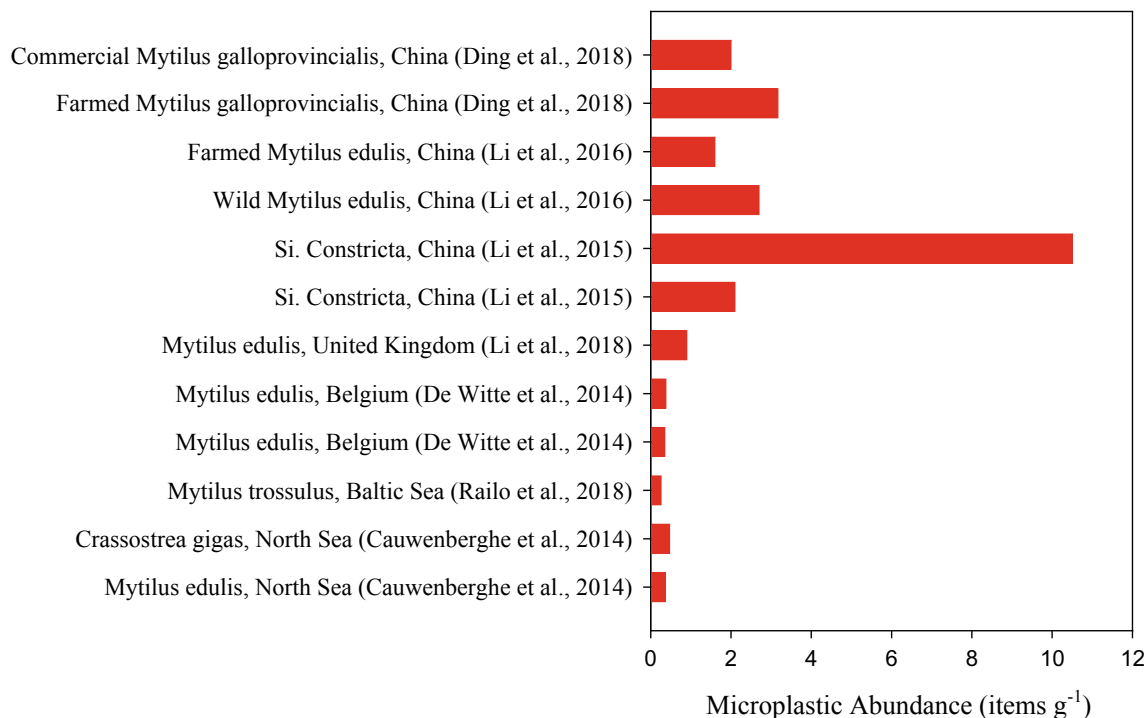


**Fig. 7** Average abundances (items  $g^{-1}$ ) of microplastics in bivalves from around the globe

approaches can be used to study the trophic transfer of MPs. One approach is to build an artificial food chain that allows to examine the trophic transfer of MPs under controlled conditions (Cedervall et al. 2012; Farrell and Nelson 2013). The other approach is to collect target organisms and their predators in a natural system, and MPs are identified and quantified to reconstruct a food chain for further assessment under field scenarios. Few literatures are currently available for the second approach.

Farrell et al. (2013) built a simple food chain, from mussels (*M. edulis*) to crabs (*Carcinus maenas*), and crabs were fed with mussels which were exposed to 0.5  $\mu\text{m}$  fluorescent polystyrene MPs. The abundance of MPs crabs peaked in 24 h after exposure, and decreased to undetectable levels at the end of the sampling period (21 days) (Farrell and Nelson 2013). This study demonstrated that trophic transfer from mussels to crabs occurred and MPs were translocated to the hemolymph, stomach, hepatopancreas, ovary, and gills of the crabs (Farrell and Nelson 2013). Cedervall et al. (2012) built an artificial freshwater food chain, from lower to higher trophic levels, consisting of algae (*Scenedesmus* sp.), zooplankton (*Daphnia magna*), and goldfish (*Carassius carassius*). Polystyrene nanoparticles (24 nm) were fed through this artificial food chain. The time to consume the same amount of zooplankton for exposed fish was twice that of controlled fish (Cedervall et al. 2012). Metabolic effects on exposed fish were also reported, including weight loss, change in the triglycerides/cholesterol ratio of blood serum, and different distribution patterns of cholesterol between muscle and liver (Cedervall et al. 2012).

A variety of Baltic Sea zooplankton taxa, including mysid shrimps, copepods, cladocerans, rotifers, polychaete larvae, and ciliates, were exposed to 10  $\mu\text{m}$  fluorescent polystyrene MPs to investigate the organisms' ability to ingest MPs (Setälä et al. 2014). It was demonstrated that MPs were transferred to mysid shrimp (*Neomysis integer*, *Mysis relicta*, and *Mysis mixta*) through the ingestion of copepods (*Eurytemora affinis*) and polychaete larvae (*Marenzelleria* spp.) exposed to MPs (Setälä et al. 2014). Santana et al. (2017) investigated the potential transfer of MPs through a multi-dimensional food web by exposing brown mussels (*Perna perna*) and 0.1–1  $\mu\text{m}$  PVC microspheres. The exposed mussels were offered to two predators, fish (*Sphoeroides greeley*) and crabs (*Callinectes ornatus*). Microplastics were found to transfer to both predators, but also rapidly depurate (Santana et al. 2017).

Despite the significant advances discussed above, additional studies are needed to comprehensively examine the trophic transfer of MPs, with considerations of particle type, size, age, and so on, as variables. Field studies are also necessary to confirm the trophic transfer potential of MPs under environmentally relevant concentrations and conditions.

## 4 Microplastics in the Atmosphere

Compared to the data on MPs in sediments, seawater, freshwater, bivalves, and fish, data on MPs in the atmosphere are scarce (Allen et al. 2019; Cai et al. 2017; Dris et al. 2015, 2016; Gasperi et al. 2018). Measured concentrations of atmospheric MPs are desirable for evaluating atmospheric deposition and transport, as well as potential health risk associated inhalation of MPs. Several studies have been conducted to measure MP abundances in the atmosphere of Paris (France) (Dris et al. 2015, 2016, 2017) and Dongguan (China) (Cai et al. 2017). Both regions have been subject to heavy anthropogenic impacts. Another study examined the occurrences and characteristics of MPs in atmospheric fallout samples from Pyrenees, a remote and pristine mountain area. It was estimated that atmospheric transport of MPs can reach a distance of 95 km (Allen et al. 2019).

Dris et al. (2016) continuously collected total atmospheric fallout (TAF), including dry and wet deposition, on building roofs at one urban and one suburban site in Paris. During the periods of one year at the urban site and 6 months at the suburban site, the atmospheric fallout of MPs ranged from 2 to 355 fibers  $\text{m}^{-2} \text{d}^{-1}$ . Generally, the TAF fluxes of MPs were higher at the urban site than at the suburban site, consistent with the difference in population density between the two areas (Dris et al. 2016). In addition, TAF of MPs during the wet weather periods was always substantially greater than that during the dry weather periods, suggesting that rainfall was an important factor influencing the atmospheric fallout fluxes of MPs (Dris et al. 2016). Dris et al. (2017) also investigated the occurrence of fibers in indoor and outdoor air, as well as indoor dust within a dense urban area of Paris. Outdoor air was sampled at the same office site where TAF monitoring took place. Indoor and outdoor air was pumped onto quartz fiber filters (1.6 mm) at a flow rate of 8  $\text{L min}^{-1}$ . Overall, MP concentrations in indoor air (1.0–60 fibers  $\text{m}^{-3}$ ) were significantly higher than those in outdoor air (0.3–1.5 fibers  $\text{m}^{-3}$ ) (Dris et al. 2017). The deposition rate of fibers in the indoor environment ranged from 1586 to 11,130 fibers  $\text{m}^{-2} \text{d}^{-1}$ , and MP concentrations in indoor dust ranged from 190 to 670 fibers  $\text{mg}^{-1}$  (Dris et al. 2017). Chemical characterization demonstrated that 29% of the fibers evaluated in TAF were plastic, with the majority being of cellulosic or natural origin (Dris et al. 2016), and that 67% of indoor fibers were naturally originated (primarily cellulosic) (Dris et al. 2017).

The concentrations of MPs ranged from 175 to 313 particles  $\text{m}^{-2} \text{d}^{-1}$  in atmospheric fallout collected from three sites of an air monitoring system in Dongguan Environmental Monitoring Central Station from October to December in 2016 (Cai et al. 2017). Visual observation

indicated that fiber was the dominant shape of suspected MP particles (Cai et al. 2017), similar to the result for MPs in the atmosphere of Paris (Dris et al. 2016). The chemical compositions of fibers and other suspected MPs in atmospheric fallout from Dongguan identified by  $\mu$ -Fourier transform infrared spectroscopy ( $\mu$ -FTIR) mainly included PE, PP, PS, and cellulose (Cai et al. 2017). Besides, there were a variety of MP shapes such as fiber, foam, fragment, and film.

Although the density of all MP types is higher than that of air, they may still be able to undergo atmospheric transport. Allen et al. (2019) suggested that MPs underwent atmospheric transport and reached Pyrenees, France. They collected 10 atmospheric fallout samples with deposition collectors in Pyrenees, France from November 2017 to March 2018 (Allen et al. 2019). Microplastic fragments, fibers, and films were found and confirmed by visual microscopic inspection as well as micro-Raman confocal microscopy in all atmospheric deposition samples collected from the Pyrenees site.

The average daily MP deposition at the Pyrenees site was  $365 \pm 69$  particles  $m^{-2} d^{-1}$  (Allen et al. 2019), with particle sizes  $\geq 5 \mu m$ . The average daily fallouts of MP particles in Paris were  $110 \pm 96$  and  $53 \pm 38$  particles  $m^{-2} d^{-1}$  (Dris et al. 2016, 2017), while that in Dongguan was  $228 \pm 43$  particles  $m^{-2} d^{-1}$  (Cai et al. 2017). Higher MP deposition at the Pyrenees site than at the Paris and Dongguan sites seemed unreasonable because Pyrenees is a remote and pristine, whereas Paris and Dongguan are densely populated. A plausible explanation for this discrepancy is that the sizes of particles counted and analyzed were different among the Pyrenees, Paris, and Dongguan studies. The sizes of particles counted and analyzed were  $\geq 100$  and  $\geq 50 \mu m$  in the two Paris studies,  $\geq 200 \mu m$  in the Dongguan study, and  $\geq 5 \mu m$  in the Pyrenees study. If only particles with sizes  $\geq 200 \mu m$  were counted in the Pyrenees study, the average daily MP deposition was  $40 \pm 20$  particles  $m^{-2} d^{-1}$ , with fibers contributing 70% to the total. The MP deposition at the Pyrenees site was lower but comparable to those of the two megacities (Allen et al. 2019), although the Pyrenees site is notably distant from urban areas.

## 5 Nanoplastics in the Environment

The occurrence of nanoplastics in the environment, either from primary or secondary sources, has rarely been investigated. Ter Halle et al. (2017) reported the presence of nanoplastics in surface water of the North Atlantic Subtropical Gyre, and suggested that modifications to the structures of plastic particles may have occurred during weathering in the environment. Owing to the extreme difficulty in extracting nano-sized plastics from environmental samples, no measurement has been made on environmental

concentrations of nanoplastics. Although the degradation of MPs may result in the formation of secondary nanoplastics, it remains a challenge to accurately quantify nanoplastic concentrations. The high specific surface areas of nanoplastics are perfectly suitable for sorption of toxic chemicals in the environment, potentially facilitating the transport and/or bioaccumulation of environmental contaminants (Liu et al. 2018).

Due to insufficient available information, the ecological risk of nanoplastics is currently considered to be below effect thresholds due to their low environmental mass concentrations (Besseling et al. 2019). However, with plastic waste inputs increasing from all anthropogenic sources, nanoplastics in the aquatic environment may soon become a viable threat to global ecosystems (Wagner and Reemtsma 2019). It was suggested that  $^{13}C$ -labeled polymers can be used to evaluate the environmental behavior of nanoplastics and their potential risks to the ecosystem (Sander et al. 2019). Overall, it remains a great challenge to quantify and track nanoplastics in the environment. Further studies concerning the occurrences, distributions, fate and ecological risks of nanoplastics are much needed.

## References

- Abu-Hilal AH, Al-Najjar TH (2009) Plastic pellets on the beaches of the northern Gulf of Aqaba, Red Sea. *Aquat Ecosyst Health* 12:461–470. <https://doi.org/10.1080/14634980903361200>
- Allen S, Allen D, Phoenix VR, Le Roux G, Durántez Jiménez P, Simonneau A, Binet S, Galop D (2019) Atmospheric transport and deposition of microplastics in a remote mountain catchment. *Nat Geosci* 12:339–344. <https://doi.org/10.1038/s41561-019-0335-5>
- Anderson PJ, Warrack S, Langen V, Challis JK, Hanson ML, Rennie MD (2017) Microplastic contamination in Lake Winnipeg. *Can Environ Pollut* 225:223–231. <https://doi.org/10.1016/j.envpoll.2017.02.072>
- Andrady AL (2011) Microplastics in the marine environment. *Mar Pollut Bull* 62:1596–1605. <https://doi.org/10.1016/j.marpolbul.2011.05.030>
- Auta HS, Emenike CU, Fauziah SH (2017) Distribution and importance of microplastics in the marine environment: a review of the sources, fate, effects, and potential solutions. *Environ Int* 102:165–176. <https://doi.org/10.1016/j.envint.2017.02.013>
- Aytan U, Valente A, Senturk Y, Usta R, Esensoy Sahin FB, Mazlum RE, Agirbas E (2016) First evaluation of neustonic microplastics in Black Sea waters. *Mar Environ Res* 119:22–30. <https://doi.org/10.1016/j.marenvres.2016.05.009>
- Baldwin AK, Corsi SR, Mason SA (2016) Plastic debris in 29 Great Lakes tributaries: relations to watershed attributes and hydrology. *Environ Sci Technol* 50:10377–10385. <https://doi.org/10.1021/acs.est.6b02917>
- Barnes DKA (2002) Invasions by marine life on plastic debris. *Nature* 416:808–809. <https://doi.org/10.1038/416808a>
- Barnes DKA, Galgani F, Thompson RC, Barlaz M (2009) Accumulation and fragmentation of plastic debris in global environments. *Philos Trans R Soc B Biol Sci* 364:1985–1998. <https://doi.org/10.1098/rstb.2008.0205>

- Besseling E, Redondo-Hasselerharm P, Foekema EM, Koelmans AA (2019) Quantifying ecological risks of aquatic micro- and nanoplastic. *Crit Rev Environ Sci Technol* 49:32–80. <https://doi.org/10.1080/10643389.2018.1531688>
- Browne MA, Crump P, Niven SJ, Teuten E, Tonkin A, Galloway T, Thompson R (2011) Accumulation of microplastic on shorelines worldwide: sources and sinks. *Environ Sci Technol* 45:9175–9179. <https://doi.org/10.1021/es201811s>
- Cózar A, Echevarría F, González-Gordillo JJ, Irigoien X, Úbeda B, Hernández-León S, Palma ÁT, Navarro S, García-de-Lomas J, Ruiz A, Fernández-de-Puelles ML, Duarte CM (2014) Plastic debris in the open ocean. *Proc Natl Acad Sci USA* 111:10239–10244. <https://doi.org/10.1073/pnas.1314705111>
- Cózar A, Martí E, Duarte CM, García-de-Lomas J, van Sebille E, Ballatore TJ, Eguíluz VM, González-Gordillo JJ, Pedrotti ML, Echevarría F, Troublé R, Irigoien X (2017) The Arctic Ocean as a dead end for floating plastics in the North Atlantic branch of the thermohaline circulation. *Sci Adv* 3:e1600582. <https://doi.org/10.1126/sciadv.1600582>
- Cai L, Wang J, Peng J, Tan Z, Zhan Z, Tan X, Chen Q (2017) Characteristic of microplastics in the atmospheric fallout from Dongguan city, China: preliminary research and first evidence. *Environ Sci Pollut Res* 24:24928–24935. <https://doi.org/10.1007/s11356-017-0116-x>
- Carbery M, O'Connor W, Palanisami T (2018) Trophic transfer of microplastics and mixed contaminants in the marine food web and implications for human health. *Environ Int* 115:400–409. <https://doi.org/10.1016/j.envint.2018.03.007>
- Carpenter EJ, Anderson SJ, Harvey GR, Miklas HP, Peck BB (1972) Polystyrene spherules in coastal waters. *Science* 178:749–750. <https://doi.org/10.1126/science.178.4062.749>
- Carpenter EJ, Smith KL (1972) Plastics on the sargasso sea surface. *Science* 175:1240–1241. <https://doi.org/10.1126/science.175.4027.1240>
- Castañeda RA, Avlijas S, Simard MA, Ricciardi A (2014) Microplastic pollution in St. Lawrence River sediments. *Can J Fish Aquat Sci* 71:1767–1771. <https://doi.org/10.1139/cjfas-2014-0281>
- Cedervall T, Hansson L-A, Lard M, Frohm B, Linse S (2012) Food chain transport of nanoparticles affects behaviour and fat metabolism in fish. *PLoS ONE* 7:e32254. <https://doi.org/10.1371/journal.pone.0032254>
- Cheung PK, Fok L, Hung PL, Cheung LTO (2018) Spatio-temporal comparison of neustonic microplastic density in Hong Kong waters under the influence of the Pearl River Estuary. *Sci Total Environ* 628–629:731–739. <https://doi.org/10.1016/j.scitotenv.2018.01.338>
- Cole M, Lindeque P, Halsband C, Galloway TS (2011) Microplastics as contaminants in the marine environment: a review. *Mar Pollut Bull* 62:2588–2597. <https://doi.org/10.1016/j.marpolbul.2011.09.025>
- Collignon A, Hecq J-H, Glagani F, Voisin P, Collard F, Goffart A (2012) Neustonic microplastic and zooplankton in the North Western Mediterranean Sea. *Mar Pollut Bull* 64:861–864. <https://doi.org/10.1016/j.marpolbul.2012.01.011>
- Dawson AL, Kawaguchi S, King CK, Townsend KA, King R, Huston WM, Bengtson Nash SM (2018) Turning microplastics into nanoplastics through digestive fragmentation by Antarctic krill. *Nat Commun* 9:1001. <https://doi.org/10.1038/s41467-018-03465-9>
- De Witte B, Devriese L, Bekaert K, Hoffman S, Vandermeersch G, Cooreman K, Robbens J (2014) Quality assessment of the blue mussel (*Mytilus edulis*): comparison between commercial and wild types. *Mar Pollut Bull* 85:146–155. <https://doi.org/10.1016/j.marpolbul.2014.06.006>
- Dekiff JH, Remy D, Klasmeier J, Fries E (2014) Occurrence and spatial distribution of microplastics in sediments from Norderney. *Environ Pollut* 186:248–256. <https://doi.org/10.1016/j.envpol.2013.11.019>
- Di Mauro R, Kupchik MJ, Benfield MC (2017) Abundant plankton-sized microplastic particles in shelf waters of the northern Gulf of Mexico. *Environ Pollut* 230:798–809. <https://doi.org/10.1016/j.envpol.2017.07.030>
- Doyle MJ, Watson W, Bowlin NM, Sheavly SB (2011) Plastic particles in coastal pelagic ecosystems of the Northeast Pacific ocean. *Mar Environ Res* 71:41–52. <https://doi.org/10.1016/j.marenvres.2010.10.001>
- Dris R, Gasperi J, Rocher V, Saad M, Renault N, Tassin B (2015) Microplastic contamination in an urban area: a case study in Greater Paris. *Environ Chem* 12:592–599. <https://doi.org/10.1071/EN14167>
- Dris R, Gasperi J, Saad M, Mirande C, Tassin B (2016) Synthetic fibers in atmospheric fallout: a source of microplastics in the environment? *Mar Pollut Bull* 104:290–293. <https://doi.org/10.1016/j.marpolbul.2016.01.006>
- Dris R, Gasperi J, Mirande C, Mandin C, Guerrouache M, Langlois V, Tassin B (2017) A first overview of textile fibers, including microplastics, in indoor and outdoor environments. *Environ Pollut* 221:453–458. <https://doi.org/10.1016/j.envpol.2016.12.013>
- Duis K, Coors A (2016) Microplastics in the aquatic and terrestrial environment: sources (with a specific focus on personal care products), fate and effects. *Environ Sci Eur* 28:2. <https://doi.org/10.1186/s12302-015-0069-y>
- Eriksen M, Mason S, Wilson S, Box C, Zellers A, Edwards W, Farley H, Amato S (2013) Microplastic pollution in the surface waters of the Laurentian Great Lakes. *Mar Pollut Bull* 77:177–182. <https://doi.org/10.1016/j.marpolbul.2013.10.007>
- Eriksen M, Lebreton LCM, Carson HS, Thiel M, Moore CJ, Borro JC, Galgani F, Ryan PG, Reisser J (2014) Plastic pollution in the world's oceans: more than 5 trillion plastic pieces weighing over 250,000 tons afloat at sea. *PLoS ONE* 9:e111913. <https://doi.org/10.1371/journal.pone.0111913>
- Farrell P, Nelson K (2013) Trophic level transfer of microplastic: *Mytilus edulis* (L.) to *Carcinus maenas* (L.). *Environ Pollut* 177:1–3. <https://doi.org/10.1016/j.envpol.2013.01.046>
- Faure F, Demars C, Wieser O, Kunz M, de Alencastro LF (2015) Plastic pollution in Swiss surface waters: nature and concentrations, interaction with pollutants. *Environ Chem* 12:582–591. <https://doi.org/10.1071/EN14218>
- Fendall LS, Sewell MA (2009) Contributing to marine pollution by washing your face: microplastics in facial cleansers. *Mar Pollut Bull* 58:1225–1228. <https://doi.org/10.1016/j.marpolbul.2009.04.025>
- Fischer EK, Paglialonga L, Czech E, Tamminga M (2016) Microplastic pollution in lakes and lake shoreline sediments—A case study on Lake Bolsena and Lake Chiusi (central Italy). *Environ Pollut* 213:648–657. <https://doi.org/10.1016/j.envpol.2016.03.012>
- Güven O, Gökdağ K, Jovanović B, Kideyş AE (2017) Microplastic litter composition of the Turkish territorial waters of the Mediterranean Sea, and its occurrence in the gastrointestinal tract of fish. *Environ Pollut* 223:286–294. <https://doi.org/10.1016/j.envpol.2017.01.025>
- Gasperi J, Wright SL, Dris R, Collard F, Mandin C, Guerrouache M, Langlois V, Kelly FJ, Tassin B (2018) Microplastics in air: are we breathing it in? *Curr Opin Environ Sci Health* 1:1–5. <https://doi.org/10.1016/j.coesh.2017.10.002>
- Gewert B, Ogonowski M, Barth A, MacLeod M (2017) Abundance and composition of near surface microplastics and plastic debris in the Stockholm Archipelago, Baltic Sea. *Mar Pollut Bull* 120:292–302. <https://doi.org/10.1016/j.marpolbul.2017.04.062>
- Goldstein MC, Rosenberg M, Cheng L (2012) Increased oceanic microplastic debris enhances oviposition in an endemic pelagic insect. *Biol Lett* 8:817–820. <https://doi.org/10.1098/rsbl.2012.0298>
- Graca B, Szewc K, Zakrzewska D, Dołęga A, Szczepłowska-Boruchowska M (2017) Sources and fate of microplastics in marine and beach sediments of the Southern Baltic

- Sea—a preliminary study. *Environ Sci Pollut Res* 24:7650–7661. <https://doi.org/10.1007/s11356-017-8419-5>
- Gregory MR (1978) Accumulation and distribution of virgin plastic granules on New Zealand beaches. *N Z J Mar Fresh* 12:399–414. <https://doi.org/10.1080/00288330.1978.9515768>
- Hurley R, Woodward J, Rothwell JJ (2018) Microplastic contamination of river beds significantly reduced by catchment-wide flooding. *Nat Geosci* 11:251–257. <https://doi.org/10.1038/s41561-018-0080-1>
- Imhof HK, Ivleva NP, Schmid J, Niessner R, Laforsch C (2013) Contamination of beach sediments of a subalpine lake with microplastic particles. *Curr Biol* 23:R867–R868. <https://doi.org/10.1016/j.cub.2013.09.001>
- Isobe A, Uchida K, Tokai T, Iwasaki S (2015) East Asian seas: a hot spot of pelagic microplastics. *Mar Pollut Bull* 101:618–623. <https://doi.org/10.1016/j.marpolbul.2015.10.042>
- Ivar do Sul JA, Costa MF (2014) The present and future of microplastic pollution in the marine environment. *Environ Pollut* 185:352–364. <https://doi.org/10.1016/j.envpol.2013.10.036>
- Ivar Do Sul JA, Costa MF, Fillmann G (2014) Microplastics in the pelagic environment around oceanic islands of the Western Tropical Atlantic Ocean. *Water Air Soil Pollut* 225:1–13. <https://doi.org/10.1007/s11270-014-2004-z>
- Jambeck JR, Geyer R, Wilcox C, Siegler TR, Perryman M, Andrady A, Narayan R, Law KL (2015) Plastic waste inputs from land into the ocean. *Science* 347:768–771. <https://doi.org/10.1126/science.1260352>
- Jang YC, Lee J, Hong S, Lee JS, Shim WJ, Song YK (2014) Sources of plastic marine debris on beaches of Korea: more from the ocean than the land. *Ocean Sci J* 49:151–162. <https://doi.org/10.1007/s12601-014-0015-8>
- Jr CJ, Burns BR, Knapp FD (1974) Plastic particles in surface waters of the northwestern Atlantic. *Science* 185:491–497. <http://www.jstor.org/stable/1738284>
- Kai Z, Xiong X, Hu H, Wu C, Bi Y, Wu Y, Zhou B, Lam KS, Liu J (2017) Occurrence and characteristics of microplastic pollution in Xiangxi Bay of Three Gorges Reservoir, China. *Environ Sci Technol*. <https://doi.org/10.1021/acs.est.7b00369>
- Kapp KJ, Yeatman E (2018) Microplastic hotspots in the Snake and Lower Columbia rivers: a journey from the Greater Yellowstone ecosystem to the Pacific Ocean. *Environ Pollut* 241:1082–1090. <https://doi.org/10.1016/j.envpol.2018.06.033>
- Kataoka T, Nihei Y, Kudou K, Hinata H (2019) Assessment of the sources and inflow processes of microplastics in the river environments of Japan. *Environ Pollut* 244:958–965. <https://doi.org/10.1016/j.envpol.2018.10.111>
- Lambert S, Wagner M (2016) Characterisation of nanoplastics during the degradation of polystyrene. *Chemosphere* 145:265–268. <https://doi.org/10.1016/j.chemosphere.2015.11.078>
- Law KL, Morét-Ferguson SE, Goodwin DS, Zettler ER, Deforce E, Kukulka T, Proskurowski G (2014) Distribution of surface plastic debris in the eastern Pacific Ocean from an 11-year data set. *Environ Sci Technol* 48:4732–4738. <https://doi.org/10.1021/es4053076>
- Lebreton LCM, van der Zwet J, Damsteeg J-W, Slat B, Andrady A, Reisser J (2017) River plastic emissions to the world's oceans. *Nat Commun* 8:15611. <https://doi.org/10.1038/ncomms15611>
- Lechner A, Keckeis H, Lumesberger-Loisl F, Zens B, Krusch R, Tritthart M, Glas M, Schludermann E (2014) The Danube so colourful: a potpourri of plastic litter outnumbers fish larvae in Europe's second largest river. *Environ Pollut* 188:177–181. <https://doi.org/10.1016/j.envpol.2014.02.006>
- Li J, Yang D, Li L, Jabeen K, Shi H (2015) Microplastics in commercial bivalves from China. *Environ Pollut* 207:190–195. <https://doi.org/10.1016/j.envpol.2015.09.018>
- Li J, Qu X, Su L, Zhang W, Yang D, Kolandhasamy P, Li D, Shi H (2016) Microplastics in mussels along the coastal waters of China. *Environ Pollut* 214:177–184. <https://doi.org/10.1016/j.envpol.2016.04.012>
- Li J, Lusher AL, Rotchell JM, Deudero S, Turra A, Brate ILN, Sun C, Shahadat Hossain M, Li Q, Kolandhasamy P, Shi H (2019) Using mussel as a global bioindicator of coastal microplastic pollution. *Environ Pollut* 244:522–533. <https://doi.org/10.1016/j.envpol.2018.10.032>
- Lima ARA, Costa MF, Barletta M (2014) Distribution patterns of microplastics within the plankton of a tropical estuary. *Environ Res* 132:146–155. <https://doi.org/10.1016/j.envres.2014.03.031>
- Liu J, Ma Y, Zhu D, Xia T, Qi Y, Yao Y, Guo X, Ji R, Chen W (2018) Polystyrene nanoplastics-enhanced contaminant transport: role of irreversible adsorption in glassy polymeric domain. *Environ Sci Technol* 52:2677–2685. <https://doi.org/10.1021/acs.est.7b05211>
- Lo H-S, Xu X, Wong C-Y, Cheung S-G (2018) Comparisons of microplastic pollution between mudflats and sandy beaches in Hong Kong. *Environ Pollut* 236:208–217. <https://doi.org/10.1016/j.envpol.2018.01.031>
- Lozoya JP, Teixeira de Mello F, Carrizo D, Weinstein F, Olivera Y, Cedrés F, Pereira M, Fossati M (2016) Plastics and microplastics on recreational beaches in Punta del Este (Uruguay): unseen critical residents? *Environ Pollut* 218:931–941. <https://doi.org/10.1016/j.envpol.2016.08.041>
- Lucia GAD, Caliani I, Marra S, Camedda A, Coppa S, Alcaro L, Campani T, Giannetti M, Coppola D, Cicero AM (2014) Amount and distribution of neustonic micro-plastic off the western Sardinian coast (Central-Western Mediterranean Sea). *Mar Environ Res* 100:10–16. <https://doi.org/10.1016/j.marenvres.2014.03.017>
- McCormick A, Hoellein TJ, Mason SA, Schluep J, Kelly JJ (2014) Microplastic is an abundant and distinct microbial habitat in an urban river. *Environ Sci Technol* 48:11863–11871. <https://doi.org/10.1021/es503610r>
- Moore C, Lattin GL, Zellers AF (2011) Quantity and type of plastic debris flowing from two urban rivers to coastal waters and beaches of Southern California. *J Integr Coastal Zone Manag* 11:65–73. <http://www.redalyc.org/articulo.oa?id=388340132008>
- Moore CJ, Moore SL, Leecaster MK, Weisberg SB (2001) A comparison of plastic and plankton in the North Pacific Central Gyre. *Mar Pollut Bull* 42:1297–1300. [https://doi.org/10.1016/S0025-326X\(01\)00114-X](https://doi.org/10.1016/S0025-326X(01)00114-X)
- Morét-Ferguson S, Law KL, Proskurowski G, Murphy EK, Peacock EE, Reddy CM (2010) The size, mass, and composition of plastic debris in the western North Atlantic Ocean. *Mar Pollut Bull* 60:1873–1878. <https://doi.org/10.1016/j.marpolbul.2010.07.020>
- Pedrotti ML, Petit S, Elineau A, Bruzaud S, Crebassa JC, Dumontet B, Marti E, Gorsky G, Cózar A (2016) Changes in the floating plastic pollution of the Mediterranean Sea in relation to the distance to land. *Plos One* 11:e0161581. <https://doi.pangaea.de/10.1594/PANGAEA.863844>
- PlasticsEurope (2017) Plastics—the Facts 2017. Analysis of European plastics production, demand and waste data
- Qu X, Su L, Li H, Liang M, Shi H (2018) Assessing the relationship between the abundance and properties of microplastics in water and in mussels. *Sci Total Environ* 621:679–686. <https://doi.org/10.1016/j.scitotenv.2017.11.284>
- Rech S, Macaya-Caquilpán V, Pantoja JF, Rivadeneira MM, Campodónico CK, Thiel M (2015) Sampling of riverine litter with citizen scientists—findings and recommendations. *Environ Monit Assess* 187:187–335. <https://doi.org/10.1007/s10661-015-4473-y>
- Reisser J, Slat B, Noble K, Plessis KD, Epp M, Proietti M, De Sonneville J, Becker T, Pattiaratchi C (2015) The vertical distribution of buoyant plastics at sea: an observational study in the North Atlantic Gyre. *Biogeosciences* 12:1249–1256. <https://doi.org/10.5194/bg-12-1249-2015>

- Sadri SS, Thompson RC (2014) On the quantity and composition of floating plastic debris entering and leaving the Tamar Estuary, Southwest England. *Mar Pollut Bull* 81:55–60. <https://doi.org/10.1016/j.marpolbul.2014.02.020>
- Sander M, Kohler H-PE, McNeill K (2019) Assessing the environmental transformation of nanoplastic through <sup>13</sup>C-labelled polymers. *Nat Nanotechnol* 14:301–303. <https://doi.org/10.1038/s41565-019-0420-3>
- Santana MFM, Moreira FT, Turra A (2017) Trophic transference of microplastics under a low exposure scenario: insights on the likelihood of particle cascading along marine food-webs. *Mar Pollut Bull* 121:154–159. <https://doi.org/10.1016/j.marpolbul.2017.05.061>
- Schmidt C, Krauth T, Wagner S (2017) Export of plastic debris by rivers into the sea. *Environ Sci Technol* 51:12246–12253. <https://doi.org/10.1021/acs.est.7b02368>
- Setälä O, Fleming-Lehtinen V, Lehtiniemi M (2014) Ingestion and transfer of microplastics in the planktonic food web. *Environ Pollut* 185:77–83. <https://doi.org/10.1016/j.envpol.2013.10.013>
- Setälä O, Magnusson K, Lehtiniemi M, Noren F (2016) Distribution and abundance of surface water microlitter in the Baltic Sea: a comparison of two sampling methods. *Mar Pollut Bull* 110:177–183. <https://doi.org/10.1016/j.marpolbul.2016.06.065>
- Song YK, Hong SH, Mi J, Kang JH, Kwon OY, Han GM, Shim WJ (2014) Large accumulation of micro-sized synthetic polymer particles in the sea surface microlayer. *Environ Sci Technol* 48:9014–9021. <https://doi.org/10.1021/es501757s>
- Song YK, Hong SH, Jang M, Han GM, Jung SW, Shim WJ (2017) Combined effects of UV exposure duration and mechanical abrasion on microplastic fragmentation by polymer type. *Environ Sci Technol* 51:4368–4376. <https://doi.org/10.1021/acs.est.6b06155>
- Sruthy S, Ramasamy EV (2017) Microplastic pollution in Vembanad Lake, Kerala, India: the first report of microplastics in lake and estuarine sediments in India. *Environ Pollut* 222:315–322. <https://doi.org/10.1016/j.envpol.2016.12.038>
- Su L, Xue Y, Li L, Yang D, Kolandhasamy P, Li D, Shi H (2016) Microplastics in Taihu Lake. *Chin Environ Pollut* 216:711–719. <https://doi.org/10.1016/j.envpol.2016.06.036>
- Suaria G, Avio CG, Mineo A, Lattin GL, Magaldi MG, Belmonte G, Moore CJ, Regoli F, Aliani S (2016) The Mediterranean plastic soup: synthetic polymers in Mediterranean surface waters. *Sci Rep* 6:37551. <https://doi.org/10.1038/srep37551>
- Tamminga M, Hengstmann E, Fischer EK (2018) Microplastic analysis in the South Funen Archipelago, Baltic Sea, implementing manta trawling and bulk sampling. *Mar Pollut Bull* 128:601–608. <https://doi.org/10.1016/j.marpolbul.2018.01.066>
- Tan X, Yu X, Cai L, Wang J, Peng J (2019) Microplastics and associated PAHs in surface water from the Feilaixia Reservoir in the Beijiang River, China. *Chemosphere* 221:834–840. <https://doi.org/10.1016/j.chemosphere.2019.01.022>
- Ter Halle A, Jeanneau L, Martignac M, Jardé E, Pedrono B, Brach L, Gigault J (2017) Nanoplastic in the North Atlantic Subtropical Gyre. *Environ Sci Technol* 51:13689–13697. <https://doi.org/10.1021/acs.est.7b03667>
- Thompson RC, Olsen Y, Mitchell RP, Davis A, Rowland SJ, Anthony WGJ, McGonigle D, Russell AE (2004) Lost at sea: where is all the plastic? *Science* 304:838. <https://doi.org/10.1126/science.1094559>
- van Cauwenberghe L, Vanreusel A, Mees J, Janssen CR (2013) Microplastic pollution in deep-sea sediments. *Environ Pollut* 182:495–499. <https://doi.org/10.1016/j.envpol.2013.08.013>
- Van Cauwenberghe L, Janssen CR (2014) Microplastics in bivalves cultured for human consumption. *Environ Pollut* 193:65–70. <https://doi.org/10.1016/j.envpol.2014.06.010>
- Van Cauwenberghe L, Claessens M, Vandegehuchte MB, Janssen CR (2015) Microplastics are taken up by mussels (*Mytilus edulis*) and lugworms (*Arenicola marina*) living in natural habitats. *Environ Pollut* 199:10–17. <https://doi.org/10.1016/j.envpol.2015.01.008>
- Vaughan R, Turner SD, Rose NL (2017) Microplastics in the sediments of a UK urban lake. *Environ Pollut* 229:10–18. <https://doi.org/10.1016/j.envpol.2017.05.057>
- Vermaire JC, Pomeroy C, Herczegh SM, Haggart O, Murphy M (2017) Microplastic abundance and distribution in the open water and sediment of the Ottawa River, Canada, and its tributaries. *FACETS* 2:301–314. <https://doi.org/10.1139/facets-2016-0070>
- Vianello A, Boldrin A, Guerriero P, Moschino V, Rella R, Sturaro A, Da Ros L (2013) Microplastic particles in sediments of Lagoon of Venice, Italy: first observations on occurrence, spatial patterns and identification. *Estuar Coast Shelf* 130:54–61. <https://doi.org/10.1016/j.ecss.2013.03.022>
- Vianello A, Da Ros L, Boldrin A, Marceta T, Moschino V (2018) First evaluation of floating microplastics in the Northwestern Adriatic Sea. *Environ Sci Pollut Res* 25:28546–28561. <https://doi.org/10.1007/s11356-018-2812-6>
- Wagner S, Reemtsma T (2019) Things we know and don't know about nanoplastic in the environment. *Nat Nanotechnol* 14:300–301. <https://doi.org/10.1038/s41565-019-0424-z>
- Wang T, Zou X, Li B, Yao Y, Li J, Hui H, Yu W, Wang C (2018) Microplastics in a wind farm area: a case study at the Rudong Offshore Wind Farm, Yellow Sea. *Chin Mar Pollut Bull* 128:466–474. <https://doi.org/10.1016/j.marpolbul.2018.01.050>
- Yamashita R, Tanimura A (2007) Floating plastic in the Kuroshio Current area, western North Pacific Ocean. *Mar Pollut Bull* 54:485–488. <https://doi.org/10.1016/j.marpolbul.2006.11.012>
- Yonkos LT, Friedel EA, Perez-Reyes AC, Ghosal S, Arthur CD (2014) Microplastics in four estuarine rivers in the Chesapeake Bay, U.S.A. *Environ Sci Technol* 48:14195–14202. <https://doi.org/10.1021/es5036317>
- Zhang K, Xiong X, Hu H, Wu C, Bi Y, Wu Y, Zhou B, Lam PKS, Liu J (2017) Occurrence and characteristics of microplastic pollution in Xiangxi Bay of Three Gorges Reservoir, China. *Environ Sci Technol* 51:3794–3801. <https://doi.org/10.1021/acs.est.7b00369>
- Zobkov M, Esiukova E (2017) Microplastics in Baltic bottom sediments: quantification procedures and first results. *Mar Pollut Bull* 114:724–732. <https://doi.org/10.1016/j.marpolbul.2016.10.060>



# Size and Composition Matters: From Engineered Nanoparticles to Ambient Fine Particles

Lung-Chi Chen and Polina Maciejczyk

## Abstract

Air pollution is a complex mixture of gaseous, volatile, and particulate matter (PM) containing inorganic and organic species. There is now abundant evidence in epidemiological and toxicological studies that air pollution contributes to the development and exacerbation of diseases of respiratory, cardiovascular, and other organs, and associated mortality. Studies showed that equal masses of PM could induce disparate health effects, suggesting that particle sizes and components may be at fault. The fine and ultrafine PM is considered to be particularly important because the small particles can be easily inhaled. Possible biological mechanisms of action leading to adverse effects include the production of inflammatory mediators in the lung causing systemic inflammation, interaction with neural receptors causing interference with the central nervous system regulation of cardiovascular function, and particle translocation via the bloodstream to other organs. This chapter reviews whether some components of the PM mixture are of a greater public health concern than others, and presents compelling evidence that trace elements are most strongly linked to the adverse effects. Air pollution has wide-ranging and harmful effects on human health and is a major issue for the global community. Further research should explore the effects of source-specific PM with more advanced approaches to exposure modeling, measurements, and statistics, which would lead to more effective legislation and interventions for greater benefits to public health.

## 1 Background on PM<sub>2.5</sub>: Global Pollution Hotspots, Multi-facets of PM<sub>2.5</sub> in Physical, Chemical, and Biological Dimensions, and Key Review Question: The Importance of Trace Metals in Exposure and Effects of PM<sub>2.5</sub>

Numerous epidemiological and laboratory studies linked particulate matter (PM) exposure to health effects (Pope et al. 2002; Lippmann 2014; Kim et al. 2015; Thurston et al. 2017) and subsequently led to worldwide regulations on air pollution. Air pollution particles penetrate deep into the lungs and cardiovascular system, causing conditions including stroke, heart disease, lung cancer, chronic obstructive pulmonary diseases and respiratory infections like pneumonia. Additionally, fine particulate matter is responsible for environmental effects such as corrosion, exterior building erosion, damage to vegetation and reduced visibility.

World Health Organization (WHO) states that outdoor and indoor air pollution is the biggest environmental risk to health as it affects practically all countries in the world, and is responsible for about one in every nine deaths annually (WHO 2016). Using the data derived from satellite measurements, air transport models and ground station monitors for more than 3000 locations, both rural and urban, the report estimated that only one-tenth of the urban population lives in areas that comply with the WHO air quality guidelines. The highest ambient air pollution levels are in the Eastern Mediterranean Region and in South-East Asia, with annual mean levels often exceeding more than 5 times WHO limits, followed by low and middle-income cities in Africa and the Western Pacific. In 2018, air pollution contributed to approximately 24% of all adult deaths from heart disease, 25% from stroke, 43% from chronic obstructive pulmonary disease and 29% from lung cancer (WHO 2018). The more recent Global Burden of Diseases, Injuries, and Risk Factors Study 2015 further updated the annual mortality due to

L.-C. Chen (✉)  
Department of Environmental Medicine, New York University  
School of Medicine, New York, NY, USA  
e-mail: [lcc4@nyu.edu](mailto:lcc4@nyu.edu)

P. Maciejczyk  
Department of Chemistry and Biochemistry, Eckerd College,  
St. Petersburg, FL, USA



PM<sub>2.5</sub> (PM with an aerodynamic diameter less than 2.5 µm) exposures to about 4.2 million per year (Cohen et al. 2017). This study also confirmed that while the global rate of mortality due to PM<sub>2.5</sub> decreased since 1990, the absolute number of deaths increased due to population growth and increased pollution in the south and east Asia.

Generally, ambient airborne PM is grouped as coarse, fine, and ultrafine particles (UFPs) with aerodynamic diameters within between 10 and 2.5 µm, less than 2.5 µm (PM<sub>2.5</sub>), and less than 0.1 µm (PM<sub>0.1</sub>), respectively. The current mass-based PM standards by the World Health Organization (WHO), U.S. Environmental Protection Agency (EPA), and European Environment Agency (EEA) apply to PM<sub>10</sub> and PM<sub>2.5</sub>. Contrastingly, the UFPs are not a criteria pollutant and thus are not routinely monitored. The reason for the specific size range standards is based on human physiology—coarse PM is mainly deposited along the conductive airways in the thorax, while nearly all of PM<sub>2.5</sub> penetrates into the gas-exchange region in bronchi where particle retention times are much longer. Both PM<sub>10</sub> and PM<sub>2.5</sub> are removed mainly by mucociliary clearance and phagocytosis. The UFPs deposit at much higher rates in the bronchioles and alveoli, where, due to their small size, they can then penetrate biological membranes, pass into the systemic circulation, overcome the placental barrier and finally diffuse into all organ systems including the brain and nervous system (Ohlwein et al. 2019; Heinzlerling et al. 2015).

A 2016 review of air quality standards in 194 countries by Kutlar et al. showed that only 39 countries worldwide have a PM<sub>2.5</sub> 24-hr (mean of 24 h) standard and 101 countries have PM<sub>10</sub> 24-hr standard. These standards vary greatly between the countries and regions, with the largest differences in air quality standards seen between high and low-income countries. A small selected subset of PM standards is shown in Table 1. Among countries with standards for 24-h averaging times for PM<sub>2.5</sub> and PM<sub>10</sub>, 21% and 46%, respectively, met the WHO guideline values (Kutlar et al. 2017).

The concentration, composition, and size distribution of atmospheric aerosol particles are temporally and spatially variable. Generally, ambient PM is a very complex mixture of different size particles from different origins, and

therefore, of different composition. Major sources of outdoor PM include fuel combustion from motor vehicles (e.g., cars and heavy-duty vehicles), heat and power generation (e.g., oil and coal power plants), industrial facilities (e.g., manufacturing factories, mines, and oil refineries), municipal and agricultural waste sites and waste incineration/burning, residential use of fuels (cooking, heating, and lighting). In some regions, additional, if not main, sources of ambient pollution are desert dust, waste burning and deforestation (WHO 2018). Furthermore, air quality is also affected by natural elements such as geographical (e.g., mountain ranges and valleys that obstruct natural air flow), meteorological and seasonal factors (e.g., amount of sunshine that enhances photochemistry and contributes to secondary aerosol formation, and relative humidity that contributes to particle growth and formation of acidic aerosols).

Although regulatory standards are mass-based, there is an overwhelming agreement that the human health effects should not be attributed simply to the total mass concentration but various PM components causing toxicities (Lippmann 2010; Lippmann et al. 2013; Cassee et al. 2013). The type and extent of health effects are investigated on their dependence on both chemical composition (such as transition metals, organic compounds, and other combustion-produced particles) and physical properties (size, particle number, and surface area). For monitoring purposes, the main constituents of PM are inorganic salts (sulfates, nitrates, ammonium, sodium chloride), organic compounds, black carbon, and mineral dust, including trace elements and metals (Adams et al. 2015). This composition is size-dependent: coarse PM is produced by abrasive physical events such as weathering, crushing, and grinding and is therefore mostly composed of minerals, bioaerosols (bacteria, pollen, fungi, vegetation litter), black smoke, and large sea salt particles. The coarse particles usually contribute the largest proportion of PM mass but little to the particle number. PM<sub>2.5</sub> is derived mainly from combustion-related sources, and thus often includes particles with a carbon core that carries organic compounds and metals, as well as secondary particles chemically transformed from oxides of sulfur and nitrogen.

Recently, there has been an increased interest in human exposure to ultrafine particles (UFPs, smaller than 0.1 µm). In

**Table 1** Selected particulate matter standards (in µg m<sup>-3</sup>)

	PM <sub>2.5</sub>		PM <sub>10</sub>	
	24-hr	Annual	24-hr	Annual
United States	35	12	150	–
Canada	28	10	–	–
European Union	–	25	50	40
China	75	35	150	70
WHO	25	10	50	20

the ambient atmosphere, UFPs originate broadly from two sources: as a submicrometer fraction of fine particle emissions, and from engineered nanomaterials. For the first group, vehicle emissions, are the primary source of the submicron ultrafine particles by both internal combustions and by operational mechanical friction in motors. The potential for exposure to these sources is very large—in the United States, approximately 45 million people live, work, or attend schools within 300 feet of a major road, airport or railroad (EPA 2014). Additionally, an average American spends about an hour in daily travel or commute, most of which takes place on major roadways. Emitted primary ultrafine particles are transformed rapidly due to coagulation, adsorption, and secondary particle formation, especially in the areas with high potential for photochemical reactions. Therefore, ultrafine particles have greater spatial and temporal variability than fine particles. The second type of sub-micron ultrafine particles, engineered nanoparticles, have become more widely used in manufactured goods and consumer products, such as food additives, pharmaceuticals, and drug delivery systems, cosmetics, as well as in materials for optical and electronic devices. The increasing popularity is due to the particle size which brings unique advantages to the products. For example, titanium or zinc oxide nanoparticles in new sun-blocks do not cause skin to appear with a white coating, as these particles do not reflect visible light. These new products eventually enter the environment through sewage (for example, washed off sunblock or silver particles from hand sanitizers) or as refuse waste. Less than 3% of incinerated nanomaterial is thought to enter the atmosphere (Keller and Lazareva 2014), which would lead to inhalation exposure to these particles as well as their combustion byproducts.

---

## 2 From Occurrence to Exposure

### 2.1 A Global Overview of Chemical Compositions of PM<sub>2.5</sub> and the Share of Trace Metals

A substantial fraction of fine and ultrafine particles is composed of primary emissions of various combustion processes such as fossil fuel combustion and high-temperature industrial processes, as well as the secondary transformation of organic volatiles from natural and anthropogenic sources. While the specific physical and chemical properties of particles, as well as the sources of these particles, are under constant investigation, it is unlikely that any single chemical component of PM is responsible for all adverse health outcomes. Many investigations prefer to focus on types of chemicals—namely ultrafine particles, bioaerosols, polycyclic aromatic compounds, and transition metals—known to have specific health effects (induction of inflammation and oxidative stress).

The chemical composition of PM<sub>2.5</sub> offers valuable information to identify the contributions of specific sources and to understand aerosol properties and processes that could affect air quality index and health. While more than 4300 cities in 108 countries have some sort of monitoring devices and contribute to WHO's ambient air quality database, Africa and some of the Western Pacific have a serious lack of air pollution data (WHO 2018). The lack of PM<sub>2.5</sub> and chemical speciation monitors is attempted to be supplemented with satellite remote sensing technology and modeling. This approach demonstrates that the addition of even a few ground-based PM monitors to more globally continuous aerosol optical depth satellite data can yield valuable improvements to PM<sub>2.5</sub> characterization on a global scale. Van Donkelaar et al. (2016) estimated that global annual average PM<sub>2.5</sub> concentration for 2010 was 32.6  $\mu\text{g m}^{-3}$ , or three times higher than the 10  $\mu\text{g m}^{-3}$  WHO guideline, with typical concentrations 20–70  $\mu\text{g m}^{-3}$  in South and East Asia. Using a population density model, they reported that only 13% of the global population lived in areas below the 10  $\mu\text{g m}^{-3}$  WHO guideline, with 52% of the high-income North America population living in cleaner air, compared to 1% or less of South Asia, East Asia, and North Africa/Middle East.

Depending on location and season, the PM<sub>2.5</sub> chemical components could vary by more than an order of magnitude between sites. For example, the SPARTAN study of the global chemical composition of PM<sub>2.5</sub> (Snider et al. 2016) involved 12 globally dispersed, densely populated urban locations in a variety of geographic regions including partial desert (Ilorin, Rehovot, Kanpur), coastline (Buenos Aires, Singapore), and developing megacities (Dhaka). The geographical variability resulted in the PM<sub>2.5</sub> mass concentrations spanning an order of magnitude, from under 10  $\mu\text{g m}^{-3}$  (e.g., Atlanta) to almost 100  $\mu\text{g m}^{-3}$  (Kanpur). The SPARTAN analysis of global chemical composition of PM<sub>2.5</sub> over periods of 2–26 months between 2013 and 2016 tabulated the major constituents as follows (relative contribution  $\pm$  SD): ammoniated sulfate (20%  $\pm$  11%), crustal material (13.4%  $\pm$  9.9%), equivalent black carbon (11.9%  $\pm$  8.4%), ammonium nitrate (4.7%  $\pm$  3.0%), sea salt (2.3%  $\pm$  1.6%), trace element oxides (1.0%  $\pm$  1.1%), water (7.2%  $\pm$  3.3%) at 35% RH, and residual matter (40%  $\pm$  24%). The crustal material was defined as elements Mg, Fe, and Al; trace elements included Zn, V, Ni, Cu, As, Se, Ag, Cd, Sb, Ba, Ce, and Pb. The “residual matter” was most likely not fully characterized as an organic fraction, some components of which are known to be toxic to humans or the environment. For example, it may contain persistent organic pollutants, a category that encompasses pesticides and polycyclic aromatic hydrocarbons, among other toxic species. Curiously, at all sites the ratio of coarse- and fine-PM mass fraction was about 1:1, thus indicating the

importance of both anthropogenic and natural sources of the pollution. It was found that ammonium sulfate correlated well with  $PM_{2.5}$  mass while other components had much higher spatial and temporal variability: nitrate absolute values range over 30-fold with additional variability attributed to season; crustal material did not show a clear pattern and was attributed to regional dust as well as (up to 80% in some urban locations) local dust; mass fractions of elemental black carbon ranged from 4% (Singapore) to 25% (Manila); trace elements and sea salt contributions were generally very small. The residual mass (mostly organic) contributed from 30 to 60% mass depending on location.

One of the persuasive studies of the spatial and temporal variation in PM in the United States comes from Bell (2012) who analyzed data on  $PM_{2.5}$  total mass and on the mass of 52 chemical components of  $PM_{2.5}$  for 187 counties in the continental U.S. for the period 2000–2005. In this study, Bell has shown that concentrations of  $PM_{2.5}$  components vary across counties and regions of the United States as well as over seasons. Her analysis of the seven components making up most of the  $PM_{2.5}$  mass found patterns similar to those in other studies. Organic carbon matter, nitrate, and elemental carbon were generally higher in the West than in the East, with some seasonal differences; sulfate was higher in the East, particularly in summer; and sodium ion appeared most prominently along the coasts. Additionally, Bell has demonstrated that relationships between daily  $PM_{2.5}$  total mass concentrations and hospitalizations for cardiovascular and respiratory disease also vary over season and region. Hospitalizations for respiratory disease were most pronounced on the second day after exposure to  $PM_{2.5}$  total mass and seasonally were largest in the winter with same-day  $PM_{2.5}$  exposures. Cardiovascular admissions in the main models were associated with same-day exposures to  $PM_{2.5}$  total mass were largest in winter and these increases were greatest across the Northeast U.S., while the seasonal model increases in cardiovascular admissions were observed only for the Northeast region and in all seasons.

Furthermore, the PM toxicity varies depending on its size distribution and chemical composition—properties associated with specific sources—and the PM health effects research is increasingly focused on source-apportionment of PM using chemical speciation data. Source-apportionment receptor models provide estimates of the contributions of various source categories to ambient air pollution at a given location at a given time. Various sources are distinguishable by the source apportionment because they have distinctive tracers and correlations that are closely associated with each source profile.

For example, further interpretation of the SPARTAN measurements with the global chemical transport model led to insights into seven sources affecting each site (Weagle et al. 2018): six primarily anthropogenic categories and one

“other sources” category. The primary anthropogenic categories, which contribute 76% of global  $PM_{2.5}$  exposures are residential energy use (21%), industry (18%), power generation (15%), agriculture (9%), transportation (8%), and open fires (5%).

The importance of such investigations is that resolution of the composition of PM into components related to emission source categories and identification of the most causal source categories and/or specific PM components responsible for most of the adverse health effects would permit more focused control of those causal  $PM_{2.5}$  components. A recent review of 280 articles published in 1966–2016 on epidemiological evidence of health effects associated with exposure to PM air pollution from five common outdoor emission sources (traffic, coal-fired power stations, diesel exhaust, domestic wood combustion heaters, and crustal dust) failed to rank them in the order of harmfulness, but indicated that PM from traffic and coal-fired power station emissions may elicit greater health effects compared to PM from other sources (Hime et al. 2018). Understanding the components and sources of  $PM_{2.5}$  that are most harmful to human health is critical for the development of air pollution regulations and environmental policies that maximize health benefits. The mortality risk estimated in the Dutch mortality cohort study for  $PM_{2.5}$  was 6% per  $10 \mu\text{g m}^{-3}$  for natural-cause mortality (Beelen et al. 2008), identical to the estimate from the American Cancer Society study (Pope et al. 2002), while rates of lung cancer associated with  $PM_{10}$  in 17 European cohorts were 22% per  $10 \mu\text{g m}^{-3}$  (Ole Raaschou-Nielsen et al. 2013). Even a 20% reduction in global anthropogenic emissions could reduce premature deaths in Europe by 54000 and in the U.S. by 27500 (Im et al. 2018).

## 2.2 Geographical Fingerprints of Metal Profiles in $PM_{2.5}$ and Implications for Site-Specific Human Exposure

A joint statement from the European Respiratory Society and American Thoracic Society seeks to further clarify a general framework for interpreting the adverse human health effects of air pollution (Thurston et al. 2017). The statement pointed out that most of the data from epidemiological studies of PM effects has been collected in Europe and North America. Even these studies, which aimed to identify which PM components and sources were associated with a variety of adverse health outcomes, met with mixed results; an unsurprising result when the differences between them are taken into account. These include variations in study time, differences in the selection of PM components and health outcomes of interest, and

uncertainty regarding estimates that stem from small data sets on PM composition and sources.

There are only a few long-term epidemiological studies that included a PM components other than PM mass (Wyzga and Rohr 2015). A study by Bell (2012) of daily hospital admissions for cardiovascular- and respiratory-related illnesses for 1999–2005 Medicare enrollees aged 65 years or older showed that only variability in elemental carbon explained variation in  $PM_{2.5}$  mass effect estimates for hospitalization. For the remaining components studied, Bell reported that greater concentrations of Ni and V in  $PM_{2.5}$  were associated with larger  $PM_{2.5}$  total mass health effect estimates for both cardiovascular and respiratory hospitalizations.  $PM_{10}$  mass associations with total non-accidental mortality were also larger in regions and seasons with higher fractions of V and notably Ni in  $PM_{2.5}$ . Lipfert et al. (2009) looked into correlations of total mortality among a group of U.S. male veterans with hypertension to several components of  $PM_{2.5}$ , including some metals, elemental carbon (EC), anions, some organic compounds, and polycyclic organic matter. They found no significant association between  $PM_{2.5}$  mass and mortality, but significant associations with “diesel particulate matter,” nitrate, EC, Ni, Pb, formaldehyde, benzene, polycyclic organic matter, while sulfate showed a significant negative association with mortality. Ostro et al. (2010, 2011) in a study of female teachers in California found all measured PM components ( $PM_{2.5}$  mass, EC, organic carbon (OC), sulfate, Fe, K, Si, Zn) correlated with ischemic heart disease deaths; but only  $PM_{2.5}$  mass, sulfate, nitrate, and Si were significantly associated with cardiopulmonary deaths and no significant associations for all-cause and pulmonary mortality. The city–season specific Poisson regression of mortality in 75 U.S. cities for 2000–2006 found that Si, Ca, and S were associated with more all-cause mortality, whereas S was related to more respiratory deaths (Dai et al. 2014). Thurston et al. (2013) used two models to examine the association between mortality among a group of individuals in the American Cancer Society cohort and multiple components of  $PM_{2.5}$  (mass, many elements, EC, OC) as well as the sources of  $PM_{2.5}$  modeled by source apportionment. For all-cause mortality, significant associations were found for the traffic and coal combustion factors,  $PM_{2.5}$  mass, As, Se, EC, and S. Respiratory mortality was significantly associated with the traffic factor,  $PM_{2.5}$  mass, Ca, Si, and OC, while associations with Cl and Ni were significantly negative. Ischemic heart disease was significantly associated with metal, traffic, and coal combustion factors,  $PM_{2.5}$  mass, As, Cl, Fe, Pb, Ni, Se, Zn, EC, and S. Subclinical markers for cardiovascular disease were examined in the Multi-Ethnic Study of Atherosclerosis cohort with no previous history of cardiovascular disease in 6 U.S. cities (Vedal et al. 2013), and were found in significant associations with  $PM_{2.5}$  mass, S, OC, and Cu for carotid intima-media thickness, and with Ni, Cu, and Ca, or V,

depending on the model, for coronary artery calcium marker. Among the  $PM_{2.5}$  components measured during 1998–2013 in the Atlanta area, water-soluble Fe had the strongest estimated effect on emergency department visits for cardiovascular diseases, while in 2008–2013, water-soluble V was associated with cardiovascular visits (Ye et al. 2018). Results from 19 European cohorts by Wang et al. (2014) found no associations between cardiovascular deaths and several measured trace elements (Cu, Fe, K, Ni, S, Si, V, and Zn). In one example of non-cardiovascular study, low birth weight of infants born to mothers living in California was associated with multiple components (including Br, Cl, Cu, EC, Fe, Pb, Mn, Ni, V, Ti, Zn, K, Na, ammonium, sulfate, and nitrate) and  $PM_{2.5}$  mass.

These studies demonstrated that metals, especially transition metals, can explain most, if not all of the health effects observed in epidemiological studies. As suggested by US EPA ISA for PM, reduction of this category of compounds would most likely lead to mitigating the health effects of air pollution (EPA 2009).

While several studies confirmed the public health benefits of clean air policies that improved air quality, the question remains on whether and what adverse effects occur at lower air pollution concentrations. As described before, the PM composition in the western hemisphere does not necessarily depict PM in other countries, for which such information is not widely available but modeled; thus, PM-health relationship derived in the developed world might not be directly applicable to the differing pollution composition and concentrations, as well as the differing demographics (e.g., age and income), of non-Western countries. To resolve such uncertainties in at least laboratory settings (sans demographic differences), several approaches could prove useful, such as a multi-cities comparison of air-volume based exposure, which would indicate the effects of PM by mass; alternatively, a multi-cities comparison of the mass-normalized health endpoints could also prove useful, indicating intrinsic PM composition effects.

For example, these approaches were used in measurements of biological oxidative potential (by macrophage reactive oxygen species (ROS) assay) associated with size-segregated airborne PM ( $PM_{10-2.5}$ ,  $PM_{2.5}$ ,  $PM_{0.25}$ ) in six urban areas of the world (Los Angeles, USA; Denver, USA; Beirut, Lebanon; Milan, Italy; Thessaloniki, Greece; Lahore, Pakistan) (Saffari et al. 2014). They found that larger ROS activity depended on mass concentration only for a coarse fraction but not for finer fractions, in which composition was more important. This was attributed to higher concentrations of water-soluble metals (most notably Fe—vehicular tracer, and Ni and V—residual oil combustion tracer, or both) and organic carbon in smaller sized PM. For coarse  $PM_{10-2.5}$  the ROS activity was generally lower, except when in presence of metals Cu, Co, and Mn from resuspended soil and dust, and vehicular abrasion.

Developed concentrator technology (Siotas et al. 1999; Gupta et al. 2004) for conducting inhalation exposure studies of concentrated ambient particles (CAPS) in laboratory animals (Maciejczyk et al. 2005), cell, and human volunteers created a new opportunity to quantitatively link the PM exposure to the biomarkers of health effects. Using a mouse model (ApoE<sup>-/-</sup> mice, bred to develop atherosclerotic plaque similar to that observed in humans with atherosclerosis) subchronically (6 h/d, 5d/wk, for 6 months) exposed to CAPS at locations with different PM<sub>2.5</sub> compositions, Chen and Nadziejko (2005) demonstrated that components attributable to source categories for residual oil combustion (Ni, V, and S), coal combustion (S and Se), and traffic (EC, Al, and P) appeared to be the most influential in altering heart rate and heart rate variability in these mice. Follow-up CAPS studies were done at five different sites across the United States which represented ambient pollutant mixtures from diverse locations and dominated by different source categories, including coal combustion, wood smoke, and traffic. In terms of atherosclerotic plaque progression, it was notable that plaque progression occurred at the three sites with exposure to coal combustion emissions and was lacking at the two sites without such exposure (Lippmann et al. 2013).

Overall, it appears that the cardiovascular effects of ambient air PM<sub>2.5</sub> are influenced, if not dominated, by their metal contents, especially the transition metals, and that nickel is likely to be a key component (Lippmann and Chen 2009).

### 2.3 Size-Specific Relative Enrichment of Anthropogenic Versus Crustal Metals Entails Implications for Element-Specific (Toxic vs. Non-toxic Metals) Exposure

While fine and ultrafine particles are mainly of anthropogenic combustion origin, coarse PM (PM<sub>10-2.5</sub>), besides some black smoke and some secondary particles, also includes the significant fraction of the mechanically generated particles from crustal sources such soil, dust from roads and building sites, and large sea salt particles. In epidemiological studies, the association between coarse PM<sub>10-2.5</sub> and health are more difficult to find (WHO 2013) since PM<sub>10-2.5</sub> is actually not measured but is calculated by subtracting measured PM<sub>2.5</sub> from measured PM<sub>10</sub>. This difficulty in separating the possible contributing effect of PM<sub>2.5</sub> increases the uncertainty in modeling the associations between coarse PM and hospital admissions. Nevertheless, EPA integrated science assessment for PM concluded that, in general, short-term coarse PM exposures had positive associations for cardiovascular and respiratory health effects and mortality (EPA 2009).

Exposure to coarse PM was linked to inflammatory effects in the lung (Wegesser et al. 2008), cardiovascular mortality (Malig and Ostro 2009), and decreased heart rate variability (Lipsett et al. 2006). Giannadaki et al. (2014) and Lelieveld et al. (2015) estimated that premature mortality attributable to natural dust is between 400 and 500 thousand per year, contributing ~18% to the total premature mortality attributable to air pollution. Locally, the contribution of natural dust can reach up to 90% of the total premature mortality due to air pollution, mostly in countries located in and around the dust belt zone in Africa, the Middle East, and Asia. The causal effect of desert dust might not necessarily be due to mineral composition or overall load—at least two studies identified the presence of microorganisms and viable pathogens in Iraq, Kuwait, and African dusts (Godleski et al. 2011; Polymenakou et al. 2008).

Clinical studies have reported that coarse particles can be as toxic as PM<sub>2.5</sub> on a mass basis (reviewed by Cassee et al. 2013). The difference in risk between coarse and fine PM may at least partially be explained by differences in intake and different biological mechanisms. However, toxicological studies on the effects of coarse particles are scarce. The few studies available usually collected PM on filters and used in vitro assays or intratracheal exposures for assessment, often in relation to the sources of emission. For example, coarse (PM<sub>10-2.5</sub>) and fine (PM<sub>2.5</sub>) PM samples from various locations in the New York City metropolitan area were assessed for their ROS response in the cell model and pro-inflammatory response in mice by oropharyngeal aspiration (Mirowsky et al. 2013). There, PM<sub>2.5</sub> was found to elicit a greater in vitro ROS response compared to PM<sub>10-2.5</sub>. Endotoxin in the NYC samples was correlated only with a pro-inflammatory-related response in mice.

Contrasting results were reported from a study of coarse and fine PM samples collected at 5 diverse sites within California (Mirowsky et al. 2015), where PM<sub>10-2.5</sub> elicited the greatest ROS response in the cells, especially for the urban locations, and also the greatest increase pro-inflammatory-related response in mice, with the exception of the rural ocean-side location. Elements associated with soil and traffic markers were most strongly linked to the adverse effects in vitro and in vivo. Interestingly, super-coarse PM (i.e., PM > 10 μm) produced as great, or more, of an inflammatory response in the mouse lung, a somewhat puzzling result since these super-coarse particles deposit largely in the upper respiratory tract. In contrast to Middle East desert dust studies, the California study only found associations between endotoxin and ROS response in the cell model failing to do so in the mouse model. Collectively this evidence points out that particle sources might be more influential than size when determining toxicity as trace elements.

### 3 From Exposure to Bioavailability

#### 3.1 Defining Bioavailability Based on Target Sites: Regional Deposition of Airborne Metals in Respiratory Tracts—Which Part of the Airway Is Vulnerable to Exposure to Inhalable Metals?

The assessment of adverse health effects of outdoor air pollution has historically focused on respiratory health outcomes. However, more recently, associations have also been reported for cardiovascular and other systemic or metabolic effects such as diabetes, neurological, and developmental outcomes. According to a joint ERS/ATC statement, the list of detectable air pollution health effects continues to expand, making a determination of the adversity of these numerous effects more and more important (Thurston et al. 2017). So the question is how do we go from respiration into multiple pathophysiological pathways that include systemic inflammation, oxidative stress, immune modulation, and epigenetic alteration? Different deposition patterns of fine and coarse particles were documented (ICRP 1994), with coarse particles having a higher deposition probability in the upper airways and the bronchial tree. Particles deposited in the upper airways are cleared rather rapidly from the respiratory tract via mucociliary clearance and macrophage transport. These deposition and clearance mechanisms explain the short-term health effects of  $PM_{10}$  and coarse PM. However, cardiovascular disease exacerbation could be activated by the autonomous nervous system via irritant receptors in the upper airways (Brook et al. 2010; Peters et al. 2006). Therefore, coarse particles may induce health effects by different mechanisms than fine and ultrafine particles and potentially relate to different health outcomes. Happonen et al. (2010) intratracheally instilled mice (10 mg/kg) with size-segregated ambient PM samples collected in six European cities over various seasons and found the overall inflammatory activity of PM decreased with particle size, such that  $PM_{10-2.5}$  and  $PM_{2.5-1}$  had a higher potency than  $PM_{1-0.2}$  and  $PM_{0.2}$ . The  $PM_{10-2.5}$  inflammatory response strongly correlated with source tracers for soil (K, Mg, Cu, Mn, Fe) and sea spray (Na, Cl, nitrate), while  $PM_{2.5-0.2}$  inflammatory response strongly correlated with oxidized organic compounds, transition metals (e.g., Fe and Cr), and source tracers for fuel oil combustion (Ni and V).

On the other end of the particle size spectrum, while larger particles such as  $PM_{10}$ ,  $PM_{10-2.5}$ , and  $PM_{2.5}$  dominate mass-based metrics, ultrafine particles (smaller than 0.1  $\mu\text{m}$ ) contribute very little to PM mass. Recent toxicological studies showed that this size fraction acts through mechanisms not shared with larger particles, but their toxicity is

depending on size, composition, surface area and surface charge (WHO 2013). The toxicity mechanism of the UFPs will be discussed later in the text.

#### 3.2 Defining Bioavailability Based on Chemical Speciation: Insoluble, Soluble Metal-Ligand Complex, Freely-Dissolved—Which Form of the Inhaled Metals Are Mostly Available for Bio-Uptake?

The problem of toxicity is rooted in PM complexity: ambient particles come in a variety of sizes, shapes, and surface coatings, all of which affect their bioactivity. For example, sulfuric acid layered ultrafine ZnO particles have been shown to give a proportionally greater pulmonary response than conventionally generated sulfuric acid mist of comparable size (Amdur and Chen 1989), suggesting that transition metals dissolved in the acid layer may be made bioavailable and render their higher pulmonary toxic.

The initial surface chemistry of the particles clearly influences their fate and distribution in biological systems upon immersion into biological fluids. The toxicity of PM may not necessarily be the cumulative toxicity of its components, since at least some of the PM components cannot dissolve in bronchial fluid and ultimately penetrate the air/blood interface. Although redox-active transition metals generally account for a small fraction of the total PM mass (10%), they are among the major drivers of PM-induced oxidative potential. Water-soluble transition metals (e.g., Fe, Ni, Cu, Cr, Mn, Zn, and V) and water-soluble organic carbon showed consistent correlations with the oxidative potential of airborne PM across different urban areas and size ranges (Saffari et al. 2014). Compared to their insoluble counterparts, soluble metals are generally more likely to quickly enter into the systemic circulation and be translocated to other organs such as the heart upon uptake in the lung. However, the extent of the solubility of all constituents of ambient PM by lung fluids is not well determined, especially for organic substances.

One of the main problems is the lack of a standardized *in vitro* bioaccessibility method, as recently pointed out in an extensive review of 96 relevant articles (Wiseman 2015). The currently favored water extraction method is practical and cheap, yet might not be physiologically relevant, especially since it hardly accounts for the effect of temperature on metal ion solubility. The aqueous leaching of metals from PM could be further hampered from additional pH effects due to hydrolysis of the ions present. The bronchial alveolar fluid, on the other hand, contains surfactant proteins, phospholipids, ions, and other substances, all of which could

affect the solubility of PM. For example, a comparison of four different Standard Reference Materials (SRMs): NIST 1648a (urban PM), BCR 038 (fly ash powder), NIES 8 (vehicle exhaust particulates) and NIST 2584 (indoor dust), reported mean increases of soluble elemental fractions in the amount of 40, 67, 39 and 59% for the SRMs extracted with a simulated biological fluid relative to water, respectively (Davies and Feddah 2003). Recognizing the limitations of aqueous extractions, the researchers rely on the use of two simulated biological fluids—Gamble's solution and artificial lysosomal fluid (ALF). The electrolytic composition of Gamble's solution was designed to be virtually identical to human interstitial lung fluid, while ALF was to simulate the acidic conditions which exist during phagocytosis by alveolar and interstitial macrophages (see review by Wiseman 2015, for variable compositions of both). Unfortunately, the different pH and composition of these leaching solutions make it difficult to cross-compare the extraction efficiencies used in different studies. For example, higher solubility of Ni, Cu, and Zn was observed in the modified Gamble's solution containing cysteine and glutathione due to the formation of soluble complexes of these metals with thiol groups (Voutsas and Samara 2002). Further complications in comparison arise from differences in length of extraction, the ratio of PM to liquid, mechanical equipment used (shaking, sonication, etc.), and sensitivity of the follow-up chemical analysis method (Wiseman 2015; Leclercq et al. 2017).

Despite these difficulties, interesting metal bioavailability results appear from a comparison of dusts collected in different locations. In one such study, three SRMs: BCR-723 (road dust collected in Austria with a particle size fraction of  $<90\ \mu\text{m}$  and a median value of  $14.6\ \mu\text{m}$ ), NIST 2710a (soil particles collected in the USA with a particle size fraction of  $<74\ \mu\text{m}$ ), and NIST 1648a (urban atmospheric particulate matter collected in the city of St. Louis, MO, USA with a particle size fraction of  $<100\ \mu\text{m}$  and a median value of  $5.85\ \mu\text{m}$ ), were selected to assess bioaccessibility of metals using several dissolution media (PBS, Gamble's solution, modified Gamble's solution and ALF) (Pelfrène et al. 2017). Total release of elements Ba, Cd, Cu, Mn, Ni, Pb and Zn in the three SRMs decreased according to the following sequence: ALF > Gamble's solution > PBS. High variability of Co and Sr bioaccessibility was recorded between the three fluids and within each fluid, while Cr was only soluble less than 10% all across. In ALF (acidic pH), metal solubilities of NIST 1648a were Cu 55%, Mn 47%, and Ni 12%, while for BCR-723 they were 65%, 5%, and 24%, respectively. The different percentages of metallic elements release could be attributed to differences in the source (St. Louis ambient PM vs. Austria road dust), and chemical tendencies of metal to form soluble complexes and transformations in the lung environment. Metal oxides (possibly formed in high-temperature combustion, but also

crustal), chlorides, carbonates can be generally easily dissolved in lung fluids, while metal sulfides, phosphates, and silicates (many of crustal origin) are common insoluble compounds. Sholkovitz et al. (2012) reflected on a remarkable systematic trend: an inherently higher solubility of Fe in aerosols derived from anthropogenic and natural combustion sources compared to lithogenic dust derived from arid continental soils. Their combined analysis for Fe total load and Fe solubility in  $\sim 1100$  samples collected by multiple researchers over the open ocean, the coastal ocean, and continental sites revealed the inverse trends for anthropogenic (low load – high solubility) and lithogenic (high load – low solubility) PM over regional and global scales despite significant differences in when and how the samples were collected and stored, and in leaching techniques and solutions that have been used to define 'soluble' iron. They also noted that the solubility of Fe (and thus, possibly of other metals) in lithogenic aerosols can increase when mixed with acidic anthropogenic aerosol (Sholkovitz et al. 2012).

In one of the few studies which examined multi-element solubility in field-collected airborne PM using simulated lung fluids, the soluble fractions of As, Ce, Co, Cr, Cu, Mn, Ni, Pb, Sb, Ti, and V were analyzed in airborne  $\text{PM}_{10}$ ,  $\text{PM}_{2.5}$  and  $\text{PM}_1$  from Frankfurt, Germany (Wiseman and Zereini 2014). Overall, filters extracted with the acidic ALF yielded more soluble metal fractions when compared to the neutral Gamble's solution. Interestingly, Sb, Pb and As were observed to be the most soluble in all airborne PM fractions. For example, after 24 h in ALF, Pb (an element of well-established health concern) had a mean soluble fraction of 96% in  $\text{PM}_{10}$ , 84% in  $\text{PM}_{2.5}$  and 78% in  $\text{PM}_1$ . Among other metals in  $\text{PM}_{10}$ ,  $\text{PM}_{2.5}$ , and  $\text{PM}_2$ , the mean soluble fraction of Ni was 52%, 25%, and 35%, respectively, while for Cu, they were consistently more than 80% all across. Leclercq et al. (2017) found that LHC-9 culture medium appears to be a good physiological proxy to human respiratory mucus collected from COPD patients for most metals. They tested the *in vitro* pro-inflammatory responses of soluble, insoluble, and total  $\text{PM}_{2.5}$ , and found that both soluble and insoluble fractions induced cell inflammatory responses although their cumulative response did not correspond to the one by the total fraction. The authors suggested that the inflammation could be not only linked to the presence of some of the metals contained in soluble and insoluble fractions of  $\text{PM}_{2.5}$ , but also to the presence of organic chemicals in its insoluble fraction.

---

## 4 From Bioavailability to Toxicity

Air pollution plays an important role in the development and exacerbation of respiratory diseases, such as asthma, chronic obstructive pulmonary disease (COPD), and lung cancer

(EPA 2009). In the past several decades, other adverse effects were documented, and the European Respiratory Society and the American Thoracic Society proposed a set of considerations of what constitutes an adverse health effect of air pollution (Thurston et al. 2017). A consensus document on behalf of the European Society of Cardiology reviewed the mechanisms and relationships between ambient air pollution and cardiovascular disease (Newby et al. 2015). Cascio (2018) succinctly summarized three principal pathways supported by epidemiological, clinical and toxicological data that explain the observed biochemical, physiological and clinical effects of PM exposure. Firstly, inhaled particulates can interact with the lung cells and initiate oxidative stress reactions leading to local and systemic inflammatory responses. For the cardiovascular system, these responses include decreased nitric oxide availability, oxidation, and alteration of the function of blood lipids, platelet activation, and prothrombotic changes in blood proteins that affect the function of blood vessels and clotting. Secondly, inhaled particulates can interact with neural receptors in the lung and activate a reflex of the autonomic nervous system that regulates blood pressure and heart rhythm. Thirdly, the UFPs can translocate across the alveolar membrane and move via bloodstream to other organs (e.g., heart, liver).

As mentioned earlier, trace elements constituents generally contribute only minimally to PM mass, yet these small amounts are biologically significant for the first proposed mechanism—activation of pro-inflammatory pathways and generation of reactive oxygen species. One of the most likely toxic components of PM<sub>2.5</sub> are transition metals such as Fe, V, Ni, Cr, Cu, and Zn due to their oxidative potential, which is related to the redox activity and ability to generate ROS in biological tissues (Lippmann and Chen 2009), which can damage DNA and disrupt cell functioning via the oxidation of proteins and peroxidation of lipids. The increase in the level of oxidative stress occurs via a two-step catalytic conversion of hydrogen peroxide into the redox-active hydroxyl radical (Pratviel 2012), and the extent of this reaction is believed to be highly dependent on the oxidation state of the transition metal and conditions of the biological fluid (e.g., pH) (Saffari et al. 2014). The oxidative potential has been suggested to be a more health-relevant metric than PM mass, which may not adequately capture regional differences in biological activity (Weichenthal et al. 2016).

For the mechanistic understanding of aerosol health effects, cellular studies investigate how PM<sub>2.5</sub> components can induce inflammation and oxidative stress. Common quantitative measures of oxidative stress are macrophage-based assay, dithiothreitol and ascorbic acid assays, iodometric spectrophotometry and electron paramagnetic/spin resonance spectrometry. However, a review by Shiraiwa et al. (2017) indicated that the relationship between the measured oxidative potential of PM

and health endpoints is not established with certainty, and might depend on the type of assays and length of exposure. For example, the glutathione-related oxidative burden but not ascorbate-related oxidative burden was associated with lung cancer mortality in the Canadian Census Health and Environment Cohort (Weichenthal et al. 2016). Nevertheless, the macrophage-based ROS assay has been applied to ambient PM collected in various places in the world, showing that the ROS activities among the sites differ by more than 1 order of magnitude (Saffari et al. 2014). A greater PM redox activity was observed in developing areas of the world, which may be due to stronger emissions of fuel oil combustion, vehicle exhaust, and biomass burning. ROS activity levels were generally higher close to sources and urban sites compared to rural locations, except in summer when comparable ROS activity was observed at rural sites (Saffari et al. 2014). Concentrations of water-soluble transition metals (e.g., Fe, Ni, Cu, Cr, Mn, Zn, and V) showed positive correlations with the ROS activity of airborne PM across different urban areas and size ranges (Daher et al. 2012; Shafer et al. 2010). A large and systematic effort (Lippmann et al. 2013) to evaluate the relative toxicity of filter-collected PM found differences in the production of ROS in human epithelial and endothelial cell lines depending on location, season, and size fraction, with the highest ROS production for samples from New York City and Los Angeles. ROS responses to ultrafine PM samples from all sites were higher than responses to coarse and fine PM samples (on an equal mass basis); responses were higher in summer for fine and ultrafine samples but higher in winter for coarse samples. Strong correlations were observed between ROS production and Cu, Sb, V, Co, Be, and Ni. A Biosampler-collected PM<sub>2.5</sub> from rural New York was studied for its oxidant generation capacity in vitro showed a relatively significant association Ni, and weaker but still significant correlations with Ba, Mn, and Fe. The single-source regression analysis showed a significant association with metal source only (Maciejczyk et al. 2010).

Ito et al. (2011) examined the effect of individual PM<sub>2.5</sub> components on mortality in New York City, and in the cold season, the components associated with residual oil burning, Ni, V, and Zn, all showed the strongest effects at lag 3, while in the warm season, strong associations were observed for secondary aerosols including OC, sulfate, and Se, which are associated with transported coal emissions. In Seattle, the components associated with mortality during cold-season were traffic (EC), residual oil burning (Ni and V), and wood burning (K) (Zhou et al. 2011). In their review, Lippmann and Chen (2009) concluded that the cardiovascular effects of ambient air PM<sub>2.5</sub> are greatly influenced, if not dominated, by their metal contents, especially the transition metals, and that nickel is likely to be a key component (Lippmann and Chen 2009).



#### 4.1 Metal-Only Particle Toxicity: Evidence and Experience from Nanotoxicology

Several decades after the enactment of Clean Air Acts in U.S and U.K the urban pollution have visibly decreased but the epidemiological studies began to show the effects of small changes in PM concentrations on cardiovascular mortality and morbidity (Dockery et al. 1995; Pope et al. 1995; Pope et al. 2002). Ultrafine particles were hypothesized to be responsible for driving the cardiovascular effects of PM (Oberdörster et al. 1995). Unfortunately, most of the PM sampling, speciation campaigns, exposure studies and epidemiology studies that have taken place in the past two decades have lacked UFP samplers. Since UFPs do not contribute substantially to the mass, they are most commonly monitored by particle number counters, and thus are somewhat difficult to separate from the mass-modeled effects of PM<sub>2.5</sub>. A recent systematic review by Ohlwein (2018) of 85 epidemiologic studies pointed to adverse short-term associations with inflammatory and cardiovascular changes, some of which were attributed to UFPs or UFPs in combination with other pollutants. For the other studied health outcomes, the epidemiological evidence on independent health effects of UFP remains inconclusive or insufficient mostly due to small numbers of participants, a lack of consistent exposure information, and short intervals between exposure and effect.

The mechanistic role of UFP in cardiovascular, genotoxic and carcinogenic effects has been studied in laboratory-created aerosols of surrogate particles (e.g., carbon black, diesel engine soot, TiO<sub>2</sub>, ZnO, and Ni). Incidentally, engineered nanomaterial industries seem to be proactively trying to predict the possible adverse effect of new materials instead of “waiting to ‘count bodies’ on the introduction of a new hazard” (Donaldson and Seaton 2012). The nano-industry has yet to define what constitutes “particle reactivity”, and lacks a single parameter that would allow it to do so. To rectify this, the industry currently proposes a number of methods to measure this, such as measurement of ROS, pH and redox potential, band gap, and in vitro dissolution. The industry has refined the particle characterization methodology to go beyond mass and number concentrations and adopted well-recognized analytical methods that can provide reliable measurements in chemical composition, aggregation, surface area, crystal structure, and other parameters (Stone et al. 2017). A portable instrument for realistic safety testing of inhaled nanoparticles in vitro was recently developed and tested with an Ag and C particles (Geiser et al. 2017).

The mechanism of UFP toxicity that lead to cardiovascular effects (atherosclerosis, stroke, myocardial infarction) as well as the subsets of symptoms and diseases (Stone et al. 2017; Allen et al. 2017; Hamanaka and Munfu 2018) follows the

same three main pathways as the inhalation and deposition of PM explained earlier in our text. First, particles interaction with neural receptors interferes with the central nervous system regulation of cardiovascular function. Second, lung inflammatory mediators cause systemic inflammation. Third, particle translocation to bloodstream carries them to other organs (e.g., heart, liver) (Stone et al. 2017; Cascio 2018).

Early work with health and safety of nanoparticles generally focused on single-component nanoparticles such as TiO<sub>2</sub>, Au, and carbon nanotubes. Some of the first studies with ultrafine TiO<sub>2</sub> particles of different sizes demonstrated an increase of translocation of smaller particles into the lung interstitium compared to larger particles (Oberdörster et al. 1994). Occupational inhalation exposure to metal nano- and micro-sized particles, e.g., tungsten carbide-cobalt dust, in hard metal manufacturing facilities and mining and drilling industries is well documented to cause “hard metal lung disease” and an increased risk of lung cancer (Armstead and Li 2016). Looking ahead, the nanoparticle industry might face the problem of ambient UFPs—increasingly complex multicomponent systems that would need to be examined for health and ecological concerns in a greater detail than their individual constituent.

Some studies have shown that engineered nanoparticles do not exhibit ecotoxicity based on their chemical and macroscopic nature, but are toxic via similar mechanisms. For example, C60 fullerene and TiO<sub>2</sub> nanoparticles have variable physicochemical properties but are both redox active and provoke oxidative stress in aquatic organisms. Furthermore, TiO<sub>2</sub> has been reported to cause neurotoxicity in the brain tissue of various fish when entering into the brain and are subsequently phagocytosed by microglial cells, which then produce ROS (Hu and Gao 2010).

The majority of preclinical and clinical studies on environmentally relevant UFPs have been conducted with diesel exhaust and diesel exhaust particles, which are a rich source of UFPs. A comprehensive review by Stone et al. (2014) provides an extensive list of effects such as airway inflammation, changes in heart rate variability and arrhythmia, and a series of vascular dysfunctions, all of which promote cardiovascular disease. The cellular and biochemical mechanisms underlying these effects are wide-ranging, with oxidative stress and inflammation being key drivers (Miller et al. 2012).

#### 4.2 The Fractional Contribution of Metals in PM<sub>2.5</sub> Mixture Effects: How Do We Quantify It?

Lippmann and colleagues used source-apportionment techniques to evaluate which specific components and source categories might be contributing most to the health effects associated with exposure to PM (Lippmann HEI report

2013). Using a mouse model of cardiovascular disease, Chen and Lippmann (Study 1 of Lippmann's HEI report 2013) observed that mice exposed to CAPS in 5 different locations in the US for 6 months showed greater plaque development in the arteries than mice exposed to filtered air, with samples collected at Manhattan (urban area with emissions from residual oil combustion, traffic, and secondary PM from coal-fired power plants) and Tuxedo (rural, mainly secondary PM from coal-fired power plants), New York, and East Lansing, Michigan (mid-west US with emissions from coal-fired power plants). In contrast, no differences between the control and CAPS-exposed mice were seen at Seattle, Washington (mainly traffic and wood smoke), and Irvine, California (mainly traffic). They found that CAPS exposures were associated with acute increases in heart rate and decreases in HRV at Manhattan and, to a lesser extent, at Tuxedo. Very few significant associations for HRV were seen at the other locations. The investigators concluded that the effects on plaque progression were most likely attributable to a coal combustion source category, and that the residual oil combustion, coal combustion, and traffic source categories contributed most to the observed acute cardiac effects. In terms of strength of associations, components attributable to source categories for residual oil combustion (Ni, V, and S), coal combustion (S and Se), and traffic (EC, Al, and P) appeared to be the most influential.

Using mouse *in vivo* and cultured cells (human lung epithelial cells and endothelial cells) *in vitro* exposures, Gordon and Chen (Study 2 of Lippmann's HEI report 2013) reported that the production of reactive oxygen species (ROS) in human epithelial and endothelial cell lines were correlated with location, season, and size fraction, with the highest ROS production for samples from Manhattan and Los Angeles. In addition, on equal mass basis, ROS responses to ultrafine PM samples from all sites were higher than responses to coarse and fine PM samples; responses were higher in summer for fine and ultrafine samples but higher in winter for coarse samples. Strong correlations were observed between ROS production and Cu, Sb, V, Co, Be, and Ni. The investigators observed an increase lung inflammation in PM-exposed mice and the lung inflammation is larger to the coarse fraction of PM than to the fine and ultrafine fractions. Interestingly, there was no correlation between *in vitro* ROS production and *in vivo* lung inflammation for the same PM sample. The investigators concluded that the composition of PM samples pointed to the traffic and residual oil combustion source categories as contributors to the observed effects.

These studies consistently identified that coal combustion, residual oil combustion, traffic and metals source categories are associated with health effects, and that variables such as location, season, and size of PM pollution are influential in the strength of the associations.

## 5 Future Perspectives

### 5.1 Role of Metals in the Formation/Thriving of Other PM<sub>2.5</sub>-Associated Components: A Catalytic Role for Organic Transformation (E.G., Radical Generation, SOA Formation)?

Some of the early studies of the mixtures of UFPs and gases to reproduce aerosols typical of primary emissions from coal combustion or smelting operations demonstrated the capacity of metal-containing particles to oxidize reactive gases and produce ultrafine acid-coated particles. For example, a ZnO–SO<sub>2</sub>–H<sub>2</sub>O (mixed at 500 °C) system showed that oxidation of SO<sub>2</sub> to H<sub>2</sub>SO<sub>4</sub> was surface catalyzed, and the amount of soluble sulfur compounds present on the surface was dependent on the ZnO concentration and not on the SO<sub>2</sub> concentration (Amdur et al. 1988). These acid-coated aerosols were used as a model of a type of primary emissions from smelters and coal combustors in the investigation of pulmonary effects in guinea pigs (Amdur and Chen 1989; Chen et al. 1992). Presence of acid in PM has been suggested as a major source of water-soluble Fe and other transition-metal ions in recent studies. For example, roadway emissions followed by secondary processing by acid were suggested as major contributors of water-soluble Fe, Cu, Mn, and Zn in Atlanta (Ye et al. 2018). Results from a series of toxicological studies designed to evaluate the health effects from various coal-fired power station emission scenarios suggest that the toxicity of PM from coal-fired power stations increases as the particles are atmospherically transformed, and transition metals play a critical role in these transformations. The amount and composition of the submicrometer aerosol depend on the source of fossil fuel used to produce electricity. For example, the dominant elements are Mg, Ca, and Fe for the lignite and Si, Fe, and Na for the bituminous coals, reflecting the differences in the composition of the mineral matter in coals of different origin (Amdur 1986). Metals such as As, Sb, Se, and Zn, which are volatile at combustion temperature, volatilize and condense preferentially on nanosized ultrafine particles (Amdur 1986). These ultrafine particles tend to be acidic and when inhaled produce decrement in pulmonary function, lung inflammation (Amdur and Chen 1989) and airway hyperresponsiveness (Chen et al. 1992). Ambient concentrations of PM<sub>2.5</sub>-sulfate are considered a reliable marker of coal-fired power plants emissions.

Oxidative stress is a general term used to describe an imbalance in a cell's redox state, such that pro-oxidant production overwhelms the endogenous antioxidant mechanisms of a cell. ROS refers to a family of molecules that are metabolites of oxygen and that, due to their high reactivity, are likely to participate in oxidation-reduction reactions (Lund 2010). While ROS form as natural by-products of a

normal metabolic redox reaction, excess ROS is a response to environmental stress and can damage cellular lipids, proteins, or DNA, thus inhibiting signal transduction pathways and normal cellular functions.

Current knowledge suggests that transition metal-containing particles are the key factors in the formation of environmentally persistent free radicals (EPFR) that are formed when combustion byproducts interact with transition metal oxide on PM (Vejerano et al. 2018). During incineration of organic materials, emitted combustion byproducts recombine to form hydrocarbons and halogenated hydrocarbons while some condense to form nanoparticles. As the temperature cools off, soot and aromatic compounds (such as phenols and halogenated benzenes) are formed. At a temperature lower than 600 °C these organic aromatic precursors get adsorbed to particle surfaces where they are catalyzed by transition metal oxides to eventually form polychlorinated dibenzofurans (PCDFs), polychlorinated dibenzo-p-dioxins (PCDDs), and polycyclic aromatic hydrocarbons (nitro-PAHs and oxy-PAHs). However, the intermediate products of these surface-mediated reactions are long-lived surface bound radicals which are resistant to reaction with molecular oxygen, and thus, environmentally persistent. In a study, Louisiana PM<sub>2.5</sub>, Gehling and Dellinger (2013) used electron paramagnetic resonance for the EPFR decay measurements and reported a fast decay of 1/e lifetime 1–21 days (attributed to the phenoxyl radical), and slow decay 21–5028 days (attributed to the semiquinone radical). The primary sink for the EPFRs in the atmosphere is their reaction with molecular oxygen, which converts EPFRs to molecular species, and the rate of this reaction depends both on the properties of the organic molecules and metal oxide surface (Vejerano et al. 2018; Feld-Cook et al. 2017).

In contrast to gas-phase free radicals, the EPFRs are stabilized on the particle surface, and thus, due to their extended lifetime, present a higher risk of inhalation exposure. Yet the toxicity of EPFRs is not well studied, most likely due to lack of use of electron paramagnetic resonance instruments. Their contribution to PM toxicity most likely gets shifted to other species such as metals or organics, depending on what is measured. For example, Biswas et al. (2009) suggested that particle oxidative potential stems from the semivolatile PM fractions, based on a remarkable reduction in oxidative potential when the semivolatile fraction was removed from diesel aerosols. However, it could also be because of the decreased EPFR formation due to the lack of organic precursors. The toxicity studies that rely on the extraction of PM would be especially biased toward other components since when extracted EPFR react in solution to form multiple molecular reaction products including catechol, hydroquinone, phenol, chlorinated phenols, dibenzo-p-dioxin, and dibenzofuran (Truong et al.

2010). Unless TOF-MS techniques are used, the conventional approach to use solvent extracts in toxicity studies might modify the toxicity of PM and explain the discrepancies between inhalation and instillation studies.

There is evidence that transition metals can possibly chelate to carbonyls and organic acids in ambient particles and form metallo-organic compounds. Such complexes contribute to aqueous phase oxidation of organic compounds and the production of water-soluble organics (Singh and Gupta 2016).

## 5.2 Identifying the Relative Importance of Inhalation in Human Aggregate Exposure to Toxic Metals—Case Analysis for As, Cd, Cu, Pb; Understand the Underlying Biogeochemical Processes that Determine the Exposure Levels of Airborne Metals - > Enhance Human Health-Oriented Understanding of the Environmental Process of Trace Metals

In a variety of large population studies, various cardiovascular and pulmonary health effects have been significantly associated with long-term average concentrations of ambient air in terms of one or more of its particle size fractions and/or of its chemical components. These associations can be verified by studies in human volunteers by intratracheal instillation of particle suspensions of known compositions. Lay et al. (1998) and Ghio et al. (1998) instilled ~5-mg doses containing both soluble and insoluble 2.6 µm Fe particle agglomerates suspended in saline into the lungs of volunteer subjects to investigate oxidative stress. BALF samples were collected from 1 to 91 days later. After 1 day, Lay et al. (1998) reported inflammatory responses, and Ghio et al. (1998) reported decreased transferrin concentrations and increased concentrations of ferritin and lactoferrin. After 4 days, iron homeostasis was normal.

When similar study protocols were applied to real-world PM samples, the observed clinical health effects, i.e., lung inflammation and injury, can be used to verify the adverse effects observed in human populations, such as those from the Utah Valley, where there was a 14-month-long strike at a steel mill complex. There were significantly lower rates of mortality and hospital admissions during the strike than in the preceding and following years (Pope et al. 1989, 1991, 1992). Analyses of the PM collected on air sampling filters during those 3 years indicated that the concentrations of many airborne metal PM components (Cu, Zn, Fe, Pb, Sr, As, Mn, and Ni) were also significantly lower during the strike interval than in the preceding and following years (Frampton et al. 1999; Ghio and Devlin 2001; Dye et al. 2001). Volunteers instilled with aqueous extracts of PM

filters while the steel mill was open had significant increases in both lung inflammation and injury in contrast to those volunteers in-stilled with an equal mass of PM extract from filters collected while the mill was closed (Ghio and Devlin 2001). Water soluble components or ionizable metals, which accounted for 20% of the PM mass, were responsible for the adverse health effects (Molinelli et al. 2002). The PM dose (500  $\mu\text{g}$ ) used in these studies was high, making it difficult to interpret these finding in relation to the risk of inhaled ambient particles in general population.

### 5.3 Forward-Looking Perspective on the Emerging Inhalable Sub-micron Particles Issues

In urban air, most UFPs are produced in vehicle exhaust and are composed of a carbon core coated with a diverse range of chemical species including redox-active transition metals and organic hydrocarbons. There is great variability in ambient UFP numbers, ranging from 500–10,000 particles/ $\text{cm}^3$  in rural areas to 7500–25,000 particles/ $\text{cm}^3$  in the urban background (Putaud et al. 2010), and with a European mean concentration of 31,500 particles/ $\text{cm}^3$  on busy streets. Depending on the type of vehicle and meteorological conditions, the large reactive surface area of exhaust UFPs can provide a reaction platform for catalytic conversion of organic radicals, sulfur, and nitrogen species chemistry, and partitioning for volatile and semi-volatile hydrocarbons. Thus, looking for causation of health effects becomes challenging in multicomponent complex systems of PM in air pollution.

Wildfires are increasingly being recognized as an important public health issue due to their UFP production. In the Western U.S. and Canada, the annual number of fires, the length of wildfire season, and the total area burned have all increased at a rapid rate over the past 30 years. Smoke from wildfires, including particles and gases, is trapped into high surface winds associated with the hot convective updraft and travels great distances to degrade air quality for communities far downwind. In 2014, wildfires in the US contributed 16.5% of fine particulate emissions for all fire, mobile, and stationary sources combined (EPA 2018). According to Verisk's (2017) Wildfire Risk Analysis, 4.5 million U.S. homes were identified at high or extreme risk of wildfire, with seven states with more than 13% of households at high or extreme risk from wildfire. Recent systematic reviews (Youssof et al. 2014; Liu et al. 2015; Reid et al. 2016) conclude that a strong association exists between exposure to wildfire smoke or wildfire  $\text{PM}_{2.5}$  and all-cause mortality and respiratory morbidity (asthma and COPD, bronchitis and pneumonia). One meta-analysis of 10 studies of wildfire-related particle exposure and respiratory health

outcomes found higher relative risk for females than for males of developing asthma and COPD, with this risk higher in adults than in children for all respiratory-related hospital or emergency departments' admissions (Kondo et al. 2019). However, significant gaps in research remain to connect wildfires beyond acute respiratory effects, such as cardiovascular mortality and morbidity, the risk for the susceptible population, long-term health effects, and consequences of exposure in children (Black et al. 2017; Reid et al. 2016; Kondo et al. 2019). Several studies have reported associations between wildfire smoke exposure and cardiac outcomes including emergency visits for heart failure (Rappold et al. 2011), out of hospital cardiac arrest (Stanley et al. 2014; Dennekamp et al. 2015) and cardiac mortality (Analitis et al. 2012; Sastry 2002). In a recent study in Dhaka City, Bangladesh, the effects of  $\text{PM}_{2.5}$  on cardiac emergency department visits, hospitalization and mortality are larger at lower  $\text{PM}_{2.5}$  concentrations, but smaller, and non-significant at higher concentrations, where biomass (e.g. crop) burning dominates, suggesting exposure biomass burning  $\text{PM}_{2.5}$  as having a lower CVD effect per  $\mu\text{g}/\text{m}^3$  than fossil fuel combustion-related  $\text{PM}_{2.5}$  (Rahman and Thurston, ISEE2019 abstract).

The size for fresh smoke particles falls in the 0.10–0.16  $\mu\text{m}$  range (a count median diameter), but fires also produce a variety of coarse mode particles, and very hot fires generate giant ash particles with diameters of up to a millimeter (Naeher et al. 2007; Reid et al. 2005). A toxicological study by Kim et al. (2014) of fine and coarse wildfire PM in mice provided direct evidence of the differential biological effects of the two size fractions of PM. The oropharyngeal aspiration of 100  $\mu\text{g}$  coarse PM/mouse causes inflammatory effects in the lung attributed to endotoxin, while the same dose of fine PM did not produce pulmonary effects, but did produce cardiovascular effects. Besides fine and UF particulates, wildfire smoke contains many air pollutants of concern for public health, such as carbon monoxide, nitrogen dioxide, ozone, polycyclic aromatic hydrocarbons, and volatile organic compounds. The chemical make-up of wildfire smoke depends on the type of biomass burned (green vs. dead vegetation, brush vs. softwood vs. hardwood) and the conditions for burning (active fire vs. smoldering).

Worldwide, indoor/outdoor cooking and heating appliances that burn wood are a major source of air pollution. In Europe 15–25% (i.e. Sweden, Finland, Germany and Austria) and 50% of  $\text{PM}_{2.5}$  in the Alpine region originates from residential biomass (primarily wood) combustion, and will become the dominant source of fine PM by 2020 with a contribution of 38% of total emissions (see review by Sigsgaard et al. 2015). Rokoff et al. (2017) reviewed 36 studies in developed countries that reported associations of household wood stove use and/or community wood smoke

exposure with pediatric health outcomes. While the use of wood stoves showed inconsistent associations with cough and wheeze and limited evidence for an association with other markers of respiratory health, there were consistent associations between higher community wood smoke and poor respiratory health in children. A conservative estimate of biomass smoke to premature mortality in Europe amounts to at least 40,000 deaths per year (Sigsgaard et al. 2015). The use of biomass, primarily for heating, is thought to be responsible for as much as 30% of PM pollution in winter in Delhi (Gordon et al. 2018). The use of traditional stoves throughout rural India and South Asia households contributes to extreme exposures well above the recommended WHO air quality guidelines.

## 6 Conclusions

### **a. Metals are minor contributors to total PM<sub>2.5</sub> mass globally, but play a multi-faceted role;**

There is clearly emerging evidence that the inhalation of some components of ambient air PM are associated with adverse health effects at concentrations near or not much higher than current ambient PM<sub>2.5</sub> mass concentrations. These components include EC, Ni, V, and Pb, and suggestive evidence exists for others, such as Al, Zn, and OC. Location, season, and size of PM are influential important variables that need to be considered when investigating the health effects of PM pollution. Many transition metals in PM are redox-active and lead to the production of reactive oxygen species in various cells in the lungs, blood and vascular tissues. This ROS production causes oxidative stress, which then leads to increased airway and systemic inflammation, and adverse cardiovascular responses. Metals also play a role in catalytic reaction leading to the formation of secondary organic aerosols, and conversion of gaseous pollutants (notably oxides of sulfur and nitrogen) to particulate phase. There is some evidence that adverse health effects are significantly associated with aerosol acidity originating from fossil fuel combustion, which could be due to its irritancy, or to its role in making metals bioavailable within the particles. Additional catalytic metal reactions lead to the formation and stabilization of long-lived organic radicals. Future studies can utilize pure materials as well as ambient air PM of mixed composition to obtain more information on the roles of specific PM components and their interactions and combined effects, and thereby identify those components most in need of control in order to reduce the health impacts of airborne PM.

### **b. Abundance and profiles of airborne trace metals infer geographical inhalation exposure disparities (exposure inequality);**

Over the past several decades, a combination of the advancements in technology and effective policies have led to a decline in air pollution in North America. Specifically, since 2010 the mandate of low-sulfur diesel fuel and vehicle emission control for diesel truck and buses in the U.S. decreased the PM and nitrogen oxide emission by 90% (HEI 2015). However, there is evidence of the environmental inequality in North America, Asia, and Africa showing that low socioeconomic status communities face higher concentrations of criteria air pollutants (Hajat et al. 2015). The results for Europe are mixed, and rapidly developing nations like India and China are understudied. This air pollution inequality may have sizeable impacts for population health—nearly 90% of air-pollution-related deaths occur in low- and middle-income countries, with nearly 2 out of 3 occurring in WHO's South-East Asia and Western Pacific regions (WHO 2016). The reasons for exposure inequality include economical (industries build factories on cheap land), political (poor communities lack political power to prevent construction of factories, landfills, and roads in close proximity), social (access to education and health services), demographic (population density and age), and other (affordability of newer cars, types of roads, etc.). Furthermore, the toxicity of particulates in different parts of the world is not necessarily the same, which might be most relevant for metals released from open-air smelting, trash burning, and less-stringently regulated industries, and for black and organic carbon compounds from combustion processes, including biomass burning and biofuel use for cooking and heating. While reported health burden estimates are based on studies conducted in North America and Europe, efforts are underway to generate locally relevant air quality and health data in developing countries (HEI 2019).

### **c. Size distribution and chemical speciation of airborne metals determines their respiratory deposition efficiency and pulmonary bioavailability and consequent toxic potencies;**

Smaller size fractions are found to be generally associated with higher intrinsic ROS activity, which may be due to a higher abundance of water-soluble metals or organics. For the human distal regions of the lungs, neither macrophage-mediated long-term clearance kinetics data nor translocation data for UFP into the circulation are currently available. Particle clearance from the lungs can also occur via transport toward lymph nodes and translocation into the blood circulation, leading potentially to accumulation in secondary organs and tissues.

**d. Metals are important toxicity contributors to PM<sub>2.5</sub>, but may not be as dominant as previously perceived.**

When black carbon and PM<sub>2.5</sub> are considered simultaneously for health effects, associations remained robust for black carbon. The review by Cassee et al. (2013) of the WHO REVIHAAP Project (2013) lists the growing evidence that links black carbon particles with cardiovascular health effects and premature mortality, for both short-term (24 h) and long-term (annual) exposures. Even when black carbon may not be the causal agent, it may operate as a universal carrier of a wide variety of combustion-derived chemical constituents of varying toxicity, including organic particles, not fully considered with PM<sub>2.5</sub> mass. Lucking et al. (2011) has shown that removing the particles from diluted diesel engine exhaust prevented adverse effects on the cardiovascular system—explained by differences in particle composition, with black carbon particles (soot) in diesel exhaust enriched with (semi)volatile organic particles and metals. There is growing information on the associations of organic carbon with health effects, and carbonaceous primary emissions are one of the important contributors to the formation of secondary organic aerosols (a significant component of the PM<sub>2.5</sub> mass). The evidence is insufficient to distinguish between the toxicity of primary and secondary organic aerosols link as a carrier of organic to metals and EPFRs in UFP or PM<sub>2.5</sub>. In the Los Angeles basin, it was found that both water-soluble and water-insoluble organic carbon as emitted by vehicular sources contribute substantially to the ROS activity of PM (Saffari et al. 2015).

**e. The shift from intrinsic toxicity of metals alone to joint interactions and combined toxicity with other PM<sub>2.5</sub> components and gaseous pollutants (total air exposure).**

A comprehensive meta-analysis of 100 studies of the association of ambient air pollution with hypertension and blood pressure (Yang et al. 2018) showed significant association of long-term exposures to PM<sub>2.5</sub> to hypertension, and of PM<sub>10</sub>, PM<sub>2.5</sub>, and NO<sub>2</sub> with diastolic blood pressure. However, any hypertension and blood pressure effects from short-term exposure to PM had to include a gaseous pollutant (SO<sub>2</sub> or NO<sub>2</sub> or both) to be significant. Acute exposure to gaseous ambient air pollution was associated with increases in morbidity and mortality within low and middle-income countries with greatest associations observed for cardiorespiratory mortality (Newell et al. 2018). Another systematic review and meta-analysis of 17 studies found positive and significant associations for air pollutants and pediatric pneumonia. While the most consistent association was for PM<sub>2.5</sub>, the highest excess risk was for SO<sub>2</sub> followed by PM<sub>2.5</sub>, O<sub>3</sub>, PM<sub>10</sub>, NO<sub>2</sub>, and CO (Nhung et al. 2017). A series of identically designed subchronic exposure animal studies compared inhalation of simulated fresh emissions from coal

combustion, diesel exhaust, gasoline exhaust, and wood smoke and found the least relative toxicity for the coal combustion (Mauderly et al. 2011). The follow-up analyses using compositional data of these exposure atmospheres pointed toward SO<sub>2</sub>, ammonia, NO<sub>x</sub>, and CO as most predictive of changes in inflammatory and vascular markers (Seilkop et al. 2012).

Reflecting on the results of the non-additive cell inflammatory responses described previously, Leclercq et al. (2017) hypothesized that the xenobiotic cell penetrance mechanisms may be different depending on how they are presented to the cells, in their soluble form or linked to particles. The relationship between chemical makeup of core particles and particle surface affects uptake, retention, translocation and the clearance within the lungs. Transition metals and PAHs are notably known to be associated with PM, either adsorbed on the surface or as an integral component of the particle core; thus, they can become bioavailable almost immediately by dissolving in somewhat neutral pH of lung fluid or somewhat later when digested by acidic phagocytosis. As a result, PM induces oxidative stress either directly via transition metals followed by inflammation by the subsequent secretion of proinflammatory mediators caused by undissolved particles, as well as by the reactive quinones arising from the metabolism of organic chemicals.

One of the major obstacles for PM health effects research is that only small amounts of PM obtained via collection is usually available. For ambient PM, it is necessary to collect and extract PM from the collector (by scraping, sonicating, or chemically extracting from a filter), which may alter the state of the PM before its use in toxicology studies. Transformation and loss of toxicologically important semivolatile compounds during sampling is also an issue that must be taken into account when testing collected PM.

A number of studies have attempted to separate the role of PM and gaseous components in the health effects associated with ambient air pollution exposure by removing PM from the mixture using high-efficiency particle filters. In a cardiovascular study of mice in Sao Paulo urban air (mostly traffic and resuspended soil sources), mild but significant vascular structural alterations compared to filtered air group where 30% NO<sub>2</sub>, 50% PM<sub>2.5</sub> (with PM<sub>0.3</sub> filter), and 100% BC were removed (Akinaga et al. 2009). However, Barrett et al. (2011) reported that acute exposure to either whole (PM plus gaseous) or just gaseous phase of simulated downwind coal combustion emissions both exacerbated various features of allergic airway responses in mice.

Gordon et al. (2012) examined various cardio physiological changes that occur with gas-phase only components of diesel exhaust and compared that to whole exhaust in rats. They concluded that it is possible that the components of whole diesel exhaust might have a greater influence on the

heart, while both filtered and whole exhaust similarly elevated pulmonary inflammation in animals. In another study in which diesel engine emission altered atherosclerotic plaque composition, the overall effect of the whole exhaust was substantial and exceeded the impact of PM alone (Campen et al. 2010). In a study that compared the effects of diluted whole diesel engine exhaust (WDE) with PM<sub>2.5</sub> CAPS, Quan et al. (2010) exposed male ApoE<sup>-/-</sup> mice 5.2 h/day, 5 days/week, for 5 months to five different exposure atmospheres: (1) FA; (2) Tuxedo, NY, PM CAPS, (mean = 110 µg/m<sup>3</sup>); (3) WDE, containing diesel exhaust particles (DEP) at 436 µg/m<sup>3</sup>; (4) diesel exhaust gases (DEG, equivalent to gases in WDE; and (5) CAPS + DEG. Atherosclerotic plaques were quantified for brachiocephalic artery cross-sections after 3 and 5 months of exposure. The results indicated that (1) DEG did *not* exacerbate progression; (2) There were *no* interactive effects between DEG and CAPS; (3) CAPS, despite having a much lower PM concentration, caused more plaque development than WDE, indicating that some components in ambient PM, not present in WDE, are responsible for the exacerbation of plaque progression by CAPS. In a human clinical study of patients with heart failure, the use of particle filter reduced the adverse effects of whole diesel exhaust on endothelial function and BNP but otherwise had no improving effect on the 6-min walking distance and arterial stiffness (Vieira et al. 2016).

**f. Future needs for holistic thinking of interactive behavior of metals, organics, and bioaerosols in atmospheric chemistry and human exposure/health; bridge biogeochemistry and environmental health for human aggregate exposure of trace metals.**

Active comprehensive research of the toxicity of ambient PM components in last several decades has not identified a single culprit component or source category that is responsible in whole or in part for the observed health effects associated with PM<sub>2.5</sub>. In fact, all the evidence points that there could be a combination of particle sizes, particle and gaseous sources, concentrations, weather patterns, geographical locations, sociodemographic factors, and sensitive population. Thus, there is a great need for accumulated knowledge to be synthesized and integrated into a holistic approach to evaluate and resolve human exposure to ambient pollutants. The priorities for improved assessments should include (1) epidemiological studies and PM monitoring in regions where such studies have not yet been performed, especially in Asia and Africa; (2) comprehensive analysis of all components (organic, inorganic, bioaerosol) including gases; (3) studies of pollution intervention or sudden pollution episodes (for examples, fires, volcanos); (4) comprehensive studies involving personal exposure monitoring; and (5) improved statistical modeling. Enhanced understanding of these related factors will lead to better targeted public health protection.

## References

- Adams K, Greenbaum DS, Shaikh R, van Erp AM, Russell AG (2015) Particulate matter components, sources, and health: systematic approaches to testing effects. *J Air Waste Manag Assoc* 65 (5):544–558. <https://doi.org/10.1080/10962247.2014.1001884>
- Akinaga LMY, Lichtenfels AJ, Carvalho-Oliveira R, Caldini EG, Dolhnikoff M, Silva LFF, De Siqueira Bueno HM, Pereira LAA, Saldiva PHN, Garcia MLB (2009) Effects of chronic exposure to air pollution from Sao Paulo city on coronary of Swiss mice, from birth to adulthood. *Toxicol Pathol* 37(3):306–314
- Allen JL, Oberdörster G, Morris-Schaffer K, Wong C, Klocke C, Sobolewski M, Conrad K, Mayer-Proschel M, Cory-Slechta DA (2017) Developmental neurotoxicity of inhaled ambient ultrafine particle air pollution: parallels with neuropathological and behavioral features of autism and other neuro developmental disorders. *Neurotoxicology* 59:140–154. <https://doi.org/10.1016/j.neuro.2015.12.014>
- Amdur MO, Chen LC, Gutty J, Lam, HF, Miller PD (1988) Speciation and pulmonary effects of acidic SO<sub>x</sub> formed on the surface of ultrafine zinc oxide aerosols. *Atmos Environ* 22(3):557–560 (1967). [https://doi.org/10.1016/0004-6981\(88\)90199-0](https://doi.org/10.1016/0004-6981(88)90199-0)
- Amdur MO, Chen LC (1989) Furnace-generated acid aerosols: speciation and pulmonary effects. *Environ Health Perspect* 79:147–150
- Analtis A, Georgiadis I, Katsouyanni K (2012) Forest fires are associated with elevated mortality in a dense urban setting. *Occup Environ Med* 69:158–162
- Armstead AL, Li B (2016) Nanotoxicity: emerging concerns regarding nanomaterial safety and occupational hard metal (WC-Co) nanoparticle exposure. *Int J Nanomedicine* 11:6421–6433
- Banerjee A, Roychoudhury A (2019) Nanoparticle-induced ecotoxicological risks in aquatic environments. In: *Nanomaterials in plants, algae and microorganisms*. Elsevier
- Barrett EG, Day KC, Gigliotti AP, Reed MD, McDonald JD, Mauderly JL, Seilkop SK (2011) Effects of simulated downwind coal combustion emissions on pre-existing allergic airway responses in mice. *Inhalation Toxicol* 23(13):792–804. <https://doi.org/10.3109/08958378.2011.609917>
- Bell ML; HEI Health Review Committee. (2012) Assessment of the health impacts of particulate matter characteristics. *Res Rep Health Eff Inst.* (161):5-38.
- Beelen R, Hoek G, van den Brandt PA, Goldbohm RA, Fischer P, Schouten LJ, Jerrett M, Hughes E, Armstrong B, Brunekreef B. (2008) Long-term effects of traffic-related air pollution on mortality in a Dutch cohort (NLCS-AIR study). *Environ Health Perspect.* 116 (2):196-202. <https://doi.org/10.1289/ehp.10767>
- Biswas S, Verma V, Sioutas C, Schauer JJ, Cassee FR, Cho AK (2009) Oxidative potential of semi-volatile and non volatile particulate matter (pm) from heavy-duty vehicles retrofitted with emission control technologies. *Environ Sci Technol* 43(10):3905–3912. <https://doi.org/10.1021/es9000592>
- Black C, Tesfaigzi Y, Bassein JA, Miller LA. (2017) Wildfire smoke exposure and human health: Significant gaps in research for a growing public health issue. *Environ Toxicol Pharmacol.* 55:186-195. <https://doi.org/10.1016/j.etap.2017.08.022>.
- Brook RD, Rajagopalan S, Pope CA 3rd, Brook JR, Bhatnagar A, Diez-Roux AV, Holguin F, Hong Y, Luepker RV, Mittleman MA, Peters A, Siscovick D, Smith SC Jr, Whitsett L, Kaufman JD; American Heart Association Council on Epidemiology and Prevention, Council on the Kidney in Cardiovascular Disease, and Council on Nutrition, Physical Activity and Metabolism. (2010) Particulate matter air pollution and cardiovascular disease: An update to the scientific statement from the American Heart Association. *Circulation.* 121 (21):2331-78. <https://doi.org/10.1161/CIR.0b013e3181d8bec1>

- Campen MJ, Lund AK, Knuckles TL, Conklin DJ, Bishop B, Young D, Seilkop S, Seagrave J, Reed MD, McDonald JD (2010) Inhaled diesel emissions alter atherosclerotic plaque composition in ApoE<sup>-/-</sup> mice. *Toxicol Appl Pharmacol* 242(3):310–317. <https://doi.org/10.1016/j.taap.2009.10.021>
- Cascio WE (2018) Wildland fire smoke and human health. *Sci Total Environ* 624:586–595. <https://doi.org/10.1016/j.scitotenv.2017.12.086>
- Cassee FR, Heroux M-E, Gerlofs-Nijland ME, Kelly FJ (2013) Particulate matter beyond mass: recent health evidence on the role of fractions, chemical constituents and sources of emission. *Inhal Toxicol* 25(14):802–812. <https://doi.org/10.3109/08958378.2013.850127>
- Chen LC, Nadziejko C (2005) Effects of subchronic exposures to concentrated ambient particles (CAPs) in mice. V. CAPs exacerbate aortic plaque development in hyperlipidemic mice. *Inhal Toxicol* 17:217–224
- Chen LC, Miller PD, Amdur MO, Gordon T (1992) Airway hyperresponsiveness in guinea pigs exposed to acid-coated ultrafine particles. *J Toxicol Environ Health* 35(3):165–174
- Cohen AJ, Brauer M, Burnett R, Anderson HR, Frostad J, Estep K, Forouzanfar MH (2017) Estimates and 25-year trends of the global burden of disease attributable to ambient air pollution: an analysis of data from the Global Burden of Diseases Study 2015. *The Lancet* 389(10082):1907–1918. [https://doi.org/10.1016/s0140-6736\(17\)30505-6](https://doi.org/10.1016/s0140-6736(17)30505-6)
- Daher N et al (2012) Characterization, sources and redox activity of fine and coarse particulate matter in Milan. *Italy Atmos Environ* 49:130–141
- Dai L, Zanobetti A, Koutrakis P, Schwartz JD (2014) Associations of fine particulate matter species with mortality in the United States: a multicity time-series analysis. *Environ Health Perspect* 122:837–842. <https://doi.org/10.1289/ehp.1307568>
- Davies NM, Feddah MR (2003) A novel method for assessing dissolution of aerosol inhaler products. *Int J Pharm* 255:175–187
- Dennekamp M, Straney LD, Erbas B, Abramson MJ, Keywood M, Smith K, Sim MR, Glass DC, Monaco AD, Haikerwal A, Tonkin AM (2015) Forest fire smoke exposures and out-of-hospital cardiac arrests in Melbourne, Australia: a case-crossover study. *Environ Health Perspect* 123(10):959–964. <https://doi.org/10.1289/ehp.1408436>
- Dockery DW, Pope CA III, Xu X, Spengler JD, Ware JH, Fay ME et al (1993) An association between air pollution and mortality in six U.S. cities. *N Engl J Med* 329:1753–1759. <https://doi.org/10.1056/nejm199312093292401>
- Donaldson K, Seaton A (2012) A short history of the toxicology of inhaled particles. *Part Fibre Toxicol* 9:13. <https://doi.org/10.1186/1743-8977-9-13>
- Dye JA, Lehmann JR, McGee JK, Winsett DW, Ledbetter AD, Everitt JI, Ghio AJ, Costa DL. (2001) Acute pulmonary toxicity of particulate matter filter extracts in rats: coherence with epidemiologic studies in Utah Valley residents. *Environ Health Perspect*. 109 Suppl 3:395–403. PMID: 11427389
- EPA U.S. (2009) Integrated science assessment for particulate matter (final report). Washington, DC, United States Environmental Protection Agency. <http://cfpub.epa.gov/ncea/cfm/recordsdisplay.cfm?deid=216546#Download>
- EPA U.S. (2012) Provisional assessment of recent studies on health effects of particulate matter exposure. U.S. Environmental Protection Agency, Washington, DC, EPA/600/R-12/056. <https://cfpub.epa.gov/ncea/isa/recordsdisplay.cfm?deid=247132>
- EPA U.S. (2014) Office of transportation and air quality. Near Roadway Air Pollution and Health: Frequently Asked Questions. EPA-420-F-14-044
- EPA U.S (2018) 2014 National Emissions Inventory. <https://gispub.epa.gov/neireport/2014/>
- Feld-Cook EE, Bovenkamp-Langlois L, Lomnicki SM (2017) Effect of particulate matter mineral composition on environmentally persistent free radical (EPFR) formation. *Environ Sci Technol* 51:10396–10402. <https://doi.org/10.1021/acs.est.7b01521>
- Frampton MW, Ghio AJ, Samet JM, Carson JL, Carter JD, Devlin RB. (1999) Effects of aqueous extracts of PM(10) filters from the Utah valley on human airway epithelial cells. *Am J Physiol*. 277(5): L960-7. <https://doi.org/10.1152/ajplung.1999.277.5.L960>.
- Gauderman WJ, Urman R, Avol E, Berhane K, McConnell R, Rappaport E, Chang R, Lurmann F, Gilliland F (2015) Association of improved air quality with lung development in children. *N Engl J Med* 372(10):905–913
- Gehling W, Dellinger B (2013) Environmentally persistent free radicals and their lifetimes in PM2.5. *Environ Sci Technol* 47(15):8172–8178. <https://doi.org/10.1021/es401767m>
- Geiser M, Jeannot N, Fierz M, Burtcher H (2017) Evaluating adverse effects of inhaled nanoparticles by realistic in vitro technology. *Nanomaterials* 7(2):49. <https://doi.org/10.3390/nano7020049>
- Ghio AJ, Carter JD, Richards JH, Brighton LE, Lay JC, Devlin RB. (1998) Disruption of normal iron homeostasis after bronchial instillation of an iron-containing particle. *Am J Physiol*. 274(3): L396-403. <https://doi.org/10.1152/ajplung.1998.274.3.L396>.
- Ghio AJ, Devlin RB. (2001) Inflammatory lung injury after bronchial instillation of air pollution particles. *Am J Respir Crit Care Med*. 164(4):704-8. PMID: 11520740
- Giannadaki D, Pozzer A, Lelieveld J (2014) Modeled global effects of airborne desert dust on air quality and premature mortality. *Atmos Chem Phys* 14(2):957–968
- Godleski JJ et al (2011) Toxicological evaluation of realistic emission source aerosols (TERESA): summary and conclusions. *Inhal Toxicol* 23(Suppl. 2):95–103
- Gordon CJ, Schladweiler MC, Krantz T, King C, Kodavanti UP. (2012) Cardiovascular and thermoregulatory responses of unrestrained rats exposed to filtered or unfiltered diesel exhaust. *Inhal Toxicol*. 24(5):296-309. <https://doi.org/10.3109/08958378.2012.670811>.
- Gupta T, Demokritou P, Koutrakis P (2004) Development and performance evaluation of a high-volume ultrafine particle concentrator for toxicological studies. *Inhal Toxicol* 16:851–862
- Hajat A, Hsia C, O'Neill MS (2015) Socioeconomic disparities and air pollution exposure: a global review. *Curr Environ Health Rep* 2(4):440–450. <https://doi.org/10.1007/s40572-015-0069-5>
- Hamanaka RB, Mutlu GM (2018) Particulate matter air pollution: effects on the cardiovascular system. *Front Endocrinol* 9:680. <https://doi.org/10.3389/fendo.2018.00680>
- Happo MS, Salonen RO, Halinen AI, Jalava PI, Pennanen AS, Dormans JA, Gerlofs-Nijland ME, Cassee FR, Kosma VM, Sillanpaa M, Hillamo R, Hirvonen MR (2010) Inflammation and tissue damage in mouse lung by single and repeated dosing of urban air coarse and fine particles collected from six European cities. *Inhal Toxicol* 22:402–416. <https://doi.org/10.3109/08958370903527908>
- Heinzerling A, Hsu J, Yip F (2015) Respiratory health effects of ultrafine particles in children: a literature review. *Water Air Soil Pollut* 227:32. <https://doi.org/10.1007/s11270-015-2726-6>
- HEI Review Panel on Ultrafine Particles (2013) Understanding the health effects of ambient ultrafine particles. HEI Perspectives 3. Health Effects Institute; Boston, MA
- Health Effects Institute (2015) Executive Summary. The Advanced Collaborative Emissions Study (ACES). Health Effects Institute; Boston, MA
- Health Effects Institute (2019) Update Winter 2019. [www.healtheffects.org/system/files/UpdateWinter2019.pdf](http://www.healtheffects.org/system/files/UpdateWinter2019.pdf)
- Hime NJ, Marks GB, Cowie CT (2018) A comparison of the health effects of ambient particulate matter air pollution from five emission sources. *Int J Environ Res Public Health* 15(6):1206. <https://doi.org/10.3390/ijerph15061206>



- Im U, Brandt J, Geels C, Hansen KM, Christensen JH, Andersen MS, Solazzo E, Kioutsioukis I, Alyuz U, Balzarini A, Baro R, Bellasio R, Bianconi R, Bieser J, Colette A, Curci G, Farrow A, Flemming J, Fraser A, Jimenez-Guerrero P, Kitwiron N, Liang C-K, Nopmongkol U, Pirovano G, Pozzoli L, Prank M, Rose R, Sokhi R, Tuccella P, Unal A, Vivanco MG, West J, Yarwood G, Hogrefe C, Galmarini S (2018) Assessment and economic valuation of air pollution impacts on human health over Europe and the United States as calculated by a multi-model ensemble in the framework of AQMEII3. *Atmos Chem Phys* 18:5967–5989. <https://doi.org/10.5194/acp-18-5967-2018>
- Ito K, Mathes R, Ross Z, Nádas A, Thurston G, Matte T (2011) Fine particulate matter constituents associated with cardiovascular hospitalizations and mortality in New York City. *Environ Health Perspect* 119:467–473. <https://doi.org/10.1289/ehp.1002667>
- Keller AA, Lazareva A (2014) Predicted releases of engineered nanomaterials: from global to regional to local. *Environ Sci Technol Lett* 1(1):65–70
- Kim KH, Kabir E, Kabir S (2015) A review on the human health impact of airborne particulate matter. *Environ Int.* 74:136–43.
- Kim YH, Tong H, Daniels M, Boykin E, Krantz QT, McGee J, Hays M, Kovalcik K, Dye JA, Gilmour MI. (2014). Cardiopulmonary toxicity of peat wildfire particulate matter and the predictive utility of precision cut lung slices. *Part Fibre Toxicol.* 11:29. <https://doi.org/10.1186/1743-8977-11-29>
- Knol AB et al (2009) Expert elicitation on ultrafine particles: likelihood of health effects and causal pathways. *Part Fibre Toxicol* 6:19
- Kutlar Joss M, Eeftens M, Gintowt E, Kappeler R, Künzli N (2017) Time to harmonize national ambient air quality standards. *Int J Public Health* 62(4):453–462. <https://doi.org/10.1007/s00038-017-0952-y>
- Kondo MC, De Roos AJ, White LS, Heilman WE, Mockrin MH, Gross-Davis CA, Burstyn I. (2019) Meta-Analysis of Heterogeneity in the Effects of Wildfire Smoke Exposure on Respiratory Health in North America. *Int J Environ Res Public Health.* 16(6). pii: E960. <https://doi.org/10.3390/ijerph16060960>.
- Lay JC, Bennett WD, Kim CS, Devlin RB, Bromberg PA. (1998) Retention and intracellular distribution of instilled iron oxide particles in human alveolar macrophages. *Am J Respir Cell Mol Biol.* 18(5):687–95. PMID: 9569239.
- Leclercq B, Alleman LY, Perdrix E, Riffault V, Happillon M, Strecker A, Lo-Guidice J-M, Garçon G, Coddeville P (2017) Particulate metal bioaccessibility in physiological fluids and cell culture media: toxicological perspectives. *Environ Res* 156:148–157. <https://doi.org/10.1016/j.envres.2017.03.029>
- Lelieveld J, Evans JS, Fnais M, Giannadaki D, Pozzer A (2015) The contribution of outdoor air pollution sources to premature mortality on a global scale. *Nature* 525(7569):367–371
- Lipfert FW, Wyzga RE, Baty JD, Miller JP (2009) Air pollution and survival within the Washington University-EPRI Veterans cohort: risks based on modeled estimates of ambient levels of hazardous and criteria air pollutants. *J Air Waste Manage Assoc* 59:473–489. <https://doi.org/10.1080/10473289.2009.10465740>
- Lippmann M, Chen LC (2009) Health effects of concentrated ambient air particulate matter (CAPs) and its components. *Crit Rev Toxicol* 39(10):865–913
- Lippmann M, Ito K, Hwang JS, Maciejczyk P, Chen LC (2006) Cardiovascular effects of nickel in ambient air. *Environ Health Perspect* 114(11):1662–1669. <https://doi.org/10.1289/ehp.9150>
- Lippmann M, Chen L-C, Gordon T, Ito K, Thurston GD (2013) National Particle Component Toxicity (NPACT) initiative: integrated epidemiologic and toxicologic studies of the health effects of particulate matter components. *Res Rep 177 Health Effects Institute, Boston, MA*
- Lippmann M. (2010) Targeting the components most responsible for airborne particulate matter health risks. *J Expo Sci Environ Epidemiol.* 20(2):117–8. <https://doi.org/10.1038/jes.2010.1>
- Lippmann M (2014) Toxicological and epidemiological studies of cardiovascular effects of ambient air fine particulate matter (PM<sub>2.5</sub>) and its chemical components: coherence and public health implications. *Crit Rev Toxicol* 44(4):299–347. <https://doi.org/10.3109/10408444.2013.861796>
- Liu JC, Pereira G, Uhl SA, Bravo MA, Bell ML (2015) A systematic review of the physical health impacts from non-occupational exposure to wildfire smoke. *Environ Res* 136:120–132
- Lucking AJ, Lundback M, Barath SL et al (2011) Particle traps prevent adverse vascular and prothrombotic effects of diesel engine exhaust inhalation in men. *Circulation* 123:1721–1728
- Lund AK (2010) Cardiovascular toxicology. In: *Comprehensive toxicology*, 2nd edn. McQueen, CA
- Maciejczyk P, Zhong M, Li Q, Xiong S, Nadziejko C, Chen LC (2005) The design of a concentrated ambient particulate matter exposure system for biometric telemetry monitoring. *Inhal Toxicol* 17:189–197
- Maciejczyk P, Zhong M, Lippmann M, Chen LC (2010) Oxidant generation capacity of source-apportioned PM<sub>2.5</sub>. *Inhal Toxicol* 2:29–36
- Malig BJ, Ostro BD (2009) Coarse particles and mortality: evidence from a multi-city study in California. *Occup Environ Med* 66:832–839
- Mauderly JL, Barrett EG, Gigliotti AP, McDonald JD, Reed MD, Seagrave J, Mitchell LA, Seilkop SK (2011) Health effects of subchronic inhalation exposure to simulated downwind coal combustion emissions. *Inhal Toxicol* 23(6):349–362
- Miller MR, Shaw CA, Langrish JP (2012) From particles to patients: Oxidative stress and the cardiovascular effects of air pollution. *Future Cardiol* 8(4):577–602. <https://doi.org/10.2217/fca.12.43>
- Mirowsky J, Hickey C, Horton L, Blaustein M, Galdanes K, Peltier RE, Chillrud S, Chen LC, Ross J, Nadas A, Lippmann M, Gordon T (2013) The effect of particle size, location and season on the toxicity of urban and rural particulate matter. *Inhal Toxicol* 25(13):747–757
- Mirowsky JE, Jin L, Thurston G, Lighthall D, Tyner T, Horton L, Galdanes K, Chillrud S, Ross J, Pinkerton KE, Chen LC, Lippmann M, Gordon T (2015) In vitro and in vivo toxicity of urban and rural particulate matter from California. *Atmos Environ* 103:256–262. <http://doi.org/10.1016/j.atmosenv.2014.12.051>
- Molinelli AR, Madden MC, McGee JK, Stonehuermer JG, Ghio AJ. (2002) Effect of metal removal on the toxicity of airborne particulate matter from the Utah Valley. *Inhal Toxicol.* 14(10):1069–86. PMID: 12396411
- Naeher LP, Brauer M, Lipsett M, Zelikoff JT, Simpson CD, Koenig JQ, Smith KR (2007) Woodsmoke health effects: a review. *Inhal Toxicol* 19(1):67–106
- Newby DE, Mannucci PM, Tell GS, Baccarelli AA, Brook RD, Donaldson K, Forastiere F, Franchini M, Franco OH, Graham I, Hoek G, Hoffmann B, Hoylaerts MF, Künzli N, Mills N, Pekkanen J, Peters A, Piepoli MF, Rajagopalan S, Storey RF (2015) ESC Working Group on Thrombosis, European Association for Cardiovascular Prevention and Rehabilitation, ESC Heart Failure Association, Expert position paper on air pollution and cardiovascular disease. *Eur Heart J* 36:83–93. <https://doi.org/10.1093/eurheartj/ehu458>
- Newell K, Kartsonaki C, Lam K, Kurmi O (2018) Cardiorespiratory health effects of gaseous ambient air pollution exposure in low and middle income countries: a systematic review and meta-analysis. *Environ Health* 17(1):41. <https://doi.org/10.1186/s12940-018-0380-3> A global access science source
- Nhung NTT, Amini H, Schindler C, Kutlar Joss M, Dien TM, Probst-Hensch N, Perez L, Kunzli N (2017) Short-term association between ambient air pollution and pneumonia in children: a systematic review and meta-analysis of time-series and case-crossover studies. *Environ Pollut* 230:1000–1008. <https://doi.org/10.1016/j.envpol.2017.07.063>

- Oberdörster G, Ferin J, Lehnert BE (1994) Correlation between particle size, in vivo particle persistence, and lung injury. *Environ Health Perspect* 102(Suppl 5):173–179
- Oberdörster G, Gelein RM, Ferin J, Weiss B (1995) Association of particulate air pollution and acute mortality: involvement of ultrafine particles? *Inhal Toxicol* 7(1):111–124
- Ohlwein S, Kappeler R, Kutlar Joss M et al. (2019) Health effects of ultrafine particles: a systematic literature review update of epidemiological evidence. *Int J Public Health*. <https://doi.org/10.1007/s00038-019-01202-7>
- Ole Raaschou-Nielsen O, Andersen ZJ, Beelen R, Samoli E, Stafogio M, Weinmayr G, Hoffmann B, Fisher P, Nieuwenhuijsen MJ, Brunekreef B, Xun WW, Katsouyanni K, Dimakopoulou K, Sommar J, Forsberg B, Modig L, Oudin A, Oftedal B, Schwarze PE, Nafstad P, De Faire U, Pedersen NL, Ostenson CG, Fratiglioni L, Penell J, Korek M, Pershagen G, Eriksen KT, Sørensen M, Tjønneland A, Ellermann T, Eeftens M, Peeters PH, Meliefste K, Wang M, Bueno-de-Mesquita B, Key TJ, de Hoogh K, Concin H, Nagel G, Vilier A, Griioni S, Krogh V, Tsai MY, Ricceri F, Sacerdote C, Galassi C, Migliore E, Ranzi A, Cesaroni G, Badaloni C, Forastiere F, Tamayo I, Amiano P, Dorronsoro M, Trichopoulou A, Bamia C, Vineis P, Hoek G (2013) Air pollution and lung cancer incidence in 17 European cohorts: prospective analyses from the European Study of Cohorts for Air Pollution Effects (ESCAPE). *Lancet Oncol* 14:813–822
- Ostro B, Lipssett M, Reynolds P, Goldberg D et al (2010) Long-term exposure to constituents of fine particle air pollution and mortality: results from the California teachers study. *Environ Health Perspect* 118:363–369. <https://doi.org/10.1289/ehp.0901181>
- Ostro B, Reynolds P, Goldberg D, Hertz A et al (2011) Erratum: assessing long-term exposure in the California teachers study. *Environ Health Perspect* 119:242–243
- Pelfrène A, Cave MR, Wragg J, Douay F (2017) In vitro investigations of human bioaccessibility from reference materials using simulated lung fluids. *Int J Environ Res Pub Health* 14(2):112
- Peters A, Veronesi B, Calderón-Garcidueñas L, Gehr P, Chen LC, Geiser M, Reed W, Rothen-Rutishauser B, Schürch S, Schulz H. (2006) Translocation and potential neurological effects of fine and ultrafine particles a critical update. *Part Fibre Toxicol*. 3:13. PMID: 16961926
- Polymenakou PN et al (2008) Particle size distribution of airborne microorganisms and pathogens during an intense African dust event in the eastern Mediterranean. *Environ Health Perspect* 116(3):292–296
- Pope CA 3rd. (1989) Respiratory disease associated with community air pollution and a steel mill, Utah Valley. *Am J Public Health*. 79(5):623-8. PMID: 2495741
- Pope CA 3rd. (1991) Respiratory hospital admissions associated with PM10 pollution in Utah, Salt Lake, and Cache Valleys. *Arch Environ Health*. 46(2):90-7. PMID: 2006899
- Pope CA 3rd, Schwartz J, Ransom MR. (1992) Daily mortality and PM10 pollution in Utah Valley. *Arch Environ Health*. 47(3):211-7. PMID: 1596104
- Pope CA III, Thun MJ, Namboodiri MM, Dockery DW, Evans JS, Speizer FE et al (1995) Particulate air pollution as a predictor of mortality in a prospective study of US adults. *Am J Respir Crit Care Med* 151:669–674. [https://doi.org/10.1164/ajrccm/151.3\\_pt\\_1.669](https://doi.org/10.1164/ajrccm/151.3_pt_1.669)
- Pope CA III, Burnett RT, Thun MJ, Calle EE, Krewski D, Ito K et al (2002) Lung cancer, cardiopulmonary mortality, and long-term exposure to fine particulate air pollution. *JAMA* 287:1132–1141. <https://doi.org/10.1001/jama.287.9.1132>
- Pratviel G (2012) Chapter 7. Oxidative DNA damage mediated by transition metal ions and their complexes. In: Sigel A, Sigel H, Sigel RKO (eds) Interplay between metal ions and nucleic acids metal ions in life sciences, pp 201–216. Springer. [https://doi.org/10.1007/978-94-007-2172-2\\_7](https://doi.org/10.1007/978-94-007-2172-2_7)
- Putaud JP, Van Dingenen R, Alastuey A, Bauer H, Birmili W, Cyrys J et al (2010) A European aerosol phenomenology - 3: physical and chemical characteristics of particulate matter from 60 rural, urban, and curbside sites across Europe. *Atmos Environ* 44(10):1308–1320. <https://doi.org/10.1016/j.atmosenv.2009.12.011>
- Quan C, Sun Q, Lippmann M, Chen LC. (2010) Comparative effects of inhaled diesel exhaust and ambient fine particles on inflammation, atherosclerosis, and vascular dysfunction. *Inhal Toxicol*. 22(9):738-53. <https://doi.org/10.3109/08958371003728057>.
- Rappold AG, Stone SL, Cascio WE et al (2011) Peat bog wildfire smoke exposure in rural North Carolina is associated with cardiopulmonary emergency department visits assessed through syndromic surveillance. *Environ Health Perspect* 119:1415–1420
- Reid JS, Koppmann R, Eck TF, Eleuterio DP (2005) A review of biomass burning emissions part II: intensive physical properties of biomass burning particles. *Atmos Chem Phys* 5:799–825
- Reid CE, Brauer M, Johnston FH, Jerrett M, Balmes JR, Elliott CT (2016) Critical review of health impacts of wildfire smoke exposure. *Environ Health Perspect* 124:1334–1343. <https://doi.org/10.1289/ehp.1409277>
- Rokoff LB, Koutrakis P, Garshick E, Karagas MR, Oken E, Gold DR, Fleisch AF. (2017) Wood Stove Pollution in the Developed World: A Case to Raise Awareness Among Pediatricians. *Curr Probl Pediatr Adolesc Health Care*. 47(6):123-141. <https://doi.org/10.1016/j.cppeds.2017.04.001>.
- Saffari A, Daher N, Shafer MM, Schauer JJ, Sioutas C (2014) Global perspective on the oxidative potential of airborne particulate matter: a synthesis of research findings. *Environ Sci Technol* 48(13):7576–7583
- Saffari A, Hasheminassab S, Wang D, Shafer MM, Schauer JJ, Sioutas C (2015) Impact of primary and secondary organic sources on the oxidative potential of quasi-ultrafine particles (PM0.25) at three contrasting locations in the Los Angeles Basin. *Atmos Environ* 120:286–296
- Sastry N (2002) Forest fires, air pollution, and mortality in southeast Asia. *Demography* 39:1–23
- Seilkop SK, Campen MJ, Lund AK, McDonald JD, Mauderly JL (2012) Identification of chemical components of combustion emissions that affect pro-atherosclerotic vascular responses in mice. *Inhal Toxicol* 24(5):270–287
- Shafer MM, Perkins DA, Antkiewicz DS, Stone EA, Quraishi TA, Schauer JJ (2010) Reactive oxygen species activity and chemical speciation of size-fractionated atmospheric particulate matter from Lahore, Pakistan: an important role for transition metals. *J Environ Monit* 12(3):704–715
- Shiraiwa M, Ueda K, Pozzer A, Lammel G, Kampf CJ, Akihiro Fushimi, ... Weber (2017) Aerosol health effects from molecular to global scales. *Environ Sci Technol* 51(23):13545–43567. <https://doi.org/10.1021/acs.est.7b04417>
- Sholkovitz ER, Sedwick PN, Church TM, Baker AR, Powell CF (2012) Fractional solubility of aerosol iron: synthesis of a global-scale data set. *Geochim Cosmochim Acta* 89:173–189. <https://doi.org/10.1016/j.gca.2012.04.022>
- Sigsgaard T, Forsberg B, Annesi-Maesano I, Blomberg A, Bølling A, Boman C, Bønløkke J, Brauer M, Bruce N, Héroux ME, Hirvonen MR, Kelly F, Künzli N, Lundbäck B, Moshhammer H, Noonan C, Pagels J, Sallsten G, Sculier JP, Brunekreef B. (2015) Health impacts of anthropogenic biomass burning in the developed world. *Eur Respir J*. 46(6):1577-88. <https://doi.org/10.1183/13993003.01865-2014>.
- Singh DK, Gupta T (2016) Role of transition metals with water soluble organic carbon in the formation of secondary organic aerosol and metallo-organics in PM1 sampled during post monsoon and pre-winter time. *J Aerosol Sci* 94:56–69. <https://doi.org/10.1016/j.jaerosci.2016.01.002>

- Sioutas C, Kim S, Chang M (1999) Development and evaluation of a prototype ultrafine particle concentrator. *J Aerosol Sci* 30:1001–1012
- Snider G, Weagle C, Murdymootoo K, Ring A, Ritchie Y et al (2016) Variation in global chemical composition of PM<sub>2.5</sub>: emerging results from SPARTAN. *Atmos Chem Phys* 16:9629–9653
- Straney L, Finn J, Dennekamp M et al (2014) Evaluating the impact of air pollution on the incidence of out-of-hospital cardiac arrest in the Perth Metropolitan Region: 2000–2010. *J Epidemiol Commun Health* 68:6–12
- Stone V, Miller MR, Clift MJD, Elder A, Mills NL, Moller P, ... Cassee FR (2017) Nanomaterials versus ambient ultrafine particles: an opportunity to exchange toxicology knowledge. *Environ Health Perspect* 125(10):106002. <https://doi.org/10.1289/ehp424>
- Thurston GD, Ito K, Lall R, Burnett RT, Turner MC, Krewski D, Shi, Y, Jerrett M, Gapstur SM, Diver WR, Pope CA III (2013) NPACT study 4 Mortality and long-term exposure to PM<sub>2.5</sub> and its components in the American cancer society's cancer prevention study II Cohort. In: National Particle Component Toxicity (NPACT) initiative: integrated epidemiologic and toxicologic studies of the health effects of particulate matter components. Res Rep 177. Health Effects Institute, Boston, MA
- Thurston GD, Kipen H, Annesi-Maesano I, Balmes J, Brook RD, Cromar K et al (2017) A joint ERS/ATS policy statement: what constitutes an adverse health effect of air pollution? An analytical framework. *Eur Respir J* 49(1):1600419. <https://doi.org/10.1183/13993003.00419-2016>
- Truong H, Lomnicki S, Dellinger B (2010) Potential for misidentification of environmentally persistent free radicals as molecular pollutants in particulate matter. *Environ Sci Technol* 44(6):1933–1939. <https://doi.org/10.1021/es902648t>
- van Donkelaar A, Martin RV, Brauer M, Hsu NC, Kahn RA, Levy RC, Lyapustin A, Sayer AM, Winker DM (2016) Global estimates of fine particulate matter using a combined geophysical-statistical method with information from satellites, models, and monitors. *Environ Sci Technol* 50(7):3762–3772
- Vedal S, Kim SY, Miller KA, Fox JR, Bergen S, Gould T, Kaufman JD, Larson TV, Sampson PD, Sheppard L, Simpson SD, Szpiro AA (2013) Section 1. NPACT epidemiologic study of components of fine particulate matter and cardiovascular disease in the MESA and WHI-OS Cohorts. In: National particle component toxicity (NPACT) initiative report on cardiovascular effects. Res Rep 178. Health Effects Institute, Boston, MA
- Vejerano EP, Rao G, Khachatryan L, Cormier SA, Lomnicki S (2018) Environmentally persistent free radicals: insights on a new class of pollutants. *Environ Sci Technol* 52:2468–2481
- Verisk (2017) Wildfire risk analysis. [https://www.verisk.com/insurance/visualize/key-findings-from-the-2017-verisk-wildfire-risk-analysis/?utm\\_source=Social&utm\\_medium=Twitter&utm\\_campaign=VeriskSM&utm\\_content=842017](https://www.verisk.com/insurance/visualize/key-findings-from-the-2017-verisk-wildfire-risk-analysis/?utm_source=Social&utm_medium=Twitter&utm_campaign=VeriskSM&utm_content=842017). Accessed 31 May 2019
- Vieira JL, Guimaraes GV, de Andre PA, Cruz FD, Saldiva PHN, Bocchi EA (2016) Respiratory filter reduces the cardiovascular effects associated with diesel exhaust exposure: a randomized, prospective, double-blind, controlled study of heart failure: the FILTER-HF trial. *JACC: Heart Failure* 4(1):55–64 <https://doi.org/10.1016/j.jchf.2015.07.018>
- Voutsas D, Samara C (2002) Labile and bioaccessible fractions of heavy metals in the airborne particulate matter from urban and industrial areas. *Atmos Environ* 36:3583–3590
- Wang M, Beelen R, Stafoggia M Raaschou-Nielsen O, Andersen ZJ, Hoffmann B, Fischer P, Houthuijs D, Nieuwenhuijsen M, Weinmayr G, Vineis P, Xun WW, Dimakopoulou K, Samoli E, Laatikainen T, Lanki T, Turunen AW, Oftedal B, Schwarze P, Aamodt G, Penell J, De Faire U, Korek M, Leander K, Pershagen G, Pedersen NL, Östenson CG, Fratiglioni L, Eriksen KT, Sørensen M, Tjønneland A, Bueno-de-Mesquita BO, Eeftens M, Bots ML, Meliefste K, Krämer U, Heinrich J, Sugiri D, Key T, de Hoogh K, Wolf K, Peters A, Cyrys J, Jaensch A, Concin H, Nagel G, Tsai MY, Phuleria H, Ineichen A, Künzli N, Probst-Hensch N, Schaffner E, Vilier A, Clavel-Chapelon F, Declercq C, Ricceri F, Sacerdote C, Marcon A, Galassi C, Migliore E, Ranzi A, Cesaroni G, Badaloni C, Forastiere F, Katsoulis M, Trichopoulou A, Keuken M, Jedynska A, Kooter IM, Kukkonen J, Sokhi RS, Brunekreef B, Katsouyanni K, Hoek G. (2014) Long-term exposure to elemental constituents of particulate matter and cardiovascular mortality in 19 European cohorts: results from the ESCAPE and TRANSPHORM projects. *Environ Int.* 66:97–106. <https://doi.org/10.1016/j.envint.2014.01.026>
- Weagle CL, Snider G, Li C, van Donkelaar A, ... and Martin RV. (2018). Global sources of fine particulate matter: interpretation of PM<sub>2.5</sub> chemical composition observed by SPARTAN using a global chemical transport model. *Environ Sci Technol* 52(20):11670–11681 <https://doi.org/10.1021/acs.est.8b01658>
- Weichenthal S, Crouse DL, Pinault L, Godri-Pollitt K, Lavigne E, Evans G, van Donkelaar A, Martin RV, Burnett RT (2016) Oxidative burden of fine particulate air pollution and risk of cause-specific mortality in the Canadian Census Health and Environment Cohort (CanCHEC). *Environ Res* 146:92–99. <https://doi.org/10.1016/j.envres.2015.12.013>
- Wegesser TC, Pinkerton KE, Last JA (2009) California wildfires of 2008: coarse and fine particulate matter toxicity. *Environ Health Perspect* 117(6):893–897. <https://doi.org/10.1289/ehp0800166>
- WHO Regional Office for Europe (2013) Review of evidence on health aspects of air pollution—REVIHAAP Project, Technical Report Copenhagen: WHO Regional Office for Europe. [http://www.euro.who.int/\\_\\_data/assets/pdf\\_file/0004/193108/REVIHAAP-Final-technical-report.pdf](http://www.euro.who.int/__data/assets/pdf_file/0004/193108/REVIHAAP-Final-technical-report.pdf)
- WHO (2016) Ambient air pollution: a global assessment of exposure and burden of disease. World Health Organization. <http://www.who.int>
- WHO (2018) 9 out of 10 people worldwide breathe polluted air, but more countries are taking action. News Release, 2 May 2018. <http://www.who.int/news-room/detail/02-05-2018-9-out-of-10-people-worldwide-breathe-polluted-air-but-more-countries-are-taking-action>
- Wiseman C (2015) Analytical methods for assessing metal bioaccessibility in airborne particulate matter: a scoping review. *Anal Chim Acta* 877:9–18. <https://doi.org/10.1016/j.aca.2015.01.024>
- Wyzga RE, Rohr AC (2015) Long-term particulate matter exposure: attributing health effects to individual PM components. *J Air Waste Manag Assoc* 65(5):523–543. <https://doi.org/10.1080/10962247.2015.1020396>
- Yang BY, Qian Z, Howard SW, Vaughn MG, Fan SJ, Liu KK, Dong GH (2018) Global association between ambient air pollution and blood pressure: a systematic review and meta-analysis. *Environ Pollut* 235:576–588. <https://doi.org/10.1016/j.envpol.2018.01.001>
- Ye D, Klein M, Mulholland JA, Russell AG, Weber R, Edgerton ES, Chang HH, Sarnat JA, Tolbert PE, Ebel Sarnat S (2018) Estimating acute cardiovascular effects of ambient PM<sub>2.5</sub> metals. *Environ Health Perspect* 126(2):027007. <https://doi.org/10.1289/ehp2182>
- Yousouf H, Liouss C, Roblou L, Assamoi EM, Salonen RO, Maesano C, Banerjee S, Annesi-Maesano I (2014) Non-accidental health impacts of wildfire smoke. *Int J Environ Res Pub Health* 11:11772–11804
- Zhou J, Ito K, Lall R, Lippmann M, Thurston G (2011) Time-series analysis of mortality effects of fine particulate matter components in Detroit and Seattle. *Environ Health Perspect* 119:461–466. <https://doi.org/10.1289/ehp.1002613>

**Transforming Environmental Chemistry  
and Toxicology to Meet the Anthropocene  
Sustainability Challenges Beyond *Silent Spring***

# Transforming Environmental Chemistry and Toxicology to Meet the Anthropocene Sustainability Challenges Beyond *Silent Spring*

Ling Jin, Guibin Jiang, and Xiangdong Li

## Abstract

This chapter revisits the development path of environmental chemistry and toxicology since the publication of *Silent Spring* in 1962. The fifty years have witnessed the transition of the subject from exposure and effect assessments based upon case chemicals in a segregated and phenomenological way toward a more predictive system science with generalized principles and translational evidences that are applicable for management references to tackle global environmental issues. This chapter further discusses the way forward that is fit for the Anthropocene sustainability challenges.

## 1 Setting the Big Scene for Environmental Chemistry and Ecotoxicology

### 1.1 The Anthropocene

*Homo sapiens* first evolved in the Pleistocene Epoch (2.6 million—11,700 years ago), marking a historical event of the Quaternary period. By the end of the epoch, humans could be found in nearly every part of the planet. The subsequent Holocene Epoch has seen the growth and impacts of the human species worldwide, development of major civilizations, and overall significant transition toward urban living in the present. It was not until the Industrial Revolution in the nineteenth century that human civilizations started to exert globally pervasive and steeply increasing influence on planet Earth, including the land surface, biosphere, and

atmosphere. Human activities have become a driving force that changes many characteristics of our environment on local, regional, and global scales, with notable examples including land use change, agriculture, fossil fuel burning, traffic emissions, and the release of industrial and commercial products. To recognize this drastic change, Nobel laureate Paul J. Crutzen and colleagues proposed a new geological epoch, the Anthropocene (Crutzen 2002) (Fig. 1). While the concept is widely accepted and increasingly used across the sciences and humanities, the actual beginning of the Anthropocene is still under debate. The proposed dates range from early human history via the nineteenth century (industrialization) to the 1960s (nuclear weapon testing and “Great Acceleration”) (Lewis and Maslin 2015; Waters et al. 2016).

As mankind’s capability to modify the natural system increases, so does his interference with and destruction to the environment. A wide range of anthropogenically induced environmental problems have thus been exacerbated worldwide, which set the historical context for the publication of Rachel Carson’s seminar volume, *Silent Spring*, in 1962. Carson describes the catastrophic effects of the insecticide dichlorodiphenyltrichloroethane (DDT) and other pesticides often used in agricultural control programs in the 1940s and 1950s. They belong to a group of persistent organic pollutants (POPs) that is now widely known as the “dirty dozen”: aldrin, chlordane, DDT, dieldrin, endrin, heptachlor, mirex, toxaphene (insecticides), polychlorinated dibenzo-p-dioxins, and polychlorinated dibenzofurans (PCDDs/PCDFs) (combustion by-products from, e.g., waste incineration or the metallurgic industry), hexachlorobenzene (insecticide, industrial chemical, and combustion by-product), as well as polychlorinated biphenyls (PCBs) (industrial chemicals and combustion by-products). Many countries have since then enacted environmental laws, an entire new research discipline has emerged, and tools to detect and predict the hazards and risks of environmental contaminants have been developed. The revolutionary element in Carson’s work was her extrapolation from

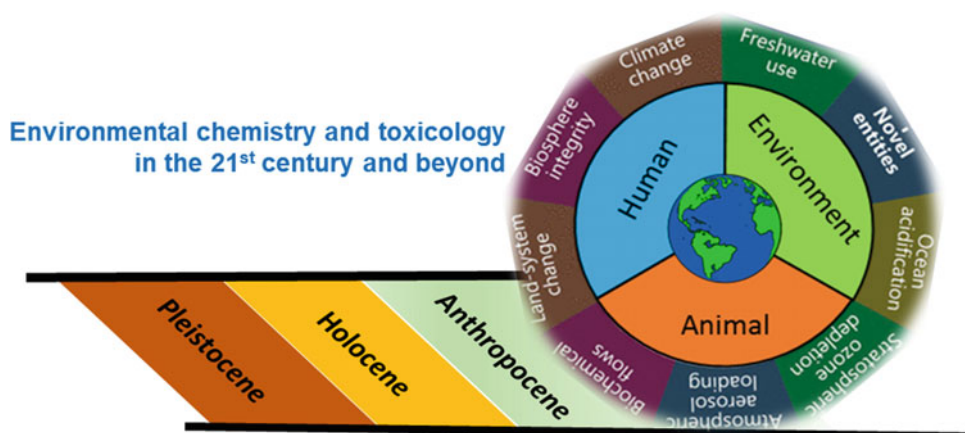
L. Jin · X.D. Li (✉)

Department of Civil and Environmental Engineering, The Hong Kong Polytechnic University, Hung Hom, Kowloon, Hong Kong  
e-mail: [cexdli@polyu.edu.hk](mailto:cexdli@polyu.edu.hk)

G.B. Jiang

State Key Laboratory of Environmental Chemistry and Ecotoxicology, Research Center for Eco-Environmental Sciences, Chinese Academy of Sciences, Beijing, China

**Fig. 1** Planetary boundaries threats and One Health in the Anthropocene epoch as the new scene for the future development of environmental chemistry and toxicology



single-organism effects to effects on the whole ecosystem and the “balance of nature”.

Carson’s work as the first publication in environmental science has far-reaching impact on what we do as environmental chemists and toxicologists. It catalyzed the separation of environmental toxicology from classical toxicology (Werner and Hitzfeld 2012). More than 50 years after *Silent Spring*, how far have we come in our efforts in understanding and managing the environmental health risks of thousands of man-made chemicals emerging in the commerce beyond the dirty dozen? Can we characterize and mitigate the consequences of multiple stressors beyond chemicals which are foreseen to be more globally pervasive in the Anthropocene? It is time to take a look at the state of environmental chemistry and toxicology and pave a way for its future.

## 1.2 Planetary Boundaries

A few years after the Anthropocene concept was proposed, Rockström et al. (2009) introduced the related idea of planetary boundaries that delimitate a “safe operating space for humanity.” The planetary boundary concept emerged from a recognition that the current magnitude of human activity can lead to impacts at a planetary scale that threaten the vital Earth system processes that allow humanity to thrive (Castree 2018). Human activities that exceed a planetary boundary disrupt the stable conditions known as the Holocene, which have supported human development over the last 12,000 years, and threaten the viability of the Earth system. Nine measurable indicators of natural processes at a planetary scale were identified, including climate change, ocean acidification, stratospheric ozone, global phosphorus and nitrogen cycles, atmospheric aerosol loading, freshwater use, land use change, biodiversity loss, and chemical pollution

(Rockström et al. 2009). For seven of these boundaries, quantitative measures and estimates of society’s margin of safety or exceedance with respect to the safe operating range were provided. Chemical agents by definition govern five of the nine planetary boundaries: ozone depletion (halocarbons), climate change ( $\text{CO}_2$ ,  $\text{CH}_4$ , and other climate-forcing agents), ocean acidification ( $\text{CO}_2$ ), the nitrogen and phosphorus cycles, and chemical pollution. Thus, it is clear that chemicals can have a variety of impacts on vital earth surface system processes.

The “chemical pollution” boundary is one of the two boundaries for which Rockström et al. provided no clear quantitative definition. Persson et al. (2013) postulated that “chemical pollution” is not a single category in the planetary boundary framework, but rather that many unknown planetary boundary issues governed by chemical or related agents may exist, which are collectively classified as “novel entities” (Steffen and Rockström 2015) (Fig. 1). Three conditions were identified that must be simultaneously fulfilled to qualify a chemical or mixtures of chemicals as a planetary boundary threat: (1) it has an unknown disruptive effect on a vital Earth system process, (2) the disruptive effect is not discovered until it is a problem at the global scale, and (3) the effect is not readily reversible (MacLeod et al. 2014). In this context, the boundary “novel entities” may also refer to new forms of particulate (e.g., airborne particulate matter, engineered nanomaterials) or microbiological stressors (e.g., pathogens, antimicrobial resistance) beyond legacy POPs and emerging chemicals of concern (e.g., antibiotics, biocides, disinfectants, and endocrine disruptors), which also reflects the broader sense of sustainability required in the Anthropocene. With this perspective, it is clear that environmental chemistry and toxicology should play a more proactive role in the development of a new and global approach to identify and manage novel entities that are planetary boundary threats in order to mitigate these global problems.

### 1.3 One Health

The Anthropocene is marked by highly coupled human and natural systems, in which human, animal, plant, and environmental health are closely interdependent (Fig. 1). The “One Health” approach was conceptualized as a global public health strategy that encourages interdisciplinary collaborative efforts to attain optimal health of people, animals, and our environment (Destoumieux-Garzón et al. 2018). Zoonotic public health emergencies, such as the outbreaks of severe acute respiratory syndrome, Middle East respiratory syndrome, H1N1 influenza, Ebola, and Zika, were among the first incidences where the One Health approach gained popularity. One Health is also prominent in several global environmental issues, such as climate change and antimicrobial resistance (AMR).

While the triad of human health, animal health, and the environment is widely advocated in the One Health framework, the environment is arguably the most dynamic and consequently the most confounding sector as evident from the examples of antibiotic resistance and climate change (Essack 2018; McEwen and Collignon 2018; Walsh 2018; Zinsstag et al. 2018). AMR has been described as the “quintessential One Health issue” as it exists in all three sectors (Robinson et al. 2016). However, the relative importance of the three sectors in the development, transmission, and prevalence of AMR are poorly understood (Berendonk et al. 2015). Antibiotic resistance is a direct consequence of the selection pressures from warranted and indiscriminate antibiotic use in human and animal health and antibiotic exposure in the environment (Vikesland et al. 2017). Use of antibiotics in animal production systems at sub-therapeutic doses for prolonged periods creates optimal conditions for bacteria to develop AMR (Zhu et al. 2013). The antibiotic resistance genes are subsequently transferred to human pathogens or commensals via humans, contaminated food, or the environment. Antibiotics used in humans and animals are frequently analogs of each other, which potentially drives the transmission of resistance between humans and animals, and there is growing evidence linking antibiotic consumption in livestock to antimicrobial resistance in the clinical settings (Liu et al. 2016). In contrast, the clinical relevance of antibiotic resistance is least well understood in the environment. Environmental bacteria, which are quantitatively the most prevalent bacteria, serve as reservoirs of resistance genes that can become incorporated into human and animal pathogens over time. These gene reservoirs are augmented by the influx of resistance genes from livestock and human waste into the environment. They are further augmented by the entry of antibiotic residues from pharmaceutical industries, intensive livestock farming,

and hospitals, which disrupt the soil and water microflora in addition to exerting selection pressure for the development of resistance. The environment is subject to variable weather patterns, particularly fluctuations in temperature, humidity, and precipitation, constituting multi-stress effects that affect bacterial ecosystems, making the environment a vacillating sector in the One Health AMR triad.

Similarly, chemical and related stressors targeted by environmental chemistry and toxicology find their manifestation in this One Health framework. The ultimate protection goals of the relevant research—the ecosystem integrity and services (clean air, water, and quality animal- and plant-derived food)—are critical environmental determinants of health. Therefore, environmental chemistry and toxicology should be encouraged to become a substantial contribution to “One Health” driven environmental research on chemical and related pollution as planetary boundary threats in the Anthropocene.

---

## 2 New Updates of Environmental Chemistry and Toxicology

### 2.1 Mixtures, Exposome, and Multiple Stressors

*Silent Spring* triggered decade-long scientific research and public campaign on the “dirty dozen” chemicals, leading to the Stockholm Convention in 2001, the very first international treaty on global efforts to reduce environmental and human exposures to what we now call “legacy POPs”. Following these landmark events, global research efforts have been in succession to characterize the sources, behaviors, fate, and biological effects of chemical pollutants from legacy POPs (Aylward and Hays 2002) to identification of new POPs (e.g., perfluoroalkyl substances) (Wang et al. 2009) and currently a wider spectrum of chemicals with diverse structures and properties (e.g., endocrine disruptors, pharmaceuticals, and personal care products) (Daughton 2014; Daughton and Ternes 1999). It is recognized that the environmental exposure occurs as complex contaminant mixtures and results in cocktail effects, although current toxicity risk assessment is still mainly based on individual chemicals.

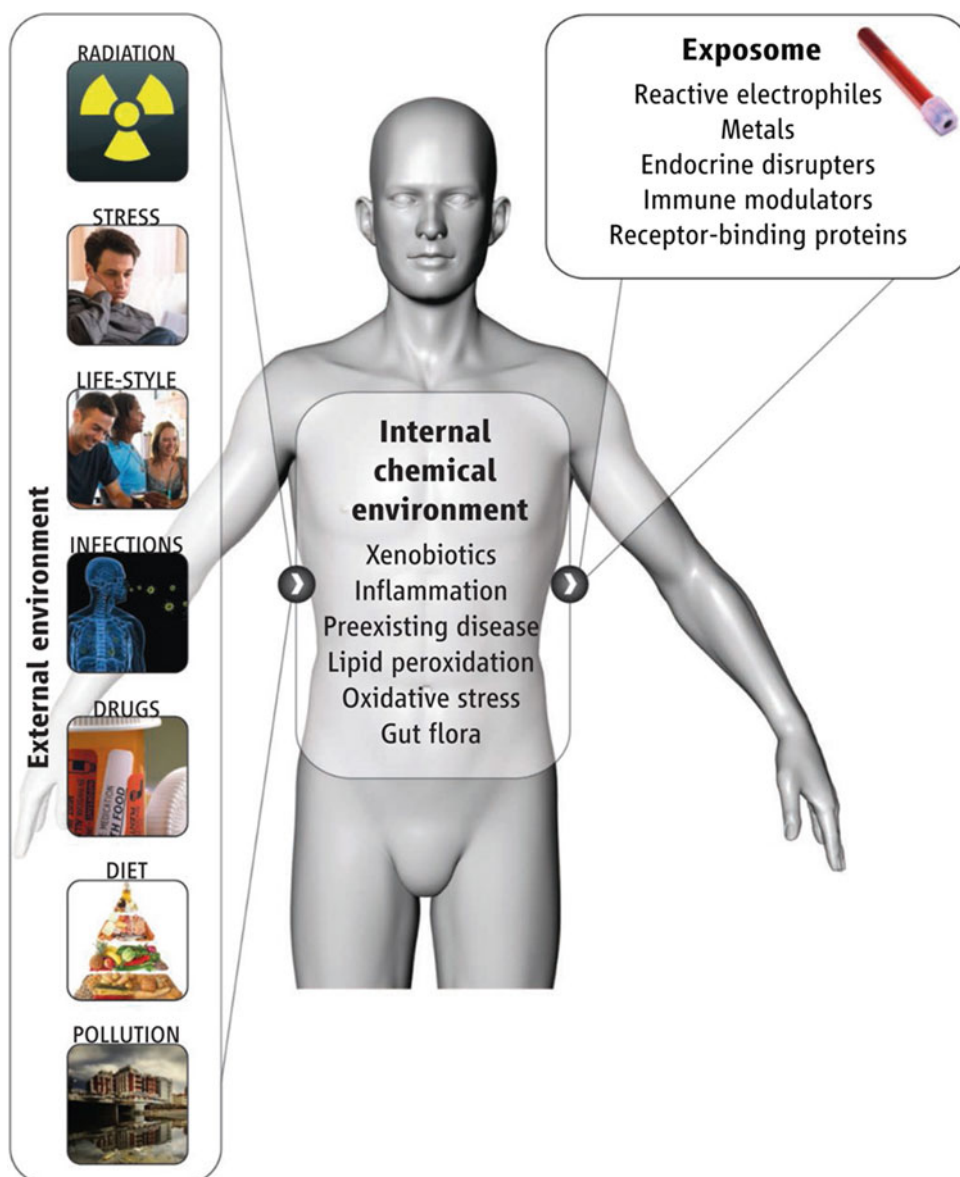
Complementary to the genome, the term “exposome” was proposed by Wild in 2005 to describe the completeness of environmental exposure in a hope to provide important clues for discovering the etiology of diseases (Wild 2005). According to Wild, the exposome encompasses environmental exposures including lifestyle factors throughout an individual’s lifetime starting from the prenatal period (Wild 2005). As such, understanding the complex interplay with

genetic susceptibility requires an accurate assessment of the exposure throughout the lifespan. Only in the presence of specific environmental exposures will the majority of genetic alterations contribute to population disease burden (Vineis et al. 2001). The exposome concept was further enriched by Rappaport and Smith (2010), who defined it as the totality of human exposures from all exogenous and endogenous sources in the “internal chemical environment.” This updated definition considers that exposures include not only those exogenous chemicals sourced from the environment (e.g., air, food, water, dust) but also those exogenous agents produced by or involved in internal physiological processes (e.g., inflammation, oxidative stress, lipid peroxidation, infections, the microbiome) (Fig. 2). The internal chemical milieu is highly dynamic throughout an individual’s life

history due to external and internal factors and processes such as aging, infections, lifestyle, preexisting diseases, etc. (Rappaport et al. 2014; Rappaport and Smith 2010).

While originally proposed in the context of human toxicology, the exposome concept can be extended analogously to wildlife and ecosystems, which is termed as “eco-exposome” (National Research Council (NRC) 2012). Similar to the extended definitions of the human exposome, the eco-exposome is described by both internal and external measures of exposure (Lioy and Smith 2013). While the exposome and eco-exposome concepts have their respective targets for humans and wildlife, the conserved targets for chemicals’ modes of action at the cellular level may allow cross-species extrapolations (Rand-Weaver et al. 2013). Thus, the exposome construct would establish an important

**Fig. 2** The essence of exposome (Reprinted with permission from Rappaport and Smith 2010)





link between human and environmental health by examining the combined effect of the complete exposure history encompassing both exogenous and endogenous agents across levels of biological organization and complexity. Shared toxicity pathways can be a basis to identify commonalities, and variations in metabolic and functional traits may explain differences (Forbes and Galic 2016; Kramer et al. 2011).

The definitions of the exposome have their specific merits depending on the angle from which exposure is viewed. On one hand, “bottom-up” strategies focus on targeted chemicals driven by specific hypotheses. On the other hand, “top-down” strategies aim at measuring the full spectrum of chemicals or their downstream products in a subject’s tissue or fluid sample (e.g., blood) as far as technically feasible (Rappaport et al. 2014; Vineis et al. 2017). Exposome research has been limited by low-throughput and costly methods, prompting the development of sensitive and high-throughput exposome analytical platforms. One of the recent advances has been using isotopically labeled biomarkers with common functional groups (e.g., phenolic hydroxyl/carboxyl/primary amine) for targeted and untargeted biomarkers coupled with an automatic computational pipeline method for identification and quantification (Jia et al. 2019). Similarly to these exposome efforts in human health, there has been a focus on exposure assessment without necessarily establishing a quantitative link to adverse effects. Human exposome and eco-exposome research face similar challenges, and therefore they can mutually benefit each other by generating mechanistic knowledge.

Conventional exposure assessment has mainly focused on exposure to environmental chemicals and related stressors. Admittedly, knowledge about microbes as agents of infectious disease had been advanced long before the start of chemical exposure science. The discovery of pathogenic microbes as causative agents in human diseases marked a revolution in the public health sector. Today, discoveries of the importance of the human microbiome as a determinant of health and disease are precipitating a second revolution. Contributions of microorganisms to both infectious and noninfectious processes merit balanced attention in environmental chemistry and toxicology. On one hand, the microbiome should be viewed as an agent of exposure in companion to chemicals (Nazaroff 2019). On the other hand, the microbiome may act as a modulator of chemical exposures by altering the chemical forms in ways that would affect their absorption, distribution, metabolism, and elimination (Koppel et al. 2017; Spanogiannopoulos et al. 2016). Gut microbiota have been found to be able to metabolize environmental chemicals (Claus et al. 2016). There is a growing body of evidence suggesting that gut microbiota are a major, yet underestimated element that must be considered

to fully evaluate the toxicity of environmental contaminants. The exposome concept provides a timely platform to incorporate both chemical and microbiological stressors and their interactions into one unified framework, thus broadening the “exposure” domain in environmental chemistry and toxicology and enhancing the discipline’s capability to contribute to improved environmental and human health.

## 2.2 Temporal Dynamics in the Equation of Environmental Chemistry and Toxicology

Traditional exposure and effect assessments often involve constant exposure to chemicals for a short period, while long-term assessments are encouraged now. However, environmental exposures change over time and space dynamically. The lack of comparisons between event-based and continuous exposure hinders the evaluation of which is more relevant for risk assessment. The predominance of low-dose exposures suggests that gradual and continuous (or sequential) exposures may well be the most relevant for sublethal effects and long-term sustainability. Event-based exposures also overlook the significance of biological resilience in toxicity development, such as the adaptive and non-adaptive properties of biological receptors. Examples of the latter include molecular networks, individuals, populations and ecological communities. Studies on the adverse outcomes under various temporal dynamics are essential for future ecotoxicology. In this sense, causal models from epidemiology and time-varying sequential exposures offer a starting point.

While chemicals in the environment are increasingly diversified, the lethality of new substitutes is consistently decreasing due to safer designs than their predecessors. Nevertheless, the perspective of a progressively diverse sublethal mixture of stressors threatens the central assumption of monotonicity. Acute mortality is a drastic outcome and it may be mostly monotonic to single chemicals. However, the sustainability of life forms requires machinery that may be adversely affected in multiple nonmonotonic ways. From gene expression to endocrine systems, or from proper display of phenological traits, successful survival of populations is replete with responses highly dependent on physiological modulation. Mediated processes often exhibit nonlinearity, and hence lack of monotonicity. Low doses of pollutants could interact with vital processes other than lethal toxicity targets, thus modulating significant sublethal effects. Numerous critical environmental transitions are attributed to the interaction of sublethal stressors. While individually negligible, sublethal contaminants in combination with one another can indirectly trigger more severe effects at population levels via adverse effects on the reproductive and immune systems. Ecotoxicology should go

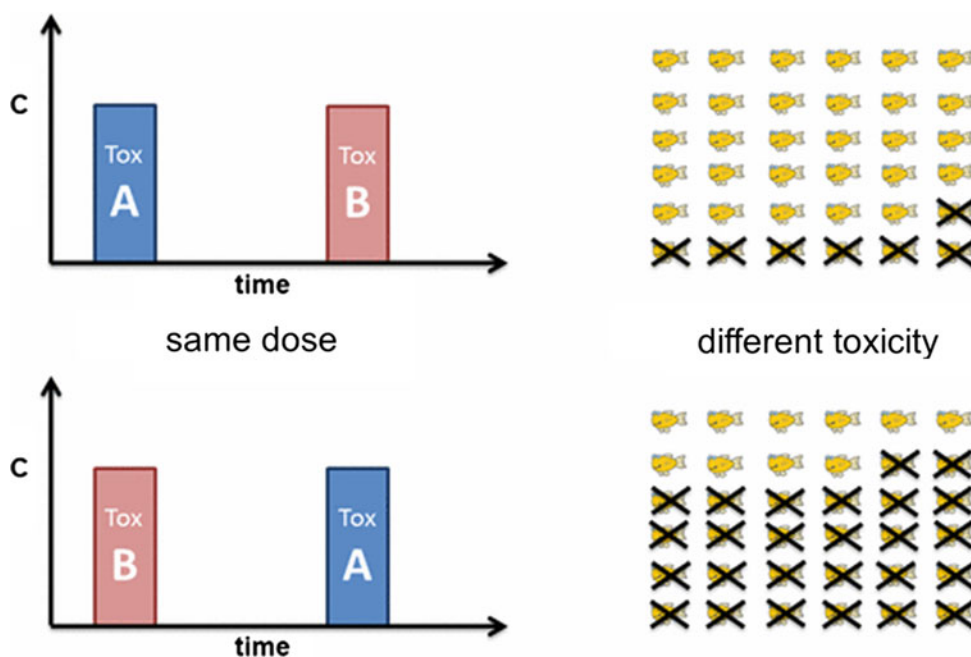
beyond lethality and focus on the resilience of biological systems.

“The dose makes the poison” is the long-held doctrine in classical toxicology and its branch disciplines. It assumes that the effect of a chemical no longer exists once cleared out of the organism, which is termed as “toxicokinetic recovery” (Ockleford et al. 2018). However, the principle overlooks toxicodynamic recovery, the process of re-establishing homeostasis, which can be fast or slow depending on the chemical (Ockleford et al. 2018). In this sense, the toxicity of chemical mixtures even as simple as two-component combinations can differ when organisms are exposed to the two toxicants in sequences that differ in order (Fig. 3). Ashauer et al. (2017) tested this hypothesis by exposing the freshwater crustacean *Gammarus pulex* to four toxicants that act on different targets (diazinon, propiconazole, 4,6-dinitro-o-cresol, 4-nitrobenzyl chloride). They found clearly different toxicity when the exposure order of two toxicants was reversed even with the same dose maintained. Slow toxicodynamic recovery caused carryover toxicity on subsequent exposures, thereby resulting in a sequence effect—but only when toxicodynamic recovery was slow relative to the interval between exposures. This suggests that carryover toxicity is a useful proxy for organism fitness and that risk assessment methods should be revised as they currently could underestimate risk (Ashauer et al. 2010). It is therefore not only the dose that makes the poison but also the exposure sequence. Furthermore, toxicodynamic models are at present not readily available for mixtures. They would be an asset to quantitatively model and predict adverse outcomes or diseases resulting from mixtures for which exposure

information is limited or where quantitative knowledge is available only for a limited number of toxic modes of action. Such models would also open an avenue toward approaching temporal issues in adverse outcome assessment such as noncontinuous or sequential exposures.

Chronological sequences on geological scales are an extended aspect of the temporal dynamics from the current prospective and retrospective risk assessments, which primarily focus on the contemporary situation with a look into its immediate past and near future. Putting future global megatrends in anthropogenically induced ecological challenges into perspective requires a comprehensive understanding of the impacts of human–natural interactions on ecosystems with respect to geological chronology. This is particularly important to meet the future demands in effective risk reduction strategies in response to the evolving stressors in the Anthropocene. It has become increasingly recognized that extrapolations based on the results of conventional toxicology studies must be tested over the long term in a natural ecosystem setting to account for increased complexity and multiple stressors. Reconstruction of environmental change through sediment cores from impacted estuaries or remote lakes may help to address some of the key knowledge gaps. It can facilitate rapid advances in our understanding of the chronic effects of pollutants on ecosystems in an environmentally realistic, multi-stressor context, when used as part of a weight-of-evidence framework with more traditional approaches in ecotoxicology. Resurrection ecology provides the most direct example of how paleolimnology can be integrated with classical toxicity testing to reveal, for example, the evolutionary responses of

**Fig. 3** An illustration of how exposure to the same combination of chemical mixture components in different time sequences results in different toxicities (Reprinted with permission from Ashauer et al. 2017)



resurrected zooplankton to chronic stressor exposures (Hairston et al. 1999). A paleo-ecotoxicological framework can leverage the recent advances in multidisciplinary technologies (e.g., isotope geochemistry, metagenomic approaches), thus providing novel insights into the most pressing questions in environmental chemistry and toxicology (Tse et al. 2018; Yin et al. 2018).

### 2.3 Predictive Continuum of Exposure and Effect Assessments

The traditional environmental chemistry and toxicology often segregate the assessment of chemical exposures from that of biological effects, thus hampering our ability to quantitatively describe the events over the continuum from sources of exposure pathways to internal and target exposures and eventual adverse outcomes. This “see-through” vision is beneficial not only to predicting the combined effects of what humans and the environment are exposed to in the perspective of fundamental science but also to more precise and effective management strategies on prioritized targets in the perspective of regulatory practice. This prompted the development of two novel concepts in the last decade, namely adverse outcome pathways (AOPs) and, subsequently, aggregate exposure pathways (AEPs), which connect the two ends of the exposome (Fig. 4).

Ankley et al. (2010) proposed the AOP conceptual construct that portrays existing knowledge concerning the linkage between a direct molecular initiating event and an adverse outcome at a biological level of organization relevant to risk assessment. The conceptual framework was developed to support the twenty-first-century risk

assessment of chemicals by providing mechanistic knowledge that links *in vitro*, *in chemico*, or *in silico* information to toxicity *in vivo* (Rusyn and Daston 2010; Yoon et al. 2012; Zhu et al. 2014). The AOP concept supports the mechanistic validation of predictive models based on the governing molecular mechanisms. Thus, high-throughput screening (HTS) data can be better used to prioritize a big library of chemicals for higher tiered testing and/or reducing the number of animal experiments. Furthermore, within a regulatory framework of integrated assessment, AOPs can support a new, more targeted safety-testing regime on focal hazards that are the most probable and relevant. To establish AOPs, subchronic or sublethal endpoints, as well as *in vitro* bioassays related to the acute and chronic effects may be used instead of apical endpoints typically assessed for regulatory purposes. Promises can be further harvested from the AOP framework as a tool for structuring knowledge or prioritization of testing as well as a quantitative predictive tool to relate exposure data to adverse outcomes (Carusi et al. 2018). However, it remains a challenge to incorporate toxicokinetics as an important determinant of toxicity in AOPs and to extrapolate to higher levels of biological organization and across species. In this connection, toxicokinetic differences at the chemical and/or species level and genetic polymorphisms among species can influence the events along an AOP cascade, thus propagating or alleviating the apical effects.

While the exposome and AOP respectively evolved in the fields of epidemiology and ecotoxicology, integrating biological responses in exposure assessment can cross-fertilize the two concepts. By considering endogenous and non-chemical stressors (e.g., microbes) and their mixture effects, the exposome can enrich the AOP concept. The exposome is

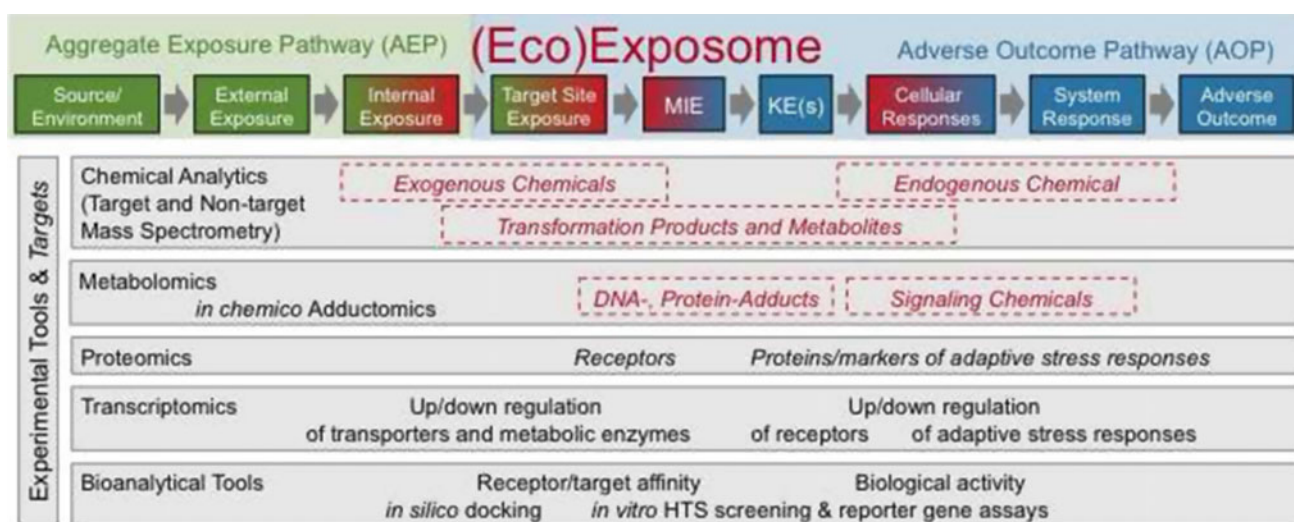


**Fig. 4** The predictive continuity from aggregate exposure pathways to exposome and adverse outcome pathways (Reprinted with permission from Escher et al. 2017)

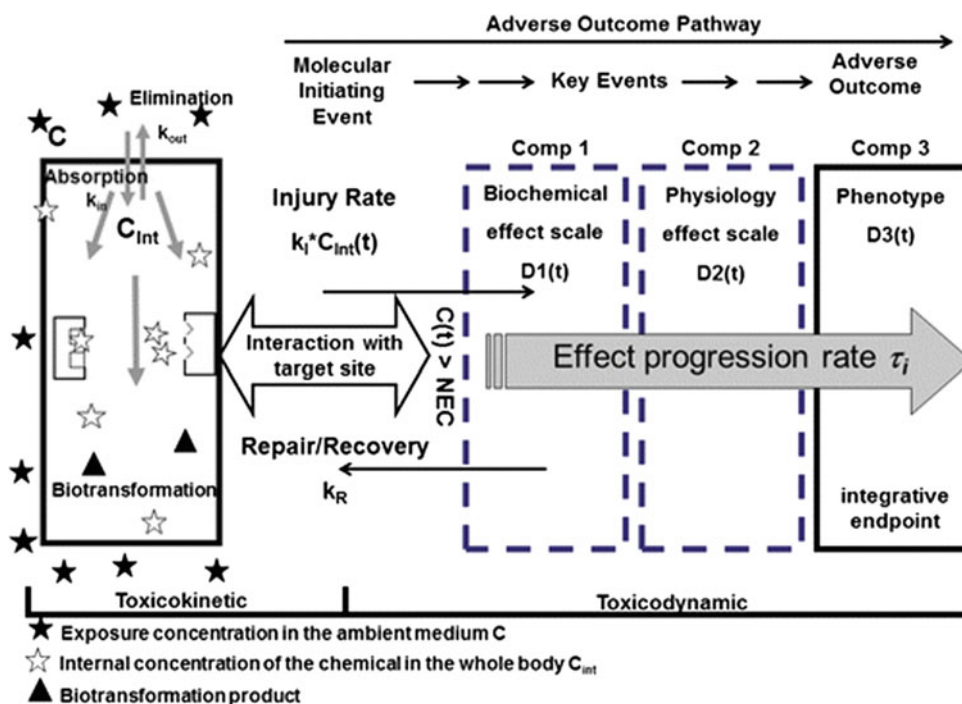
constructed specifically for individuals' totality of lifetime while the AOP concept is focused on biological mechanisms and pathways. The temporal dimension of the exposome is in part embedded in the AOP construct. Life-stage specificity or chronic toxicity, for example, would address effects that are related to long-term or potentially repeated exposure scenarios and biological responses. In principle, the requirements for AOPs to be used for mixtures do not differ significantly from those for individual chemicals (Altenburger et al. 2015). However, different molecular initiating events (MIEs) may trigger similar adverse outcomes, as those MIEs could act jointly on the same key event (KE) or they could have more complex interactions. This phenomenon has been observed with the interactive role of low-dose mixtures in carcinogenesis (Goodson et al. 2015). Therefore, studies should focus on those KEs that may augment the bioactivity of different compounds binding to different target sites while yet converging into the same adverse outcome (Vogs and Altenburger 2016).

In addition to downstream consequences of the exposome, categorizing upstream exposure pathways that shape the exposome will make the source-pathway-exposure-effects link intact. The AEP concept has been developed as the natural and complementary companion in the exposure sciences to the AOP concept in the toxicological sciences (Teeguarden et al. 2016). AEPs comprise a sequence of KEs from source via external exposure (including environmental and dietary exposure) to exposure in the organism, termed target site exposure, which is the crucial step linked to the MIEs in the AOP (Tan et al. 2018). Similar to AOPs, AEPs help to

organize exposure information from exogenous source to internal target site, setting the stage for inferring target concentrations of the chemicals with a predictive linkage to biological effects (Hines et al. 2018). The AEP conceptually considers toxicokinetic processes leading to exposure at the site of action. This is in consistency with the vision of exposure science to resolve the movement of chemicals from external sources to target sites by covering all levels of physical and biological organization.

Chemicals and microbiomes in the exposome constitute not only the exogenous agents transported into the body and their metabolites but also adducts with cellular constituents and other endogenous compounds, as well as signaling molecules formed as part of the pathway of toxicity or adaptive stress responses. The formation of chemical adducts can be classified as MIEs, while endogenous chemicals (e.g., ROS, nitric oxide, ATP, glutathione) formed or altered as part of the stress responses can be categorized as KEs. In this connection, some endogenous chemicals of the exposome get involved in defence against external insults rather than in the development of a disease. However, the internal chemical response of stressed/perturbed organisms (e.g., due to an infection or an unhealthy lifestyle) may potentially lower the repair capacities, which may result in the next downstream event. These specific cases should be addressed in future studies. Overall, aligning the chemicals in the exposome to the various steps of the AEP/AOP will help to quantify time-resolved exposure and effect events and thus establish the mechanistic link between the exposome and adverse health outcomes (Fig. 5).

**Fig. 5** Toxicokinetic–toxicodynamic models to quantify time-resolved exposure and effect events (Reprinted with permission from Vogs and Altenburger 2016)



### 3 Targeting the Big Questions

#### 3.1 How Can We Characterize the Chemical Use, Emissions, Fate, and Exposure Over Spatiotemporal Scales?

The lack of a specific spatiotemporal context is one of the limitations associated with the current environmental risk assessment framework of chemicals, which is often performed in a generalized manner. Retrieving data on the emissions, fate, and exposure of chemicals at high spatiotemporal resolutions may offer to map the lifetime exposure of organisms in reality, and provide a better predictive link to the impacts of such exposures. Novel insights into chemical exposure can be accelerated by increasingly available technologies in analytical (e.g., nontarget analysis), computational (e.g., high-resolution spatial models), sensor (e.g., remote sensing, passive sampling devices, miniaturized mobile sensors), and automation domains (e.g., robotics) (Hollender et al. 2017; Lohmann et al. 2017; Nyhan et al. 2016; Pennington et al. 2005; Shen et al. 2013). These technologies would facilitate (1) characterization of human and wildlife exposures to the overlooked diversity of chemicals, (2) quantification of chemical pollution at unprecedentedly higher spatiotemporal resolutions, and (3) access to hostile environments or systems that have been difficult to sample or access in the past. Smart use of available technologies coupled with big data analytics (Dafforn et al. 2016) will facilitate our understanding of the magnitude of human and ecological exposure to contaminants and consequent risks to ecosystem integrity and human health, which in turn helps prioritize mitigation targets and measures.

#### 3.2 How Can We Extrapolate Adverse Effects Across Levels of Biological Organization?

The scope of current regulatory toxicity studies is often confined within effect measurements on individual organisms exposed to chemicals. Therefore, these studies are not truly driven by protection goals, as they do not include the impacts on higher levels of biological organization, such as populations, communities, and ecosystem services. Extrapolation of effects across levels of biological organization is thus urgently needed. Mechanistic effect models offer a way to this end. For example, toxicokinetic–toxicodynamic models and quantitative AOPs extrapolate chemical concentrations or MIEs to individual-level effects (Ankley et al. 2010; Jager et al. 2011), dynamic energy budget models extrapolate changes in physiological responses to vital rates (Baas et al. 2018), individual-based and population models extrapolate

individual-level effects to population-level consequences (Forbes et al. 2011), food web models extrapolate effects on populations to community-level consequences (Lombardo et al. 2015), and ecological production functions extrapolate from changes in biophysical structure or processes to ecosystem functions driving ecosystem services. Recent advances include the development of good modeling practice; the integration of the toxicokinetic–toxicodynamic, dynamic energy budget, individual-based model approaches, and the use of scenarios and trait-based approaches to improve the general applicability of models. In addition to approaches for extrapolating across levels of biological organization, there are emerging computational approaches for extrapolating across species based on the conservation of key biological traits and molecular processes. The use of these approaches in environmental risk assessment is limited, and considerable research is still required to make the models suitable for regulatory risk assessment. In particular, more in-depth knowledge is required of mechanistic linkages between different levels of biological organization and increased availability of trait data for species that are relevant to key protection goals.

#### 3.3 How Can We Quantify the Effects of Multiple Stressors on Ecosystems and Integrate Stressor Interactions in Environmental Risk Assessments?

The global change in the Anthropocene subjects ecosystems to a multitude of stressors induced by nature and humans. The increasing complexity renders it challenging to quantify and predict their interactive effects. A wide array of approaches, including in situ toxicity identification and evaluation (Burton and Nordstrom 2004), molecular diagnostic tools (Dafforn et al. 2016), eco-epidemiology (Posthuma et al. 2016), and Bayesian network relative risk models (Landis et al. 2017) can generate multiple lines of evidence required to distinguish the effects of multiple stressors on ecosystems. However, the limited ecological information over sufficient spatiotemporal scales hampers our ability to distinguish chemical effects from natural variability and to establish robust causal links between exposure and effect. Such limited understanding of the combined effects of multiple stressors on ecosystems further hampers the development of sound risk assessment and effective management strategies. To improve the situation, the use of emerging high-throughput technologies from remote sensing (Chariton et al. 2016) and ecogenomics sequencing (Zhang 2019) would enable a more rapid and economical collection of ecological datasets than the current laborious physical and chemical monitoring on a similar or

even greater scale. However, as these methods evolve, care must be taken to ensure that the granularity and scale, as well as relevance and narrative intent, of different measures are properly taken into account. To establish causality, field surveys and weight-of-evidence approaches alone are not sufficient; a combination of field surveys and laboratory experiments is also required.

Accounting for multi-stressor effects on individuals, populations, and communities is one of the most perplexing goals of environmental risk assessment, though it can no longer be avoided in the face of increasingly complex global sustainability challenges (Kapo et al. 2014). The current practice either focuses on a single stressor or a limited number of stressors in a few model species under controlled conditions over limited timescales in prospective environmental risk assessments or characterizes the impacts that already occurred on ecosystems for which causality is virtually impossible to infer for individual stressors (Fischer et al. 2013; Hommen et al. 2010). This is the current dilemma in prospective and retrospective environmental risk assessments. Many chemical (e.g., pH), physical (e.g., temperature, sedimentation), and biological (e.g., parasitism, invasive species) stressors may enhance or reduce the impact of anthropogenic chemical exposures on dynamic and complex ecosystems. Interactions among these stressors can influence the bioavailability of chemical contaminants and subsequent uptake, transformation, and elimination, and may thus lead to antagonistic or synergistic effects on individual organisms (Karlsson et al. 2017). The ecosystem may be rendered more or less resilient to anthropogenic chemical pollution as a result of stressor-induced alterations in phenology, species tolerance, community composition, and biotic interactions (Rohr et al. 2016). Therefore, it is imperative to develop mechanistic exposure and models to account for multi-stressor effects in environmental risk assessment. The models should quantify stressor interactions at relevant spatiotemporal scales and enable extrapolation across levels of biological organization. This would require an integration of the results from simulation experiments at realistic environmental scenarios and from field studies capturing wide stressor gradients over geographical coverages (Beketov and Liess 2012). An advanced understanding of stressor interactions would facilitate the development of mechanistic models that allow combined exposure and effect assessment.

### **3.4 How Can We Enhance the Predictability of Risk Assessments Against Increasing Environmental Complexity and Spatiotemporal Scales?**

Stressors can be transported considerable distances from the point of release and may be distributed across multiple

habitats. Spatiotemporal variations in stressor exposure mirror the variation in the distribution of biological species, ecological processes, and the ecosystem services they provide, which determines the variability and context dependence of risk. It depends on the location, type, and quality of habitats and the exposure to stressors within the landscape. Current environmental risk assessment frameworks do not take into account the environmental complexity that drives spatiotemporal variation in risks at different scales. Current approaches that adopt “realistic worst-case” assumptions are more conservative than realistic. The validity of these assumptions would mean either inadequate or excessive protection. A more spatially defined environmental risk assessment would allow for better targeted allocation of resources to interventions where protection is most needed. Overly simple models do not represent important aspects of the system’s dynamics and create large biases. Overly complex models require a priori knowledge of species and environmental interactions and require a vast amount of parameterization to specify detailed dynamics, thus bring about large parameter uncertainty. An alternative approach to building complex models is to develop scenarios that are defined in terms of landscape structure and environmental conditions, incorporate spatial and temporal variability, and link to protection goals (Rico et al. 2016). Landscape ecotoxicology provides a conceptual framework integrating mechanistic exposure and effect modeling. The availability of spatiotemporally explicit datasets offers a prime opportunity to develop mapping and modeling tools that can make real-time predictions in a spatially defined fashion (Focks 2014).

---

## **4 Vision for Environmental Chemistry and Toxicology in the Twenty-First Century and Beyond**

Over 50 years have passed since Carson’s work, and the practice of simply identifying new chemicals, reporting high concentrations and finding new toxic mechanisms no longer fulfills the mission of utilizing chemistry and toxicology to tackle global environmental issues. Reductionist approaches are unlikely to provide timely solutions for the many pressing sustainability challenges. Future research must be driven by a specific practical purpose and question from a holistic perspective. The increasing complexity of stressors and sustainability challenges requires a radically novel theory that can deal with complex problems. This is where the complexity theory fits in. The theory shows that nearly all rules applicable to individual nodes are not relevant to a network, and complex systems often have an underlying simplicity. Therefore, the connectivity of nodes affected is more important than the particular properties of individual

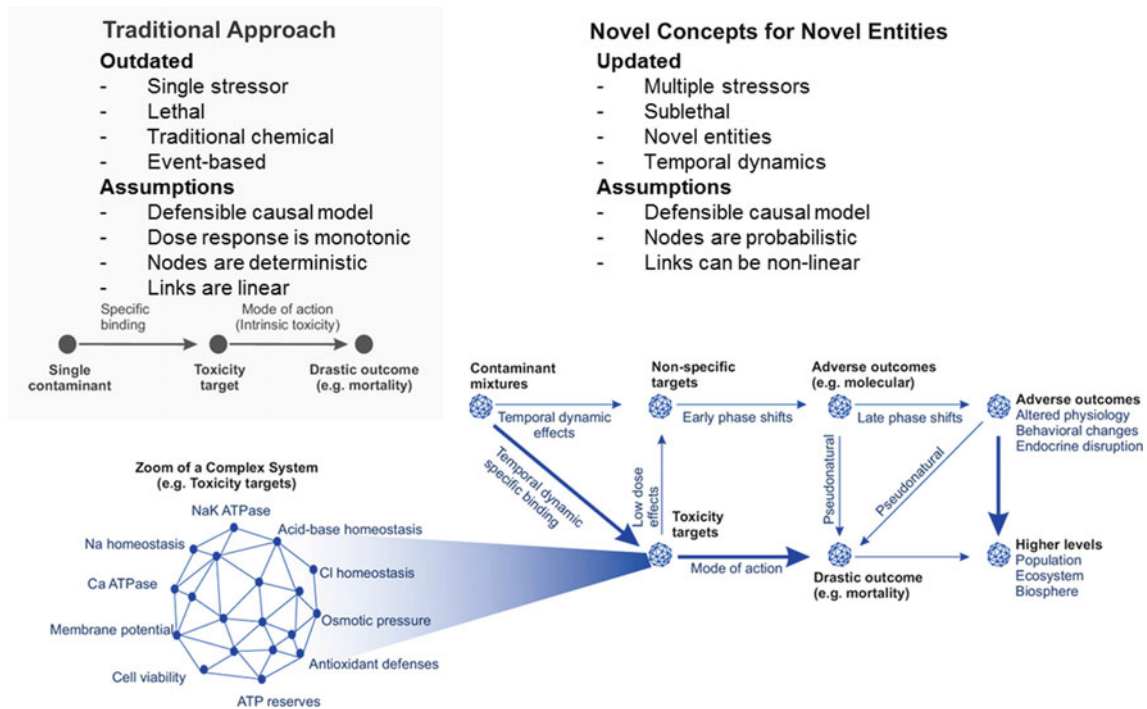


**Fig. 6** Paradigm shift of environmental chemistry and toxicology to fit for the Anthropocene complex sustainability challenges in the twenty-first century and beyond (Adapted with permission from de Souza Machado et al. 2019)

contaminants, which means that effects on more central parts are more likely to trigger systemic responses. This novel approach is a complex system where novel entities of planetary boundary threats affect biological systems initiating responses at various and interacting levels (Fig. 6). We hereby make the following recommendations:

- Shift the focus of environmental chemistry and toxicology from individual contaminants to the resilience of biological systems using the concepts of complexity theory and causal inference and investigation of emergent properties that cannot be predicted alone by the individual parts of the system;
- Contemplate the plethora of stressors, particularly those falling within the planetary boundary threats in the Anthropocene, in their temporal dynamic interactions with both specific and nonspecific targets that trigger apical effects in a probabilistic manner; and
- Develop mechanistic models combining exposure and effects assessments, in which a network of nodes is connected by nonlinear structured causal equations that allow the whole system to respond when in stressed conditions so as to generate more effective management strategies in response from a system perspective.

A paradigm shift from current analytical reductionism to a holistic view would accelerate the transformation of

environmental chemistry and toxicology into predictive science that can generalize the spatiotemporal continuity in the real-world scenarios. In this way, we can make environmental chemistry and toxicology an integral part of the interdisciplinary contributions to tackle the Anthropocene sustainability challenges in the twenty-first century and beyond.

## References

- Altenburger R, Ait-Aissa S, Antczak P, Backhaus T, Barceló D, Seiler TB, Brion F, Busch W, Chipman K, de Alda ML, de Aragão Umbuzeiro G, Escher BI, Falciani F, Faust M, Focks A, Hilscherova K, Hollender J, Hollert H, Jäger F, Jahnke A, Kortenkamp A, Krauss M, Lemkine GF, Munthe J, Neumann S, Schymanski EL, Scrimshaw M, Segner H, Slobodnik J, Smedes F, Kughathas S, Teodorovic I, Tindall AJ, Tollefsen KE, Walz KH, Williams TD, Van den Brink PJ, van Gils J, Vrana B, Zhang X, Brack W (2015) Future water quality monitoring—Adapting tools to deal with mixtures of pollutants in water resource management. *Sci Total Environ* 512–513:540–555. <https://doi.org/10.1016/j.scitotenv.2014.12.057>
- Ankley GT, Bennett RS, Erickson RJ, Hoff DJ, Hornung MW, Johnson RD, Mount DR, Nichols JW, Russom CL, Schmieder PK, Serrano JA, Tietge JE, Villeneuve DL (2010) Adverse outcome pathways: a conceptual framework to support ecotoxicology research and risk assessment. *Environ Toxicol Chem* 29:730–741. <https://doi.org/10.1002/etc.34>
- Ashauer R, Hintermeister A, Caravatti I, Kretschmann A, Escher BI (2010) Toxicokinetic and toxicodynamic modeling explains carry-over toxicity from exposure to diazinon by slow organism

- recovery. *Environ Sci Technol* 44:3963–3971. <https://doi.org/10.1021/es903478b>
- Ashauer R, O'Connor I, Escher BI (2017) Toxic mixtures in time—The sequence makes the poison. *Environ Sci Technol* 51:3084–3092. <https://doi.org/10.1021/acs.est.6b06163>
- Aylward LL, Hays SM (2002) Temporal trends in human TCDD body burden: decreases over three decades and implications for exposure levels. *J Expo Anal Environ Epidemiol* 12:319–328. <https://doi.org/10.1038/sj.jea.7500233>
- Baas J, Augustine S, Marques GM, Dorne JL (2018) Dynamic energy budget models in ecological risk assessment: from principles to applications. *Sci Total Environ* 628–629:249–260. <https://doi.org/10.1016/j.scitotenv.2018.02.058>
- Beketov MA, Liess M (2012) Ecotoxicology and macroecology—Time for integration. *Environ Pollut* 162:247–254. <https://doi.org/10.1016/j.envpol.2011.11.011>
- Berendonk TU, Manaia CM, Merlin C, Fatta-Kassinos D, Cytryn E, Walsh F, Bürgmann H, Sørum H, Norström M, Pons MN, Kreuzinger N, Huovinen P, Stefani S, Schwartz T, Kisand V, Baquero F, Martinez JL (2015) Tackling antibiotic resistance: the environmental framework. *Nat Rev Microbiol* 13:310–317. <https://doi.org/10.1038/nrmicro3439>
- Burton GA, Nordstrom JF (2004) An in situ toxicity identification evaluation method part I: laboratory validation. *Environ Toxicol Chem* 23:2844–2850. <https://doi.org/10.1897/03-409.1>
- Carusi A, Davies MR, De Grandis G, Escher BI, Hodges G, Leung KMY, Whelan M, Willett C, Ankley GT (2018) Harvesting the promise of AOPs: an assessment and recommendations. *Sci Total Environ* 628–629:1542–1556. <https://doi.org/10.1016/j.scitotenv.2018.02.015>
- Castree N (2018) Anthropocene and planetary boundaries. In: *International encyclopedia of geography*. Wiley, Oxford, UK, pp 1–18. <https://doi.org/10.1002/9781118786352.wbieg0027.pub2>
- Chariton AA, Sun M, Gibson J, Webb JA, Leung KMY, Hickey CW, Hose GC (2016) Emergent technologies and analytical approaches for understanding the effects of multiple stressors in aquatic environments. *Mar Freshw Res* 67:414–428. <https://doi.org/10.1071/MF15190>
- Claus SP, Guillou H, Ellero-Simatos S (2016) The gut microbiota: a major player in the toxicity of environmental pollutants? *NPJ Biofilms Microbiomes* 3:17001. <https://doi.org/10.1038/npjbiofilms.2016.3>
- Crutzen PJ (2002) Geology of mankind. *Nature* 415:23. <https://doi.org/10.1038/415023a>
- Dafforn KA, Johnston EL, Ferguson A, Humphrey CL, Monk W, Nichols SJ, Simpson SL, Tulbure MG, Baird DJ (2016) Big data opportunities and challenges for assessing multiple stressors across scales in aquatic ecosystems. *Mar Freshw Res* 67:393–413. <https://doi.org/10.1071/MF15108>
- Daughton CG (2014) The Matthew effect and widely prescribed pharmaceuticals lacking environmental monitoring: case study of an exposure-assessment vulnerability. *Sci Total Environ* 466–467:315–325. <https://doi.org/10.1016/j.scitotenv.2013.06.111>
- Daughton CG, Ternes TA (1999) Pharmaceuticals and personal care products in the environment: agents of subtle change? *Environ Health Perspect* 107(Suppl 6):907–938. <https://doi.org/10.1289/ehp.99107s6907>
- de Souza Machado AA, Wood CM, Kloas W (2019) Novel concepts for novel entities: updating ecotoxicology for a sustainable anthropocene. *Environ Sci Technol* 53:4680–4682. <https://doi.org/10.1021/acs.est.9b02031>
- Destoumieux-Garzón D, Mavingui P, Boetsch G, Boissier J, Darriet F, Duboz P, Fritsch C, Giraudoux P, Le Roux F, Morand S, Paillard C, Pontier D, Sœur C, Voituron Y (2018) The one health concept: 10 years old and a long road ahead. *Front Vet Sci* 5:14. <https://doi.org/10.3389/fvets.2018.00014>
- Escher BI, Hackermüller J, Polte T, Scholz S, Aigner A, Altenburger R, Böhme A, Bopp SK, Brack W, Busch W, Chadeau-Hyam M, Covaci A, Eisenträger A, Galligan JJ, Garcia-Reyero N, Hartung T, Hein M, Herberth G, Jahnke A, Kleinjans J, Klüver N, Krauss M, Lamoree M, Lehmann I, Luckenbach T, Müller GW, Müller A, Phillips DH, Reemtsma T, Rolle-Kampczyk U, Schüürmann G, Schwikowski B, Tan YM, Trump S, Walter-Rohde S, Wambaugh JF (2017) From the exposome to mechanistic understanding of chemical-induced adverse effects. *Environ Int* 99:97–106. <https://doi.org/10.1016/j.envint.2016.11.029>
- Essack SY (2018) Environment: the neglected component of the One Health triad. *Lancet Planet Heal* 2:e238–e239. [https://doi.org/10.1016/s2542-5196\(18\)30124-4](https://doi.org/10.1016/s2542-5196(18)30124-4)
- Fischer BB, Pomati F, Eggen RIL (2013) The toxicity of chemical pollutants in dynamic natural systems: the challenge of integrating environmental factors and biological complexity. *Sci Total Environ* 449:253–259. <https://doi.org/10.1016/j.scitotenv.2013.01.066>
- Focks A (2014) The challenge: landscape ecotoxicology and spatially explicit risk assessment. *Environ Toxicol Chem* 33:1193. <https://doi.org/10.1002/etc.2568>
- Forbes VE, Calow P, Grimm V, Hayashi TI, Jager T, Katholm A, Palmqvist A, Pastorok R, Salvito D, Sibly R, Spromberg J, Stark J, Stillman RA (2011) Adding value to ecological risk assessment with population modeling. *Hum Ecol Risk Assess* 17:287–299. <https://doi.org/10.1080/10807039.2011.552391>
- Forbes VE, Galic N (2016) Next-generation ecological risk assessment: predicting risk from molecular initiation to ecosystem service delivery. *Environ Int* 91:215–219. <https://doi.org/10.1016/j.envint.2016.03.002>
- Goodson WH, Lowe L, Carpenter DO, Gilbertson M, Ali AM, de Cerain Salsamendi AL, Lasfar A, Carnero A, Azqueta A, Amedei A, Charles AK, Collins AR, Ward A, Salzberg AC, Colacci A, Olsen AK, Berg A, Barclay BJ, Zhou BP, Blanco-Aparicio C, Bagloli CJ, Dong C, Mondello C, Hsu CW, Naus CC, Yedjou C, Curran CS, Laird DW, Koch DC, Carlin DJ, Felsher DW, Roy D, Brown DG, Ratovitski E, Ryan EP, Corsini E, Rojas E, Moon EY, Laconi E, Marongiu F, Al-Mulla F, Chiaradonna F, Darroudi F, Martin FL, Van Schooten FJ, Goldberg GS, Wagemaker G, Nangami G, Calaf GM, Williams G, Wolf GT, Koppen G, Brunborg G, Kim Lyerly H, Krishnan H, Hamid HA, Yasaei H, Sone H, Kondoh H, Salem HK, Hsu HY, Park HH, Koturbash I, Miousse IR, Ivana Scovassi A, Klaunig JE, Vondráček J, Raju J, Roman J, Wise JP, Whitfield JR, Woodrick J, Christopher JA, Ochieng J, Martinez-Leal JF, Weisz J, Kravchenko J, Sun J, Prudhomme KR, Narayanan KB, Cohen-Solal KA, Moorwood K, Gonzalez L, Soucek L, Jian L, D'Abronzo LS, Lin LT, Li L, Gulliver L, McCawley LJ, Memeo L, Vermeulen L, Leyns L, Zhang L, Valverde M, Khatami M, Romano MF, Chapellier M, Williams MA, Wade M, Manjili MH, Leonart M, Xia M, Gonzalez MJ, Karamouzian MV, Kirsch-Volders M, Vaccari M, Kuemmerle NB, Singh N, Cruickshanks N, Kleinstreuer N, Van Larebeke N, Ahmed N, Ogunkua O, Krishnakumar PK, Vadgama P, Marignani PA, Ghosh PM, Ostrosky-Wegman P, Thompson P, Dent P, Heneberg P, Darbre P, Leung PS, Nangia-Makker P, Cheng QS, Brooks Roberg R, Al-Temaimi R, Roy R, Andrade-Vieira R, Sinha RK, Mehta R, Vento R, Di Fiore R, Ponce-Cusi R, Dornetshuber-Fleiss R, Nahta R, Castellino RC, Palorini R, Hamid RA, Langie SAS, Eltom S, Brooks SA, Ryeom S, Wise SS, Bay SN, Harris SA, Papagerakis S, Romano S, Pavanello S, Eriksson S, Forte S, Casey SC, Luanpitpong S, Lee TJ, Otsuki T, Chen T, Massfelder T, Sanderson T, Guarnieri T, Hultman T, Dormoy V, Otero-Marah V,



- Sabbisetti V, Maguer-Satta V, Kimryn Rathmell W, Engström W, Decker WK, Bisson WH, Rojanasakul Y, Luqmani Y, Chen Z, Hu Z (2015) Assessing the carcinogenic potential of low-dose exposures to chemical mixtures in the environment: the challenge ahead. *Carcinogenesis* 36(Suppl 1):S254–S296. <https://doi.org/10.1093/carcin/bgv039>
- Hairston NG, Lampert W, Cáceres CE, Holtmeier CL, Weider LJ, Gaedke U, Fischer JM, Fox JA, Post DM (1999) Lake ecosystems: rapid evolution revealed by dormant eggs. *Nature* 401:446. <https://doi.org/10.1038/46731>
- Hines DE, Edwards SW, Conolly RB, Jarabek AM (2018) A Case study application of the aggregate exposure pathway (AEP) and adverse outcome pathway (AOP) frameworks to facilitate the integration of human health and ecological end points for cumulative risk assessment (CRA). *Environ Sci Technol* 52:839–849. <https://doi.org/10.1021/acs.est.7b04940>
- Hollender J, Schymanski EL, Singer HP, Ferguson PL (2017) Nontarget screening with high resolution mass spectrometry in the environment: ready to go? *Anal Bioanal Chem* 407:6237–6255. <https://doi.org/10.1021/acs.est.7b02184>
- Hommen U, Baveco JM, Galic N, van den Brink PJ (2010) Potential application of ecological models in the European environmental risk assessment of chemicals I: review of protection goals in EU directives and regulations. *Integr Environ Assess Manag* 6:325–337. <https://doi.org/10.1002/ieam.69>
- Jager T, Albert C, Preuss TG, Ashauer R (2011) General unified threshold model of survival—A toxicokinetic-toxicodynamic framework for ecotoxicology. *Environ Sci Technol* 45:2529–2540. <https://doi.org/10.1021/es103092a>
- Jia S, Xu T, Huan T, Chong M, Liu M, Fang W, Fang M (2019) Chemical isotope labeling exposome (CIL-EXPOSOME): one high-throughput platform for human urinary global exposome characterization. *Environ Sci Technol* 53:5445–5453. <https://doi.org/10.1021/acs.est.9b00285>
- Kapo KE, Holmes CM, Dyer SD, De Zwart D, Posthuma L (2014) Developing a foundation for eco-epidemiological assessment of aquatic ecological status over large geographic regions utilizing existing data resources and models. *Environ Toxicol Chem* 33:1665–1677. <https://doi.org/10.1002/etc.2557>
- Karlsson MV, Carter LJ, Agatz A, Boxall ABA (2017) Novel approach for characterizing pH-dependent uptake of ionizable chemicals in aquatic organisms. *Environ Sci Technol* 51:6965–6971. <https://doi.org/10.1021/acs.est.7b01265>
- Koppel N, Rekdal VM, Balskus EP (2017) Chemical transformation of xenobiotics by the human gut microbiota. *Science* 356:eag2770. <https://doi.org/10.1126/science.aag2770>
- Kramer VJ, Etterson MA, Hecker M, Murphy CA, Roesijadi G, Spade DJ, Spromberg JA, Wang M, Ankley GT (2011) Adverse outcome pathways and ecological risk assessment: bridging to population-level effects. *Environ Toxicol Chem* 30:64–76. <https://doi.org/10.1002/etc.375>
- Landis WG, Ayre KK, Johns AF, Summers HM, Stinson J, Harris MJ, Herring CE, Markiewicz AJ (2017) The multiple stressor ecological risk assessment for the mercury-contaminated South River and upper Shenandoah River using the Bayesian network-relative risk model. *Integr Environ Assess Manag* 13:85–99. <https://doi.org/10.1002/ieam.1758>
- Lewis SL, Maslin MA (2015) Defining the anthropocene. *Nature* 519:171–180. <https://doi.org/10.1038/nature14258>
- Lioy PJ, Smith KR (2013) A discussion of exposure science in the 21st century: a vision and a strategy. *Environ Health Perspect* 121:405–409. <https://doi.org/10.1289/ehp.1206170>
- Liu Y-Y, Wang Y, Walsh TR, Yi L-X, Zhang R, Spencer J, Doi Y, Tian G, Dong B, Huang X, Yu L-F, Gu D, Ren H, Chen X, Lv L, He D, Zhou H, Liang Z, Liu J-H, Shen J (2016) Emergence of plasmid-mediated colistin resistance mechanism MCR-1 in animals and human beings in China: a microbiological and molecular biological study. *Lancet Infect Dis* 16:161–168. [https://doi.org/10.1016/S1473-3099\(15\)00424-7](https://doi.org/10.1016/S1473-3099(15)00424-7)
- Lohmann R, Muir D, Zeng EY, Bao LJ, Allan IJ, Arinaitwe K, Booij K, Helm P, Kaserzon S, Mueller JF, Shibata Y, Smedes F, Tsapakis M, Wong CS, You J (2017) Aquatic global passive sampling (AQUA-GAPS) revisited: first steps toward a network of networks for monitoring organic contaminants in the aquatic environment. *Environ Sci Technol* 51:1060–1067. <https://doi.org/10.1021/acs.est.6b05159>
- Lombardo A, Franco A, Pivato A, Barausse A (2015) Food web modeling of a river ecosystem for risk assessment of down-the-drain chemicals: a case study with AQUATOX. *Sci Total Environ* 508:214–227. <https://doi.org/10.1016/j.scitotenv.2014.11.038>
- MacLeod M, Breitholtz M, Cousins IT, De Wit CA, Persson LM, Rudén C, McLachlan MS (2014) Identifying chemicals that are planetary boundary threats. *Environ Sci Technol* 48:11057–11063. <https://doi.org/10.1021/es501893m>
- McEwen SA, Collignon PJ (2018) Antimicrobial resistance: a one health perspective. *Microbiol Spectr* 6. <https://doi.org/10.1128/microbiolspec.ARBA-0009-2017>
- National Research Council (NRC) (2012) Exposure science in the 21st century: a vision and a strategy. National Academic Press, Washington, DC
- Nazaroff WW (2019) Embracing microbes in exposure science. *J Expo Sci Environ Epidemiol*. <https://doi.org/10.1038/s41370-018-0075-4>
- Nyhan M, Grauwil S, Britter R, Misstear B, McNabola A, Laden F, Barrett SRH, Ratti C (2016) “Exposure track”—The impact of mobile-device-based mobility patterns on quantifying population exposure to air pollution. *Environ Sci Technol* 50:9671–9681. <https://doi.org/10.1021/acs.est.6b02385>
- Ockleford C, Adriaanse P, Berny P, Brock T, Duquesne S, Grilli S, Hernandez-Jerez AF, Bennekou SH, Klein M, Kuhl T, Laskowski R, Machera K, Pelkonen O, Pieper S, Smith RH, Stemmer M, Sundh I, Tiktak A, Topping CJ, Wolterink G, Cedergreen N, Charles S, Focks A, Reed M, Arena M, Ippolito A, Byers H, Teodorovic I (2018) Scientific opinion on the state of the art of Toxicokinetic/Toxicodynamic (TKTD) effect models for regulatory risk assessment of pesticides for aquatic organisms. *EFSA J* 16:e05377. <https://doi.org/10.2903/j.efsa.2018.5377>
- Pennington DW, Margni M, Ammann C, Jolliet O (2005) Multimedia fate and human intake modeling: spatial versus nonspatial insights for chemical emissions in Western Europe. *Environ Sci Technol* 39:1119–1128. <https://doi.org/10.1021/es034598x>
- Persson LM, Breitholtz M, Cousins IT, de Wit CA, MacLeod M, McLachlan MS (2013) Confronting unknown planetary boundary threats from chemical pollution. *Environ Sci Technol* 47:12619–12622. <https://doi.org/10.1021/es402501c>
- Posthuma L, Dyer SD, de Zwart D, Kapo K, Holmes CM, Burton GA (2016) Eco-epidemiology of aquatic ecosystems: separating chemicals from multiple stressors. *Sci Total Environ* 573:1303–1319. <https://doi.org/10.1016/j.scitotenv.2016.06.242>
- Rand-Weaver M, Margiotta-Casaluci L, Patel A, Panter GH, Owen SF, Sumpter JP (2013) The read-across hypothesis and environmental risk assessment of pharmaceuticals. *Environ Sci Technol* 47:11384–11395. <https://doi.org/10.1021/es402065a>
- Rappaport SM, Barupal DK, Wishart D, Vineis P, Scalbert A (2014) The blood exposome and its role in discovering causes of disease. *Environ Health Perspect* 122:769–774. <https://doi.org/10.1289/ehp.1308015>
- Rappaport SM, Smith MT (2010) Epidemiology. Environment and disease risks. *Science* 330:460–461. <https://doi.org/10.1126/science.1192603>

- Rico A, Van den Brink PJ, Gylstra R, Focks A, Brock TC (2016) Developing ecological scenarios for the prospective aquatic risk assessment of pesticides. *Integr Environ Assess Manag* 12:510–521. <https://doi.org/10.1002/ieam.1718>
- Robinson TP, Bu DP, Carrique-Mas J, Fèvre EM, Gilbert M, Grace D, Hay SI, Jiwakanon J, Kakkar M, Kariuki S, Laxminarayan R, Lubroth J, Magnusson U, Thi Ngoc P, Van Boeckel TP, Woolhouse MEJ (2016) Antibiotic resistance is the quintessential one health issue. *Trans R Soc Trop Med Hyg* 110:377–380. <https://doi.org/10.1093/trstmh/trw048>
- Rockström J, Steffen W, Noone K, Persson Å, Chapin FS, Lambin E, Lenton TM, Scheffer M, Folke C, Schellnhuber HJ, Nykvist B, de Wit CA, Hughes T, van der Leeuw S, Rodhe H, Sörlin S, Snyder PK, Costanza R, Svedin U, Falkenmark M, Karlberg L, Corell RW, Fabry VJ, Hansen J, Walker B, Liverman D, Richardson K, Crutzen P, Foley J (2009) Planetary boundaries: exploring the safe operating space for humanity. *Ecol Soc* 14:32. <https://doi.org/10.5751/ES-03180-140232>
- Rohr JR, Salice CJ, Nisbet RM (2016) The pros and cons of ecological risk assessment based on data from different levels of biological organization. *Crit Rev Toxicol* 46:756–784. <https://doi.org/10.1080/10408444.2016.1190685>
- Rusyn I, Daston GP (2010) Computational toxicology: realizing the promise of the toxicity testing in the 21st century. *Environ Health Perspect* 118:1047–1050. <https://doi.org/10.1289/ehp.1001925>
- Shen H, Huang Y, Wang R, Zhu D, Li W, Shen G, Wang B, Zhang Y, Chen Y, Lu Y, Chen H, Li T, Sun K, Li B, Liu W, Liu J, Tao S (2013) Global atmospheric emissions of polycyclic aromatic hydrocarbons from 1960 to 2008 and future predictions. *Environ Sci Technol* 47:6415–6424. <https://doi.org/10.1021/es400857z>
- Spanogiannopoulos P, Bess EN, Carmody RN, Turnbaugh PJ (2016) The microbial pharmacists within us: a metagenomic view of xenobiotic metabolism. *Nat Rev Microbiol* 14:273–287. <https://doi.org/10.1038/nrmicro.2016.17>
- Steffen BW, Rockström J (2015) Planetary boundaries: guiding human development on a changing planet. *Science* 347:1259855. <https://doi.org/10.1126/science.1259855>
- Tan YM, Leonard JA, Edwards S, Teeguarden J, Paini A, Egeghy P (2018) Aggregate exposure pathways in support of risk assessment. *Curr Opin Toxicol* 9:8–13. <https://doi.org/10.1016/j.cotox.2018.03.006>
- Teeguarden JG, Tan Y-M, Edwards SW, Leonard JA, Anderson KA, Corley RA, Kile ML, Simonich SM, Stone D, Tanguay RL, Waters KM, Harper SL, Williams DE (2016) Completing the link between exposure science and toxicology for improved environmental health decision making: the aggregate exposure pathway framework. *Environ Sci Technol* 50:4579–4586. <https://doi.org/10.1021/acs.est.5b05311>
- Tse TJ, Doig LE, Tang S, Zhang X, Sun W, Wiseman SB, Feng CX, Liu H, Giesy JP, Hecker M, Jones PD (2018) Combining high-throughput sequencing of *sed*a DNA and traditional paleolimnological techniques to infer historical trends in cyanobacterial communities. *Environ Sci Technol* 52:6842–6853. <https://doi.org/10.1021/acs.est.7b06386>
- Vikesland PJ, Pruden A, Alvarez PJJ, Aga D, Bürgmann H, Li X, Manaia CM, Nambi I, Wigginton K, Zhang T, Zhu Y-G (2017) Toward a comprehensive strategy to mitigate dissemination of environmental sources of antibiotic resistance. *Environ Sci Technol* 51:13061–13069. <https://doi.org/10.1021/acs.est.7b03623>
- Vineis P, Chadeau-Hyam M, Gmuender H, Gulliver J, Herceg Z, Kleinjans J, Kogevinas M, Kyrtopoulos S, Nieuwenhuijsen M, Phillips DH, Probst-Hensch N, Scalbert A, Vermeulen R, Wild CP (2017) The exposome in practice: design of the EXPOsOMICS project. *Int J Hyg Environ Health* 220:142–151. <https://doi.org/10.1016/j.ijheh.2016.08.001>
- Vineis P, Schulte P, McMichael AJ (2001) Misconceptions about the use of genetic tests in populations. *Lancet* 357:709–712. [https://doi.org/10.1016/S0140-6736\(00\)04136-2](https://doi.org/10.1016/S0140-6736(00)04136-2)
- Vogs C, Altenburger R (2016) Time-dependent effects in algae for chemicals with different adverse outcome pathways: a novel approach. *Environ Sci Technol* 50:7770–7780. <https://doi.org/10.1021/acs.est.6b00529>
- Walsh TR (2018) A one-health approach to antimicrobial resistance. *Nat Microbiol* 3:854–855. <https://doi.org/10.1038/s41564-018-0208-5>
- Wang T, Wang Y, Liao C, Cai Y, Jiang G (2009) Perspectives on the inclusion of perfluorooctane sulfonate into the Stockholm convention on persistent organic pollutants. *Environ Sci Technol* 43:5171–5175. <https://doi.org/10.1021/es900464a>
- Waters CN, Zalasiewicz J, Summerhayes C, Barnosky AD, Poirier C, Gałuszka A, Cearreta A, Edgeworth M, Ellis EC, Ellis M, Jeandel C, Leinfelder R, McNeill JR, Richter DDB, Steffen W, Syvitski J, Vidas D, Wagemann M, Williams M, Zhisheng A, Grinevald J, Odada E, Oreskes N, Wolfe AP (2016) The anthropocene is functionally and stratigraphically distinct from the holocene. *Science* 351:aad2622. <https://doi.org/10.1126/science.aad2622>
- Werner I, Hitzfeld B (2012) 50 years of ecotoxicology since silent spring—A review. *GAIA - Ecol Perspect Sci Soc* 21:217–224. <https://doi.org/10.14512/gaia.21.3.13>
- Wild CP (2005) Complementing the Genome with an “Exposome”: the outstanding challenge of environmental exposure measurement in molecular epidemiology. *Cancer Epidemiol Biomarkers Prev* 14:1847–1850. <https://doi.org/10.1158/1055-9965.EPI-05-0456>
- Yin R, Guo Z, Hu L, Liu W, Hurley JP, Lepak RF, Lin T, Feng X, Li X (2018) Mercury inputs to Chinese marginal seas: impact of industrialization and development of China. *J Geophys Res Ocean* 123:5599–5611. <https://doi.org/10.1029/2017JC013691>
- Yoon M, Campbell JL, Andersen ME, Clewell HJ (2012) Quantitative in vitro to in vivo extrapolation of cell-based toxicity assay results. *Crit Rev Toxicol* 42:633–652. <https://doi.org/10.3109/10408444.2012.692115>
- Zhang X (2019) Environmental DNA shaping a new era of ecotoxicological research. *Environ Sci Technol* 53:5605–5612. <https://doi.org/10.1021/acs.est.8b06631>
- Zhu H, Zhang J, Kim MT, Boison A, Sedykh A, Moran K (2014) Big data in chemical toxicity research: the use of high-throughput screening assays to identify potential toxicants. *Chem Res Toxicol* 27:1643–1651. <https://doi.org/10.1021/tx500145h>
- Zhu Y-G, Johnson TA, Su J-Q, Qiao M, Guo G-X, Stedtfeld RD, Hashsham SA, Tiedje JM (2013) Diverse and abundant antibiotic resistance genes in Chinese swine farms. *Proc Natl Acad Sci USA* 110:3435–3440. <https://doi.org/10.1073/pnas.1222743110>
- Zinsstag J, Crump L, Schelling E, Hattendorf J, Maidane YO, Ali KO, Muhammed A, Umer AA, Aliyi F, Nooh F, Abdikadir MI, Ali SM, Hartinger S, Mäusezahl D, de White MBG, Cordon-Rosales C, Castillo DA, McCracken J, Abakar F, Cercamondi C, Emmenegger S, Maier E, Karanja S, Bolon I, de Castañeda RR, Bonfoh B, Tschopp R, Probst-Hensch N, Cissé G (2018) Climate change and one health. *FEMS Microbiol Lett* 365:fny085. <https://doi.org/10.1093/femsle/fny085>